7th ICANAS 2024

INTERNATIONAL CONFERENCE ON ADVANCES IN NATURAL AND APPLIED SCIENCES

17-20 APRIL 2024 — **ANTALYA / TÜRKİYE**

BOOK of ABSTRACTS & PROCEEDINGS

7th ICANAS 2024
INTERNATIONAL CONFERENCE ON ADVANCES IN NATURAL AND APPLIED SCIENCES
17-20 APRIL 2024 ANTALYA / TÜRKİYE

Chief Editor | Önder ŞİMŞEK
Executive Editors | Abdulkerim KARABULUT
Ahmet ÖZMEN
Mustafa Tolga YURTCAN
Technical Editors | Hülya AKINCIOĞLU
Burak ALAYLAR
Tuba AYDIN
Bünyamin AYGÜN
Esra KADANALI
Aydın KIZILASLAN
Zeynep UZUNOĞLU
Book Cover Design | Ahmet ÇAĞAN

All papers published in this abstract book have been peer reviewed.

Dear colleagues,

On behalf of the Scientific and Organizing Committee, following the six tremendously successful ICANAS conferences we have held in IC Hotels Green Palace, Antalya, we are pleased to invite you to participate in the 7th International Conference on Advances in Natural and Applied Sciences (ICANAS 2024) that will be held in Antalya at the summit of Anatolia on 17-20 April 2024.

ICANAS 2024 stands for International Conference on Advances in Natural and Applied Sciences open to researchers from all over the world working in the fields of Natural and Applied Sciences. It serves as a platform to present the latest research results, to exchange new ideas and application experiences, to discuss challenging issues, to establish research relations and to find global partners for future collaboration. ICANAS 2024 is a non-profit scientific organization. Exclusive scientific committee and organizing committee of the conference are to ensure that the congress is conducted following high academic standards. We hope that the conference results provide significant contribution to the global knowledge in the relevant scientific fields.

We are proud that ICANS 2024 is taking place in Antalya, with the support of the İbrahim Çeçen Foundation and with the auspices of Ağrı İbrahim Çeçen University. For their precious financial support, I also like to thank all of the scientific institutions and commercial sponsors listed in the program.

We thank you for your participation and hope that this conference will provide an excellent chance to network with leading scientists from around the globe in the stimulating atmosphere of the venue on the Antalya.

We hope that everyone's stay is enjoyable and productive.

Best regards,

Prof. Dr. Önder ŞİMŞEK

Conference Chair

Distinguished Rector, esteemed guests, and valued academics,

Welcome to the 7th International Conference on Advances in Natural and Applied Sciences!
In the history of mankind, behind every great breakthrough there is a scientific discovery. From flame to electrical energy, from the discovery of the microscope to the exploration of space, scientific knowledge has always been the source of progress and enlightenment.

At ICANAS 2024, we are here to continue this blessed tradition and change the world together in the light of scientific knowledge. This conference, where distinguished academics from all over the world come together to share the latest research findings in biology, physics, engineering, health sciences and many other fields, exchange ideas and set out together to new horizons, is an important platform not only for knowledge sharing and scientific advancement, but also for finding solutions to global problems.

We need the power of science and collaboration to solve humanity's biggest problems, such as climate change, food security and the energy crisis. I sincerely believe that this conference, which is also important to demonstrate the unifying power of science and the importance of working together to find common solutions to these challenges, will help build a brighter and more prosperous future in the light of science.

Dear Participants,
As İbrahim Çeçen Foundation, we believe that "everyone who lives in this country owes a debt of heart to this country." We are involved in many areas such as education, health, employment, support for disadvantaged groups as well as sport, culture and art.
Our goal is to create a qualified society and we see education as the basis for this. For this reason, Ağrı İbrahim Çeçen University, which we founded in 2007 and donated to the state, has developed into an important education and research center for our region and our country since its establishment.

With our scholarship program, one of the priority activities of our foundation, we have contributed to the education of 16 thousand young people so far. This academic year, we will continue to support 1,500 scholarship holders. With the "Community Service" requirement, we want to make our scholarship holders aware of social responsibility. In this context, we try to open new horizons for them by organizing various educational projects, international programs and meetings.

In addition to Ağrı İbrahim Çeçen University, we have also built permanent works such as 5 elementary school, a girls' dormitory in Ağrı and a training kitchen for the catering department. With the IC-Career Bridge Project, we aim to contribute to the career development and employment of our scholarship holders by bringing IC Group companies together with university faculties.

As the IC Foundation, our common goal is for our university to serve society by keeping up with the times through scientific research. To contribute to the realization of this goal, I would like to highlight the Article Incentive Awards, which we established 12 years ago and which have become one of our traditional contributions, increasing every year. All academics from our university who publish on national and international platforms in the natural and social sciences are rewarded by the Foundation. When we decided to provide this support, our aim was to reward scientific publications and at the same time encourage more.

When I look at the increasing number of publications today, I can see that we made the right decision. The journals for natural and social sciences, which have continued for 8 years, are published twice a year and have given our university a great academic boost, contributing significantly to the publications of academics in certain fields. In addition to these journals, we

as a foundation are also happy to support national and international congresses and symposia. The building inspection laboratory, which will be used for earthquake studies, and the cell culture laboratories, that will be used for health research, are among the technical support we have donated to our university this year. We also felt that the biggest solution for Ağrı's public health is the medical school within the university. Within the framework of the protocol we signed with our Rectorate, we continue to support the scientists of the Faculty of Medicine. Our university has stood by our side and given us strength in all these endeavors. Hosting you, dear universities, with this international congress that we are opening today is the best example of this.

It is very meaningful for us to see that Ağrı İbrahim Çeçen University joins forces with other educational institutions and scholars by supporting the production and exchange of knowledge in the international community. For this reason, we were very excited when the Icanas International Conference on Advances in Basic and Applied Sciences was organized for the first time. The congress, which we started to support with this initial conviction and enthusiasm, has ensured its sustainability with the efforts of our academicians and is now reaching its 7th year. I wholeheartedly congratulate you on this success. I sincerely believe that you, our esteemed academicians and the students you educate will be individuals who research, produce, ask questions, respect human rights and freedoms, and act with scientific understanding for the benefit of society.

Distinguished guests
The ICANAS conference that we are organizing here today is an important event that will raise the visibility of our university on the international stage and promote the production and exchange of scientific knowledge. We believe that this conference will bring together academics from different disciplines to discuss the latest developments in basic and applied sciences and to establish new collaborations.

We think it is very valuable that ICANAS 2024 will share the latest research findings in many fields such as biology, mathematics, physics, chemistry, architecture, engineering, health sciences, agriculture and food sciences. Bringing together academics from different disciplines on this platform, sharing new ideas and practical experiences is also crucial for building research relationships and finding global partners for future collaboration.

We believe that ICANAS 2024 will make a valuable contribution to the development of scientific knowledge and the promotion of research in this field. We hope that this conference will be an inspiring and useful experience for all participants.

I would like to thank the Agri Ibrahim Çeçen University and all those who contributed to the ICANAS conference and wish that the conference will be useful and inspiring for all participants.

Günseli ÇEÇEN

IC Foundation Chairperson

ICANAS 2024

ORGANIZATION

Honorary Board
Prof. Dr. Abdulhalik KARABULUT, Rektor, Ağrı İbrahim Çeçen University
İbrahim ÇEÇEN, IC Investment Holding Board Chairman

Chair
Prof. Dr. Önder ŞİMŞEK, Ağrı İbrahim Çeçen University

Organizing Committee
Prof. Dr. Metin AKGÜN, Ağrı İbrahim Çeçen Üniversitesi
Prof. Dr. Hülya AKINCIOĞLU, Ağrı İbrahim Çeçen Üniversitesi
Prof. Dr. Rıdvan DURAK, Atatürk Üniversitesi
Prof. Dr. Mucip GENİŞEL, Ağrı İbrahim Çeçen Üniversitesi
Prof. Dr. Murat GÜNEY, Ağrı İbrahim Çeçen Üniversitesi
Prof. Dr. İbrahim HAN, Ağrı İbrahim Çeçen Üniversitesi
Prof. Dr. Fatma YALÇIN, Ağrı İbrahim Çeçen Üniversitesi
Assoc. Prof. Dr. Burak ALAYLAR, Ağrı İbrahim Çeçen Üniversitesi
Assoc. Prof. Dr. Bünyamin AYGÜN, Ağrı İbrahim Çeçen Üniversitesi
Assoc. Prof. Dr. Tuba AYDIN, Ağrı İbrahim Çeçen Üniversitesi
Assoc. Prof. Dr. Safinur ÇELİK, Atatürk Üniversitesi
Assoc. Prof. Dr. Esra KADANALI, Ağrı İbrahim Çeçen Üniversitesi
Assoc. Prof. Dr. Abdulkerim KARABULUT, Erzurum Teknik Üniversitesi
Assoc. Prof. Dr. Aydın KIZILASLAN, Ağrı İbrahim Çeçen Üniversitesi
Assoc. Prof. Dr. Mustafa Tolga YURTCAN, Atatürk Üniversitesi
Assoc. Prof. Dr. Murat YILDIRIM, Atatürk Üniversitesi
Assist. Prof. Dr. Üyesi Akın AKINCIOĞLU, Ağrı İbrahim Çeçen Üniversitesi
Assist. Prof. Dr. Nimetullah ALDEMİR, Ağrı İbrahim Çeçen Üniversitesi
Assist. Prof. Dr. Dilan ÖZMEN ÖZGÜN, Ağrı İbrahim Çeçen Üniversitesi
Assist. Prof. Dr. Rüya SAĞLAMTAŞ, Ağrı İbrahim Çeçen Üniversitesi
Assist. Prof. Dr. Zeynep UZUNOĞLU, Ağrı İbrahim Çeçen Üniversitesi
Dr. Meral DİNÇER, IC Vakfı Genel Müdürü
Lecturer Ahmet ÇAĞAN, Ağrı İbrahim Çeçen Üniversitesi
Lecturer Ahmet ÖZMEN, Ağrı İbrahim Çeçen Üniversitesi
Derya ŞİMŞEK, Atatürk Üniversitesi

Secretariat
Assist. Prof. Dr. Nimetullah ALDEMİR, Ağrı İbrahim Çeçen University
Lecturer Ahmet ÇAĞAN, Ağrı İbrahim Çeçen University
Lecturer Ahmet ÖZMEN, Ağrı İbrahim Çeçen University

Scientific Board

Prof. Dr. Metin AKGÜN, Ağrı İbrahim Çeçen University, Türkiye
Prof. Dr. Hülya AKINCIOĞLU, Ağrı İbrahim Çeçen University, Türkiye
Prof. Dr. Gonca ALAK, Atatürk University, Türkiye
Prof. Dr. Hakan ARSLAN, Ondokuz Mayıs University, Türkiye
Prof. Dr. Sanaa BARDAWEEL, University of Jordan, Amman
Prof. Dr. Zeki BAYRAMOĞLU, Selçuk University, Türkiye
Prof. Dr. Cevdet COŞKUN, Giresun University, Türkiye
Prof. Dr. Suat ÇELİK, Atatürk University, Türkiye
Prof. Dr. Uğur ÇEVİK, Karadeniz Technical University, Türkiye
Prof. Dr. Oğuz DOĞAN, Necmettin Erbakan University, Türkiye
Prof. Dr. Rıdvan DURAK, Atatürk University, Türkiye
Prof. Dr. Melek EKİNCİ, Atatürk University, Türkiye
Prof. Dr. Mehmet ERTUĞRUL, Karadeniz Technical University, Türkiye
Prof. Dr. Müjde ERYILMAZ, Ankara University, Türkiye
Prof. Dr. Kadir ESMER, Marmara University, Türkiye
Prof. Dr. Hikmet GEÇKİL, Inonu University, Türkiye
Prof. Dr. Mucip GENİŞEL, Ağrı İbrahim Çeçen University, Türkiye
Prof. Dr. Süleyman GÖKSU, Atatürk University, Türkiye
Prof. Dr. Medine GÜLLÜCE, Atatürk University, Türkiye
Prof. Dr. İnci GÜLTEKİN, Atatürk University, Türkiye
Prof. Dr. İbrahim HAN, Ağrı İbrahim Çeçen University, Türkiye
Prof. Dr. Mehmet Akif HAŞILOĞLU, Ağrı İbrahim Çeçen University, Türkiye
Prof. Dr. Kenan KARAGÖZ, Ağrı İbrahim Çeçen University, Türkiye
Prof. Dr. Alper Cihan KONYALIOĞLU, Atatürk University, Türkiye
Prof. Dr. Turgay KORKUT, Sinop University, Türkiye
Prof. Dr. Zeliha KÜÇÜKYUMUK, Isparta University of Applied Sciences, Türkiye
Prof. Dr. Aliev Fikret Ahmadali OGLU, Azerbaijan State University, Azerbaijan
Prof. Dr. Nilüfer OKUR AKÇAY, Ağrı İbrahim Çeçen University, Türkiye
Prof. Dr. Furkan ORHAN, Ağrı İbrahim Çeçen University, Türkiye
Prof. Dr. Lütfi ÖKSÜZ, Süleyman Demirel University, Türkiye
Prof. Dr. Selda ÖRS CIRIK, Atatürk University, Türkiye
Prof. Dr. Lütfi ÖZYÜZER, Izmir Institute of Technology, Türkiye
Prof. Dr. Riyazali Zafarali SAYYED, KBC North Maharashtra University, India
Prof. Dr. Hilal M. ŞEHİTOĞLU, Çanakkale Onsekiz Mart University, Türkiye
Prof. Dr. Rahime ŞİMSEK, Hacettepe University, Türkiye
Prof. Dr. Kadriye URUÇ PARLAK, Ağrı İbrahim Çeçen University, Türkiye
Prof. Dr. Handan UYSAL, Atatürk University, Türkiye
Prof. Dr. Ali YILDIZ, Atatürk University, Türkiye
Assoc. Prof. Dr. Osman AĞAR, Karamanoğlu Mehmetbey University, Türkiye
Assoc. Prof. Dr. Ahmet Gökhan AĞGÜL, Ağrı İbrahim Çeçen University, Türkiye
Assoc. Prof. Dr. Özlem AKGÜL, Eğe University, Türkiye

ICANAS 2024

ICANAS 2024

Assoc. Prof. Dr. Murat YILDIRIM, Ağrı İbrahim Çeçen University, Türkiye
Assoc. Prof. Dr. Mustafa Tolga YURTCAN, Atatürk University, Türkiye
Assist. Prof. Dr. O. Collins AIREMWEN, Cyprus International University, North Cyprus
Assist. Prof. Dr. Akın AKINCIOĞLU, Ağrı İbrahim Çeçen University, Türkiye
Assist. Prof. Dr. Agostinho ALMEIDA, Porto University, Portekiz
Assist. Prof. Dr. Neblea Monica ANGELA, Pitesti University, Romania
Assist. Prof. Dr. Cemalettin AYGÜN, Karadeniz Technical University, Türkiye
Assist. Prof. Dr. Neslihan Balcı, Gümüşhane University, Türkiye
Assist. Prof. Dr. Aykut COŞKUN, Bayburt University, Türkiye
Assist. Prof. Dr. Emine Serap ÇAĞAN, Ağrı İbrahim Çeçen University, Türkiye
Assist. Prof. Dr. Mehmet Ali ÇELİK, Ağrı İbrahim Çeçen University, Türkiye
Assist. Prof. Dr. Tülay DİZİKISA, Ağrı İbrahim Çeçen University, Türkiye
Assist. Prof. Dr. Dilek ERKMEN VATANSEVER, Ağrı İbrahim Çeçen University, Türkiye
Assist. Prof. Dr. Kübra FETTAHOĞLU, Ağrı İbrahim Çeçen University, Türkiye
Assist. Prof. Dr. Elife KAYA, Kahramanmaraş Sütçü İmam University, Türkiye
Assist. Prof. Dr. Beyza Ecem ÖZ BEDİR, Ankara Yıldırım Beyazıt University, Türkiye
Assist. Prof. Dr. Tuba ÖZDEMİR SANCI, Ankara Yıldırım Beyazıt University, Türkiye
Assist. Prof. Dr. Bülent ŞENGÜL, Bayburt University, Türkiye
Assist. Prof. Dr. Dilan ÖZMEN ÖZGÜN, Ağrı İbrahim Çeçen University, Türkiye
Assist. Prof. Dr. Bilge ÖZTÜRK, Bayburt University, Türkiye
Assist. Prof. Dr. Arzu ÖZTÜRK KESEBİR, Ağrı İbrahim Çeçen University, Türkiye
Assist. Prof. Dr. Mohammed Naithel RADHI, University Of Thi-Qar, Iraq
Assist. Prof. Dr. Rüya SAĞLAMTAŞ, Ağrı İbrahim Çeçen University, Türkiye
Assist. Prof. Dr. Ferhan ŞAHİN, Ağrı İbrahim Çeçen University, Türkiye
Assist. Prof. Dr. Emine TERZİ, Ankara Yıldırım Beyazıt University, Türkiye
Assist. Prof. Dr. Zeynep UZUNOĞLU, Ağrı İbrahim Çeçen University, Türkiye
Assist. Prof. Dr. Mustafa YAŞAR, Alparslan University, Türkiye
Assist. Prof. Dr. Casim YAZICI, Ağrı İbrahim Çeçen University, Türkiye
Assist. Prof. Dr. Melek ZOR, Ağrı İbrahim Çeçen University, Türkiye
Assist. Prof. Dr. Aziz AHMAD, Jaipur College of Pharmacy, India
Assist. Prof. Dr. Shivam BHARTIYA, Jain University, India
Uzm. Dr. Mehmet GÜMÜŞTAŞ, İstanbul Başakşehir Çam and Sakura City Hospital, Türkiye
Dr. Abdülkadir KESKİN, İstanbul Medeniyet University, Türkiye
Assist. Prof. Dr. Venkata Suresh PONNURU, Chalapathi Institute of Pharmaceutical Sciences, India

GENERAL INFORMATION ON ICANAS 2024

CONFERENCE VENUE

IC Hotels Green Palace – Kundu Mahallesi Yaşar Sobutay Cad No:432, 07070 Aksu/Antalya, Türkiye

TOPICS

Agriculture and Food Sciences
Architecture and Engineering
Biology
Chemistry
Genetic
Health Sciences
Mathematics and Science Education
Mathematics
Physics

Invited Talks

Antioxidants and Their Potential as Medicines for Some Metabolic Diseases

İlhami Gülçin[1]

[1]*Aataturk University, Erzurum, Turkiye, ORCID: (https://orcid.org/0000-0001-5993-1668)*

Antioxidants are frequently added to foods for presentation of the radical chain reactions and oxidation. They inhibit the initiation and propagation step leading to the termination of the reaction and delay the oxidation process.[1] A variety of foods and beverages of vegetable origin contain a large spectrum of phenolic compounds like curcumin and resveratrol. Among them, curcumin is a phenolic compound and a major component of Curcuma longa, which used for hundreds of years as a flavor, color, and preservative. Curcumin has significant medicinal potential. This nutraceutical compound reported to possess therapeutic properties against a variety of diseases ranging from cancer to cystic fibrosis.[2] On the other hand, resveratrol (3,5,4'-trans-trihydroxystilbene), a natural product, is known to affect a broad range of intracellular mediators. resveratrol has been identified as the major active stilbene phytoalexins and is presumed to be beneficial for human health. Resveratrol is a naturally occurring phytoalexin in the fruits and leaves of edible plants, peanuts, mulberries, and especially grapes. It is currently in the limelight all over the world due to its beneficial effects on the human body. [3] Recently, phenolic compounds have attracted much attention due to their significant medicinal potentials including treatment of some metabolic diseases like Alzheimer's disease, glaucoma and diabetes. In this presentation, we determined and argued the antioxidant activity of some natural phenolic compounds including curcumin and resveratrol in various in vitro antioxidant assays. Their antioxidant potential will be compared to some standard and synthetic antioxidants including BHA, BHT, α-tocopherol and trolox.

References

[1] İ. Gulcin, 2020. Antioxidants and antioxidant methods-An updated overview, Arch. Toxicol., 94(3), (2020) 651-715.

[2] T. Ak, I. İ. Gulcin, 2008. Antioxidant and radical scavenging properties of curcumin, Chem. Biol. Interact., 174 (2008) 27–37.

[3] İ. Gülçin, 2010. Antioxidant properties of resveratrol: A structure-activity insight. Innov. Food Sci. Emerg. Technol.11 (2010) 210-218.

Bioremediation of saline soil using sustainable microbial technology: Success story from lab to land

N. K. Arora

Department of Environmental Science, School of Earth and Environmental Sciences
Babasaheb Bhimrao Ambedkar University, Lucknow 226025, Uttar Pradesh, India
ORCID: 0000-0001-9412-663X

Climate change, global warming and pollution are the greatest threats to mankind, affecting the food security and environmental sustainability. Reports show that about 3.6 billion people already live in areas highly susceptible to climate change. World Health Organization reports that between 2030 and 2050, around 250000 deaths are expected due to climate change induced stresses such as drought, heat, diseases, pollution etc. The Intergovernmental Panel on Climate Change's (IPCC) Sixth Assessment Report (AR6) highlighted that climate risks are appearing sooner and are more severe than expected, however the actions taken are unsatisfactory and minimal. The United Nations Sustainable Development Goals are also lagging far behind their targets and are on the verge of losing their aim to limit the average temperature rise to 2° C. The increasing weather extreme events have led to severe land degradation enhancing the risk of soil degradation. Soil salinization is one of the most detrimental abiotic stresses, affecting one billion hectares of land accounting for 7% of global area and an annual loss of USD 27.3 billion. According to the Intergovernmental Science-Policy Platform on Biodiversity and Ecosystem Services (IPBES) and the U.S. Agency for International Development (USAID), salt-affected regions have increased from 45 million hectares to almost 1 billion hectares since the 1990s, thereby hitting hard the agricultural output. Physical and chemical solutions proposed to remediate saline lands are unsustainable.

Plant growth promoting microbes are beneficial soil entities living in in close proximity to roots and having complex associations with plants. The complex signaling and interaction between plants and microbes help in amelioration of stresses and inducing growth of plants under hostile and non-hostile conditions. We checked and selected diverse groups of salt-tolerant plant growth promoting microbes (ST-PGPM) for their remediation and growth promotion attributes under saline conditions. Selected strains showed plant growth promoting activities such as production of phytohormones, assimilation of nutrients and various salt stress ameliorating activities such as antioxidant activity, osmoregulation, exopolysaccharide production. The selected PGPM were used to design novel bioformulations for saline. The novel bioinoculants were tested using various crops

under different saline conditions. These products were applied to crops like cereals, staple crops, paddy, oilseed, legumes, vegetables, and their growth and productivity were checked along with improvement in soil quality. Over the years promising results were obtained and soils showed complete remediation along with increased productivity of crops. The developed bioinoculants can be cheap and sustainable solution to remediate saline fields and increase the economic status of farmers leading to food and economic security.

Keywords: Bioremediation, Salinity, PGPM, Novel Bioformulation, Sustainable Development Goals

Enhancing Radiation Protection: A Comparative Analysis of Heavy Metal Oxides in Glass Shielding Systems

M.I. SAYYED[1,2]

[1]*Department of Physics, Faculty of Science, Isra University, Amman – Jordan*
[2]*Renewable Energy and Environmental Technology Center, University of Tabuk, Tabuk 47913, Saudi Arabia.*

This study delves into the efficacy of various glass systems, integrated with heavy metal oxides, in providing radiation shielding, aiming to contribute significantly to the development of safer, more efficient protective materials in environments exposed to ionizing radiation. Recognizing the pivotal role of glass compositions in mediating radiation absorption, we systematically investigate the attenuation characteristics of several glass systems, each doped with different heavy metal oxides such as lead oxide (PbO), bismuth oxide (Bi2O3), and tungsten oxide (WO3). Through a comprehensive experimental setup, we measure the gamma-ray and neutron shielding efficiencies, employing a range of energies relevant to medical, industrial, and research applications.

Our findings reveal that the incorporation of heavy metal oxides into glass matrices markedly enhances their shielding capabilities, attributable to the high atomic numbers and densities of these additives. Notably, glasses doped with bismuth oxide exhibit superior performance, presenting a promising lead-free alternative to traditional radiation shielding materials. Furthermore, the study explores the trade-offs between optical transparency and shielding efficiency, addressing the critical demand for transparent, yet protective barriers in various applications.

By providing a detailed comparative analysis, this work offers valuable insights into the design and optimization of glass-based shielding systems, emphasizing the potential of heavy metal oxide doping as a strategic approach to improving radiation protection. Our results hold profound implications for the advancement of safe, effective, and environmentally friendly shielding materials, paving the way for their application in medical imaging, nuclear safety, and beyond.

Configurations and Conformations: an Achilles Heel of Structure Elucidation of Natural Products

A. Kijjoa

Instituto de Ciências Biomédicas Abel Salazar and CIIMAR, Universidade do Porto, Portugal,
ORCID: http://orcid.org/0000-0002-3321-1061

Chirality is a key feature of natural products, which is crucial for their biological/pharmacological activities. Although many important classes of natural products such as xanthones, anthraquinones, flavonoids, coumarins and some phenolics, do not possess chiral center, and are major targets of a majority of natural products chemists, there is a large portion of natural products, possessing one or more chiral centers, that serves as a source of diverse diastereoisomers with different chemical and biological properties. Therefore, it is necessary to unequivocally establish the absolute configuration of each chiral center by either X-ray crystallography or chiroptical methods. Another type of stereoisomers is atropisomerism which arises because of hindered rotation about a single bond, where energy differences due to steric strain or other contributors create a barrier to rotation that is high enough to allow for isolation of individual conformers. Many natural products display this phenomenon. Many natural products also contain amide bonds whose rotation can produce several rotamers that exhibit different ^{1}HNMR signals. Finally, some of natural products that contain a particular type of flexible ring can also adopt various conformations which gives different and peculiar NMR signals. Therefore, the objective of the present paper is to demonstrate the examples of the determination of the absolute configurations of some complex natural products and to determine different atropisomers by ^{1}H and ^{13}CNMR methods as well as to demonstrate the effects of conformations on the appearances of the NMR signals.

Dual Coumarin-Based Inhibitors of Carbonic Anhydrases and Monoamine Oxidase B Against Neurodegenerative Disorders

S. Carradori

Department of Pharmacy, University "G. d'Annunzio" of Chieti-Pescara, ORCID: 0000-0002-8698-9440

Recent research has revealed that some clinically approved carbonic anhydrase (CA) inhibitors can prevent the Aβ-induced increase in Reactive Oxygen Species (ROS) and mitochondrial dysfunction in vitro, limiting neuronal apoptosis. In addition, it was shown that the activity of monoamine oxidase B (MAO-B) elicit ROS production, leading to the alteration of the cholinergic system and the formation of amyloid plaques. Thus, dual inhibitors of human CAs and MAO-B were designed to tackle multiple pathways involved in Alzheimer's disease (AD) and prevent $A\beta_{1\text{-}42}$-associated neurotoxicity. The multitarget drug design strategy merged a reversible MAO-B inhibitor (coumarin) with benzenesulfonamide fragments as highly effective CA inhibitors. Among our designed derivatives, some 7-substituted coumarins demonstrated the best dual-targeting activity in the nanomolar range against hCAs and hMAO-B. The most effective multitarget compounds successfully counteracted Aβ-related toxicity, reversed ROS formation, and restored the mitochondrial functionality in SH-SY5Y neuroblastoma cells. Computational analyses and other *in silico* approaches were conducted to elucidate the structure−activity relationships and pharmacokinetics for planning *in vivo* studies. Further research in this area could open new scenarios for novel therapeutic interventions for AD and related conditions.

Abstracts

Nuclear Radiation Shielding Properties of Newly Developed Composite Metal Foams: Role of TeO$_2$ Addition and Foam Type

R. Durak[1] and A. Araz[1]

[1]*Atatürk University, Faculty of Science, Erzurum, Türkiye, ORCID: 0000-0002-3935-176X*

In current study, a new composite material was produced by filling open-cell aluminum foams with additives and the role of TeO$_2$ amount in the additive, changing of thickness and pore size of the foam on the radiation shielding efficiency of this material was investigated. The aluminum foams with 30 mm thickness 2 pores/cm and 10 mm thickness 16 pores/cm pore sizes encoded A1-A5 and B1–B5 respectively were filled with different mixtures which have Epoxy(60) -B$_2$O$_3$(20)- CeO$_2$ (20-x)-TeO$_2$(x); (x; 0, 5, 10, 15 and 20 wt%) chemical compositions. The measurements of this study were carried out in three different experimental systems. Ultra Ge detector was used for gamma measurements and the samples were bombarded with 241Am, 133Ba, and 137Cs radioactive sources. Measurements were made for photon energy of 6 MV (~ 2 MeV) using a linear accelerator for X-ray measurements. BF3 gas neutron detector and 241Am-Be neutron source were used for neutron measurements. The linear attenuation coefficients (LAC) of the samples and further photon protection parameters derived from LAC were computed with the data acquired from those measurements. The MAC, Zeff and Ne values of the samples decreased with the rising in the percentage of TeO2 added to the epoxy mixture. Moreover, energy absorption (EABF) and exposure (EBF) buildup factors in the energy range of 0.015-15 MeV were computed up to 40 mean free path (MFP). It was concluded that the 20% TeO$_2$ added samples had the least EABF value. Finally, the shielding potential of the prepared samples against fast neutrons was assessed by performing equivalent dose measurements (EAD) and calculating macroscopic cross section (∑R) values. It was observed that the ∑R values decreased with the increase in the TeO$_2$ percentage in the additive and it was determined that the B5 sample had the highest absorption dose rate of 44%. Generally, it was concluded that the samples in the B series, which are thinner and have more pores, have better radiation attenuation capabilities.

Keywords: Composite metal foam, TeO$_2$, shielding, mass attenuation coefficient, buildup factor

Base-State Properties of N-Electron Quantum Dot Structures Interacting Within the Morse Potential

R. Durak[1] and R.A. Raoof[1]

[1]Atatürk University, Faculty of Science, Erzurum, Türkiye, ORCID: 0000-0002-3935-176X

In this study, ground state properties such as electron density, chemical potential, kinetics and Hartree energy etc. of a quantum dot (QD) system, which contains a large number of interacting electrons confined in Morse potential ($V(r) = V_0(1 - e^{-br})^2$, V_0 and b constants), are investigated depending on the V_0 and b boundary parameters. To that end, firstly, the electron density for the two-dimensional electron gas interacting with the limited Coulomb potential in the Morse potential at $T = 0$ K is expressed using Fermi-Dirac functions. Then, the density expression is combined with the Poisson equation to obtain the Thomas-Fermi equation for the interacting system. The solution of the Thomas-Fermi equation is numerically carried out. The effect of electron interaction on the ground state properties of the system was determined by taking $V_e = 0$ in the numerical operation. When the results were compared with the non-interacting ($V_e = 0$) results, it was concluded that the depth and curvature of the confinement potential significantly changed the intensity of electron interactions and thus the overall system properties.

Synthesis of Triazole Compounds from Azide-derived Oxazolidinone Compounds

A. Yıldırım[1] and Z. Odabaş[1]

[1]Marmara University, Faculty of Science, Chemistry Department, Kadıköy, İstanbul ORCID: 0000-0003-1701-1606

Oxazolidinones have a unique mechanism of bacterial protein synthesis inhibition and constitute a relatively new class of antimicrobial agents. Oxazolidinones [1] have wide usage areas due to their biological activities. In the last few years, interest in the synthesis of oxazolidinones has increased considerably due to their biological activity. Optically pure oxazolidinones [2] play key roles in the synthesis of different types of düğse, antibiotic, antidepressant, antihistamine, antifungal or antibacterial activities. Another reason why compounds bearing the oxazolidinone ring have become the focus of attention is that they inhibit protein synthesis, which is of great importance far living things. This project, endoperoxide compounds were synthesized from 1,3-diene compounds by photooxygenation method. Af ter the resulting endoperoxide compounds were converted into hydroxy ketones with NEt3, oxazolidinone derivatives were synthesized from α,β-unsaturated hydroxy ketones using CSI. The synthesis of biologically important azide-derived oxazolidinone compounds from oxa compounds has been achieved in high yields. After these steps, triazole molecules [3] will be synthesized from azide-derived compounds by the click reaction,

Key Words: Phthalocyanine, oxo-bridged, metal, metal-free

References

[1] Bach, T., Schlummer, B. and Harms, K., 2001. - A European Journal, 7 (12), 2581-2594.

[2] Laserna, V., Guo, W. and Kleij, A.W., 2015. Advanced Synthesis & Catalysis, 357 (13), 2849-2854.

[3] Demaray, Jeffrey A., et al. "Synthesis of triazole-oxazolidinones via a one-pot reaction and evaluation of their antimicrobial activity." Bioorganic & medicinal chemistry letters 18.17 (2008): 4868-4871.

Investigation of Inhibition Effects of Some Flavonoids on Cholesterol Esterase

V. Comaklı[1], A. Oztekin[2], S. Adem[3], S. Tasbası[4], Z. Yardımcı[4] and G. Bas[5]

[1]Department of Nutrition and Dietetics, Faculty of Health Sciences, Agri Ibrahim Cecen University, Agri-TURKEY, ORCID: 0000-0003-2109-6702
[2]Department of Medical Services and Techniques, Vocational School of Health Services, Agri Ibrahim Cecen University, Agri-TURKEY, ORCID: 0000-0003-1418-179X
[3]Department of Chemistry, Faculty of Sciences, Cankiri Karatekin University, Cankiri-TURKEY, ORCID:0000-0003-2146-5870
[4]Department of Chemistry, Postgraduate Education Institute, Agri Ibrahim Cecen University, Agri-TURKEY
[5]Department of Chemistry, Postgraduate Education Institute, Cankiri Karatekin University, Cankiri-TURKEY,

Cholesterol esterase (CE; EC 3.1.1.13), synthesized by the gall bladder, plays a considerable role in both the hydrolysis of exogenously taken cholesterol esters and the carrying of free cholesterol from micelles to intestinal absorptive cells (Zhao et al., 2022). CE is found in a small number of mammals, with the inclusion of humans (John et al., 2010). This enzyme hydrolyzes sterol esters, separating them into fatty acids and sterols. Additionally, it carries out hydrolysis reactions of diverse substrates, including triglycerides, phospholipids, and fat-soluble vitamins (Sivashanmugam et al., 2013). Flavonoids are natural compounds that have a polyphenolic structure and are widely found in vegetables, fruits, bark, flowers, roots, stems, grains, wine, and tea (Guven et al., 2019). In this study, the inhibitory effects of myricetin, scutellarin, 6-hydroxyflavone, baicalein, and morin flavonoids on the CE enzyme were investigated. According to the results, the IC50 values of myricetin, scutellarin, 6-hydroxyflavone, baicalein, and morin were found to be 26 µM, 11 µM, 28 µM, 22 µM, and 64 µM, respectively. Consequently, it was observed that scutellarin was the most effective compound, and this compound noticeably inhibited the CE in addition to being used as an anti-inflammatory and antioxidant.

Key words: Cholesterol esterase, Flavonoids

References

[1] Guven, H., Arici, A., & Simsek, O. (2019). Flavonoids in Our Foods: A Short Review. *Journal of Basic and Clinical Health Sciences Basic Clin Health Sci*, *3*, 96–106.

[2] John, S., Thangapandian, S., Sakkiah, S., & Lee, K. W. (2010). Discovery of potential pancreatic cholesterol esterase inhibitors using pharmacophore modelling, virtual screening, and optimization studies. Taylor & FrancisS John, S Thangapandian, S Sakkiah, KW LeeJournal of Enzyme Inhibition and Medicinal Chemistry, 2011•Taylor & Francis, 26(4), 535–545.

[3] Sivashanmugam, T., Muthukrishnan, S., Umamaheswari, M., Asokkumar, K., Subhadradevi, V., Jagannath, P., & Madeswaran, A. (2013). Discovery of potential cholesterol esterase inhibitors using in silico docking studies. ||| Bangladesh Journal of Pharmacology|||, 8(3).

[4] Zhao, S., Wu, Y., & Hu L. (2022). Identification and synthesis of selective cholesterol esterase inhibitor using dynamic combinatorial chemistry. *Elsevier*, *119*.

Draft

Assessment of Fall Risk in the Postpartum Period by Adapting the Postpartum Period Fall Risk Scale

E.S. Çağan[1], R. Taşkın[1], E. Solmaz[1], A. Ekşioğlu[2], Z. Baykal Çağan[2] and E. Eminov[1]

[1]Ağrı Ibrahim Cecen University, Ağrı, Turkey, ORCID: 0000-0002-3261-0431
[2]Ege University, İzmir, Turkey, ORCID: 0000-0002-8769-3289

The study was aimed to evaluate the fall risk in women during the postpartum period by adapting the postpartum fall risk scale into Turkish. The research is methodological and cross-sectional. The population of the study consisted of women (n: 272) hospitalized in the postpartum service in a hospital in the eastern region of Turkey. Research data were analyzed in the IBM SPSS (Statistical Package for the Social Sciences) 23.0 package program. It has been determined that 31.2% of the participants are in the 20-24 age group, and the average age is 26.75±6.00. It has been found that 58.5% of women are primary school graduates, 93.4% are not working, and 71.0% have health insurance. When the obstetric histories of women were examined, it was determined that 33.5% had a cesarean section birth, and 94.5% of these women had a cesarean section with spinal anesthesia. The postpartum period fall risk scale mean score of the participants was determined as 1.27±1.70. It was determined that there was a significant relationship between the type of birth and the risk of postpartum falls, and the risk of postpartum falls was significantly higher in those who had a cesarean section. It is thought that the postpartum period fall risk assessment scale will facilitate the assessment of fall risk in puerperant women.

Keywords: Falling, postpartum, scale

References

[1] Vriz GB, Soriani N, Postai D, Piras GN, Masè C, Comoretto RI, et al. A simple instrument to assess the risk of falling in postpartum women: The SLOPE Scale (riSk of faLling in pOstPartum womEn). Journal of Obstetrics and Gynaecology.2021;1-6

[2] Gaffey AD. Fall prevention in our healthiest patients: assessing risk and preventing injury for moms and babies. Journal of Healthcare Risk Management.2015;34(3), 37-40.

[3] Simpson KR. Patient falls in the perinatal setting. MCN: The American Journal of Maternal/Child Nursing.2010;35(6), 364.

Ornithological Potential of Foça (İzmir)

E. Azizoğlu[1] and E. Çelik[2]

[1]*Department of Plant and Animal Production, Çölemerik Vocational School, Hakkari University, Hakkari, 30100, Turkey, ORCID: 0000-0002-4895-4298*
[2]*Hunting and Wildlife Program, Department of Forestry, Vocational School of Technical Sciences, Igdir University, Igdir, 76000, Turkey, ORCID: 0000-0003-1274-4122*

In this study, bird species in Foça and its immediate surroundings were investigated. The research which kept nearly two years occurred between March 2019 and September 2021. As a result of the observations, 155 bird species belonging to 14 orders and 44 families were recorded in Foça and its surroundings. When the migration status of the species was evaluated, it was determined that 60 species were residant (R), 67 species were summer visitors (SV), 21 species were transit migrants (T) and 7 species were winter visitors (WV). According to IUCN conservation criteria, it was determined that 2 species are Vulnerable (VU), 3 species are Near Threatened (NT) and 150 species are Least concern (LC).

References

[1] İ. Kiziroğlu, 2015. Türkiye Kuşları Cep Kitabı, Sarıyıldız Ofset ve Matbaacılık, Ankara, 577.

[2] O. Onmuş, M. Sıkı, 2011. Gediz Deltası'nda (İzmir-Türkiye) üreyen ve kışlayan Kıyı Kuşlarının (Yağmurcunlar) populasyon büyüklükleri, dağılımları ve mevsimsel değişimleri, Turk Journal Zoology, 35(5) 615-629.

[3] M. Sıkı, 2002. The birdsof Gediz Delta-Izmir Bird Paradise[GedizDeltasi- Izmir Kus Cenneti Kuslari]'- EcologyandEnvironment/EkolojiÇevreDergisi,2002:1300-1361.

Poisonous Plants; Van Case Study

M. Mukemre[1] and N.A. Ertas[2]

1Hakkari University, Yüksekova Vocational School, Department of Plant and Animal Production, Hakkari, Türkiye, ORCID: 0000-0001-6154-6603
2Hakkari University, Vocational School of Health Services, Department of Medical Services and Techniques, Hakkari, Türkiye, ORCID: 0000-0003-3590-5961

In Eastern Anatolia, due to its geographical location and structure, as well as the dominance of rural lifestyle and economic reasons, local people benefit from wild plants for food and treatment purposes. As a result of negative experiences, it has become clear that a significant part of these plants are poisonous. Especially the local people living in rural areas such as Van, which is our study area, can cause serious poisoning if they come into contact with or use poisonous plants, which are similar to plants used for food or treatment purposes. Therefore, ethnotoxic information about the poisonous plants detected in the province of Van, as well as the local names of the plants, their poisonous parts, their poisonous dose and their poisonous effects, were revealed. The ethnotoxic information data was collected over ten years period (2014-2023) based on structured face-to-face interviews with local healers (320 informants) identified with their long practice in traditional medicine using toxic plants. As a result of the research, a total of 54 poisonous plant taxa belonging to 21 families and local information about these taxa were determined. The study revealed that in traditional medicine, only 33 vernacular (common) names were in use to describe these 54 plant taxa. Out of the traditionally known 46 ethnotoxic plants only 15 are utilized for medicinal purposes. The application of toxic plants in folk medicine is based on (i) strict dose and (ii) utilization of the second fraction of decoction or infusion. The highest degree of consensus among the traditional healers was recorded in regards to the effects of toxic botanicals on nervous system (ICF: 0.96). The ethnobotanical data collected in this study may provide valuable leads for the identification of novel and efficient pharmaceutical agents.

References

[1] Baytop, T. Türkiye'nin tıbbı ve zehirli bitkileri. İstanbul Universitesi (1963).

[2] Kocabaş, Y. Z. Türkoğlu (Kahramanmaraş) ilçe florasında bulunan zehirli bitkiler. Turkish Journal of Science and Health, 1(1), 42-51 (2020).

[3] Yılmaz, O. Bursa yöresinde yetişen önemli zehirli bitkilerin toksikolojik özellikleri (Doctoral dissertation, Bursa Uludag University (Turkey) (1990).

Investigated Study of Anemia in Pregnant Women

H.B. Farhood[1]

[1]*Chemistry department, College of science, University of Thi-Qar, Iraq, ORCID: 0000-0003-1856-2207*

Pregnancy is a natural time for physiological changes that promote fetal growth and get the mother ready for labor and delivery. While some of these alterations affect typical biochemical values, others could resemble the signs and symptoms of a specific illness. It's critical to distinguish between pathology associated with a disease and normal physiological changes in order to better comprehend the situation and take appropriate action. One of the most frequent medical conditions that pregnant women deal with is anemia. Hemoglobin concentration is the foundation for the World Health Organization's classification of anemia. Pregnancy-related anemia can occur for a variety of reasons, including medical, socioeconomic, etc. This study was designed to investigate the role of anemia and some chemical parameters such as vitamin D and iron in pregnant women. The comparison was made between two age groups of pregnant women, the first group A from 18 to 25 years, and the second group B from 26 to 33 years, in addition to comparing it with a control group of non-pregnant women in the same age group. Anemia was measured through hemoglobin levels, which were significantly decreased in group B compared to group A and the control. Iron and vitamin D levels were also significantly decreased, as in the case of hemoglobin.

Keywords: Anemia, hemoglobin, iron, pregnant, vitamin D

Investigation of The Healing Effect of Melatonin On Deltamethrin Applied Mouse Primary Hepatocyte Culture

B. Ergoz Azizoglu[1], E. Kaval Oguz[2], A.R. Oguz[3], N. Ozok[3], Z. Alkan[3], E. Orgi[3], A. Yesilbas[3] and A.N. Erdemir[3]

[1]Vocational School Crop and Animal Production Dairy and Livestock Breeding Program, Hakkari University, Hakkari, Türkiye, ORCID: 0000-0002-7002-3801
[2]Department of Science Education, Van Yüzüncü Yıl University, Van, Türkiye, ORCID: 0000-0003-0196-2693
[3]Department of Biology, Van Yüzüncü Yıl University, Van, Türkiye, ORCID: 0000-0001-6431-0508, ORCID: 0000-0002-6733-211X, ORCID: 0000-0003-2591-0839, ORCID: 0000-0002-5246-5438, ORCID: 0000-0002-6410-9019, ORCID: 0000-0002-7135-0214

In this study, the healing effect of the melatonin hormone on the harmful effects of deltamethrin, a pyrethroid pesticide used extensively in the world and in Turkey, on mouse liver cells was investigated. In the study, hepatocytes from Balb/C mice were isolated by a two-stage perfusion method. The proportion of live hepatocytes isolated was over 85%. The isolated cells were cultured with different doses of deltamethrin (1 and 10 µM) and melatonin (100 µM) for 48 hours. At the end of the culture, hepatocytes were extracted at 24 and 48 hours and Malondialdehyde (MDA), total oxidation (TOS), total antioxidation (TAS), and DNA damages (8-hydroxy-2'-deoxyguanosine (8-OHdG)) were examined. While an increase in MDA, TOS, and DNA damage was observed in the deltamethrin administered groups, a decrease in TAS level was observed. It was determined that the applied deltamethrin had no effect on cell viability throughout the application period. It was observed that melatonin administered together with deltamethrin reduced the toxic effect of deltamethrin. In this study, it can be said that melatonin has a protective effect against deltamethrin-induced damage in mouse hepatocyte cells.

References

[1] Agathokleous, E., Kitao, M., & Calabrese, E. J. 2019. New insights into the role of melatonin in plants and animals. Chemico-biological interactions, 299, 163-167.
[2] Arora, D., Siddiqui, M. H., Sharma, P. K., & Shukla, Y. 2016. Deltamethrin induced RIPK3-mediated caspase-independent non-apoptotic cell death in rat primary hepatocytes. Biochemical and biophysical research communications, 479(2), 217-223.
[3] Cassone, W. M. 1990. Effects of melatonin on vertebrate circadian systems. Trends Neurosci. 13: 457-63.

Determination of Metabolite Profile and Enzyme Inhibitor Activities of Different Extracts from Pitaya

N. Dinç[1] and R. Sağlamtaş[2]

[1]Medical Services and Techniques Department, Agri, Türkiye
[2]Central Research and Application Laboratory, Agri, Türkiye, ORCID: 0000-0002-4400-2302

Dragon fruit (Hylocereus spp.), also known as pitaya or pitahaya, is a tropical and subtropical plant belonging to the Cactaceae family. Hylocereus undatus, which has a reddish bark and white pulp, and Hylocereus polyrhizus, which has a purple bark and pulp, are the two species of this plant that are most widely used for commercial purposes [1,2]. In this study, water, methanol, ethanol, acetone, ethyl acetate, dichloromethane, and n-hexane extracts were prepared from the inner part of Hylocereus polyrhizus using the meceration method. The in vitro effects of the extracts on the critical metabolic enzymes, including acetylcholinesterase (AChE) and butyrylcholinesterase (BChE) were investigated. In addition, in this study, the phytochemical profile of pitaya and the content analysis of its ethanol extract were determined by LC-MC/MC. To determine enzyme inhibition in extracts, half maximum inhibition concentration values (IC50) were calculated. Tacrine was used as a positive control for both enzymes. Experiments were performed in triplicate. The IC50 values of pitaya extracts were calculated as 16.92±0.19 mg/mL-62.45±1.13 mg/mL for AChE and 31.27±0.43 mg/mL-58.56±0.28 mg/mL for BChE. According to the study results, it was determined that ethanol and methanol extracts of pitaya had a stronger inhibitory effect on AChE and BChE enzymes than other extracts. It can be thought that including pitaya fruit in daily nutrition can be used as a protective against chronic diseases such as Alzheimer's and Parkinson's.

References

[1] Le Bellec, F., Vaillant, F., & Imbert, E. (2006). Pitahaya (Hylocereus spp.): a new fruit crop, a market with a future. *Fruits*, *61*(4), 237-250.

[2] Sağlamtaş, R. (2023). Investigation of the inhibition effect of pitaya (hylocereus guatemalensis) bark extracts on some metabolic enzymes. *Gümüşhane Üniversitesi Fen Bilimleri Dergisi*, *13*(3), 595-604.

Compilation of Innovative Studies Conducted Between 2020-2024 on Newborn Health

B. Kaya[1], R. Taşkın[1], E. Solmaz[1] and E.S. Çağan[1]

Ağrı Ibrahim Cecen University, Ağrı, Turkey, ORCID: 0000-0002-2515-479X, ORCID: 0000-0001-5176-157X, ORCID: 0000-0003-1962-8669, ORCID: 0000-0002-3261-0431

The purpose of this study is an examination of innovative studies on newborn health between 2020-2024. Innovative studies on newborn health (2020-2024) were reviewed. The literature was examined through Google Scholar and PubMed with the keywords "newborn, new, device, produce". 17 thousand 600 studies in Google Scholar and 16 studies in PubMed were found. 11 studies found as a result of the literature review were examined. As a result of the literature review, innovative products were developed in nine of the studies and innovative methods were developed in two of them. In the study of Presti et al. (2020), an FMRI-compatible smart device was developed to measure palmar grasping actions in newborns. Kuwelker et al. (2021) used probiotics to reduce infections and deaths and prevent colonization with extended-spectrum beta-lactamase (ESBL)-producing bacteria among newborns in Tanzania. Reis et al. (2022) performed neonatal skin maturity medical device validation for gestational age estimation. Abdul Rahim et al. (2020) monitored the newborn's heart rate and SpO2 using the InfaWrap device. Coffey and Wollen (2022) conducted non-clinical desktop performance testing of a very low-cost non-electric bubble continuous positive airway pressure (bcpap) and mixer device designed for neonatal respiratory support. Vitral et al. (2023) calculated the gestational age in lowbirth weight newborns using the optical skin reflection method. Ditai et al. (2021) designed a new device for neonatal resuscitation with intact placental circulation at birth. Nakadi et al. (2020) developed a simple and direct atomic absorption spectrometry method for the direct determination of Hg in dried blood spots and dried urine spots prepared using various microsampling devices. According to the literature on innovative studies in newborn health between 2020-2024, it was concluded that the studies were mostly created by developing a new device/product.

Keywords: Newborn, new, device, produce

References

[1] Lo Presti, Daniela, Dall'Orso, Sofia, Muceli, Silvia, Arichi, Tomoki, Neumane, Sara, Lukens, Anna, Sabbadini, Riccardo, Massaroni, Carlo, Caponero, Michele Arturo, Formico, Domenico, Burdet, Etienne, Schena, Emiliano. "An fmri compatible smart device for measuring palmar grasping actions in newborns." *Sensors* 20.21 (2020): 6040.

[2]   Kuwelker, Kanika, Langeland, Nina, Löhr, Iren Hoyland, Gidion, Joshua, Manyani, Joel, Moyo, Sabrina John, Blomberg, Bjorn, Klingenberg, Claus. "Use of probiotics to reduce infections and death and prevent colonization with extended-spectrum beta-lactamase (ESBL)-producing bacteria among newborn infants in Tanzania (ProRIDE Trial): study protocol for a randomized controlled clinical trial." *Trials* 22.1 (2021): 312.

[3]   Vitral, Gabriela Luiza Nogueira, Romanelli, Roberta Maia de Castro, Reis, Zilma Silveira Nogueira, Guimaraes, Rodney Nascimento, Dias, Ivana, Mussagy, Nilza, Taunde, Sergio, Neves, Gabriela, Silveira, Jose, Carolina Nogueira de Sao, Pantaleao, Alexandre Negrao, Pappa, Gisele Lobo, Gaspar, Juliano de Souza, Lopes de Aguiar, Regina Amelia Pessoa. "Gestational age assessed by optical skin reflection in low-birth-weight newborns: Applications in classification at birth." Frontiers in Pediatrics 11 (2023): 1141894.

Comparison of Elemental Analysis, Nutritional Values and Health Risk Assessment of Some Commercial Dried Fruits and Natural Dried Fruits

M.E. Şeker[1] and A. Erdoğan[2]

[1]Giresun University, Program of Medicinal and Aromatic Plants, Espiye, 28600 Giresun, Türkiye, ORCID: 0000-0003-4463-6898
[2]University Application and Research Center For Testing and Analysis (EGE MATAL), Bornova, 35100 Izmir, Türkiye, ORCID: 0000-0002-3174-7970

The consumption of dried fruit is suggested for health due to its high content of essential micro and macro nutrients. This work employed inductively coupled plasma mass spectrometry (ICP-MS) to conduct elemental analysis [1] on commercially available tropical dried fruits, namely pineapple, ginger, kiwi, mango, and coconut. A comparison was made between the acquired findings and the naturally dried outcomes of the identical fruits. The findings were utilized in order to ascertain the recommended daily allowances (RDAs) and evaluate the degrees of health risk [2]. The corresponding elements' values are as follows:

Samples		Elements (mg kg^{-1})						
		Na	Mg	K	Ca	Mn	Fe	Zn
Pineapple	Commercial-1	3297	33	122	330	1.8	10	6
	Commercial-2	3660	76	195	587	1.6	6	6
	Natural dried fruits	95	1488	10118	3054	237	22	23
		Na	Mg	K	Ca	Mn	Fe	Zn
Ginger	Commercial-1	876	68	278	1447	14	6	3
	Commercial-2	2268	42	547	617	0.3	20	4
	Natural dried fruits	211	2384	26514	845	27	36	12
		Na	Mg	K	Ca	Mn	Fe	Zn
Kiwi	Commercial-1	5266	83	1223	1827	1.4	21	5
	Commercial-2	4889	85	1221	1815	1.1	21	9
	Natural dried fruits	463	847	20584	2053	3.3	18	10
		Na	Mg	K	Ca	Mn	Fe	Zn
Mango	Commercial-1	2241	50	207	777	0.5	8	1.2
	Commercial-2	2549	53	319	752	0.5	12	2,5
	Natural dried fruits	39	451	7123	1251	7	17	7.1
		Na	Mg	K	Ca	Mn	Fe	Zn
Coconut	Commercial-1	223	9	31	67	0.1	3	7
	Commercial-2	295	17	47	99	0,6	11	5
	Natural dried fruits	404	1024	6659	201	24.9	40	17

Standard deviations for analyzes are below %5, n=3

The amount of potentially toxic elements (As, Pb, Cd, Cr, Ni) were also determined in all samples in order to make a health risk assessment [3]. For all samples, the target hazard quotient (THQ) and hazard index (HI) remained below 1, the carcinogenic risk (CR) remained below 1 x 10^{-6}. It is noteworthy that for some elements the results of naturally dried fruits are up to 100 times higher than those of commercial ones.

References

[1] A. Erdoğan, A., M. E. Şeker, S.D. Kahraman (2023). Evaluation of environmental and nutritional aspects of bee pollen samples collected from East Black Sea region, Turkey, via elemental analysis by ICP-MS. Biological Trace Element Research, 201(3), 1488-1502.

[2] Şeker, M. E. (2023). Elemental analysis and health risk assessment of different hazelnut varieties (Corylus avellana L.) collected from Giresun-Turkey. Journal of Food Composition and Analysis, 122, 105475.

[3] Exposure to potentially toxic elements through ingestion of canned non-alcoholic drinks sold in Istanbul, Türkiye: A health risk assessment study. Journal of Food Composition and Analysis, 121, 105361.

Investigation of the Inhibitory Activity of Pyrazoline Derivatives Against the BChE Enzyme

D. Özmen Özgün[1], R. Sağlamtaş[2], İ. Babacan[3] and H.İ. Gül[1]

[1]Ağrı İbrahim Çeçen University, Faculty of Pharmacy, Department of Pharmaceutical Chemistry, Ağrı, Türkiye, ORCID: 0000-0002-8574-9672, ORCID: 0000-0001-6164-9602
[2]Ağrı İbrahim Çeçen Unıversity, Vocational School of Health Services, Central Research and Application Laboratory, Ağrı, Turkey, ORCID: 0000-0002-4400-2302
[3]Ağrı İbrahim Çeçen Unıversity, Faculty of Pharmacy, Ungdergraduate Student, Ağrı, Türkiye

Dementia is a neurodegenerative disease that significantly affects a person's memory, behaviour and mental state. The most prominent symptoms of Alzheimer's disease are the progressive weakening of memory functions, such as memory loss, difficulty speaking, disorientation, and the inability to carry out daily personal needs [1]. Currently, the treatments developed for Alzheimer's disease are aimed at regulating the decline of the cholinergic system, preventing the disease and generally treating the symptoms. One of the treatments for the disease is cholinesterase inhibition. The mechanism of action of cholinesterase inhibitors is to improve cognitive function and prevent disease by regulating the amount of acetylcholine in the cholinergic system [2]. However, due to the high side effects of cholinesterase inhibitors, there is a need for new compounds that do the same job with fewer side effects. Studies have shown that pyrazole derivatives, which are chalcone analogues with different functional properties, inhibit the BChE enzyme [3]. This study aims to investigate the synthesis and bioactivities of pyrazoline derivative compounds with more selective and minimised side effects that may be effective in the treatment of Alzheimer's disease using a medicinal chemistry approach.

IC50 values and Ki values were determined to measure the level of BChE enzyme inhibition. Tacrine was used as a positive control. For BChE, the Ki values of 4-[5-aryl-3-phenyl-4,5-dihydro-1H-pyrazol-1-yl] benzenesulfonamide derivatives were calculated as 0.291±0.008 μM-1.567±0.021 μM. The synthesized pyrazole derivatives demonstrated inhibitory effects on the BChE enzyme. It is thought that these molecules will make significant contributions

References

[1] Yıldırım E.R., Ulusoy Güzeldemirci N, 2023. Recent advances of cholinesterase inhibitors playing a critical role in the treatment of alzheimer's disease (2020-2022). Sağlık Bilimlerinde İleri Araştırmalar Dergisi 6.2 (2023): 197-209.

[2] Z. Demir ve F. Türkan, 2022. Asetilkolinesteraz ve Bütirilkolinesteraz Enzimlerinin Alzheimer Hastalığı ile İlişkisi, Journal of the Institute of Science and Technology. (2022): 2386-2395.

[3] D. Ozmen Ozgun, H. I. Gul, C. Yamali, H. Sakagami, I. Gulcin, M. Sukuroglu ve C. Supuran, 2019. Synthesis and bioactivities of pyrazoline benzensulfonamides as carbonic anhydrase and acetylcholinesterase inhibitors with low cytotoxicity, Bioorganic chemistry 84 (2019): 511-517.

Candidate Drugs for Alzheimer's Disease: Pyrazole Derivatives

D. Özmen Özgün[1], R. Sağlamtaş[2], <u>E. Doğru</u>[3] and H.İ. Gül[1]

[1]Ağrı İbrahim Çeçen University, Faculty of Pharmacy, Department of Pharmaceutical Chemistry, Ağrı, Türkiye, ORCID: 0000-0002-8574-9672, ORCID: 0000-0001-6164-9602
[2]Ağrı İbrahim Çeçen Unıversity, Vocational School of Health Services, Central Research and Application Laboratory, Ağrı, Turkey, ORCID: 0000-0002-4400-2302
[3]Ağrı İbrahim Çeçen Unıversity, Faculty of Pharmacy, Ungdergraduate Student, Ağrı, Türkiye

Alzheimer's disease is a chronic, slowly progressive disease characterized by a specific impairment of intellectual capacity in various areas such as learning, memory, language and speech skills, reading and writing ability, and progressive loss of neuronal function and structural deterioration. Alzheimer's is the most well-known cause of dementia. No drug has yet been discovered for the definitive treatment of the disease. Current medications are used to relieve symptoms, reduce severity, and slow the progression of the disease. If not prevented, there will be an increasing number of people diagnosed with the disease in the coming years [1]. Pyrazole derivative compounds have a wide range of biological activities [2]. This study aims to synthesize and investigate the bioactivities of pyrazoline derivative compounds with reduced side effects and more effective disease-specific pyrazoline derivatives for the treatment of Alzheimer's disease using a medicinal chemistry approach and to discover new drug candidate molecules. IC50 values and Ki values were determined to measure the level of AChE enzyme inhibition. Tacrine was used as a positive control. For AChE, the Ki values of 4-[5-aryl-3-phenyl-4,5-dihydro-1H-pyrazol-1-yl] benzenesulfonamide derivatives were calculated as 0.072 ± 0.002 µM-0.749 ± 0.037 µM. The synthesized pyrazole derivatives demonstrated inhibitory effects on the AChE enzyme. It is thought that these molecules will make significant contributions to the treatment of chronic diseases such as Alzheimer's and Parkinson's.

References

[1] Z. Demir ve F. Türkan, 2022. Asetilkolinesteraz ve Bütirilkolinesteraz Enzimlerinin Alzheimer Hastalığı ile İlişkisi, Journal of the Institute of Science and Technology. (2022): 2386-2395.

[2] D. Ozmen Ozgun, H. I. Gul, C. Yamali, H. Sakagami, I. Gulcin, M. Sukuroglu ve C. Supuran, 2019. Synthesis and bioactivities of pyrazoline benzensulfonamides as carbonic anhydrase and acetylcholinesterase inhibitors with low cytotoxicity, Bioorganic chemistry 84 (2019): 511-517.

Identification and Antimicrobial Activity of Streptomyces Bacteria Isolated from Some Areas of the Zap River

I. Aslan[1], M. Ertas[2] and Ş.B. Taylan[3]

[1]Hakkari University, Graduate Education Institute, Department of Biology, Hakkari, Türkiye
[2]Hakkari University, Yuksekova Vocational School, Department of Chemistry and Chemical Processing, Cosmetic Technology Program, Hakkari, Türkiye, ORCID: 0000-0003-3537-6078
[3]Hakkari University, Vocational School of Health Service, Department of Medical Services and Techniques, Environmental Health Program, Hakkari, Türkiye, ORCID: 0000-0002-8158-4487

Twenty-six Streptomyces were isolated from the sediments of the Zap River using the serial dilution technique. All isolates were first screened for antibacterial activity and 2 were found to be active against a group of test bacteria. ZP003 and ZP010 strains were selected for taxonomic characterization and identification as they have moderate to high antibacterial activity. Secondary metabolites of effective isolates were extracted and inhibition zones and minimum inhibition concentration (MIC) values were determined. As a result of the comparative 16S rRNA gene sequence analysis, it was determined that the ZP003 strain was similar to 99.72% Streptomyces albus, and the ZP010 strain was 99.86% similar to Streptomyces cyaneus. Based on its morphological and physiological characteristics and 16S rDNA sequence homology data, ZP003 was identified as Streptomyces albus and ZP010 as Streptomyces cyaneus.

References

[1] Chater, K. F. Recent advances in understanding Streptomyces. F1000Research, 5 (2016).

[2] Chevrette, M. G., Carlson, C. M., Ortega, H. E., Thomas, C., Ananiev, G. E., Barns, K. J., ... & Currie, C. R. The antimicrobial potential of Streptomyces from insect microbiomes. Nature communications, 10(1), 516 (2019).

[3] Quinn, G. A., Banat, A. M., Abdelhameed, A. M., Banat, I. M. Streptomyces from traditional medicine: Sources of new innovations in antibiotic discovery. Journal of medical microbiology, 69(8), 1040-1048 (2020).

[4] Á. Baricz, D.K. Dimitrov, H. Orhan, N. Yağmur, 2016. Radii of starlikeness of some special functions, Proc. Amer. Math. Soc. 144(8) (2016) 3355–3367. Ozdemir, K., Ogun, E., Ertas, M., Acar, S., Atalan, E. Identification of biodiversity of some Streptomyces species and determination of a restriction fragment length polymorphism (RFLP) profile of 16S rDNA gene region. Journal of Animal and Veterinary Advances, 13 (16): 978-988 (2014).

Removal and Detoxification of Congo Red Dye from Aqueous Solutions Using Fraxinus excelsior L. (Oleaceae) Biosorbent

E. Güllüce[1], Y. Gülşahin[1], İ. Çolak[1], M. Karadayı[2] and M. Güllüce[2]

[1]Institute of Natural and Applied Sciences, Atatürk University, Erzurum, Turkey, ORCID: 0000-0003-2290-3799; ORCID: 0000-0002-3770-2116; ORCID: 0000-0002-3500-260X
[2]Department of Biology, Faculty of Science, Atatürk University, Erzurum, Turkey, ORCID: 0000-0002-5957-8259; ORCID: 0000-0002-5957-8259

Pollution of water resources by synthetic dyes is seen as one of the most important environmental problems. These synthetic dyes are used in various industries such as textiles, paper and cosmetics. When the wastewater resulting from the synthetic dyes used by these industries is discharged to the receiving environment without treatment, both the color of the synthetic dyes negatively affects the water quality and they pose another serious environmental problem due to its serious harmful effects such as toxic, mutagenic and carcinogenic [1]. In recent years, the biosorption process has been used to remove synthetic dyes from aqueous solutions because it is sustainable and environmentally friendly. The biosorption process has become an innovative process for removing synthetic dyes from aqueous solutions using various bioorganic wastes abundant in nature [2]. The aim of our study was to use the biosorption process to remove Congo red dye from aqueous solutions using the Fraxinus excelsior L. (Oleaceae) (FEO) biosorbent. In this study, parameters such as contact time, pH, biosorbent dose and initial dye concentration were investigated. In addition, isotherm and kinetic studies were also carried out. According to the results of the studies carried out at pH: 6, biosorbent dose: 1 g, initial dye concentration: 10 mg/L and stirring speed: 150 rpm; Using FEO biosorbent, it was removed 92% Congo red dye from aqueous solutions. In isotherm studies; Langmuir, Freundlich, Temkin and Elovich isotherm studies were carried out. A higher correlation coefficient was found for the Langmuir isotherm ($R2=0.903$) compared to other isotherms. In kinetic studies, the correlation coefficient of the pseudo-second-order kinetic model ($R2=0.991$) was found to be higher than the pseudo-first-order kinetic model ($R2=0.924$). Moreover, alterations in phytotoxic and genotoxic properties of effluents before and after treatment were monitored by using seed germination assay, Allium test and Ames/Salmonella test systems. In conclusion, FEO biosorbent was determined as an effective, inexpensive, sustainable and eco-friend biosorbent for removal and detoxification of synthetic anionic dyes from aqueous solutions.

References

[1] F. Deniz, E. Tezel Ersanli, 2022. A novel biowaste-based biosorbent material for effective purification of methylene blue from water environment, International Journal of Phytoremediation. 24(12) (2022) 1243–1250.

[2] E. Gulluce, M. Karadayi, M. Gulluce, G. Karadayi, V. Yildirim, D. Egamberdieva, B. Alaylar, (2020). Bioremoval of methylene blue from aqueous solutions by *Syringa vulgaris* L. hull biomass, Environmental Sustainability. 3 (2020) 303–312.

Removal of Congo Red Dye from Aqueous Solutions Using Robinia pseudoacacia L. (Fabaceae) Fruits Biosorbent; Isotherm and Kinetic Studies

E. Güllüce[1], Y. Gülşahin[1], M. Karadayı[2] and M. Güllüce[2]

[1]Institute of Natural and Applied Sciences, Atatürk University, Erzurum, Turkey, ORCID: 0000-0003-2290-3799; ORCID: 0000-0002-3770-2116
[2]Department of Biology, Faculty of Science, Atatürk University, Erzurum, Turkey, ORCID: 0000-0002-5957-8259; ORCID: 0000-0002-5957-8259

The industrial revolution has been a great step towards increasing the welfare of humanity. However, the discharge of wastewater from various industrial processes has brought up a serious problem. The wastewater of industries such as cosmetics, wool and textiles, which use toxic synthetic dyes, causes serious damage to the environmental ecology when discharged into the receiving environment without treatment [1]. Therefore, these wastewaters that harm human health and the environment must be treated. There are various conventional wastewater treatment processes such as membrane, filtration, coagulation and flocculation. Since these processes have disadvantages, such as being high-cost and using hazardous chemicals, there was a need to search for a new process. In recent years, the biosorption process has come to the fore as a sustainable and effective method for treatment synthetic dyes from aqueous solutions [2]. The aim of our study was to use the biosorption process to remove Congo red dye from aqueous solutions using *Robinia pseudoacacia* L. (Fabaceae) (RPF) biosorbent. In this study, Congo red dye was removed 80% from aqueous solutions using RPF biosorbent under optimum experimental conditions (pH: 6, biosorbent dose: 1 g, initial dye concentration: 10 mg/L and stirring speed: 150 rpm). In addition to parameters affecting biosorption such as pH, contact time, biosorbent dose and initial dye concentration, isotherm and kinetic studies were also investigated. Langmuir, Freundlich, Temkin and Elovich isotherm modeling were used in isotherm studies. According to the results of isotherm studies, the correlation coefficient of the Langmuir isotherm (R^2=0.997) was found to be higher than other isotherm modeling. Pseudo-first-order and pseudo-second-order kinetic models were used in kinetic studies, and the correlation coefficient of the pseudo-second-order kinetic model (R^2=0,999) was found to be higher. Consequently, RPF biosorbent can be used to remove Congo red dye from aqueous solutions due to its advantages such as low-cost, effective removal efficiency and sustainability.

References

[1] E. Güllüce, T.Y. Koç, M. Güllüce, M. Karadayı, (2022). Isolation of Methylene Blue from Aqueous Solution Using a *Fraxinus Excelsior* L. (Oleaceae) Based Biosorbent: Isotherm, Kinetics, and Thermodynamics, Analytical Letters. 56(3) (2022) 422–432.

[2] K. Cappuccio de Castro, V.F. Cintra Leme, F.H. Moreti Souza, G.O. Barros Costa, G. Espirito Santos, L.R. Vedovelo Litordi, G.S. Silva Andrade, (2021). Performance of inactivated *Aspergillus oryzae* cells on dye removal in aqueous solutions, Environmental Technology & Innovation. 24 (2021) 101828.

Determination of Science Perceptions of Students With Special Education Through Drawing

P. Mete[1], S. Çakabay[2]

[1]Atatürk Üniversitesi/Temel Eğitim, Erzurum, Türkiye, ORCID: 0000-0002-3075-2575
[2]Milli Eğitim, Bingöl, Türkiye, ORCID: 0000-0001-6898-9159

Purpose: The aim of this research is to assess and interpret the perceptions of children with special needs towards science lessons using their drawings. Additionally, it emphasizes the significance of perspectives related to the science education of children with special needs and highlights how these perspectives can contribute to the success of these children in science lessons.

Methodology: This research employs the case study method, which is one of the qualitative research methods. Descriptive analysis method is preferred for data analysis, and through this method, information obtained is summarized to reach an understanding of perceptions related to science. In this context, data obtained through student drawings are meticulously examined to comprehend the perceptions of special education students towards science lessons.

Findings: In Figure 1, elements such as animal diversity, electrical circuits, home and construction, plant components, human figures, clouds and weather, traffic signs, and safety represent topics in biology, physics, architecture, botany, ecology, atmosphere, and technology. Figure 2, while exploring the theme of space and different life forms, references astronomy, biology, and space science with elements like star clusters, planets, aliens, the sun, and animals resembling insects. Figure 3 combines the natural world and living beings with elements of biology, environmental science, and geology, while Figure 4 and Figure 5 point to various subjects such as meteorology, botany, architectural science, and ecology with different natural landscapes. Finally, Figure 6 encompasses various themes of life sciences such as biology, botany, entomology, and astronomy with elements like giant flowers, rabbits, sheep, houses, trees, butterflies, roosters, birds, grass, flowers, and the sun.

Conclusion: Various science subjects such as animal diversity, electrical circuits, homes and construction, plant elements, human figures, clouds and weather, traffic signs, and safety have been represented in different forms in students' drawings. This diversity indicates students' interests in different disciplines of science and their expressions of perceptions on these subjects. The information obtained by considering individual differences can guide the analysis of drawings of special education students, assisting in determining students' specific areas of interest.

The Impact of Genistein on Human Carbonic Anhydrase Isoenzymes (hCA I and II)

L. Durmaz[1] and İ. Gülçin[2]

[1]*Erzincan Binali Yıldırım University, Çayırlı Vocational School, Medical Services and Technical Department, Erzincan, Türkiye, ORCID: 0000-0002-3773-5751*
[2]*Atatürk University, Faculty of Science, Department of Chemistry, Erzurum, Türkiye, ORCID: 0000-0001-5993-1668*

Carbonic anhydrases (CAs, carbonate dehydratases) are ubiquitous metalloenzymes present in eukaryotes and prokaryotes. They reversible for hydration of carbon dioxide (CO_2) and water to produce bicarbonate (HCO_3^-) and proton (H^+) [1]. Genistein, a phytoestrogen in all the legumes, is isoflavone and has many important beneficial effects in terms of health [2]. In the beginning primarily, the in vitro effects of coumarin derivative including Genistein determined on human erythrocyte carbonic anhydrase isoenzymes (hCA I and II) were investigated. For this aim, hCA I, and II isoenzymes were purified from human erythrocytes by Sepharose-4B-L-Thyrosine affinity column chromatography. For determination of the enzyme purity, SDS-PAGE was performed and single band was observed for each isoenzyme. After that, the inhibition effects of the Genistein on hCA I and II were determined and IC_{50} and K_i values were calculated. In our study, for hCA I isoenzyme, IC_{50} and K_i values were found 208.42 μM and 139.23 μM, respectively. The same parameters were calculated as 218.13 μM and 320.13 μM, for hCA II isoenzyme. Acetazolamide was used as standards for both of CA isoenzymes [3].

Keywords: Genistein, Carbonic Anhydrase, Enzyme Inhibition, Enzyme Purification

References

[1] İ. Gülçin, 2020. Antioxidants and antioxidant methods-An updated overview. Archives of Toxicology, 94(3), 651-715.

[2] L. Durmaz, 2015. Some coumarin derivatives: Their antioxidant capacities and investigation of their effects on human carbonic anhydrase isoenzymes (hCA I and II) and acetylcholinesterase enzymes, Atatürk University Graduate School of Natural and Applied Sciences, Department of Chemistry, Ph.D. Thesis, Erzurum (2015).

[3] L. Durmaz, İ. Gülçin, P. Taslimi, B. Tüzün, 2023. Isofraxidin: Antioxidant, anticarbonic anhydrase, anticholinesterase, antidiabetic, and in silico properties, ChemistrySelect, 8(34) (2023) 1-12.

Basic and Simple Step Synthesis and Characterization of Novel Hydrazide Derivatives Containing 4-Methylsulfonate Ester Scaffold
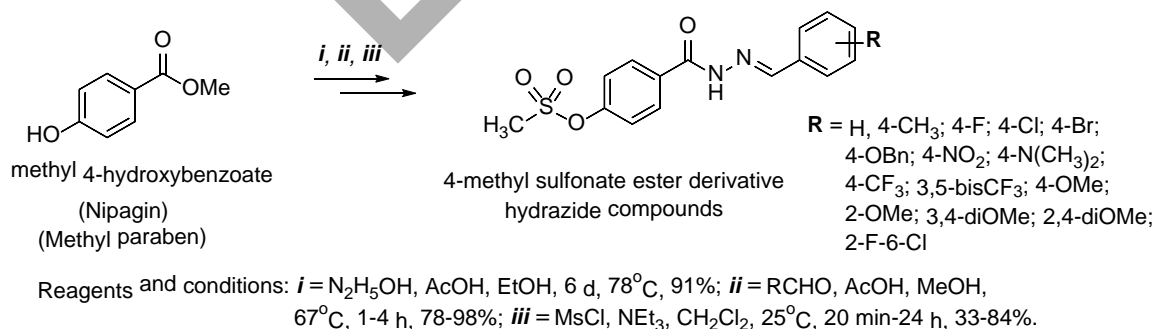
A. Köse[1], H. Şenol[2] and N. Ulusoy Güzeldemirci[3]

[1]Aksaray University, Faculty of Science and Letters, Department of Chemistry, Aksaray, Turkey, ORCID: 0000-0003-2448-3716
[2]Bezmilem Vakif University, Faculty of Pharmacy, Department of Pharmaceutical Chemistry, İstanbul, Turkey, ORCID: 0000-0002-8333-035X
[3]İstanbul University, Faculty of Pharmacy, Department of Pharmaceutical Chemistry, İstanbul, Turkey, ORCID: 0000-0002-4495-4282

Hydrazides are chemical compounds with the formula $R-NR^1-NR^2R^3$. Despite having numerous R groups, it is commonly known in the literature as acyl and aroyl. Hydrazides are compounds that have been investigated for many years and have gained popularity in the recent decade. These substances are designed for use as COX 1-2 inhibitors, analgesic, anti-inflammatory, anti-mycobacterial, anti-cancer, etc. [1]. In this work, fifteen new hydrazide derivative compounds containing 4-methyl sulfonate ester scaffold were synthesized in three steps starting from the methyl 4-hydroxybenzoate (Nipagin). To synthesize these compounds, fifteen benzaldehyde derivatives with different substituted groups were purchased and condensed with 4-hydroxybenzohydrazide which is a hydrazide derivative of nipagin to produce phenolic hydrazides in high yields. The phenolic hydrazides were also converted to sulfonate esters with triethylamine (NEt_3) and methane sulfonyl chloride (MsCl) in dichloromethane and fifteen hydrazide derivatives were gained, all being new.

methyl 4-hydroxybenzoate
(Nipagin)
(Methyl paraben)

4-methyl sulfonate ester derivative hydrazide compounds

R = H, 4-CH$_3$; 4-F; 4-Cl; 4-Br; 4-OBn; 4-NO$_2$; 4-N(CH$_3$)$_2$; 4-CF$_3$; 3,5-bisCF$_3$; 4-OMe; 2-OMe; 3,4-diOMe; 2,4-diOMe; 2-F-6-Cl

Reagents and conditions: ***i*** = N$_2$H$_5$OH, AcOH, EtOH, 6 d, 78°C, 91%; ***ii*** = RCHO, AcOH, MeOH, 67°C, 1-4 h, 78-98%; ***iii*** = MsCl, NEt$_3$, CH$_2$Cl$_2$, 25°C, 20 min-24 h, 33-84%.

References

[1] **a)** A.A. Abdel-Aziz, L.A. Abou-Zeid, K.E.H. ElTahir, R.R. Ayyad, M.A. El-Sayed, 2016. Synthesis, anti-inflammatory, analgesic, COX-1/2 inhibitory activities and molecular docking studies of substituted 2-mercapto-4(3H)-quinazolinones., Eur. J. Med. Chem., 121 (2016) 410–421. **b)** M.G. Mamolo, V. Falagiani, D. Zampieri, L. Vio, E. Banfi, G. Scialino, 2003, Synthesis and antimycobacterial activity of (3,4-diaryl-3H-thiazol-2-ylidene)-hydrazide derivatives, Il Farmaco, 58(9) (2003) 631–637. **c)** M. Taha, S.A. Ali Shah, M. Afifi, M. Zulkeflee, S. Sultan, A. Wadood, F. Rahim, N.H. Ismail, 2017, Morpholine hydrazone scaffold: Synthesis, anticancer activity and docking studies, Chin. Chem. Lett. 28(3), (2017) 607–611.

Renewable Energy, Agriculture and CO_2 Emission Relationship: Turkey's Example

B. Açdoyuran[1], M. Beşer[1] and N.Ö. Beşer[1]

[1]*Agri Ibrahim Cecen University, Agri, Turkey, ORCID: 0000-0003-1513-1110, ORCID: 0000-0002-8487-4586, ORCID: 0000-0002-6738-3638*

In recent decades, the increase in greenhouse gas emissions has led to environmental degradation becoming a major global issue. The agricultural sector has a significant impact on the generation of greenhouse gases, and CO_2 in particular accounts for a large share of these gases. Tillage on agricultural land releases organic carbon into the air, leading to an increase in the amount of CO_2 in the atmosphere. The aim of this study is to empirically examine the relationship between agriculture, renewable energy and CO_2 emissions in Turkey. For this purpose, agriculture, renewable energy, CO_2 emissions and gross national product per capita data covering the period 1990-2020 were used in this study. Johansen cointegration test was used in the study and then cointegration estimation results for FMOLS, DOLS and CCR models were obtained. Then, Granger Causality test was applied. According to the findings of the study, a 1% increase in renewable energy reduces CO_2 by approximately 0.28% according to FMOLS findings, approximately 0.36% according to DOLS findings and approximately 0.27% according to CCR findings. According to another result of the study, a 1% increase in agriculture increases CO_2 by approximately 0.12% according to FMOLS findings, approximately 0.22% according to DOLS findings and approximately 0.12% according to CCR findings. The results of the study reveal that the agricultural sector increases CO_2 emissions and renewable energy reduces them. Therefore, steps can be taken to reduce the contribution of the agriculture sector to GHG emissions, such as promoting sustainable agricultural practices and renewable energy, and increasing productivity.

Cancer Healing Effects of Natural Organosulfur Compounds Originating in Turkey

Ü. Polat Korkunç[1], H. Çalık[2], R. Çakır Koç[2] and E. Karakuş[1]

[1]Yıldız Technical University, Faculty of Arts and Science, Department of Chemistry, İstanbul, Türkiye, ORCID: 0000-0001-6942-9532, ORCID: 0000-0002-7730-3304
[2]Yıldız Technical University, Faculty of Chemical and Metallurgical Engineering, İstanbul, Türkiye, ORCID: 0000-0002-9509-7866, ORCID: 0000-0002-8545-9878

Garlic, scientifically known as Allium sativum, is a plant belonging to the Liliaceae family. It has been used for many years due to its diverse biological and therapeutic characteristics. These vegetables are rich in organosulfur compounds (OSCs)1,2,3. The aim of this study is to investigate the anticancer effects of natural organosulfur compounds originating from our country. The anticancer properties of Kastamonu Taşköprü garlic were assessed applying both water-soluble and oil-soluble extraction techniques. Anticancer effects were examined on NIH/3T3 (ATCC; CRL-1658), Caco-2 human colorectal cancer (ATCC; HTB-37), and MCF-7 human breast cancer (ATCC; HTB-22) cell lines. According to these extraction methods, the cell viability and cytotoxic effects of the extractions were analysed. As a result of the examination of anticancer effects, it was determined that the anticancer effects of Kastamonu Taşköprü garlic soluble in oil had higher anticancer effects than water-soluble garlic extracts.

References

[1] Jones A. T., Oldham H., and Graz M., O13 Quantitative analysis of an oil based natural compound extracted from plasma, Biochemical Pharmacology 2017; 139: 113–114.

[2] Hu B., Hu H., Pu C., Wei Z. Wang, Q. et al., Three new flavonoid glycosides from the aerial parts of Allium sativum L. and their anti-platelet aggregation assessment. Natural Product Research 2022; 36(23): 5940-5949.

[3] Padmini R., Uma Maheshwari Nallal V., Razia M., Sivaramakrishnan S. et al., Cytotoxic effect of silver nanoparticles synthesized from ethanolic extract of Allium sativum on A549 lung cancer cell line, Journal of King Saud University- Science 2022; 34(4): 102001-102008.

Investigation of the Effects of Tomentosin Against Septic Heart Damage Model Due to Cecum Ligation and Perforation in Rats

M. Cellat[1], C.T. İşler[2], T. Aydın[3], T. Kutlu[4], M. Etyemez[1] and M. Güvenç[1]

[1]Hatay Mustafa Kemal Üniversitesi Veteriner Fakültesi Fizyoloji A.D, Hatay, Türkiye, ORCID: 0000-0003-2559-096X, ORCID: 0000-0003-0497-1878, ORCID: 0000-0002-9716-0697

[2]Hatay Mustafa Kemal Üniversitesi Veteriner Fakültesi Cerrahi A.D, Hatay, Türkiye, ORCID: 0000-0002-1910-8316

[3]Ağrı İbrahim Çeçen Üniversitesi Eczacılık Fakültesi Farmakognozi A.D, Ağrı, Türkiye, ORCID: 0000-0002-7653-6480

[4]Hatay Mustafa Kemal Üniversitesi Veteriner Fakültesi Patoloji A.D, Hatay, Türkiye, ORCID: 0000-0002-8771-1256

Sepsis is a systemic inflammatory response syndrome caused by infection, trauma, burns, and surgery. Dysfunction syndrome occurring in the heart and other organs is the most common complication and the main cause of death in sepsis patients. In sepsis, an exaggerated inflammatory response results in the production of pro-inflammatory cytokines, chemokines, and other inflammatory mediators. Tomentosin, a phytochemical found in Inula species belonging to the Asteracea family, has various pharmacological properties and is prescribed in Chinese medicine to treat numerous diseases. This study aimed to investigate the effects of tomentosin in a sepsis model caused by cecal ligation and puncture in rats. For this purpose, male Wistar albino rats were used in the study. For the sepsis model, cecum ligation and perforation were performed. At the same time, the protective effects of different doses of tomentosin (12,5mg/kg, 25 mg/kg and 50 mg/kg) were also investigated. In the study, cardiac tissue oxidative damage and antioxidant activity markers and proinflammatory cytokines were examined. At the end of the study, it was determined that MDA levels, which are a marker of oxidative damage, increased, GSH.Px and CAT activities, which are antioxidant activity parameters, decreased, and TNF-α and IL-6 levels increased in the cecal ligation group. However, in the group treated with high dose tomentosin, TNF-Alpha, IL-6 and MDA levels as well as GSH.Px and CAT activities were observed to be similar to the control group. As a result, it can be said that tomentosin has protective effects on heart damage caused by sepsis in rats with its antioxidant and anti-inflammatory properties.

Determination of in vitro anti-diabetic properties of Ractopamine

N. Aydemir[1] and H. Akıncıoğlu[2]

[1]*Agri İbrahim Çeçen University, Faculty of Arts and Science, Department of Molecular Biology and Genetics Agri, Turkey,*
[2]*Agri İbrahim Çeçen University, Faculty of Arts and Science, Department of Chemistry Agri, Turkey,*
ORCİD: 0000-0001-5453-0953

Diabetes mellitus (diabetes) reduces the quality of life, negatively affecting human health and leading to various complications. Worldwide, especially with the increasing prevalence of obesity, the number of diabetes patients is increasing every day [1]. There are different approaches to the treatment of the disease, and the use of α-glucosidase and α-amylase enzyme inhibitors is just one of these approaches. The drugs used in the treatment of the disease have side effects, and this situation also troubles patient health in other ways.[2] Studies are progressing towards more effective and less side-effect drug search. Our study was planned for this purpose. In the study, the inhibitory effects of Ractopamine molecule on α-glucosidase and α-amylase enzymes were investigated. The ractopamine molecule is a molecule belonging to the group of β-agonists. The results of the studies IC50 for α-amylase, IC50 for α-glucosidase, and Ki value were calculated of the ractopamine molecule . The results are given in Table 1.

	α-Amylase		α-Glucosidase		
	IC_{50} (μM)	R^2	IC_{50} (μM)	R^2	K_i (μM)
Ractopamine	68.36±0.07	0.99	82.43	0.98	24.81±8.18
Acarbose	7.93± 0.04	0.96	159.6	0.90	155.37±47.75

Table 1. Ractopamine molecule's IC50 and Ki results

Acarbose was used as a positive control for both enzymes in the studies. When the IC50 values of ractopamine were compared with acarbose, ractopamine gave 10 times better results than acarbose, especially for the α-amylase enzyme. It is considered by us that the strong inhibitory potential of the ractopamine molecule could be guiding in other scientific studies and especially in the field of new drug design.

Keywords: α-Amilase, α- Glucosidase, Ractopamine, IC50

References

[1] Aktas, A., Barut Celepci, D., Gok, Y., Taslimi, P., Akincioglu, H., & Gulcin, I. (2020). A novel Ag-N-heterocyclic carbene complex bearing the hydroxyethyl ligand: Synthesis, characterization, crystal and spectral structures and bioactivity properties. Crystals, 10(3), 171.

[2] El Sayed, H., Farahat, M. M., Awad, L. F., Balbaa, M., Yusef, H., Badawy, M. E., & Abd Al Moaty, M. N. (2022). New 4-(arylidene) amino-1, 2, 4-traizole-5-thiol derivatives and their acyclo thioglycosides as α- glucosidase and α-amylase inhibitors: Design, synthesis, and molecular modelling studies. Journal of Molecular Structure, 1259, 132733.

The photoelectrical performances of WS₂-based photodiode

N. Karabulut[1,2] and Abdulkerim Karabulut[3]

[1]Department of Electric and Energy, Technical Science Vocational School, Atatürk University, Erzurum, Turkey, ORCID: 0009-0006-0832-0692
[2]Department of Photonics, Graduate School of Sciences, Erzurum Technical University, Erzurum 25050, Turkey
[3]Department of Basic Sciences, Erzurum Technical University, Erzurum, Turkey, ORCID: 0000-0003-1694-5458

In this study, a photodiode was fabricated using the WS_2 interfacial layer coated between Au metal and p-Si semiconductor, and its electrical behavior against light was characterized in detail. The current-voltage and transient photocurrent measurements under different light intensities were used to determine the relevant characteristics. As a result of the study, it was found that while the ideality factor value was 1.49 in the dark, it increased to 2.26 when the light intensity to which the device was exposed was 100 mW/cm^2. However, the barrier height value also decreased from 0.81 eV to 0.68 eV. Additionally, it was determined that the highest rectification was in the measurement performed in a dark environment. The fabricated device showed rectifying behavior and hence the obtained experimental values showed that the fabricated device complies with thermionic emission theory and therefore the electrical parameters were evaluated using thermionic emission theory [1-3]. As a result of the analyses, it has been confirmed that the produced device and WS_2 material can be used in optoelectronic technology, especially in photodiode and photodetector applications.

Keywords: Photodiode, WS2, Electrical properties, Thermionic emission theory

References

[1] B.A. Gozeh, A. Karabulut, A. Yildiz, F. Yakuphanoglu, 2018. Solar light responsive ZnO nanoparticles adjusted using Cd and La Co-dopant photodetector, Journal of Alloys and Comp., 732 (2018) 16-24.

[2] İ. Dökme, 2011. The analysis of I–V characteristics of Schottky diodes by thermionic emission with a Gaussian distribution of barrier height, Microelectronics Reliab., 51(2) (2011) 360-364.

[3] Ş. Karataş, Ş. Altındal, A. Türüt, A. Özmen, 2003. Temperature dependence of characteristic parameters of the H-terminated Sn/p-Si (100) Schottky contacts, Applied Surface Sci., 217(1-4) (2003) 250-260.

Growth of Cerium Oxide via Pulsed Electron Deposition as a Thin Film

T.A. Alqutamy[1] and M.T. Yurtcan[1,2]

[1]Department of Nanoscience and Nanoengineering, Graduate School of Natural and Applied Sciences, Atatürk University, 25240, Erzurum, Turkey
[2]Department of Mathematics & Science Education, Kazim Karabekir Education Faculty, Atatürk University, 25240, Erzurum, Turkey

In this study, pulsed electron deposition was utilized to develop cerium oxide thin films on $LaAlO_3$ substrates at temperatures ranging from room temperature to higher values with 100 °C steps [1]. CeO_2 pellet is used as a target, pressure is fixed to 15 mTorr with 99.999% pure oxygen and 15 kV used for electron source. $LaAlO_3$ and CeO_2 has a good lattice match [2]. The thin film quality is verified by X-ray diffraction and the morphology of the thin films was examined using a scanning electron microscope.

References

[1] Mustafa Tolga YURTCAN, 2021, Deposition of grid-like single-crystal Ce2O3 thin films on LaAlO3(100) substrate by pulsed laser deposition, Journal of Materials Science: Materials in Electronics, Volume 32, pages 3854–3862, (2021),2-5

[2] Yen-Teng Ho, Kuo-Shu Chang, Kou-Chen Liu, Li-Zen Hsieh, Mei-Hui Liang, 2013, Room temperature epitaxial growth of (001) CeO2 on (001) LaAlO3 by pulsed laser deposition, Journal of CRYSTAL Research & Technology, Volume48, Issue5,(2013),2-3

Fractional Order Memristor Based PID Control Systems

S. Beyzade[1] and Ö. Atan[2]

[1]Agrı Ibrahim Cecen University, Agrı, Turkey, ORCID: 0009-0002-6145-1780
[2]Van Yuzuncu Yıl University, Van, Turkey, ORCID: 0000-0001-6443-9600

Memristors, also known as lossy circuit elements until 2008, are electronic circuit components that exhibit behavior based on the distribution between electrical flux and magnetic flux in an electronic circuit. The performance and efficiency of systems modeled with fractional order memristors increase. These models are used in controller design because they are known to improve overall performance in the literature. In this study, it was determined that fractional order memristors have a wider stability range and many advantages in their applications in PID control systems. It has been established that fractional order memristors have operating principles in a wider stability area, and it has been determined that these elements can be used as analog control elements in PID control systems. Additionally, it has been found that these factors increase the performance of fractional order memristors in PID control systems, and they have positive effects on control algorithms.

Quantitative Analysis of Ursolic Acid in Lavandula Stoechas Extracts and Bioactivity Studies

T. Aydın[1], R. Sağlamtaş[2], M. Gümüştaş[3], M. Genişel[1], C. Kazaz[4] and A. Çakır[5]

[1]Ağrı İbrahim Çeçen University, Faculty of Pharmacy, Ağrı, Türkiye, ORCID: 0000-0002-7653-6480, ORCID: 0000-0002-9339-9334

[2]Ağrı İbrahim Çeçen University, Vocational School of Health Services, Ağrı, Türkiye, ORCID: 0000-0002-4400-2302

[3]Başakşehir Çam and Sakura City Hospital, Pediatric Cardiology Department, Istanbul, Türkiye, ORCID: 0000-0002-4846-5398

[4]Atatürk University, Faculty of Science, Erzurum, Türkiye, ORCID: 0000-0002-5249-0895

[5]Kilis 7 Aralık University, Faculty of Science, Kilis, Türkiye, ORCID: 0000-0003-1672-1438

In this study, the ursolic acid contents of different extracts of Lavandula stoechas, popularly known as ''karabaş otu'', were analyzed. For this purpose, after purifying ursolic acid from the methanol extract of the plant sample, its chemical structure was characterized. At the same time, methanol, ethanol, dichloromethane:methanol (1:1, v/v), acetone, ethyl acetate, diethyl ether and chloroform extracts of Lavandula stoechas were prepared by the maceration method, and the ursolic acid contents in the extracts were determined quantitatively by HPLC. By calculating IC50 values, the inhibitory effects of ursolic acid and the extracts were also determined on α-glucosidase, acetylcholinesterase (AChE), butyrylcholinesterase (BChE), and human carbonic anhydrase I (hCAI) and II (hCAII) enzymes. The study's findings showed that the methanol extracts had the lowest ursolic acid level, 8.34 g/100 g extract, whereas the other extracts had ursolic acid contents ranging from 19.11 to 14.58 g/100 g extract. According to the study results, extracts and ursolic acid inhibited the α-glucosidase enzyme at different rates. However, the present results showed that pure ursolic acid (IC50=4.75 mg/ml) was more potent inhibitor than extracts (IC50=16.20-49.86 mg/ml). It was found in the study that ursolic acid and its extracts were extremely weak neuroprotective agents. Furthermore, ursolic acid and the extract were found to have no inhibitory effects on the hCAI and hCAII enzymes.

Biomimetic Approach: Innovative Design Solutions from Structures Inspired by Nature

A. Çelik [1,2], Y. Seçer Kavasoğlu[2], B. Atik[2], H. Kovacı[2], Y. B. Bozkurt[2], Y. Uzun[1,2], M. Aslan Çakır[3], Ş.M.Tüzemen[2]

[1]Atatürk University, Technology Development Area (ATA Teknokent), Erzurum, Turkey, ORCID: 0000-0002-8096-0794 ORCID: 0000-0002-5134-7640
[2]Ataturk University, Faculty of Engineering, Department of Mechanical Engineering, Erzurum, Turkey, ORCID: 0000-0002-8096-0794 ORCID: 0000-0003-4671 ORCID: 0000-0003-2117-9284 ORCID: 0000-0002-9053-3593 ORCID: 0000-0003-3859-9322 ORCID: 0000-0002-5134-7640
[3]Erzincan Binali Yıldırım University, Faculty of Engineering and Architecture, Department of Mechanical Engineering, Erzincan, Turkey, ORCID: 0000-0002-3826-8390

Structures that have developed over the long process of evolution in nature offer a wide range of extraordinary mechanical, hydrodynamic, optical and electrical properties, especially those found in complex organic structures. This provides an important source of inspiration in the design of next-generation structural materials. Modifications to the interfacial structure, composition and micro/nano properties of materials are being investigated to prevent damage, and studies are being carried out on the development of new materials. This approach has recently attracted the attention of researchers and aims to give materials the desired mechanical properties, inspired by nature (biomimetic). Biomimetic is defined as an innovative approach in which human beings develop new technologies by taking inspiration from the structures and strategies of living organisms in nature in search of sustainable solutions. The main purpose of this approach is to analyze the characteristics of living things in nature using certain engineering methods and to transform these characteristics into usable designs for human needs. If examples need to be given; Velcro used in shoes, clothing and many industrial applications is inspired by burdock. Another biomimetic example is the Kingfisher bird, which was used to solve the noise problem that occurs at high speeds in the Japanese Shinkansen high-speed trains. In another case, when the skin of a shark was examined, the presence of microscale textures was observed. Micro/nano- riblets on the surface of the shark enable it to move very fast and exhibit high friction performance. Another interesting example is that the front part of the Concorde plane was inspired by the nose structure of dolphins in order to reduce the friction caused by the air. In addition, many examples such as the hydrophobic structure of the lotus flower, the high adhesion of the Geico lizard, and the tensile flexibility of spider silks can be cited. Considering all these situations, it is thought that the field of biomimetic should be examined in more detail. For this purpose, this study analyzes which features of biomimetic, which guides the production and design processes of bio design-oriented approaches, can be used in designs and for what purposes.

References

[1] Anonymous, (2022b). https://www.sciencenews.org/article/how-math-helps-explain-delicatepatterns-dragonfly-wings (Access date: 11 July 2022).

[2] Anonymous, (2022c). https://www.argevetasarim.com/dogadan-esinlenilerek-gelistirilen-teknolojiler-biyomimetik/helikopter- yusufcuk (Erişim Tarihi: 11.07.2022).

[3] Benyus, J.M. (1997). Biomimicry: Innovation inspired by nature. New York: William Morrow and Comp, Inc., 320 pp

[4] Lakhtakia, A., Hesselberg, T., Metze, A.-L., Lenau, T.A., 2018. Paradigms for biologically inspired design. Bioinspiration, Biomimetics, and Bioreplication VIII.

[5] Li, Q., Zeng, Q., Shi, L., Zhang, X., & Zhang, K. Q. (2016). Bio-inspired sensors based on photonic structures of Morpho butterfly wings: a review. Journal of Materials Chemistry C, 4(9), 1752-1763.

[6] Meyers, M. A., Chen, P. Y., Lin, A. Y. M., & Seki, Y. (2008). Biological materials: structure and mechanical properties. Progress in materials science, 53(1), 1-206.

[7] Meyers, M. A., Chen, P. Y., Lopez, M. I., Seki, Y., & Lin, A. Y. (2011). Biological materials: A materials science approach. Journal of the mechanical behavior of biomedical materials, 4(5), 626-657.

[8] Naleway, S. E., Porter, M. M., McKittrick, J., & Meyers, M. A. (2015). Structural design elements in biological materials: application to bioinspiration. Advanced materials, 27(37), 5455-5476.

[9] Wang, J., Chen, H., Sui, T., Li, A., & Chen, D. (2009). Investigation on hydrophobicity of lotus leaf: Experiment and theory. Plant science, 176(5), 687-695.

[10] Fu, Y. F., Yuan, C. Q., & Bai, X. Q. (2017). Marine drag reduction of shark skin inspired riblet surfaces. Biosurface and Biotribology, 3(1), 11-24.

[11] Bar-Cohen, Y. (2006). Biomimetics—using nature to inspire human innovation. Bioinspiration & biomimetics, 1(1), P1.

Influence of Fire Temperature and Bar Diameter on the Mechanical Performance of Steel Reinforcement in Reinforced Concrete Structures

C. Yazici[1] and F.M. Özkal[2]

[1]Department of Construction, Ağrı İbrahim Çeçen University, Ağrı, Turkey, ORCID: 0000-0002-2061-4275
[2]Department of Civil Engineering, Atatürk University, Erzurum, Turkey, ORCID: 0000-0002-5552-283X

This study investigates the influence of fire temperature and bar diameter on the mechanical performance of steel reinforcement, a crucial component in reinforced concrete (RC) structures [1]. Twenty tensile tests were conducted on plain rebar specimens (Φ8-20) exposed to varying temperatures (23°C, 400°C, 500°C, 600°C, and 700°C). The results indicate a positive correlation between bar diameter and strength retention after fire exposure. The mechanical characteristics of fire-protected materials following exposure to elevated temperatures offer essential information for fire resistance investigations in steel structures. In fires within storage rack systems, localized collapse modes can trigger the complete collapse of the entire warehouse [2]. Thicker bars exhibited superior strength at elevated temperatures compared to their thinner counterparts. This can be attributed to their higher heat capacity, allowing them to absorb more thermal energy before reaching critical temperatures. The selected fire temperatures provide valuable insights: no strength reduction was observed at room temperature (23°C), while an increase in strength was observed for the 20 mm bar at 400°C, whereas the 8 mm bar exhibited a decrease in strength. These findings suggest that selecting larger diameter reinforcement can be a strategy to enhance the fire resistance of RC members. The relationship between diameter, temperature, and strength was established for both bar sizes, with maximum stress values at 400, 500, 600, and 700°C being 91.93%, 59.52%, 25.36%, and 11.82% for the 8 mm bar and 101.02%, 63.08%, 40.66%, and 12.15% for the 20 mm bar, respectively. This information is expected to contribute to the design of fire-resistant RC structures with enhanced safety and structural integrity.

References

[1] B. Aliş, C. Yazici, and F. Mehmet Özkal, "Investigation of Fire Effects on Reinforced Concrete Members via Finite Element Analysis," ACS Omega, vol. 7, no. 30, pp. 26881–26893, Aug. 2022.

[2] C. Yazici, F. Mehmet Özkal, S. Nazif Orhan, and B. Kaan Cirpici, "Reformative Effects of Intumescent Coating on the Structural Characteristics of Cold-Formed Steel," ACS Omega, vol. 7, no. 46, pp. 42560–42569, Nov. 2022.

Enhancing Concrete Strength with Waste Metal Fibers: A Study on Mechanical Properties and Workability

C. Yazici[1] and E. Yılmaz[1]

[1]Department of Construction, Ağrı İbrahim Çeçen University, Ağrı, Turkey, ORCID: 0000-0002-2061-4275; ORCID: 0009-0003-3511-0728

This research delves into the utilization of waste metal fibers derived from lathe waste as a sustainable solution to enhance both the compressive strength and workability of concrete. The study encompasses an extensive exploration of various proportions of metal fibers, including 0.5%, 1%, 1.5%, and 2%, incorporated into concrete mixes. Compressive strength evaluations were conducted at both 7 and 28 days to comprehensively assess the performance of the concrete specimens [1],[2]. The findings of this study reveal enhancement in compressive strength with the incorporation of waste metal fibers, showcasing promising results compared to conventional concrete mixes lacking fiber reinforcement. However, a concurrent observation of diminishing workability was noted with the increasing addition of metal fibers [3]. This adverse effect on workability necessitates a balanced consideration between strength enhancement and workability optimization in concrete mix design processes. This research contributes significantly to the fields of construction engineering and sustainability by shedding light on the potential of waste metal fibers in sustainable concrete production. By providing insights into the dual effects of enhancing strength while compromising workability, this study addresses a critical aspect of sustainable materials utilization in construction practices. The findings presented herein pave the way for further research and development aimed at refining concrete mix designs to achieve optimal performance while minimizing environmental impact through the utilization of recycled materials.

References

[1] M Barbuta, A Timu, L Bejan, RD Bucur, (2018). Mechanical properties of fly ash polymer concrete with different fibers. Materiale plastice, 55(3), 405-409.

[2] G Pachideh, M Gholhaki (2020). An experimental investigation into effect of temperature rise on mechanical and visual characteristics of concrete containing recycled metal spring. Structural concrete, 22(1), 550-565.

[3] M Ali, MJC Opulencia, T Chandra, S Chandra (2022). An environmentally friendly solution for waste facial masks recycled in construction materials. Sustainability, 14(14), 8739.

Effect of Heat Stress on Male Rat Kidney Catalase Enzyme

E. Senturk[1], and H. Ustundag[2]

[1]Agri Ibrahim Cecen University, Faculty of Medicine, Agri, Turkey, ORCID: (0000-0003-2082-6478)
[2]Erzincan Binali Yildirim University, Faculty of Medicine, Erzincan, Turkey, ORCID: (0000-0003-3140-0755

Catalase (CAT), an enzyme prevalent in almost all oxygen-exposed living organisms including bacteria, plants, and animals, serves to catalyze the breakdown of H_2O_2 into water and oxygen. This enzyme plays a crucial role in shielding cells from oxidative harm caused by reactive oxygen species (ROS) [1]. When the ambient temperature exceeds 25°C, disturbances arise, upsetting the balance between body temperature and heat dissipation. This phenomenon, referred to as heat stress (HS), poses significant risks to both human and animal well-being, resulting in considerable economic losses in public health services and livestock production [2]. In this study, the change of heat stress on male rat kidney catalase enzyme activity was observed. In this research, 18 male Sprague Dawley rats were utilized as experimental subjects. These rats were randomly divided into three groups: the control group (CG), which remained untreated at the normal temperature of 24±2 °C, the HS group 1 (HS1) subjected to 8 hours of daily exposure at 30 °C, and the HS group 2 (HS2) subjected to 8 hours of daily exposure at 35 °C. Following the completion of the heat-stress regimen on day 14, the rats were euthanized under ether anesthesia, and tissue samples from the kidney were collected for analysis. CAT activity measurement was performed according to the Aebi method [3]. Consequently, the findings demonstrated that heat stress (HS) had an adverse effect on the oxidant/antioxidant equilibrium in the kidney tissues of rats.

Key Words: Antioxidant, catalase, heat stress, kidney.

References

[1] P. Chelikani, I. Fita, P.C. Loewen, 2004. Diversity of structures and properties among catalases. CMLS, Cell. Mol. Life Sci. 61 (2004) 192-208.

[2] Y. Lin, L. Yang, M. Luo, 2021. Physiological and subjective thermal responses to heat exposure in northern and southern Chinese people. Build. Simul. 14 (2021) 1619-1631.

[3] H. Aebi, 1984. Catalase invitro. Methods Enzymol. 105 (1984) 121-126.

Role of Acetylcholinesterase Enzyme in Muscle Cells

E. Senturk[1], M. Senturk[2,3] and F. Sayır[1]

[1]*Agri Ibrahim Cecen University, Faculty of Medicine, Agri, Turkey, ORCID: 0000-0003-2082-6478, ORCID: 0000-0003-2864-9496*
[2]*Agri Ibrahim Cecen University, Faculty of Pharmacy, Agri, Turkey, ORCID: 0000-0002-9638-2896*
[3]*Oxford University, Chemistry Research Laboratory, Oxford, United Kingdom, ORCID: 0000-0002-9638-2896*

Acetylcholinesterase (AChE) stands as a key player among cholinergic enzymes, predominantly residing at the postsynaptic neuromuscular junctions, notably within muscles and nerves. Its primary function entails the swift breakdown or hydrolysis of acetylcholine (ACh), a neurotransmitter naturally present in the body, into acetic acid and choline [1]. Operating as a pivotal regulator, AChE effectively halts neuronal transmission and signaling across synapses, thereby curtailing the dispersal of ACh and the subsequent activation of adjacent receptors [2]. AChE is also present in skeletal muscle, exhibiting distribution patterns that appear to be associated with the muscle type (such as fast-twitch or slow-twitch) and their particular roles [3]. When a neural signal propagates and stimulates a cellular membrane, it triggers the release of the neurotransmitter acetylcholine. This action leads to a conformational shift in the ACh receptor and prompts the release of calcium ions from the membrane. These calcium ions further stimulate nerve and muscle fibers by inducing alterations in phospholipids. In essence, the initial signal mediated by ACh sets off a cascade that amplifies and propagates cellular signaling downstream [2,4].

References

[1] S.F. McHardy, H.L. Wang, S.V. McCowen, M.C. Valdez, 2017. Recent advances in acetylcholinesterase Inhibitors and Reactivators: an update on the patent literature (2012-2015). Expert Opin. Ther. Pat. 27(4) (2017) 455-476.

[2] A. Trang, P.B. Khandhar, 2023. Physiology, Acetylcholinesterase. In: StatPearls. Treasure Island (FL): StatPearls Publishing; 2024.

[3] S. Brimijoin, 1983. Molecular forms of acetylcholinesterase in brain, nerve and muscle: nature, localization and dynamics. Prog. Neurobiol. 21(4) (1983) 291-322.

[4] W. Leuzinger, 1969. Structure and function of acetylcholinesterase. Prog. Brain. Res. 31 (1969) 241-245.

Investigating The Effectiveness of Augmented Reality (Ar) Technology Supported Science Activities in Preschool Children: Solar System

M. Coşgun Demirdağ[1] and A. Taşgın[1]

[1]Department of Educational Sciences, Atatürk University, Erzurum, Türkiye ORCID: 0000-0003-2652-020X, ORCID: 0000-0002-3704-861X

This study examines the effect of science activities using augmented reality technology on preschool students. The study sample consisted of 21 preschool students in the age group of 5 years studying in a kindergarten in a province in eastern Turkey. The research method is a mixed method in which quantitative and qualitative data are used together. In the study where the nested mixed method was adopted, the pretest-posttest semi-weak experimental design was adopted in the quantitative design, and a case study was adopted in the qualitative part. The Solar System Knowledge Test, prepared by the researchers whose validity and reliability studies were conducted, was used as a pre-test. In the experimental application, DEVAR and AG Science Cards were shown to the students in groups of 4 on tablets. The observation form prepared by the researchers was used during the applications. The observation form consisted of questions related to cognitive, affective, and psychomotor domains during the students' use of AR. The Solar System Knowledge Test was reapplied as a post-test at the end of five weeks. In the results of the quantitative data, a significant difference was found between the pre-test and post-test scores. According to the results, there was an increase of 47 points in students' learning of the concepts in the solar system. In the qualitative data, observations and interviews showed that preschool children generally liked AR technology-supported activities, positively affecting their learning of solar system concepts.

Keywords: Preschool Education, Science Education, Augmented Reality (AR) Technology, Solar System, Mixed Method

References

[1] R. Azuma, 1997. A survey of augmented reality. Presence: Teleoperators and Virtual Environments. 6(4) (1997) 355-385.

[2] J. Garzón, 2017. An overview of twenty-five years of augmented reality in education. Multimodal Technologies and Interaction. 5(7) (2021) 37.

   [3]   J.W. Creswell, 2014. Research design: Qualitative, quantitative, and mixed methods approaches, (4th ed.) (2014) Sage.

Characterization of the Gibberellic Acid-Stimulated in Arabidopsis (GASA) Gene Family in Quinoa

E. Yiğider[1]

[1]Ataturk University, Erzurum, Turkey, ORCID: 0000-0002-6896-0193

The Gibberellic acid-stimulated in Arabidopsis (GASA) peptide family is widely distributed among plants and regulates plant growth stages and signal transduction in response to different environmental stresses [1]. The presence of the GASA gene has been detected in some plants but has not been studied in quinoa. This study evaluated the genome-wide analysis and functional identification of the GASA gene family members in quinoa (Chenopodium quinoa Willd.) and their responses to abiotic stresses. In the genome of quinoa, 20 GASA genes were identified and characterized. The molecular weight (MW) of GASA proteins varied from 10.06 to 36.29 kDa, their amino acid (aa) lengths ranged from 95 to 333, and their theoretical isoelectric point (pI) values varied from 4.44 to 9.73. Between 2 and 7 exons are estimated for CqGASA genes, with an average of 3. Phylogenetic relationships between Arabidopsis thaliana, Spinacia oleracea, and Chenopodium quinoa GASA genes were determined and it was observed that they were divided into three main groups. GASA genes had segmental and tandem duplicate gene pairs, and they were subjected to negative selection pressure during the evolutionary process. Using RNAseq data, expression profiles of CqGASA genes were determined in the root and shoot tissue of the Q68 genotype of quinoa during salinity stress. This study is significant for comprehending the biological functions of GASA genes in quinoa. According to the findings of this study, it was noted that GASA genes have the potential to play a role in the growth and development of quinoa, as well as in response to abiotic challenges experienced by the organism. This study, the first to examine the GASA gene family in quinoa, may benefit plant biotechnology and molecular biology.

References

[1] S. Rezaee, M. Ahmadizadeh, P. Heidari, 2020. Genome-wide characterization, expression profiling, and post-transcriptional study of GASA gene family, Gene Rep., 20 (2020) 100795.

Genome-Wide Analysis and Characterization of PIP5K (Phosphatidylinositol-4-Phosphate 5-Kinase) Gene Family of Phaseolus Vulgaris L.

S. Ucar[1], E. Yaprak[1], A.S. Aygören[1], S. Muslu[1], E. Yiğider[2], A.G. Kasapoğlu[1], E. İlhan[1] and M. Aydın[2]

[1]Erzurum Teknik Üniversitesi, Türkiye, ORCID: 0000-0002-7629-02064
[1]Erzurum Teknik Üniversitesi, Türkiye, ORCID: 0000-0002-8753-494X
[1]Erzurum Teknik Üniversitesi, Türkiye, ORCID: 0000-0002-6264-9935
[1]Erzurum Teknik Üniversitesi, Türkiye, ORCID: 0000-0003-4777-0726
[2]Atatürk Üniversitesi, Türkiye, ORCID: 0000-0002-6896-0193
[1]Erzurum Teknik Üniversitesi, Türkiye, ORCID: 0000-0002-6447-4921
[1]Erzurum Teknik Üniversitesi, Türkiye, ORCID: 0000-0002-8404-7900
[2]Atatürk Üniversitesi, Türkiye, ORCID: 0000-0003-1091-0609

PIP5Ks are important enzymes in the phosphatidylinositol signaling system that contributes to plant development and growth and play a role in responses to both biotic and abiotic stress factors. [1][2]. In this study, genome-wide analysis and characterization of *PIP5K* gene family members belonging to bean (Phaseolus vulgaris L.) plant were investigated. Twenty genes have been identified in the bean genome. The identified PIP5K gene family members were named PvPIP5K. According to analysis, *PvPIP5K-7* with the highest molecular weight of 98.53 kDa, and *PvPIP5K-16* with the lowest molecular weight of 10.54 kDa were found among the *PvPIP5K* proteins. In addition, the theoretical isoelectric points vary between 4.41 and 9.31, and the highest isoelectric point PvPIP5K-3 was obtained. The amino acid numbers of *PvPIP5Ks* are between 452 to 2466. As a result of gene duplication analyzes, *PvPIP5K-2/PvPIP5K-11*, *PvPIP5K-3/PvPIP5K-9*, *PvPIP5K-4/PvPIP5K-17*, and *PvPIP5K-14/PvPIP5K-15* genes were identified as duplicated genes. The Ka/Ks ratio of genes with was duplicated genes found to be less than 1. In gene structure analyses, the *PvPIP5K-10* gene had the highest number of exons, while the gene with the lowest number was *PvPIP5K-18*. Again, the highest number of introns belonged to the PvPIP5K-10 gene with 15, while the PvPIP5K-18 gene among the genes did not contain any introns. The phylogenetic tree forming 3 groups was drawn using common bean, Glycine max. and Arabidopsis PIP5K proteins. The protein-protein interactions of the *PIP5K* proteins were determined. The analysis of the data obtained from public databases was performed under salt and drought stress conditions, the lowest expression profile was found in the *PvPIP5K-2* gene in salt applications. On the other hand, when drought application was evaluated, the highest expression was detected in the *PvPIP5K-8* gene. The results of this study will provide a potential biotechnological resource and additional information for a better understanding of the molecular basis of the *PIP5K* gene family in the common bean plant.

References

[1] J. M. Ugalde, C. Rodriguez-Furlán, R. De Rycke, L. Norambuena, J. Friml, G. León, R. Tejos, 2016. Phosphatidylinositol 4-phosphate 5-kinases 1 and 2 are involved in the regulation of vacuole morphology during Arabidopsis thaliana pollen development, Plant Science. 250 (2016) 10-19.Á. Baricz, D.K. Dimitrov, I. Mezö, 2016. Radii of starlikeness and convexity of some q-Bessel functions, J. Math. Anal. Appl. 435 (2016) 968–985.

[2] Z. Zhang, Y. Li, K. Huang, W. Xu, C. Zhang, H. Yuan, 2020. Genome-wide systematic characterization and expression analysis of the phosphatidylinositol 4-phosphate 5-kinases in plants, Gene. 756 (2020) 144915.

Molecular Docking Analysis of Luteolin Derivatives as SARS-CoV-2 Inhibitors

Y. Gülşahin[1], Ş. Aksu[2] and M. Karadayı[2]

[1]Atatürk University, Graduate School of Natural and Applied Sciences, Erzurum, Türkiye, ORCID: 0000-0002-3770-2116
[2]Kafkas University, Department of Molecular Biology and Genetics, Kars, Türkiye, ORCID: 0000-0002-0844-5130
[3]Atatürk University, Department of Biology, Erzurum, Türkiye, ORCID: 0000-0002-2473-0409

SARS-CoV-2 (severe acute respiratory syndrome coronavirus 2) is a positive-sense single-stranded RNA virus that has been the cause of COVID-19, one of the most important pandemics in human history [1]. Research on the combat against SARS-CoV-2 is commonly accepted as vital for treatment of recent symptoms, reducing mortality and preventing new pandemics in the near future. In this respect, molecular docking is a powerful tool that enables the discovery of potential inhibitors of target viral receptors that play a critical role in the development of viral disease [2]. Thus, the present study was conducted to search new SARS-CoV-2 inhibitors by using molecular docking tools.

For this aim, molecular structures of luteolin, a well-known natural bioactive molecule, and it 73 derivatives obtained from ZINC, a database of commercially-available compounds for molecular docking. Then, structural minimization of each ligand was performed with UCSF Chimera 1.17.3 and ligand preparation was finished by using AutoDockTools 1.5.7. The target receptor SARS-CoV-2 3CL protease was obtained from RCSB Protein Data Bank (PDB: 6M2N) and its preparation was also done by using AutoDockTools 1.5.7. Docking studies were performed by AutodockVina and visualized by BIOVIA Discovery Studio Visualizer. According to the results, luteolin and its tested derivatives showed a high binding affinity to SARS-CoV-2 3CL protease. The best scores are obtained from Luteolin 6-C-Rutinoside (-10.7 kcal/mol), Luteolin 4'-Glucoside 7-Galacturonide (-10.6 kcal/mol), Scolymoside (-10.5 kcal/mol), Chrysoeriol 7-Rutinoside (-10.5 kcal/mol) and Luteolin-3',7-Diglucoside (-10.4 kcal/mol). Consequently, the present study showed that luteolin derivatives have significant inhibitory potential on the SARS-CoV-2 3CL protease and this finding valuable for development of new treatment strategies for COVID-19 and combat against new viral pandemics.

References

[1] M. Ciotti, M. Ciccozzi, A. Terrinoni, W.C. Jiang, C.B. Wang, S. Bernardini, 2020. The COVID-19 pandemic. Critical reviews in clinical laboratory sciences, Results Math., 57(6) (2020) 365-388.

[2] W. Wang, C. Yang, J. Xia, N. Li, W. Xiong, 2023. Luteolin is a potential inhibitor of COVID-19 An in silico analysis, Medicine. 102.38 (2023): e35029.

Diagnosis of Autoimmune Diseases: Detecting the Presence of ANA using the IIF method

K. Cavusoglu[1], and M. H. Uyanik[1]

[1]Ataturk University, Faculty of Medicine, Erzurum, Turkey, ORCID: 0009-0000-3206-1025, ORCID: 0000-0002-0759-9832

Autoimmune disease refers to approximately a hundred different defined clinical conditions caused by the body's immune system, the exact causes of which are not yet fully known, resulting from interactions between genetic and environmental factors, and can target any tissue or organ. Autoimmune diseases are diseases that have gained importance today because they can be diagnosed more easily. Antinuclear antibodies (ANA) have been guiding and helpful in the diagnosis of autoimmune diseases for many years. Today, different methods are used to detect ANA. The accepted gold standard for detecting ANA is the indirect immunofluorescence (IIF) method using HEp-2 (HEp-2000) cells as a substrate. The reliability of the results obtained with this method is of great importance for disease diagnosis.[1] At this point, the two most important factors are reliable HEp-2 cell series and reliable microscopic evaluation. The ANA IIF method is an in-vitro diagnostic method in which cell or tissue sections are used as the solid phase and specific antibodies are investigated in the patient's serum. It is the most commonly used method for detecting ANA. With the IIF method, immunological interactions against antigens specific to the mitotic and cytoplasmic area, as well as the nuclear area inside the cell, are detected. [2]. In order to ensure international standardization in ANA IIF reporting, a total of 29 different Anti Cell (AC) patterns, including 15 nuclear patterns, 9 cytoplasmic patterns and 5 mitotic patterns, have been defined by international consensus (ICAP, International Consensus on Antinuclear Antibody Pattern). While some of these patterns have been shown to be related to autoimmune diseases at different levels, a relationship has not yet been established for some of them. Therefore, the diagnostic effect of a positive ANA result is at different levels in autoimmune diseases and is also useful in the monitoring and prognosis of some diseases. ANA measured by the IIF method is guiding in the detection of many antigens. However, it is possible to demonstrate the relationship of determined patterns with some clinical diseases with monospecific tests. The IIF method is based on the binding of the antibody in the patient's serum to the antigen and the binding of the fluorescently labeled anti-human antibody to this complex. In this method, slides are used as the solid phase, and various cells or tissues are fixed on these slides. Patient serum is dropped onto these commercially prepared slides and incubated in accordance with the recommendations of each manufacturer. Following washing with buffer solution, FITC labeled anti-human antibody (conjugate) is added and incubation and washing are repeated. Subsequently, glycerol is dropped onto the slide, covered with a coverslip, and examined under a

fluorescence microscope. Titration is given and reported according to the fluorescence intensity of the samples examined. [1,3].

References

[1] Agmon-Levin N, Damoiseaux J, Kallenberg C, Sack U, Witte T, Herold M, et al. International recommendations for the assessment of autoantibodies to cellular antigens referred to as anti nuclear antibodies. Ann Rheum Dis 2013;73:17-23. 2. Maliler M, Meroni PL, Bossuyt X,

[2] Fritzler MJ. Current concepts and future directions for the assessment of autoantibodles to celi ular antigens referred to as anti-nuclear antibodies. J Immunol Res 2014; Article ID 315179.

[3] Meroni PL, Biggioggero M, Pierangeli SS, Sheldon J, Zegers 1, Borghi MO. Standardization of autoantibody testing: a paradigm for serology in rheumatic diseases. Nat Rev Rheumatol 2014;10:35-43.

The First Synthesis of New N-Substituted α-Amino Acid Methyl Ester Derivatives and Investigation of Their Inhibitor Effects on AChE and BChE

K. Coşkun Çalışır[1,2,3], A. Çağan[2], A. Akıncıoğlu[2] and H. Akıncıoğlu[2,3]

[1]*Ağrı İbrahim Çeçen University Graduate Education Institute Biochemistry PhD, 04100-Agri, TURKEY*
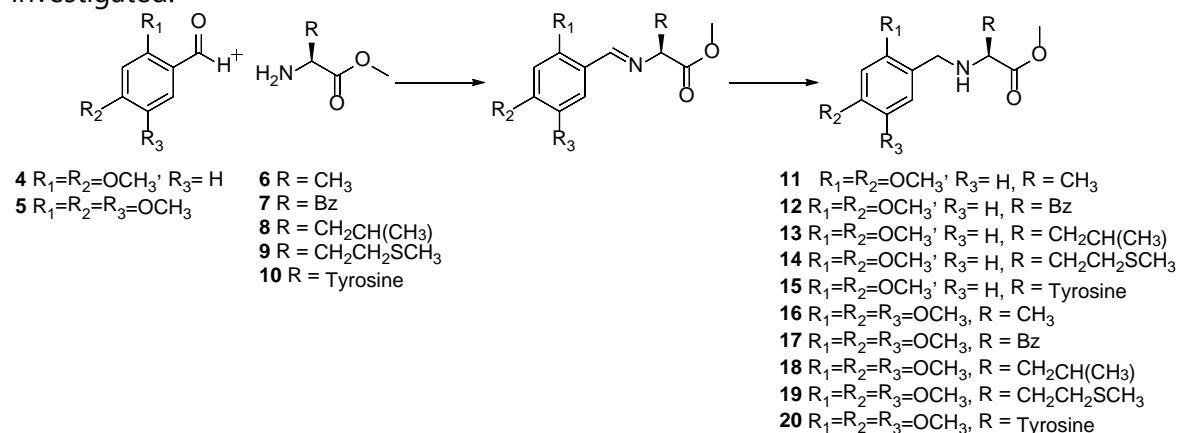[2]*Ağrı İbrahim Çeçen University, Central Researching Laboratory, 04100-Agri, TURKEY*
[3]*Ağrı İbrahim Çeçen University, Faculty of Arts and Sciences, 04100-Agri, TURKEY*

Amino acids are the building blocks of life. It's also known that many compounds derived from amino acids have various biological activities. For example, Ademetionine (1) is used in metabolic reactions and has anti-inflammatory properties in the treatment of chronic liver disease[1]. Betaine (2) reduces high blood homocysteine levels in patients with homocystinuria[2]. Acivicin (3) has antineoplastic properties that are used in cancer treatment[3].

1 Ademetionine   **2** Betain   **3** Acivicin
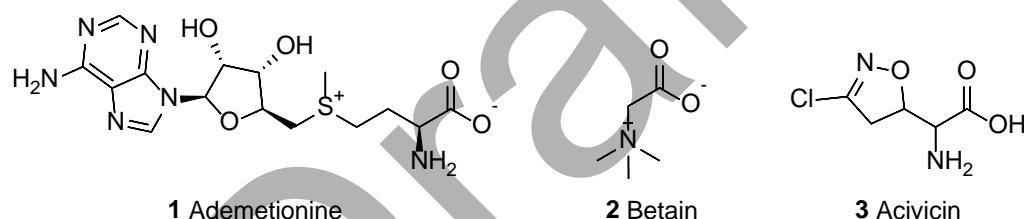
Due to the various biological activities of amino acids, in this study, the relevant imine derivatives obtained as a result of the reaction of aldehydes 4 and 5 with α-amino acid methyl ester derivatives 6-10 were reduced to obtain *N*-substituted α-amino acid methyl ester derivatives 11-20. Furthermore, AChE and BChE inhibition effects of 11-20 were investigated.

4 $R_1=R_2=OCH_3$, $R_3=$ H
5 $R_1=R_2=R_3=OCH_3$

6 R = CH_3
7 R = Bz
8 R = $CH_2CH(CH_3)$
9 R = $CH_2CH_2SCH_3$
10 R = Tyrosine

11 $R_1=R_2=OCH_3$, $R_3=$ H, R = CH_3
12 $R_1=R_2=OCH_3$, $R_3=$ H, R = Bz
13 $R_1=R_2=OCH_3$, $R_3=$ H, R = $CH_2CH(CH_3)$
14 $R_1=R_2=OCH_3$, $R_3=$ H, R = $CH_2CH_2SCH_3$
15 $R_1=R_2=OCH_3$, $R_3=$ H, R = Tyrosine
16 $R_1=R_2=R_3=OCH_3$, R = CH_3
17 $R_1=R_2=R_3=OCH_3$, R = Bz
18 $R_1=R_2=R_3=OCH_3$, R = $CH_2CH(CH_3)$
19 $R_1=R_2=R_3=OCH_3$, R = $CH_2CH_2SCH_3$
20 $R_1=R_2=R_3=OCH_3$, R = Tyrosine

References

[1] Almasio, P., & Pagliaro, L. (1993). Ademetionine: the state of the art and future prospects. Annali Italiani di Medicina Interna: Organo Ufficiale Della Societa Italiana di Medicina Interna, 8, 52S-55S.

[2] Craig, S. A. (2004). Betaine in human nutrition. The American journal of clinical nutrition, 80(3), 539-549.

[3] Ali, I., Wani, W. A., Haque, A., & Saleem, K. Glutamic acid and its derivatives: candidates for rational design of anticancer drugs. Future Med. Chem, 2013, 5(8), 961-978.

Diagnosis of Wegener's Granulomatosis: Antineutrophil Cytoplasmic Antibodies

E. Binici[1], K. Cavusoglu[1] and M.H. Uyanik[1]

[1]Ataturk University, Faculty of Medicine, Erzurum, Turkey, ORCID: 0009-0002-0834-8063, ORCID: 0009-0000-3206-1025, ORCID: 0000-0002-0759-9832

Granulomatosis with polyangiitis (GPA), more commonly known as Wegener's Granulomatosis, is an autoimmune disease characterized by lung and kidney involvement and ear-nose-throat symptoms, with a high mortality rate in untreated patients [1]. GPA is a rare disease whose prevalence is estimated to be 3/100,000 people; It is more common in Scandinavian countries. GPA affects both genders. Although the average age of occurrence is 45, elderly and pediatric cases have also been reported. One of the key features of GPA is the presence of cytoplasmic Antineutrophil cytoplasmic antibodies (ANCA) against proteinase 3 in approximately 90% of systemic forms and 50% of localized forms. PR3-ANCAs are highly specific for GPA and therefore have high diagnostic value. ENT symptoms are usually symptoms that reveal the disease, and chronic sinusitis or rhinitis is common. Although pulmonary symptoms are non-specific, cough, dyspnea, chest pain and hemoptysis may be observed. Chest X-ray and CT scan show one or more unilateral or bilateral nodules in half of the cases. It is vital to check for hematuria and proteinuria in diagnosis and at every follow-up examination. If it is not detected and treated in time, it can progress to serious kidney failure. Since partial or complete recovery can be achieved with treatment, it is important to treat it quickly. It is very important to investigate the presence of ANCAs with diffuse cytoplasmic fluorescence against PR3 and, much less frequently, myeloperoxidase, which is a critical component of GPA for diagnosis and monitoring, in 75% of cases. Enzyme-Linked ImmunoSorbent Assay (ELISA) and/or Indirect immunofluorescence (IFF) methods can be used to detect the presence of ANCA antibodies in laboratory diagnosis. The IIF method is preferred as a screening test for ANCA [1,2]. For this purpose, ethanol-stained human neutrophils are used as substrates for ANCA screening. With the IIF method, it is investigated microscopically whether there is a reaction against neutrophil granulocytes and the staining in the perinuclear and cytoplasmic areas of neutrophil granulocytes. Cytoplasmic staining in neutrophil granulocytes; cANCA and perinuclear stainings are called pANCA. GPA treatment is based on a combination of corticosteroids, and cyclophosphamide or rituximab, which allows attenuation of remission [3].

References

[1] Xavier Puéchal, Granulomatosis with polyangiitis (Wegener's), Joint Bone Spine, Volume 87, Issue 6, 2020, Pages 572-578, ISSN 1297-319X.

[2] Garlapati P, Qurie A. Granulomatosis With Polyangiitis. 2022 Dec 5. In: StatPearls [Internet]. Treasure Island (FL): StatPearls Publishing; 2024 Jan–. PMID: 32491759.

[3] Cartin-Ceba R, Peikert T, Specks U. Pathogenesis of ANCA-associated vasculitis. Curr Rheumatol Rep. 2012 Dec;14(6):481-93. doi: 10.1007/s11926-012-0286-y. PMID: 22927039.

Understanding the Role of Matrix Metalloproteinase-12 in Lung Cancer as a Potential Drug Target

S.K. Bardaweel[1]

[1]*School of Pharmacy, Department of Pharmaceutical Science, University of Jordan*

Lung cancer continues to be the leading cause of cancer death worldwide, often due to its late diagnosis and rapid progression. Despite advances in the available treatment approaches for lung cancer, the 5-year survival rate remains marginal [1]. Matrix metalloproteinases (MMPs) are zinc-dependent proteases that have been broadly investigated in extracellular matrix (ECM) breakdown and remodeling. Matrix metalloproteinase 12 (MMP12), a member of the matrix metalloproteinase family, has well-documented roles in lung pathological states. Moreover, recent studies linked the elevated expression of MMP12 to increased invasiveness, angiogenesis, and poor prognosis in lung cancer. However, despite the sufficient evidence on MMP12 overexpression in human lung cancer, its exact role in the development and progression of cancer remains an area of dispute [2,3]. In this work, we applied systems biology approach, to study the network biology of MMP12 and derive gene-disease hypotheses linking MMP12 to lung cancer to identify lung cancers and lung cancer cell lines that can be targeted with MMP12 inhibitors, in addition to identifying biomarkers for monitoring disease treatment with MMP12 inhibitors or MMP12 silencing. Ligand and structure-based drug design approaches were used to generate drug discovery hypotheses regarding MMP12 binding pockets and high-confidence model-based virtual screening hits that were validated experimentally.

References

[1] Breathnach, O.S., Freidlin, B., Conley, B., Green, M. R., Johnson, D. H., Gandara, D. R., Johnson, B. E.. Twenty-two years of phase III trials for patients with advanced non-small-cell lung cancer: Sobering results. *Journal of Clinical Oncology* 2001, *19*, 1734-1742.

[2] Wong, D.T., Todd, R., Tsuji, T., Donoff, R.B. Molecular biology of human oral cancer. *Crit. Rev. Oral Biol. Med.* 1996, *7*, 319-328.

[3] Bertini, I.; Calderone, V.; Fragai, M.; Giachetti, A.; Loconte, M.; Luchinat, C.; Maletta, M.; Nativi, C.; Yeo, K.J. Exploring the subtleties of drug-receptor interactions: the case of matrix metalloproteinases. *J. Am. Chem. Soc.* 2007, *129*, 2466-2475, doi:10.1021/ja065156z.

Effect of different Chip Ratios on Metal Quality via Rotary Degassing

A. Koşatepe[1], Ç. Yüksel[2], A. Taşer[1], M.E. Kalçık[1]

[1]Ağrı İbrahim Çeçen University Patnos Vocational School
[2]Atatürk University, Department of Metallurgical and Materials Engineering, Erzurum

The recyclability of aluminum and its alloys is considerably high. Therefore, the motivation of this study was originated by considering that the engineering materials currently in use are raw materials as scrap for melting process. Degassing, a routine procedure during melting, was carried out by purging only inert nitrogen gas without using any rafinationflux, and the measurements of liquid metal quality were applied depending on the varying chip quantities. The rotary degassing procedure was performed over a period of 5 min at a constant speed of 450 rpm and a constant flow rate of 10 l/min.Four different metal baths were prepared with metal charges of 75% primary + 25% chips, 50% primary+ 50% chips, 25% primary+ 75% chips and 100% chips with no primary ingots. Bifilm Index, a technique for measuring oxide films before and after rotary degassing, was used to evaluate the extent to which metal qualities changed. The values of Bifilm Index were 71.67 mm, 146.38 mm, 221.34 mm and 278.98 mm before the rotary degassing process and 36.33 mm, 78.76 mm, 148.86 mm and 123.08 mm after the process, respectively. When analyzed before and after the specimens of Bifilm Index, it is observed that there is an improvement of 49.31% of 25% scrap ratio, 46.19% of 50% scrap ratio, 32.75% of 75% scrap ratio and 44.12% of 0% scrap ratio. The scatters here were entirely due to the coincidence of these double oxides with the inert gas bubbles formed in the rotary degassing procedure and floating ability of these bubbles to these oxides from suspended locations to the surface. This study is presented as a clear proof that significant improvements in liquid metal quality can be achieved by purging only an inert gas in an environmentally friendly way without the use of any kind of flux compounds.

Keywords: Aluminum, Liquid metal quality, Rotary degassing

Metabolite Profiling and Enzyme Inhibitory Activity Potential of Different Extracts from Papaver Triniifolium

R. Demirdağ[1], R. Sağlamtaş[2], V. Çomakli[1], H. Akincioğlu[3], E. Yerlikaya[4], Y. Karagöz[5]

[1]*Agri İbrahim Çeçen University ,Faculty of Health, Nutrition and Dietetics, Department, Agri, Türkiye*
[2]*Agri İbrahim Çeçen University, Medical Services and Techniques Department, Agri, Türkiye*
[3]*Agri İbrahim Çeçen University, Faculty of Science and Letters, Chemistry Department, Agri, Türkiye*
[4]*Siirt University, Faculty of Health, Nutrition and Dietetics, Department, Siirt, Türkiye*
[5]*Agri İbrahim Çeçen University, Faculty of Pharmacy, Dept Pharmaceut Bot., Agri, Türkiye*

The Papaveraceae family, which can grow in various ecosystems, includes both annual and perennial species. The Papaver genus is naturally distributed in regions with a Mediterranean climate. Papaver triniifolium, a species of papaver, is a biennial plant native to Türkiye [1,2]. This plant, which was the study material, was collected from Ağrı-Türkiye. The collected plants were dried at room temperature and ground into a powder. The maceration method was used to extract *P. triniifolium* from methanol, ethanol, methanol-dichloromethane, ethyl acetate, dichloromethane, and n-hexane. The *in vitro* effects of the extracts on metabolic enzymes, including acetylcholinesterase (AChE) and butyrylcholinesterase (BChE), were investigated. Additionally, in this study, LC-MC/MC was used to determine the phytochemical profile of the methanol extract of *P. triniifolium*. The IC_{50} values were determined to measure the level of enzyme inhibition in the extracts. Tacrine served as a positive control for both enzymes. The experiments were conducted in triplicate. The IC_{50} values of P. triniifolium extracts were calculated as 62.10±0.11 µg/mL -75.97±0.65 µg/mL for AChE and 98.17±0.28 µg/mL-226,51±0.78 µg/mL for BChE. The best inhibitory effect for both enzymes was found in methanol extract. According to the results, *P. triniifolium* extracts had an inhibitory effect on AChE and BChE enzymes. It can be thought that the *P. triniifolium* plant can be used as a preventive measure against chronic diseases such as Alzheimer's and Parkinson's.

Keywords: Acetylcholinesterase, Butyrylcholinesterase, LC-MC/MC, *P. triniifolium*,

References

[1] Sari, A., Gray, A. I., & Sarıyar, G., (2006). Two new benzylisoquinoline alkaloids from Papaver triniifolium. Nat. pro. res, 20(5), 493-496.

[2] Atay M., Sari, A., Sarıyar, G., (2015). Alkaloıds and Chromosome Numbers of Papaver Polychaetum and P.Trınıifolıum. Jour of Fac of Pharm of Istanbul University, 32, 59-62.

Validity and Reliability Study of the Gender-Friendly Breastfeeding Knowledge Scale: A Methodological Study

R. Taşkın[1], E.S. Çağan[2] and A. Ekşioğlu[3]

[1]Ağrı Ibrahim Cecen University, Ağrı, Turkey, ORCID: 0000-0001-5176-157X
[2]Ağrı Ibrahim Cecen University, Ağrı, Turkey, ORCID: 0000-0002-3261-0431
[3]Ege University, İzmir, Turkey, ORCID: 0000-0002-8769-3289

Purpose: This study aimed to adapt the Gender-Friendly Breastfeeding Knowledge Scale into Turkish.

Methods: The research is of a methodological type. 256 students participated in the research. The data collection process involved the descriptive characteristics questionnaire and the Gender-friendly Breastfeeding Information Scale. In the analysis of the data, IBM SPSS (Statistical Package for the Social Sciences) 25.0, AMOS 22.0 package programs were utilized.

Results: In the adaptation of the scale to Turkish, language, scope, and structural validity analyses were conducted. The Scope Validity Ratio was found to be 0.77, and the scope validity index was found to be 0.94. The KMO result of the scale was 0.769, and the Bartlett test value was determined to be $X2: 643.889$, $p: 0.00$. As a result of the exploratory factor analysis, 4 items were excluded from the analysis. As a result of this analysis, 14 items were grouped under two dimensions and explained 37.48% of the total variance. With the confirmatory factor analysis, it was determined that the fit index results obtained from the sample were significant. The Cronbach's alpha value was found to be 0.74.

Conclusion: The research concluded that the scale is a valid and reliable measuring tool that can be applied to the Turkish population.

Keywords: Breastfeeding, Knowledge, Scale, Reliability, Validity

References

[1] Gupta, A., Aravindakshan, R., Sathiyanarayanan, S., Naidu, N. K., Santhoshi, K. N. ve Kakkar, R. (2021). Validation of Gender Friendly Breastfeeding Knowledge scale among young adults. *Journal of Preventive Medicine and Hygiene*, 62(4), 892-903. https://doi.org/10.15167/2421-4248/jpmh2021.62.4.2032.

[2] Leshi, O., Samuel, F. O. ve Ajakaye, M. O. (2016). Breastfeeding knowledge, attitude and intention among female young adults in Ibadan, Nigeria. *Open Journal of Nursing*, 6(1), 11-23. http://doi.org/ 10.4236/ojn.2016.61002.

[3] North, K., Gao, M., Allen, G. ve Lee, A. C. (2022). Breastfeeding in a global context: epidemiology, impact, and future directions. *Clinical Therapeutics,* 44(2), 228-244. https://doi.org/10.1016/j.clinthera.2021.11.017

[4] Terzi, Y. Anket, güvenilirlik–geçerlilik analizi. *Ondokuz Mayıs Üniversitesi,* 01 Aralık 2022, https://personel. omu. edu. tr/docs/ders_dokumanlari/1030_32625_1500.pdf adresinden erişildi.

[5] Alpar, R. (2018). *Applied statistics and validity-reliability studies with examples from sports, health and education*. Ankara: Detay Publishing.

The Effect of Pet Ownership on Postpartum Maternal Attachment

E. Solmaz[1], R. Raşkın[2], E.S. Çağan[3] and E. Sari[4]

[1]Ağrı Ibrahim Cecen University, Ağrı, Turkey, ORCID: 0000-0003-1962-8669
[2] Ağrı Ibrahim Cecen University, Ağrı, Turkey, ORCID: 0000-0001-5176-157X
[3] Ağrı Ibrahim Cecen University, Ağrı, Turkey, ORCID: 0000-0002-3261-0431
[4] Van Yuzuncu Yil University, Van, Turkey, ORCID: 0000-0002-8769-3289

This study was conducted to examine the effect of pet ownership on postpartum maternal attachment. The number of studies focusing on the relationship between pet ownership and mental health during pregnancy and postpartum period is limited. The study was a cross-sectional research conducted online via survey method between October 2022 and March 2023. A total of 86 mothers with babies aged between 0-6 months participated in the study, including 49 pet owners (37 cat, 8 dog, 4 bird) and 35 non-pet owners. In data collection, sociodemographic characteristics introduction form and mother attachment scale were used. Statistical Package for Social Sciences (SPSS) for Windows 25.0 was used to analyze the data. It was found that 75.5% of pet-owning mothers had cats and 6.1% reported that owning a pet affected their pregnancy. The average maternal attachment scale score for pet-owning mothers was 97.26±6.59, and for non-pet owning mothers it was 97.82±4.57. There was no statistically significant difference between the two groups. The study found no difference in maternal attachment levels between mothers who own pets and those who do not. It is thought that this may be due to the increasing anxiety of mothers about their childcare responsibilities.

References

[1] Adhikari, A., Jacob, N.K., Hansen, A.R., Wei, Y., Snook, K., Liu, F., Zhang, J. (2019). Pet ownership and the risk of dying from lung cancer, findings from an 18 year follow-up of a US national cohort. *Environ. Res.* 173, 379–386.

[2] Beetz, A., Uvnäs-Moberg, K., Julius, H., & Kotrschal, K. (2012). Psychosocial and psychophysiological effects of human-animal interactions: the possible role of oxytocin. *Frontiers in Psychology*, *3*, 234.

Numerical Solution of One Nonlinear Fourth-Order Integro-Differential Parabolic Equation Using Machine Learning

B. Tabatadze[1], T. Chkhikvadze[2], T. Jangveladze[2,3] and Z. Kiguradze[2,4]

[1]*European University, Georgia*
[2]*Ivane Javakhishvili Tbilisi State University, Georgia*
[3]*Georgian Technical University, USA*
[4]*Missouri University of Science and Technology, USA*

In [1] reduction of the well-known Maxwell system [2] of differential equations to the form of integro-differential equations was first performed. The mentioned reduced model has the following form

$$\frac{\partial H}{\partial t} = -rot\left[a\left(\int_0^t |rot\,H|^2 d\tau\right)rot\,H\right],$$

(1)

where, $H = (H_1, H_2, H_3)$ is the vector of the magnetic field. Some qualitative and structural properties of solutions of (1) type systems are established in many works. For more detail information see, for example, [3], [4] and references therein.

The presented work discusses a natural mathematical generalization of the scalar analog of the integro-differential model (1). In particular, the corresponding fourth-order integro-differential equation is investigated. Some properties of the corresponding initial-boundary value problems are studied in this note. The investigated model has the following form:

$$\frac{\partial u}{\partial t} + \frac{\partial^2}{\partial x^2}\left\{\left[1 + \left(\int_0^t \left(\frac{\partial^2 u}{\partial x^2}\right)^2 d\tau\right)\frac{\partial^2 u}{\partial x^2}\right]\right\} = f,$$

(2)

$$u(0,t) = u(1,t) = 0,$$

(3)

$$\frac{\partial u}{\partial t}(0,t) = \frac{\partial u}{\partial t}(1,t) = 0,$$

(4)

$$u(x,0) = u_0(x).$$

(5)

In equation (2) and in the initial condition (5), f and u_0 are given functions of their arguments. The stability and uniqueness of the solution of the initial-boundary value problem (2) - (5) is studied. Numerical solutions are found using the machine learning algorithms [5].

References

[1] Gordeziani D., Dzhangveladze T., Korshiya T. Existence and uniqueness of the solution of a class of nonlinear parabolic problems (Rus sian). Differ. Uravn, 19, 7 (1983), 1197-1207. English translation: Differ. Equ., 19, 7 (1984), 887-895.

[2] Landau L., Lifschitz E. Electrodynamics of Continuous Media, Course of Theoretical Physics, Moscow, 1957.

[3] Jangveladze T., Kiguradze Z., Neta B. Numerical Solution of Three Classes of Nonlinear Parabolic Integro-Differential Equations. Elsevier, 2016, ACADEMIC PRESS, ISBN: 978-0-12-804628-9. Elsevier/Academic Press, Amsterdam, 2015. 254 p.

[4] Jangveladze T. Investigation and Numerical Solution of Nonlinear Partial Differential and Integro-Differential Models Based on System of Maxwell Equations. Mem. Differential Equations Math. Phys., 76 (2019), 1-118.

[5] Raissi M., Perdikaris P., Karniadakis G. E., Physics informed deep learning (Part I): data-driven solutions of nonlinear partial differential equations. arXiv 1711.10561, 2017.

Development of New Metal Matrix Composite Materials with Tungsten Addition and Determination of Their Nuclear Radiation Protection

B. Aygün[1], A. Karabulut[2], Ö. Şimşek[3] and E. Kuşburak[4]

[1]) *Department of Electronics and Automation, Vocational School, Agri Ibrahim Cecen University, Agri, Turkey*
ORCID: 0000-0002-9384-1540
[2]*Department of Physics, Faculty of Science, Atatürk University, Erzurum, Turkey and Agri Ibrahim Cecen University Rectorate, Agri, Turkey*
[3]*Mathematics & Science Education, Faculty of Education, Agri Ibrahim Cecen University, Agri, Turkey*
[4]*Hayrettin Atmaca Anatolian High School, Agri, Turkey*

In this study, new metal matrix composite materials with high temperature resistance and the ability to shield gamma and fast neutron radiation were developed and produced. The productions were carried out using the powder metallurgy method with materials including Aluminum (Al), Cobalt (Co), Boron Carbide (B4C), Chromium (Cr), Nickel (Ni), Iron (Fe), Tungsten (W), Titanium Boride (TiB2), Titanium Carbide (TiC), Aluminum Oxide (Al2O3), Molybdenum (Mo), and Zirconium (Zr). The effective removal cross-section, half-value layer, mean free path, and transmission rate, which are neutron protection parameters for fast neutrons, were theoretically calculated using Monte Carlo simulation with the GEANT4 code. Additionally, the dose rates absorbed by all samples were determined using an Am[241]-Be fast neutron source. The gamma-ray mass attenuation coefficients, linear attenuation coefficients, half-value layer effective atomic numbers, and shielding parameters were theoretically determined. By comparing the results with 316LN nuclear stainless steel, it was determined that all new types of metal matrix composite materials exhibit capabilities for absorbing both gamma and fast neutron radiation. It is suggested that these new types of metal matrix composite materials can be utilized for shielding purposes in nuclear applications.

Numerical Solution of Two Systems of Nonlinear Partial Differential Equations Using Machine Learning

M. Gagoshidze[1], T. Jangveladze[1,2] and Z. Kiguradze[2,3]

[1]Ivane Javakhishvili Tbilisi State University, Georgia
[2]Georgian Technical University, Georgia
[3]Missouri University of Science and Technology, USA

Numerous scientific works, monographs, and textbooks are devoted to the research of the system of nonlinear partial differential equation. One model of such type, describing the process of electromagnetic field penetration in the substance is a well-known system of Maxwell equations [1]:

$$\frac{\partial H}{\partial t} = -rot(v_m\, rot\, H), \tag{1}$$

$$c_v \frac{\partial \theta}{\partial t} = v_m (rot\, H)^2, \tag{2}$$

where $H = (H_1, H_2, H_3)$ is a vector of the magnetic field, θ is temperature, v_m characterizes the electro-conductivity of the substance. As a rule, these coefficient are functions of the argument θ. Equations (1) describe the process of diffusion of the magnetic field while equation (2) expresses the change of the temperature at the expense of Joule heating. Many important processes are described applying the abovementioned Maxwell's system (see, e.g., [2-4] and references therein). System (1), (2) does not take into account many physical effects. For a more thorough description, first of all it is desirable to take into consideration heat conductivity. In this case, together with (1) instead of (2) the following equation is considered [1]

$$c_v \frac{\partial \theta}{\partial t} = v_m (rot\, H)^2 + \nabla(k\nabla\theta), \tag{3}$$

where k is a coefficient of heat conductivity. This coefficient is a function of θ as well. This abstract investigates decomposition schemes for (1), (2), and (1), (3) multidimensional models using machine learning algorithms [5]. Computer realizations have been implemented for above-mentioned decomposition schemes. Results from computer experiments are compared with theoretical conclusions and corresponding analyses are carried out.

References

[1] Landau L., Lifschitz E. Electrodynamics of Continuous Media. Course of Theoretical Physics. Pergamon Press, 1984, 474 p.

[2] Sun D., Manoranjan V., Yin H.-M., Numerical solutions for a coupled parabolic equations arising induction heating processes. Discrete Contin. Dyn. Syst. Supplement, (2007), 956-964.

[3] Jangveladze T., Investigation and Numerical Solution of Nonlinear Partial Differential and Integro-Differential Models Based on System of Maxwell Equations. Mem. Differential Equations Math. Phys., 76 (2019), 1-118.

[4] Jangveladze T., Kiguradze Z., Neta B. Numerical Solution of Three Classes of Nonlinear Parabolic Integro-Differential Equations, Elsevier, 2016, ACADEMIC PRESS, ISBN: 978-0 12-804628-9. Elsevier/Academic Press, Amsterdam, 2015.

[5] Raissi M., Perdikaris P., Karniadakis G. E., Physics informed deep learning (Part I): data-driven solutions of nonlinear partial differential equations. arXiv 1711.10561, 2017; https://arxiv.org/abs/1711.10561.

Analysing The Agricultural Emissions Performance of The World's 20 Largest Economies

E. Kadanali[1] and F.C. Dikmen[2]

[1]Ağrı İbrahim Çeçen University, Ağrı, Türkiye, ORCID: 0000-0001-6899-4935
[2]Ağrı İbrahim Çeçen University, Ağrı, Türkiye, ORCID: 0000-0002-4697-0761

Today, increasing global awareness of climate change is driving interest in analysing trends in energy use and carbon dioxide (CO_2) emissions from different sectors (Zhou et al., 2010). The drive to mitigate global warming and reduce greenhouse gas emissions is a concern for most economies around the world (Balsalobre-Lorente et al., 2019). At the regional level, farm gate emissions in 2020 are reported to be highest in Oceania (71%), Asia (50%) and the Americas (43%) (FAO, 2022). Land use change made the largest contribution in Africa (44%), while pre- and post-production processes made the largest contribution in Europe (53%) (FAO, 2022). It is stated in the literature that agricultural food systems account for one third of total anthropogenic greenhouse gas emissions (GHG) (Crippa vd, 2021; Tubiello vd., 2021). Tubiello et al. (2021) found that three-quarters of carbon emissions in the agri-food system come from pre- and post-production activities such as production, transport, processing and waste disposal. However, they found that the remainder was due to land-use change at the boundaries of conversion of natural ecosystems to agricultural land.

The aim of this study is to analyse the carbon emissions performance of the 20 most developed economies in the world as a result of their agricultural activities. For this purpose, multi-criteria decision-making methods were used. Multi-criteria decision-making methods allow evaluating many criteria together. The agricultural emissions of countries are assessed according to different criteria. Therefore, multi-criteria decision making methods can be applied. Data on the variables Farm Gate, Agricultural Land, Pre and Post Agrifood System and Livestock as criteria in the study were obtained from the FAO statistics. Entropy, CRITIC and MEREC methods, which are multi-criteria decision making methods, were used to analyse the data. The carbon emissions performance of 20 of the world's developed economies in the agricultural sector was analysed according to the defined criteria. The criteria or priority weights calculated according to the entropy values were 0,06% for pre- and post-production, 13% for the agri-food system, 19% for the farm gate, 29% for emissions from agricultural land and 34% for emissions from livestock. When the importance weights of the criteria were calculated using the CRITIC method, it was found that the pre- and post-production criterion ranked first with 43%. It was determined that the second place was 16% emissions from livestock. In third place, farm gate and farmland emissions were found to have equal weight at 15%. The weight of the agri-food system criteria was also calculated at 11%. MEREC results regarding the importance weights of the criteria are as follows. Agri-food system and farm gate (%22) were found to have equal weight. Likewise, emissions from agricultural land and

emissions from livestock criteria (%20) were determined with the same weight. The pre-post production criterion (%16) has the lowest weight.

References

[1] D. Balsalobre-Lorente, O.M Driha, F.V., Bekun, O.A. Osundina, 2019. Do agricultural activities induce carbon emissions? The BRICS experience. Environmental Science and Pollution Research, 26, 25218-25234.

[2] M. Crippa, E. Solazzo, Guizzardi, D., F. Monforti-Ferrario, F.N. Tubiello, A. Leip, 2021. Food systems are responsible for a third of global anthropogenic GHG emissions. Nature Food, 1–12. https://doi.org/10.1038/s43016-021-00225-9

[3] FAO. 2022. Greenhouse gas emissions from agri-food systems – Global, regional and country trends, 2000–2020. FAOSTAT Analytical Brief No. 50. Rome.

[4] F.N. Tubiello, C.Rosenzweig, G. Conchedda, K. Karl, , J. Gütschow, , P.Xueyao, et al. 2021. Greenhouse gas emissions from food systems: building the evidence base. Environmental Research Letters.

[5] P. Zhou, B. W.Ang, J.Y.Han, 2010. Total factor carbon emission performance: a Malmquist index analysis. Energy Economics, 32(1), 194-201.

High Temperature Resistant Insulation Composite Materials for Radiation Protection

B. Aygün[,1], A. Karabulut[2], S. Beyzade[1]

[1][1]Department of Electronics and Automation, Vocational School, Agri Ibrahim Cecen University, Agri, Turkey
ORCID: 0000-0002-9384-1540
[2]Department of Physics, Faculty of Science, Atatürk University, Erzurum, Turkey and Agri Ibrahim Cecen University Rectorate, Agri, Turkey

In this study, new type insulation composite materials with excellent resistance to temperature, corrosion, oxidation, and mechanical effects were designed and produced. The parameters for neutron radiation shielding (total macroscopic cross sections, effective removal cross sections, mean free path, half-value layer, and neutron transmission number) were determined using CERN Monte Carlo simulation Geant4 code. The dose rates absorbed by the materials were determined experimentally using a [241]Am-Be neutron source with an average energy of 4.5 MeV and an activity of 74 GBq, along with a BF_3 gas detector. Both simulation and experimental measurements were compared with paraffin and traditional concrete. Shielding parameters for gamma radiation, such as mass attenuation coefficient, effective atomic number, mean free path, and half-value layer (HVL), were calculated using WinXCom software. Additionally, radiation levels in areas traversed by high-voltage lines and in large transformer centers were determined. Electrical conductivity was determined to demonstrate suitability for use in these areas. It was determined that these new radiation protective composite materials could be used as shielding material for neutron and gamma radiation in nuclear medicine, transportation and storage of radioactive waste, nuclear power plants, and high-voltage areas.

Obtaining Graphene/Graphitic Structures on Catalyst Surfaces by CVD and PECVD Method

<u>M.T. Yurtcan</u>[1, 2], E. İgman[3], A. Güzel[1] and O. Simsek[2,4]

[1]*Department of Nanoscience and Nanoengineering, Graduate School of Natural and Applied Sciences, Atatürk University, 25240, Erzurum, Turkey*
[2]*Department of Mathematics & Science Education, Kazim Karabekir Education Faculty, Atatürk University, 25240, Erzurum, Turkey*
[3]*Department of Electronics and Automation, Technical Sciences Vocational College, Bayburt University, 69000 Bayburt, Turkey*
[4]*Central Application and Research Laboratory (MERLAB), Agri Ibrahim Cecen University, 04100 Agri, Turkey*

Graphene and graphitic structures were created by using chemical vapor deposition method and plasma-assisted chemical vapor deposition method on copper catalyst surfaces with the help of methane, argon and hydrogen gases [1]. Copper surfaces were annealed at 1000 C before deposition, and the growth temperature was 1000 C in the chemical deposition method and 750 C in the Plasma-assisted chemical vapor deposition method [2]. Optical images of the surfaces were taken and the most suitable conditions were tried to be determined with the help of Raman spectroscopy [3].

References

[1] Ö. Bayram, E. İgman, O. Simsek, 2019. CVD ve PECVD tekniği kullanilarak bakir folyolar üzerinde grafen nanoyapilarin elde edilmesi ve karakterizasyonu, Niğde Ömer Halisdemir Üniversitesi Mühendislik Bilimleri Dergisi, 8(2) (2019) 1126-1134.

[2] O. Bayram, O. Simsek, 2019. Vertically oriented graphene nano-sheets grown by plasma enhanced chemical vapor deposition technique at low temperature, Ceramics International, 45 (11) (2019) 13664-13670.

[3] O. Bayram, 2019. A study on 3D graphene synthesized directly on Glass/FTO substrates: Its Raman mapping and optical properties, Ceramics International, 45 (14) (2019) 16829-16835.

Species Determination of Microorganisms Isolated in Blood Culture

F. Cimen Acikgul[1]

[1]Ağrı İbrahim Çeçen University, Department of Medical Microbiology, Ağrı- Türkiye
ORCID:0000-0002-8904-1444

Bloodstream infection and sepsis are still significant causes of morbidity and mortality today[1]. Our study aimed to identify the microorganisms growing in blood culture and reveal their species profiles.

Aerobic and anaerobic blood culture bottles (n: 2,088), both pediatric and adult, sent to our laboratory from various units of our hospital between November 2022 and April 2023, were incubated in a fully automated blood culture device (Render, Shandong, China). Samples giving positive signals were plated on blood, EMB, and SDA agars, which were incubated at 370C for 18-24 hours. Tests such as Gram staining, catalase, coagulase, and oxidase were executed. Species identification was performed on the VITEC (Biomeriux, France) device.

Growth was detected in 400 samples in 2,088 blood culture bottles, with 99 pediatric and 301 adult blood samples. In 400 samples, 272 (68%) Gr(+), 112 (28%) Gr(-) bacteria and 16 (4%) yeast cells were grown. Among the 190 (63%) grams (+) bacteria in adult blood culture, 164 were Staphylococcus, 17 Enterococcus, and 9 Streptococcus bacteria. The most isolated species among 97 (32%) Gr(-) bacteria were determined to be Klebsiella pneumonia (31%) and E.coli (25%). Candida spp (71%) and Candida albicans (29%) were isolated in 14 (5%) samples. Proportionally similar findings were detected in pediatric blood culture bottles: 83(83%) Gr(+), 15(15%) Gr(-) bacteria, and 2(2%) Candida-type microorganisms. While 242(60.5%) Staphylococci were isolated in a total of 400 samples, 51(21%) of them were identified as S.aureus and 191(79%) as coagulase-negative staphylococci (CNS). The most frequently isolated bacterial species were determined as CNS.

Production and identification of microorganisms as soon as possible guide the clinician in choosing empirical treatment. In addition, timely initiation of antibiotic treatment is vital for patients as it reduces mortality [2].

References

[1] A.M. Peri, P.N.A. Harris, D.L. Paterson, 2022. Clin Microbiol Infect. Feb;28(2):195-201. doi: 10.1016/j.cmi.2021.09.039. Epub 2021 Oct 20.PMID: 34687856 Review.

[2] A. Balıkçı, Z. Belas, A. Eren Topkaya, 2013. Mikrobiyol Bul; 47(1): 135-140.

Investigation of the Wastewater of Organized Industrial Zone by Jet Loop Membrane Bioreactor System

B.Y. Aydin[1], S. Uzuner[2] and B. Farizoglu[3]

[1] Balıkesir University Institute of Science and Technology Environmental Engineering Department, Balıkesir,
ORCID: 0000-0001-6707-5507
[2]Balıkesir University Faculty of Engineering Department of Environmental Engineering , Balıkesir, Türkiye,
ORCID: 0000-0002-5715-6490
[3]Balıkesir University Faculty of Engineering Department of Environmental Engineering , Balıkesir, Türkiye,
ORCID: 0000-0001-5777-9412

Organized Industrial wastewater has a very complex structure and therefore the use of advanced technology systems is more convenient than conventional systems. Real industrial wastewater taken from the existing treatment unit located in Balıkesir Organized Industrial Zone, which has a very high organic matter concentration, was achieved at a high rate with the JLMBR system, whose design was completed with the high-performance cross-flow ceramic membrane obtained in the laboratory environment.

Balıkesir Organized Industrial Zone wastewater, which has a very high organic matter concentration, has reached a high treatment efficiency with the JLMBR system, whose design was completed with a cross-flow ceramic membrane module established in a laboratory environment. In this study, 98% purification efficiency was achieved at 11.7 kg COD/m^3.day and approximately 5 hours of retention time. Considering the MLSS concentration, which reached up to 7.9 g/L during the study, it was observed that this system offered the opportunity to increase the sludge age. It is also predicted that the cost of sludge treatment will decrease in a facility where this system will be used. High quality effluent was obtained from the UF membrane unit operated with the cross flow mode used in the system, with AKM=0 at all times. When this system is used in areas with complex wastewater content due to various areas, it provides output water in a smaller area, at a lower cost and of much higher quality compared to large systems.

References

[1] M.T. Santos, & P. A. Lopes, "Sludge recovery from industrial wastewater treatment. Sustainable Chemistry and Pharmacy", 29, 100803. Sludge recovery from industrial wastewater treatment, 2022.

[2] S. Udayakumar, & K. Praveen, "Advancements in industrial wastewater treatment by integrated membrane technologies. In Integrated Environmental Technologies for Wastewater Treatment and Sustainable Development", pp. 369-382, Elsevier, 2022.

[3] E. Hualpa-Cutipa, R. A. S. Acosta, S. Sangay-Tucto, X. G. M. Beingolea, G. T. Gutierrez, & I. N. "Zabarburú, Recent trends for treatment of environmental contaminants in wastewater: An integrated valorization of industrial wastewater", "In Integrated Environmental Technologies for Wastewater Treatment and Sustainable Development", (pp. 337-368). Elsevier, 2022.

[4] S.B. Doltade, Y. J. Yadav, & N. L. Jadhav, "Industrial wastewater treatment using oxidative integrated approach", "South African Journal of Chemical Engineering", 40, 100-106, 2022.

[5] J. Wagner, "Membrane Filtration Handbook Practical Tips and Hints by Chem. Eng Second Edition, Revision 2", 2001.

[6] J. Schwinge, P. R. Neal, D. E. Wiley, D. F. Fletcher, A.G. Fane, "Spiral wound modules and spacers: Review and analysis. Journal of Membrane Science. Elsevier", 2004.

[7] D. K. Jain, A. N. Patwari, M. B. Rao, A. A. Khan, "Liquid circulation characteristics in jet loop reactors. The Canadian Journal Of Chemical Engineering", 68, 1047–1051, 1990.

[8] M. Velan, T. K Ramanujam, "Gas-liquid mass transfer in a down flow jet loop reactor. Chem. Eng. Science", 47, 2871–2876, 1992.

[9] G. Padmavathi, K. R. Rao, "Influence of geometry on gas holdups in a reversed flow jet loop reactor. The Canadian Journal Of Chemical Engineering", 71, 94–100, 1993.

[10] E. S. Gaddis, A. Vogelpohl, "The impinging-stream reactor: a high performance loop reactor for mass transfer controlled chemical reactions. Chem. Eng. Science", 47, 2877–2882, 1992.

[11] U. Wachsmann, N. Rabiger, And A. Vogelpohl, "The compact reactor- a newly developed loop reactor with a high mass transfer performance. Ger. Chem. Eng." 8, 411-418, 1984.

[12] A. Vogelpohl, " Wastewater treatment by the HCR-Process. Acta Biotechnol", 20, 2, 119–128, 2000.

[13] B. Farizoglu, B. Keskinler, E. Yıldız, A. Nuhoglu, "Cheese whey treatment performance of an aerobic jet loop membrane bioreactor. Process Biochemistry", 39, 2283–2291, 2004.

The Evaluation of HERV-K Gene Expression in Doxorubicin-treated MCF-7 Breast Cancer Cell Line

B. Cakmak Guner[1], M. Yilmazer[2] and V.C. Ozalp[3]

[1]Ankara University, Faculty of Medicine, Department of Medical Biology, Ankara, Türkiye, ORCID: 0000-0003-4340-0867
[2]Istanbul University, Faculty of Science, Department of Molecular Biology and Genetics, Istanbul, Türkiye, ORCID: 0000-0003-4382-3763
[3]Atılım University, Faculty of Medicine, Department of Medical Biology, Ankara, Türkiye, ORCID: 0000-0002-7659-5990

Cancer has become a major public health problem worldwide. According to the data of the International Agency for Research on Cancer (IARC) in 2022, approximately 20 million new cancer cases and 9.7 million cancer-related deaths occurred. In the last 5 years, 7.8 million women were diagnosed with breast cancer and it made breast cancer the most common cancer worldwide [1,2]. Drugs such as doxorubicin, cyclophosphamide, methotrexate, and fluorouracil are frequently used in chemotherapy [3]. Doxorubicin, one of the most commonly used drugs in the treatment of breast cancer, inhibits the topoisomerase II enzyme and prevents replication. In this case, the cell is directed to apoptosis [4]. Resistance to anti-cancer agents such as doxorubicin develops in various breast cancer cases. However, it has been shown that doxorubicin causes a decrease in the expression of genes related to cell proliferation and anti-apoptotic genes in the breast cancer cell line MCF-7 [5]. Human endogenous retroviruses (HERV) are retroviruses that have existed in the human genome for millions of years, and HERV proteins appear to be expressed in various types of cancer [6]. While the expressions of HERV genes are not observed in normal breast tissues, there appears to be an increase in the expression of these genes in breast cancer. It has been reported in various studies that these mobile genetic elements can be used as a diagnostic biomarker [7,8]. In this study, alterations in the expression of the HERV-K *env*, *pol*, and *gag* genes were investigated in the breast cancer cell line MCF-7 treated with doxorubicin at 0.4 µM concentration. Analysis of the gene expression of HERV-K in breast cancer showed that doxorubicin treatment was altered HERV-K gene expression levels.

References

[1] C. Wild, E. Weiderpass, B.W. Stewart, 2020. World cancer report: cancer research for cancer prevention. International Agency for Research on Cancer.
[2] World Health Organization, (2023, July 12). "Breast cancer". Retrieved from https://www.who.int/news-room/fact-sheets/detail/breast-cancer

[3] H.B. Muss, D.A. Berry, C.T. Cirrincione, M. Theodoulou, A.M. Mauer, A.B. Kornblith ,... E.P. Winer, 2009. Adjuvant chemotherapy in older women with early-stage breast cancer, N. Engl. J. Med. 360(20) (2009) 2055-2065.

[4] R.L. Momparler, M. Karon, S.E. Siegel, F. Avila, 1976. Effect of adriamycin on DNA, RNA, and protein synthesis in cell-free systems and intact cells, Cancer Res. 36(8) (1976) 2891-2895.

[5] V. Ergin, İ. Doğan Turaçlı, A. Cumaoğlu, A. Yar, A. Ekmekçi, E. Menevşe, A. Menevse, 2011. The effects of Monensin and Doxorubicin on cell survıval and gene expressions in MCF-7 cell line, J. Exp. Clin Med. 28(2) (2011) 59-63.

[6] M. Gonzalez-Cao, P. Iduma, N. Karachaliou, M. Santarpia, J. Blanco, R. Rosell, 2016. Human endogenous retroviruses and cancer, Cancer Biol. Med. 13(4) (2016) 483.

[7] M. Tourang, L. Fang, Y. Zhong, R.C. Suthar, 2021. Association between Human Endogenous Retrovirus K gene expression and breast cancer, Cell. Mol. Biomed. Rep. 1(1) (2021) 7-13.

[8] B. Liang, T. Yan, H. Wei, D. Zhang, L. Li, Z. Liu, ... J. Leng, 2024. HERVK-mediated regulation of neighboring genes: implications for breast cancer prognosis. Retrovirology 21(1) (2024) 4.

# Synthesis of Novel Amino Acid Methyl Ester Derivatives and Investigation of AChE and BChE Inhibition Properties

D. Toğrul[1], A. Çağan[2], A. Akıncıoğlu[2] and H. Akıncıoğlu[3]

[1]Ağrı İbrahim Çeçen University, Department of Molecular Biology and Genetics, Faculty of Arts and Sciences, 04100-AĞRI, TÜRKİYE
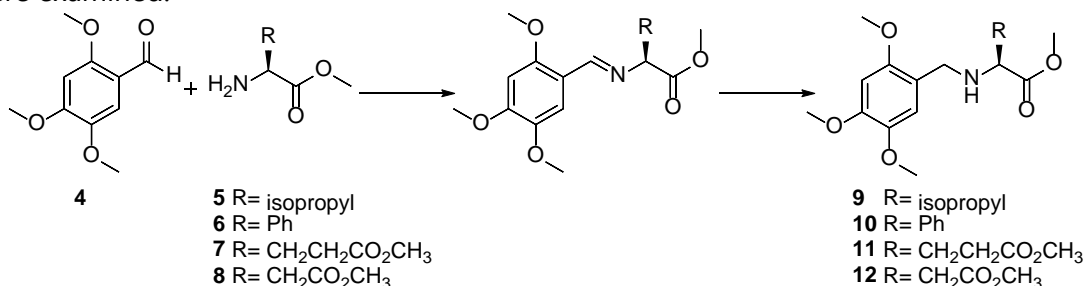[2]Ağrı İbrahim Çeçen University, Central Researching Laboratory, 04100-AĞRI, TÜRKİYE
[3]Ağrı İbrahim Çeçen University, Faculty of Arts and Sciences, 04100-AĞRI, TÜRKİYE

Amino acids, as known, are the basic building blocks that form proteins. Therefore, they have great biological importance. It is also known in the literature that they have many different biological activities. For example, Carglumic Acid (**1**) is a N-acetylglutamate (NAG) analog used in the treatment of acute and chronic hyperammonemia in patients with N-acetylglutamate synthase (NAGS) deficiency [1]. The derivative of alanine, Glufosinate (**2**), exhibits herbicidal properties [2]. Also, an amino acid methyl ester derivative **3**, which has MAO-A and MAO-B inhibition, has been reported in the literature [3].

1 Carglumic Acid   **2** Glufosinate   **3**
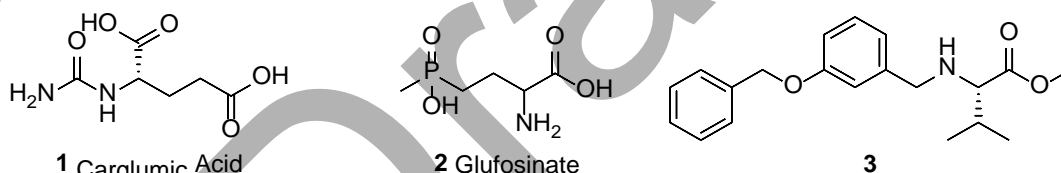
Due to the diverse biological activities of amino acids, in this study, the imine derivatives were obtained from the reaction of amino acid methyl ester derivatives **5-8** with 2,4,5-trimethoxybenzyl aldehyde (**4**). The imine derivatives were reduced with $NaBH_4$ or $NaCNBH_3$ to obtain the corresponding N-(2,4,5-trimethoxybenzyl)-substituted α-amino acid derivatives **9-12**. In addition, AChE and BChE enzyme inhibition properties of **9-12** were examined.

4

5 R= isopropyl
6 R= Ph
7 R= $CH_2CH_2CO_2CH_3$
8 R= $CH_2CO_2CH_3$

9 R= isopropyl
10 R= Ph
11 R= $CH_2CH_2CO_2CH_3$
12 R= $CH_2CO_2CH_3$

References

[1] Elpeleg, O., Shaag, A., Ben-Shalom, E., Schmid, T., & Bachmann, C. (2002). N-acetylglutamate synthase deficiency and the treatment of hyperammonemic encephalopathy. Annals of Neurology: Official Journal of the American Neurological Association and the Child Neurology Society, 52(6), 845-849.

[2] Hall, C. J., Mackie, E. R., Gendall, A. R., Perugini, M. A., & Soares da Costa, T. P. (2020). amino acid biosynthesis as a target for herbicide development. Pest Management Science, 76(12), 3896-3904.

[3] Akıncıoğlu, A. (2024). Design, synthesis, in silico, and in vitro evaluation of novel benzyloxybenzene substituted (S)-α-amino amide derivatives as cholinesterases and monoaminoxidases inhibitor. Drug Development Research, 85(2), e22161.

An Example Design Model of Wireless Power Transfer Using ANSYS Maxwell and Simplorer

M.A. Çelik[1]

[1]*Agrı Ibrahim Cecen University, Vocational School, Electrical and Energy Department, Agri, Türkiye,*
ORCID:0000-0001-9221-1099

Traditionally, electrical power is transmitted from a power source to a load through wired connections, but with the development of Wireless Power Transfer (WPT) technology, this paradigm is changing. WPT is the process of transferring electrical energy from a source to a receiver without a physical connection. Among the reasons for the increasing popularity of WPT today are its effects in facilitating human life and the absence of cable complexity. WPT technology enables energy transfer using various methods such as electromagnetic induction, magnetic resonance, or radio frequency (RF) transmission. Electromagnetic induction transfers energy through a magnetic field, while magnetic resonance technology enables energy transmission over longer distances and with higher efficiency using the resonance principle. RF transmission, on the other hand, can transmit energy using microwaves or radio waves. In the magnetic resonance method, the frequency of the magnetic field between the transmitter and receiver coils is tuned to the resonance frequency to achieve maximum energy transmission. Additionally, the ability to transfer energy without being affected by obstacles has made this method useful in many applications. Different simulation programs like CST Studio Suite, ANSYS Maxwell/Simplorer, COMSOL Multiphysics can be used to simulate wireless power transfer systems. In this study, co-simulation was carried out with ANSYS Maxwell and Simplorer to determine the design of WPT coils, electromagnetic field interaction and performance of the system, and co-simulation steps were presented in detail.

Keywords: ANSYS Maxwell, Simplorer, Wireless Power Transfer, Co-simulation

Synthesis And in silico Docking Studies of New Benzene Sulfonamides Towards Investigation of hCA and AChE

A. Çağan[1], A. Akıncıoğlu[1], R. Elati[2], N. Öztaşkın[3] and S. Göksu[3]

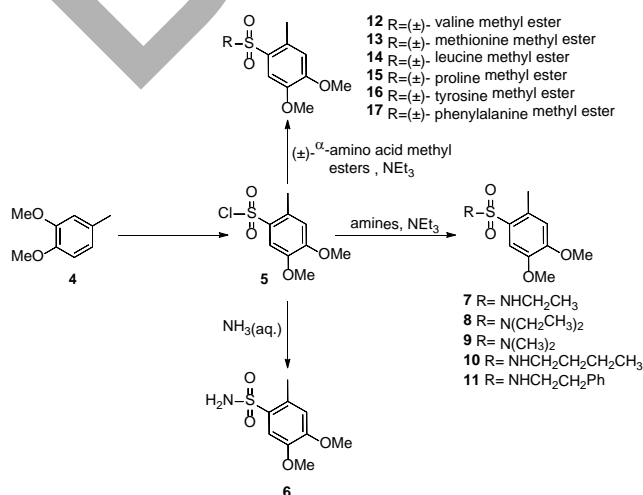[1]Ağrı İbrahim Çeçen University, Central Researching Laboratory, 04100-Agri, TURKEY
[2]LaboratoryofAppliedChemistryand Environment (LCAE), Faculty of Sciences, University Mohammed the first, Oujda, Morocco
[3]DepartmentofChemistry, Faculty of Science, Atatürk University, Erzurum, Turkiye

Sulfonamides, initially used in synthetic organic and medicinal chemistry [1], have a wide range of uses including as anti-microbial [2], anti-diabetic [3], and anti-inflammatory [4] compounds. Over 150 sulfonamide drugs exist today. Examples include sumatriptan (**1**) for migraines [5], dorzolamide (**2**) for glaucoma [6], and sulfamethoxazole (**3**) for urinary tract infections and Crohn's disease [7].
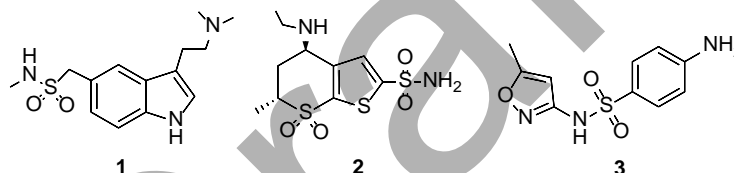
In this study, due to the wide range of biological activities of sulfonamides, a series of new sulfonamides were synthesized starting from 1,2-dimethoxy-4-methylbenzene (**4**). In silico docking studies were also carried out with hCA and AChE enzymes.

12 R=(±)- valine methyl ester
13 R=(±)- methionine methyl ester
14 R=(±)- leucine methyl ester
15 R=(±)- proline methyl ester
16 R=(±)- tyrosine methyl ester
17 R=(±)- phenylalanine methyl ester

(±)-α-amino acid methyl esters , NEt$_3$

amines, NEt$_3$

7 R= NHCH$_2$CH$_3$
8 R= N(CH$_2$CH$_3$)$_2$
9 R= N(CH$_3$)$_2$
10 R= NHCH$_2$CH$_2$CH$_3$
11 R= NHCH$_2$CH$_2$Ph

NH$_3$(aq.)

References

[1] S. Mondal, S. Malakar. Synthesis of sulfonamide and their synthetic and therapeutic applications: Recent advances. Tetrahedron, 2020, 76, 131662.

[2] T. Nasr, S. Bondock, S. Eid. Design, synthesis, antimicrobial evaluation and molecular docking studies of some new thiophene, pyrazole and pyridone derivatives bearing sulfisoxazole moiety. Eur. J. Med. Chem., 2014, 84, 491-504.

[3] Y. Du, Y. Zhang, H. Ling, Q. Li, J. Shen. Discovery of novel high potent and cellular active ADC type PTP1B inhibitors with selectivity over TC-PTP via modification interacting with C site. Eur. J. Med. Chem., 2018, 144, 692-700.

[4] H. Suleyman, E. Cadirci, A. Albayrak, Z. Halici. Nimesulide is a Selective COX-2 Inhibitory, Atypical Non-Steroidal Anti-Inflammatory Drug. Curr. Med. Chem. 2008, 15, 278 – 283.

[5] Pierce M, Marbury T, O'Neill C, Siegel S, Du W, Sebree T (June). Zelrix: a novel transdermal formulation of sumatriptan. Headache. 2009, 49, 817–825.

[6] H. Kubinyi. Chance favors the prepared mind--from serendipity to rational drug design. J Recept Signal Transduct Res. 1999, 19, 15–39.

[7] M. E. Falagas, K. Z. Vardakas, Ni. S. Roussos. Trimethoprim/sulfamethoxazole for Acinetobacter spp.: A review of current microbiological and clinical evidence. Int. J. Antimicrob. Agents, 2015, 46, 231–241.

Comparative Analysis of New Monoamine Oxidases (A and B) from Pan troglodytes

G. Budak[1], H. Akıncıoğlu[2] and E. Karataşl[1]

[1]Ağrı İbrahim Çeçen University, Patnos Vocational School Ağrı Turkey, ORCID: 0009-0007-4203-3926, ORCID: 0000-0001-6848-7618
[2]Ağrı İbrahim Çeçen University, Faculty of Science and Letters, Ağrı, Turkey, ORCID: 0000-0001-5453-0953

Monoamine oxidase A (MAOA) and B (MAOB) are enzymes found in mammals that are attached to the outer membrane of mitochondria [1]. There are two main forms of MAO: MAOA and MAOB. MAOA primarily metabolizes serotonin, norepinephrine, and dopamine. MAOA and MAOB are important targets for drug development, particularly in the treatment of neurological and psychiatric disorders. This has led to pharmaceutical companies highly valuing specific MAO inhibitors. The development of these inhibitors has facilitated the creation of the biocatalytic method for producing enantiopure amines, which are crucial building blocks in the pharmaceutical industry [2]. In this study, it was aimed to elucidate new MAOAs for heterologous expression in yeast systems via *in silico* analysis. The specific *maoa* and *maob* genes to be used have been identified through the NCBI and UniProt databases. Studies have focused on *maoa* and *maob* genes of the *Pan troglodytes*, known as the chimp, is a species of great ape native to the forests and savannahs of tropical Africa. Results of comparative analyses (Expasy Swissmodel and NCBI BLAST), signal peptide content (Signal IP 4.1), glycosylation sites (NetNGlyc 1.0), ligand binding points, and domain properties (PyMOL) were examined, and monoamine oxidases characteristics of the related genes were determined. According to result of additional BLAST and alignment applications with the protein sequences of the major studies, related genes will be synthesized on pPIC9K vector by GeneScript Inc commercially. PCR processes will be applied, and band formation will be observed in agarose gel analysis. In future studies, it is planned to accomplish heterologous production, purification, and kinetic calculations of the enzymes in *Pichia pastoris* GS115.

References

[1] Salach, J. I. (1979) Monoamine oxidase from beef liver mitochondria: Simplified isolation procedure, properties, and determination of its cysteinyl flavin content. Arch. Biochem. Biophys. 192,128–137.

[2] Ghislieri, D., Houghton, D., Green, A. P., Willies, S. C., & Turner, N. J. (2013). Monoamine oxidase (MAO-N) catalyzed deracemization of tetrahydro-β-carbolines: Substrate dependent switch in enantioselectivity. Acs Catalysis, 3(12), 2869-2872.

Gas Sensor Applications of Metal Oxide Nanostructures Synthesized by Cost-Effective USP Method

M.E. Güldüren[1], H. Güney[2], D. İskenderoğlu[3], S. Morkoç Karadeniz[4] and S. Sarıtaş[5]

[1]Ağrı İbrahim Çeçen University, Vocational School, Ağrı, Turkey
[2]Atatürk University, Hınıs Vocational School, Erzurum, Turkey
[3]Atatürk University, Kazım Karabekir Education Faculty, Erzurum, Turkey
[4]Erzincan Binali Yıldırım Universit, Physics Department, Erzincan, Turkey
[5]Atatürk University, İspir Hamza Polat Vocational School, Erzurum, Turkey

Research in materials at the nanoscale has experienced exponential growth in recent decades due to the unique physical and chemical properties exhibited by these nanostructures, properties often absent in their bulk counterparts. The structural, optical and electrochemical properties of these nanoscale metal oxide films can be further tailored by doping them with transition metals (TMs) like Fe, Co, Ni, Cr, Mn, etc., which can modulate defect sites such as oxygen vacancies and charge carrier density within the host material. Additionally, various deposition techniques, including sol-gel processes, hydrothermal methods, pulsed laser deposition, RF-DC magnetron sputtering, and the ultrasonic spray pyrolysis (USP) method, can be employed to fabricate doped metal oxide thin films. Among these methods, the USP approach stands out for its ease of control and cost-effectiveness, not requiring expensive equipment like vacuum chambers. In this study, we investigate the structural, optical and H2 gas sensor effects of transition metal doping on the USP grown metal oxide nanocrystals.

Keywords: XRD, Uv-vis spectroscopy, Semiconductor thin films, H2 gas sensors.

Characterization and Supercapacitor Analysis of Metal Oxide Semiconductor Thin Films Grown by USP Method

M.E. Güldüren[1], H. Güney[2], D. İskenderoğlu[3], S. Morkoç Karadeniz[4] and K. Çınar Demir[5]

[1]Ağrı İbrahim Çeçen University, Vocational School, Ağrı, Turkey
[2]Atatürk University, Hınıs Vocational School, Erzurum, Turkey
[3]Atatürk University, Kazım Karabekir Education Faculty, Erzurum, Turkey
[4]Erzincan Binali Yıldırım University, Physics Department, Erzincan, Turkey
[5]Atatürk University, Art & Science Faculty, Erzurum, Turkey

In recent years, the production and characterization of materials at the nano-scale have garnered significant attention within the scientific community. This surge in interest is primarily due to the fact that as particle size diminishes to the nanometer scale, the physical and chemical properties of many materials undergo profound transformations. Consequently, nano-sized metal oxide semiconductors have become a focal point of research due to their intriguing properties, particularly in electronic devices, heterogeneous catalysts, gas sensing systems, etc. Furthermore, impurity doping has emerged as a highly effective method for tailoring material properties to specific requirements. Various techniques have been employed to prepare metal oxide nanoclusters, including vacuum thermal evaporation, molecular beam epitaxy, spin coatings, chemical bath deposition, electron beam evaporation, and sol-gel processes. However, these conventional growth methods often incur high costs, particularly when fabricating nanostructures on a large scale. To address this challenge, we utilize the ultrasonic spray pyrolysis (USP) method to fabricate metal oxide nanoparticles doped with different concentrations of impurities. This method offers the advantage of requiring no sophisticated experimental setup. Subsequently, we present the corresponding structural, optical, and photocatalytic assessments of these nanoparticles.

Keywords: Metal oxide thin films, optical band gap, SEM, PL spectrum, supercapacitors

Plants Defense Enzymes

Ş. Taşbaşı[1], F.N. Coşkun[2], K. Karagöz[3], A. Öztekin[3] and B. Alaylar[4]

[1]Department of Chemistry, Postgraduate Education Institute, Agri Ibrahim Cecen University, Agri-TURKEY, ORCID: 0000-0001-9093-3928
[2]Department of Molecular Biology and Genetics, Postgraduate Education Institute, Agri Ibrahim Cecen University, Agri-TURKEY, ORCID: 0009-0008-3986-3096
[3]Department of Molecular Biology and Genetics, Faculty of Science and Letters, Agri Ibrahim Cecen University, Agri-TURKEY, ORCID: 0000-0003-1908-5836, ORCID: 0000-0003-1908-5836
[4]Department of Medical Services and Techniques, Vocational School of Health Services, Agri Ibrahim Cecen University, Agri-TURKEY, ORCID: 0000-0003-1418-179X

Plants are exposed to insect and pathogen attacks in daily life, and therefore most plants use different defense mechanisms [1]. Some of these defense mechanisms comprise lignification, suberization, and callose accumulation within the cell wall, along with phenolic compounds, phytoalexins, and pathogenesis-related (PR) proteins. Plants benefit from certain enzymes to strengthen their defense mechanisms. These defense enzymes include peroxidase, chitinase, polyphenol oxidase, phenylalanine ammonia-lyase (PAL) and β-1,3-glucanase [2]. Peroxidases, which belong to the PR protein family, limit the spread of intercellular infection by producing reactive oxygen species [3]. Chitinases are enzymes that develop a defense mechanism against plant pathogens by breaking down chitin [4]. Polyphenol oxidases are catalyze the conversion of hydroxyphenols into quinone derivatives, thus helping to protect the plant against pathogens by leading to the formation of molecules with antimicrobial effects. [5,6]. PAL, found in higher plants, yeasts, fungi, ferns, and algae, are enzymes that catalyze the non-oxidative deamination of L-phenylalanine into trans-cinnamic acid and ammonia. Additionally, PAL plays a role in the biosynthesis of various secondary metabolites, such as lignin, flavonoids, and coumarins, as they are rate-limiting enzyme in the phenylpropanoid pathway of plants [7]. β-1,3-glucanases, which belong to the PR-2 protein family and exhibit endo-type enzyme properties, catalyze the formation of glucan oligosaccharides by cutting β-1-3 glycoside bonds along the β-glucan chain [8,9]. Plants have developed various defense mechanisms to protect themselves against environmental factors like pathogens. One of these mechanisms is the enzymatic methods. Plants strengthen their cell walls using various enzymes, such as peroxidase, β-1,3-glucanase, chitinase, phenylalanine ammonia-lyase, and polyphenol oxidase, to protect themselves against biotic factors.

Key words: Plants, Enzymes

References

[1] Usha Rani, P., & Jyothsna, Y. (2010). Biochemical and enzymatic changes in rice plants as a mechanism of defense. *Acta Physiologiae Plantarum*, *32*, 695-701.

[2] Prasannath, K. (2017). Plant defense-related enzymes against pathogens: a review.

[3] Passardi, F., Cosio, C., Penel, C., & Dunand, C. (2005). Peroxidases have more functions than a Swiss army knife. *Plant cell reports*, *24*, 255-265.

[4] Jalil, S. U., Mishra, M., & Ansari, M. I. (2015). Current view on chitinase for plant defence.

[5] Shi, C., Dai, Y., Xia, B., Xu, X., Xie, Y., & Liu, Q. (2001). The purification and spectral properties of polyphenol oxidase I fromNicotiana tabacum. *Plant Molecular Biology Reporter, 19*, 381-382.

[6] Mayer, A. M., & Harel, E. (1979). Polyphenol oxidases in plants. *Phytochemistry*, *18*(2), 193-215.

[7] Kawatra, A., Dhankhar, R., Mohanty, A., & Gulati, P. (2020). Biomedical applications of microbial phenylalanine ammonia lyase: Current status and future prospects. *Biochimie*, *177*, 142-152.

[8] Wessels, J. G. H., & Sietsma, J. H. (1981). Fungal cell walls: a survey. In Plant carbohydrates II: extracellular carbohydrates (pp. 352-394). Berlin, Heidelberg: Springer Berlin Heidelberg.

[9] Wu, J., Yang, R., Gao, M., Zhang, H., & Zhan, X. (2021). Synthesis of functional oligosaccharides and their derivatives through cocultivation and cellular NTP regeneration. *Advances in applied microbiology*, *115*, 35-63.

Inhibition Effect of Chromenopyridine Derivatives on Some Metabolic Enzymes

A. Öztürk Kesebir[1], H. Akıncıoğlu[2] and V. Çomaklı[2]

[1]Agri Ibrahim Cecen University, Vocational School of Patnos, Agri, Patnos, Türkiye. ORCID: 0000-0003-2603-7509
[2]Ağrı İbrahim Çeçen University, Faculty of Arts and Science, 04100 Ağrı, Turkiye, ORCID: 0000-0001-5453-0953
[3]Agri Ibrahim Cecen University, Faculty of Health Sciences, Agri, Türkiye ORCID: 0000-0003-2109-6702

Chromenopyridine is a versatile structural motif found in various polyheterocycles with applications in biology as estrogenic, antibacterial and anticancer agents and biosensors. Due to these properties, it is of great importance to investigate chromenopyridine derivatives on the activities of enzymes identified as targets in many diseases [1-4]. The pentose phosphate pathway (PPP) is a metabolic pathway in cells that produces NADPH and pentose sugars. NADPH plays an important role in maintaining cellular redox balance and defense against reactive oxygen species (ROS) [5]. In study, investigated the inhibition effect of 4 different chromenopyridine derivatives on Glucose 6-phosphate dehydrogenase and 6-phosphogluconate dehydrogenase, two important enzymes of PPP pathway. All derivatives exhibited competitive inhibition on 6PGD, with Ki values ranging from 1.77 to 8.3 µM. Derivatives 2 and 3 exhibited competitive inhibition on G6PD, whereas derivatives 1 and 4 exhibited noncompetitive inhibition. The Ki value was calculated between 0.06 and 2.05 µM. The results obtained indicate that chromenopyridine derivatives are good candidates for the treatment of oxidative stress-related diseases.

References

[1] F.A. El-Essawy, AAS. El-Etrawy 2014. Synthesis of New Chromeno [4, 3-b] pyrazolo [4, 3-e] pyridines Derivatives with Antimicrobial Evaluation. J. Heterocycl. Chem. 51, 191–195.

[2] W. Huang, W. Lin, X. Guan 2014. Development of ratiometric fluorescent pH sensors based on chromenoquinoline derivatives with tunable pKa values for bioimaging. Tetrahedron Lett. 55, 116–119

[3] [3] Z. Hu, C Wang, D. Sitkoff, N.L. Cheadle, S. Xu, J.K. Muckelbauer, L.P. Adam, R.R. Wexler, M.L. Quan 2020. Identification of 5H-chromeno[3,4-c]pyridine and 6H-isochromeno[3,4-c]pyridine derivatives as potent and selective dual ROCK inhibitors. Bioorg Med Chem Lett. 2020.

[4] X. Liu, Y. Li, X. Ren, Q. Yang, Y. Su, L. He, X. Song 2018. Methylated chromenoquinoline dyes: synthesis, optical properties, and application for mitochondrial labeling. Chem. Commun. 54, 1509–1512.

[5] Zhang H, Zhang H, Wang S, Ni Z, Wang T. 2019. 1-Hydroxy-8- methoxy-anthraquinon reverses cisplatin resistance by inhibiting 6PGD in cancer cells. Open Life Sci. 14(1): 454-61.

Examining the Reflection of Occupational Health and Safety Topics on Vocational and Technical High School Curriculum Objectives

Ö. Karabulut[1,2] and P. Baykan[1]

[1]Ağrı İbrahim Çeçen University, Ağrı, Türkiye, ORCID: 0000-0002-9208-2589, ORCID: 0000-0001-5279-3872
[2]Atatürk University, Erzurum, Türkiye

Occupational health and safety (OHS) topics being included in the school curriculum is considered important for the development of a culture of health and safety in society. Especially in Vocational and Technical Schools, which have a mission of vocational training, it is necessary to provide students with not only basic knowledge and skills related to their profession but also competencies in health and safety. It is noted that larger injury cases among young workers in workplaces are due to lack of awareness of work-related hazards (Miller and Kaufman, 1998; Linker et al., 2005). Therefore, educational practices that will contribute to the creation of awareness of danger and risk among students should be included in the curriculum programs of vocational and technical schools. Developing school-based OHS teaching programs in this direction is seen as an intervention strategy to prevent occupational injuries among young workers (Balanay et al., 2014). In this context, this study aimed to examine the reflection of occupational health and safety topics in the curriculum outcomes of vocational and technical schools published by the Ministry of National Education. The study was conducted using document analysis method. Vocational education curriculum documents published by the Ministry of National Education were used as the data source. The OHS analysis units were determined as Health, Risk, Safety, Precaution, Emergency, Security, Protection, Occupational Health and Safety, Danger, Duties and Responsibilities, Equipment, and Traffic Rules. All curriculum programs were analyzed within the framework of these analysis units. When examining vocational high school curricula, a total of 173 outcomes were identified across 32 fields. The curriculum emphasizes the need to implement OHS measures and impart knowledge and skills in the field. However, these lessons are introductory units that serve as a warning about occupational health and safety rules. In vocational high school curriculum programs, including outcomes aimed at behavioral change, not just knowledge, will help students develop the ability to assess risks and make safe decisions for both themselves and others.

References

[1] Miller, M. E., & Kaufman, J. D. (1998). Occupational injuries among adolescents in Washington State, 1988–1991. American Journal of Industrial Medicine, 34(2), 121–132.

[2] Linker, D., Miller, M. E., Freeman, K. S., & Burbacher, T. (2005). Health and safety awareness for working teens: Developing a successful, statewide program for educating teen workers. Family and Community Health, 28(3), 225–238.

[3] Balanay, J. A. G., Adesina, A., Kearney, G. D., & Richards, S. L. (2014). Assessment of occupational health and safety hazard exposures among working college students. American Journal of Industrial Medicine, 57(1), 114–124

Psychological Safety in Workplaces

S. Erk[1] and P. Baykan[1]

[1]Ağrı İbrahim Çeçen University, Ağrı, Türkiye, ORCID: 0009-0001-1450-4459, ORCID: 0000-0001-5279-3872

In today's workplace environments, occupational health and safety measures encompass not only physical safety but also the psychological well-being of employees. Psychological safety perception indicates the level of comfort employees feel psychologically when expressing their views believed to be beneficial for the organization and sharing innovative ideas within the organization (Yener, 2014). Based on this, employees' perceptions of psychological safety regarding occupational health and safety can be considered a key factor in Occupational Health and Safety processes. This study aimed to highlight the importance of employees' perceptions of psychological safety in creating a safer environment in workplaces. In workplaces where psychological safety perception is high, employees feel safe enough to proactively identify potential hazards and confidently express their ideas to the management for preventive measures to be taken. Psychological safety can make a difference between narrowly avoiding an industrial accident and experiencing a catastrophic one or between strong job performance and a dramatic, headline-grabbing failure (Edmondson, 2018). This situation allows efforts to increase workplace safety to be planned more effectively based on identified risks. Moreover, employees' perceptions of psychological safety can influence their trust in occupational health and safety policies and practices, encouraging better compliance with these policies and effective continuation of OHS practices.

References

[1] Edmondson, A., 2018. The Fearless Organization: Creating Psychological Safety in the Workplace for Learning, Innovation and Growth. NJ: John Wiley& Sons.

[2] Yener S. (2014), Özel Ortaöğretim Kurumlarında Paylaşılan Liderlik Davranışı ve İştenAyrılma Niyeti Arasındaki İlişkide Psikolojik Güvenlik Algısının Aracı Değişken İlişkisinin Araştırılması, (Yayımlanmamış Doktora Tezi), Haliç Üniversitesi, İstanbul.

Performing Risk Analysis Evaluation in The Faculty of Dentistry

E. Urkan[1] and E. Senemtaşı Ünal[1]

[1]*Ağrı İbrahim Çeçen University, Ağrı, Türkiye, ORCID: 0009-0000-9552-9051, ORCID: 0000-0002-8530-9423*

In every type of business, there are various factors that adversely affect the health of employees to a greater or lesser extent. Due to these adverse conditions in workplaces, employees experience work accidents or contract occupational diseases (TMMOB, 2016). The healthcare sector, in particular, is one of the work areas that poses significant dangers and risks in terms of occupational health and safety. Employees in this sector are exposed to risks in many areas (biological, chemical, physical, ergonomic, psychosocial). According to research conducted in our country, these problems can reach significant proportions, and therefore, employees may face difficulties in performing their occupational duties (Saygun, 2012). Therefore, risk analysis is an important step in preventing or reducing damage proactively by identifying risks beforehand (Erdal, 2021). This study was conducted to determine the risks faced by employees in a dentistry faculty in their work environment. For this purpose, risk assessment was performed using the Fine Kinney risk method, one of the risk analysis methods. The Fine-Kinney method is a technique that ranks risks and hazards according to probability, severity, and frequency parameters, and describes the risk according to the result diagram (Özgür, 2013). Risk analysis was conducted in a total of 10 activity areas in the Dentistry Faculty, including Oral, Dental and Maxillofacial Surgery, Periodontology Operating Room, Pedodontics Department, Radiology Department, Restorative Dentistry, Endodontics Department, Orthodontics Department, First Examination Department, and Prosthodontics Department. According to the results of the risk analysis, a total of 638 risks were identified, including 71 insignificant risks, 233 potential risks, 189 significant risks, 102 substantial risks, and 43 intolerable risks. Measures and solutions to be taken in accordance with the legislation for these identified risks are presented.

References

[1] Erdal, Y. ve Özdemir, A. (2021). Diş Hekimliği Fakültesinin İş Sağlığı ve Güvenliği Açısından Analizi: Risk Değerlendirme Örneği. Uşak Üniversitesi Fen ve Doğa Bilimleri Dergisi, 5 (2), 137-156. DOI: 10.47137/usufedbid.924036.

[2] Özgür, M. (2013). Metal sektöründe risk analizi uygulaması. İzmir: Çalışma ve Sosyal Güvenlik Bakanlığı İş Teftiş Kurulu Başkanlığı.

[3] Saygun, M. (2012). Sağlık Çalışanlarında İş Sağlığı Ve Güvenliği Sorunları. TAF Preventive Medicine Bulletin, 11(4).

[4] TMMOB Makina Mühendisleri Odası, Oda Raporu (2018). İşçi sağlığı ve iş güvenliği. Ankara, Yayın No: Mmo/689, Isbn: 978-605-01-1183-5, 8. Baskı, 232.

Office Environments: Ergonomic Risks and Musculoskeletal Diseases

M.S. Ulusoy[1] and E. Senemtaşı Ünal[1]

[1]Ağrı İbrahim Çeçen University, Ağrı, Türkiye, ORCID: 0009-0007-0476-1973, ORCID: 0000-0002-8530-9423

With the advancement of technology, the widespread use of computers in every field, intensive use of accessories such as keyboards and mice, and the prevalence of mobile devices, factors have emerged that expose workers to various health problems in the hand, wrist, and arm regions. Especially considering that individuals working in office environments are required to work long hours at computers, it is evident that the dimensions of the health problems that may arise as a result of this exposure are quite serious. This study aims to identify the ergonomic risks and measures to be taken for possible musculoskeletal system diseases that employees may encounter in office environments. According to research, disorders such as carpal tunnel syndrome, tennis elbow, and tendinitis are among the frequently seen health problems. Especially in office environments where computer use is intensive, factors such as non-ergonomic work arrangements, incorrect sitting positions, and improper positioning of computer equipment increase the likelihood of employees encountering these health problems (Barr, Barbe & Clark, 2004; Kroemer and Robiette, 1968). Individuals with these health problems are more likely to experience loss of workforce, decreased work efficiency, and unwanted workloads and long-term rest needs in the workplace. Moreover, if these health problems are not treated, they can become chronic and lead to long-term loss of workforce. In this context, it is of great importance for office workers to develop effective strategies to minimize the risks to their hand, wrist, and arm health and to create a healthy and efficient working environment. Epidemiological and ergonomic analyses of hand, wrist, and arm diseases are critically important for understanding the risks faced by office workers. Therefore, it is seen that keyboard and mouse ergonomics in long-term computer use are a determining factor in the development of diseases such as carpal tunnel syndrome and wrist tendinitis.

References

[1] Barr, A. E., Barbe, M. F., & Clark, B. D. (2004). Work-related musculoskeletal disorders of the hand and wrist: epidemiology, pathophysiology, and sensorimotor changes. Journal of orthopaedic & sports physical therapy, 34(10), 610-627.

[2] Kroemer, K. E., & Robinette, J. C. (1968). Ergonomics in the design of office furniture: A review of European literature.

A Combined Biochemical and Bioinformatic Analysis of a New Subtilisin from Hyperthermophilic Archaeon Thermococcus Piezophilus

Ü.Z. Üreyen Esertaş[1]

[1]*Ağrı İbrahim Çeçen University, Faculty of Medicine Ağrı, Turkey, 0000-0001-9897-5313*

Subtilisin is a type of protease (an enzyme that digests proteins), initially derived from Bacillus subtilis. Subtilisins belong to the subtilase family and are widely used in both the detergent industry due to their ability to break down proteins at high temperatures and alkaline pH levels, and in biotechnological applications for protein engineering and synthesis [1]. Enzymes produced by hyperthermophiles, which are bacteria and archaea thriving at temperatures above 80°C, exhibit high thermal stability, maintaining their structure and function at elevated temperatures where others would denature. These hyperthermophilic enzymes perform optimally under high-temperature conditions, employing the same biochemical catalytic processes as their counterparts found in organisms that prefer moderate temperatures (mesophiles) [2]. In the current study, it has been aimed to produce a new hyperthermophilic subtilisin enzyme that can be used in several industry. For this purpose, after bioinformatics analysis, the specific gene (tpsub) from thermophilic archea Thermococcus piezophilus was determined. After codon optimization according to Escherichia coli, the gene will be constructed in pET28b+ plasmid and commercially synthesize. Biochemical characterization and usage for industrial applications potential will be determined as future experiment plans.

References

[1] Su, Y., Liu, C., Fang, H., & Zhang, D. (2020). Bacillus subtilis: a universal cell factory for industry, agriculture, biomaterials and medicine. Microbial cell factories, 19, 1-12.

[2] Vieille, C., & Zeikus, G. J. (2001). Hyperthermophilic enzymes: sources, uses, and molecular mechanisms for thermostability. Microbiology and molecular biology reviews, 65(1), 1-43.

In silico Screening and Heterologous Expression of a Polyethylene Terephthalate Hydrolase from Micromonospora inositola Involved in Plastic Biodegradation

E. Karataş[1]

[1]Ağrı İbrahim Çeçen University, Patnos Vocational School, Ağrı, Turkey, 0000-0001-6848-7618

Polyethylene terephthalate (PET), a quintessential polymer, exhibits noteworthy physicochemical attributes, including elevated durability and cost-effectiveness, rendering it indispensable across diverse industrial domains such as packaging (bottles), textile fibers, and containment solutions. The escalating reliance on plastics, particularly single-use items, has catalyzed interest in sustainable management approaches. Consequently, the advent of innovative technologies and methodologies for the treatment of plastic refuse is imperative to mitigate these challenges. The application of enzymatic hydrolysis for the degradation of synthetic polymers is posited as a potentially superior and ecologically benign alternative to the prevailing practices [2]. In the context of this study, the primary objective was to clone a novel gene encoding the Polyethylene Terephthalate Hydrolase (PETase) enzyme from Micromonospora inositola, characterized as a mesophilic bacterium that forms an aerial mycelium. To achieve this aim, bioinformatic analyses were conducted to elucidate the catalytic and structural attributes of the enzyme, facilitating the appropriate submission of the gene to the UniProt database. Following the processes of DNA isolation and gene cloning, the gene was successfully incorporated into the pET28a vector, and the resultant construct was transformed into Escherichia coli BL21(DE) cells. In subsequent stages, following the successful expression of the PETase enzyme, its biochemical characterization and potential for industrial applications will be assessed.

References

[1] Yang, S. B., Yoo, Y. J., Kim, E. S., & Choi, S. (2022). Heterologous Expression of Streptomyces PETase Gene Involved in PET Biodegradation.

[2] Almeida, E. L., Carrillo Rincón, A. F., Jackson, S. A., & Dobson, A. D. (2019). In silico screening and heterologous expression of a polyethylene terephthalate hydrolase (PETase)-like enzyme (SM14est) with polycaprolactone (PCL)-degrading activity, from the marine sponge-derived strain Streptomyces sp. SM14. Frontiers in Microbiology, 10, 476617.

Synthesis of Novel 2-arylidene-2,3-dihydro-1H-inden-1-amine Compounds

K. Aksu[1]

[1]Ordu University Faculty of Science and Arts, Department of Chemistry, Ordu, Turkey, ORCID: 0000-0002-2729-2168

Chalcone is a naturally occurring chemical compound that belongs to the flavonoid family. It has gained significant attention due to its diverse pharmacological properties. Chalcones and their derivatives possess a wide range of pharmacological properties due to the presence of a reactive α,β-unsaturated carbonyl group. These properties include antiproliferative, antifungal, antibacterial, antiviral, antileishmanial, and antimalarial effects [1]. Benzylamines are useful organic compounds with important biological activities in the central nervous system [2]. Aminoindanes are bicyclic aromatic amines that have garnered significant attention in medicinal chemistry and neuroscience due to their structural similarity to neurotransmitters like dopamine and serotonin. For example, indatralin is a non-selective monoamine transporter inhibitor that has been reported to block the reuptake of dopamine, norepinephrine, and serotonin, showing similar effects to cocaine. These compounds display a range of pharmacological activities, such as modulation of dopamine and serotonin, making them a valuable foundation for designing new psychoactive agents [3]. Due to the aforementioned properties, this study aimed to synthesise two different novel 2-arylidene-2,3-dihydro-1H-inden-1-amine compounds obtained from suitable chalcone derivatives which are considered to display various bioactivities.

References

[1] N. A. A. Elkanzi, H. Hrichi, R. A. Alolayan, W. Derafa, F. M. Zahou, and R. B. Bakr, "Synthesis of Chalcones Derivatives and Their Biological Activities: A Review," *ACS Omega*, vol. 7, no. 32. American Chemical Society, pp. 27769–27786, Aug. 16, 2022. doi: 10.1021/acsomega.2c01779.

[2] M. B. H. Youdim, M. Fridkin, and H. Zheng, "Bifunctional drug derivatives of MAO-B inhibitor rasagiline and iron chelator VK-28 as a more effective approach to treatment of brain ageing and ageing neurodegenerative diseases," in *Mechanisms of Ageing and Development*, Feb. 2005, pp. 317–326. doi: 10.1016/j.mad.2004.08.023.

[3] Y. S. Cho *et al.*, "Antidepressant indatraline induces autophagy and inhibits restenosis via suppression of mTOR/S6 kinase signaling pathway," *Sci Rep*, vol. 6, Oct. 2016, doi: 10.1038/srep34655.

The inhibition Effect of Some Piperidine Derivatives on Acetylcholinesterase Enzyme

N. Balcı[1] and İ. Gülçin[2]

[1]Gümüşhane University Şiran Dursun Keleş Health Services Vocational School, 29100-Gümüşhane, Turkey, ORCİD: 0000-0002-1798-5550
[2]Atatürk University, Faculty of Science, 25240-Erzurum, Turkey, ORCİD:0000-0001-5993-1668

Falling levels of neurotransmitter acetylcholine are linked to symptoms of Alzheimer's disease. Acetylcholine (ACh), released by nerve endings, controls muscle contraction when it binds to receptors. The acetylcholinesterase (AChE) controls ACh levels by breaking it down [1]. AChE inhibitors are essential in the biochemical processes of the human body, notably in the brain. They stop AChE enzyme breaking down acetylcholine, increasing availability [2].

Piperidine ring, a nitrogen-bearing heterocyclic compound, is a natural product and is found almost everywhere (Figure 1).
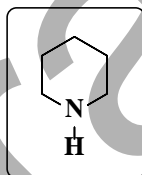
Figure 1. Piperidine moiety

Piperidine scaffold has great biological activities and plays important roles in metabolism [3]. Piperidine and its derivatives like alogliptin, ritalin, and risperidone are current drugs containing the piperidine moiety that reduce schizophrenia in children and treat diabetes [4]. Also, Donepezil is a piperidine derivative used in the treatment of Alzheimer's disease [1]. Besides, piperidine core is used in various therapeutic agents such as anti-rheumatic, antihistaminic, anticancer, anti-inflammatory, antimicrobial, and analgesic drugs. Piperidine and its derivatives include the heterocyclic moiety commonly found in FDA-approved drugs [6]. This study investigates the effects of some piperidine derivatives on AChE enzymes as in vitro. AChE activity was realized according to the Ellman's method [7]. AChE activity (%)-[Piperidine derivatives] graphs were drawn, and IC_{50} was calculated from this graphs. Inhibition type and K_i values were determined from the Lineweaver-Burk graphs [8]. The IC_{50} values were calculated as 0.0136, 0.081 and 0.0079 µM for 4-amino-1 –benzyl piperidine, 4-aminopiperidine and ethyl-4-amino carboxy piperidine, respectively. On the other hand, K_i values from Lineweaver-Burk graphs were calculated as 0.0126 ±0.0002, 0.045±0.011 and 0.0049±0.0014 µM for 4-amino-1-benzyl piperidine, 4-aminopiperidine and ethyl-4-amino carboxy piperidine, respectively. All of the compounds showed competitive inhibition.

References

[1] H. Akıncıoğlu, İ. Gülçin, 2020. Potent acetylcholinesterase inhibitors: Potential drugs for Alzheimer's disease. Mini Reviews in Med. Chem., 20(8), 703-715.

[2] M.O. Karaytuğ, N. Balcı, F. Türkan, M. Gürbüz, M.E. Demirkol, Z. Namlı, İ. Gülçin, 2023. Piperazine derivatives with potent drug moiety as efficient acetylcholinesterase, butyrylcholinesterase, and glutathione S-transferase inhibitors. J. Biochem. Mol. Toxicol., 37.2:23259.

[3] S. Das, G. Brahmachari, 2013. Ni (ClO$_4$).6H$_2$O: An efficient catalyst for one-pot synthesis of densely functionalized piperidine scaffolds via multicomponent reaction in ethanol at room temperature. Org. Biomol. Chem., 1, 33-46.

[4] R. Aeluri, M. Alla., V.R. Bommena, R. Murthy, N. Jain, 2012. Synthesis and Antiproliferative Activity of Polysubstituted Tetrahydropyridine and Piperidin-4-one-3-carboxylate Derivatives. Asian J. Organic Chem. 1:71-79.

[5] M. M., Abdelshaheed, I. M Fawzy, H. I. El-Subbagh, K. M. Youssef, 2021. Piperidine nucleus in the field of drug discovery. Future J. Pharm. Sci. 7, 1-11.

[6] E. Vitaku, D.T. Smith, J.T. Njardarson, 2014. Analysis of the structural diversity, substitution patterns, and frequency of nitrogen heterocycles among U.S. FDA approved pharmaceuticals. J Med Chem 57, 10257–10274.

[7] G. L. Ellman, K.D. Courtney, V. Andres Jr, R.M. Featherstone, 1961. A new and rapid colorimetric determination of acetylcholinesterase activity. Biochem. Pharmacol, 7(2), 88-95.

[8] H. Lineweaver, D. Burk, 1934. The determination of enzyme dissociation constants. J. Am. Chem. Soc. 56(3), 658-666.

Gastric Ulcer

B. Öztürk Karagöz

[1]Ağrı İbrahim Çeçen University School of Medicine, Department of Internal Medical Sciences, Department of Medical Pharmacology, Ağrı, Türkiye, ORCID: 0000-0001-7187-1557

Peptic ulcer has two subtypes: duodenal and gastric ulcers. Gastric ulcer is one of the digestive system diseases that affects approximately 5-10% of people worldwide [1] and has serious complications, often recurrent and life-threatening [2]. Gastric ulcer is caused by long-term smoking [3], continuous use of non-steroidal anti-inflammatory drugs, excessive production of hydrochloric acid and pepsin, helicobacter pylori infection, and genetic predisposition (endogenous aggressive factors). Mucin, bicarbonate, antioxidants, prostaglandins, nitric oxide, and growth factors (endogenous defence factors) form a defence line to prevent gastric ulcer [1]. An imbalance between these two factor groups leads to the disruption of the mucosal protective barrier, resulting in stomach ulcers [1, 4]. In addition, advancing age [5], an unbalanced diet, the consumption of spicy foods and acidic drinks, and long-term alcohol use may also contribute to gastric mucosal damage and stomach ulcers [3]. The diagnosis and treatment of stomach ulcers vary depending on the patient and the course of the disease. Stomach ulcer treatment strategies include administration of various drugs, such as antacids, anticholinergic drugs, proton pump inhibitors, and histamine H2 receptor antagonists [6]. Proton pump inhibitors are the primary treatment for stomach ulcers. It is imperative to increase the pH level of the stomach to heal the gastric mucosa. If a patient is diagnosed with a Helicobacter pylori infection, it is essential to undergo antibiotic treatment [7]. This review has been prepared mostly based on studies conducted in the last 10 years and aims to bring together up to date knowledge on gastric ulcer formation, known possible mechanisms and treatment strategies, and to provide compiled and updated information to researchers.

References

[1]. Aman, R.M., R.A. Zaghloul, and M.S. El-Dahhan, Formulation, optimization and characterization of allantoin-loaded chitosan nanoparticles to alleviate ethanol-induced gastric ulcer: in-vitro and in-vivo studies. Sci Rep, 2021. 11(1): p. 2216.

[2]. Li, H., A. Zhao, R. Xu, et al., A Meta-Analysis of the Prevalence of Peptic Ulcer in Chinese Adults. 2022.

[3]. Li, A., Progress of Research on the Effect of Dietary Care on Patients with Gastritis and Gastric Ulcers. Journal of Clinical and Nursing Research, 2024. 8(2): p. 201-205.

[4]. Huang, Z., Y. Shi, H. Wang, et al., Protective Effects of Chitosan-Bilirubin Nanoparticles Against Ethanol-Induced Gastric Ulcers. Int J Nanomedicine, 2021. 16: p. 8235-8250.

[5]. Kavitt, R.T., A.M. Lipowska, A. Anyane-Yeboa, et al., Diagnosis and Treatment of Peptic Ulcer Disease. Am J Med, 2019. 132(4): p. 447-456.

[6]. Anter, H.M., H. Abu, II, W. Awadin, et al., Novel chitosan oligosaccharide-based nanoparticles for gastric mucosal administration of the phytochemical "apocynin". Int J Nanomedicine, 2019. 14: p. 4911-4929.

[7]. Majumdar, D. and S. Looi, Helicobacter pylori infection and peptic ulcers. Medicine, 2024.

A Molecular Docking Study on the Methylene Blue Toxicity

Y. Gülşahin[1], İ. Çolak[2], G. Karadayı[3], E. Güllüce[4], M. Karadayı[5] and M. Güllüce[6]

[1]Atatürk University, Graduate School of Natural and Applied Sciences, Erzurum, Türkiye, ORCID: 0000-0002-3770-2116, ORCID: 0000-0002-3500-260X, ORCID: 0000-0003-2290-3799
[3]Atatürk University, Department of Molecular Biology and Genetic, Erzurum, Türkiye, ORCID: 0000-0003-2044-9609
[5]Atatürk University, Department of Biology, Erzurum, Türkiye, ORCID: 0000-0002-2473-0409, ORCID 0000-0002-5957-8259

Methylene blue is a synthetic thiazine dye that is easily soluble in water. Due to its easy water solubility and chemical stability, the range of uses of methylene blue extends from use in the textile, pharmaceutical, paper, dyeing, printing and dye industries to its use as a therapeutic agent [1]. However, methylene blue is an environmental pollutant that accumulates in nature along with industrial wastes. It is also known to be highly toxic to living things, depending on the exposure dose [2]. Since there are limited studies on the mechanisms of methylene blue toxicity in the literature, both experimental and bioinformatic studies are needed to elucidate these mechanisms. For this reason, our current study aimed to determine the relationship between methylene blue and DNA and very-long-chain fatty acid (VLCFA) synthesizing proteins using molecular docking. For this purpose, research has been conducted on the mechanism of action of methylene blue using the molecular docking approach. For molecular docking, 3D molecular structures of DNA and the target proteins involved in VLCFA pathways were obtained from RCSB Protein Data Bank (PDB IDs: 1BNA,1I01, 1HND, 4JQC and 6N3P). They were further processed to prepare for docking studies by using AutoDockTools (ver. 1.5.7). The structure of methylene blue was obtained from Drugbank Database (DB09241). The structure minimization of the ligand was done by using UCSF Chimera (ver. 1.17.3) and the preparation step was finished by AutoDockTools. Finally, docking studies were performed by AutodockVina and visualized by BIOVIA Discovery Studio Visualizer (ver 24.1.0). According to molecular docking analysis, the best scores for a high binding affinity of methylene blue to target receptors are B-DNA (-7.1 kcal/mol), Beta-Ketoacyl-Acp Synthase III (-6.6 kcal/mol), Beta-Ketoacyl [ACP] Reductase (-7.9 kcal/mol), (D) Enoyl-(Acyl-Carrier-Protein) Reductase (-8.2 kcal/mol) and 3-Hydroxyacyl-(Acyl-Carrier-Protein) Dehydratase (-8.0 kcal/mol). As a result, molecular mechanisms of the toxicity were shown for the target receptors by using molecular docking approach for the first time. The results of this study are valuable in understanding the mechanism of action of methylene blue on VLCFA synthesis and DNA. It will also shed light on future studies in the development of alternative solutions against toxicity.

References

[1]   I. Khan, K. Saeed, I. Zekker, B. Zhang, A.H. Hendi, A. Ahmad, S. Ahmad, N. Zada, H. Ahmad, L.A. Shah 2022. Review on Methylene Blue: Its Properties, Uses, Toxicity and Photodegradation, Water. 14(2) (2022) 242.

[2]   E.B. Santoso, R. Ediati, Y. Kusumawati, H. Bahruji, D.O. Sulistiono, D. Prasetyoko 2020. Review on recent advances of carbon based adsorbent for methylene blue removal from waste water, Materials Today Chemistry. 16 (2020).

Parietin Protects Against H_2O_2-induced Oxidative Stress Damage in Erythrocytes.

Y. Karagöz[1], M. Genişel[2] and N. Uzun[3]

[1]Ağrı İbrahim ÇeÇen University, Faculty of Pharmacy, Department of Pharmaceutical Botany, Ağrı, Türkiye, https://orcid.org/0000-0002-4835-4508; https://orcid.org/0000-0002-9339-9334
[2]Ağrı İbrahim Çeçen University Faculty of Pharmacy, Department of Clinical Pharmacy, Ağrı, Türkiye https://orcid.org/0000-0002-9763-7643

In this study, we collected the lichen Xanthoria elegans within the borders of Ağrı province and isolated parietin from this lichen. Characterization of parietin was carried out according to literature [1] using standardized TLC in three standard solutions and determination of melting point. We examined parietin's impact on oxidative damage in erythrocytes through examination of malondialdehyde (MDA) levels, hemolysis, superoxide dismutase (SOD) activity, catalase (CAT) activity, glutathione (GSH) levels [2-4]. We also examined morphological features of erythrocytes under microscope. Ascorbic acid (AA) was used as positive control. Our findings suggest that 10 and 50 mM parietin reduced the MDA level in the oxidative damage process caused by H2O2 and this effect was statistically equivalent to AA. Parietin reduced the percentage of hemolysis, and prevented the deformities that occur in erythrocytes. It also brought about a statistically significant increase in SOD activity, statistically in the same band as AA. GSH content did not change significantly. We observed a similar stability in CAT activity. These two observations suggest that parietin protected cellular GSH content, probably through direct interaction with H2O2. When used at a concentration of 100 mM, parietin did not produce desirable results. The data obtained from this experiment puts Xanthoria elegans and parietin forward as sources of antioxidant biomolecules and activities.

References

[1] Huneck, S. and I. Yoshimura, *Identification of lichen substances*. 1996, Berlin ; New York: Springer. xi, 493 p.

[2] Beauchamp, C. and I. Fridovich, *Superoxide dismutase: improved assays and an assay applicable to acrylamide gels*. Anal Biochem, 1971. **44**(1): p. 276-87.

[3] Chang, D., et al., *Serum antioxidative enzymes levels and oxidative stress products in age-related cataract patients*. Oxid Med Cell Longev, 2013. **2013**: p. 587826.

[4] Liu, H., H. Ding, and G. Hou, *Quercetin inhibits hydroperoxide-induced peroxidation of human red blood cells*. Journal of Guangdong Medical College, 2003. **20**(4): p. 317-318.

Characterization of Mn-Doped MgO Thin Films Produced via Successive Ionic Layer Adsorption Reaction Method

A. Taşer

[1]*Ağrı İbrahim Çeçen University, Patnos Vocational School, Ağrı, Turkey, 0000-0003-4563-160X*

Metal oxide semiconductors are crucial materials in various fields such as electronics, optoelectronics, and energy applications. These materials are preferred for their high electrical conductivity, optical transparency, and chemical stability. Among these semiconductors, metal oxides like zinc oxide (ZnO), titanium dioxide (TiO_2), and magnesium oxide (MgO) are particularly noteworthy. Metal oxide semiconductors typically possess wide band gaps, making them suitable for applications such as solar cells and photocatalysts. Moreover, these materials are resistant to high temperatures and corrosive environments, hence they are widely used in applications like sensors and protective coatings [1].

MgO stands out among metal oxide semiconductors due to its high dielectric constant, excellent thermal conductivity, and high chemical stability [4]. MgO thin films can be produced by various methods such as Physical Vapor Deposition (PVD), Chemical Vapor Deposition (CVD), Sol-Gel, and Successive Ionic Layer Adsorption and Reaction (SILAR). Each method offers different advantages for controlling properties of the film like thickness, morphology, and crystallinity. For instance, the SILAR method is known for its low cost and ease of application [2].

This study presents the fabrication of magnesium oxide (MgO) nanostructures, both with and without manganese (Mn) doping, utilizing the SILAR technique. Comprehensive characterization was carried out employing an array of analytical methods, including ultraviolet-visible (UV-vis) spectroscopy, X-ray diffraction (XRD) and scanning electron microscopy (SEM), These results underscore the effectiveness of the SILAR method for Mn doping of MgO thin films and highlight the potential of Mn-modified MgO nanostructures in enhancing the performance of optoelectronic devices.

References

[1] Güney, H., & İskenderoğlu, D. (2018). Synthesis of MgO thin films grown by SILAR technique. Ceramics International, 44(7), 7788-7793.

[2] Talukdar, T. K., Liu, S., Zhang, Z., Harwath, F., Girolami, G. S., & Abelson, J. R. (2018). Conformal MgO film grown at high rate at low temperature by forward-directed chemical vapor deposition. Journal of Vacuum Science & Technology A, 36(5).

Investigation of Nuclear Radiation Shielding Properties of Glass/Al/WS₂ Composites Produced by RF Sputtering Method

U. Perişanoğlu[1,2*]

[1]*Hakkari University, Hakkari, Turkey, ORCID: 0000-0003-4110-2241*
[2]*Ataturk University, Erzurum, Turkey, ORCID: 0000-0003-4110-2241*

In this study, aluminum (Al) and tungsten disulfide (WS2) were grown on conventional glass by RF Sputtering Method at different growth times. The samples obtained after this process were evaluated for their nuclear radiation shielding properties due to their superior surface properties, chemical resistance, heat resistance and higher density than the base material. Aluminum is a widely used material in radiation shielding, especially due to its light weight and high strength. Tungsten is effective element for absorbing radiation due to its high density. For this purpose, transmission measurements were performed for the samples produced using an Ultra Ge detector and a Ba-133 radioactive source emitting photons in the 81-383 keV energy range. The mass attenuation coefficients (MAC) of the samples were obtained by evaluating the spectra. Subsequently, other gamma shielding parameters were derived from the MAC values. Equivalent neutron dose reduction percentages and effective removal cross sections of the samples were also found. The sample grown with 10 min Al and 5 min WS2 was found to be the best radiation attenuator. In general, the findings of this study will contribute to the radiation shielding materials literature by increasing the effectiveness of the material with a new synthesis approach.

Investigation of Gamma Radiation Attenuation Properties of Tungsten and Molybdenum High-Speed Steels

V. Sola[1], B. Aygün[2], Y. Özdemir[3]

[1]Department of Motor Vehicles and Transportation Technologies, Horasan Vocational School, Atatürk University, Erzurum, Turkey ORCID: 0000-0002-7117-5719
[2]Department of Electronics and Automation, Vocational School, Agri Ibrahim Cecen University, Agri, Turkey
[3]Department of Physics, Faculty of Science, Atatürk University, Erzurum, Turkey

Ionizing radiation has adverse effects that can extend to the extent of causing cancer in human health. Taking necessary safety measures and controlling this radiation during its use provides significant conveniences to humans in nuclear medicine, electricity generation, industry, and various research fields. The IAEA develops and implements various safety standards to minimize the potential health effects of leaks that may occur during work for this purpose. In this study, the gamma radiation absorption properties of the most commonly used tungsten and molybdenum high-speed steels were determined theoretically. For this purpose, important shielding parameters such as linear attenuation coefficients (LAC), mass attenuation coefficients (MAC), half-value layer (HVL), and mean free path (MFP) were calculated using WinXCom. It was observed that increasing the tungsten content in the steels enhances their ability to absorb gamma radiation. Accordingly, it was determined that Tungsten (18-4-1) steel could be used as a protective material against gamma radiation in nuclear medicine, radioactive waste storage facilities, and nuclear power plants where gamma radiation is prevalent.

Impact of Feature Selection on Energy Forecasting Machine Learning Models

E. Arslan[1], E. Karayürek[2], Z.O. Yüksek[3] and Ş. Koyun Yılmaz[4]

[1]Metric Software and Consulting, İstanbul, Türkiye, ORCID: 0000-0002-1812-1236, ORCID: 0009-0005-6918-6725, ORCID: 0009-0005-0508-3874, ORCID: 0000-0002-2589-3568

Today, we live in an energy-dependent world. The COVID-19 pandemic illustrated the importance of energy security for the manufacturing industry. Securing the energy resources for production has further implications than facility shutdowns. It affects operational and environmental costs and eventually affects local and global economies. Forecasting energy consumption is crucial for production operations from budget planning to production planning. Given the impact on production operations and environmental costs, the need for models that accurately predict energy consumption is evident. Studies show that data-driven forecasting models focus mostly on time-series analysis, some with additional features. Machine learning models perform subpar to the conventional models such as linear regression for the time-series analysis approach. When additional features such as weather or indoor conditions of a building are accounted for, the accuracy of conventional models decreases. Additional features increase the non-linearity of the problem, making machine learning models perform better. Increasing the number of features may increase the forecast accuracy, but it comes with pitfalls. Features should be engineered carefully to avoid these pitfalls e.g. increased model complexity, a longer time for computing, and increased data storage costs. In this study, we investigate possible features for energy consumption forecast models while comparing their contribution to model performance.

References

[1] S.-Y. Shin, H.-G. Woo, 2022. Energy Consumption Forecasting in Korea Using Machine Learning Algorithms, Energies 15 (13) 4880.

[2] A. González-Briones, G. Hernández, J. M. Corchado, S. Omatu, M. S. Mohamad, 2019. Machine Learning Models for Electricity Consumption Forecasting: A Review, 2nd International Conference on Computer Applications & Informations Security (ICCAIS)., 1-6.

[3] N. Wei, C. Li, X. Peng, F. Zeng, X. Lu, 2019. Conventional Models and Artificial Intelligence-Based Models for Energy Consumption Forecasting: A Review, J. of Petroleum Sci. And Eng. 181 (2019) 106187.

[4] M. Bourdeau, X.G. Zhai, E. Nefzaoui, X. Guo, P. Chatellier, 2019. Modeling and Forecasting Building Energy Consumption: A Review of Data-Driven Techniques, Sustainable Cities and Society 48 (2019) 101533.

[5] M.A.M. daut, M.Y. Hassan, H. Abdullah, H.A. Rahman, M.P. Abdullah, F. Hussin, 2017. Building Electrical Energy Consumption Forecasting Analysis Using Conventional and Artificial Intelligence Methods: A Review, Renewable and Sustainable Energy Reviews 70 (2017) 1108-118.

Serum Albumin Synthesis of Modified Jujube (Zizyphus jujuba) Quantum Dot and Determination of Its Effect on Various Cancer Cells

M.N. Canbolat[1], E. Taşğın[2], H. Nadaroğlu[3], and A. Babagil[4]

[1]Department of Nano-Science and Nano-Engineering, Institute of Science and Technology, Ataturk University, 25240 Erzurum, Turkey
[2]Faculty of Health Sciences, Atatürk University, Erzurum, Türkiye, ORCID: 0000-0001-5292-8992,
[3]Erzurum Vocational School of Technical Sciences, Atatürk University, Erzurum, Türkiye,
ORCID: 0000-0002-0536-4212

In recent years, research conducted with complementary therapy approaches has mainly focused on the use of plant-derived compounds with anti-cancer properties in cancer treatment, with particular emphasis on green synthesis methodologies involving quantum dots (QDs) [1,2]. In the green synthesis method where carbon quantum dots (CQDs) are obtained within the scope of nanotechnological methods, nanoparticles are synthesized by using natural resources because they are economical, environmentally friendly, non-toxic and have high biocompatibility. They are also used as auxiliary agents in cancer treatment [3,4].

In this research, it was aimed to obtain quantum dots from Jujube (Zizyphus jujuba) fruit, which has high antioxidant capacity, by hydrothermal green synthesis method, to increase their effectiveness by using them together with albumin, an important carrier protein in metabolism, and to determine their effectiveness on cells by applying them to healthy and some cancer cell lines.

Characterizations of the synthesized CQDs were performed using the transmission electron microscopy (TEM), Fourier Transform Infrared Spectroscopy (FT-IR) and X-Ray diffraction analysis (XRD) methods. CQDs obtained using jujube fruit and CQDs modified with albumin were applied to quantum dots HeLa (human cervical cancer), A549 (non-small cell lung cancer) and HDF (human dermal fibroblast/healthy cell lines cell lines, and their entry into the cells was monitored and their cytotoxic effects were determined. MTT assay was used as a viability assay to evaluate the in vitro activities of the synthesized compounds.

Additionally, cupric ion reducing antioxidant capacity (CUPRAC) determination, iron (Fe3+) ion reducing antioxidant power (FRAP) determination and 1,1-diphenyl-2-picrylhydrazil (DPPH) free radical scavenging analyzes were performed for the antioxidant activities of the synthesized quantum dots.

In conclusion, this study shows that CQDs from Jujube fruit extract were successfully synthesized by green synthesis approach. Modification of these CQDs with albumin has been shown to increase their antioxidant capacity and be effective against both healthy and cancerous cells. These findings highlight the potential of CQDs from Jujube fruit as effective agents in biomedical applications, especially in cancer treatment. This study

highlights that future research may be an alternative approach to increasing the effectiveness of drugs administered through CQDs and using them in cancer treatments.

References

[1] J. Fathalizadeh, V. Bagheri, H. Khorramdelazad, M.K. Arababadi, A. Jafarzadeh, M. Mirzaei, 2015. Induction of apoptosis by pistachio (pistacia vera l.) hull extract and its molecular mechanisms of action in human hepatoma cell line HepG2, Cell Mol. Biol. 61(7) (2015)128-34.

[2] K. Atacan, G. Nuray, A. Azize, H. Nadaroğlu, 2023. Novel green synthesis of Ag2S from Diospyros kaki and its application for efficient photocatalytic hydrogen evolution, Molecular Cat. 544 (2023) 113140.

[3] J. Chang, B. Yu, W.M. Saltzman, M. Girardi, 2023. Nanoparticles as a therapeutic delivery system for skin cancer prevention and treatment. JID Innovations. 3(4) 2023 100197.

[4] M.R. Abedini, N. Erfanian, H. Nazem, S. Jamali, R. Hoshyar, 2016. Anti-proliferative and apoptotic effects of Ziziphus Jujube on cervical and breast cancer cell, AJP. 6(2) (2016) 142.

Effects of Metformin on Human GSK3β Gene Expression in Fission Yeast

M. Yilmazer[1], M. Gokcay[2], S. Canbazoglu[3], C. Akkulah[4] and S. Karaer Uzuner[5]

[1] *Istanbul University, Faculty of Science, Department of Molecular Biology and Genetics, Istanbul, Türkiye,*
ORCID: 0000-0003-4382-3763, ORCID: 0009-0002-3457-1031, ORCID: 0009-0007-8489-1371
ORCID: 0009-0005-1284-669X, ORCID: 0000-0002-2914-7431

Glycogen synthase kinase-3β (GSK-3β) was discovered as a kinase that phosphorylates glycogen synthase, but it plays a role in many cellular processes including glucose metabolism, intracellular signal transduction, and cell division [1]. GSK-3β is very effective in glucose metabolism and is known to interact with the insulin hormone, which regulates blood sugar by taking glucose into the cell [2,3]. Increased activity of GSK-3β can cause metabolic disorders such as glucose intolerance [1]. This case indicates the importance of the regulatory role of GSK-3β on glucose metabolism for a healthy metabolism. Metformin, which has a glucose level-lowering effect, is used in the early-stage treatment of type 2 diabetes [4]. Fission yeast, Schizosaccharomyces pombe (S. pombe), a single-celled eukaryotic model organism, is preferred in research to understand mammalian cellular processes [5]. In this study, metformin was treated to S. pombe cells heterologously expressing the human GSK3β gene [6], and the gene expression levels of hxk2, fbp1, and GSK3β, which play a role in glucose metabolism, were analyzed in comparison with the control group. The presence of metformin caused alterations in gene expression profile in cells.

Keywords: Human GSK3β gene, glycogen synthase kinase 3, diabetes, metformin, fission yeast.

References

[1] L. Wang, J. Li, L.J. Di, 2021. Glycogen synthesis and beyond, a comprehensive review of GSK3 as a key regulator of metabolic pathways and a therapeutic target for treating metabolic diseases, Med. Res. Rev. 42(2) 946-982.

[2] A. Ullah, N. Ali, S. Ahmad, S.U. Rahman, S. Alghamdi, A.M. Bannunah, ... M.U.K. Sahibzada, 2021. Glycogen synthase kinase-3 (GSK-3) a magic enzyme: it's role in diabetes mellitus and glucose homeostasis, interactions with fluroquionlones. A mini-review, Braz. J. Biol. 83, e250179.

[3]   D.M. Teli, A.K. Gajjar, 2023. Glycogen Synthase Kinase-3: A Potential Target for Diabetes, Bioorg. Med. Chem. 117406.

[4]   T.E. LaMoia, G.I. Shulman, 2021. Cellular and molecular mechanisms of metformin action, Endocr. Rev. 42(1), 77-96.

[5]   J. Hayles, P. Nurse, 2018. Introduction to fission yeast as a model system. Cold Spring Harb. Protoc. 2018(5), pdb-top079749.

[6]   M. Yılmazer, S.K. Uzuner, 2024. Effects of Glucose on the Cellular Respiration in Fission Yeast Expressing Human GSK3B Gene, Trak. Univ. J. Nat. Sci. 25(1).

Draft

Effect of Proton Pump Inhibitors (PPI) on The Tissues

S.N. Parlak

Ağrı İbrahim Çeçen University School of Medicine, Basic Medical Sciences, Department of Histology and Embryology, Ağrı, Türkiye, ORCID: 0000-0001-9577-986X

The stomach is a tubular organ located in the upper left part of the abdominal cavity, between the esophagus and duodenum. The pepsin enzyme, which plays a role in the digestion of proteins, becomes active in the stomach when pH is 3 and below 3 [1]. Strong acidic environment in the stomach is a physiological necessity for effective digestion.

Parietal cells are pyramidal-shaped, acidophilic-staining cells located in the crypts of the gastric mucosa epithelium. These cells synthesize stomach acid (HCl) through proton pumps in their membranes. They lower the pH level in the stomach with the HCl they synthesize. They increase the effectiveness of digestive enzymes in and prevent the entry of pathogens to stomach [2].

Proton Pump Inhibitors (PPI) are a group of medications used to suppress stomach acid long-term [3]. It contains chemicals ending in 'prazole'. PPI group drugs suppress stomach acid by inhibiting proton pumps in the membrane of parietal cells, but proton pumps are not only found in the membrane of parietal cells of the stomach. There are also proton pumps in mitochondria, which are found in every cell of the body. The proton pumps in mitochondria create an electrical potential, enabling the production of ATP energy molecules from carbohydrates and fats through aerobic respiration [4]. If the functions of proton pumps are blocked by PPI, cells cannot obtain sufficient energy. In this case, oxygen-free breathing is used to obtain energy. Since the efficient way of obtaining energy in other cells of the body will be blocked, this can lead to many health problems. Although PPI is said to be specific to the proton pump in gastric parietal cells, studies show that it also has effects on cells outside the stomach [5,6]. Due to their chemical structure, these drugs can also bind to proton pumps in other cells. PPIs form irreversible bonds with proton pumps.

This review aims to provide up-to-date information on the effects of PPI drug use on tissues such as stomach, intestines, bones, vessels and brain.

References

[1]. Hsu M, Safadi AO, Lui F. Physiology, stomach. StatPearls [Internet]: StatPearls Publishing; 2023.

[2]. Smith, J. L. 2003. ''The role of gastric acid in preventing foodborne disease and how bacteria overcome acid conditions'', Journal of food protection, 66(7), 1292-1303.

[3]. Ali T, Roberts DN, Tierney WM. Long-term safety concerns with proton pump inhibitors. The American journal of medicine. 2009;122(10):896-903.Kavitt, R.T., A.M. Lipowska, A. Anyane-Yeboa, et al., Diagnosis and Treatment of Peptic Ulcer Disease. Am J Med, 2019. 132(4): p. 447-456.

[4]. Schultz, B. E., & Chan, S. I. 2001. ''Structures and proton-pumping strategies of mitochondrial respiratory enzymes'', Annual review of biophysics and biomolecular structure, 30(1), 23-65.

[5]. Moayyedi, P., Leontiadis, G. I. 2012. ''The risks of PPI therapy'', Nature reviews Gastroenterology & hepatology, 9(3), 132-139.

[6]. Novotny, M., Klimova, B., & Valis, M. 2019. ''PPI long term use: risk of neurological adverse events? '', Frontiers in Neurology, 9, 1142.

Investigation of the Inhibition Effect of Some Indole Derivative Molecules on hCA-I and hCA-II Isoenzymes

G. Oktay[1], H.Akıncıoğlu[2]

[1]Agri İbrahim Çeçen University, Midwifery Department, Faculty of Health Sciences Agri, Turkey,
[2]Agri İbrahim Çeçen University, Faculty of Arts and Science, Department of Chemistry Agri, Turkey,
ORCİD: 0000-0001-5453-0953

Enzymatic or non-enzymatic antioxidants present in metabolism try to prevent the destruction caused by oxidative damage through various mechanisms. Indole-3-carbinol (I3C) and 3-3' Diindolylmethane (DIM) molecules that we will use in the study are found in cardamom, broccoli, zucchini and cauliflower and have high antioxidant and anticancer activity [1]. Carbonic anhydrase family (CA, EC 4.2.1.1), which contains zinc and is a metalloenzyme, catalyzes the reversible reaction that provides the conversion between carbon dioxide and bicarbonate ion. This reaction is associated with many physiological diseases, especially tumorigenesis, glaucoma and diabetes [2]. Within the scope of the study, hCAI-II isoenzymes were first purified by Sepharose-4B-L-Tyrosine affinity column chromatography. Then, the inhibition effect of I3C and DIM molecules on hCA-I and hCA-II isoenzymes was investigated by the esterase method [2]. By evaluating the results, IC50 and Ki values of the molecules were calculated for each enzyme.The results are given in Table 1.

	hCA-I			hCA-II		
	IC_{50} (µM)	R^2	K_i (µM)	IC_{50} (µM)	R^2	K_i (µM)
I3C	175,97	0,9091	115,21±23,13	238,39	0,9882	427,05±294,33
DİM	14,648	0,8524	16,04±2,31	426,9	0,926	261,66±128,6
(AZA)*	67,9	0,9689	39,6±20,8	160,30	0,8102	122,50±47,71

Table 1. IC_{50} and K_i results for I3C and DIM molecules   *:nM

AZA was used as a positive control for isoenzymes in the studies. It is considered by us that inhibitory potential of molecules could be guiding in other scientific studies and especially in the field of new drug design.

Keywords: DİM, IC3 ,hCA-I and hCA-II

References

[1] İ. Binici, E. E., Akıncıoğlu, H., & Kılınç, N. (2023). Indole-3-carbinol (I3C): Inhibition Effect on Monoamine Oxidase A (MAO-A), Monoamine Oxidase B (MAO-B) and Cholinesterase Enzymes, Antioxidant Capacity and Molecular Docking Study. *ChemistrySelect*, *8*(33),

[2] A Orhan, F., & Akincioglu, H. (2020). Determination of carbonic anhydrase enzyme activity in halophilic/halotolerant bacteria. *Applied Soil Ecology*, *155*, 103650.

Isolation and Characterization of ACC Deaminase Producing Endophytic Pantoea ssp. from Origanum vulgare L. ssp. vulgare

Y. Dil [1], B. Alaylar [2]

[1]Institute of Natural and Applied Sciences, Ataturk University, Erzurum, Türkiye, yuxel61@hotmail.com
Orcid ID: 0000-0002-2238-061X
[2]Department of Molecular Biology and Genetic, Faculty of Arts and Sciences, Agri Ibrahim Cecen University, Agri, Türkiye, Orcid ID: 0000-0001-6737-3440

Ethylene known as an important hormone that coordinates plant development through numerous mechanisms such as breaking dormancy, root formation, elongation and differentiation, leaf abscission and senescence, fruit ripening, and nodule formation etc. Ethylene hormone supports developmental events at certain concentrations while inhibiting these developmental events at other concentrations (1). Plants produce high levels of ethylene in response to stress conditions such as drought, salinity, and temperature. This high amount of ethylene inhibits root development, increases leaf abscission, and enhances aging in plants by preventing auxin transport. Microorganisms that promote plant growth limit ethylene production by synthesizing 1-aminocyclopropane-1-carboxylic acid (ACC) deaminase enzyme in response to elevated ethylene concentrations (2). The ACC deaminase produced by microorganisms cleaves ACC, the precursor of ethylene, into α-ketobutyrate and ammonia, thereby reducing the amount of ethylene produced under stress conditions and promoting plant growth. In this context, Origanum vulgare L. ssp. vulgare plants collected from different natural areas of Erzurum province and brought to the laboratory under aseptic conditions. Different parts of plant samples were prepared for surface sterilization such as root, leave and stem. Then, each part of the plant sample was inoculated onto Nutrient Agar (NA) medium to isolate endophytic bacteria. The ACC deaminase activities of the isolated strains were measured by using the colorimetric ninhydrin-ACC assay method (3,4). Genomic DNA isolations were performed for bacterial isolates showing high activity in this test. According to the assay 6 potential isolates were determined. The 16S rRNA regions of the obtained genomic DNA were amplified by PCR using universal primers 27F (5'-AGAGTTTGATCCTGGCTCAG-3') and 1492R (5'-GGTTACCTTGTTACGACTT-3') under in vitro conditions. When the sequence analysis of 16S rRNA were evaluated 6 potential Pantoea ssp. strains were determined such as 2 Pantoea sp., P. agglomerans, P. eucalypti, P. hericii and P. vagans.

References

[1] del Carmen Orozco-Mosqueda, M., Glick, B. R., & Santoyo, G. (2020). ACC deaminase in plant growth-promoting bacteria (PGPB): An efficient mechanism to counter salt stress in crops. Microbiological Research, 235, 126439.

[2] Afridi, M. S., Mahmood, T., Salam, A., Mukhtar, T., Mehmood, S., Ali, J., ... & Chaudhary, H. J. (2019). Induction of tolerance to salinity in wheat genotypes by plant growth promoting endophytes: Involvement of ACC deaminase and antioxidant enzymes. Plant Physiology and Biochemistry, 139, 569-577.

[3] Penrose, D. M., & Glick, B. R. (2003). Methods for isolating and characterizing ACC deaminase-containing plant growth-promoting rhizobacteria. Physiologia plantarum, 118(1), 10-15.

[4] Li, Z., Chang, S., Lin, L., Li, Y., & An, Q. (2011). A colorimetric assay of 1-aminocyclopropane-1-carboxylate (ACC) based on ninhydrin reaction for rapid screening of bacteria containing ACC deaminase. Letters in applied microbiology, 53(2), 178-185.

Investigation of Endophytic Siderophore Producing Mucor sp. from Origanum vulgare L. ssp. vulgare

Y. Dil [1], B. Alaylar [2], M. Güllüce [3], M. Karadayı[3], V. Yıldırım[3], S. Doğan[1]

[1]Institute of Natural and Applied Sciences, Ataturk University, Erzurum, Türkiye, yuxel61@hotmail.com
Orcid ID: 0000-0002-2238-061X
[2] Department of Molecular Biology and Genetic, Faculty of Arts and Sciences, Agri Ibrahim Cecen University, Agri, Türkiye, balaylar@agri.edu.tr Orcid ID: 0000-0001-6737-3440
[3] Department of Biology, Faculty of Sciences, Ataturk University, Erzurum, Türkiye

Iron (Fe) is an essential element necessary for plant life, found in soil in an insoluble form. In plants, it is needed for many metabolic processes, such as serving as a cofactor to enzymes, photosynthesis, oxidative phosphorylation, and the electron transport chain. Plants cannot easily access the Fe element found in various forms in the soil, such as ferric oxides, so they produce siderophores. These are low molecular weight biological molecules that make iron accessible in the soil (1). Plants produce phyto-siderophores, but these siderophores show less affinity to the ferric form of Fe (Fe+3) compared to microbial siderophores. As a result, competition begins for the Fe element between plants and pathogenic microorganisms in the environment (2). Endophytic fungi, through the siderophores they produce, contribute to the Fe in the environment for their hosts and promote their development (3). In this study, Origanum vulgare L. ssp. vulgare plant samples were collected from various areas around the province of Erzurum. Plant samples brought to the laboratory under aseptic conditions and surface sterilization was applied to these plants (4). Subsequently, root, leave and stem parts of the plants were dissected into small pieces and inoculated onto Potato Dextrose Agar (PDA) media at 0.1 g each. The resulting fungi were purified, and for the determination of their siderophore production capabilities, they were inoculated onto Chrome Azurol S (CAS) agar media. The fungi isolated from O. vulgare formed yellow-orange-colored zones of various sizes on CAS agar, indicating siderophore production by these isolates (5). Subsequently, DNA isolations were performed for the isolates producing siderophores, and their ITS regions were amplified in vitro using universal primers ITS1 forward (5'-TCCGTAGGTGAACCTGCGG-3') and ITS4 reverse (5'-TCCTCCGCTTATTGATATGC-3'). According to the sequence analysis results, it was determined that 3 isolates belonged to Mucor sp.

References

[1] Ferreira, M. J., Silva, H., & Cunha, A. (2019). Siderophore-producing rhizobacteria as a promising tool for empowering plants to cope with iron limitation in saline soils: a review. Pedosphere, 29(4), s. 409-420.

[2] Chowdappa, S., Jagannath, S., Konappa, N., Udayashankar, A. C., & Jogaiah, S. (2020). Detection and characterization of antibacterial siderophores secreted by endophytic fungi from *Cymbidium aloifolium*. Biomolecules, 10(10), 1412.

[3] Ghosh, S. K., Bera, T., & Chakrabarty, A. M. (2020). Microbial siderophore–A boon to agricultural sciences. Biological Control, 144, 104214.

[4] Zhao, Y. (2012). Auxin biosynthesis: a simple two-step pathway converts tryptophan to indole-3-acetic acid in plants. Molecular plant, 5(2), 334-338.

[5] Louden, B. C., Haarmann, D., & Lynne, A. M. (2011). Use of blue agar CAS assay for siderophore detection. Journal of microbiology & biology education, 12(1), s. 51-53.

Shielding Performance of Lightweight Nickel Foam/MoS₂ Composites

E. Kavaz Perişanoğlu[1], U. Perişanoğlu[2]

[1]*Ataturk University, Erzurum, Turkey, ORCID: 0000-0002-7016-2510*
[2]*Hakkari University, Hakkari, Turkey, ORCID: 0000-0002-7016-2510*

In this study, MoS2 was nano-walled on nickel foam by RF sputtering at 1 min, 2.5 min and 5 min. The obtained composite samples were irradiated with 241Am-point radioactive source and the transmitted photons were counted with Ultra Ge detector. After evaluating the spectra, mass attenuation coefficients (MAC) were calculated. Other photon attenuation parameters were derived by utilizing MAC values. Neutron dose measurements were then performed. It was observed that the composite with 5 min MoS2 grown on Ni Foam was more successful in radiation attenuation. the study contributes valuable insights and materials innovations to the shielding literature, potentially leading to more effective, versatile, and sustainable radiation shielding solutions for a range of applications.

Ag Dopant Effect on Supercapacitor Applications of Mn₃O₄ Thin Film Grown by Silar Method

M. Albayrak[1], H. Güney[2], S. Sarıtaş[3]

[1]Department of Electric and Energy, Vocational School Ağrı İbrahim Çeçen University, Ağrı - Turkey
[2]Deparments of Medical Services and Techniques, Hınıs Vocational School Ataturk University, Erzurum-Turkey
[3]Department of Electric and Energy, İspir Hamza Polat Vocational School Ataturk University, Erzurum-Turkey

Ag dopant effect on Mn3O4 thin films were grown on different ITO substrates at room temperature using the SILAR method. By varying the additive ratios during synthesis, the effects on the structural, morphological, and optical properties of the material were thoroughly evaluated and analyzed. The structural analysis was carried out using experimental techniques such as XRD, Raman spectroscopy and EDAX, optical properties by Ultraviolet-Visible Wavelength Optical Absorption Method and the morphological properties were examined by scanning SEM. Additionally, the capacitive properties were assessed through cyclic voltammetry (CV) and galvanostatic charge/discharge (GCD) testing. The specific capacitance of the undoped Mn3O4 thin film was measured to be approximately 230 F g-1 at a current density of 1 A g-1, with a noticeable increase observed with higher doping levels.

Key words: Ag dopant, Mn₃O₄, SILAR.

Effect Cd Dopant on Supercapacitor Applications of Mn₃O₄ Thin Film Grown by Silar Method

M. Albayrak[1]

[1]*Department of Electric and Energy, Vocational School, Ağrı İbrahim Çeçen University, Ağrı - Turkey*

The impact of Cd doping on Mn3O4 thin films was investigated, which were deposited on various ITO substrates at room temperature using the SILAR method. By modifying the additive ratios during synthesis, we thoroughly examined the effects on the structural, morphological, optical, and capacitive properties of the material. Structural analysis employed experimental techniques such as X-ray diffraction (XRD), Raman spectroscopy, and EDAX. Optical properties were assessed using Ultraviolet-Visible Wavelength Optical Absorption Method, while morphological characteristics were observed through scanning electron microscopy (SEM). Additionally, capacitive properties were analyzed using cyclic voltammetry (CV) and galvanostatic charge/discharge (GCD) techniques. The specific capacitance of the pristine Mn3O4 thin film was found to be approximately 230 F g-1 at a current density of 1 A g-1, with a noticeable enhancement observed upon increasing levels of doping.

Key words: Cd dopant, Mn₃O₄, Supercapacitor, SILAR.

Enhancing Water Quality Monitoring: Development of Carbon Nanotube-Functionalized Quartz Crystal Sensors for Trace Detection of Cadmium and Lead Ions

A. Altındal[1] and E. Kam[2]

[1]Istanbul Technical University, Physics Engineer, Istanbul, Turkiye, 0000-0002-2185-4094
[2]Istanbul Technical University Energy Institute, Istanbul, Turkiye. 0000-0001-5850-5464

As it is known, water is one of the most vital natural resources on Earth. In parallel with the developments in the industrial activity, the pollution of water resources by heavy metal ions such as Cadmium (Cd) and Lead (Pb) has become a threat to ecosystem and human health. It is well known that when HMIs present in excess than permissible exposure limit in living organisms cause various disorders and diseases in immune, nervous, and gastrointestinal systems. Therefore, the establishment of selective sensing techniques for trace level of heavy metal ions has great importance for ensuring both human health and ecological balance.

In this study, it was aimed to develop sensors to detect low concentrations of Cd and Pb in water resources. For this purpose, as transducer, AT-cut quartz crystals vibrating in the thickness shear mode with a fundamental resonant frequency of 10 MHz with gold (Au) electrodes was used. Carbon nanotube was used as the sensing layer. Our preliminary studies showed that carbon nanotube functionalized quartz crystals have great potential for the detection of Cd and Pb ions in water samples.

Keywords: Quartz crystal, heavy metal ions, adsorption, mass changes

Analysis of Teacher Needs Regarding the Science Course Conducted in Support Education Rooms

A. Kızılaslan[1], D. Şimşek[2], E. Durmaz[3]

[1]Agri Ibrahim Cecen University, Agri, Turkey, ORCID: 0000-0003-3033-9358
[2]Sabanci Secondary School, Erzurum, Turkey, ORCID: 0009-0008-5060-4618
[3]Mahmutlar Selçuklu Ortaokulu

This research, designed in a phenomenological model, aimed to determine the opinions of science teachers regarding support education room practices. The sample of the study consists of 20 teachers who work at east of Turkey in the 2023-2024 academic year and teach science education in the support education room with at least one student who needs special education throughout their professional experience. Semi-structured interview form was used as the main data collection tool in the research. In this study conducted in the form of focus group interviews, the data were subjected to content analysis. According to the research findings, it has been determined that teachers focus more on the academic success of students in the support education room. In terms of teaching methods and techniques, teachers focus on methods such as lecture, question-answer and demonstration, and use question-answer/oral and test/written exams as measurement and evaluation tools. It has been determined that they use It was observed that the main problems faced by science teachers in the support education room were physical conditions. While the most common answer to the advantages of the support education room was academic success, socialization problems and loss of motivation came to the fore as disadvantages. It was concluded that while science teachers made suggestions regarding support education room practices, they emphasized the provision of materials and the necessary training of teachers.

Assessing the Impact of Industrial Pollution on Environmental and Public Health: A Study on Heavy Metal and Radiation Contamination in Altınoluk and Edremit Using Laser-Induced Breakdown Spectroscopy (LIBS)

Z.Ü. Yumun[1], M. Önce[2], H. Ozen[3],

[1]*Tekirdağ Namık Kemal University, Çorlu Faculty of Engineering, Department of Environmental Engineering, Tekirdağ, Türkiye. ORCID ID: https://orcid.org/0000-0003-0658-0416*
[2]*Tekirdağ Namık Kemal University, Saray Vocational School, Department of Land Registry and Cadastre, Tekirdağ, Türkiye, ORCID ID: https://orcid.org/0000-0001-9621-3630*
[3]*Topkapı Istanbul University Management and Information Systems Istanbul, Turkiye. https://orcid.org/0009-0005-5594-621X*

This research was conducted to identify industrial pollution, specifically focusing on heavy metal and radiation contamination in the Altınoluk and Edremit areas. The study emphasizes the environmental and health impacts of elements that have existed since the earth's formation. The rapid industrialization following the Industrial Revolution, coupled with continuous population growth, has significantly increased the dispersion of various chemical components into the environment, leading to a marked increase in heavy metal pollution on the earth's crust. The escalation in levels of heavy metal and radiation pollution has consequently increased exposure levels in living organisms, posing a significant threat to health due to their toxic and carcinogenic effects once certain thresholds are exceeded.

Understanding the levels of heavy metal presence in a region is of paramount importance for public health. This study utilizes Laser-Induced Breakdown Spectroscopy (LIBS) to determine the presence of heavy metals. The LIBS method has increased its use in environmental analysis because it performs analysis quickly, on-site and with a small number of samples. The method's effectiveness in detecting and analyzing environmental pollutants underscores the critical need for continuous monitoring and evaluation of industrial pollution to mitigate its adverse effects on both the environment and human health. The findings highlight the urgent need for strategies to manage and reduce exposure to these hazardous elements, thereby safeguarding public health and preserving environmental integrity.

Keywords: heavy metal, pollution, environment, health.

Development and Validation of a UHPLC–ESI–MS/MS Method for the Simultaneous Determination of Organic Acids and Phenolic Compounds in Filipendula vulgaris, Polygonum divaricatum, Hypericum linarioides and Rheum ribes

H. Can[1], L. Güven[2], F. Demirkaya Miloğlu[3] and A. M. Abd El-Aty[4]

[1]Atatürk University, Erzurum, Turkiye, ORCID: 0000-0002-5723-2959, ORCID: 0000-0002-3189-6415, ORCID: 0000-0001-5729-7181, ORCID: 0000-0001-6596-7907

This study examined biologically active and pharmaceutically important phytochemicals utilizing reliable and reproducible analytical methods for traditional medicinal plants. Due to plant extracts' vast chemical variety, effective identification methods are essential. This work aimed to create and verify a reliable UHPLC-ESI-MS/MS technique for analyzing organic acids (OAs) and phenolic compounds (PCs). OAs and PCs were separated chromatographically on a C18 reversed-phase column using gradient elution of water and acetonitrile with 0.1% formic acid. These chemicals were detected on a triple quadrupole tandem mass spectrometer using a negative electrospray ionization source. Validation results show the approach is linear ($r^2 \geq$ 0.9986), sensitive (LOQ: 1.08 µg/L-10.79 µg/L), precise (RSD%≤2.73), and true (RE% < 1.53) for plant OAs and PCs. Successfully implemented UHPLC-ESI-MS/MS technology for qualitative and quantitative analysis of OAs and PCs in Turkish plants, commonly used in traditional medicine. We found 12 OAs and PCs in F. vulgaris, 12 in P. divaricatum, 9 in H. linarioides, and 11 in R. ribes. The highest gallic acid content was found in F. vulgaris (925.67 µg/g extract) and R. ribes (1358.78 µg/g extract), while H. linarioides (730.66 µg/g extract) and P. divaricatum (4003.02 µg/g extract) had greater quinic acid levels. In conclusion, the UHPLC-ESI-MS/MS approach can simultaneously analyze and quantify 2 OAs and 33 PCs in plants, making it a useful tool for assessing traditional medicinal plant efficacy.

Angiogenesis Related Roles of Induced Pluripotent Stem Cells in Wound Healing

H. Ocak[1], A. Özen[2]

[1]Ağrı İbrahim Çeçen University, Faculty of Medicine, Basic Medical Sciences, Department of Anatomy, Ağrı, Türkiye, ORCID:0000-0002-0288-4167
[2]Ankara University, Faculty of Veterinary Medicine, Department of Histology-Embryology, Ankara, Türkiye, ORCID:0000-0002-9678-0018

Wound healing is a type of regeneration involving 4 consecutive stages: haemostasis, inflammation, proliferation and remodeling. Occuring mainly in proliferative phase vasculature formation is a vital step for wound healing. Induced pluripotent stem cells (iPSCs) have invaluable capacity for tissue regeneration and wound healing because of their ability to differentiate into multiple cell lineages, lack of immune rejection and ethical concerns.

Studies in the literature could be divided to 4 groups: cellular differentiation based, exosome based, scaffold-biomaterials based and gene based studies. First group of studies involve differentiation of iPSCs to smooth muscle cells (SMCs), epithelial cells (ECs), keratinocytes. Mainly these iPSCs derived SMCs enhanced wound healing via angiogenesis by increasing growth factors and cytokines such as bFGF, VEGF (1, 2), cellular proliferation, survival of hiPSCs and macrophage polarization (2), collagen deposition, macrophage infiltration (3), increased blood vessel density and growth factors (4).

iPSCs derived exosomes-microvesicles improved wound healing by improved collagen I and III levels, reduced inflammation (5), thickening epidermis and increased collagen deposition and α-smooth muscle actin (α-SMA) together with CD31 (6), increased number of nerve fibers and α-SMA and CD31 (7). In another study they increased wound healing by improved collagen-elastin deposition and vessel density (8).

Collagen scaffolds with hIPSCs derived SMCs healed wound by epidermal and dermal thickening, enhanced cytokines and growth factors (9). Human skin substitute with fibroblasts and keratinocytes improved wound healing by neovascularization, and blood vessel invasion from wound bed (10).

When integrin β1 was knocked out in iPSCs, it resulted with improved iPSCs migration and survival, angiogenesis, blood perfusion and consequently wound healing (11).

References

[1] Sasson DC, Islam S, Duan K, Dash BC, Hsia HC, 2023. TNF-α Preconditioning Promotes a Proangiogenic Phenotype in hiPSC-Derived Vascular Smooth Muscle Cells. Cell Mol Bioeng. 2023 Apr 8;16(3):231-240.

[2] Gorecka J, Gao X, Fereydooni A, Dash BC, Luo J, Lee SR, Taniguchi R, Hsia HC, Qyang Y, Dardik A, 2020. Induced pluripotent stem cell-derived smooth muscle cells increase angiogenesis and accelerate diabetic wound healing. Regen Med. 2020 Feb;15(2):1277-1293.

[3] Clayton ZE, Tan RP, Miravet MM, Lennartsson K, Cooke JP, Bursill CA, Wise SG, Patel S, 2018. Induced pluripotent stem cell-derived endothelial cells promote angiogenesis and accelerate wound closure in a murine excisional wound healing model. Biosci Rep. 2018 Jul 31;38(4):BSR20180563.

[4] Kim KL, Song SH, Choi KS, Suh W, 2013. Cooperation of endothelial and smooth muscle cells derived from human induced pluripotent stem cells enhances neovascularization in dermal wounds. Tissue Eng Part A. 2013 Nov;19(21-22):2478-85.

[5] Bakhshandeh B, Jahanafrooz Z, Allahdadi S, Daryani S, Dehghani Z, Sadeghi M, Pedram MS, Dehghan MM, 2023. Transcriptomic and in vivo approaches introduced human iPSC-derived microvesicles for skin rejuvenation. Sci Rep. 2023 Jun 20;13(1):9963.

[6] Li J, Gao H, Xiong Y, Wang L, Zhang H, He F, Zhao J, Liu S, Gao L, Guo Y, Deng W, 2022. Enhancing Cutaneous Wound Healing Based on Human Induced Neural Stem Cell-derived Exosomes. Int J Nanomedicine. 2022 Dec 5;17:5991-6006.

[7] Kobayashi H, Ebisawa K, Kambe M, Kasai T, Suga H, Nakamura K, Narita Y, Ogata A, Kamei Y, 2018. ＜Editors' Choice＞ Effects of exosomes derived from the induced pluripotent stem cells on skin wound healing. Nagoya J Med Sci. 2018 May;80(2):141-153.

[8] Zhang J, Guan J, Niu X, Hu G, Guo S, Li Q, Xie Z, Zhang C, Wang Y, 2015. Exosomes released from human induced pluripotent stem cells-derived MSCs facilitate cutaneous wound healing by promoting collagen synthesis and angiogenesis. J Transl Med. 2015 Feb 1;13:49.

[9] Dash BC, Setia O, Gorecka J, Peyvandi H, Duan K, Lopes L, Nie J, Berthiaume F, Dardik A, Hsia HC, 2020. A Dense Fibrillar Collagen Scaffold Differentially Modulates Secretory Function of iPSC-Derived Vascular Smooth Muscle Cells to Promote Wound Healing. Cells. 2020 Apr 14;9(4):966.

[10] Abaci HE, Guo Z, Coffman A, Gillette B, Lee WH, Sia SK, Christiano AM, 2016. Human Skin Constructs with Spatially Controlled Vasculature Using Primary and iPSC-Derived Endothelial Cells. Adv Healthc Mater. 2016 Jul;5(14):1800-7.

[11] Ren Y, Liu J, Xu H, Wang S, Li S, Xiang M, Chen S, 2022. Knockout of integrin β1 in induced pluripotent stem cells accelerates skin-wound healing by promoting cell migration in extracellular matrix. Stem Cell Res Ther. 2022 Jul 30;13(1):389.

Investigation of the Effects of Different Colored Black Peppers on Cholinesterases

Y. Hasanoğlu[1], R. Sağlamtaş[2]

[1]Agri İbrahim Çeçen University, Faculty of Education, Agri, Türkiye,0000-0001-8139-6331
[2]Agri İbrahim Çeçen University, Medical Services and Techniques Department, Agri, Türkiye, 0000-0002-4400-2302

Black pepper (Piper nigrum L.), also known as the "king of spices," is one of the most popular spices in the world and is beneficial for health [1]. Black pepper seeds were classified into four distinct types: green, black, red, and white. These variations are determined by the level of ripeness at which the seeds are gathered, and the specific processing procedure employed for the fruits[2,3]. In this study, methanol, ethanol, dichloromethane, and n-hexane extracts were prepared using the maceration method for red and white peppers. In vitro, the effects of the extracts on critical metabolic enzymes including acetylcholinesterase (AChE) and butyrylcholinesterase (BChE) were investigated. To determine enzyme inhibition in the extracts, half-maximal inhibitory concentration values (IC50) were calculated. Tacrine was used as a positive control for both enzymes. The experiments were performed in triplicate. The IC50 values of white pepper extracts for AChE were 29.36 ± 0.59 µg/mL for the ethanol extract and 22.87 ± 0.93 µg/mL for the methanol extract. The IC50 value for BChE was 10.97 ± 0.83 µg/mL-71.44 ± 1.45 µg/mL. In contrast, the IC50 values of red pepper extracts for AChE were 45.59 ± 0.89 µg/mL for ethanol extract and 51.33 ± 1.53 µg/mL for methanol extract, for BChE, it was calculated as 17.77 ± 0.86 µg/mL- 92.4 ± 2.54 µg/mL. The n-hexane and DCM extracts did not inhibit AChE activity.

According to the study results, it was determined that ethanol and methanol extracts of white and red peppers had a more substantial inhibitory effect on AChE and BChE enzymes than other extracts. It can be thought that including black peppers of different colors in daily consumption can protect against chronic diseases such as Alzheimer's and Parkinson's disease.

Keywords. White and Red Black Pepper, Cholinesterases, Enzyme Inhibition

References

[1] Butt, M.S.; Pasha, I.; Sultan, M.T.; Randhawa, M.A.; Saeed, F.; Ahmed, W. Black Pepper and Health Claims: A Comprehensive Treatise. *Crit Rev Food Sci Nutr* 2013, *53*, doi:10.1080/10408398.2011.571799.

[2] Abukawsar, M.M.; Saleh-e-In, M.M.; Ahsan, M.A.; Rahim, M.M.; Bhuiyan, M.N.H.; Roy, S.K.; Ghosh, A.; Naher, S. Chemical, Pharmacological and Nutritional Quality

Assessment of Black Pepper (Piper Nigrum L.) Seed Cultivars. *J Food Biochem* 2018, *42*, doi:10.1111/jfbc.12590.

[3] Liu, H.; Zheng, J.; Liu, P.; Zeng, F. Pulverizing Processes Affect the Chemical Quality and Thermal Property of Black, White, and Green Pepper (Piper Nigrum L.). *J Food Sci Technol* 2018, *55*, doi:10.1007/s13197-018-3128-8.

2D MoS₂/MoO₂ nanocomposite structures growth control by Chemical Vapor Deposition

H.F. Budak[1]

[1]East Anatolia High Technology Application and Research Center, Atatürk University, Erzurum, Turkey, 25050,

The Chemical vapor deposition (CVD) is a widely used method in recent years to grow graphene-like two-dimensional (2D) TMDC and metal oxide structures. In this study, MoS2/MoO2 composite thin films were fabricated using CVD growth sulfur and MoO3 powder sources at 750 ℃. MoO2 structures with different thicknesses and 2D vertical MoS2 structures on the surface were grown by CVD and the effect of different growth time and distance between sulfur and MoO3 powder sources was systematically investigated. It was observed that different growth conditions caused changes in the morphology of the MoS2/MoO2 composite structures. Nanosheet, nanosheet and nanowall structures grown horizontally and vertically were imaged by SEM. As the CVD growth time increased, an increase in larger and thicker horizontal plate-like structures was observed. In MoS2/MoO2 grown for less time, mixed vertical and horizontal nanostructures were observed. The structural and cytochiometric changes of MoS2/MoO2 composite nanostructures were investigated by SEM-EDS as the distance between the powder sources affects the variation of the CVD reaction zone. The structural and optical properties of the grown composite structures were evaluated by micro-Raman and photoluminescence spectroscopic analysis. 2H MoS2 peaks and monoclinic MoO2 crystal structures were determined by XRD analysis. In addition, chemical analysis of the MoS2/MoO2 composite structures grown by CVD was carried out by XPS. abstract is a succinct summary of your study's purpose, main point, method, findings, and conclusions.

Understanding Positive Psychology: Past, Present, and Future Perspectives

M. Yıldırım[1]

[1]Department of Psychology, Agri Ibrahim Cecen University, Ağrı, Türkiye, ORCID: 0000-0003-1089-1380.

Positive psychology aims to understand the factors that foster human well-being and flourishing. Since its emergence, it has undergone significant transformation and growth. This study seeks to present an overview of the past, present, and future perspectives of positive psychology. In the early 2000s, positive psychology emerged as a response to traditional psychology, which primarily focuses on psychological diseases, pathology and dysfunction. Its early years were influenced by efforts to determine and understand the elements that contribute to happiness, life satisfaction, fulfilment, and human functioning by focusing on various concepts such as resilience, gratitude, flow, and character strengths. In contemporary times, positive psychology has been applied to many disciplines with extensive applications across diverse domains, including clinical psychology, education, organizational psychology, and public health. Scholars and practitioners continue to explore novel research avenues and practices within positive psychology, investigating topics such as mindfulness, positive relationships, purpose in life, and the cultural influences on flourishing and well-being. Various positive practices like gratitude exercises, resilience- and mindfulness-based techniques, and strengths-focused coaching have gained popularity as approaches for enhancing well-being, flourishing, and optimal positive human functioning. The future of positive psychology holds promise for further innovation and advancement. As the field continues to progress, researchers are interested in uncovering the underlying mechanisms of well-being, flourishing and positive functioning from an interdisciplinary perspective with fields such as neuroscience, social work, sociology, economics, environment, and public health.

Keywords: Positive psychology, past, present, future.

Social Support, Religiosity, and Death Distress after Maraş Earthquake

A. Güler[1]

[1]Department of Sociology, Agri Ibrahim Cecen University, Ağrı, Türkiye, ORCID: 0000-0002-0317-8221.

Earthquakes are natural disasters affecting the mental health of the general public, not only survivors, within national borders in many aspects. The present study aimed to investigate the mediating role of social support in the relationships between religiosity and death distress. The study included 424 participants ranging in age from 18 to 65 years (mean = 35.21 ± 9.85) who were residing in Turkey and completed the self-reported measures of social support, religiosity, and death distress, namely death anxiety, death depression, and death obsession, using a web-based online format. The results indicated that religiosity significantly predicted social support, indicating that individuals reporting higher levels of religiosity also tended to report higher levels of social support. Additionally, social support significantly predicted death distress, suggesting that higher levels of social support were associated with lower levels of death distress. This suggests that social support partially mediated the relationship between religiosity and death distress, indicating that higher levels of religiosity were associated with higher levels of social support, which in turn were associated with lower levels of death distress. These findings underscore the importance of social support-based interventions that reduce death distress in times of natural disasters. Post-disaster interventions should aim to focus on the existing social support networks within religious communities while also providing targeted strategies to diminish the symptoms of death distress and promote well-being.

Keyword: Social support; religiosity; death anxiety; death depression; death obsession

Advancements in Aluminium Alloys: The Future Unfolded by in situ Powder Metallurgy

M. Varol[1,2]

[1]Ağrı İbrahim Çeçen University, Patnos Vocational School, Ağrı, Turkey, ORCID: 0000-0002-0595-8379
[2]Atatürk University, Institute of Science, Erzurum, Turkey

As industries demand materials that offer a superior blend of mechanical strength, lightweight properties, and corrosion resistance, the evolution of aluminium alloys through innovative manufacturing techniques has become a focal point of materials science research. This study delves into a comprehensive review of recent advancements, synthesizing findings from leading studies to present a cohesive overview of the state-of-the-art in aluminium alloy development. The review highlights how in situ powder metallurgy has emerged as a pivotal technology, enabling the precise control of alloy compositions and microstructures. This method facilitates the direct incorporation of reinforcing phases during the alloy manufacturing process, leading to materials with enhanced properties that are tailored for specific applications [1]. Our synthesis of the literature reveals significant strides in achieving improved tensile strength, ductility, and resistance to environmental degradation, thereby underscoring the potential of in situ powder metallurgy to meet and exceed the performance benchmarks set by traditional alloy fabrication methods. The review also identifies emerging trends and gaps in the current research landscape, proposing directions for future investigation that could further unlock the capabilities of aluminium alloys to address the complex challenges of modern engineering applications. In conclusion, by reviewing the latest studies, this study not only charts the progress in aluminium alloys facilitated by in situ powder metallurgy but also sets the stage for the next leaps forward in materials science [2]. It showcases the transformative potential of this approach, envisioning a future where materials are not only stronger and more durable but also more harmoniously aligned with the principles of sustainability and efficiency.

References

[1] Schramm Deschamps, I., dos Santos Avila, D., Vanzuita Piazera, E., Dudley Cruz, R. C., Aguilar, C., & Klein, A. N. (2022). Design of in situ metal matrix composites produced by powder metallurgy—A critical review. Metals, 12(12), 2073.

[2] Kondoh, K., Oginuma, H., Kimura, A., Matsukawa, S., & Aizawa, T. (2003). In-situ synthesis of Mg2Si intermetallics via powder metallurgy process. Materials Transactions, 44(5), 981-985.

The Relationship Between Hearing Loss and Dementia

G.B. Göçer[1]

[1]Department of Otorhinolaryngology, Bulanık State Hospital, Muş, Turkey, ORCID: 0000-0002-5295-547X

Dementia and hearing loss are common conditions in the aging population and often coexist [1]. Presbycusis means bilateral age-related hearing loss. In literal terms, presbycusis means "old hearing" or "elder" hearing. It is defined as sensorineural hearing loss caused by aging [2]. Dementia is a neurological condition characterized by the gradual death of brain cells, resulting in a decline in cognitive functions or thinking skills. Dementia is one of the leading causes of disability worldwide. It affects approximately 6.5% of the population over the age of 65. More than 135 million people are expected to be affected by 2050. Unfortunately for people with dementia curative treatments are not yet available. Current treatment strategies only improve symptoms and do not change the course of the disease. However, we know that the risk of dementia decreases with social changes, improvements in living conditions and good cardiovascular risk management. Similarly, rehabilitation of hearing loss also reduces the risk of dementia [3-9]. The relationship between cognitive changes and hearing loss is controversial in the literature. Although some studies indicate that there is a relationship between hearing loss and cognitive changes in people with cognitive impairment [10-12] on the contrary, some other studies say that there is no relationship between them. [13-15]. With age, mild or severe hearing loss may occur. If left untreated, moderate or greater hearing losses affect communication. It can cause isolation from social life, depression and dementia. These effects can be largely reversed with rehabilitative treatment. Hearing aids, assistive listening devices, and cochlear implants can be applied. Hearing aids are not used enough due to reasons such as cost and current social attitudes. Cochlear implantation can be applied in cases where hearing aids do not provide benefit. Cochlear implant application is the preferred treatment method that gives excellent results even at the age of eighty [6].

Keywords: Hearing loss, Dementia, presbycusis

References

1.   Matthews, F.E., et al., *A two-decade comparison of prevalence of dementia in individuals aged 65 years and older from three geographical areas of England: results of the Cognitive Function and Ageing Study I and II*. The Lancet, 2013. **382**(9902): p. 1405-1412.

2.   Fransen, E., et al., *Age-related hearing impairment (ARHI): environmental risk factors and genetic prospects.* Experimental gerontology, 2003. **38**(4): p. 353-359.

3.   Baird, A. and S. Samson, *Music and dementia.* Progress in brain research, 2015. **217**: p. 207-235.

4.   Ferri, C.P., et al., *Global prevalence of dementia: a Delphi consensus study.* The lancet, 2005. **366**(9503): p. 2112-2117.

5.   Norton, S., et al., *Potential for primary prevention of Alzheimer's disease: an analysis of population-based data.* The Lancet Neurology, 2014. **13**(8): p. 788-794.

6.   Gates, G.A. and J.H. Mills, *Presbycusis.* The lancet, 2005. **366**(9491): p. 1111-1120.

7.   Huang, C.-Q., et al., *Chronic diseases and risk for depression in old age: a meta-analysis of published literature.* Ageing research reviews, 2010. **9**(2): p. 131-141.

8.   Lin, F.R., et al., *Hearing loss and incident dementia.* Archives of neurology, 2011. **68**(2): p. 214-220.

9.   Brookmeyer, R., et al., *Forecasting the global burden of Alzheimer's disease.* Alzheimer's & dementia, 2007. **3**(3): p. 186-191.

10.   Wei, J., et al., *Hearing impairment, mild cognitive impairment, and dementia: a meta-analysis of cohort studies.* Dementia and geriatric cognitive disorders extra, 2018. **7**(3): p. 440-452.

11.   Valentijn, S.A., et al., *Change in sensory functioning predicts change in cognitive functioning: Results from a 6-year follow-up in the Maastricht Aging Study.* Journal of the American Geriatrics Society, 2005. **53**(3): p. 374-380.

12.   Peters, C.A., J.F. Potter, and S.G. Scholer, *Hearing impairment as a predictor of cognitive decline in dementia.* Journal of the American Geriatrics Society, 1988. **36**(11): p. 981-986.

13.   Gennis, V., et al., *Hearing and cognition in the elderly: new findings and a review of the literature.* Archives of Internal Medicine, 1991. **151**(11): p. 2259-2264.

14.   Anstey, K.J., M.A. Luszcz, and L. Sanchez, *Two-year decline in vision but not hearing is associated with memory decline in very old adults in a population-based sample.* Gerontology, 2001. **47**(5): p. 289-293.

15.   Gussekloo, J., et al., *Sensory impairment and cognitive functioning in oldest-old subjects: the Leiden 85+ Study.* The American Journal of Geriatric Psychiatry, 2005. **13**(9): p. 781-786.

Synthesis of Triazole Compounds from Azide-derived Oxazolidinone Compounds

A. Yıldırım[1], S.H. Atalay[1] Z. Odabaş[1]

[1]Marmara University, Faculty of Science, Chemistry Department, Kadıköy/İstanbul ORCID: 0000-0003-1701-1606, 0009-0004-3367-8376, 0000-0002-0647-0404

Oxazolidinones have a unique mechanism of bacterial protein synthesis inhibition and constitute a relatively new class of antimicrobial agents. Oxazolidinones [1] have wide usage areas due to their biological activities. In the last few years, interest in the synthesis of oxazolidinones has increased considerably due to their biological activity. Optically pure oxazolidinones [2] play key roles in the synthesis of different types of düğse, antibiotic, antidepressant, antihistamine, antifungal or antibacterial activities. Another reason why compounds bearing the oxazolidinone ring have become the focus of attention is that they inhibit protein synthesis, which is of great importance far living things.

GENERAL PROCEDURE

This project, endoperoxide compounds were synthesized from 1,3-diene compounds by photooxygenation method. Af ter the resulting endoperoxide compounds were converted into hydroxy ketones with NEt3, oxazolidinone derivatives were synthesized from α,β-unsaturated hydroxy ketones using CSI. The synthesis of biologically important azide-derived oxazolidinone compounds from oxa compounds has been achieved in high yields. After these steps, triazole molecules [3] will be synthesized from azide-derived compounds by the click reaction

Keywords: Phthalocyanine, oxo-bridged, metal, metal-free

References

[1] Bach, T., Schlummer, B. and Harms, K., 2001. - A European Journal, 7 (12), 2581-2594.

[2] Laserna, V., Guo, W. and Kleij, A.W., 2015. Advanced Synthesis & Catalysis, 357 (13), 2849-2854.

[3] Demaray, Jeffrey A., et al. "Synthesis of triazole-oxazolidinones via a one-pot reaction and evaluation of their antimicrobial activity." *Bioorganic & medicinal chemistry letters* 18.17 (2008): 4868-4871.

Antioxidant, and Enzyme Inhibition Effects of Chia (Salvia hispanica) Seed Oil: A Comprehensive Phytochemical Screening Using LC-HR/MS, GC/MS, and GC-FID

M. Mutlu[1], Z. Bingöl[2], E.M. Özden[3], E. Köksal[4], A. Erturk[5], A. C. Gören[6], S. Alwasel[7], S. Ahmed El-Sohaimy [8], and İ. Gulcin[9]

[1]Vocational School of Applied Sciences, Gelişim University, Istanbul 34315, Turkey; muzaffermutlu@hotmail.com
[2]Department of Medical Services and Techniques, Tokat Vocational School of Health Services, Gaziosmanpasa University, 60250-Tokat, Turkey; https://orcid.org/0000-0003-3373-779X
[3]Department of Chemistry, Faculty of Science, Ataturk University, Erzurum 25240, Turkey; https://orcid.org/0000-0002-9259-5704
[4]Department of Chemistry, Faculty of Science and Arts, Erzincan Binali Yildirim University, Erzincan 24100, Turkey; https://orcid.org/0000-0003-0853-566X
[5]Department of Pharmacy Services, Hınıs Vocational School, Ataturk University, Erzurum 25600, Turkey; https://orcid.org/0000-0002-1750-1966
[6]Department Chemistry, Faculty of Sciences, Gebze Technical University, Kocaeli 41400, Turkey; https://orcid.org/0000-0002-5470-130X
[7]Department of Zoology, College of Science, King Saud University, Riyadh 11451, Saudi Arabia; https://orcid.org/0000-0002-0626-2306
[8]Food Technology Department, Arid Land Cultivation Research Institute (ALCRI), City of Scientific Research and Technological Applications (SRTA-City), New Borg El-Arab, Alexandria P.O. Box 21934, Egypt
[9]Department of Technology and Organization of Public Catering, Institute of Sport, Tourism, and Service, South Ural State University (SUSU), 454080 Chelyabinsk, Russia
https://orcid.org/0000-0002-8877-6414
*Correspondence: igulcin@atauni.edu.tr; Tel.: +90-4422314375; https://orcid.org/0000-0001-5993-1668

Plants are integral to human well-being providing food, fiber, medicine, feed, industrial material and ornamental and cultural services. Research has reported the role of plants in enhancing the quality of human life. Their medicinal properties, nutritional value, air-purifying abilities, and contribution to biodiversity make them vital for human well-being.[1] Plants contain bioactive compounds such as flavonoids, alkaloids, terpenes, and polyphenols that have demonstrated therapeutic properties. These compounds are called secondary metabolites and may have antioxidant, anti-inflammatory, antimicrobial, analgesic, and other beneficial effects on the body. [2,3]

In this study, the antioxidant and anti-Alzheimer properties of Chia (Salvia hispanica) seed oil (CSO) were determined for the first time. Three different reduction (CUPRAC, FRAP, and Fe3+ reducing) and two different radical scavenging methods were used to determine the antioxidant properties of CSO.

It exhibited higher antioxidant activity than vitamins E and C in the CUPRAC method. In the DPPH scavenging method, CSO showed higher activity than BHT, a standard antioxidant. The anti-Alzheimer's disease properties of CSO were determined by

inhibition of acetylcholinesterase (AChE) enzyme and its IC50 value (17.60 µg/mL) was found to be close to the IC50 value of tacrine (8.82 µg/mL), the standard inhibitor of the enzyme. Inhibition properties of α-glycosidase and human carbonic anhydrase II (hCA II) enzymes were also studied. It was understood that CSO inhibited both enzymes at a lower rate than standard inhibitors. Also, total phenolic and flavonoid contents of CSO were determined as 784.44 µg gallic acid equivalent (GAE)/mL oil and quercetin 150.00 µg quercetin equivalent (QE)/mL oil, respectively. In addition, LC-HRMS chromatography application was performed to understand the phenolic content of CSO. It was determined that isosacuranetin (29.07 mg/L oil) was the most abundant polyphenolic compound in the structure of the plant. On the other hand, the amount of seven polyphenolic compounds (Ascorbic acid, Fumaric acid, Rutin, Apigenin-7-glycoside, Quercetin, Salicylic acid and Caryophyllene oxide) of the studied remained below the detectable amount.

References

[1] Marselle MR, Hartig T, Cox DTC, de Bell S, Knapp S, Lindley S, et al. Pathways linking biodiversity to human health: A conceptual framework. Environ Int. 2021;150: 106420. https://doi.org/10.1016/j.envint.2021.106420

[2] Seyedsayamdost MR. Toward a global picture of bacterial secondary metabolism. J Ind Microbiol Biot. 2019; 46: 301-311. https://doi.org/10.1007/s10295-019-02136-y,

[3] Tran N, Pham B, Le L. Bioactive compounds in anti-diabetic plants: from herbal medicine to modern drug discovery. Biol. 2020; 28: 252-82. https://doi: 10.3390/biology9090252.

Full Texts

Cellulase-Producing Bacteria from Lake Van

S. Gurkok[1], A.A. Yılmaz[2]

[1]Department of Biology, Science Faculty,
Ataturk University, Erzurum, Turkey, ORCID: 0000-0002-2707-4371
[2]1Institute of Natural and Applied Sciences,
Atatürk University, Erzurum, Turkey, ORCID: 0000-0001-9071-7897

Abstract

Enzymes, essential biocatalysts, govern numerous biological processes within living cells, with cellulase standing out as a crucial type orchestrating the enzymatic hydrolysis of cellulose. Cellulases are a group of intricate enzyme systems that primarily include endo-glucanase, exo-glucanase, and β-glucosidase enzymes. They are pivotal players in the hydrolysis of cellulose which is an insoluble, fibrous, crystalline complex biopolymer of glucose. This hydrolysis process transforms cellulose into its end product, glucose, with successive conversion steps involving the breakdown of cellulose molecules into shorter polysaccharides and, ultimately, into monosaccharides. Cellulose hydrolysis is quite important for many industrial processses. Therefore, cellulases show great potential in a wide-ranging industrial application areas including food processing, textile and laundry industries, biofuel production, paper and pulp manufacturing, and environmental pollutant treatment.

Cellulases are widespread across plants, fungi, and bacteria; however, microorganisms take precedence in industrial enzyme production due to their rapid growth, controllable cultivation conditions, and advantageous enzymatic characteristics. In certain instances, enzymes capable of functioning under extreme conditions may be necessary, depending on the specific application area. To acquire such enzymes, extremophilic organisms are actively sought after as the source of enzymes. Therefore, this study focuses on screening, isolating and identifying an efficient alkaline cellulase from extremophilic bacteria thriving in the basic pH environment of Lake Van to evaluate its potential applications in various biotechnological processes.

Keywords: Microbial cellulase, alkaliphilic cellulase, cellulose, *Bacillus pumilus*, Lake Van

Introduction

Cellulose, a product of photosynthesis, stands as one of the most abundant polymers on Earth [1]. Cellulases are complex enzyme systems represented by three enzyme groups, endoglucanase (CMCase), exoglucanase and β-glucosidase [2] and have pivotal roles in hydrolysis of cellulose polymers.

Cellulase producer organisms can be found across different domains of life, however, microorganisms take precedence in industrial enzyme production due to their rapid growth, controllable cultivation conditions, and advantageous enzymatic characteristics. Bacillus species such as *Bacillus subtilis* and *B. pumilus, and Clostridium* spp are among the bacteria exhibiting cellulolytic activity [3]. *Trichoderma reesei*, *Aspergillus niger* and *Aspergillus oryzae*, and some *Penicillium* strains are known as cellulase producing fungi [4,5] and *Saccharomyces spp*. can also exhibit cellulolytic activity [6]. Among actinomycetes, *Streptomyces spp.* have been reported to produce cellulase [7].

Microbial cellulases show great potential in a wide-ranging application such as textile and laundry industries, biofuel production, food processing, paper and pulp manufacturing, and environmental pollutant treatment [8]. These organisms have adapted to diverse environments and contribute to the breakdown of cellulose in nature by exhibiting cellulase production as part of their metabolic process. The diversity of cellulase-producing microbes provides enzyme sources with different properties for different applications in these industries, and the discovery of new cellulase-producing microorganisms is of great importance for the advancement of biotechnological applications and improvement of industrial processes to be carried out under different conditions. For example, in industries such as laundry and detergent production, alkaliphilic enzymes such as proteases, lipases and amylases are prefered [9,10,11]. Alkaliphilic cellulase are also advantageous due to their compatibility with alkaline cleaning agents. These enzymes work effectively in the presence of detergents, ensuring effective stain removal or biopolishing, and improving the overall performance of cleaning products. Therefore, the objective of this research was to isolate alkaline cellulase-producing bacteria suitable for prospective applications in alkaline environments. To achieve this goal, Van Lake, characterized by elevated pH values, was utilized as the source of alkaliphilic bacterial isolates.

Material and Methods

Materials

Carboxymethyl cellulose - agar was used to examine whether pure cultures have cellulase activity based on cellulolytic zone formation. It was prepared by adding 1% carboxymethyl cellulose to nutrient agar medium and pH was adjusted to 9. It was sterilized by autoclaving at 121 °C at 1.5 atmospheric pressure for 15 min. Then, when the medium cooled, it was transferred to sterile petri dishes and made ready for use.

Carboxymethyl cellulose - broth was used as a liquid cellulase production medium. Carboxymethyl cellulose - broth contains 10 g CMC, 0.2 g $MgSO_4.7H_2O$, 5 g NaCl, 10 g peptone, 2 g yeast extract, 1 g K_2HPO_4 and 0.1 g $CaCl_2$, pH 9. 100 mL each was transferred to the flasks and sterilized by autoclaving at 121 °C at 1.5 atmospheres pressure for 15 minutes.

DNS solution was prepared by mixing two solutions. The first solution was prepared by dissolving 1 g of DNS in 20 mL of 2 N NaOH and the second solution was prepared by dissolving 30 g of Na-K-tartrate in 50 mL of pure water. It was used to stop the enzyme reaction and to quantitatively determine the activity of the enzyme.

Congo Red (0.1%) was prepared by dissolving 0.1 g Congo Red in 100 mL distilled water. It was used to determine cellulase activity on solid medium, to stain the medium and to monitor zone formation.

Substrate solution was freshly prepared by dissolving 1% carboxymethyl cellulose in 50 mM Glycine-NaOH buffer. It was used as substrate for carboxymethyl cellulase (endo-β-1-4-glucanase) activity.

Methods

Sample Collection and Isolation of Bacteria

Water samples from Lake Van were taken in sterile falcon tubes. The samples were inoculated directly or diluted in sterile phosphate buffer saline at various ratios and plated in petri dishes containing nutrient agar. Samples were incubated at 30 °C for 3 days. Individual colonies were picked and streaked onto new nutrient agar plates for purification. Glycerol stocks were prepared in nutrient broth containing 20% glycerol and cryopreserved at -86 °C.

Selection of Cellulase Producing Isolates

Screening cellulase producing isolates was performed by qualitative cellulase activity determination. In order to select the isolates with cellulase activity, pure cultures were inoculated into carboxymethyl cellulose - agar medium and incubated at 30 °C for 48-72 hours. After incubation, 0.1% Congo red was poured onto the colonies to observe zone formation and stained for 15 min. Then the stain was removed and the petri plate was washed with 1 M NaCI solution for 30 minutes. The diameters of the cellulolytic zones formed around the isolates were measured and the ones forming the widest zones were determined [12].

Quantitative Cellulase Activity Assay

Isolates showing the widest cellulolytic zone formation on carboxymethyl cellulose - agar were selected and incubated in 250 mL erlen mayers containing 100 mL carboxymethyl cellulose - broth at 30 ºC, 180 rpm for 24, 48, 72, 96 and 120 hours. At the end of incubation, 2 mL of the cultures were taken and placed in eppendorf tubes. After centrifugation at 6000 rpm and 4 °C for 10 min, the supernatant was separated from the cell content and prepared to be used as crude enzyme. The substrate solution was prepared by heating in a 35 °C water bath for 5 min before use. 0.5 mL of substrate solution and 0.5 mL of crude enzyme were mixed and homogenized and incubated in a

35 °C water bath for 30 min. At the end of incubation, 1 mL of DNS reagent was added to the reaction mixture, boiled in water for 5 min and the reaction was stopped. The boiled samples were allowed to cool at room temperature. The absorbance of the samples was measured at 540 nm wavelength in a spectrophotometer [13] and carboxymethyl cellulase activity was calculated according to the glucose standard graph. The amount of glucose released as a result of the cellulase reaction was calculated by standard glucose curve prepared with different concentrations of pure glucose. One unit of cellulase activity (1 U) was evaluated as the amount of enzyme that produced 1 µmol glucose in 1 min under the assay conditions. Experiments were performed in three replicates.

Identification of Cellulase Producing Isolate

According to qualitative and quantitative cellulase activity determinations, the bacterial isolate with the highest cellulase activity was selected and morphological (colony color and shape, cell shape, Gram staining, KOH) and biochemical (oxidase, amylase, protease, hemolysis, H_2O_2 catalase, urease, lipase, asparaginase, glutaminase, maltose, etc.) properties were determined by classical methods. Molecular characterizations of the selected isolate were carried out through 16S rDNA sequence analysis.

Results

Isolation of Bacteria

As a result of the isolation studies, 60 isolates were obtained from Lake Van and used for qualitative cellulase determination.

Determination of Cellulase Activities of the Isolates

As a result of qualitative cellulase activity determinations of the isolates on carboxymethyl cellulose - agar, 19 cellulase producer isolates were selected. Figure 1 shows examples of isolates forming the widest cellulolytic zone. The most prominent cellulolytic zones were observed in isolates coded V2 (7 mm), V3 (8 mm), V4 (4 mm), V7 (9 mm), VS1 (4 mm), VS13 (6 mm), VS15 (4 mm), VS20 (11 mm) and B6 (5 mm).
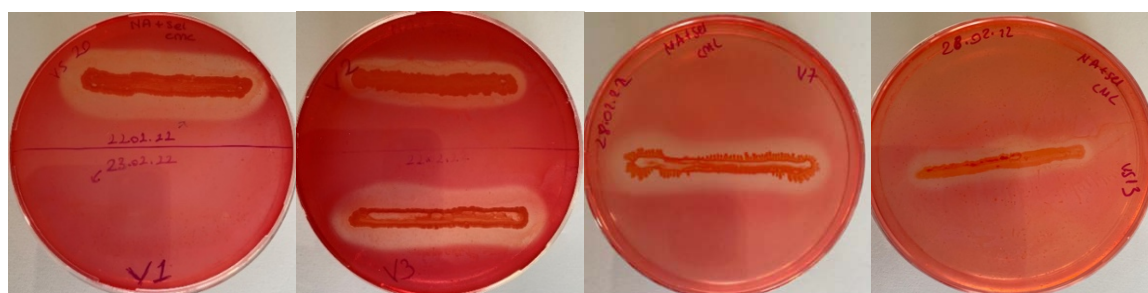
Figure 1. Cellulotic zones formed by the isolates obtained from Lake Van after incubation in carboxymethyl cellulose - agar medium at 30 °C for 48 hours

Quantitative Determination of Cellulase Activity of Bacterial İsolates

Quantitative activity determinations were performed with 6 isolates (V2, V3, V7, VS13, VS20 and B6) selected according to the zone diameters they formed on carboxymethyl cellulose - agar. Isolates were incubated in NB medium for 24 hours to prepare a pre-culture. At the end of incubation, 1 mL of the bacteria grown in nutrient broth medium was taken and incubated in 250 mL flasks containing 100 mL carboxymethyl cellulose - broth medium at 30 ºC, 180 rpm for 120 hours. At the end of the incubation periods, cellulase activity of the isolates was determined by DNS method and the isolate with the highest activity was determined.

Figure 2. Cellulase activities of Lake Van bacterial isolates during 120 hours of incubation at 30 °C in CMC-B medium.

Figure 3. Microbial growth of Lake Van bacterial isolates during 120 hours of incubation at 30 °C in CMC-B medium

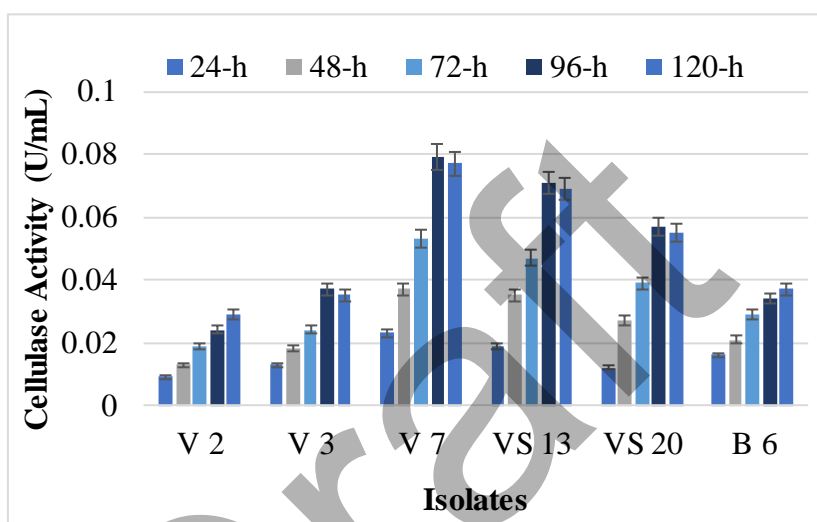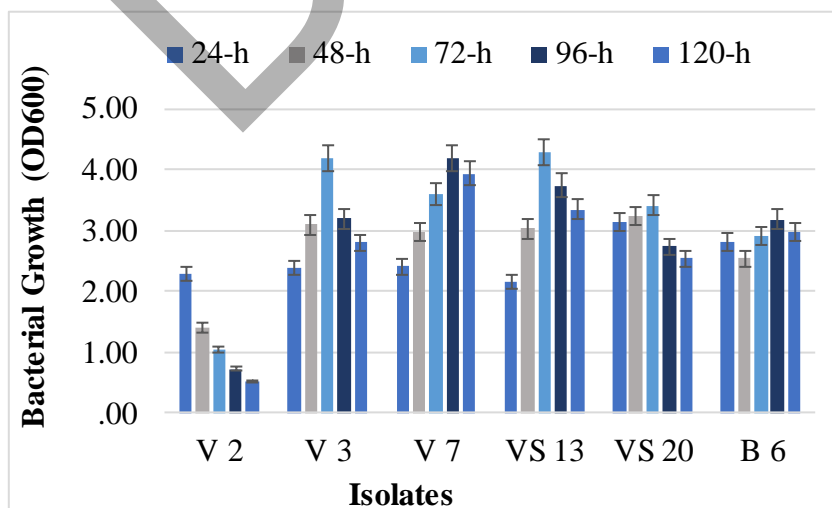Isolate V7 was selected as the best cellulase producer based on the zone diameter formed in carboxymethyl cellulose - agar and the quantitative cellulase activity results shown in Figure 2. Carboxymethyl cellulase activity of V7 isolate was found to be 0.079 U/mL after 96 h incubation. In Figure 3, the growth patterns of the isolates are given.

Identification of The Cellulolytic Isolate

The characterization of isolate V7 was firstly performed by classical methods. The motile and bacillus-shaped V7 isolate was found to have Gram-positive cell wall structure and small, smooth-edged, rod, cream colored colonies. It was positive for oxidase, hemolysis, catalase, protease, lipase, KOH, asparaginase, maltose, L-arabinose, D-xylose and myo-inositol and negative for amylase, glutaminase and urease.

The sequence obtained as a result of molecular characterization of the isolate coded V7 by analysis of the 16S rDNA region was compared with the sequences in the NCBI database. The isolate was identified as *Bacillus pumilus* VLC7 and GenBank number OR415888.1 was assigned for the isolate.

In the next stage of the study, the purification and characterization of the cellulase obtained from *Bacillus pumilus* VLC7 will be performed and the potential biotechnological applications of the enzyme will be evaluated.

Conclusions

In conclusion, our investigation into alkaliphilic isolates from Lake Van revealed that among the isolates tested (V2, V3, V7, VS13, VS20, and B6), isolate V7 demonstrated the most extensive cellulolytic activity, forming the widest cellulolytic zone and exhibiting the highest cellulase activity. Further analyses identified isolate V7 as *Bacillus pumilus* VLC7 through classical and molecular methods. The morphological and biochemical characteristics of *B. pumilus* VLC7 were determined, providing valuable insights into its Gram-positive, bacillus-shaped, and cream-colored features, as well as its positive and negative reactions to various enzymatic tests.

Moving forward, the subsequent phase of our study will focus on the purification and detailed characterization of the cellulase enzyme derived from *B. pumilus* VLC7. This crucial step will enable us to unravel the enzyme's functional properties, shedding light on its potential applications in various biotechnological processes. The anticipated outcomes will contribute to our understanding of the cellulase's specific attributes and pave the way for evaluating its efficacy in practical applications.

References

[1] L. Liu, W.C. Huang, Y. Liu, M. Li, 2021. Diversity of cellulolytic microorganisms and microbial cellulases. Int. Biodeterior. Biodegrad. 163 (2021) 105277.

[2] R. Singh, A.A. Saati, H. Faidah, F. Bantun, N.A. Jalal, S. Haque, A.K. Rai, M. Srivastava, 2023. Prospects of microbial cellulase production using banana peels wastes for antimicrobial applications. Int. J. Food Microbiol. 388 (2023) 110069.

[3] A.S. Kurt, D. Cekmecelioglu, 2023. Bacterial cellulase production using grape pomace hydrolysate by shake-flask submerged fermentation. Biomass Conver. Biorefin. 13(8) (2023) 6981-6988.

[4] C. Conesa, L. Seguí, P. Fito, (2018). Hydrolytic performance of Aspergillus niger and *Trichoderma reesei* cellulases on lignocellulosic industrial pineapple waste intended for bioethanol production. Waste Biomass Valorization 9 (2018) 1359-1368.

[5] X. Lu, X. Li, J. Zhao, 2024. Improving enzymatic efficiency of β-glucosidases in cellulase system by altering its binding behavior to the insoluble substrate during bioconversion of lignocellulose. Bioresour. Technol. 391 (2024) 129974.

[6] J. van Dyk, J.F. Görgens, E. van Rensburg, 2024. Enhanced ethanol production from paper sludge waste under high-solids conditions with industrial and cellulase-producing strains of *Saccharomyces cerevisiae*. Bioresour. Technol. 394 (2024) 130163.

[7] J.A. John, E. Selvarajan, 2023. Genomic analysis of lignocellulolytic enzyme producing novel *Streptomyces* sp. MS2A for the bioethanol applications. Int. J. Biol. Macromol. 250 (2023) 126138.

[8] R. Ranjan, R. Rai, S.B. Bhatt, P. Dhar, 2023. Technological road map of Cellulase: A comprehensive outlook to structural, computational, and industrial applications. Biochem. Eng. J. (2023) 109020.

[9] A. Hemsinli, S. Gurkok, 2024. Evaluation of a novel purified and characterized alkaline protease from the extremophile *Exiguobacterium alkaliphilum* VLP1 as a detergent additive. Biotechnol. J. 19, (2024) e2300441.

[10] S. Gurkok, M. Ozdal, 2021. Purification and characterization of a novel extracellular, alkaline, thermoactive, and detergent-compatible lipase from *Aeromonas caviae* LipT51 for application in detergent industry. Protein Expr. Purif. 180 (2021) 105819.

[11] S. Gurkok, 2019. Microbial enzymes in detergents: A review. Int. J. Sci. Eng. Res. 10(9) (2019) 75-81.

[12] H.R. Gohel, C.N. Contractor, S.K. Ghosh, V.J. Braganza, 2014. A comparative study of various staining techniques for determination of extra cellular cellulase activity on carboxy methyl cellulose (CMC) agar plates. Int. J. Curr. Microbiol. Appl. Sci. 3(5) (2014) 261-266.

[13] G. Miller, 1959. Use of dinitrosalicylic acid reagent for determination of reducing sugar. Anal. Chem. 31(3) (1959) 426-428

Isolation and Identification of Amylase-Producing Strain

S. Gurkok[1], F. Akbas[2] and M. Ozdal[3]

[1]Department of Biology, Science Faculty, Ataturk University, Erzurum, Turkey, ORCID: 0000-0002-2707-4371, ORCID: 0000-0001-8800-1128
[2]1Institute of Natural and Applied Sciences, Atatürk University, Erzurum, Turkey, ORCID: 0000-0003-3787-0213

Abstract

Amylase enzymes are a class of enzymes that hydrolyse the starch into simpler sugars such as maltose and glucose. These enzymes are widely found in various organisms, including plants, animals, and microorganisms. Among the diverse sources of amylase enzymes, microbial enzymes, derived from bacteria and fungi, hold significant advantages over their counterparts from plants and animals.

Microbial amylase enzymes offer versatility, stability, and scalability, making them indispensable for a wide array of industrial applications. The aim of this study was to investigate the efficient and economical production of amylase enzyme with a good microbial source and the biotechnological application areas of the enzyme produced. In line with this aim, firstly isolation of amylase producing bacteria from potatoes was targeted. It was aimed to select and identify the best amylase producer among the isolated amylolytic bacteria.

Keywords: Microbial amylase, starch, potato, *Priestia megaterium*

Introduction

Amylases, which hydrolyse starch into simpler sugars such as maltose and glucose, are enzymes commonly found in a variety of organisms, including plants, animals and microorganisms [1]. Among the diverse sources of amylase enzymes, microbial enzymes, derived from bacteria and fungi, hold significant advantages over their counterparts from plants and animals.

Microbial amylase enzymes exhibit several key advantages, including high stability under a range of environmental conditions, such as pH and temperature fluctuations. This stability makes them more adaptable for industrial applications where varying conditions may be encountered. Additionally, microbial enzymes can be produced on a large scale through fermentation processes, offering cost-effective and sustainable production methods.

The applications of microbial amylase enzymes span across various industries [2]. In the food industry, these enzymes are essential for processes like baking, brewing, and starch processing [3]. Amylases also find applications in the detergent industry, where they contribute to the removal of starch-based stains [4]. Moreover, microbial amylases play a crucial role in biofuel production by breaking down starch into fermentable sugars for ethanol production [5].

In summary, microbial amylase enzymes offer versatility, stability, and scalability, making them indispensable for a wide array of industrial applications. The aim of this study was to investigate the efficient and economical production of amylase enzyme with a good microbial source and the biotechnological application areas of the enzyme produced. In line with this aim, firstly isolation of amylase producing bacteria from potatoe was targeted. It was aimed to select the best amylase producer among the isolated amylolytic bacteria.

Material and Methods

Materials

Starchy nutrient agar (SNA) was used for screening the amylase activity of the isolates. 20 g NA was dissolved in 1 L distilled water, 1% (10 g) soluble starch was added and sterilized at 121 °C for 15 minutes at 1.5 atm pressure.

Starch (Substrate) solution (1%) was prepared by dissolving 1 g soluble starch in 100 mL pH 7 sodium phosphate buffer.

Lugol solution was used to screen amylase activity on SNA medium containing 1% soluble starch.

DNS (Dinitro salicylic acid) (1%) was used to determine the amount of reducing sugar released as a result of the amylase enzyme reaction and to stop the reaction. 1 g DNS was dissolved in 50 mL deionized water, then 30 g Na-K-Tartrate and 20 mL 2 N NaOH were added and mixed thoroughly in a magnetic stirrer. The final volume was made up to 100 mL with distilled water [6].

Liquid amylase production (LAP) medium was used for quantitative amylase activity determinations of the isolates. 3 g yeast extract and 10 g soluble starch were dissolved in distilled water and the volume was completed to 1 L. Then 100 mL each was transferred to 250 mL flasks and sterilized at 121 °C for 15 minutes at 1.5 atm pressure.

Sodium phosphate buffer (100 mM, pH 7.0) was prepared by dissolving 15,487 g $Na_2HPO_4.7H_2O$ and 5,827 g $NaH_2PO_4.H_2O$ in distilled water to a concentration of 100 mM. The final volume was completed to 1 L.

Methods

Isolation of Bacteria from Potatoes

Bacterial isolates used in this study were isolated from potatoes. The samples were taken in sterile glass tubes from potatoes kept in the refrigerator and at room temperature for 15 days. For bacterial isolation, potato pieces were mixed in distilled water in sterile glass tubes, and dilutions were made at various ratios. Petri dishes containing NA medium were inoculated dropwise. The inoculated petri dishes were kept in an oven at 30 °C for 3 days and the microorganisms that grew were screened for amylase activity. Colonies thought to be different from the cultures growing on NA medium were isolated and purified by inoculation on fresh NA media. Purified cultures were stored in glycerol stocks at -80 °C.

Screening of Isolates for the Detection of Amylase-Producing Bacteria

For the screening of microorganisms producing the amylase enzyme, SNA media containing 1% soluble starch were inoculated with isolates. They were incubated in an oven at 30 °C for 1-3 days [7]. Bacterial colonies were stained with lugol solution. Amylolytic zone formation was observed around bacterial isolates that hydrolyse starch by synthesizing amylase enzyme. Bacterial isolates forming clear hydrolysis zone were considered as amylase positive. The isolates with the largest zones were selected and quantitative enzyme activity determination was performed with these bacteria.

Amylase Production in Liquid Media and Quantitative Amylase Activity Assay

Quantitative amylase activity determinations of amylase producers forming the widest hydrolysis zone were measured spectrophotometrically according to their ability to hydrolyse soluble starch used as their substrate. 1 mL of inoculum culture was inoculated into 100 mL of LAP media and incubated at 150 rpm and 30 °C. Amylase activities were checked for 4 days to determine the maximum level of amylase production.

After incubation, 1 mL of the liquid cultures were centrifuged at 6000 rpm for 10 minutes to remove bacteria and the supernatant was used as crude enzyme solution. In the sample tube, 0.5 mL of substrate solution and 0.5 mL of crude enzyme solution were placed. In the control tube, 0.5 mL substrate solution and 0.5 mL buffer (0.1 M sodium phosphate buffer, pH 7) were added. The prepared tubes were incubated in a water bath at 30 °C for 10 min. After incubation, 1 mL of DNS solution was added to each tube to stop the reaction and placed in boiling water for 5 minutes. The colour change in the tubes in boiling water was observed depending on the amount of maltose released. The tubes were removed from the boiling water and allowed to cool to room temperature. The optical density (OD) of the tubes at room temperature was measured in a 540 nm wavelength spectrophotometer (Shimadzu, Japan) and the enzyme activity was calculated according to the maltose standard graph [6].

Classical and Molecular Identification of Amylase Producer Isolate

Biochemical, morphological, and physiological tests were performed for the identifications of the selected isolate by classical methods. Morphological tests included the examinations of the colour and the shape of the colonies, the shape of the cells, Gram reaction, and KOH reaction. Biochemical tests included oxidase, catalase, haemolysis, urease, lipase, cellulase, protease, asparaginase, glutaminase activities in addition to, arabinose, maltose, and xylose fermentation reactions. Molecular identification of the selected isolate was performed by 16S rDNA sequence analysis. DNA sequences obtained were compared with existing data using the Blast Search Program of the National Center for Biotechnology Information (NCBI) data bank, similarities were determined and GenBank numbers were obtained.

Results

Isolation of Bacteria from Potatoes

Forty bacteria were isolated from potatoes kept at room temperature and refrigerator for 15 days and pure cultures were prepared and stored in glycerol stocks at -80 °C.

Amylase Activities of the Isolates

The amylase production potential of 40 purified bacterial isolates was determined by treatment with lugol solution after growth on SNA medium containing 1% soluble starch. An amylolytic transparent zone was observed in 25% of the tested bacteria. Isolates B5 (18 mm), B19 (5 mm), B22 (21 mm), B27 (14 mm) and B31 (12 mm) shown in Figure 1 were selected according to the width of the zone diameters on solid medium and used for quantitative amylase activity determination.

The 5 isolates with the largest amylolytic zone diameter in SNA were incubated in LAP medium and amylase activity determinations were performed. Activity calculations were made using the standard maltose graph. As shown in Figure 2, it was determined that the isolate with the highest activity was isolate B22 with 0.76 U/mL.

Identification of The Amylase Producing Isolate

Among the isolates whose amylase activities were compared, the bacterium coded B22, which formed the widest zone on SNA medium and had the highest activity in LAP medium, was identified by classical methods and 16S rDNA sequencing as *Priestia megaterium* strain SFA strain and received GenBank accession number OR415891.1.

Isolate B22 was observed to form cream coloured, shiny and round colonies and was immobile. It was Gram (+), haemolysis (-), catalase (+), urease (-), lipase (-), cellulase (+), asparaginase (+), and glutaminase (+). It was also able to ferment xylose, maltose, and arabinose sugars.

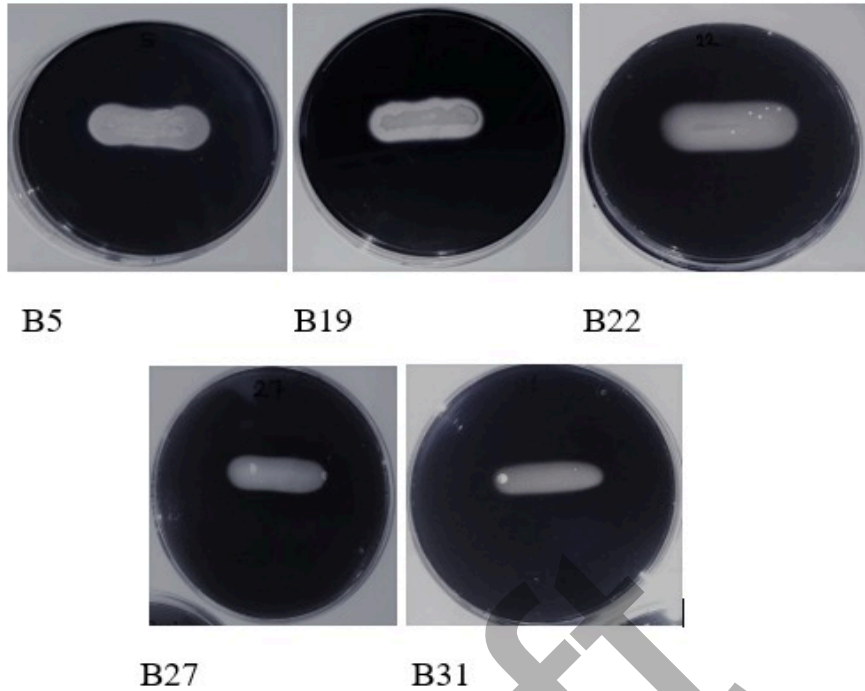**Figure 1.** Amylolytic zones observed after 2 days of incubation on SNA at 30 °C with isolates obtained from potato
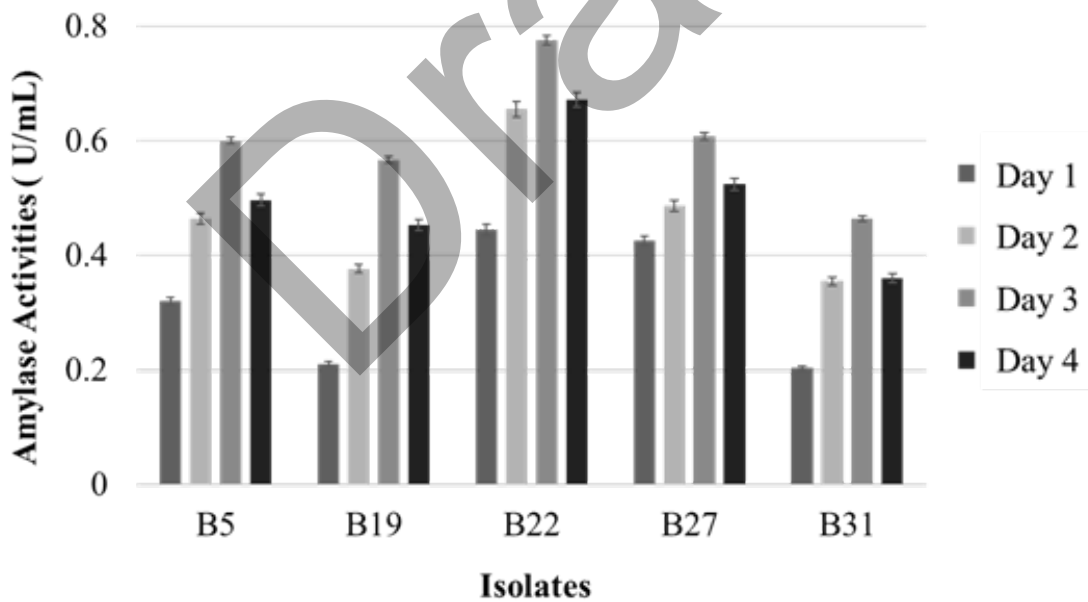

Figure 2. Amylase activities of bacterial isolates in liquid amylase production (LAP) medium at 30 °C.

The next phase of the investigation will involve the purification and characterization of the *P. megaterium* strain SFA amylase as well as assessment of the enzyme's possible biotechnological uses.

Conclusions

In conclusion, the isolation and identification of *Priestia megaterium* strain SFA from potatoes have yielded valuable insights into its amylase production potential. Through meticulous experimentation and analysis, isolate B22 emerged as a prominent candidate, exhibiting significant amylase activity. The characterization of this strain opens avenues for further research, particularly in understanding its enzymatic capabilities and exploring potential biotechnological applications. The findings underscore the importance of microbial diversity in natural environments and highlight the potential of bacterial isolates for industrial and scientific purposes. Moving forward, the purification and characterization of the *P. megaterium* SFA amylase hold promise for use in various fields. This study represents a crucial step towards harnessing the enzymatic potential of microorganisms for sustainable development and technological innovation.

References

[1] X. Ban, Y. Guo, B. Kaustubh, C. Li, Z. Gu, K. Hu, Z. Li, 2023. The Global amylase research trend in food science technology: A data-driven analysis. Food Rev. Int. 39(5) (2023) 2492-2506.

[2] M. Shad, N. Hussain, M. Usman, M.W. Akhtar, M. Sajjad, 2023. Exploration of computational approaches to predict the structural features and recent trends in α-amylase production for industrial applications. Biotechnol. Bioeng. 120(8) (2023) 2092-2116.

[3] M.A. Farooq, S. Ali, A. Hassan, H.M. Tahir, S. Mumtaz, S. Mumtaz, 2021. Biosynthesis and industrial applications of α-amylase: A review. Arch. Microbiol. 203 (2021) 1281-1292.

[4] S. Gürkök, 2019. Microbial enzymes in detergents: a review. Int. J. Sci. Eng. Res. 10(9) (2019) 75-81.

[5] D.B. Arya, S.G.T. Vincent, N. Balagurusamy 2022. Physiology of Ethanol Production by *Clostridium thermocellum*. Bioethanol: Biochemistry and Biotechnological Advances, (2022) 43.

[6] G. Miller, 1959. Use of dinitrosalicylic acid reagent for determination of reducing sugar. Anal. Chem. 31(3) (1959) 426-428.

[7] R. Singh, V. Kumar, V. Kapoor, 2014. Partial purification and characterization of a heat stable α-amylase from a thermophilic actinobacteria, *Streptomyces* sp. MSC702. Enzyme Res. (2014).

Acetylcholinesterase, Butyrylcholinesterase, and α-Amylase Enzymes Inhibitory Potentials of Cichorium Pumilum Extracts

E. Kaya[1], Ö. Narlı[2] and E. Kök[3]

[1]*Department of Food Processing, Technical Sciences Vocational School, Kahramanmaras Sutcu Imam University, Kahramanmaras, Türkiye, ORCID: 0000-0001-7213-3601*
[2,3]*Department of Bioengineering and Sciences, Institute of Natural and Applied Sciences, Kahramanmaras Sutcu Imam University, Kahramanmaras, Türkiye,* [2]*ORCID: 0000-0003-1218-019,* [3]*ORCID: 0009-0009-9339-5964*

Abstract

Cichorium pumilum, a member of the Astreacea family, is a perennial bushy plant species common to the Eastern Mediterranean region that produces blue or lavender blossoms. *Cichorium* species have many bioactive components. In this study, the in vitro inhibitory potentials of extracts of the aerial parts of *C. pumilum* prepared in solvents of different polarities (water, ethanol, and ethyl acetate) on acetylcholinesterase (AChE), butyrylcholinesterase (BChE), and α-amylase enzymes were investigated. According to the results of the study, ethanol extract showed the highest inhibitory effect on both AChE (IC$_{50}$:10.86 µg/mL) and BChE enzymes (IC$_{50}$:18.05 µg/mL), respectively. Additionally, it was found that the water extract demonstrated the most potent inhibitory impact on α-amylase, with an IC$_{50}$ value of 35.19 µg/mL. These findings indicate that the extracts have anticholinergic and antidiabetic properties, emphasizing the need for further in vivo investigations for the treatment of diseases caused by associated enzymes.

Keywords: Enzyme inhibition, acetylcholinesterase, butyrylcholinesterase, α-amylase

Introduction

Cichorium pumilum Jacq. is a member of the Asteraceae family. The Asteraceae family has three subfamilies. These are the Barnadesioideae, Cichorioideae, and Asteroideae. *Cichorium* species plants belong to the subfamily Cichorioideae. This family includes *C. intybus*, *C. endivia*, *C. bottae*, *C. spinosum*, *C. calvum* and *C. pumilum* [1]. *C. pumilum* (often known as chicory) has lavender or blue-colored flowers. It is a bushy perennial plant occasionally referred to as dwarf chicory [2]. *Cichorium* species are widely used in traditional medicine.

The chemical composition of *Cichorium* species consists of phenolic and polyphenolic compounds, fatty and organic acids and essential oils. Furthermore, research on these species has shown that they possess different pharmacological activities such as

antioxidant, antiproliferative, anti-inflammatory, antibacterial, antihyperglycemic, antidiabetic, and hepatoprotective effects [3].

In recent years, chicory has also been widely used in the food industry. This plant has also long been consumed by people as a vegetable [4]. As an example, chicory roots have gained popularity as a coffee replacement, replacing traditional brews in many parts of the World [5]. One of the most important molecules found in chicory root, inulin, has been the focus of a great deal of research about the prebiotic effect it displays [6]. *C. pumilum* leaves are utilized in the Eastern Mediterranean regions for the treatment of several health conditions, including diabetes, bacterial infections, poisoning, and rheumatism [7].

Many chronic diseases, including diabetes and Alzheimer's disease, are linked to the types and quality of foods consumed. In particular, secondary metabolites such as phenolic structures of various plant-based products are reported to be beneficial against such chronic diseases [8]. It is important to investigate the biological activity of *Cichorium* Species consumed as food. Furthermore, phenolic compounds are known to influence biological processes in cells by inhibiting certain metabolic enzymes.

Alzheimer's disease (AD) is a complex, progressive, and multifaceted neurological illness. Cholinesterase inhibitor treatment for Alzheimer's disease patients improves cognitive, behavioral, and functional symptoms [9]. However, because the inhibitory drugs utilized have numerous negative effects, various natural inhibitors of the acetylcholinesterase enzyme have been investigated.

Diabetes mellitus (DM) is a metabolic disease characterized by hyperglycemia due to a lack of insulin or resistance. Herbal extracts and their ingredients have received wide attention in clinical settings as safe antioxidants and potential inhibitors of important metabolic enzymes. For example, α-glycosidase and α-amylase are critical digestive enzymes involved in carbohydrate metabolism. They play a significant role in decreasing high blood sugar levels (hyperglycemia) in diabetic patients [10]. Plants are traditionally used to treat diseases, including diabetes. The species *Cichorium endivia* [11] and *Cichorium intybus* [12,13], which belong to the Cichorium family, have been reported for having antidiabetic effects.

The main objective of this study was to determine the possible inhibitory effects of different polarity extracts (water, ethanol, and ethyl acetate) prepared from the aerial parts of *C. pumilum* against AChE, BChE, and α-amylase enzymes. In the literature, it was observed that studies investigating *C. pumilum*'s inhibitory effect on enzymes associated with Alzheimer's disease were limited. The purpose of evaluating these inhibitory effects is to demonstrate the plant's potential antidiabetic and neuroprotective properties.

Material and Methods

Plant Materials

The *Cichorium pumilum* Jacq. plant used in this study was collected from the Hasanaga region of Kahramanmaras in September 2022. The species identification of the plant was made by Asst. Prof. Alper UZUN (Kahramanmaras Sutcu Imam University, Faculty of

Forestry, Türkiye). It was deposited at the Kahramanmaras Sutcu İmam University Faculty of Forestry Herbarium (KASOF) with herbarium number KASOF-3903.

Extracts Preparation

The plant, which were pulverized in a laboratory grinder, were taken at 10 grams each and mixed homogeneously with 200 mL of ultrapure water, ethanol, and ethyl acetate solvents in a magnetic stirrer for 24 hours. Then, all extracts were filtered in turn. The ethanol and ethyl acetate extracts were separated from their solvents using an evaporator. The plant's water extract was frozen at 20°C and then lyophilized.

Acetylcholinesterase/ Butyrylcholinesterase inhibition studies

Water, ethanol, and ethyl acetate extracts of the aerial parts of *C. pumilum* were examined for their effects on acetylcholinesterase and butyrylcholinesterase enzymes using the Ellman method [14].

In the study, control tubes and sample tubes were prepared. Acetylthiocholine iodide/ butyrylthiocholine iodide, DTNB, Tris-HCl, purified water, AChE/BChE enzyme and extracts were added to the tubes and mixed. After the reaction started, the mixtures' absorbance was measured at 412 nm. The activity (%)-[extract] graph was drawn using the obtained data. IC_{50} values were calculated using the graph.

α-amilase inhibition studies

The antidiabetic potential of the plant was assessed by examining the inhibitory effects of water, ethanol, and ethyl acetate extracts on the α-amylase enzyme. α-amylase inhibition experiments were performed using previously reported methods [15].

Sodium phosphate buffer (10 mM, pH:6.9, 0.006 M NaCl) was prepared. The extracts were diluted in ethanol to make stock solutions containing different concentrations. α-amylase enzyme (1.5 μl enzyme) was prepared by dissolving in 10 ml sodium phosphate buffer. The test tubes were filled with buffer, sample, and enzyme solutions and incubated for 25 minutes at 37°C. Next, a 1% starch solution was added to test tubes and incubated at 37°C for 25 minutes. After that, DNS solution was added, and all test tubes were placed in a boiling water bath for 5 minutes. After the tubes were vortexed, their absorption was measured to at 540 nm. The results were calculated as IC_{50} values.

Result and Discussıon

Many treatments used to relieve symptoms of disorders such as Alzheimer's, diabetes, and obesity include the inhibition of metabolic enzymes [16]. In this context, cholinesterases have been associated with several neurodegenerative diseases, such as Alzheimer's disease. There has also been a lot of research on the metabolic enzyme inhibition potential of pharmaceuticals and natural extracts.

This study was investigated the inhibitory effects of water, ethanol, and ethyl acetate extracts of *C. pumilum* on the enzymes acetylcholinesterase, butyrylcholinesterase, and α-amylase. The results are shown in Table 1 with IC_{50} values.

Table 1. The enzyme inhibition results (IC_{50} values) of the extracts on AChE, BChE anda α-amylase enzymes

Compounds	AChE(µg/mL)		BChE(µg/mL)		α-amylase(µg/mL)	
	IC_{50}	r^2	IC_{50}	r^2	IC_{50}	r^2
Water extract	15.60	0.9654	30.15	0.9514	35.19	0.9923
Ethanol extract	10.86	0.9912	18.05	0.9346	44.32	0.9715
Ethyl acetate extract	29.26	0.9732	38.12	0.9596	59.55	0.9803

In this study, the ethanol extract shown significant inhibition on AChE/BChE, with IC_{50} values of 10.86 µg/mL (r^2: 0.9912) and 18.05 µg/mL (r^2: 0.9346), respectively. Ethyl acetate extract showed the weakest effect on both the AChE and BChE enzymes (Table 1). Previous study has indicated that extracts obtained from the roots of *Cichorium intybus* L. exhibit a potent inhibitory effect on the AChE enzyme [17]. As can be seen in the study, extracts containing significant phytochemicals are thought to inhibit cholinesterase enzymes and may be useful in the treatment of neurodegenerative illnesses.

Inhibition of AChE/BChE and α-amylase enzymes plays important roles in the treatment of Alzheimer's disease, hyperglycemia, and diabetes [18]. In this study (Table 1), it was found that the water extract of *C. pumilum* exhibited the most effective inhibitory effect against α-amylase. However, ethyl acetate extract demonstrated the lowest inhibitory effect against α-amylase. In another study, water extract of *Cichorium endivia* leaves also showed inhibitory effect on the α-amylase enzyme [11]. The results of this study are in agreement with previous studies on the inhibition effects of different *cichorium* species on α-amylase activities.

Conclusions

The study found that extracts of *C. pumilum* at different polarity inhibited AChE, BChE, and α-amylase enzymes. These findings indicate that *C. pumilum* has potential neuroprotective and antidiabetic properties. The results will contribute to a better knowledge of *C. pumilum's* biological activities and will help in the search for promising natural therapeutic agents, particularly for the treatment of chronic illnesses like Alzheimer's disease and diabetes.

References

[1] A.M Kiers, T.H Mes, R. van der Meijden, K.Bachmann, 2000. A search for diagnostic AFLP markers in *Cichorium* species with emphasis on endive and chicory cultivar groups, Genome. 43(3) (2000) 470–476.

[2] W. Al Khateeb, E.Hussein, L. Qouta, M. Alu'datt, B. Al-Shara, A. Abu-Zaiton, 2012. In vitro propagation and characterization of phenolic content along with antioxidant and antimicrobial activities of *Cichorium pumilum* Jacq, Plant Cell, Tissue Organ Cult. (PCTOC). 110 (2012) 103-110.

[3] Z. Boghrati, E. Zibaee, Z. Ayati, M.S. Amiri, M. Ramezani, T. Jamialahmadi, A. Sahebkar, 2021. Ethnomedicinal Uses, Phytochemistry and Pharmacology of Different *Cichorium* Species (Asteraceae): A Review, Pharmacol. Prop. Plant- Deriv. Nat. Prod. Implic. Hum. Health. (2021) 501-546

[4] C.L. Pouille, D. Jegou, C. Dugardin, B. Cudennec, R. Ravallec, P. Hance, C. Rambaud, J.L. Hilbert, A. Lucau-Danila, 2020. Chicory root flour–A functional food with potential multiple health benefits evaluated in a mice model, J. Funct. Foods. 74 (2020) 104174

[5] D. Komes, A. Bušić, A. Vojvodić, A. Belščak-Cvitanović, M. Hruškar, 2015. Antioxidative potential of different coffee substitute brews affected by milk addition, Eur. Food Res. Technol. 241(2015) 115-125.

[6] C.L. Pouille, S. Ouaza, E. Roels, J. Behra, M. Tourret, R. Molinié, J.X. Fontaine, D. Mathiron, D. Gagneul, B. Taminiau, G. Daube, R. Ravallec, C. Rambaud, J.L. Hilbert, B. Cudennec, A. Lucau-Danila, 2022. Chicory: Understanding the effects and effectors of this functional food, Nutrients. 14(5) (2022) 957.

[7] H. Azaizeh, B. Saad, K. Khalil, O. Said, 2006. The state of the art of traditional Arab herbal medicine in the Eastern region of the Mediterranean: a review, Evidence-Based Complementary Altern. Med. 3 (2006) 229-235.

[8] P. Taslimi, E. Köksal, A.C. Gören, E. Bursal, A. Aras, Ö. Kılıç, S. Alwasel, İ. Gülçin, 2020. Anti-Alzheimer, antidiabetic and antioxidant potential of *Satureja cuneifolia* and analysis of its phenolic contents by LC-MS/MS, Arabian J. Chem. 13(3) (2020) 4528-4537.

[9] M.H. Oh, P.J. Houghton, W. K. Whang, J.H. Cho, 2004. Screening of Korean herbal medicines used to improve cognitive function for anti-cholinesterase activity, Phytomedicine. 11(6) (2004) 544-548.

[10] Z. Bingol, H. Kızıltaş, A.C. Gören, L. Polat Kose, M. Topal, L. Durmaz, S.H. Alwasel, I. Gulcin, 2021. Antidiabetic, anticholinergic and antioxidant activities of aerial parts of shaggy bindweed (*Convulvulus betonicifolia* Miller subsp.)–profiling of phenolic compounds by LC-HRMS, Heliyon. 7(5) (2021).

[11] Z.H. Kamel, I. Daw, M. Marzouk, 2011. Effect of *Cichorium endivia* leaves on some biochemical parameters in streptozotocin-induced diabetic rats, Aus. J. Basic. And App Sci. 5(7) (2011) 387-96.

[12] A.S. Alkofahi, K.K. Abdul-Razzak, K.H. Alzoubi, O.F. Khabour, 2017. Screening of the Anti-hyperglycemic activity of some medicinal plants of Jordan, Pak. J. Pharm. Sci. 30(3) (2017) 907-913.

[13] A. Dalar, I. Konczak, 2014. *Cichorium intybus* from Eastern Anatolia: Phenolic composition, antioxidant and enzyme inhibitory activities. Ind. Crops Prod. 60 (2014) 79-85.

[14] G.L. Ellman, K.D. Courtney, V. Andres, R.M.A. Featherston, 1961. New and rapid colorimetric determination of acetylcholinesterase activity, Biochem. Pharmacol. 7 (1961) 88–95.

[15] M. Akyüz, L. Yabo-Dambagi, T. Kılıc, A. Cakır, 2022. Antidiabetic, neuroprotective and antioxidant potentials of different parts of *pistacia terebinthus* fruits, S. Afr. J. Bot. 147(2022) 443–456.

[16] G. Luisi, A. Stefanucci, G. Zengin, M.P. Dimmito, A. Mollica, 2018. Antioxidant and tyrosinase inhibitory in vitro activity of amino acids and small peptides: New hints for the multifaceted treatment of neurologic and metabolic disfunctions, Antioxidants. 8(1) (2018) 7.

[17] A. Jaśkiewicz, G. Budryn, M. Carmena-Bargueño, H. Pérez-Sánchez, 2022. Evaluation of Activity of Sesquiterpene Lactones and Chicory Extracts as Acetylcholinesterase Inhibitors Assayed in Calorimetric and Docking Simulation Studies, Nutrients. 14(17) (2022) 3633.

[18] G. Zengin, M.J. Rodrigues, H.H. Abdallah, L. Custodio, A.Stefanucci, M.Z. Aumeeruddy, A. Mollicae, K.R.R. Rengasamyg, M. F. Mahomoodally, 2018. Combination of phenolic profiles, pharmacological properties and in silico studies to provide new insights on *Silene salsuginea* from Turkey, Comput. Biol. Chem. 77(2018) 178-186.

A Promising Approach to Recover Non-arable Soils with Different Contaminants: Bacterial Bioremediation

D. Efe[1]

[1]*Espiye Vocational School, Giresun University, Giresun, Türkiye, ORCID: 0000-0003-4230-6780*

Nowadays, the soil has been subjecting excessive contamination all over the World because of uncontrolled industrialization. Considering the increasing world population, it is obvious that the need for food will increase day by day and humanity will face hunger [1]. In this context, recovering non-arable agricultural lands because of different contaminants such as aliphatic and aromatic hydrocarbons, chlorinated solvents, pesticides, and heavy metals is a vital necessity [2]. For this reason, researchers have intensely focused on bacterial bioremediation due to the bacteria's adaptation to all conditions such as extreme hot or cold, acidic or basic, contaminated with harmful chemicals, without nutrients, the advantages of their adaptation, their degrading or remediating capability of the contaminants [3]. It is aimed to give an overview of bacterial bioremediation (its advantages and disadvantages, application areas, etc.) in this paper.

Key words: non-arable, bioremediation, heavy metal, bacteria

Introduction

Nowadays, the global soil pollution has become one of the major threats to the ecosystem and the world population [1]. The main causes of the soil pollution are the substances such as toxic heavy metals, petroleum, and polythenes produced by the different industries including mining, electricity and battery generation, textile industry. The soil is the basis of the life, as the soil provides habitat for millions of organisms including bacteria, fungi, plants, animals, human beings. The continuation of the food chain, which is essential for the survival of all living things, is because the soil is a suitable environment for the growing of plants by serving as nutrient element reservoir [2]. The human population is globally estimated to be 8 billion by 2050 and 11 billion by 2100, respectively. As a result of excessively increasing world population and industrialization, it is obviously seen that not only natural life but also people will be in danger of food shortage and hunger in the future [3]. Anyway, the non-degradable pollutants such as heavy metals, polythenes, and polychlorinated biphenyls cause many health diseases such as cancer, damages of nervous system, liver, and kidney because of their mutagenic and oxidant effects [4]. At this point, the researchers have been giving great attention to protect arable soils and remediate non-arable soils, which play a vital role to produce food and feed the growing global population [5].

In the past, there have been used conventional remediation methods including physical (excavation, landfilling, and washing) and chemical methods. Physical remediation methods are high costly and time consuming. Chemical remediation methods mostly use large amounts of chemicals and produce toxic products [6-8].

Among different strategies to remediate the contaminated soils, bioremediation defined as degradation of pollutants via biological mechanisms, is the most promising approach because of many advantages such as being effective, cost effective, environment-friendly, and practical. The bioremediation processes have been performing by using algae, fungi, and bacteria to remove, degrade or render harmless the pollutants [9, 10]. Bacteria have great biodiversity with the ability to adapt almost every environments, which are extremely cold, hot, acidic, basic, salty, contaminated, etc. To utilize bacteria in bioremediation is more advantageous than the others as they can be used in every different environmental conditions and support insect control, nutrient recycling, and plant growth promotion with bioremediation [11-14].

The different application methods of bacterial bioremediation are adding bacteria or bacterial metabolites (enzymes, biosurfactants, etc.) into the contaminated soils to reduce or transform the contaminants [15]. Although adding bacterial metabolites to the soil for its remediation yields in a very short time, its sustainability is challenging as continuous addition of metabolites to the environment is required to continue the process. Therefore, the most preferred method is the direct addition of bacteria with bioremediation potential to the contaminated soil or providing the best possible conditions for the used bacteria in the remediation process [15, 16]. Biostimulation and bioaugmentation are the most common methods used in in situ bioremediation. Biostimulation is to increase and stimulate the natural microorganism population with the bioremediation potential by optimizing bacterial living conditions via nutrient addition, aeration, supplying optimum temperature and pH [17]. The main advantage of this method is that the process is performed by indigenous bacteria that are perfectly adapted to the environment and well distributed within the soil. On the other hand, the main disadvantage is that growth promotion of the other bacteria with no bioremediation potential and then formation creating a competition between the useful bacteria and the useless bacteria for the process. The difficulties in distributing the necessary factors such as nutrients, oxygen, etc. evenly in the environment is another disadvantage [18].

In some cases, the native indigenous bacteria have no pathway to dispose of the contaminants and applying biostimulation does not provide any benefit recover the soil or the population size may not have enough individuals to show its effect on soil remediation. Therefore, if the indigenous bacterial population is not sufficient, bioaugmentation should be preferred instead of biostimulation. In biougmentation process, the indigenous or exogenous microbial culture that can neutralize or degrade the contaminants and generally isolated from contaminated environment is added in to soil. The success of this approach depends on the properties of bacterial cultures such as their survival in hostile and contaminated area, viability during storage and maintaining

genetic stability, competitiveness with indigenous microorganisms, mobility through the soil pores [18].

The researchers have been still trying with great interest to increase the efficiency of bioremediation processes. Recently, some studies have indicated to use combination of bioaugmentation and biostimulation methods mostly results in higher remediation rates. Because the addition of appropriate bacteria to the soil and their stimulation for the best performance by optimizing their requirements will speed up the amerolization process of the soil. In addition, the used bacteria can be genetically modified by gene engineering techniques to increase their ability yield [19, 20].

Conclusions

Bioremediation is a more environment-friendly, cheaper, and promising method than physical and chemical remediation methods to recover non-usable and contaminated agricultural lands. The two different bioremediation approaches, bioaugmentation and biostimulation, have advantages and disadvantages relative to each other. However, it is seen that it would be useful to choose the method of bioremediation or to combine two methods regarding the properties of the soil and contaminant. In addition, to ensure continuity of the soil remediation, it is vital to determine by laboratory and field trials essential nutrient needs (carbon, phosphorous, iron, carbonates, nitrogen, oxygen or another electron acceptor) and optimum conditions (temperature, pH, salt concentration) for bacterial growth and activating. The method of bioremediation and the bacteria to be to utilize should be chosen according to the obtained results from the optimum conditions experiments for bacteria. Because, the more the optimum conditions needed by the bacteria parallel the natural state of the contaminated soil, the more efficient, inexpensive and effortless the bioremediation process will be.

In conclusion, it is a clear fact that the researchers will continue to conduct new research to increase bioremediation efficiency in the future.

References

[1] FAO:202. Global assessment of soil pollution-summary for policy makers. Report. Reme: FAO: 2020.

[2] E.C. Brevik, T.J. Sauer, 2015 The past, present, and future of soils and human health studies, Soil. 1 (2015), 35-46.

[3] United Nations, Department of Economic and Social Affairs, Population Division, 2019. World Population Prospects 2019: Highlights (ST/ESA/SER.A/423). (https://www.un.org/development/desa/publications/world-population-prospects-2019 highlights.html.)

[4] , J. Briffa, E. Sinagra, R. Blundell, 2020. Heavy metal pollution in the environment and their toxicological effects on humans. Heliyon 6 (2020), e04691.

[5] W.L. Silver, T. Perez, A. Mayer, A.R. Jones, 2021. The role of soil in the contribution of food and feed. Phil. Trans. R. Soc. B 376 (2021), 20200181.

[6] E.V. Lau, S. Gan, H.K Ng, P. Eong, 2014. Extraction agents for the removal of polycyclic aromatic hydrocarbons (PAHs) from soil in soil washing technologies. Environ. Pollut. 184 (2014), 640-649.

[7] C. Liu, H. Shi, C. Wang, Y. Fei, Z. Han,2022. Thermal Remediation of Soil Contaminated with Polycyclic Aromatic Hydrocarbons: Pollutant Removal Process and Influence on Soil Functionality. Toxics. 10(8) (2022), 474-486.

[8] B. Ranc, P.Faure, V. Croze, C. Lorgeoux, M.O. Simonnot,2017. Comparison of the effectiveness of soil heating prior or during in situ chemical oxidation (ISCO) of aged PAH-contaminated soils. Environ. Sci. Pollut. Res. 24 (2017), 11265-11278.

[9] S. Bala, D. Garg, B.V. Thirumalesh, M. Sharma, K. Sridhar, B.S. Inbaraj, M. Tripathi, 2022. Recent Strategies for Bioremediation of Emerging Pollutants: A Review for a Green and Sustainable Environment. Toxics. 10(484) (2022), 1-24.

[10] A. Hussain, F. Rehman, H. Rafeeq, M. Waqas, A. Asghar, N. Afsheen, A. Rahdar, M. Bilal, H.M. Iqbal, 2022. In-situ, Ex-situ, and nano-remediation strategies to treat polluted soil, water, and air-A review. Chemosphere 289 (2022), 133252.

[11] M. Tripathi, S.K. Garg, 2014. Dechlorination of chloroorganics, decolorization and simultaneous bioremediation of Cr^{6+} from real tannery effluent employing *indigenous Bacillus cereus* isolate. Environ. Sci. Pollut. Res. 21 (2014), 5227-5241.

[12] D. Efe, 2020. Potential Plant Growth-Promoting Bacteria with Heavy Metal Resistance. Curr Microbiol. 77(12) (2020), 3861-3868.

[13] D. Kour, T. Kaur, R. Devi, A. Yadav, M. Singh, D. Joshi, 2021. Beneficial microbiomes for bioremediation of diverse contaminated environments for environmental sustainability: Present status and future challenges. Environ. Sci. Pollut. Res. 28 (2021), 24917-24939.

[14] M.J. Krzmarzick, D.K. Taylor, X. Fu, A.L. McCutchan, 2018. Diversity and niche of archaea in bioremediation. Archaea. 2018 (1), 1-17.

[15] M. Tyagi, M.M. da Fonseca, C.C. de Carvalho, 2010. Bioaugmentation and biostimulation strategies to improve the effectiveness of bioremediation processes. Biodegradation. 2011 2 (2011),231-241.

[16] A.S. Nwankwegu, L. Zhang, D. Xie, C.O. Onwosi, W.I. Muhammad, C.K. Odoh, K. Sam, J.N. Idenyi, 2021. Bioaugmentation as a green technology for hydrocarbon pollution remediation. Problems and prospects. J Environ Manage. 15 (304) (2022), 114313.

[17] , R. Margesin, F. Schinner, 2001. Bioremediation (natural attenuation and biostimulation) of diesel-oil-contaminated soil in an alpine glacier skiing area. Appl. Environ. Microbiol. 67 (2001), 3127-3133.

[18] G.O. Adams, P.T. Fufeyin, S.E. Okoro, I. Ehinomen, 2015. Bioremediation, Biostimulation and Bioaugmention: A Review. J. bioremediat. biodegrad. 3(1), (2015), 28-39.

[19] S. Abdulsalam, A.B. Omale, 2009.Comparison of Biostimulation and Bioaugmentation Techniques for the Remediation of Used Motor Oil Contaminated Soil. BABT. 52(3), (2009), 747-754.

Effects of β-arbutin on Apoptosis and Cell Cycle A549 and H1299 Lung Cancer Cells

E. Terzi[1]

[1]Institution, City, Country, ORCID: (in Segoe UI, 9 pt, italic style)
[1]Ankara Yildirim Beyazit University Medical Faculty Medical Biology Department, Ankara, Türkiye, ORCID: 0000-0001-9106-3848

Abstract

Lung cancer is a type of cancer that causes 2.2 million new cases and 1.8 million deaths in 2020, leading cause of cancer-related deaths in both men and women. [1]. Most lung cancer patients are diagnosed in advanced stages where the chance of treatment is difficult. Up to now, imaging techniques and treatment options are being enhanced to decrease lung cancer mortality. Due to the toxic effects of conventional cancer treatment methods on healthy cells, bioactive phytochemicals have recently attracted great attention for their medical uses [2]. β-Arbutin is a hydroquinone-β-D-glucopyranoside phytochemical commonly found in plants [3]. Since β-Arbutin does not have side effects such as irritation and sensitivity, it is commonly used as a skin whitening agent [4]. In addition, it also has biological properties such as anti-oxidant, anti-microbial, anti-inflammatory and anti-cancer [5]. This study was aimed to determine the effect of β-Arbutin on apoptosis and cell cycle in A549 and H1299 lung cancer cells. For this purpose, A549 and H1299 lung cancer cells were cultured. The WST-1 test was used to identify the optimum dose of β-Arbutin on A549 and H1299 cells. To determine the apoptotic and cell cycle effects, flow cytometry was performed. Statistical significance level was accepted $p \leq 0.05$. According to the these data, the doses of β-Arbutin were found to be 4,060 mM and 3,879 mM for the A549 and H1299 cells, respectively, at the 24h. It has been observed that β-Arbutin induces apoptosis in lung cancer cells ($p < 0,0001$ for A549 cell line, $p < 0,0001$ for H1299 cell line) and arrests the cell cycle at the G1 stage for A549 and H1299 cell lines. As a result of this study, it can be said that β-Arbutin reduces cell viability in lung cancer cells and induces apoptosis through the caspase 3/7 pathway.

Keywords: Lung cancer, β-Arbutin

Introduction

Lung cancer has high morbidity and mortality rates and ranks among the most prevalent forms of cancer, globally. Based on histological categorization, lung cancer is classified into two main types: small cell lung cancer (SCLC) and non-small cell lung cancer (NSCLC) [6]. SCLC is a high-grade neuroendocrine tumor that accounts for approximately 15% of all lung cancers. It is characterized by high proliferative rate, early metastasis and poor

prognosis [7]. NSCLC is the most common subtype of lung cancer, comprising around 85-90% of all cases. NSCLC consists of many subtypes, including lung squamous adenocarcinoma, lung squamous carcinoma, and large cell lung cancer [8]. The prevalence of lung cancer is elevated in nations with a high prevalence of tobacco consumption, with tobacco use being responsible for over 80% of lung cancer cases. Other risk factors for lung cancers are secondhand smoke, asbestos, air pollution and arsenic [9]. Treatment of lung cancer in the early stages is surgical resection of the tumor along with adjuvant therapy. Treatment methods used in advanced disease stages are chemotherapy and radiotherapy. Chemotherapy agents used in the treatment of lung cancer have limitations such as nonspecific targeting, low bioavailability, and the development of drug resistance. Although there are many treatment methods for lung cancer, these treatment methods still face great difficulties. Therefore, there is a need to develop new and effective treatment strategies for lung cancer [10]. Natural compounds are bioactive molecules obtained from plants and show high levels of bioavailability. They have unique chemical structures and have higher levels of potency than synthetically produced compounds [11]. In recent years, natural products have begun to be used as drug derivatives in traditional medicine and studies have been carried out to evaluate these compounds. Numerous studies have shown that natural compounds can provide anticancer effects against the mechanisms that cause lung cancer development [12]. Arbutin is a compound with a structure in which a D-glucose molecule is linked to hydroquinone. It can appear in the form of α-, β-, or γ-. β-Arbutin is a natural compound obtained from plants such as wheat, grapes and bearberry, where the β anomer of D-glucose is bonded to hydroquinone (Figure 1) [13]. β-Arbutin inhibits melanin formation and tyrosinase activity in skin cells without affecting cell proliferation. It can also accelerate the excretion of melanin, thus reducing skin pigmentation. It does not show side effects such as toxicity, irritation or sensitivity. So it can be a cosmetic product as a cream formulation [14]. In addition, it can be used in the treatment of urinary tract infections and as an antioxidant. Also, β-Arbutin has anti-inflammatory and anti-tumor activities [15]. In vitro studies have demonstrated that β-Arbutin has a cytotoxic effect against many cell lines such as bladder, bone, brain, breast, cervical, colon, stomach, liver, prostate and skin cancer [5]. In this study, the effects of β-Arbutin were determined on apoptosis and cell cycle in lung cancer cell lines, in parallel with the studies in the literature.

Materials and Methods

Cell culture

Human lung cancer cell lines A549 and H1299 were obtained from American Type Culture Collection (ATCC). A549 cell line was cultured in high glucose DMEM medium (Dulbecco's Modified Eagle Medium) (Capricorn) containing %10 FBS (Fetal Bovine Serum) (Capricorn) and 1% penicilin streptomycin at 37°C and 5% CO_2 conditions. H1299 cell line was cultured in RPMI (Capricorn) medium containing %10 FBS and 1% penicilin streptomycin at 37°C and 5% CO_2 conditions. Passage was performed when the density of cells reached 80-90%. Trypsin-EDTA (Gibco) was used to detach cells while passaging.

Isolation of β-arbutin

β-arbutin was purified from the aerial parts of *Onobrychis buhseana* collected from Nakhchivan region. The dried and ground plant sample was extracted by maceration with an ethanol solvent and then separated into fractions by thin layer and silica gel column chromatography methods. β-arbutin was highly purified from the sub-fractions, its chemical structure was characterized by 1H and 13C NMR spectroscopic methods [16].

Preparation of β-Arbutin

β-Arbutin was prepared by dissolving in dimethyl sulfoxide (DMSO) as a 100 mM stock solution. It was tested at 24th and 48th hours at concentrations 0, 2.5, 5, 10, 20, 30 mM respectively.

Cytotoxicity Analysis

WST-1 test was performed to determine the effective doses of β-Arbutin on A549 and H1299 cell lines. A549 and H1299 cells were seeded in 96-well plates and β-Arbutin was applied to the cells at 2.5, 5, 10, 20, 30 mM concentrations, respectively. 10 µL of WST-1 solution (Cayman Chemical) was added to each well and the cells were incubated at 37°C for 2-4 hours. In the final stage of the test, measurements were made at 450 nm wavelength on the Thermo Varioskan device. Inhibitory dose (IC_{50} value) that inhibit 50% of the cells were calculated in the Graphpad Prism 9.1.0 program.

Annexin V/PI Analysis

β-Arbutin was applied to A549 and H1299 cells at doses of 3,879 mM, 4,060 mM respectively and treated for 24h. At the end of incubation, cells were detached with Trypsin-EDTA. After that, collected cells were washed with PBS and binding buffer was added at a 1:1 ratio. Cells were placed in a 12x75 mm polystyrene tube. Then, 1X Annexin Binding buffer and 5 µl Annexin V-Fluorescent Isothiocyanate (Annexin V-FITC) and Propidium Iodide (PI) were added to each tube. The cells were incubated at room temperature for 15 minutes and then measurements were made with an ACEA novocyte flow cytometry device (Agilent). After the analysis, the living cells were evaluated as PI (-), Annexin V (-); early apoptotic cells were evaluated as PI (-), Annexin V (+); Late apoptotic cells were evaluated as PI (+), Annexin V (+), and necrotic cells were evaluated as PI (+), Annexin V (-).

Caspase 3/7 Analysis

TheAat Bioquest Cell Meter Caspase 3/7 Activity Apoptosis Assay Kit was utilized to demonstrate that A549 and H1299 cells use the caspase 3/7 apoptotic pathway. A549 and H1299 cells were treated with β-Arbutin and incubated. After incubation, collected live and dead cells were studied according to the Aat Bioquest Cell Meter Caspase 3/7

Activity Apoptosis Assay protocol. Measurements were made on the ACEA Novocyte (Agilent) flow cytometry device.

Cell Cycle Analysis

β-Arbutin was applied to A549 and H1299 cells at doses of 3,879 mM, 4,060 mM respectively and treated for 24h. At the end of incubation, cells were detached with Trypsin-EDTA and centrifuged in PBS. The cells were fixed with 70% ethanol at 4°C for 20 minutes and then washed twice with PBS. To stain the DNA, the cells were treated with propidium iodide (PI). To achieve the best DNA resolution, the cells were treated with RNase, since PI can also attach to double-stranded RNA. Then the cells were exposed to a solution of 40 mg/mL of PI, 0.1% NP-40, and 20 mg/mL of RNase A for 30 minutes at 4°C in the dark. The DNA content of both the control and β-Arbutin treated cells were measured with an ACEA novocyte flow cytometry device (Agilent).

Results

Determination of the effective β-Arbutin dose in A549 and H1299 lung cancer cells

β-Arbutin was applied to A549 and H1299 lung cancer cells at doses of 0, 2.5, 5, 10, 20, 30 mM at the 24th and 48th hour and the appropriate cytotoxic dose for the cells was determined.

According to WST-1 results, the viability rates for A549 cells treated with β-Arbutin for 24 hours at concentrations of 0, 2.5, 5, 10, 20, 30 mM were %100, %57.71, %36.12, %29.29, %14.76, %13.06, respectively. For A549 cells treated with β-Arbutin for 48 hours at concentrations 0, 2.5, 5, 10, 20, 30 mM, the viability rates were %100, %48, %36, %30.15, %12.27, %7.46, respectively (Figure 2).

For H1299 cells treated with β-Arbutin for 24 hours, the viability rates were %100, %57,78, %42,39, %15,98, %13,41, %12,47 at concentrations of 0, 2.5, 5, 10, 20, 30 mM, respectively. For H1299 cells treated with β-Arbutin for 48 hours, the viability rates were %100, %45, %35.3, %18.2, %16.12, %13.51 at concentrations of 0, 2.5, 5, 10, 20, 30 mM, respectively (Figure 3).

Based on these findings, it was determined that the appropriate β-Arbutin dose for A549 and H1299 cells were 4.060 mM and 3.879 mM at the 24h, respectively.

Determination of the effects of β-Arbutin on the cell viability and apoptosis of A549 and H1299 cells by Annexin V/PI Analysis

To determine the effects of β-Arbutin on apoptosis and cell viability in A549 and H1299 cells, flow cytometry was performed using propidium iodide (PI) and Annexin V/FITC. The cells were divided into two groups: the control group and the β-Arbutin tretated group.

β-Arbutin-treated A549 and H1299 cells showed a significant increase in apoptosis compared to the control group (p<0,0001 for A549 cell line, p<0,0001 for H1299 cell line). Additionally, a significant decrease in cell viability was observed in β-Arbutin-treated A549 and H1299 cells compared to the control group (p<0,0001 for A549 cell line, p<0,0001 for H1299 cell line) (Figure 4, 5).

Determination of the effect of β-Arbutin on A549 and H1299 lung cancer cell death by caspase 3/7 Analysis

After Annexin V/PI analyses, caspase 3/7 activation was examined in control group, β-Arbutin treated A549 cells and β-Arbutin treated H1299 cells by flow cytometry. It was observed that caspase 3/7 activity was significantly increased in A549 and H1299 cells treated with β-Arbutin compared to the control group (p<0,0001 for A549 cell line, p<0,0001 for H1299 cell line) (Figure 6).

Determination of the effect of β-Arbutin on cell cycle in A549 and H1299 cells

The changes of cell cycle in A549 and H1299 cells were observed by flow cytometry after treatment with β-Arbutin. The percentage of control cells for the A549 cell line was 59.01, 23.50, 15.38 for the G1, S, and G2 phases, and 83.25, 12.31, 4.11 for the β-Arbutin treated A549 cells, respectively. The percentages of control cells for the H1299 cell line were 44.98, 37.61, 16.70 for the G1, S, and G2 phases and 61.17, 30.37, 8.35 for the β -Arbutin treated H1299 cells respectively. According to these findings, it can be said that β -Arbutin arrests the cell cycle at the G1 stage for A549 and H1299 cell lines (Figure 7).

CONCLUSİON

In this study, the effects of β-Arbutin on apoptosis and cell cycle in A549 and H1299 lung cancer cells were demonstrated. β-Arbutin has been observed to induce apoptosis and arrest the cell cycle in A549 and H1299 cells. It has been determined that β-Arbutin shows very effective results when applied to lung cancer cells.

ACKNOWLEDGEMENT
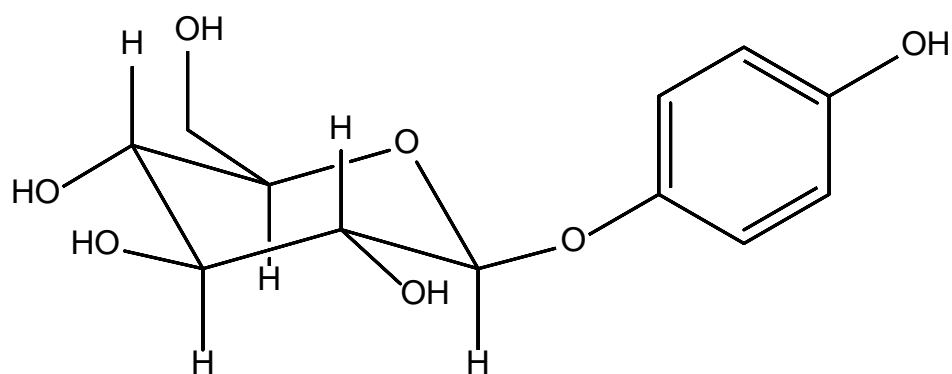
FIGURES

Figure 1. Structure of β-Arbutin
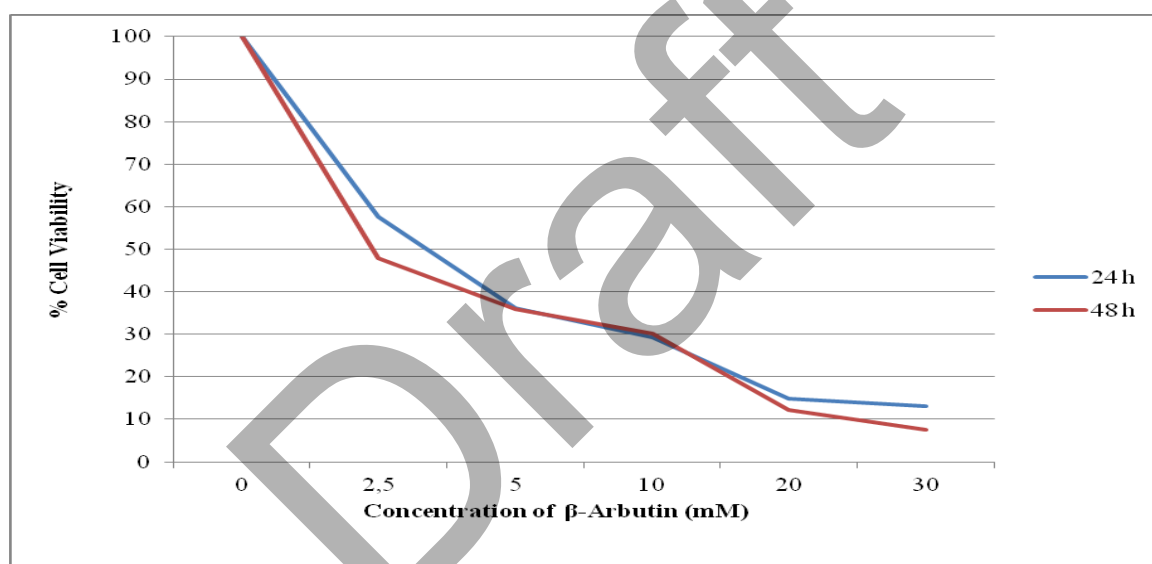
Figure 2. Cell viability graph of A549 cells treated with different concentrations of β-Arbutin for 24h and 48h.
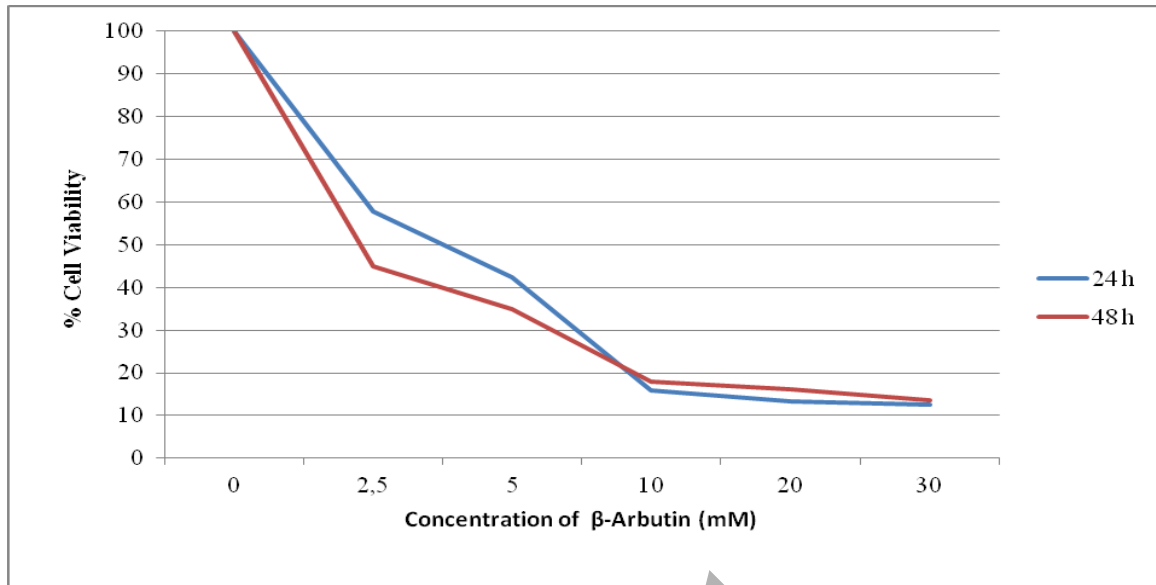
Figure 3. Cell viability graph of H1299 cells treated with different concentrations of β-Arbutin for 24h and 48h.
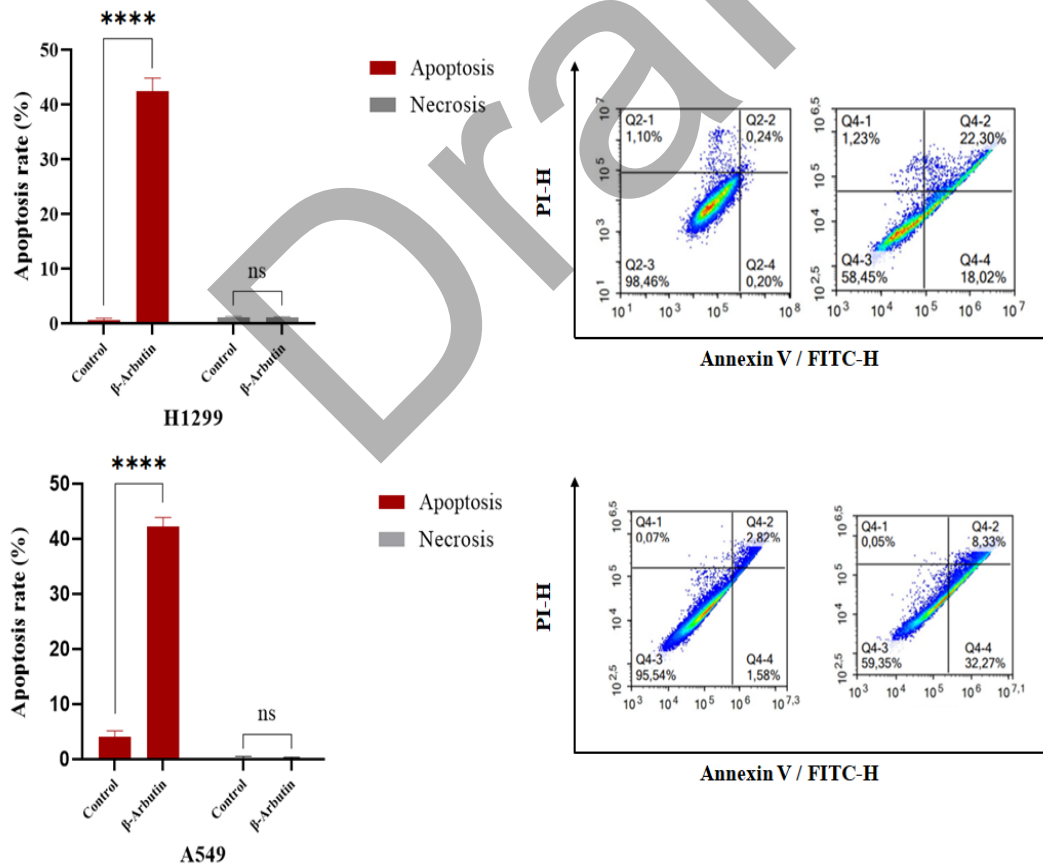
Figure 4. Determination of the effects of β-Arbutin on apoptosis in A549 and H1299 lung cancer cells.
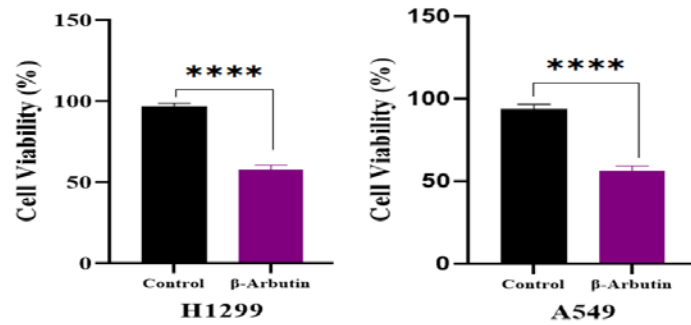
Figure 5. Determination of the effects of β-Arbutin on cell viability in A549 and H1299 lung cancer cells.
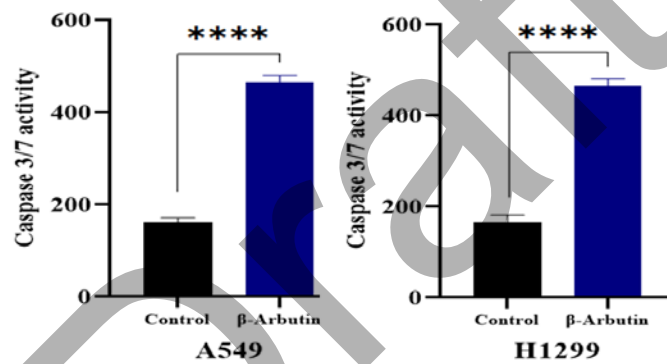
Figure 6. Determination of the effects of β-Arbutin on caspase 3/7 activity in A549 and H1299 lung cancer cells.
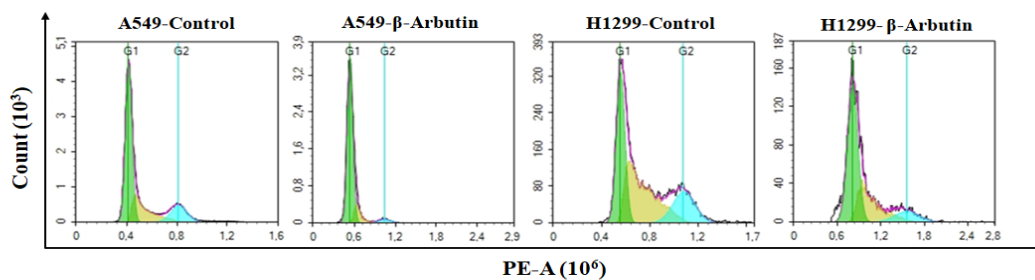
Figure 7. Effects of β-Arbutin on cell cycle in A549 and H1299 lung cancer cells.

References

[1]   M. B. Schabath and M. L. Cote, "Cancer progress and priorities: Lung cancer," *Cancer Epidemiol. Biomarkers Prev.*, vol. 28, no. 10, pp. 1563–1579, 2019, doi: 10.1158/1055-9965.EPI-19-0221.

[2]   C. Xie *et al.*, "Resveratrol suppresses lung cancer by targeting cancer stem-like cells and regulating tumor microenvironment," *J. Nutr. Biochem.*, vol. 112, p. 109211, 2023, doi: 10.1016/j.jnutbio.2022.109211.

[3]   N. An *et al.*, "Establishing a growth-coupled mechanism for high-yield production of β-arbutin from glycerol in Escherichia coli," *Bioresour. Technol.*, vol. 369, no. December 2022, p. 128491, 2023, doi: 10.1016/j.biortech.2022.128491.

[4]   N. An *et al.*, "High-yield production of β-arbutin by identifying and eliminating byproducts formation," *Appl. Microbiol. Biotechnol.*, vol. 107, no. 20, pp. 6193–6204, 2023, doi: 10.1007/s00253-023-12706-x.

[5]   L. Nahar, A. Al-Groshi, A. Kumar, and S. D. Sarker, "Arbutin: Occurrence in Plants, and Its Potential as an Anticancer Agent," *Molecules*, vol. 27, no. 24, pp. 1–22, 2022, doi: 10.3390/molecules27248786.

[6]   W. D. Travis *et al.*, "The 2015 World Health Organization Classification of Lung Tumors," *J. Thorac. Oncol.*, vol. 10, no. 9, pp. 1243–1260, Sep. 2015, doi: 10.1097/JTO.0000000000000630.

[7]   C. M. Rudin, E. Brambilla, C. Faivre-Finn, and J. Sage, "Small-cell lung cancer," *Nat. Rev. Dis. Prim.*, vol. 7, no. 1, p. 3, Jan. 2021, doi: 10.1038/s41572-020-00235-0.

[8]   H. M. Abdelaziz *et al.*, "Inhalable particulate drug delivery systems for lung cancer therapy: Nanoparticles, microparticles, nanocomposites and nanoaggregates," *J. Control. Release*, vol. 269, no. November 2017, pp. 374–392, 2018, doi: 10.1016/j.jconrel.2017.11.036.

[9]   K. Chaitanya Thandra, A. Barsouk, K. Saginala, J. Sukumar Aluru, and A. Barsouk, "Epidemiology of lung cancer," *Współczesna Onkol.*, vol. 25, no. 1, pp. 45–52, 2021, doi: 10.5114/wo.2021.103829.

[10]   Y. Li, B. Yan, and S. He, "Advances and challenges in the treatment of lung cancer," *Biomed. Pharmacother.*, vol. 169, p. 115891, Dec. 2023, doi: 10.1016/j.biopha.2023.115891.

[11]   L. Singh, K. Dua, S. Kumar, D. Kumar, and S. Majhi, "Targeting Molecular and Cellular Mechanisms in Tuberculosis," in *Targeting Cellular Signalling Pathways in Lung Diseases*, Singapore: Springer Singapore, 2021, pp. 337–353. doi: 10.1007/978-981-33-6827-9_14.

[12]   S. Kumar, A. K. Sharma, H. Lalhlenmawia, and D. Kumar, "Natural Compounds Targeting Major Signaling Pathways in Lung Cancer," in *Targeting Cellular Signalling Pathways in Lung Diseases*, Singapore: Springer Singapore, 2021, pp. 821–846. doi: 10.1007/978-981-33-6827-9_37.

[13]   Y. C. Boo, "Arbutin as a skin depigmenting agent with antimelanogenic and antioxidant properties," *Antioxidants*, vol. 10, no. 7, pp. 1–22, 2021, doi: 10.3390/antiox10071129.

[14]   X.-X. Li, L.-D. Du, and G.-H. Du, "Arbutin," in *Natural Small Molecule Drugs from Plants*, Singapore: Springer Singapore, 2018, pp. 667–670. doi: 10.1007/978-981-

10-8022-7_107.

[15] A. Garcia-Jimenez, J. A. Teruel-Puche, J. Berna, J. N. Rodriguez-Lopez, J. Tudela, and F. Garcia-Canovas, "Action of tyrosinase on alpha and betaarbutin: A kinetic study," *PLoS One*, vol. 12, no. 5, pp. 1–19, 2017, doi: 10.1371/journal.pone.0177330.

[16] S. Jafarova, T. Aydın, C. Isayev, R. Saglamtas, C. Kazaz. " Inhibitory Effects of Ethanol Extract of *Onobrychis buhseana* from Nakhchivan and its major component β-Arbutin on Acetylcholinesterase, Butyrlcholinesterase and α-Glucosidase enzymes," 5th International Conference On Life And Engineering Sciences, Alanya, Turkey. ICOLES 2022 Abstract Book.

Investigation of Ilicic Acid on Apoptosis and Cell Cycle in Different Stages of Bladder Cancer Cells

T. Ozdemir Sanci[1]

[1]*Ankara Yildirim Beyazit University Medical Faculty Histology and Embryology Department, Ankara, TÜRKİYE*
ORCID: 0000-0002-9468-4719

Abstract

Bladder cancer is a type of cancer that results in high morbidity and mortality rates. It ranks among the top ten most prevalent cancers globally. The incidence of bladder cancer is influenced by demographic shifts, including population expansion and aging [1]. Currently, treatment modalities for bladder cancer include radical or transurethral resection of the bladder and lymph nodes, complemented by chemotherapy and radiotherapy [2]. Natural products obtained from plants act important roles in drug discovery due to their wide chemical diversity and complex structures. These products serve as leading compounds in the treatment of many health problems such as cancer, infectious diseases, inflammation and pain [3]. Ilicic acid is a natural compound belonging to the sesquipertene lactone group [4]. There are very few studies published in the literature about ilicic acid. It has been suggested that ilicic acid and its derivatives may have anti-cancer and anti-inflammatory effects [5]. In this study we aimed to investigate the effects of ilicic acid on apoptosis and cell cycle in different stages of bladder cancer cells. Therefore HTB9 and HT1376 bladder cancer cells were cultured. The WST-1 test was used to determine the optimal dose of ilicic acid on HTB9 and HT1376 cells. Flow cytometry was performed to define the apoptotic and cell cycle effects. Statistical significance levels were accepted as $p \leq 0.05$. According to the these data, the doses of ilicic acid were found to be 0.3874 mM and 1.287 mM for the HTB9 and HT1376 cells, respectively, at 24h. It has been investigated that ilicic acid induces apoptosis in bladder cancer cells ($p < 0.0001$ for HTB9 cell line, $p < 0.0001$ for HT1376 cell line) and arrests the cell cycle at the G2 and S stages for HTB9 and HT1376 cell lines, respectively. In conclusion, it was observed that ilicic acid reduces cell viability in bladder cancer cells and induces apoptosis through the caspase 3/7 pathway.

Keywords: Bladder cancer, Ilicic acid, Apoptosis, Cell Cycle

Introduction

Bladder cancer is a type of cancer that shows high morbidity and mortality rates. 573,278 people were diagnosed with bladder cancer in 2020 according to the World Health Organization. By 2040, the number is expected to roughly double. The bladder wall consists of 5-7 layers of epithelial cells containing umbrella cells called urothelium on the surface and connective tissue and muscle bundles underneath these cells. Urothelial cells

are the main source of bladder cancer and account for approximately 95% of the entire disease [6]. Urothelial carcinoma consists of two main groups with different clinical outcomes and treatment options: non-muscle-invasive bladder cancer and muscle-invasive bladder cancer [7]. A number of risk factors have been identified for bladder cancer. Risk factors other than geography and age vary between genders. The most common of these risk factors are carcinogens exposed to smoking [8]. For non-muscle-invasive bladder cancer, resection of the tumor is performed followed by immunotherapy with intravesical Bacillus Calmette-Guerin (BCG) vaccine and intravesical chemotherapy. The treatment option for muscle-invasive bladder cancer is multimodal therapy, including neoadjuvant chemotherapy and radical cystectomy. For advanced disease, the best treatment method is cisplatin-based chemotherapy [9].

Today, anticancer drugs show toxicity not only against tumor cells but also against normal cells. Therefore, studies have led to the search for drugs that are toxic to cancer cells but have no effect on normal cells. Since plants are sources of materials with high biological activity, they have been used as part of alternative medicine in many parts of the world. In addition, many anticancer drugs isolated from plant sources have been tested on various cell lines, experimental animals and included in clinical studies. There has been a noticeable increase in the number of natural compounds discovered in recent years [10].

Sesquipertene lactones are secondary metabolites found in plants. They are found in more than 5000 known plants in the plant kingdom. They are most commonly found in the Asteraceae family. A limited number of studies in the literature have focused on the anti-cancer and anti-inflammatory effects of sesquipertene lactones. Traditional medical studies have led to the use of sesquiterpene lactones as active ingredients for treatments such as diarrhoea, burns, cognition and neurodegeneration [11]. Ilicic acid is a natural compound belonging to the sesquiterpene lactone group. Ilicic acid is one of the main components of the aireal parts of plants. Ilicic acid has anti-inflammatory properties. Its anti-cancer feature has been reported in only one study in the literature. In the study, it was reported that ilicic acid showed a cytotoxic effect against SK-MEL melanoma and A549 lung cancer cell lines [12], [13], [14]. In this study, we determined the effects of ilicic acid, a phytochemical from the sesquiterpene lactone group, on cytotoxicity, apoptosis and cell cycle in non-muscle-invasive HTB9 and muscle-invasive HT1376 bladder cancer cell lines.

Materials and Methods

Cell culture

The human bladder cancer cell lines HTB9 (non-muscle-invasive), and HT1376 (muscle-invasive) were gifted from Dr. Serap Erkek Ozhan from the Ozhan Lab at İzmir Biomedicine and Genome Center. HTB9 and HT1376 cells were cultured in RPMI 1640 and DMEM with high glucose, respectively, supplemented with 10% fetal bovine serum and 1% penicillin. The cells were maintained at 37°C in a humidified environment enriched with 5% CO_2.

Isolation of Ilicic Acid

Ilicic acid was isolated from the aerial parts of the *Inula viscosa*. The dried and ground herb sample (500 g) was macerated with ethanol (1.5 L) for 24 hours and filtered. After repeating the same procedure five times, the filtrates were combined. After ethanol was removed by a rotary evaporator, the obtained extract (98 g) was fractionated by silica gel column chromatography ($CHCl_3$:acetone (90:10)). Crystallization occurred when (11.7 g) acetone was added to the sub-fractions 26-55. The nuclear magnetic resonance (NMR) chemical structure of the crystals, which were thoroughly washed with acetone, was characterized as ilicic acid (210 mg). Ilicic acid was highly purified from the sub-fractions, its chemical structure was characterized by ^{1}H and ^{13}C NMR spectroscopic methods (Figure 1).

Ilicic acid: ^{1}H-NMR (dmso-d6, 400 MHz): δ (ppm) 5.98 (d, J=1.09, H13a), 5.52 (s, H13b), 2.48 (m, H7α), 1.86 (bd, J=12.44, H6), 1.59 (m, H1), 1.56 (m, H9), 1.43 (m, H2), 1.28 (m, H8), 1.16 (dt, H3), 1.03 (m, H5), 0.91 (s, H15), 0.81 (s, H14).

^{13}C-NMR (dmso-d6), 100 MHz): δ (ppm) 168.9 (C12), 147.1 (C11), 122.3 (C13), 70.7 (C4), 54.8 (C5), 45.0 (C9), 43.6 (C3), 41.1 (C1), 40.2 (C7), 34.7 (C10), 27.8 (C8), 26.8 (C6), 23.1 (C15), 20.4 (C2), 19.2 (C14).

Preparation of Ilicic Acid

Ilicic acid was prepared by dissolving in dimethyl sulfoxide (DMSO) as a 10 mM stock solution. It was tested at 24h and 48h at concentrations of 0, 0.1, 0.2, 0.5, 1, 1.5, 2, 3 mM.

WST-1 test

WST-1 was performed to evaluate the impact of ilicic acid on the viability of bladder cancer cells HTB9 and HT1376. The cells were seeded into 96-well plates at a concentration of 2×10^4 cells per well and incubated for 24h. After incubation, Ilicic acid was applied to the cells at the concentrations of 0, 0.1, 0.2, 0.5, 1, 1.5, 2, 3 mM for 24h and 48h. After the treatment period, 10 µl of WST-1 (Cayman Chemical, 10008883) was added to each well and incubated for 4h. Then the absorbance was measured at 450 nm using an ThermoVarioskan Microplate Reader. The data was analyzed using GraphPad Prism 9.1.0 software to calculate the inhibitor doses (IC_{50}) needed to achieve 50% inhibition of cell viability.

Apoptosis Assay

For the apoptosis assay, HTB9 and HT1376 bladder cancer cells were seeded into 6-well plates. The cell lines were treated with ilicic acid at the following concentrations; 0.3874 mM for HTB9, and 1.278 mM for HT1376 bladder cancer cells. After the incubation period, the dead cells were collected. The cells adhered to the plate were detached using trypsin-EDTA. After that, all cells were collected, washed with PBS, and the concentration was adjusted to 1×10^5 cells in 100 µl. Then, the resulting cell solution was transferred into 12x75 mm polystyrene tubes, and 5 µl of Annexin V-FITC and propidium iodide (PI) were added along with 1X Annexin Binding Buffer. After incubating at room temperature

for 15 minutes, the cells were analyzed using an ACEA Novocyte (Agilent) flow cytometry device. The flow cytometric analysis allowed us to differentiate cell populations. The cells that tested negative for both PI and Annexin V were classified as alive, while those testing negative for PI but positive for Annexin V were categorized as early apoptotic cells. Cells that were positive for both PI and Annexin V were classified as late apoptotic, and cells that tested positive for PI but negative for Annexin V were considered necrotic.

Caspase 3/7 Activity Assay

TheAat Bioquest Cell Meter Caspase 3/7 Activity Apoptosis Assay Kit was utilized to demonstrate that HTB9 and HT1376 cells use the caspase 3/7 apoptotic pathway. HTB9 and HT1376 cells were treated with ilicic acid at the concentrations of 0.3874 mM and 1.278 mM, respectively and then incubated. After incubation, collected live and dead cells were studied according to the Aat Bioquest Cell Meter Caspase 3/7 Activity Apoptosis Assay protocol. Measurements were made on the ACEA Novocyte (Agilent) flow cytometry device.

Cell Cycle Assay

HTB9 and HT1376 cells, both treated with ilicic acid and untreated were harvested using trypsin-EDTA, then centrifuged and resuspended in PBS. The cells were fixed initially by incubating them with 70% ethanol at 4°C for 20 minutes and then washed twice with PBS. To stain the DNA, the cells were treated with propidium iodide (PI). To achieve the best DNA resolution, we treated the cells with RNase. Then, the cells were exposed to a solution of 40 mg/mL of PI, 0.1% NP-40, and 20 mg/mL of RNase A for 30 minutes at 4°C in the dark. After that, the DNA content of both the control and ilicic acid treated cells were measured with an ACEA novocyte flow cytometry device (Agilent).

Results

Effective Ilicic acid dose in HTB9 and HT1376 bladder cancer cells

HTB9 and HT1376 bladder cancer cells were treated with ilicic acid at doses of 0, 0.1, 0.2, 0.5, 1, 1.5, 2, 3 mM at the 24h and 48h, respectively and the appropriate cytotoxic dose for the cells was determined.

The viability rates for HTB9 cells treated with ilicic acid for 24 hours at concentrations of 0, 0.1, 0.2, 0.5, 1, 1.5, 2, 3 mM were 100, %77.06, %58.17, %19.12, %18.59, 1%7.53, %14.34, %12.4 respectively. For HTB9 cells treated with ilicic acid for 48 hours at concentrations 0, 0.1, 0.2, 0.5, 1, 1.5, 2, 3 mM, the viability rates were %100, %70.03, %45.2, %20.02, %18, %15.3, %13.2, %10 respectively (Figure 2).

For HT1376 cells treated with ilicic acid for 24 hours, the viability rates were %100, %97, %89, %49.89, %47.62, %41.17, %29.83, %23.34 at concentrations of 0, 0.1, 0.2, 0.5, 1, 1.5, 2, 3 mM, respectively. For HT1376 cells treated with ilicic acid for 48 hours, the viability

rates were %100, %88, %47.3, %45.4, %40, %33.2, %25 %20 at concentrations of 0, 0.1, 0.2, 0.5, 1, 1.5, 2, 3 mM, respectively (Figure 3).

The effects of ilicic acid on the cell viability and apoptosis of HTB9 and HT1376 bladder cancer cells by Annexin V/PI Analysis

Flow cytometry was performed using propidium iodide (PI) and Annexin V/FITC to determine the effects of ilicic acid on apoptosis and cell viability in HTB9 and HT1376 cells.

Ilicic acid treated HTB9 and HT1376 cells showed a significant increase in apoptosis compared to the control group (p<0,0001 for HTB9 cell line, p<0,0001 for HT1376 cell line). Additionally, a significant decrease in cell viability was observed in ilicic acid treated HTB9 and HT1376 cells compared to the control group (p<0,0001 for HTB9 cell line, p<0,0001 for HT1376 cell line) (Figure 4, 5).

The effect of ilicic acid on HTB9 and HT1376 bladder cancer cell death by caspase 3/7 Analysis

According to the caspase 3/7 analysis, it was observed that caspase 3/7 activity was significantly increased in HTB9 and HT1376 cells treated with ilicic acid compared to the control group (p<0,001 for HTB9 cell line, p<0,0001 for HT1376 cell line) (Figure 6).

The effect of ilicic acid on cell cycle in HTB9 and HT1376 bladder cancer cells

The changes of cell cycle in HTB9 and HT1376 bladder cancer cells were observed by flow cytometry after treatment with ilicic acid. The percentage of control cells for the HTB9 cell line was 54.94, 32.37, 6.74 for the G1, S, and G2 phases, and 44,21 , 30.39, 25.41 for the ilicic acid treated HTB9 cells, respectively. The percentages of control cells for the HT1376 cell line were 56.55, 29.24, 7.8 for the G1, S, and G2 phases and 51.01, 39.91, 8.95 for the ilicic acid treated HT1376 cells respectively. According to these findings, it can be said that ilicic acid arrests the cell cycle at the G2 stage for HTB9 and S stage for HT1376 bladder cancer cells (Figure 7).

Conclusion

This study was aimed to investigate the effects of ilicic acid on the apoptosis and cell cycle in the HTB9 and HT1376 bladder cancer cells. Ilicic acid has a very notable effect on the apoptosis and the cycle of the HTB9 and HT1376 bladder cancer cells. There is a limited of study in the literature about the effects of ilicic acid on cancer cells. So that the study is preliminary for showing the apoptotic and cell cycle effect of ilicic acid on bladder cancer cells.

Acknowledgement
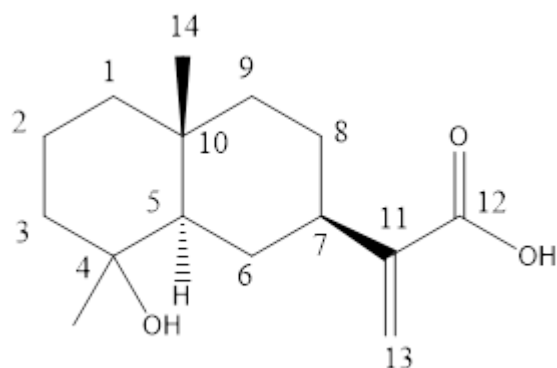
FIGURES

Figure 1. Chemical structure of ilicic acid
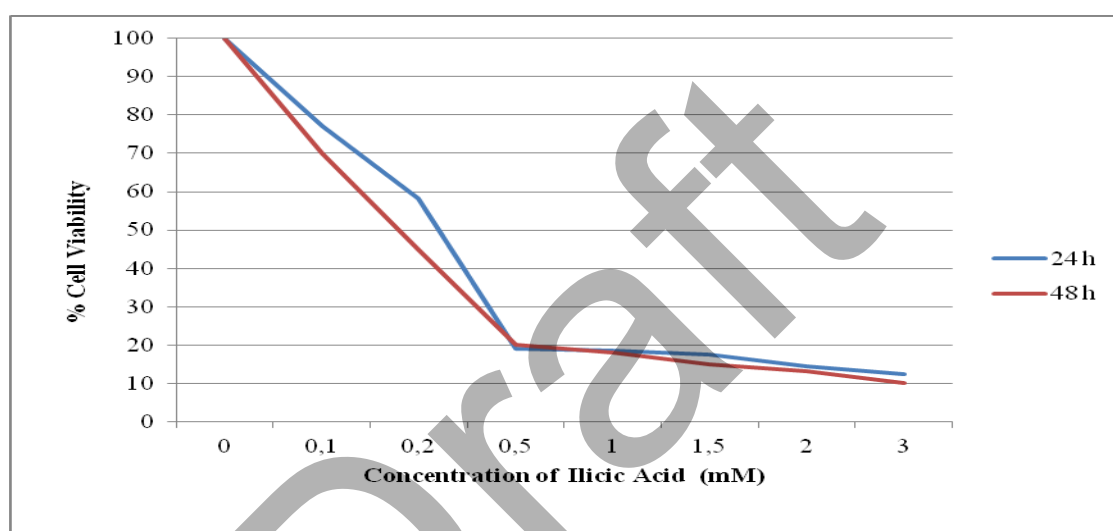
Figure 2. The effect of various concentrations of Ilicic acid on the cell viability of HTB9 cells.
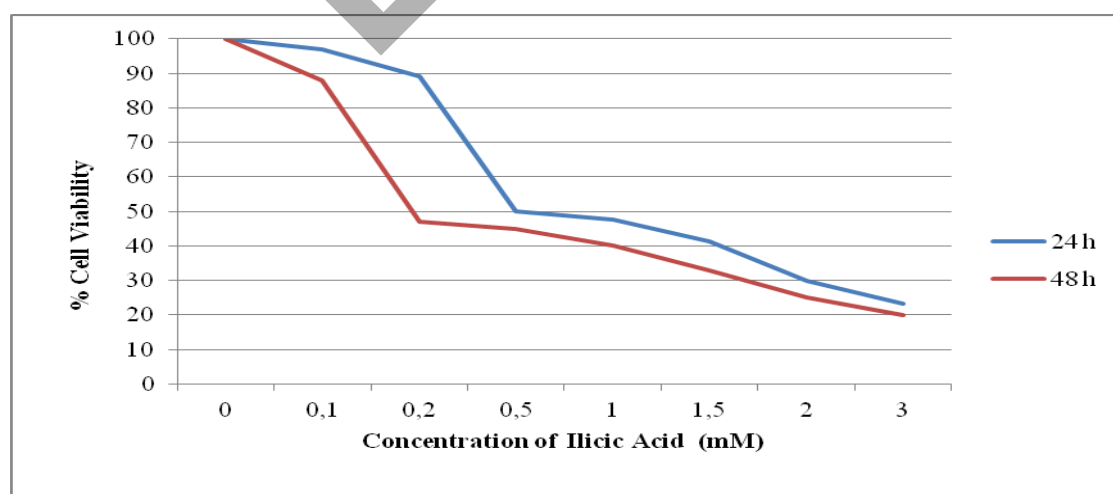
Figure 3. The effect of various concentrations of Ilicic acid on the cell viability of HT1376 cells
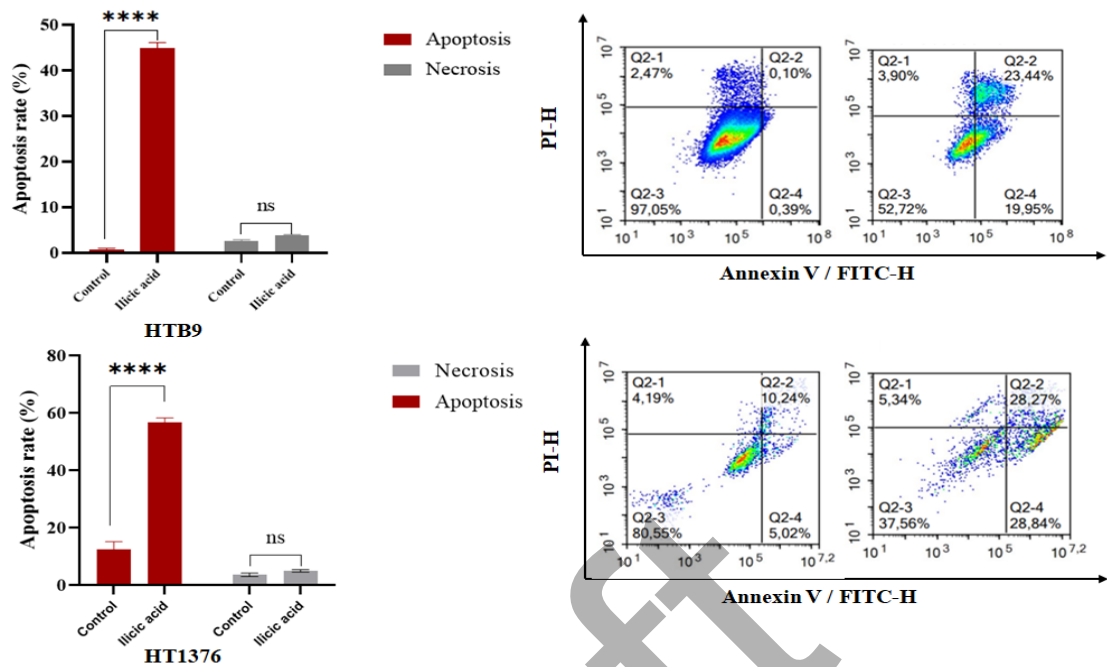
Figure 4. Determination of the effects of ilicic acid on apoptosis in HT1376 and HTB9 bladder cancer cells.
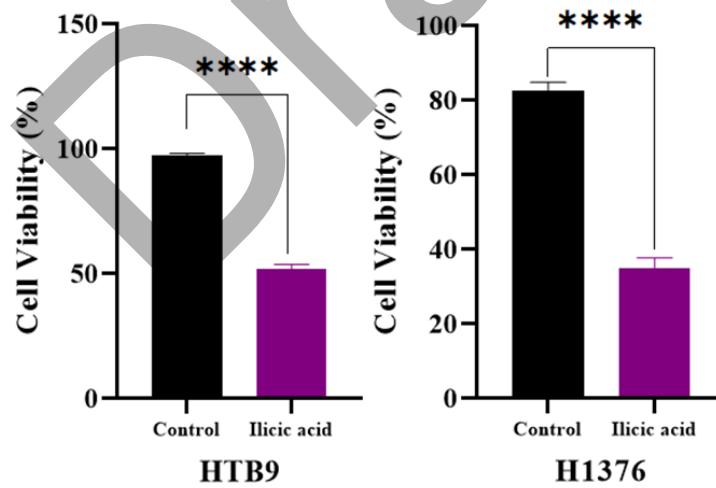
Figure 5. Determination of the effects of ilicic acid on cell viability in HTB9 and HT1376 bladder cancer cells.
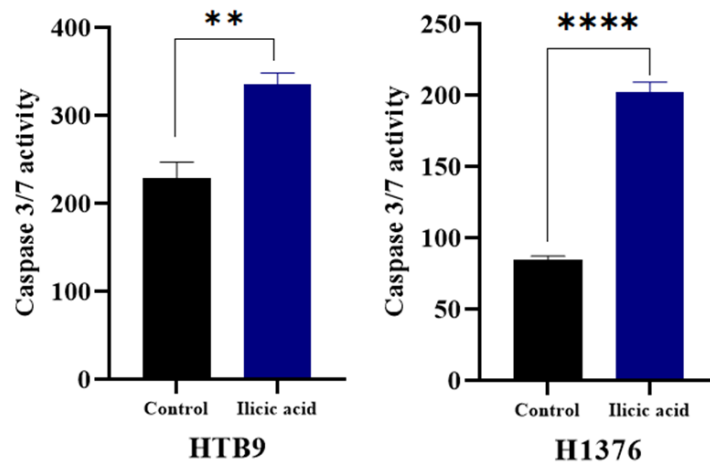
Figure 6. Determination of the effects of ilicic acid on cell viability in HTB9 and HT1376 bladder cancer cells.
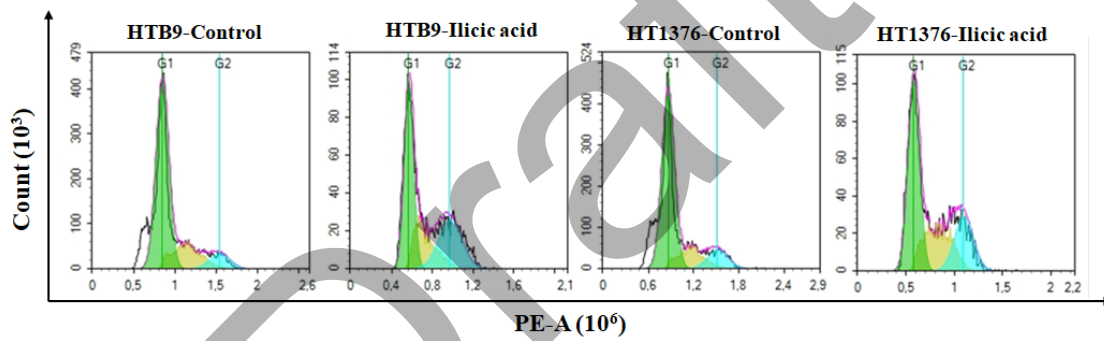
Figure 7. Effects of ilicic acid on cell cycle in HTB9 and HT1376 bladder cancer cells.

References

[1] L. M. C. van Hoogstraten, A. Vrieling, A. G. van der Heijden, M. Kogevinas, A. Richters, and L. A. Kiemeney, "Global trends in the epidemiology of bladder cancer: challenges for public health and clinical practice," *Nat. Rev. Clin. Oncol.*, vol. 20, no. 5, pp. 287–304, May 2023, doi: 10.1038/s41571-023-00744-3.

[2] Y. Shi, B. J. Mathis, Y. He, and X. Yang, "The Current Progress and Future Options of Multiple Therapy and Potential Biomarkers for Muscle-Invasive Bladder Cancer," *Biomedicines*, vol. 11, no. 2, p. 539, Feb. 2023, doi: 10.3390/biomedicines11020539.

[3] E. Coy-Barrera, I. V. Ogungbe, and T. J. Schmidt, "Natural Products for Drug Discovery in the 21st Century: Innovations for Novel Therapeutics," *Molecules*, vol. 28, no. 9, p. 3690, Apr. 2023, doi: 10.3390/molecules28093690.

[4] L. G. León, O. J. Donadel, C. E. Tonn, and J. M. Padrón, "Tessaric acid derivatives induce G2/M cell cycle arrest in human solid tumor cell lines," *Bioorg. Med. Chem.*, vol. 17, no. 17, pp. 6251–6256, Sep. 2009, doi: 10.1016/j.bmc.2009.07.053.

[5] D. T. Nguyen *et al.*, "Biochemical Conservation and Evolution of Germacrene A Oxidase in Asteraceae," *J. Biol. Chem.*, vol. 285, no. 22, pp. 16588–16598, May 2010, doi: 10.1074/jbc.M110.111757.

[6] L. Dyrskjøt *et al.*, "Bladder cancer," *Nat. Rev. Dis. Prim.*, vol. 9, no. 1, p. 58, Oct. 2023, doi: 10.1038/s41572-023-00468-9.

[7] L. Tran, J.-F. Xiao, N. Agarwal, J. E. Duex, and D. Theodorescu, "Advances in bladder cancer biology and therapy," *Nat. Rev. Cancer*, vol. 21, no. 2, pp. 104–121, Feb. 2021, doi: 10.1038/s41568-020-00313-1.

[8] J. Dobruch and M. Oszczudłowski, "Bladder Cancer: Current Challenges and Future Directions," *Medicina (B. Aires).*, vol. 57, no. 8, p. 749, Jul. 2021, doi: 10.3390/medicina57080749.

[9] A. M. Kamat *et al.*, "Bladder cancer," *Lancet*, vol. 388, no. 10061, pp. 2796–2810, Dec. 2016, doi: 10.1016/S0140-6736(16)30512-8.

[10] A. Lichota and K. Gwozdzinski, "Anticancer Activity of Natural Compounds from Plant and Marine Environment," *Int. J. Mol. Sci.*, vol. 19, no. 11, p. 3533, Nov. 2018, doi: 10.3390/ijms19113533.

[11] M. Chadwick, H. Trewin, F. Gawthrop, and C. Wagstaff, "Sesquiterpenoids Lactones: Benefits to Plants and People," *Int. J. Mol. Sci.*, vol. 14, no. 6, pp. 12780–12805, Jun. 2013, doi: 10.3390/ijms140612780.

[12] A. F. Barrero, M. M. Herrador, P. Arteaga, and J. V. Catalán, "Ilicic Acid as a Natural Quiron for the Efficient Preparation of Bioactive α- and β-Eudesmol," *European J. Org. Chem.*, vol. 2009, no. 21, pp. 3589–3594, Jul. 2009, doi: 10.1002/ejoc.200900438.

[13] X. Wu, B. Vogler, W. A. Haber, and W. N. Setzer, "A Phytochemical Investigation of Nectandra membranacea from Monteverde, Costa Rica," *Nat. Prod. Commun.*, vol. 1, no. 6, p. 1934578X0600100, Jun. 2006, doi: 10.1177/1934578X0600100607.

[14] B. E. Abu Irmaileh, A. M. F. Al-Aboudi, M. H. Abu Zarga, F. Awwadi, and S. F. Haddad, "Selective phytotoxic activity of 2,3,11β,13-tetrahydroaromaticin and ilicic acid isolated from Inula graveolens," *Nat. Prod. Res.*, vol. 29, no. 10, pp. 893–898, May 2015, doi: 10.1080/14786419.2014.955489.

Determination of Herniarin Effects on Apoptosis and Cell Cycle in Pancreas Ductal Adenocarcinoma Cells

B.E. Oz Bedir[1]

[1]Ankara Yildirim Beyazit University Medical Faculty, Ankara, Türkiye, ORCID: 0000-0002-0596-834X

The third most common cause of cancer-related mortality is pancreatic cancer. Pancreatic cancer primarily manifests as pancreatic ductal adenocarcinoma (PDAC) [1]. Before 2040, PDAC is expected to overtake colorectal cancer, overtaking only lung cancer as the primary cause of lung cancer. Because of the disease's rapid local growth and early systemic dissemination, this condition has a bad prognosis. Only 10-15% of individuals have local disease at presentation, compared to 50-60% with distant metastatic disease and 25-30% with regional disease [2]. The disease's rising prevalence highlights the pressing need to find and apply fresh treatment approaches that will help the majority of patients [3]. Herniarin (7-methoxycoumarin) is a member of the coumarin family and is known for its ability to regulate cellular processes. It also has anti-bacterial, anti-inflammatory, anti-oxidant, and anti-cancer activities [4]. The aim of this study is to determine of herniarin effects on apoptosis and cell cycle in pancreas ductal adenocarcinoma cells. In this study, PANC1 and MIA PaCa-2 cells were cultured. The WST-1 test was used to perform the optimum dose of Herniarin on pancreas ductal adenocarcinoma cells. Moreover, to determine the apoptotic and cell cycle effects of Hernarin on pancreas ductal adenocarcinoma cells, flow cytometry was conducted. Statistical significance level was accepted as $p \leq 0.05$. According to the findings, Herniarin doses were found to be 221.9 µM and 190.6 µM for PANC1 and MIA PaCa-2 cells at the 24h, respectively. Herniarin stimulates apoptosis in pancreas ductal adenocarcinoma cells ($p < 0.0001$ for PANC1 cells, $p < 0.001$ for MIA PaCa-2 cells) and arrests the cell cycle at S and G2 phase for MIA PaCa-2 and PANC1 cells, respectively. As a result of study, Herniarin decreases cell viability and stimulates apoptosis via caspase 3/7 pathway in pancreas ductal adenocarcinoma cells.

Keywords: Pancreatic cancer, Herniarin, Apoptosis, Cell cycle

Introduction

Pancreatic cancer (PC) ranks seventh in the world in terms of cancer mortality and is the 12th most common disease worldwide. It is also linked to a significant number of years lost to death; in 2017, its disability-adjusted life years were estimated to be 9.1 million worldwide. Because of its poor survival rate and extremely aggressive behavior, it continues to pose a serious worldwide health threat [5] Pancreatic ductal adenocarcinoma (PDAC) is the predominant kind of pancreatic cancer, accounting for over 90% of cases. Pancreatic cancer is the clinical term for adenocarcinoma, a malignant tumor developed in the epithelial cells of glandular structures in the pancreatic ductal cells. Despite being the 10th most frequent disease, PDAC is the seventh main cause of cancer death worldwide due to the dismal survival rates [6]. Surgery, chemotherapy, and radiation therapy are examples of current standard of care treatments that are still only partially successful because PDAC has shown a strong resistance to these modalities. Furthermore, although early surgical resection may be a curative treatment, 80% of patients who get surgery experience a recurrence of the illness, and PDAC usually manifests in a late stage due to nonspecific symptoms. Recent developments in immunotherapy and targeted medicines have caused a paradigm change in the way cancer care is treated [7].

Phytochemicals have regained prominence in the cancer drug research sector in recent times, owing to their remarkable efficacy and minimal toxicity. Several coumarin derivatives against cancers, including pancreatic, stomach, and colon tumors have been reported [8]. Herniarin (7-methoxycoumarin) is one of the coumarins, which are specific secondary metabolites obtained from plants that may have medicinal properties (Figure 1). Herniarin, a member of the coumarin family found in a wide range of plants, has a variety of biological characteristics [9], [10]. Herniarin's function in controlling important cellular processes highlights its potential as a cancer agent because of its benzopyran-2 one ring structure [11].
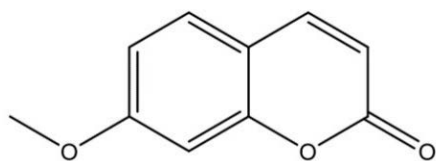
Figure 1. Chemical structure of herniarin.

This study aimed to examine the effect of herniarin on PDAC cells. The effects of herniarin on the cell viability of PDAC cells were investigated, and the effects of herniarin on the cell cycle were examined.

Materials and Methods

Reagents and chemicals

All chemicals for the herniarin extraction and isolation processes was bought from Tekkim and Isolab. Trypsin-EDTA (Gibco), DMEM (Dulbecco's Modified Eagle Medium) (Capricorn), PBS (Bioshop), FBS (Fetal Bovine Serum) (Capricorn) and DMSO (Merck) were used for growing the cells. WST-1 assay (Cayman Chemical) was used for cytotoxicity experiment.

Plant material

The aerial parts of the cultivated plant A. dracunculus L.(Asteraceae) were collected from the Erzurum (Turkey) center in June 2020. A sample of the plant has been preserved in the Atatürk University herbarium (ATA-9783) [12].

Isolation of herniarin

The 500g dried and ground herb sample was macerated in 1.5 L of methanol for 24 hours before being filtered. The filtrates were mixed after five iterations of the same process. The resulting extract (57 g) was fractionated using silica gel column chromatography (ethylacetate-methanol10:0, 9:1, 8:2, v/v) following the removal of methanol using a rotary evaporator. From the subfractions (14–25), herniarin (130 mg) was refined using crystal structure. 1D, 1H, and 13 CNMR spectra were used to analyze the herniarin's chemical structure. The 1H and 13C NMR spectra of herniarin are provided in our earlier research [10].

Cell culture

The pancreatic ductal adenocarcinoma cell lines PANC1 and MIA PaCa-2 were obtained from American Tissue Cell Culture (ATCC). PANC-1 and MIA PaCa-2 are cell lines commonly used for pancreatic cancer. It is known that both MIA PaCa-2 and PANC-1 are poorly differentiated and PANC-1 is derived from a patient with metastasis, but the metastatic status of the patient from which MIA PaCa-2 is derived is unclear [13]. The cells were grown in high-glucose DMEM supplemented with 1% penicillin and 10% fetal

bovine serum. The cells were kept in a humidified atmosphere with 5% CO_2 enrichment at 37°C. The sub-confluent cultures were subcultured using trypsin-EDTA (0.25% trypsin) in accordance with the manufacturer's instructions once they had attained an 80-90% density. An Olympus IX73 microscope was used to take all of the microscopy images.

WST-1 assay

WST-1 assay was used to evaluate the effect of herniarin on the viability of pancreatic ductal adenocarcinoma cell lines PANC1 and MIA PaCa-2. All cells were seeded into 96-well plates at a concentration of 2×10^4 cells per well and incubated them for 24h and 48h. Then, all cells were washed with PBS and treated them with herniarin at different concentrations (0, 5, 10, 50, 100, 250, 500, 1000 μM) for 24h and 48h. After process, 10 μl of WST-1 solution was added to each well. Next, cell-containing wells were placed in a CO_2 incubator and incubated them for 4 hours at 37°C. Then, the plate was measured the absorbance at 450 nm using a spectrophotometer. The inhibitor dosages (IC_{50}) required to induce 50% inhibition of cell viability were determined by analyzing the data collected with GraphPad Prism 9.1.0 software.

Apoptosis assay

PANC1 and MIA PaCa-2 cells were seeded into 6-well plates for apoptosis assay. Herniarin treatment was done 221.9 μM for PANC1 cells and 190.6 μM for MIA PaCa-2 cells. The dead cells were collected after the incubation period and Trypsin-EDTA was used to detached from the surface. Then, all cells were collected and washed with PBS. The final volume was adjusted to 1×10^5 cells in 100 μl. Following that, the cell solution was put into 12 x 75 mm polystyrene tubes, and 1X Annexin Binding Buffer, 5 μl of Annexin V-FITC, and propidium iodide (PI) were added. 15 minutes later, the cells were analyzed using an ACEA NovoCyte flow cytometry device from Agilent. According to our earlier research, cells that tested negative for Annexin V but positive for PI were classified as early apoptotic cells, whereas those that tested negative for PI but positive for Annexin V were classified as living cells. Cells that tested positive for PI but negative for Annexin V were categorized as necrotic, whereas those that tested positive for both substances were categorized as late apoptotic.

Caspase 3-7 activity assay

Cells were seeded as 5×10^5 cells per well in 6-well plates and incubated overnight. Herniarin added 221.9 μM for PANC1 cells and 190.6 μM for MIA PaCa-2 cells. Then, all cells were collected in 0.5 ml of medium and subsequently incubated for an hour at 37°C

with a caspase 3-7 detection reagent. The cells were then washed and resuspended in 0.5 mL of assay buffer. The NovoCyte D3000 (Agilent) flow cytometry device was used to detect the activity of caspase 3-7 in the cells.

Cell cycle analysis

PANC1 and MIA PaCa-2 cells with treated/untreated with herniarin were detached using trypsin-EDTA. Then, cell suspension was centrifuged and resuspended in PBS. After fixing the cells for the first time, they were twice washed with PBS and then incubated with 70% ethanol for 20 minutes at 4°C. Propidium iodide (PI), a fluorescent dye, was applied to the cells in order to stain the DNA. The cells were incubated for 30 minutes at 4°C in the dark with a solution containing 40 mg/mL of PI, 0.1% NP-40, and 20 mg/mL of RNase A. Then, DNA content of both the control and treated cells were measured using a flow cytometer.

Statistical analysis

Statistical analyses were performed using the GraphPad Prism 9.1 software. Student's t-test was used for pairwise comparisons. Also, the two-way ANOVA test was used to compare the levels across two categorical variables. The statistical significance was accepted as p<0.05.

Results

Cytotoxic effects of herniarin for PANC1 and MIA PaCa-2 cells

The optimal cytotoxic dose for PANC1 and MIA PaCa-2 pancreatic cancer cells was found by applying herniarin at 0, 5, 10, 50, 100, 250, 500, and 1000 µM on the 24th and 48th hour of incubation. According to WST-1 results, the viability rates for PANC1 cells treated with Herniarin for 24 hours at concentrations of 0, 5, 10, 50, 100, 250, 500 and 1000 µM were found 100%, 96.81%, 92.22%, 91.05%, 73.51%, 42.61%, 25.25% and 19.2% respectively. For PANC1 cells treated with herniarin for 48 hours, the viability rates were 100%, 85.09%, 75.06%, 54.08%, 37.97%, 35.04%, 29.5% and 25.76%, respectively, at concentrations of 0, 5, 10, 50, 100, 250, 500 and 1000 µM. For MIA-PaCa cells treated with herniarin for 24 hours at concentrations of 0, 5, 10, 50, 100, 250, 500 and 1000 µM, the viability rates were 100%, 93.96%, 87.41%, 82.96%, 72.23%, 37.95%, 23.03% and 19.06%, respectively. Herniarin treatment for 48 hours at doses of 0, 5, 10, 50, 100, 250, 500, and 1000 µM resulted in 100%, 85.31%, 84.53%, 49.29%, 37.23%, 34.88%, 26.47%, and 21.71% viability rates for MIA-PaCa cells. Based on the provided results, the Herniarin

optimal doses for PANC1 and MIA-PaCa pancreatic cancer cells were determined to be 221.9 µM and 190.6 µM, respectively, at the 24h (Figure 2A-B).
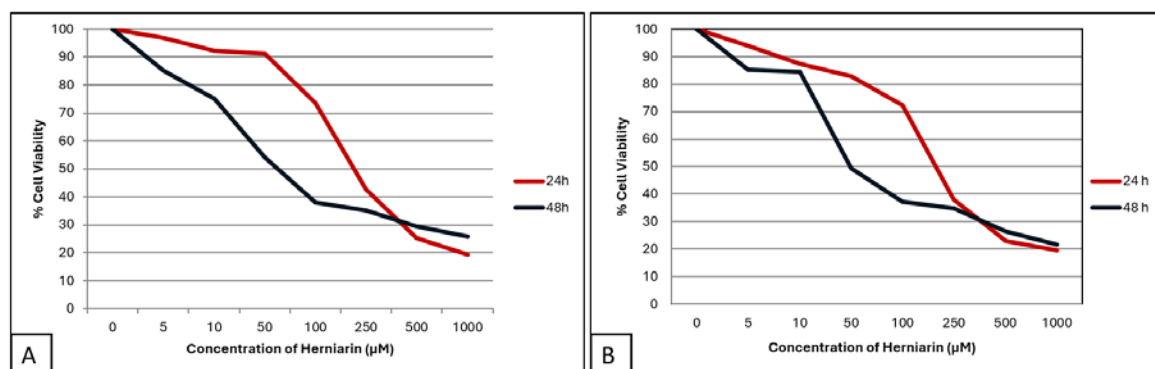
Figure 2. The effect of various concentrations of herniarin on the cell viability. A) The effect of various concentrations of herniarin on the cell viability of PANC1 cells. B) The effect of various concentrations of herniarin on the cell viability of MIA PaCa-2 cells.

The Impact of herniarin on apoptosis and cell viability in PANC1 and MIA PaCa-2 cells

To determine the effects of herniarin on apoptosis and cell viability in pancreatic cancer cells, flow cytometry was performed using propidium iodide (PI) and Annexin V/FITC. The cells were divided into two groups: the control group and the herniarin-treated group. A significant increase in apoptosis was observed in herniarin-treated pancreatic cancer cells compared to control groups. However, a more significant increase was observed in PANC1 cells than in MIA-PaCa cells. (for PANC-1; $p < 0.0001$, for MIA-PaCa; $p < 0.001$) (Figure 3). Additionally, a significant decrease in cell viability was observed in PANC1 and MIA-PaCa cells treated with herniarin. However, the decrease in PANC1 cells was found to be more significant than in MIA-PaCa cells (for PANC1; $p < 0.001$, for MIA-PaCa; $p < 0.01$) (Figure 4).
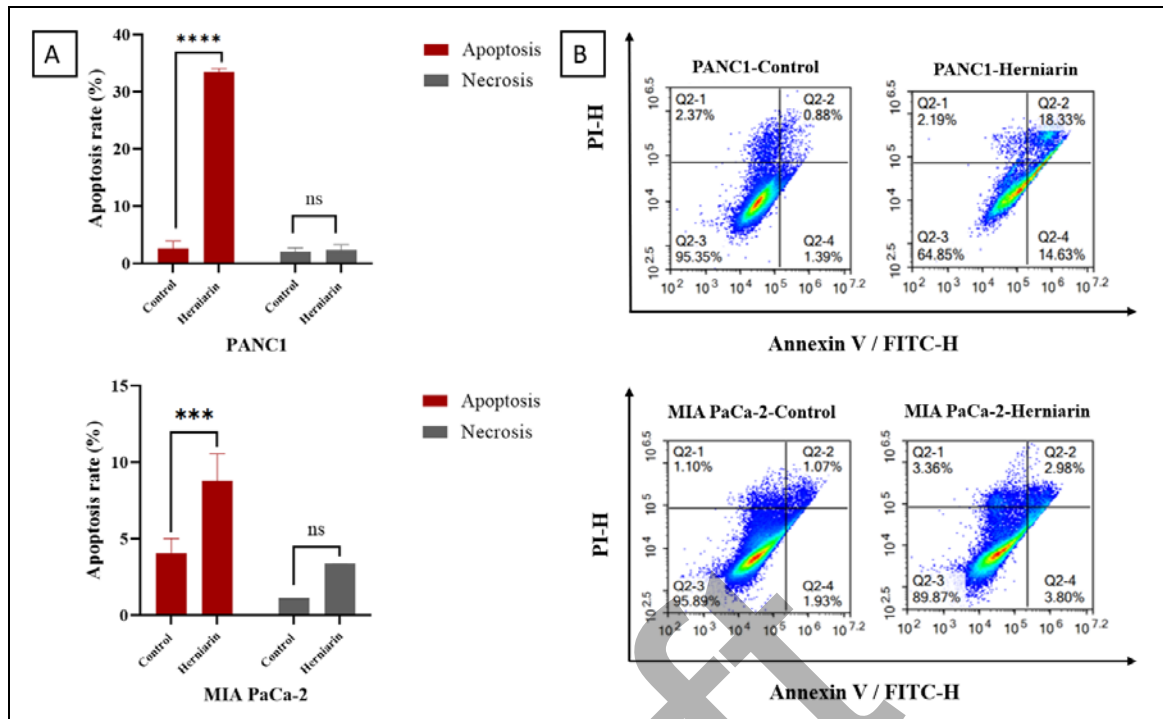
Figure 3. The effect of herniarin on apoptosis in PANC1 and MIA PaCa-2 cells. A) % apoptotic rate of PANC1 and MIA PaCa-2 cells. Herniarin stimulates apoptosis in PANC1 and MIA PaCa-2 cells (for PANC-1; $p<0.0001$, for MIA-PaCa; $p<0.001$). B) The percentages of early and late apoptotic cells, necrotic cells and cell viability were analyzed using flow cytometry. Annexin V-PI staining was performed following herniarin treatment in PANC1 and MIA PaCa-2 cells.
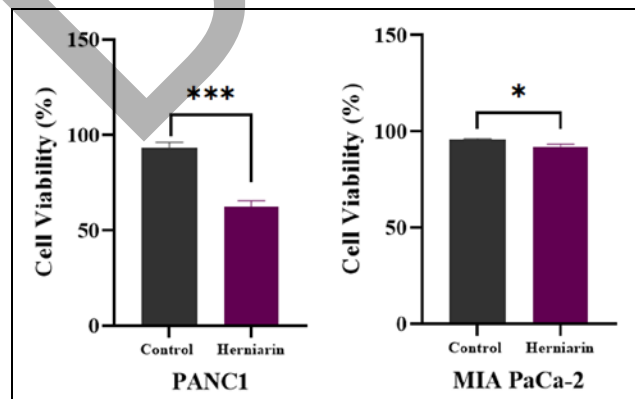
Figure 4. Herniarin reduces cell viability in PANC1 and MIA PaCa-2 cells (for PANC-1; $p<0.001$, for MIA-PaCa; $p<0.05$).

After Annexin V/PI analyses, caspase 3/7 activation was examined in the control group and herniarin-treated groups by flow cytometry. Significantly increased caspase 3/7

activity was observed in the herniarin-treated group compared to the control group (for PANC1; p<0.0001, for MIA-PaCa; p<0.001) (Figure 5).
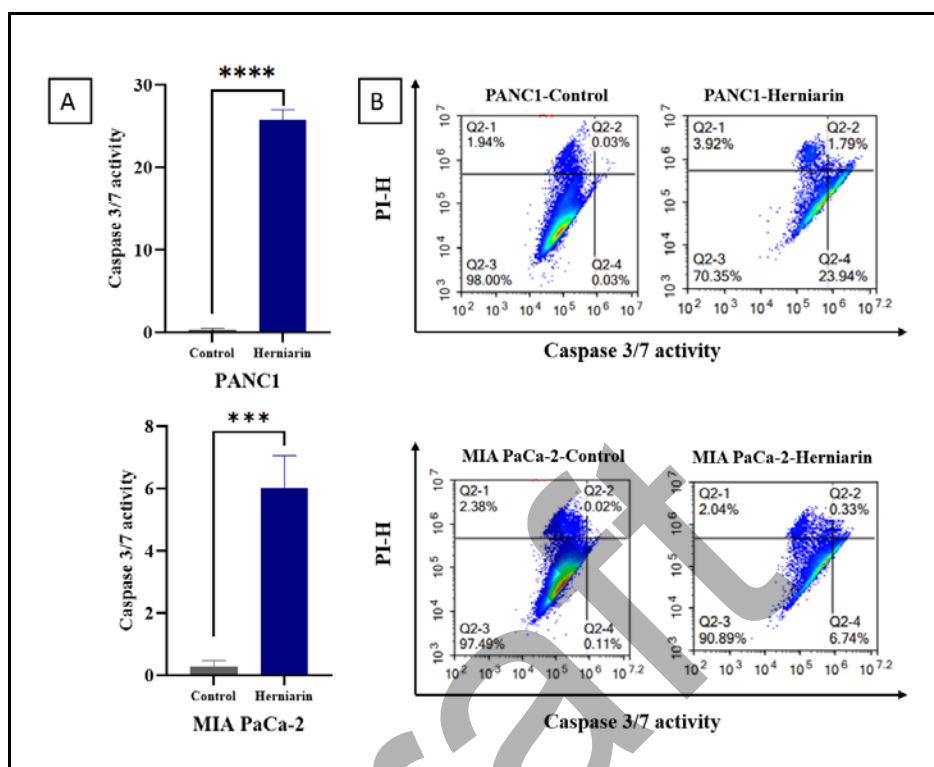
Figure 5. Caspase 3/7 activation as an apoptotic marker in PANC1 and MIA PaCa-2 cells. A) Herniarin effects caspase 3/7 acitivities significantly in PANC1 and MIA PaCa-2 cells (for PANC1; p<0.0001, for MIA-PaCa; p<0.001). B) Caspase 3/7 activities in these cell lines were analyzed by flow cytometry.

Determination of the effect of herniarin on cell cycle in PANC1 and MIA PaCa-2 cells

Following the treatment of herniarin, flow cytometry was used to evaluate alterations in the cell cycle of PANC1 and MIA PaCa-2 cells. At various phases of the cell cycle, herniarin causes cell cycle arrest. For the G1, S, and G2 phases of the PANC1 cell line, the percentage of control cells was 37.51, 37.53, 24.64, and for the PANC1 herniarin group, it was 36.73, 22.69, and 38.95. For the G1, S, and G2 phases of the MIA PaCa-2 cell line, the percentage of control cells was 56.53, 26.61, 16.14, and for the MIA PaCa-2 herniarin group, it was 41.17, 35.61, and 20.93, respectively. These findings show that herniarin triggers G2 arrest in PANC1, S arrest in MIA PaCa-2. These findings demonstrate the potency of herniarin in the cancer cell cycle (Figure 6).
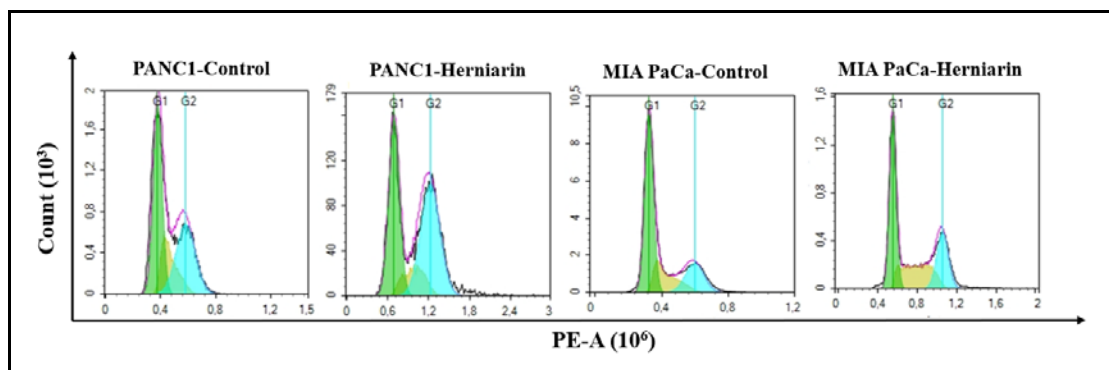
Figure 6. Effect of herniarin on cell cycle.

Conclusions

There will undoubtedly be an increase in pancreatic cancer cases in the coming years. Molecular research into the treatment of pancreatic cancer must accelerate given the disease's high mortality rate and the difficulty of early diagnosis. In this study, it was determined that herniarin reduces cell viability on pancreatic cells and increases cell death by inducing apoptosis. With this study, it is thought that herniarin will be a promising agent in the treatment of cancer.

Acknowledgement

References

[1] C. J. Halbrook, C. A. Lyssiotis, M. Pasca di Magliano, and A. Maitra, "Pancreatic cancer: Advances and challenges," *Cell*, vol. 186, no. 8, pp. 1729–1754, Apr. 2023, doi: 10.1016/j.cell.2023.02.014.

[2] H. M. Kolbeinsson, S. Chandana, G. P. Wright, and M. Chung, "Pancreatic Cancer: A Review of Current Treatment and Novel Therapies," *J. Investig. Surg.*, vol. 36, no. 1, Dec. 2023, doi: 10.1080/08941939.2022.2129884.

[3] H. Wei and H. Ren, "Precision treatment of pancreatic ductal adenocarcinoma," *Cancer Lett.*, vol. 585, p. 216636, Mar. 2024, doi: 10.1016/j.canlet.2024.216636.

[4] T. Ozdemir Sanci, E. Terzi, B. E. Oz Bedir, M. Gumustas, T. Aydin, and A. Cakir, "Effect of herniarin on cell viability, cell cycle, and Erk protein levels in different stages of bladder cancer cells," *Chem. Biodivers.*, Jan. 2024, doi: 10.1002/cbdv.202301645.

[5] J. Huang *et al.*, "Worldwide Burden of, Risk Factors for, and Trends in Pancreatic Cancer," *Gastroenterology*, vol. 160, no. 3, pp. 744–754, Feb. 2021, doi: 10.1053/j.gastro.2020.10.007.

[6] J.-X. Hu *et al.*, "Pancreatic cancer: A review of epidemiology, trend, and risk

factors," *World J. Gastroenterol.*, vol. 27, no. 27, pp. 4298–4321, Jul. 2021, doi: 10.3748/wjg.v27.i27.4298.

[7]   E. M. Anderson, S. Thomassian, J. Gong, A. Hendifar, and A. Osipov, "Advances in Pancreatic Ductal Adenocarcinoma Treatment," *Cancers (Basel).*, vol. 13, no. 21, p. 5510, Nov. 2021, doi: 10.3390/cancers13215510.

[8]   A. M. D. Delkhah, E. Karimi, and S. Farivar, "Herniarin-loaded solid lipid nanoparticles: promising molecular mechanism and therapeutic potential against pancreatic cancer line," *Mol. Biol. Rep.*, no. 0123456789, 2023, doi: 10.1007/s11033-023-08560-9.

[9]   M. Salehcheh, O. Safari, M. J. Khodayar, H. Mojiri-Forushani, and M. Cheki, "The protective effect of herniarin on genotoxicity and apoptosis induced by cisplatin in bone marrow cells of rats," *Drug Chem. Toxicol.*, vol. 45, no. 4, pp. 1470–1475, Jul. 2022, doi: 10.1080/01480545.2020.1842883.

[10]   T. Aydin, H. Akincioglu, M. Gumustas, I. Gulcin, C. Kazaz, and A. Cakir, "human monoamine oxidase (hMAO) A and hMAO B inhibitors from Artemisia dracunculus L. herniarin and skimmin: human mononamine oxidase A and B inhibitors from A. dracunculus L.," *Zeitschrift fur Naturforsch. - Sect. C J. Biosci.*, vol. 75, no. 11–12, pp. 459–466, 2020, doi: 10.1515/znc-2019-0227.

[11]   S. B. Patil, "Medicinal significance of novel coumarin analogs: Recent studies," *Results Chem.*, vol. 4, no. February, p. 100313, 2022, doi: 10.1016/j.rechem.2022.100313.

[12]   T. O. Sanci, E. Terzi, B. E. Oz Bedir, M. Gumustas, T. Aydin, and A. Cakir, "Effect of herniarin on cell viability, cell cycle, and Erk protein levels in different stages of bladder cancer cells," *Chem. Biodivers.*, Feb. 2024, doi: 10.1002/cbdv.202301645.

[13]   Shen *et al.*, "Differentially Expressed microRNAs in MIA PaCa-2 and PANC-1 Pancreas Ductal Adenocarcinoma Cell Lines are Involved in Cancer Stem Cell Regulation," *Int. J. Mol. Sci.*, vol. 20, no. 18, p. 4473, Sep. 2019, doi: 10.3390/ijms20184473.

Investigation and Simulation of Horizontal Axis Wind Turbine Blade Optimization Methods

K. Ozbek[1], K. Gelis[1] and O. Ozyurt[1]

[1]Bolu Abant Izzet Baysal University,Mechanical Engineering, Bolu, Türkiye, ORCID: 0000-0002-5475-8111, ORCID: 0000-0001-8612-2233, ORCID: 0000-0001-9148-3463

Abstract

Wind energy is one of the most important renewable energy sources that is used widely around the world. The increase in energy demand and fossil fuel emissions has led to an increase in studies on renewable energy. This study analyses and compares blades designed with different airfoils and optimization methods in small wind turbines. In the study, open source QBlade software was used. NACA 4412, NACA 4415, NACA 2415 and NREL S822 airfoils, which are frequently used by researchers in small-scale wind turbines, were preferred as airfoils. When the results obtained are evaluated, it can be seen that the blades with the NREL 822 airfoil give better results in small wind turbines.

Keywords: Blade Optimization, Wind Turbine Blade Design, QBlade, Blade Analysis

Introduction

Wind energy is one of the most important renewable energy sources that are extensively used worldwide. The increase in energy demand and fossil fuel emissions has led to an increase in studies on renewable energy. Many researchers from the industrial sector are working on different designs to increase the efficiency and performance of wind turbines. The use of renewable energy sources has a promising future in reducing emission values. In order to meet the increasing energy demand, it has become imperative to increase the use of clean and efficient energy. Unlike fossil fuels, renewable energy sources are constantly renewed by natural processes and offer an environmentally friendly alternative [1].

For many years, energy needs of people have been met from non-renewable fossil fuels such as coal, oil and natural gas. However, the limited nature of these resources and their negative effects on the environment during their extraction and use have led researchers to search for alternative energy sources that do not harm the environment. There is a global trend towards renewable energy sources. However, it shows that the dependence on fossil fuels in some sectors will continue until 2050 [2]. However, diverse renewable energy sources hold great promise for reducing dependence on traditional fossil fuels.

Wind energy, one of the renewable energy sources, stands out as an advantageous solution especially in large-scale systems. Wind energy plays an important role in the global transition to renewable energy use, especially with its cost competitiveness in high wind regions [3]. The large capacity wind turbines have designs that are accepted by universally with high efficiency systems. However, there is no recognized wind turbine with an optimum design, especially at low wind speeds and rpm.

Researchers have conducted many studies on different blade geometries in order to obtain maximum kinetic energy from the wind [4]–[6]. In order to increase the efficiency of the blades, different optimization methods and effective designs are needed. The efficiency of wind turbines increases with the ability of the blades to capture wind energy. Factors such as wind speed, tip speed ratio, Reynolds number, airfoil geometry, number of blades and blade length are factors in blade designs.[7]. Understanding and optimizing these parameters is critical to improving the efficiency of wind turbines.

Many different software can be used in blade designs and simulation processes. Software such as Ansys Fluent, QBlade, FAST, Blade Comp are commonly used. Among these software, QBlade software is the most frequently used application where fast results can be achieved. Researchers have concluded that the results obtained from QBlade software in the studies conducted in this field are highly consistent with the experimental data [7]. QBlade is an open-source software that provides a comprehensive solution for the design, simulation, and aerodynamic calculations of horizontal and vertical axis wind turbine blades. Betz [8]and Schmitz (Glauert) [9]theories are used in blade optimization.

In this study, a comparative analysis of different airfoils and optimization methods for a wind turbine with a capacity of 2 kW was carried out. In the study, blade designs and analyses were performed with QBlade software. Blade profiles (NACA 4412, NACA 4415, NACA 2415 and NREL S822) which are preferred by researchers at low capacities were selected as blade profiles. Betz and Schmitz methods have been used in wind turbine blade optimization and examined comparatively.

Theoretical Formulation

The Blade Element Momentum (BEM) method is recognized as a fundamental method for examining the aerodynamic properties of wind turbine blades. In the BEM method, the blade is divided into sections and the forces acting on each section are calculated separately. The parameters used in the calculations of horizontal axis wind turbines are explained below. Aerodynamic lift and drag forces on the blades are calculated using Eq. (1) and Eq. (2).

$$C_l = \frac{F_l}{0.5 * \rho_\infty * V_\infty^2 * A} \tag{1}$$

$$C_d = \frac{F_d}{0.5 * \rho_\infty * V_\infty^2 * A} \tag{2}$$

Where, ρ_∞ (kg/m³) is the air density, V_∞ (m/s) is wind speed, F_l (N) is lift force, F_d (N) is drag force, and A (m²)is the cross section area. In wind turbines, the power factor is calculated by dividing the power output by the wind power. The power factor is affected by many factors such as mechanical efficiency, gearbox efficiency, generator efficiency and electrical efficiency [5]. The power factor is calculated using Eq. (3) and Eq. (4).

$$C_p = \frac{P_{gen}}{\rho_\infty * V_\infty^2 * A} \tag{3}$$

$$P_{gen} = 2\,\rho\,A\,V_\infty^3\,a\,(1-a)^2 \tag{4}$$

Where a is defined as the axial induction factor. This factor represents the reduction in wind speed between the free flow and the turbine rotor. Based on this, the power coefficient can be rewritten as in Eq. (5).

$$C_p = 4\,a\,(1-a)^2 \tag{5}$$

The power that can be obtained from wind turbines is calculated using Eq. (6).

$$P = \frac{1}{2}\,\rho\,A\,V_\infty^3\,C_p \tag{6}$$

Analysis and optimization of blade

In this study, the airfoils previously used in different studies were preferred. The airfoils were selected to have operating characteristics especially at low turbine capacities. Cross sections of the selected airfoils are presented in Figure 1.

Airfoil Design Module

	Foil Name	Thickness (%)	at (%)	Camber (%)	at (%)	Points	LE Flap (deg)	Show	Ponts	Centerline	Style
1	NACA 2415	14.92	29.80	2.00	40.90	201	0.00	√	☐	☐	
2	NACA 4412	11.94	29.50	4.00	40.50	201	0.00	√	☐	☐	
3	NACA 4415	14.92	30.10	4.00	40.60	201	0.00	√	☐	☐	
4	NREL S822	16.00	39.20	1.90	59.20	66	0.00	√	☐	☐	
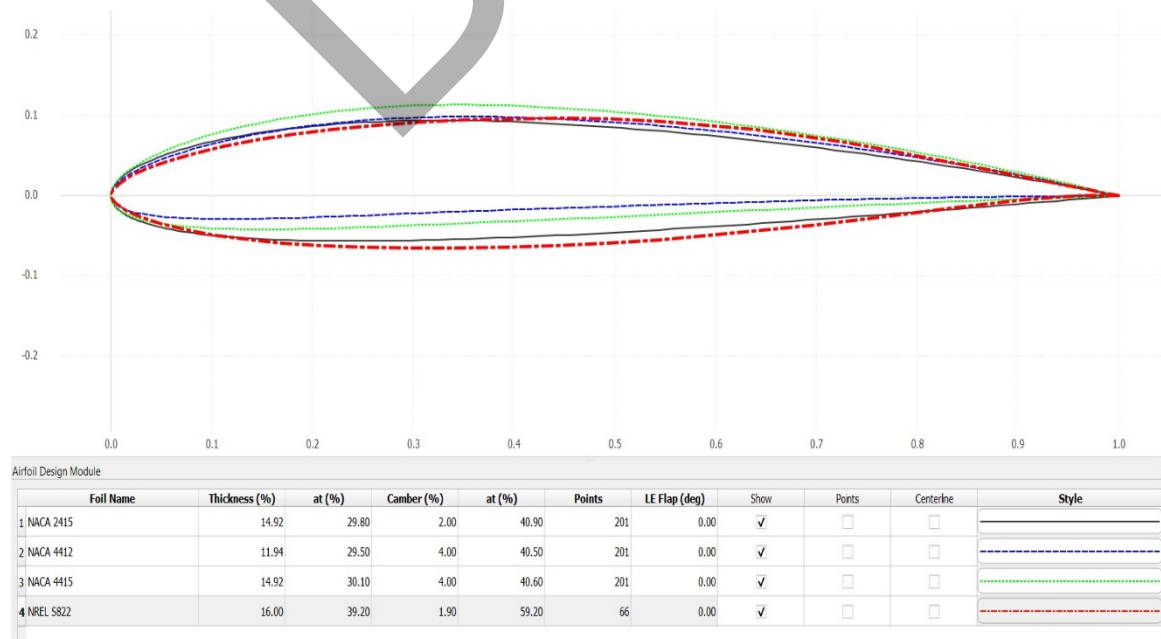
Figure 1. Airfoils and cross-sectional views used in the study

In Qblade software, NACA profiles are included in the software infrastructure. The coordinates of the profiles other than the NACA profile were defined in the software and included in the comparison. After defining the airfoils, lift and drag coefficients should be computed to be used in the calculations. In this study, airfoils were analysed for Reynolds number 1000000 and free flow turbulence value Ncrit=0,9. Aerodynamic polar plots provide information about the lift and drag forces of an airfoil at different angles of attack. The lift and drag forces of the airfoils for the specified values are presented in Figure (2).
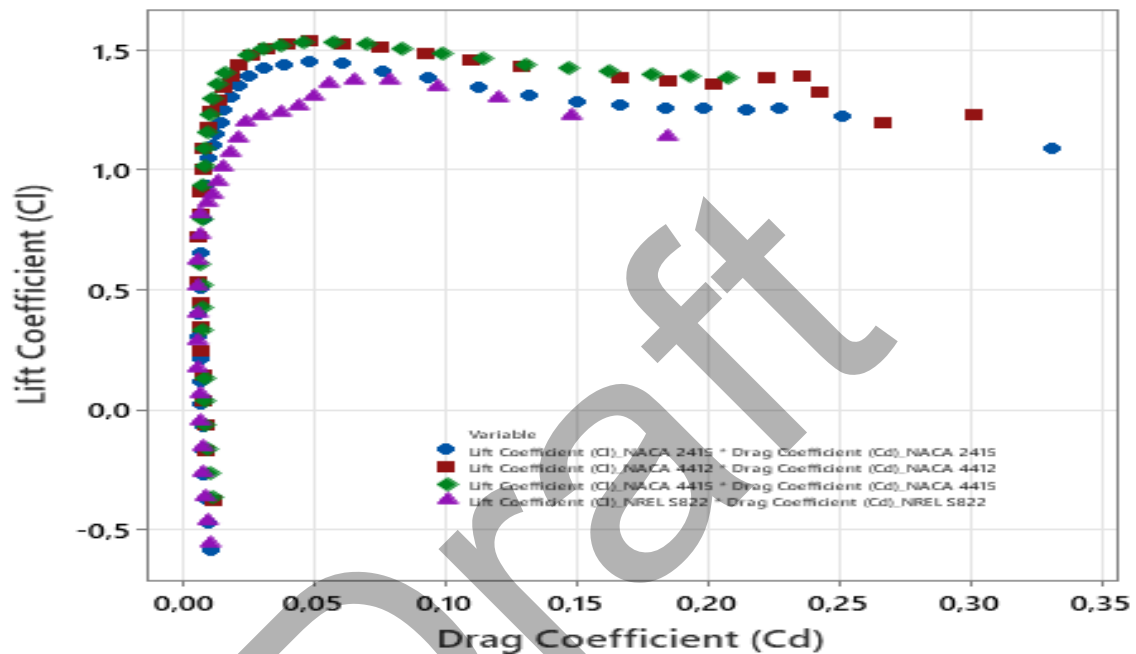
Figure 2. Lift and drag forces of airfoils

In order to make optimization in airfoil designs, it is necessary to know at which angles of attack the airfoils have the maximum glide ratio (Cl/Cd). In cases with high glide ratio, the power that can be obtained from the blade will be higher. Therefore, the angle of attack with maximum glide ratio should be computed for each airfoil. Figure (3) shows the glide ratios of the airfoils at different angles of attack. The analyses are performed for cases where the angle of attack varies from -5° to 30°.

When the results in Figure (3) are analyzed, it is seen that NACA 4412, NACA 4415 and S822 profiles reach the maximum glide ratio at 5° and NACA 2415 profile at 7°. 4412 profiles have the highest glide ratio with 131,08. The results obtained here were used to optimize the blades.
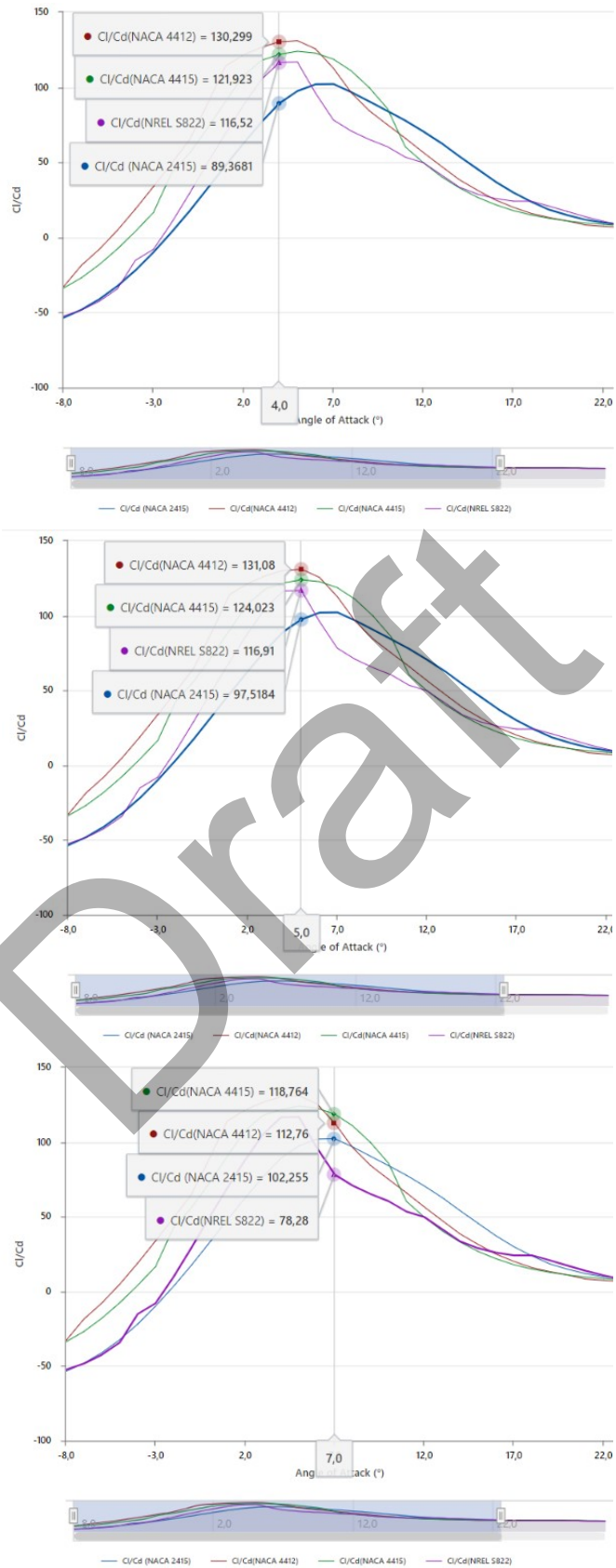
Figure 3. Glide ratios of the airfoils at different angle of attack

In this study, 3 cases were analyzed for each airfoil. The first case is the case where no optimization procedures are performed; the second case is the case where the wings are optimized according to the Schmitz method (Type 1); the third case is the situation where the Betz optimization method is applied to the blades (Type 2).

A total of 12 cases were comparatively analyzed. With the application of each optimization method, changes occurred in the design of the blades. As an example, the wing designed using the NREL S822 airfoil without optimization, with Type 1 and Type 2 optimization is presented in Figure 4.

For the 2-kW wind turbine, the blade length was determined as 1.2 meters. The same blade length was used in all airfoils. In case no optimization was used, the twist angle was defined into the system as 0.

Profile: NRELS822

Swept Area: 6.03 m^2

Without Optimisation

Schmitz Optimisation (Type 1)

Betz Optimisation (Type 2)
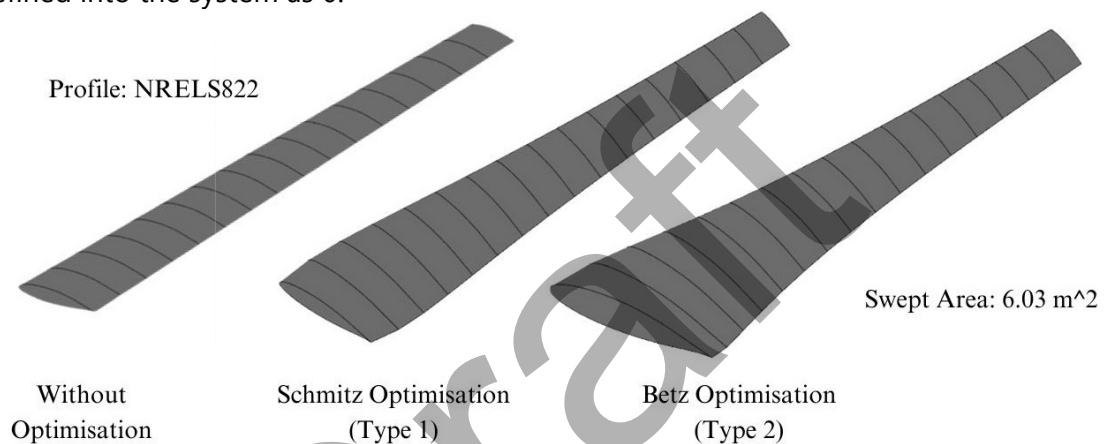
Figure 4. Variation of wings according to optimization types (NREL S822)

Chord lengths and twist angles of the blades for all cases are presented in Table 1. Each blade is divided into 17 equal sections with 0.075m spacing. When designing a wing, 10 to 20 sections are sufficient for optimization. [1]. In the designs, the number of parts can be increased towards the root or tip parts of the blades. During the optimization, the angles of attack specified in Figure 3 were taken into consideration.

Another important issue in blade design is the Tip Speed Ratio (TSR) on the blade. The larger tip speed ratio, the smaller the blade designs become, and the desired power values can be obtained at higher speeds. Considering the average wind speeds in our country, TSR is accepted as 5 for all designs.

In the designs, it is aimed to reach a capacity of 2 kW at 500 rpm when the wind speed is 10 m/s. Based on this, the TSR ratio was determined. Blades with low TSR ratio start to rotate and generate energy at lower wind speeds. When both optimization methods are examined, it is seen that the Chord lengths of the root parts of the blades are longer in the Betz optimization method.

Table 1. Chord and twist angles of the wings according to the positions

Position (m)	NACA 4412						NACA 4415					
	Without Optimization		Type 1		Type 2		Without Optimization		Type 1		Type 2	
	Chord (m)	Twist (°)	Chord (m)	Twist (°)	Chord (m)	Twist (°)	Chord (m)	Twist (°)	Chord (m)	Twist (°)	Chord (m)	Twist (°)
0,00	0,20	0,00	0,28	29,17	0,53	38,39	0,20	0,00	0,27	27,17	0,52	37,39
0,08	0,20	0,00	0,29	23,56	0,45	29,31	0,20	0,00	0,28	22,56	0,44	28,31
0,15	0,19	0,00	0,28	19,00	0,39	22,69	0,19	0,00	0,27	18,00	0,38	21,69
0,23	0,19	0,00	0,27	15,32	0,34	17,77	0,19	0,00	0,26	14,31	0,33	16,76
0,30	0,18	0,00	0,25	12,33	0,30	14,01	0,18	0,00	0,24	11,32	0,29	13,01
0,38	0,18	0,00	0,23	9,89	0,26	11,08	0,18	0,00	0,22	8,88	0,26	10,08
0,45	0,17	0,00	0,21	7,87	0,24	8,74	0,17	0,00	0,20	6,86	0,23	7,74
0,53	0,17	0,00	0,20	6,18	0,22	6,84	0,17	0,00	0,19	5,18	0,21	5,84
0,60	0,16	0,00	0,18	4,75	0,20	5,26	0,16	0,00	0,18	3,75	0,19	4,26
0,68	0,16	0,00	0,17	3,53	0,18	3,93	0,16	0,00	0,16	2,53	0,18	2,93
0,75	0,15	0,00	0,16	2,48	0,17	2,79	0,15	0,00	0,15	1,48	0,16	1,79
0,83	0,15	0,00	0,15	1,57	0,16	1,82	0,15	0,00	0,14	0,56	0,15	0,82
0,90	0,14	0,00	0,14	0,77	0,15	0,97	0,14	0,00	0,13	-0,23	0,14	-0,02
0,98	0,14	0,00	0,13	0,06	0,14	0,23	0,14	0,00	0,13	-0,95	0,13	-0,76
1,05	0,13	0,00	0,12	-0,57	0,13	-0,42	0,13	0,00	0,12	-1,57	0,12	-1,42
1,13	0,13	0,00	0,12	-1,14	0,12	-1,01	0,13	0,00	0,11	-2,14	0,12	-2,03
1,20	0,12	0,00	0,11	-1,64	0,12	-1,53	0,12	0,00	0,11	-2,64	0,11	-2,53

Position (m)	NACA 2415						NREL S822					
	Without Optimization		Type 1		Type 2		Without Optimization		Type 1		Type 2	
	Chord (m)	Twist (°)	Chord (m)	Twist (°)	Chord (m)	Twist (°)	Chord (m)	Twist (°)	Chord (m)	Twist (°)	Chord (m)	Twist (°)
0,00	0,20	0,00	0,29	26,17	0,53	35,39	0,20	0,00	0,30	26,30	0,50	33,03
0,08	0,20	0,00	0,29	20,56	0,46	26,31	0,20	0,00	0,29	20,34	0,41	24,16
0,15	0,19	0,00	0,28	16,00	0,39	19,69	0,19	0,00	0,27	15,77	0,34	18,07
0,23	0,19	0,00	0,27	12,31	0,34	14,77	0,19	0,00	0,25	12,25	0,93	13,71
0,30	0,18	0,00	0,25	9,32	0,30	11,01	0,18	0,00	0,22	9,49	0,26	10,47
0,38	0,18	0,00	0,23	6,88	0,27	8,08	0,18	0,00	0,20	7,30	0,23	7,98
0,45	0,17	0,00	0,21	4,86	0,24	5,74	0,17	0,00	0,19	5,53	0,20	6,02
0,53	0,17	0,00	0,20	3,18	0,22	3,84	0,17	0,00	0,17	4,07	0,18	4,43
0,60	0,16	0,00	0,18	1,75	0,20	2,26	0,16	0,00	0,16	2,86	0,17	3,20
0,68	0,16	0,00	0,16	1,53	0,18	0,93	0,16	0,00	0,15	1,83	0,15	2,04
0,75	0,15	0,00	0,16	-0,51	0,17	-0,20	0,15	0,00	0,14	0,94	0,14	1,11
0,83	0,15	0,00	0,15	-1,43	0,16	-1,17	0,15	0,00	0,13	0,18	0,13	0,32
0,90	0,14	0,00	0,14	-2,23	0,15	-2,02	0,14	0,00	0,12	-0,47	0,12	-0,36
0,98	0,14	0,00	0,13	-2,94	0,14	-2,76	0,14	0,00	0,11	-1,06	0,11	-0,97
1,05	0,13	0,00	0,13	-3,57	0,13	-3,42	0,13	0,00	0,11	-1,58	0,11	-1,50
1,13	0,13	0,00	0,12	-4,13	0,12	-4,01	0,13	0,00	0,10	-2,04	0,10	-1,98
1,20	0,12	0,00	0,11	-3,64	0,11	-3,53	0,12	0,00	0,10	-2,46	0,10	-2,40

Results

In accordance with the parameters determined for different airfoils, blade designs and analyses were performed using QBlade software. Under this heading, the results obtained from the analyses will be presented and evaluated comparatively. Tip Speed Ratio- Cp graph is presented in Figure 5.
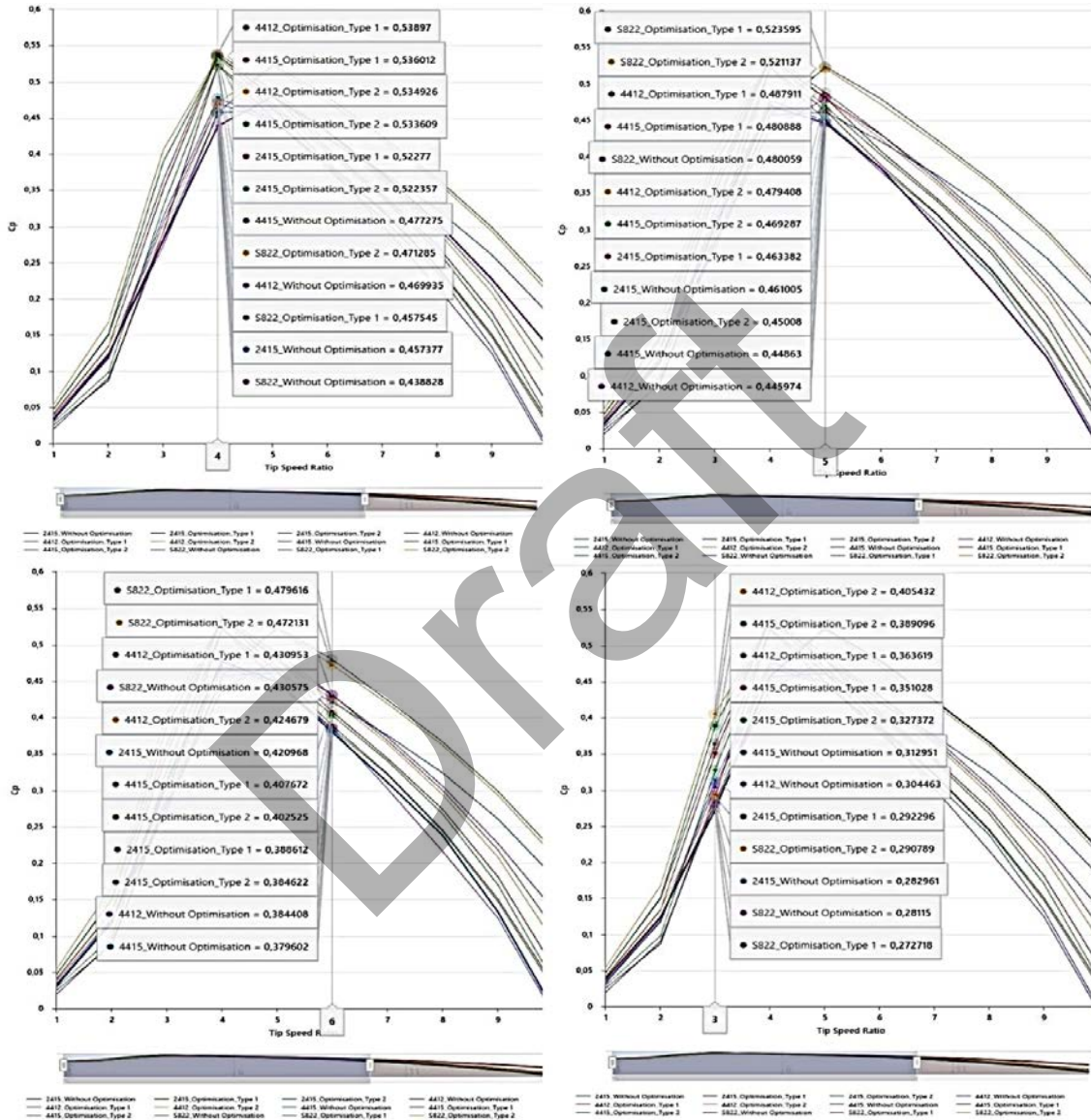
Figure 5. TSR (λ)-C$_p$ plot for different airfoils and optimization methods

When the graphs obtained in Figure 5 are examined, it is seen that the Schmitz optimized wing with NACA 4412 profile has the highest power coefficient with 0,538 for TSR 4 value. It can be said that NACA 4412, NACA 4415 give better results than other profiles at low TSR values. This TSR value, which is used to obtain power especially at low wind speeds, is not preferred because it increases the material and labour prices since it increases the blade surface too much. For TSR 5, the Schmitz optimized blade with NREL

S822 profile was found to give the highest value with 0,523. Both optimization methods of S822 gave better results than other airfoils. For TSR 6 value, the Schmitz optimized wing with NREL 822 profile gave the highest value with a power coefficient of 0,497. In general, when the graphs are analyzed, it can be said that the wing with NREL S822 profile gives better results. TSR-Power graphs for different airfoils and optimization methods are presented in Figure 6.
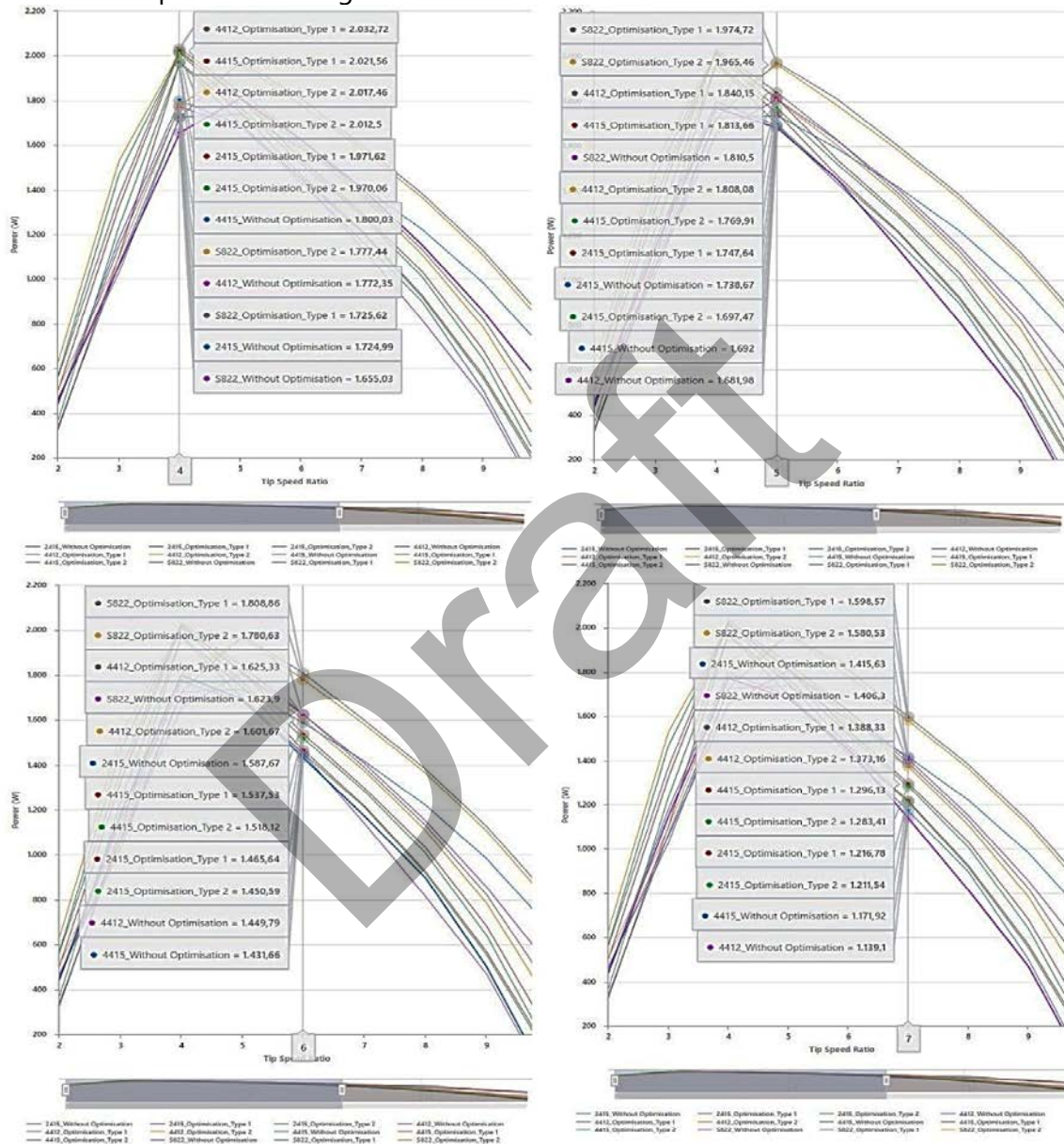
Figure 6. TSR (λ)-Power plot for different airfoils and optimization methods

When Figure 6 is examined, it is seen that the NACA 4412 profile with Schmitz optimization for TSR 4 is the blade type with the highest energy output with 2032,72 W. For TSR 5, TSR 6 and TSR 7 values, it is seen that the wings with NREL S822 profile, which are Schmitz optimized, have the highest power output with 1974,72 W, 1808,86 W and 1598,57 W, respectively. In general, when the blade designs are analyzed, it can be said that the blades with NREL S822 profile give better results in low-speed systems.

Conclusions

In this study, blades designed for small scale wind turbines using different airfoils and optimization methods are analyzed and comparatively investigated. Open source QBlade software was used in the study. NACA 4412, NACA 4415, NACA 2415 and NREL S822 blades, which are frequently used by researchers in small-scale wind turbines, were preferred as blade profiles. When the results obtained are evaluated, it is seen that blades with NREL 822 airfoil give better results in small-scale wind turbines. Within the scope of the study, Schmitz and Betz methods, which are blade optimization methods, were also evaluated. In the results obtained, it was seen that Schmitz optimized blades gave better results. In addition, it was observed that the chord length of the systems using Betz optimization method was longer than the Schmitz method.

References

[1]   M. R. Islam, L. Bin Bashar, and N. S. Rafi, "Design and Simulation of A Small Wind Turbine Blade with Qblade and Validation with MATLAB," *2019 4th Int. Conf. Electr. Inf. Commun. Technol. EICT 2019*, vol. 3, no. December, pp. 1–6, 2019, doi: 10.1109/EICT48899.2019.9068762.

[2]   P. E. Brockway, A. Owen, L. I. Brand-Correa, and L. Hardt, "Estimation of global final-stage energy-return-on-investment for fossil fuels with comparison to renewable energy sources," *Nat. Energy*, vol. 4, no. 7, pp. 612–621, 2019, doi: 10.1038/s41560-019-0425-z.

[3]   Z. Wang, A. Ozbay, W. Tian, and H. Hu, "An experimental study on the aerodynamic performances and wake characteristics of an innovative dual-rotor wind turbine," *Energy*, vol. 147, pp. 94–109, 2018, doi: 10.1016/j.energy.2018.01.020.

[4]   M. Alaskari, O. Abdullah, and M. H. Majeed, "Analysis of Wind Turbine Using QBlade Software," *IOP Conf. Ser. Mater. Sci. Eng.*, vol. 518, no. 3, 2019, doi: 10.1088/1757-899X/518/3/032020.

[5]   A. I. Altmimi, A. Aws, M. J. Jweeg, A. M. Abed, and O. I. Abdullah, "An Investigation of Design and Simulation of Horizontal Axis Wind Turbine Using QBlade," *Meas. Sci. Rev.*, vol. 22, no. 6, pp. 253–260, 2022, doi: 10.2478/msr-2022-0032.

[6]   K. Deghoum *et al.*, "Optimization of Small Horizontal Axis Wind Turbines Based on Aerodynamic, Steady-State, and Dynamic Analyses," *Appl. Syst. Innov.*, vol. 6, no. 2, pp. 1–19, 2023, doi: 10.3390/asi6020033.

[7]   T. John, "Horizontal Axial Wind Turbine Blade Design Using Ansys Fluent," *J. Multidiscip. Eng. Sci. Stud.*, vol. 2, no. 8, pp. 798–803, 2016.

[8]   A. Betz, *Wind energy and its utilization through windmills*, Vol.2. Göttingen: Vandenhoeck & Ruprecht., 1926.

[9]   G. Schmitz, "Theory and design of windwheels with an optimum performance," *Zeitschrift der Univ. Rostock*, vol. 56, 1955.

Comparative Analysis of Technical and Economic Aspects of Solar Tracking System and Fixed Tilt Angle Photovoltaic Systems for Bolu Province

K. Ozbek[1], K. Gelis[1] and O. Ozyurt[1]

[1]Bolu Abant Izzet Baysal University,Mechanical Engineering, Bolu, Türkiye, ORCID: 0000-0002-5475-8111, ORCID: 0000-0001-8612-2233, ORCID: 0000-0001-9148-3463

Abstract

The increasing global need for energy and the gradual depletion of fossil fuels increase the importance of renewable energy-sourced power plants. In this study, a high capacity solar power plant in Bolu province, which is located in the 3rd degree day zone in the Western Black Sea region of Turkey, has been comparatively analysed in terms of technical and economic aspects. In grid-connected solar power plants, the cases where the panels are fixed angle and have a single axis tracking system are analysed. Although technically single axis tracking systems seem to be partially advantageous, economically it can be said that fixed systems have much advantages. The results obtained show that fixed tilt angle systems will be more suitable for Bolu province.

Keywords: PVSyst, Mega Scale PV Plant, Solar Tracking Systemi, Fixed Angle Fotovoltaic System

Introduction

The increase in global population and energy consumption has made it important to increase the utilisation rates of sustainable energy sources. Globally, the demand for energy increases by approximately 4 per cent each year [1]. Today, most of the demand for energy is obtained from fossil fuels such as coal and natural gas. However, due to the limited lifespan of fossil fuel resources and the damage they cause to the environment, the trend towards renewable energy sources has increased [2].

The use of renewable energy sources is increasing globally. Approximately 250 GW of renewable energy-sourced plants are installed every year, and solar power plants constitute a large part of this. By 2025, the capacity of installed solar power plants is projected to account for 60% of all renewable energy-sourced plants [3].

Turkey meets most of its fossil-based raw material needs from other countries. Due to the increasing raw material prices, it can be said that Turkey's energy investments have been directed towards renewable energy based power plants in recent years. Although the share of renewable energy is increasing with the current investments, approximately

55% of electricity generation is obtained from fossil fuel-based power plants. Only 3.7% of Turkey's electricity demand can be supplied from solar power plants [4]. In 2021, Turkey signed the Paris Agreement, which has global targets against climate change. In this direction, it can be said that the orientation towards renewable energy sources and investments will increase day by day. Photovoltaic power plants with minimum operating and maintenance costs can serve for 25 years. Although the solar potential of our country is more than many countries, it is seen that it has less capacity in terms of installed power.

The systems used in solar power plants are affected by many parameters. Optimum system equipment and systems should be determined for each region and city. At this stage, optimum systems can be determined and designed with different software. PVSyst software is one of these software. PVSyst software has the capacity to perform comprehensive analyses for a solar power plant to be established in a selected region. When the studies in the literature are examined, it is seen that the analysis results are highly compatible with real-time data. In addition, the software can also be analysed for situations where solar radiation tracking systems are used. In some studies conducted in the literature using PVSyst software, real-time data and simulation results were analysed comparatively. They concluded that the results obtained from simulation are highly compatible with real-time data [5]–[8].

In this study, a high-capacity solar power plant in Bolu province, which is located in the 3rd degree day zone in the Western Black Sea region of Turkey, has been comparatively analysed from a technical and economic point of view. The capacity of the solar power plant is selected as 1 MW. In addition, the cases where the photovoltaic panels have a fixed angle system and a single axis tracking system are comparatively analysed..

Methodology

Climate data for Bolu province are taken from Meteonorm 7.2 database. Bolu province is located at 40.73° Latitude, 31.60° Langtitude and Altitude 722. Table 1 shows the climate data for Bolu province.

Table 1. Climatic data of Bolu province

Months	Monthly Solar Radiation(kWh/m²)	Temperature (°C)	Wind Speed (m/s)
January	40,1	1,1	1,11
February	55,0	2,0	1,20
March	96,2	5,9	1,40
April	128,4	10,0	1,40
May	165,2	14,7	1,29
June	177,6	18,0	1,29
July	194,0	21,3	1,30
August	177,3	21,6	1,39

September	131,5	16,6	1,26
October	87,7	12,5	1,08
November	55,7	7,0	1,10
December	38,5	2,9	1,09
Average	1347,2	11,1	1,20

The IEC 61724 standard is a standard used to measure the performance of photovoltaic systems. It implements a series of methods to evaluate the performance of photovoltaic systems. The parameters used in the evaluation of a system according to IEC 61724 standard are presented in Eq. (1)-Eq. (8).

DailyArray Yield $\quad\quad\quad\quad \frac{E_{DC,d}}{P_{PV}}$ [kWh/kW/day] $\quad\quad\quad\quad\quad\quad\quad$ (1)

Array Yield: $\quad\quad\quad Y_{(A,m)} = \frac{1}{N}\sum_{d=1}^{N} Y_{(A,d)}$ [kWh/kW/month] $\quad\quad\quad$ (2)

PV System Yield: $\quad\quad Y_{(f,m)} = \frac{1}{N}\sum_{d=1}^{N} Y_{(f,d)}$ [kWh/kW/month] $\quad\quad\quad$ (3)

Reference Yield: $\quad\quad\quad Y_{(r)} = \frac{H_i}{G_{stc}}$ [kWh/kW/year] $\quad\quad\quad\quad\quad\quad$ (4)

Performance Ratio: $\quad\quad\quad\quad\quad\quad\quad\quad\quad\quad\quad\quad\quad R_p = \frac{Y_f}{Y_r}$ (%)
(5)

PV Module Efficiency: $\quad\quad\quad\quad\quad\quad\quad\quad\quad\quad \eta_{PV} = \frac{E_{AC}}{H_i\,x\,A_{PV}}$ (%)
(6)

Invertor Efficiency: $\quad\quad\quad\quad\quad\quad\quad\quad\quad\quad\quad \eta_{Inv} = \frac{P_{AC}}{P_{DC}}$ (%)
(7)

Total Efficiency: $\quad\quad\quad\quad\quad\quad\quad\quad\quad\quad\quad \eta_{tot} = \eta_{PV}\,x\,\eta_{inv}$ (%)
(8)

where $E_{DC,d}$ is DC energy generation in a day, P_{PV} is the power of the PV plant, N is the number of days, $E_{AC,d}$ is Ac energy output in a day, E_{AC} is AC energy output and A_{PV} is the area of PV module.

Grid connected solar power plants consist of PV arrays, Combiner Box, DC/AC inverter, Utility Meter, Transformer. In this study, the photovoltaic panels are fixed and single axis tracking system is used. For a 1 MW capacity solar power plant, an area of approximately 6000 m^2 is required [9].

The optimum panel angle for Bolu was determined as 33°. For the case of a two-axis tracking system, the tracking system is planned to operate between a minimum of 10° and a maximum of 80°. Details about the optimum panel angle are presented in Figure 1.
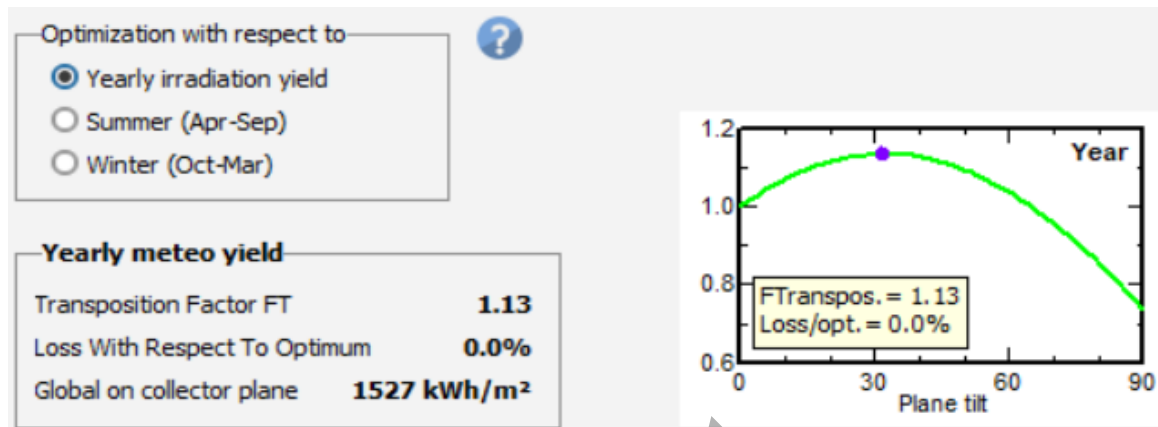
Figure 1. Optimum panel angle for Bolu province

AE400DGLM6-72 of AE Solar, which is available in Turkey, was preferred as solar panel. The same panels were used in both systems. The characteristic graphs of the selected panel are presented in Figure 2. The characteristics of the panel are presented below.

- Max Power Point (Pmpp): 400,7 W ;Max Power Point Current (Impp): 9,78 A; Short- Circuit Current (Isc): 10,32 A; Temperature Coefficient: -0,36 %/°C; Max Power Point Voltage (Vmpp): 41 V; Open Circuit Voc= 49,7 V
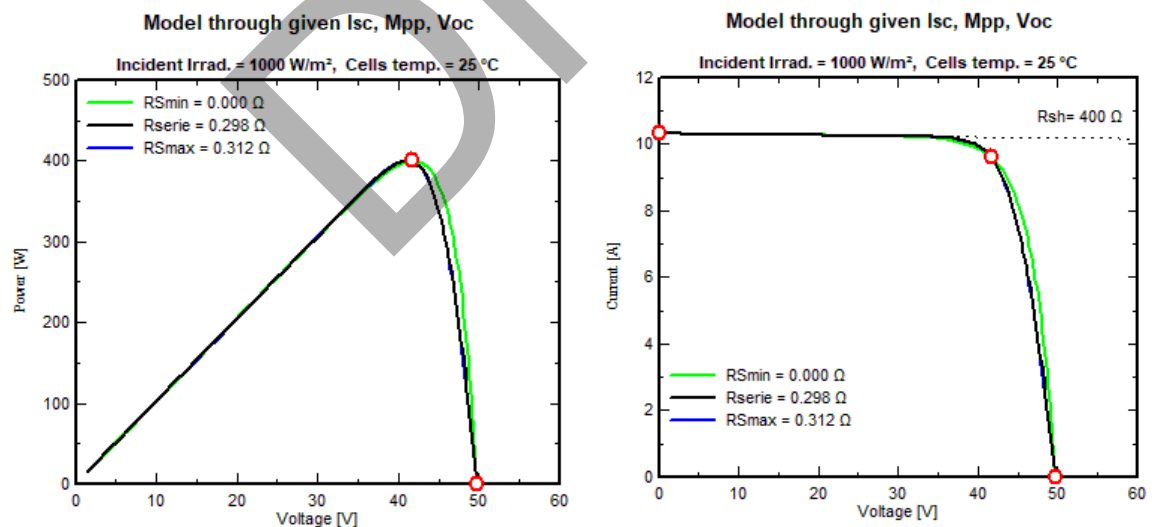
Figure 2. Characteristic graphs of the selected photovoltaic panel

It is seen that the panels reach the maximum power value with 400 W at 1000 W / m² radiation value. SG1000 MX 1000 kW inverter produced by Sungrow brand was preferred as inverter. The DC voltage range of the inverter is 550-850 V and the maximum efficiency is 98%.

Results

In this study, the design and simulations of a solar power plant with a capacity of 1 MW for Bolu province were carried out. The analyses have been performed for the case where the panels have a fixed tilt angle and the panels have a solar ray tracking system, and the results are evaluated comparatively. In both systems, 2500 photovoltaic panels were used to provide the desired capacity.

Normalised production values depending on months for both cases are presented in Figure 3(a) and Figure 3(b).
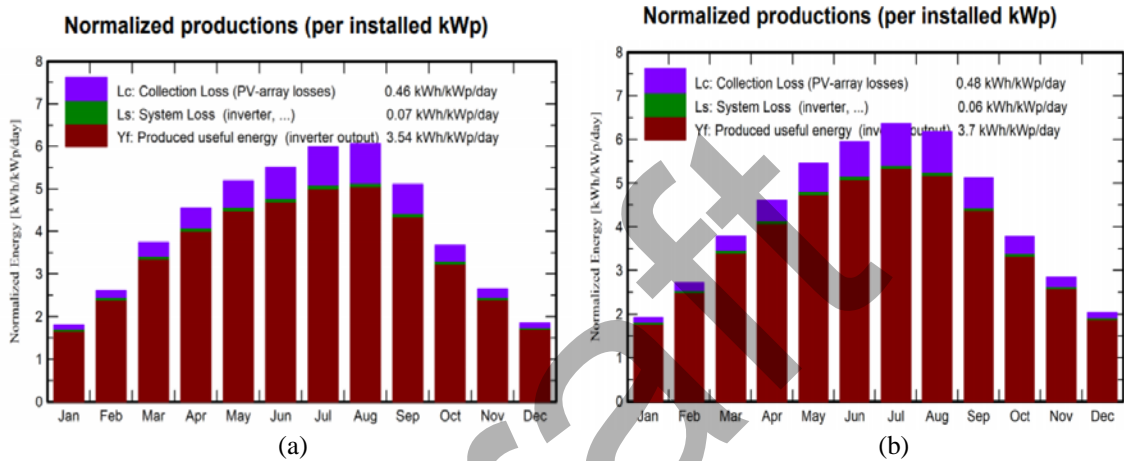
Figure 3. Normalised production values of photovoltaic systems according to months (a): fixed angle system; (b) single axis tracking system

When the graphs in Figure 3 are evaluated, it is concluded that the daily normalised production of the solar power plant with the tracking system is higher and the system losses are lower. Performance ratios of both systems are given in Figure 4.
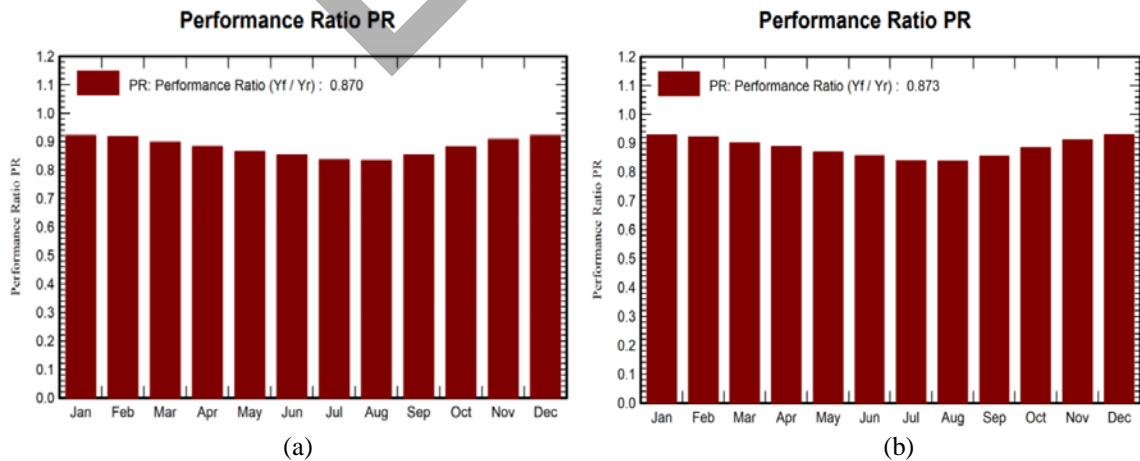
Figure 4. Performance ratios of photovoltaic systems according to months (a): fixed angle system; (b) single axis tracking system

When the Performance Ratios given in Figure 4 are analysed, it is seen that the performances of the systems in both cases give almost the same results. The performance ratio of the power plant with single axis tracking system is higher. The comparison of the annual energy production of both systems is given in Table 2.

Table 2. Annual energy production of the systems

System	Produced Energy (MWh/year)	Specific Production (kWh/kWp/year)	Performance Ratio (%)
Fixed Angle PV	1291	1292	86,96
Single Axis Tracking PV	1350	1351	87,34

When the data in Table 2 are analysed, it is seen that the annual production of the single axis tracking system is higher. When analysed technically, it is concluded that the single axis tracking system produces more energy for Bolu province.

From an economic point of view, the equipment used in both systems and their costs are presented in Table 3.

Table 3. System Cost Details

Description	Unit Price
PV Modules	196 $
Support Modules (For Fixed)	26,25 $
Support Modules (For Single Axis Tracking System)	120,15 $
Invertor	32500 $
Engineering	3000$
Permitting	6500 $
Global Installation cost per module	19900 $
Transport	10000 $
Wiring	10000 $
Land Cost	120000$
Salaries (per year)	8000 $
Cleaning (per year)	5000 $
Security (per year)	1000 $

Economic analyses of fixed angle solar power plants and solar power plants with single axis tracking system have been made. Calculations are made for the case where the solar power plant has a service period of 25 years. The initial investment cost is analysed for the case where the entire initial investment cost is met from equity capital for both scenarios. Based on the tariffs of electricity distribution companies in Turkey, it is predicted that the energy will be sold to companies at a price of 0.12 USD/kWh. Annual cash flow summary for solar power plants with fixed angle and single axis tracking system are given in Figure 5(a) and Figure 5(b).
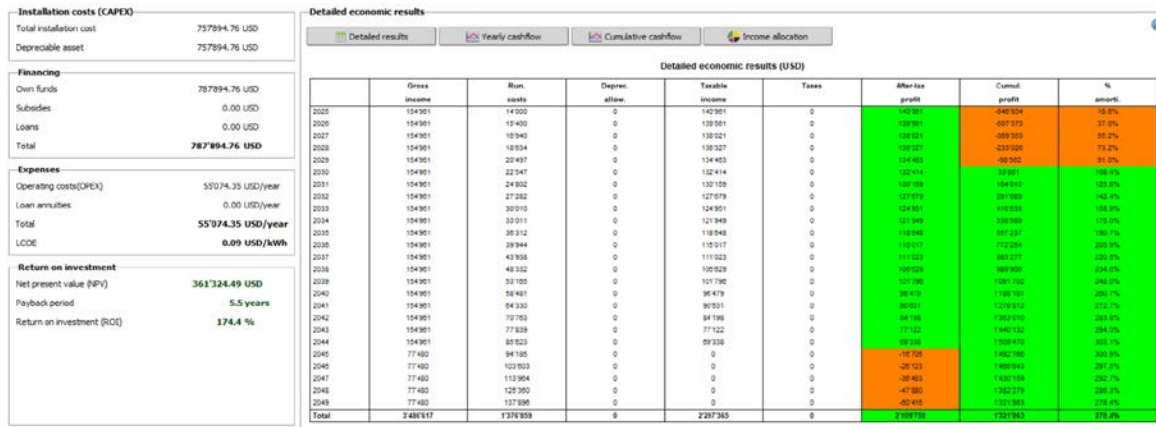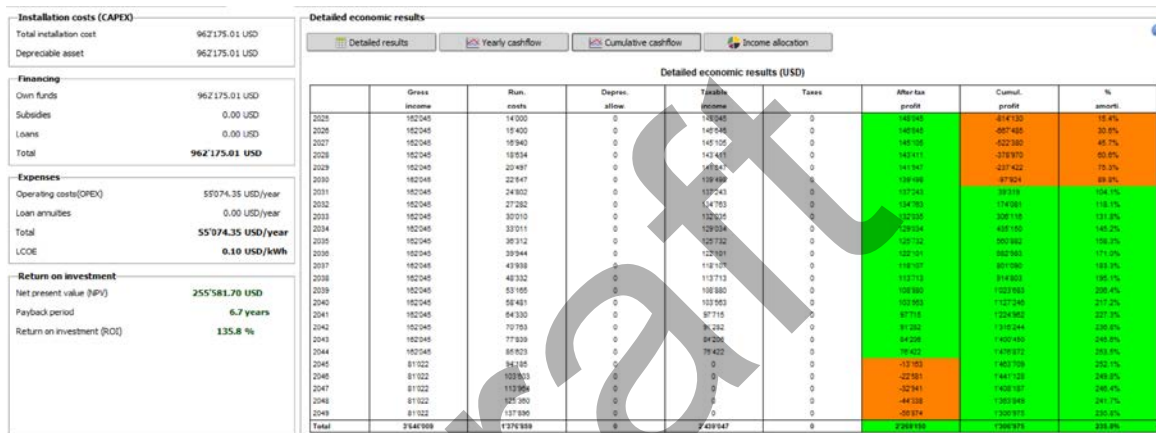
Figure 5. Annual cash flow for solar power plants with fixed angle and single axis tracking system (a): fixed angle system; (b) single axis tracking system

When Figure 5 is analysed, it is seen that the payback period of the fixed angle system is lower than the single axis tracking system. While the payback period of the fixed angle system is 5.5 years, the payback period of the single axis tracking system is 6.7 years. The initial investment cost of the single axis tracking system is 22% higher than the fixed angle system. When the Return of Investment (ROI) values of both systems were analysed, it was seen that the ROI value of the fixed angle system was higher. When the results obtained are evaluated in general, it is seen that the uniaxial tracking system is disadvantageous for Bolu province. The fact that the initial investment costs, payback periods are high and ROI values are low has led to the conclusion that single axis tracking systems are not suitable for Bolu province.

Conclusions

In this study, a high capacity solar power plant in Bolu province, which is located in the 3rd degree day zone in the Western Black Sea region of Turkey, has been comparatively analysed from a technical and economic point of view. The capacity of the solar power plant is selected as 1 MW. When analysed from a technical point of view, it is seen that partially more energy can be produced than the plants with a single axis tracking system.

When the systems are analysed economically, it is seen that the fixed system has much more advantages. The minimal increase in energy production does not cover the increase in costs. Based on this, it is concluded that single axis tracking systems are not feasible for Bolu province.

Acknowledgement: The author(s) declared no potential conflicts of interest with respect to the research. author-ship. and/or publication of this article.

References

[1]   IEA, "Energy Efficiency 2021," 2021. [Online]. Available: https://webstore.iea.org/download/direct/4259

[2]   D. Okello, E. E. Van Dyk, and F. J. Vorster, "Analysis of measured and simulated performance data of a 3.2 kWp grid-connected PV system in Port Elizabeth, South Africa," *Energy Convers. Manag.*, vol. 100, pp. 10–15, Aug. 2015, doi: 10.1016/j.enconman.2015.04.064.

[3]   IEA, "Renewables 2020," IEA,PARIS, 2020. [Online]. Available: https://www.iea.org/reports/renewables-2020

[4]   TEIAS, "Installed Capacity Report (2022-01)," Ankara, 2022. [Online]. Available: https://www.teias.gov.tr/tr-TR/kurulu-guc-raporlari

[5]   D. Dey and B. Subudhi, "Design, simulation and economic evaluation of 90 kW grid connected Photovoltaic system," *Energy Reports*, vol. 6, pp. 1778–1787, Nov. 2020, doi: 10.1016/j.egyr.2020.04.027.

[6]   H. Vidal, M. Rivera, P. Wheeler, and N. Vicencio, "The analysis performance of a grid-connected 8.2 kwp photovoltaic system in the patagonia region," *Sustain.*, vol. 12, no. 21, pp. 1–16, 2020, doi: 10.3390/su12219227.

[7]   Z. Corba, B. Popadic, D. Milicevic, B. Dumnic, and V. A. Katic, "A long-term condition monitoring and performance assessment of grid connected PV power plant with high power sizing factor under partial shading conditions," *Energies*, vol. 13, no. 18, p. 4810, Sep. 2020, doi: 10.3390/en13184810.

[8]   R. Srivastava, A. N. Tiwari, and V. K. Giri, "Performance evaluation of parking integrated grid-connected photovoltaic system located in Northern India," *Environ. Dev. Sustain.*, vol. 23, no. 4, pp. 5756–5775, Apr. 2021, doi: 10.1007/s10668-020-00845-4.

[9]   B. Tripathi, P. Yadav, S. Rathod, and M. Kumar, "Performance analysis and comparison of two silicon material based photovoltaic technologies under actual climatic conditions in Western India," *Energy Convers. Manag.*, vol. 80, pp. 97–102, Apr. 2014, doi: 10.1016/j.enconman.2014.01.013.

[10]   A. I. Altmimi, A. Aws, M. J. Jweeg, A. M. Abed, and O. I. Abdullah, "An Investigation of Design and Simulation of Horizontal Axis Wind Turbine Using QBlade," *Meas. Sci. Rev.*, vol. 22, no. 6, pp. 253–260, 2022, doi: 10.2478/msr-2022-0032.

[11]   M. R. Islam, L. Bin Bashar, and N. S. Rafi, "Design and Simulation of A Small Wind Turbine Blade with Qblade and Validation with MATLAB," *2019 4th Int. Conf. Electr. Inf. Commun. Technol. EICT 2019*, vol. 3, no. December, pp. 1–6, 2019, doi: 10.1109/EICT48899.2019.9068762.

Enhancement of Corrosion Resistance for Biodegradable Pure Magnesium by Anodization Processes

Ş.M. Tüzemen[1], Y.B. Bozkurt[1], H. Kovacı[1,2], Z. Halıcı[3], A. Çelik[1]

[1]*Atatürk University, Department of Mechanical Engineering, Erzurum, Turkey, ORCID: 0000-0003-0400-5602, ORCID: 0000-0003-3859-9322, ORCID: 0000-0002-8096-0794*
[2]*Ataturk University, East Anatolia High Technology Application and Research Center (DAYTAM), Erzurum, Turkey ORCID: 0000-0002-9053-3593*
[3]*Ataturk University, Department of Pharmacology, Erzurum, Turkey ORCID: 0000-0001-6854-6059*

Abstract

Magnesium and its alloys have been preferred since 2000's as an alternative to Titanium, Cobalt-Chromium and Austenitic Stainless Steel metals and alloys, which are frequently preferred in implant and prosthesis applications. These materials have biodegradable properties in terms of biocompatibility and bring many advantages in medical applications with these properties. However, the control of the degradability properties of magnesium and its alloys is very important in terms of healing times and mechanical strength in implant applications. Since the degradation processes of Mg and its alloys such as corrosion, wear resistance, fatigue strength, biocompatibility are also related to their surfaces, surface treatments can be applied to control this situation. Anodic oxidation, also known as anodization, is the process of forming a stable and protective oxide film with adjustable nano- or micro-scale thickness on metals, including Mg and its alloys. In this study, anodization of pure magnesium samples was carried out using an environmentally friendly medium of 10 M NaOH electrolyte solution. In order to investigate the effect of additives on the degradation property during the anodization process, 1 g/L h-BN additive was added to the electrolyte solution. For comparison, untreated-Mg, anodized-Mg and h-BN doped anodized-Mg samples were subjected to corrosion tests in stimulated body fluid (SBF). The test results showed that the anodization process increased the corrosion resistance, while the h-BN doping increased this effect more.

Keywords: Pure Magnesium, Biodegradable, Corrosion, Anodization, h-BN.

Introduction

Magnesium (Mg) and its alloys are biomaterials that have attracted attention for biodegradable in-body implant applications since the early 2000s [1]. Other attractive properties of Mg are that it has mechanical properties close to human cortical bone and does not exhibit magnetic properties in terms of medical imaging [2]. Due to all these

superior properties, implants produced from Mg and its alloys are biodegradable after the damaged tissue heals, eliminating the need for a repeat surgical procedure. This situation allows for both economical and healthier implant applications [3]. When Mg and its alloys degrade, they release Mg^{2+} ion, which is one of the most abundant cations in intracellular and extracellular fluids in the body and is necessary for the formation of bone/dental tissue [4]. However, since Mg is a highly active element, its corrosive degradation in the body must be controlled. Surface treatments are applied to improve the corrosive properties of Mg and its alloys [5].

Anodization is an electrochemical surface treatment often applied to Mg and its alloys that allows to grow a stable and protective oxide film of adjustable thickness [4], [5]. This surface treatment takes place in an electrolytic cell. During the process, the anode (+ pole) is selected as the working electrode and the cathode (- pole) as the counter electrode, and direct current is applied by means of a power supply to the anode and cathode located at a certain distance in the electrolyte [6]. As with all metals subjected to anodization, the anodic behavior of Mg and its alloys and the properties of the oxide film formed depend on the alloy composition, applied current/voltage, time and parameters such as composition, concentration and pH of the electrolyte [7]. While acidic media is generally preferred in the anodization process, the stability of the oxide films formed in acidic media in Mg and its alloys and their poor antibacterial properties have led researchers to basic electrolytes. In addition, the ability to incorporate different additives into the structure during the anodization process makes this process more attractive than other surface treatments [6], [7].

Hexagonal boron nitride (hBN) exhibits insulating properties due to the strong covalent bonding of boron and nitrogen atoms in hexagonal form, and relative elastic properties due to the bonding of these hexagonal forms in layers with weak van der Waals forces between them, allowing the layers to slide. Insulation and sliding properties of the surface in terms of abrasion resistance are among the other properties desired in in-body implants. In addition, hBN is a non-toxic, chemically inert and environmentally friendly material [9]. Studies also show that hBN doping enhances the antibacterial effect in in vivo implants [10], [11].

In this study, the anodization potential of Mg in environmentally friendly NaOH electrolyte for biodegradable implant applications and the effect of h-BN doping, which is highly biocompatible, were investigated. The study aimed to improve the corrosion resistance of the surface and accordingly, untreated, anodized, and h-BN doped anodized Mg samples were subjected to corrosion tests in stimulated body fluid (SBF).

Materials and Methods

Within the scope of this study, in order to make a comparison, pure magnesium samples prepared with a diameter of 1.5 mm and a thickness of 3 mm were subjected to anodization process for 20 minutes by applying a constant voltage of 10 V in 10 M 150 ml NaOH and 10 M 100 ml NaOH solutions containing 1g/L h-BN. After surface

treatment, corrosion tests were performed on untreated Mg, anodized Mg, and h-BN doped anodized Mg samples. During the anodization process, Mg electrode was used as anode and graphite electrode was used as cathode. The compounds and species formed on the surface by anodization of magnesium are shown by the reactions given in (1), (2), and (3).

$$Mg \longrightarrow Mg^{2+} + 2e^- \tag{1}$$

$$Mg^{2+} + 2OH^- \longrightarrow Mg(OH)_2 \tag{2}$$

$$Mg(OH)_2 \longrightarrow MgO + H_2O \tag{3}$$
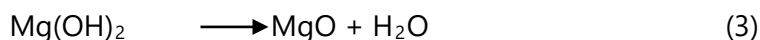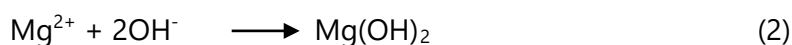
After surface treatment, untreated, anodized, and h-BN doped anodized Mg samples were subjected to corrosion tests in artificial body fluid (SBF) whose components are given in **Table 1**. The corrosion tests were carried out with a 3-electrode system with Mg samples as working electrode, graphite rod as counter electrode and Ag/AgCl reference electrode. The tests were started by measuring the Open Circuit Potential (OCP) for 1800 seconds. Electrochemical Impedance Spectroscopy, Cyclic Potentiodynamic Polarization and again Electrochemical Impedance Spectroscopy analyses followed. Test results and graphs are given in detail in the next section.

Table 1. Compounds of SBF (pH=7.4)

Ion Concentrations	Counts
Na^+ (mmol L^{-1})	142
K^+ (mmol L^{-1})	5.0
Ca^{2+} (mmol L^{-1})	2.5
Mg^{2+} (mmol L^{-1})	1.5
HCO_3^- (mmol L^{-1})	4.2
Cl^- (mmol L^{-1})	147
HPO_4^{2-} (mmol L^{-1})	1
SO_4^{2-} (mmol L^{-1})	0.5
Tris (g L^{-1})	6.069

Results and Discussions

Surface images after anodization are given in **Figure 1**. **Figure 1 (a)** shows the untreated, **(b)** the anodized, and **(c)** the hBN doped anodized pure Mg samples. It was observed that the surface became dull and rougher after coating.
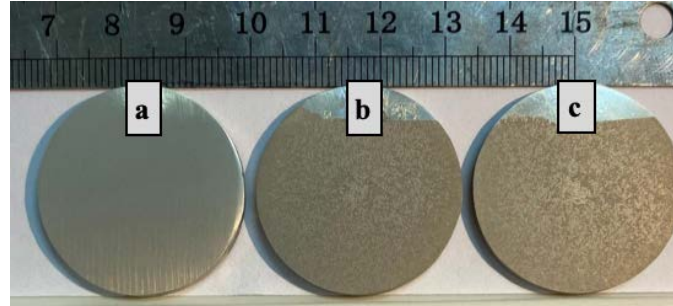
Figure 1. (a) Untreated, **(b)** anodized, and **(c)** hBN doped anodized pure Mg samples.

The results of the corrosion tests are given graphically. In the **Figure 2**, OCP diagrams are given as time-voltage and it is seen in the graph that the open circuit potential increases with the anodization process compared to the untreated sample and the hBN additive supports this increase more.
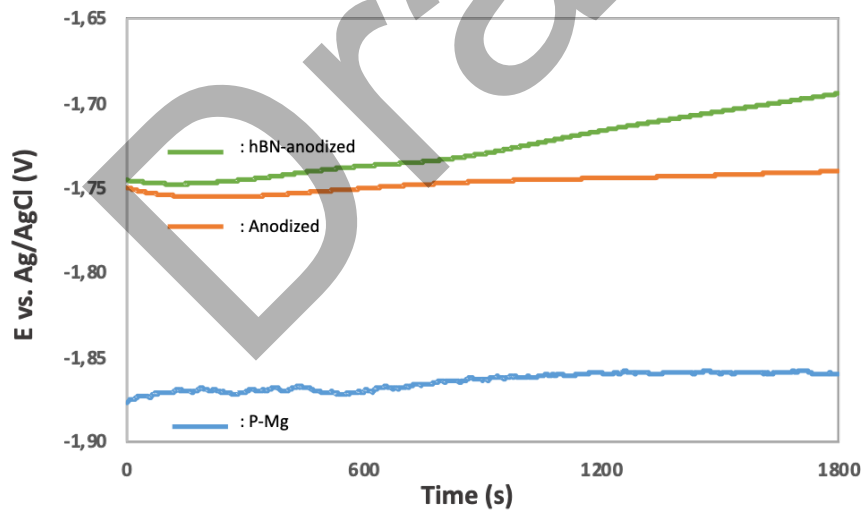
Figure 2. Open Circuit diagrams of samples

Figure 4 shows the electrochemical impedance spectroscopy (EIS) analysis results of all samples before cyclic polarization. When all these curves are examined, it is observed that the anodization process increases the corrosion resistance. **Figure 4 (a)** shows that the capacitive loop expands in the surface treated samples and this increases the corrosion resistance [6]. In **Figure 4 (c)**, the highest phase angle is observed in the hBN-anodized sample and it is seen that the highest corrosion resistance is obtained in the hBN doped structure among these three samples. When all these curves are examined, it is observed that the anodization process increases the corrosion resistance.
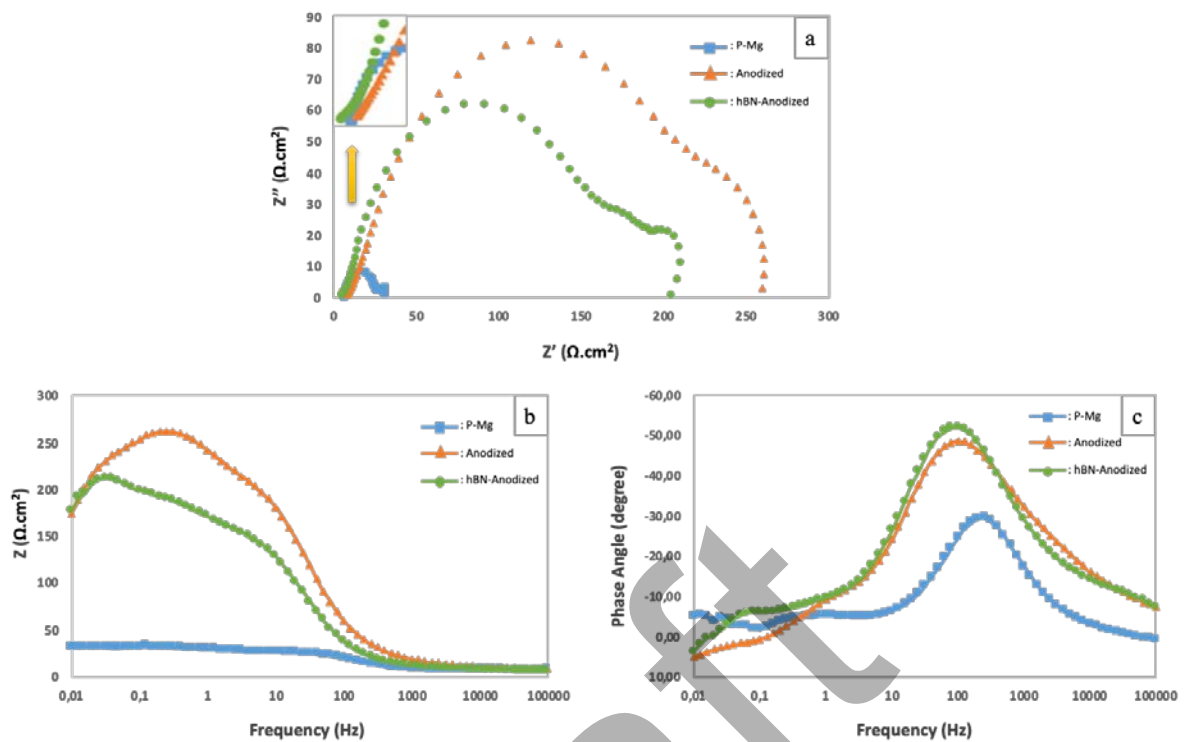
Figure 3. (a) Nyquist, **(b)** Bode, and **(c)** phase angle curves of all samples before cyclic polarization.

Figure 4 shows the cyclic polarization diagrams of untreated, anodized and h-BN doped anodized Mg samples. As it is known, the increase in corrosion resistance is realized by shifting the graph of the sample to the left and upwards along the voltage-current density graph in this diagram, that is, the corrosion voltage and current density approach the more positive regions [1]. As can be seen from the diagram, the surface treatments increased the corrosion resistance of biodegradable magnesium.
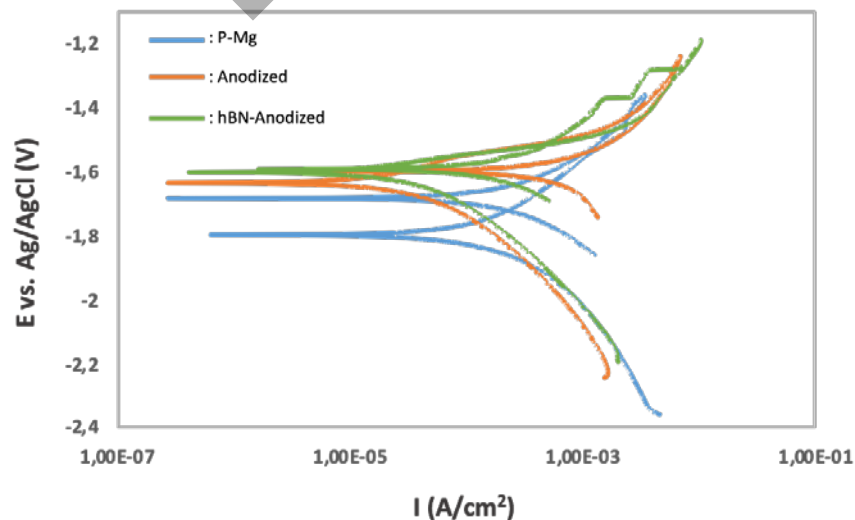
Figure 4. Cyclic polarization diagrams of samples

In **Table 2**, solution-interface beta values, corrosion current, corrosion voltage and corrosion rate of cyclic polarization tests are given. It was observed that the current and voltage values of hBN-anodized Mg were lower than the other samples and the process increased the corrosion resistance. It was also observed that the lowest corrosion rate value of mm loss per year occurred in the hBN-anodized sample.

Table 2. Compounds of SBF (pH=7.4)

Samples	Beta A (V/decade)	Beta C (V/decade)	Icorr (A/cm^2)	Ecorr (V)	Corrosion rate (mpy)
Untreated	413.6e-3	299.6e-3	232.0e-6	-1.800	209.0
Anodized	151.5e-3	196.2e-3	30.10e-6	-1.630	27.08
hBN-anodized	63.30e-3	141.1e-3	17.20e-6	-1.600	15.52

Figure 5 shows the changes that occur on the surfaces of untreated, anodized, and hBN-anodized Mg samples after corrosion. In **Figure 5 (a)**, the untreated surface appears lighter because an oxide layer is formed, while the anodized and hBN-anodized surfaces appear darker because they are already covered with an oxide film.
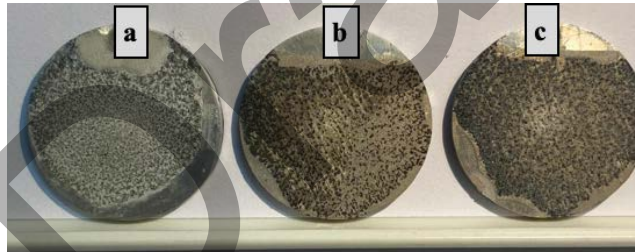
Figure 5. (a) Untreated, **(b)** anodized, and **(c)** hBN doped anodized pure Mg samples after corrosion tests.

Conclusions

The test results showed that the anodization process increased the corrosion resistance, while the h-BN doping increased this effect more. As a result of the analysis, it was confirmed that the corrosion resistance was increased by anodization process and hBN additive and that this process applied to biodegradable pure Mg can provide control of the degradation process. It is thought that more controlled structures can be obtained with this process in intra-body implants to be produced from pure Mg.

References

[1] Y.B. Bozkurt, A. Çelik, 2022. Tailoring biodegration rate of AZ31 magnesium alloy, Electrochimica Acta, 435 (2022) 141403.

[2] A.F. Cipriano, J. Lin, C. Miller, A. Lin, M.C.C. Alcaraz, P. Soria, H. Liu, 2017. Anodization of magnesium for biomedical applications – Processing, characterization, degradation and cytocompatibility, Acta Biomaterialia, 62 (2017) 397-417.

[3] L. Meng, X. Liu, L. Liu, Q. Hong, Y. Cheng, F. Gao, J. Chen, Q Zhang, C. Pan, 2022. Comparative Investigation of the Corrosion Behavior and Biocompatibility of the Different Chemical Conversion Coatings on the Magnesium Alloy Surfaces, Metals, 12(10) (2022) 1644.

[4] D. Peixoto Barbosa, G. Knörnschild, 2009. Anodization of Mg-alloy AZ91 in NaOH solutions, Surface and Coatings Technology, 203(12) (2009) 1629-1636.

[5] D. Xue, Y. Yun, M.J. Schulz, V. Shanov, 2011. Corrosion protection of biodegradable magnesium implants using anodization, Materials Science and Engineering: C, 31(2) (2011) 215-223.

[6] S.A. Salman, M. Okido, 2013. Anodization of magnesium (Mg) alloys to improve corrosion resistance, Editor(s): Guang-Ling Song, In Woodhead Publishing Series in Metals and Surface Engineering, Corrosion Prevention of Magnesium Alloys, Woodhead Publishing, (2013), 197-231.

[7] A. Hussain, C. Gautam, A. Jafri, V.K. Mishra, A. Madheshiya, A. Gautam, M.K. Singh, R.K. Gautam, M. Gupta, Md. Arshad, R. Vajtai, P.M. Ajayan, 2020. Formation of multifunctional ZrO2–MgO-hBN nanocomposite for enhanced bone regeneration and E coli bacteria filtration applications, Ceramics International, 46(14) (2020) 23006-23020.

[8] A. Gnanavelbabu, M. Prahadeeswaran, R. Rai, N.S. Ross, M.K. Gupta, 2023. Tribo-corrosive wear behaviour of squeeze-casted Mg/TiN/hBN composite under different ageing temperature, Tribology International, 187 (2023) 108748.

[9] J. Eichler, C. Lesniak, 2008. Boron nitride (BN) and BN composites for high-temperature applications, J. Eur. Ceram. Soc., 28 (5) (2008) 1105-1109.

[10] M. Ikram, I. Jahan, A. Haider, J. Hassan, A. Ul-Hamid, M. Imran, J. Haider, A. Shahzadi, A. Shahbaz, S. Ali, 2020. Bactericidal behavior of chemically exfoliated boron nitride nanosheets doped with zirconium, Appl. Nanosci., 10 (7) (2020) 2339-2349.

[11] A.M. Kumar, M.Y. Khan, A. Khan, M.A. Hussein, H. Dafalla, S.H. Jang, S. Ramakrishna, 2022. Novel polymer nanocomposite based on polypyrrole and ZrO2 reinforced BN nanosheets: prospective utilization as implant coatings for TiNbZr bio-implant alloy, Mater. Chem. Phys., 287 (2022) 126205.

Examination on the Tribological Properties of hBN Doped Anodized Pure Magnesium

Ş.M. Tüzemen[1], Y.B. Bozkurt[1], Y. Uzun[1], H. Kovacı[1,2], A. Çelik[1]

[1]Atatürk University, Department of Mechanical Engineering, Erzurum, Turkey, ORCID: 0000-0003-0400-5602, ORCID: 0000-0003-3859-9322, ORCID: 0000-0002-5134-7640, ORCID: 0000-0002-8096-0794
[2]Ataturk University, East Anatolia High Technology Application and Research Center (DAYTAM), Erzurum, Turkey ORCID: 0000-0002-9053-3593

Magnesium and its alloys have recently been widely used in the aviation, aerospace, aircraft, automobile and medical industries due to their low density and light weight. However, these materials also have low hardness values and very low wear resistance. Therefore, Mg and its alloys are tried to improve their wear resistance either by adding additives to their structures to obtain alloys and composites or by surface treatments. In terms of surface treatments, coating the surface with a lubricant structure can improve wear resistance, lubricants are classified as solid and liquid lubricants. The use of Mg and its alloys with solid lubricants instead of liquid lubricants is considered more suitable due to their application areas and low corrosion resistance. Solid lubricants are structures that offer a slippery surface thanks to their layered structure without the need for a liquid medium. In this sense, hexagonal Boron Nitride (hBN), which is a 2D material group, is used as a solid lubricant with Van der Waals bonds that facilitate sliding between hexagonal layers. Within the scope of this study, in order to make a comparison, pure magnesium samples prepared with a diameter of 1.5 mm and a thickness of 3 mm were subjected to anodization process for 20 minutes by applying a constant voltage of 10 V in 10 M 150 ml NaOH and 10 M 100 ml NaOH solutions containing 1g/L hBN. After surface treatment, wear tests were performed on untreated Mg, anodized Mg and hBN doped anodized Mg samples. As a result of the tests, friction coefficient-time graphs and wear rates were analyzed. In line with the graphs and wear rates obtained, it was observed that the lowest wear rate belonged to the hBN doped anodized Mg sample.

Keywords: Pure Magnesium, Tribology, Anodization, hBN, Solid Lubricant.

Introduction

Magnesium is the third structural metal after aluminum and iron and the eighth most abundant metal on earth. Magnesium and its alloys are lighter than aluminum and iron due to their low density (~1.74 g/cm3) [1]. In addition, these materials have many superior properties such as good machinability, vibration damping, high specific strength and specific stiffness [2]. Therefore, magnesium and its alloys have attracted attention in the automotive and aircraft industries due to their light weight and high specific strength to improve energy efficiency. Despite all these superior properties, magnesium has the

disadvantages of low ductility, poor wear and corrosion resistance due to its hexoganol cubic structure [3].

Tribology is the study of friction, wear, lubrication and their interrelationships between contacting structures and is closely related to energy consumption, material loss and reliability [4]. Therefore, tribological energy loss and material consumption can be prevented mainly through surface engineering, lubrication, wear-resistant materials and design [5]. Surface engineering and lubrication technologies are the primary methods to improve tribological performance. With surface engineering, it is possible to obtain surfaces with superior tribological properties without affecting the mechanical properties of the base material [6]. Lubrication aims to minimize friction and wear between liquid and solid lubricants and contact surfaces. The deterioration of the structure of liquid lubricants at high temperatures and the fact that they are not preferred in places where there is no gravity have led tribology studies interested in lubrication to solid lubricants [7]. Hexagonal boron nitride (hBN), which can be preferred as a solid lubricant thanks to its lamellar structure, has attracted attention in tribology studies in recent years due to the fact that its structure does not deteriorate at high operating temperatures, is chemically inert and provides high conductivity [8].

In this study, the effect of anodization treatment of Mg, which is widely preferred in the automotive and aircraft industries due to its light weight and strength, with solid lubricant hBN on the wear resistance in dry environment was investigated. In order to make a comparison in the study, untreated, anodized and hBN-anodized samples were subjected to wear tests and it was observed that the highest wear resistance occurred in the hBN-anodized Mg sample.

Materials and Methods

As part of this study, pure magnesium samples with a diameter of 1.5 mm were sliced with a thickness of 3 mm, then the surfaces of the samples were made smooth and bright with 60, 200, 400, 800 and 1200 grit SiC sandpaper. The prepared samples were then anodized in 10 M NaOH and 10 M NaOH solutions containing 1g/L h-BN with voltage and time parameters of 10 V - 20 minutes. Untreated, undoped and doped samples were characterized by x-ray diffraction. After the characterization study, all samples were subjected to reciprocating wear test under 1 N load for 30 min. The graphs obtained as a result of the characterization analysis and tests are given in the next section and are examined in detail.

Results and Discussions

X-ray diffraction patterns of all samples are given in **Figure 1.** The 2theta peaks in the XRD patterns confirm that the anodization process and the peak values obtained in the hBN doped anodized samples confirm that the hBN doping was successfully performed.
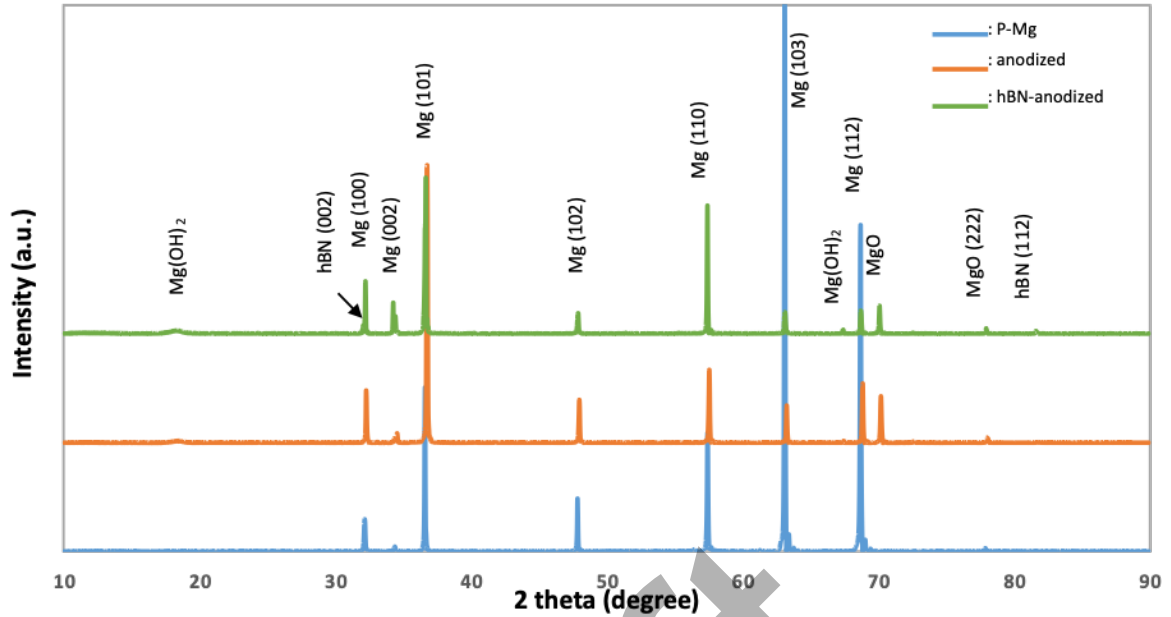
Figure 1. XRD patterns of all samples.

Figure 2 shows the coefficient of friction-time graphs obtained as a result of wear tests. Although it is thought that the wear resistance will increase as the coefficient of friction (COF) value decreases, as can be seen from the graph, the smooth and softer untreated surface caused the COF graph to be more wavy [1]. The investigations confirm that the surface treatments applied to the hBN-anodized and anodized Mg specimens increase the wear resistance of the hBN-anodized and anodized Mg specimens, although the COF values are higher, the graphs are less wavy.
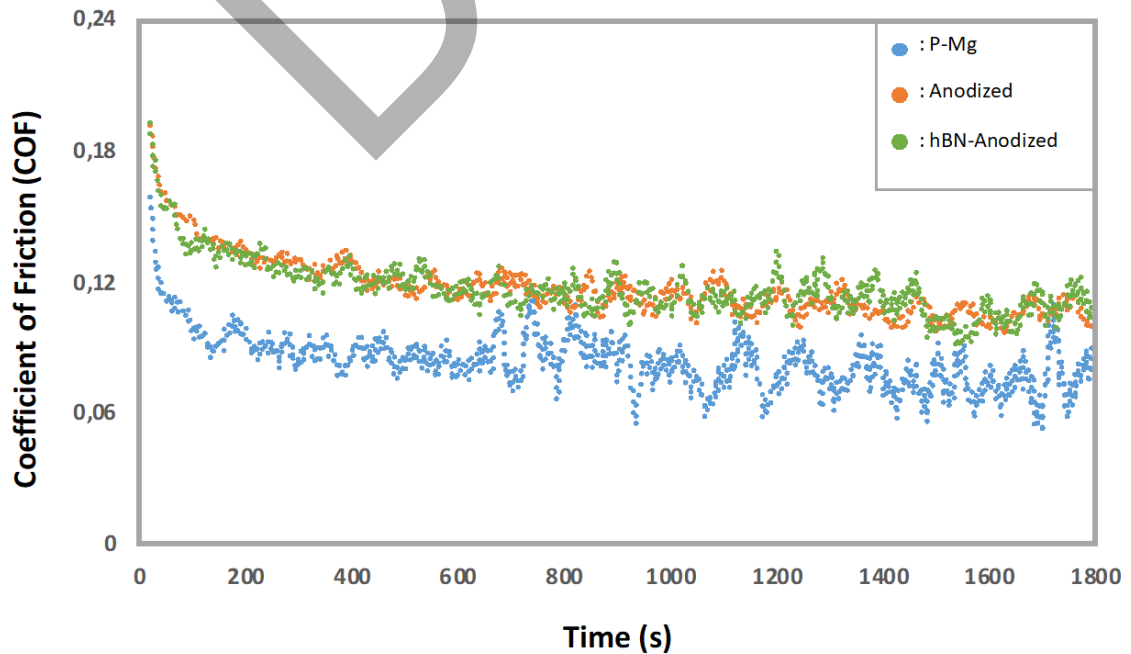
Figure 2. Coefficient of friction-time graphs of all samples

In **Figure 3**, the wear rates of all samples are given as column graphs. When the values are examined, it is seen that the least load-based wear loss occurs in the hBN doped anodized sample.
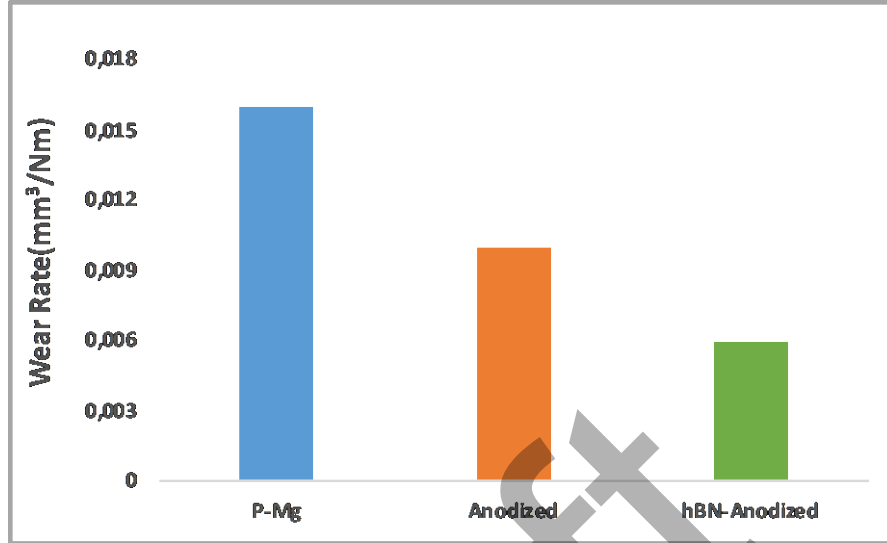
Figure 3. Column graph of wear rate according to specimens.

Conclusions

The wear values obtained as a result of the study confirm that hBN doping together with the anodization process increases the wear resistance. It shows that the hBN doped surface treatment can be used as a solid lubricant and that such easily applicable and economical coatings can be applied to Mg and its alloys in the industry.

References

[1] A. Çelik, Y.B. Bozkurt, 2022. Improvement of tribological performance of AZ31 biodegradable alloy by TiN-based PVD coatings, Tribology International, 173 (2022) 107684.

[2] S. Yue, J. Huang, Y. Ni, L. Shen, Y. Huang, D. Fan, J. Liu, 2024. Enhancing microstructural, mechanical, and tribological behavior of AZ31B magnesium alloy through friction stir processing, Journal of Materials Research and Technology, 29 (2024) 1441-1452.

[3] A. Amanov, O.V. Penkov, Y.-S. Pyun, D.-E. Kim, 2012. Effects of ultrasonic nanocrystalline surface modification on the tribological properties of AZ91D magnesium alloy, Tribology International, 54 (2012) 106-113.

[4] R. Kumar, I. Hussainova, R. Rahmani, M. Antonov, 2022. Solid Lubrication at High-Temperatures—A Review. Materials, 15(5) (2022) 1695.

[5] Q. Huang, X. Shi, Y. Xue, K. Zhang, C. Wu, 2023. Recent progress on surface texturing and solid lubricants in tribology: Designs, properties, and mechanisms, Materials Today Communications, 35 (2023) 105854.

[6] D. Peixoto Barbosa, G. Knörnschild, 2009. Anodization of Mg-alloy AZ91 in NaOH solutions, Surface and Coatings Technology, 203(12) (2009) 1629-1636.

[7] A. Gnanavelbabu, M. Prahadeeswaran, R. Rai, N.S. Ross, M.K. Gupta, 2023. Tribo-corrosive wear behaviour of squeeze-casted Mg/TiN/hBN composite under different ageing temperature, Tribology International, 187 (2023) 108748.

[8] J. Eichler, C. Lesniak, 2008. Boron nitride (BN) and BN composites for high-temperature applications, J. Eur. Ceram. Soc., 28 (5) (2008) 1105-1109.

Modeling and Altitude Control of the Ground Effect Vehicle

T.A.T. Al Maatoq[1] and K. Orman[2]

[1]Erzincan Binali Yıldırım University, Erzincan, Turkiye, ORCID: 0009-0008-5842-9762
[2]Erzincan Binali Yıldırım University, Erzincan, Turkiye, ORCID: 0000-0002-7236-9988

Ground effect aerial vehicle's (GEV) have the ability to fly over the water surface thanks to the aerodynamic effect created between the wings of the vehicle and the surface. The distinguishing feature of these vehicles is that they have higher efficiency compared to ordinary aircraft and higher speed than sea vehicles, and they can also take off and land on water or land. It is very difficult for traditional vehicles such as ships used in maritime transportation to reach the speeds of ground effect aircraft, which can reach speeds of more than 100 km/h with an acceptable fuel efficiency. On the other hand, it has many advantages such as being able to be used in military fields. They can be of great importance for civilian transportation, especially over short distances between coastal cities. Today, ground effect vehicles are considered as promising transportation vehicles that should be taken into consideration for the near future.

The purpose of this study is to examine Ground Effect Vehicles and their control structures. In order to use ground effect in the most efficient way, height control was applied to the obtained vehicle model. As a controller, the PI controller, which basically acts as a low-pass filter and has the ability to filter out high-frequency noise in the system, has been tested and simulation results are presented.

Keywords: GEVs, Altitude Control, PI Controller.

Introduction

Ground effect vehicle (GEV) is an innovative transportation system that uses the ground effect phenomenon to provide high speed and more efficient travel thanks to the aerodynamic interaction between the vehicle's wings and the water surface. The distinguishing feature of these vehicles is that they have higher efficiency compared to ordinary aircraft and higher speed compared to sea vehicles, and they can also take off and land on water or land. Additionally, they can be used in both civilian and military missions [1].

Today, GEVs are considered as promising transportation vehicles that should be taken into consideration for the near future. It is unlikely that conventional vehicles such as ships used in maritime transportation can reach the speeds of ground-effect vehicles, which can reach speeds of more than 100 km/h with acceptable fuel efficiency. Vehicles such as hydrofoil boats or speedboats can only reach these speeds, but these vehicles

are not used in the field of transportation. In air transportation, high operating costs such as landing-takeoff runways, airport and fuel efficiency occur. Another factor that should be taken into consideration is that the amount of payload that can be carried will increase due to ground effect.

The development of ground effect vehicles began in the 1920s, when the German physicist Carl Wieslsberger defined how ground effects worked, which had a great impact on the flight dynamics of aircraft, and proposed and developed some ideas about ground effects. Many terms exist today to describe such an aircraft. Russian R. Alekseev used the name "Ekranoplan" (French ékran = screen and Russian nizkolet = low-flying vehicle) [2]. Belavin used the name "Ekranolet" (vehicle that can enter and exit the ground effect) [3]. The popularly used name WIG means Wing in Ground Effect. It was defined as WISES - Surface Wing Effect Ship by Japanese S. Kubo. American Bertelson GEM was used to mean Ground Effect machine. The terms Flaircraft and Tandem-Aerofoil Boat were suggested by Gunther Jorg. Lippisch aircraft derivatives developed by Hanno Fischer are called Airfish. The vehicles produced by Techno Trans are called Hydrowing. S. Hooker introduced the term Wingship, which describes huge WIG vehicles [4].

In order to control the Ground Effect Aircraft, all external forces including aerodynamic effects, gravitational forces, thrust force and their moments must be taken into account. As a common method when developing control algorithms, the system is first linearized and a controller is designed for the resulting linear system, then the parameters of the developed controller are adjusted and used for the non-linear system [5]. There are different control methods applied in the literature. PID controller has been considered as the most common control approach [6],[7],[8]. However, approaches such as the cost function calculation method [9] and the Model-based predictive control method [10] have also been discussed. Although the perspectives vary when applying these control methods, the control variables of the Ground Effect Aircraft are designed by controlling the 3 Euler angles (Pitch, Roll and Yaw) and altitude.

In this study, a mathematical model that accurately represents the dynamics and aerodynamic properties of a GEV was created and a PI controller was applied for the height control of the GEV. Additionally, simulation results are presented to see the effects of ground effect on the system.

Ground Effect and Mathematical Modeling of Ground Effect Vehicle

Ground effect can be expressed as the increase in the lift force effect (L) and the decrease in the drag force (D) effect when the wing of the aircraft approaches the ground. In order for a wing to produce positive lift, the static pressure on the lower side of the wing must be higher than that on the upper side [11]. On the wing tips; the high pressure area at the bottom meets the low pressure area at the top. Thus, air flow occurs from the lower side to the upper side around the wing tip. This is called a wing tip vortex. The energy stored in these vortices is lost and this is expressed as drag for the aircraft. As the GEV approaches the water surface, there is not enough space for the vortices on the wings to

fully form. Vortices are also pushed outward by the water surface. Thus, the effective aspect ratio of the wing is higher than the geometric aspect ratio, fig 1. [11].
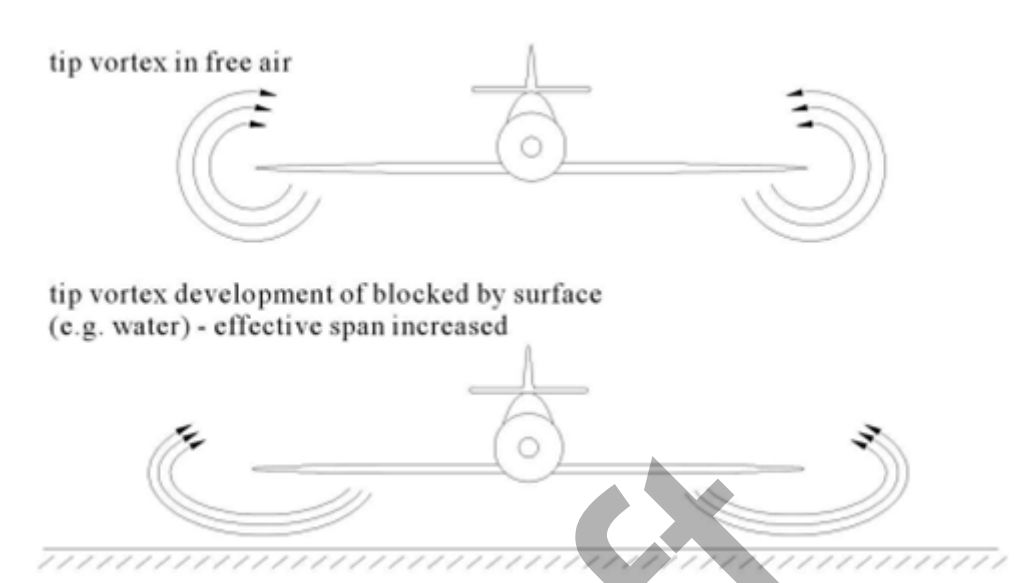
Figure 1. Vortex and Span dominated ground effect [10].

In the study first presented by Weisselsberger, the increase in lift force was calculated with a parameter (σ), assuming that the drag induced by the aircraft's proximity to the ground decreased. [12].

$$\sigma = \frac{1 - 0.66\frac{h}{l}}{1.05 + 3.7\frac{h}{l}} \tag{1}$$

Here h represents the height of the aircraft above the water surface and l represents the wingspan (which holds well from $h/l = 1/15$ to $h/l = 1/2$). The increasing aspect ratio ($\widehat{AR}$) when ground effect occurs is defined as:

$$AR = \frac{l^2}{s} \quad \text{and} \quad \widehat{AR} = \frac{AR}{1-\sigma} \tag{2}$$

Here s represents the wing area. In another study showing similar results [13]; drag due to lift coefficient and lift coefficient (C_{L0} is the lift coefficient at zero angle of attack);

$$C_{D_L} = (1 - \sigma)\frac{C_L^2}{\pi\widehat{AR}} \tag{3}$$

$$C_L = \frac{2\pi}{1+\frac{2}{AR}}\alpha + C_{L0} \tag{4}$$

While creating the mathematical model of the GEV, it is aimed to develop a 6-DOF non-linear dynamic model in which all forces and moments, including ground effect,

aerodynamic effects, thrust force, gravity, atmospheric elements and mass inertia are included. The nonlinear equations of motion of the GEV are developed by applying Newton's second law and the law of conservation of linear momentum. The vehicle is assumed to be a rigid body with six degrees of freedom (Figure 2).
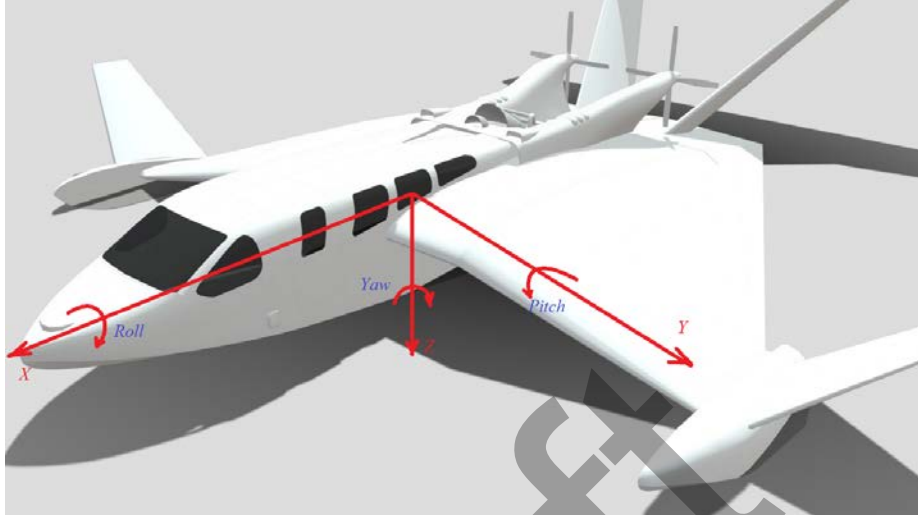
Figure 2. Ground Effect Vehicle and its axes (Airfish 8)[14].

Three translation axes (X, Y and Z) define the movement of the center of mass, and three rotation axes (Roll-φ, Yaw-θ and Roll-ψ) define the orientation of the vehicle. The equations are written on a fixed axis system that moves with the GEV and is centered at the GEV's center of mass. The following constraints are generally taken into consideration when modeling: The mass of the GEV is assumed to be constant (no change in mass due to fuel consumption). That is, the center of gravity does not change during the simulation, the Earth is assumed to be stationary (no rotation), and the curvature of the Earth is neglected.

The body axis equations of GEV are as follows [15];

- Force Equations

$$\dot{u} = vr - \omega q - g\,sin\theta + \frac{F_x}{m} \tag{5}$$

$$\dot{v} = ur + \omega p + g\,cos\,\theta\,sin\,\phi + \frac{F_y}{m} \tag{6}$$

$$\dot{\omega} = uq + vp + g\,cos\,\theta\,cos\,\phi + \frac{F_z}{m} \tag{7}$$

It should also be noted that the lift force (*L*) due to ground effect must be replaced by $\hat{L} = L(1 - \sigma)$.

- Moment Equations

$$\dot{p} = \left[\begin{array}{l} (I_y I_z - I_z^2 - I_{xz}^2)qr + I_z L \\ + I_{xz}(I_x + I_y + I_z)pq + I_{xz}N \end{array} \right] / I_x I_z - I_{xz}^2 \qquad (8)$$

$$\dot{q} = [(I_z - I_x)pr - I_{xz}(p^2 - r^2) + M]/I_y \qquad (9)$$

$$\dot{r} = \left[\begin{array}{l} (I_x^2 - I_x I_y + I_{xz}^2)pq + I_{xz}L \\ - I_{xz}(I_x - I_y + I_z)qr + I_x N \end{array} \right] / I_x I_z - I_{xz}^2 \qquad (10)$$

- Kinematic Equations

$$\dot{\phi} = p + (r \cos\phi + q \sin\phi) \tan\theta \qquad (11)$$

$$\dot{\theta} = q \cos\phi - r \sin\phi \qquad (12)$$

$$\dot{\psi} = (r \cos\phi + q \sin\phi) / \cos\theta \qquad (13)$$

- Trajectory Equations

$$\dot{x}_g = u \cos\theta \cos\psi + (\sin\phi \sin\theta \cos\psi - \cos\phi \sin\psi)$$
$$+ \omega (\cos\phi \sin\theta \cos\psi + \sin\phi \sin\psi) \qquad (14)$$

$$\dot{y}_g = u \cos\theta \sin\psi + v (\sin\phi \sin\theta \sin\psi + \cos\phi \cos\psi)$$
$$+ \omega (\cos\phi \sin\theta \sin\psi - \sin\phi \cos\psi) \qquad (15)$$

$$- \dot{h}_g = -u \sin\theta + u \sin\phi \cos\theta + \omega \cos\phi \cos\theta \qquad (16)$$

Altitude Control of GEV
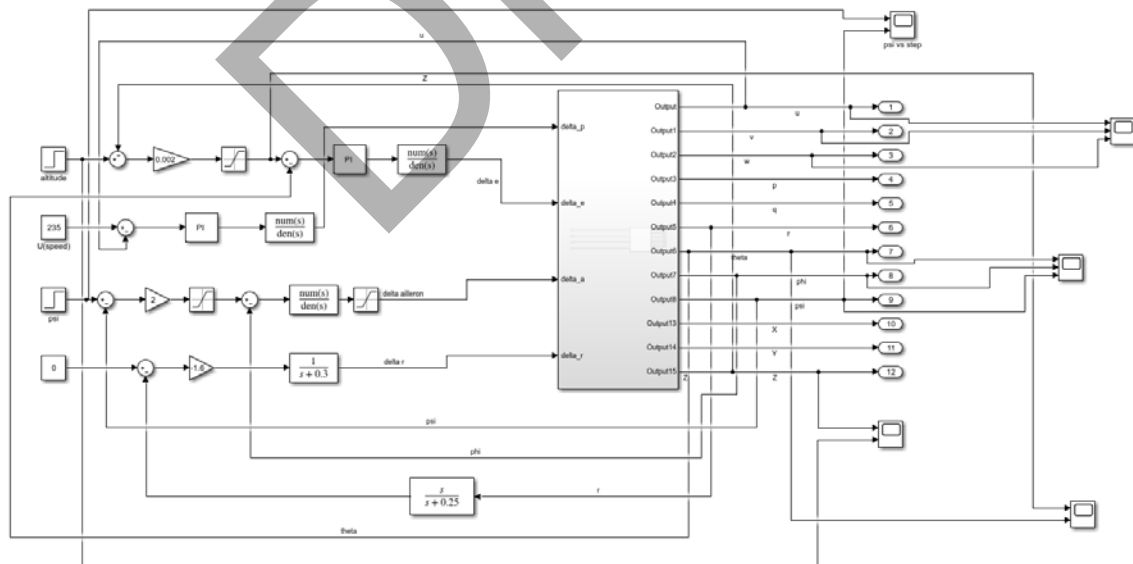
Figure 3. Altitude and Speed Control of GEV

In this section, a nonlinear model of the GEV is considered and simulation results are presented to show the performance of the conventional PI controller in the height

control of the GEV. Conventional PI type controllers have been used in many industrial applications, especially in autonomous vehicles and unmanned vehicle applications [16],[17],[18]. In addition, the cases where the ground effect defined in Eq. (1) is not taken into account and the cases where it is taken into account are compared. Controller parameters (K_p and K_i) were determined by trial and error method. Figure 4 shows the ground effect parameter (σ) given in Eq. (1) according to altitude. As the altitude value decreases within the specified range, the parameter value also increases.
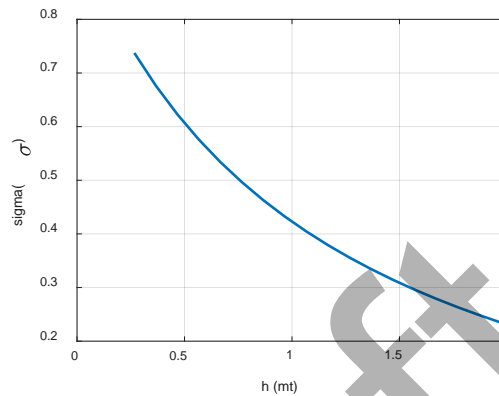
Figure 4. Sigma (σ) relative to altitude

Figure 5 shows the lift coefficient (C_L) and drag coefficient (C_D) values given in Eq. (3) and Eq. (4) according to the height. As the altitude value decreases within the specified range, the lift coefficient value increases and the drag coefficient value decreases.

(a) (b)
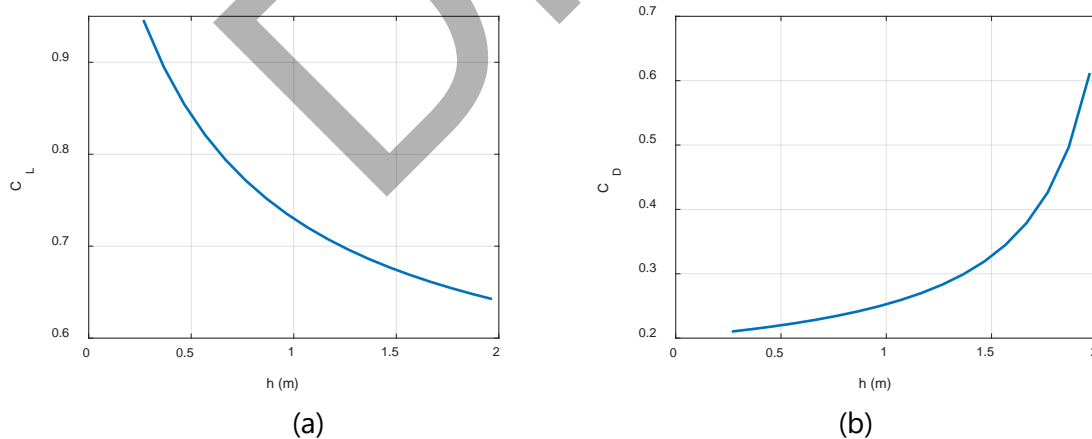
Figure 5. C_L (a) and C_D (b) relative to altitude

Figure 6 shows the movement of the GEV in the altitude range determined as the area where ground effect occurs. The PI controller gave successful results in terms of reaching the reference and eliminating the error in trajectory tracking.
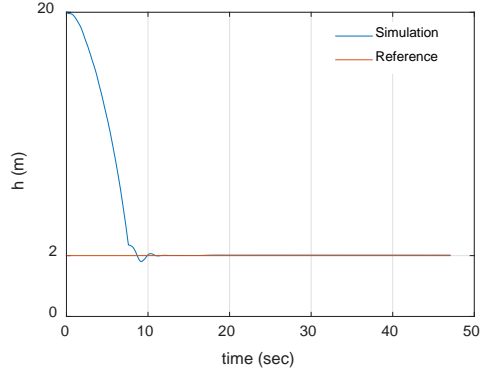
Figure 6. GEV's altitude

In Figure 7, the control signal of the PI controller is presented for cases where the ground effect is not taken into account (a) and when it is taken into account (b). A low change in the average amplitude of the control signal was observed. On the other hand, it was observed that the oscillations in the control signal decreased.
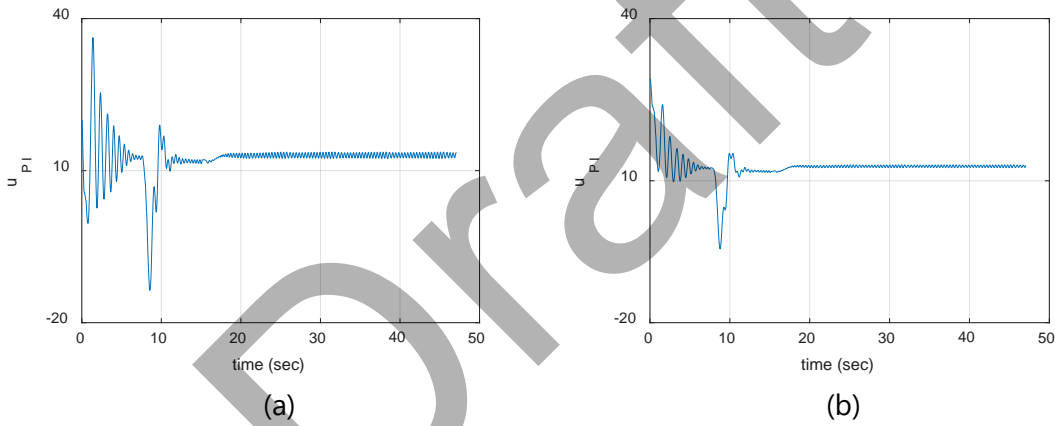
Figure 7. Controller signal; without Ground Effect (a) and with Ground Effect (b)

Conclusion

In this study, the altitude control performance of a ground effect aircraft was tested through simulation. Conventional PI controller was used for altitude control. Simulation results showed that the traditional PI controller was successful in reference tracking. Additionally, the effects of ground effect on controller performance are also presented. This result, shown in Figure 7, can be expressed as an increase in the lift force and a decrease in the drag force due to the ground effect in the system. In future studies, it is planned to focus on developing new controllers by taking into account the ground effect.

References

[1] T. A. T, Al Maatoq, K. Orman, 2023, Modern Elektrik Teknolojileri: Tasarım, Optimizasyon ve Güvenlik II, Prof. Dr. Eyyüp GÜLBANDILAR, Editör, BİDGE Yayınları, Ankara, ss.5-19.

[2] Wikipedia, 2020. Eranoplane. Retrieved on 11.04.2024 from https://tr.wikipedia.org/wiki/Ekranoplan.

[3] N. I. Belavin, 1968. Letauschie Suda-ekranoplany. Katera I Yakhty no. 15.

[4] S. Hooker, 1982. Wingships: Prospect for High-Speed Oceanic Transport, Jane's All the World's Surface Skimmers, Jane's Information Group, Coulsdon, UK.

[5] N. Kornev, K. Matveev, 2003. Complex numerical modeling of dynamics and crashes of wing-in-ground vehicles. In 41st Aerospace sciences meeting and exhibit (p. 600).

[6] A. Nebylov, V. Nebylov, 2007. New design methods and results for automatically controlled WIG. DOI:10.13009/EUCASS2019-174.

[7] A. Ghafoor, 2015, Wıng In Ground Effect Vehıcle: Modellıng And Control. Master Thesis, METU, Ankara, Turkiye.

[8] Y. Mei, S. Su, X. Shan, P. Yu, H. Wang, 2022. High Precision Height Control for Wing-in-Ground Crafts. International Journal of Aerospace Engineering.

[9] R. Shabani, G. Nalcaci, M.K. Leblebicioglu, M. Ermis, 2020. Cost Function Determination for a WIG in Predefined Path and Height Using Conjugate Gradient Method. In 2020 IEEE 6th International Conference on Control Science and Systems Engineering (ICCSSE) (s. 172-177). IEEE.

[10] D. Patria, C. Rossi, R.A.S. Fernandez, S. Dominguez, 2021. Nonlinear control strategies for an autonomous wing-in-ground-effect vehicle. Sensors, 21(12), 4193.

[11] T. Abramowski, 2007. Numerical investigation of airfoil in ground proximity. Journal of theoretical and applied mechanics, 45(2), 425-436.

[12] C. Wieselsberger, 1922. Wing Resistance near the Ground. NACA TM No. 77.

[13] M. LeSueur, 1935. Ground Effect on the Take-Off and Landing of Airplanes, NACA TM No. 771.

[14] FS-8. The WIG page. 2008. Archived from the original on July 18, 2011. Retrieved on 11.04.2024 from https://web.archive.org/web/20110718175215/http://www.se-technology.com/wig/html/main.php?open=showpic&code= &pic=360

[15] H. Ji, J. Yan, Y. Zhao, Y. Zhu, J. Wang, D. Zuo, 2021. Control system design for WIG aircraft on the wavy water surface. In 2021 International Conference on Control, Automation and Information Sciences (ICCAIS) 567-571.

[16] K. Orman, A. Başçi, A. Derdiyok, 2016. Speed and Direction Angle Control of Four Wheel Drive Skid-Steered Mobile Robot by Using Fractional Order PI Controller. ELEKTRONIKA IR ELEKTROTECHNIKA, vol.22, no.5, 14-19.

[17] K. Orman, 2022. Design of a Memristor-Based 2-DOF PI Controller and Testing of Its Temperature Profile Tracking in a Heat Flow System. IEEE ACCESS , vol.10, no.10 , 98384-98390.

[18] K. Orman, A. Derdiyok, 2015. Kalman Filtresi ile PI Kontrolün Mikro İnsansız Hava Aracı'nın Gerçek Zamanlı Yörünge Takibine Uygulanması. TOK'15 Otomatik Kontrol Ulusal Toplantısı Pamukkale Üniversitesi , (Denizli, Turkey), 598-602.

Pre-Service Science Teachers' Views on Model and Model-Based Instruction

Ç.N. Özkan[1], S. Okumuş[2]

[1]*Kazım Karabekir Educational Institute, Erzurum, Türkiye, ORCID: 0000-0002-6349-9692*
[2]*Kazım Karabekir Educational Institute, Erzurum, Türkiye, ORCID: 0000-0001-6271-8278*

Abstract

This study aims to evaluate pre-service science teachers' views on models and model-based instruction. The research was conducted with a quasi-experimental design. The sample of the study consisted of 14 pre-service science teachers studying at Atatürk University. Since the sample selection was based on volunteerism, convenience sampling was used. A pre-test was administered to 14 volunteer pre-service teachers and then they were given training on models and model-based instruction. During the training process, theoretical and practical information was given on models, types of models, the importance of models in science education, modeling, and model-based learning and teaching. The training lasted 7 hours. A post-test was administered at the end of the training. In addition, pre-service science teachers' opinions on the use of models were taken before and after the training. The attitude scale of pre-service science teachers towards the model and a view form use were used as data collection tools. At the stage of analyzing the data obtained from the research, the normality of the data was checked first. A dependent sample t-test was used in the analysis process. There was no significant difference between the pre and post-test scores (p>.05). It is thought that the fact that the pre-service science teachers had previously seen information about models in their lessons affected this situation. In addition, according to the interview form conducted, pre-service science teachers were favorable to the use of models before the training. At the end of the training, they showed positive opinions about the training. According to the results, it was inferred that there was not a big difference after the training since the pre-service teachers already cared about the models.
Keywords: Model, model-based instruction, pre-service science teachers

Introduction

Science is a large part of the knowledge that students use to understand the world they interact with [1]. With science, students get to know nature and nature relations. Since the science course is intertwined with life, the use of only wooden chalk and books as

course materials may cause students to perceive science as a boring course. Since it is not possible to appeal to different senses at the same time in the traditional education environment, the use of materials with auditory and visual content will make the lesson more attractive [2]. It is thought that the student's interest in the lesson will increase in an educational environment enriched with such content. Models are frequently used to make science lessons more attractive.

Models form the basis of all the information available in science and models are seen as an integral part of the science course [3]. For this reason, integrating models and model-based instruction approaches into science lessons will be more effective than in the traditional education environment. Models provide students with the opportunity to experience the parts of a subject or concept that they cannot fully visualize in their minds by hearing, seeing, and touching the parts they have trouble understanding and help permanent learning to take place [4]. In addition, models allow the subject to be perceived in a different dimension than it is normally perceived and abstract events or ideas to become concrete and more visible [5].

In studies examining the effect of using models in education on student achievement, it was concluded that lessons taught using models were more effective than other methods [6]. As the studies on the importance of using models in lessons increased, a theory on the use of models was needed and the model-based instruction approach was developed [7]. According to Hanke and Huber (2008), if students do not accept an instructional strategy, they will not participate, pay attention, and consequently will not learn the lesson. Therefore, it is important to integrate models into the lesson with this approach. Model-based instruction involves individuals creating mental models, testing this information, and then reinforcing or rejecting it [8]. The general stages of model-based instruction are given in Table 1.

Table 1. Model-based instruction phases [7]

Process	Stage	Description
Learning	Mental model construction	Mental provocation	Learning starts with a new situation.
		Remembering preliminary information	Prior knowledge is used to understand the new situation.
		Search for new information	More information is gathered about the new situation.
		Integration in a mental model	The new situation is combined with existing knowledge in a mental model.
	Schematization	For knowledge to be understood without the mental model construction process, the mental model construction process is experienced repeatedly.

To support learning in model-based instruction, these sub-processes should be taken into account and therefore model-based instruction (MOMBI) was developed [9]. The MOMBI has five stages in parallel with the stages of model-based instruction [7]. How the MOMBI stages should be carried out in the lesson is given in Table 2 below.

Table 2. Basic stages of MOMBI [7].

Phase	Content
Provocation	Activities such as justifying why the new concept or situation to be learned should be learned, presenting information that contradicts existing knowledge, and making the need for learning felt are carried out.
Activation	Questions are asked and reminders are made to utilize students' prior knowledge about the new concept. At this stage, the basis for learning is created.
Presentation	The teacher is the most active and the teaching process is carried out with conceptual models based on MOMBI. In this process, pictures, concept maps, tables, different internet resources, experts or libraries, etc. can be utilized. For this purpose, methods such as including activities to eliminate misconceptions, etc. are utilized.
Scaffolding	Asking questions about the information acquired, giving hints, taking into account the differences of the students, and guiding them are carried out.
Practice	The mental model development processes are repeatedly renewed for students to assimilate the mental models they have constructed.

In the process of this research, pre-service science teachers (PST) were given training on models and model-based instruction by expert faculty members from different universities. In this respect, it differs from other studies. This study aims to determine the attitudes and opinions of PSTs towards models and model-based instruction. In line with this purpose, answers to these questions were sought.

1- Is there a difference in PSTs' attitudes towards the use of models before and after the training?

2- What are the opinions of PST about the use of models?

2. METHOD

Design

In this study, a quasi-experimental design was used since it was aimed to evaluate the attitudes and opinions of PST towards model and model-based instruction.

Sample

The sample of the study consists of PST studying at Atatürk University. A total of 14 students voluntarily participated in the study. In the selection of the sample in the process of the project numbered TÜBITAK 123K603, convenience sampling was used since volunteering was essential.

Data Collection Tool

PSTs' The Scale of Attitude Towards Model Use (SATMU) developed by Harman and Alat (2015) was used as a data collection tool. This scale consists of 55 items in a five-point

Likert type. 27 of these items are reverse items. The Cronbach Alpha reliability coefficient of the attitude scale was calculated as .94.

In addition, a total of 9 questions, 4 before the training and 5 after the training were asked in the interview before and after the training. The questions were prepared by taking expert opinion.

Process

This study was conducted with 14 volunteer PST from the Atatürk University science education department who participated in the training given within the scope of the 1001 project numbered 123K603. Before the training, the pre-test of SATMU was applied to the PST. A 7-hour training on model and model-based instruction was given to PST by expert academicians from different universities. In this training process, in addition to theoretical knowledge, applications were also included, and interactive lessons were provided. The content of the training included models, model design, mental models, model-based instruction, and their applications. At the end of the training, SATMU was applied as a post-test. In addition, PSTs' opinions about models and model-based instruction were taken before and after the training. Visuals related to the training are given in Figure 1.

Figure 1: Visuals from practical training

Data Analysis

In the quantitative data analysis phase, the normality of the data was first checked. For this purpose, the Shapiro-Wilk test was performed and skewness and kurtosis values were examined. The normality values of the pre-test and post-test data of SATMU are as follows.

Table 3. Normality values of the SATMU (Shapiro-Wilk)

	Statistics	df	p
Pre-test	,831	14	,012
Post-test	,932	14	,323

According to Table 3, it is seen that normality was not achieved in the pre-test p=0.012 (p<0.05). For this, the skewness and kurtosis values of the pre-test data were also examined. Accordingly, skewness was determined as -2.53 and kurtosis as 1.83. It is stated that skewness and kurtosis values can be stretched up to +3, and -3 values for normal distribution [10]. Accordingly, the data were accepted as normal. Since the distribution of the data was normal, a dependent sample t-test was used to compare the pre-post data.

Content analysis was used to analyze qualitative data. Accordingly, the interview results were divided into themes and codes and organized. The themes and codes were coded separately by two researchers and the agreement between the coders was checked with Miles & Huberman's (1994) formula and the agreement was ensured [11,12].

3. FINDINGS AND RESULTS

First of all, the data obtained from the SATMU were presented. Accordingly, the findings of the dependent sample t-test applied to the pre and post-test data are given in Table 4.

Table 4. Dependent sample t-test results

	N	X̄	Sd	t	p
Dependent sample t-test	14	257,78	16,02	-,967	,351

According to Table 4, there was no significant difference between the pre- and post-test results of the SATMU data p>0.05 (p=.351).

The interview questions and answers before the PST were trained are presented.

The results of the interviews conducted with the PST in the research are presented by dividing them into themes and codes.

In the first question, the PST were asked *"What are your views on the concept of model and the use of models in science education? Explain."* The question was asked. The answers to the PST are given in Table 5.

Table 5. Findings related to the First Question (pre)

Theme	Code	PST	f	%
Facilitation	Embodiment	PST1, PST3, PST7, PST9, PST10, PST11, PST13	7	49.7
	Making the Lesson interesting	PST8	1	7.1
	Easy understanding	PST2, PST4, PST7, PST12	4	28.4
	Simplification	PST10, PST11, PST14	3	21.3
Persistence	Ensuring Course Retention	PST1, PST4, PST6, PST10	4	28.4
Student-Centered	Making students active	PST5	1	7.1

According to Table 5, 49.7% of the PSTs stated that it made the lesson concrete, 28.7% stated that it made the lesson easy to understand, 28.7% stated that it ensured retention and 7.1% stated that it made the students active and made the lesson interesting.

In the second question, PST was asked *"Have you designed a model to be used in science before? a. If yes, can you explain how you prepared it? b. If no, would you like to design a model for science lessons? Why?"* and the answers are given in Table 6.

Table 6. Findings related to the Second Question (pre)

	PST	f	%
Yes	PST3, PST14	2	14.2
No	PST1, PST2, PST4, PST5, PST6, PST7, PST8, PST9, PST10, PST11, PST12, PST13	12	85.2

According to Table 6, 85% of the PSTs stated that they had never designed a model before.

In the third question, *"What do you think about model-based instruction (MBI)? Explain."* The question was directed and the answers are given in Table 7.

Table 7. Findings related to the Third Question (pre)

Theme	Code	PST	f	%
Facilitation	Embodiment	PST2, PST3, PST7, PST12	4	28.4
	Making the lesson interesting	PST1, PST13, PST14	3	21.3
	Easy Understanding	PST2, PST5, PST6, PST8, PST11,	5	35.5
Persistence	Ensuring Course Retention	PST10, PST11	2	14.2

According to Table 7, 35% of the PST stated that it made the lesson easier to understand, 28% stated that it made the lesson concrete, 21% stated that it made the lesson interesting, and the others stated that it increased the permanence of the lesson.

In the fourth question, *"Have you prepared a course content for MBI before? a. If yes, can you explain how you prepared it? b. If your answer is no, would you like to prepare MBI-oriented course content for the science course? Why?"* and the answers are given in Table 8.

Table 8. Findings related to the Fourth Question (pre)

	PST	f	%
Yes	PST9	1	7.1
No	PST1, PST2, PST3, PST4, PST5, PST6, PST7, PST8, PST10, PST11, PST12, PST13, PST14	13	92.3

According to Table 8, 92% of the PST stated that they had not prepared course content for MBI before.

In this section, the interview questions and answers after the PST were trained are presented.

In the first question, *"What do you think about the adequacy of the information about the model and MBI in the training process, explain with examples."* The question was directed and the answers are given in Table 9.

Table 9. Findings related to the First Question (post)

Theme	Code	PST	f	%
Qualification	Information was sufficient	PST1, PST3, PST5, PST6, PST7, PST8, PST9, PST10, PST11, PST13, PST14	11	78.1
	Activities were sufficient	PST2, PST12	2	14.2
Interaction	Interaction with students	PST4	1	7.1

According to Table 9, all of the PST thought that the content presented in the training was sufficient.

In the second question, *"Were the practices related to the model and MBI in the training process sufficient? Why? Explain."* the answers are given in Table 10.

Table 10. Findings related to the Second Question (post)

Theme	Code	PST	f	%
Qualification	Activities were sufficient	PST1, PST2, PST3, PST4, PST5, PST6, PST7, PST8, PST10, PST13, PST14	11	78.1
	Activities were not enough	PST9, PST12	2	14.2
Interaction	Interaction with students	PST11	1	7.1

According to Table 10, while 85% of the PST thought that the practices were sufficient, 15% stated that the activities were not sufficient.

In the third question, *"After the training, do you feel competent in designing activities related to MBI? Explain."* The question was directed and the answers are given in Table 11.

Table 11. Findings related to the Third Question (post)

	PST	f	%
Yes	PST1, PST2, PST3, PST4, PST6, PST7, PST8, PST9, PST10, PST11, PST12, PST13, PST14	13	92.3
No	PST5	1	7.1

According to Table 11, 92% of the PST stated that they felt competent in preparing IST activities after the training.

In the fourth question *"What are the positive aspects of the training given to you? Explain."* The question was directed and the answers are given in Table 12.

Table 12. Findings related to the Fourth Question (post)

Theme	Code	PST	f	%
Useful	Informative	PST1, PST5, PST6, PST9, PST10, PST13, PST14	7	49.7
	Eye-opening	PST2, PST3, PST4, PST10	4	28.4
	Funny	PST1, PST7, PST11, PST12	4	28.4
	Interactive	PST1, PST8, PST9, PST11	4	28.4

According to Table 12, all of the PSTs stated that they found the training useful.

In the fifth question, *"What are the deficiencies you see about the training process? Explain."* The question was directed and the answers are given in Table 13.

Table 13. Findings related to the Fifth Question (post)

Theme	Code	PST	f	%
Time	Insufficient	PST1, PST8, PST12, PST13	4	28.4
Hardware	Technological devices cannot work	PST2, PST3, PST9, PST11	4	28.4

According to Table 13, 28% of the PST stated that time was limited, and 28% stated that they had problems using technological devices such as computers.

4. CONCLUSIONS

It was aimed to evaluate PSTs' views on models and MBI in this study. According to the findings, there was no significant difference between the t-test results before and after the training given to the PST. Considering the answers given in the interview forms of the PST, they had developed positive attitudes towards models and MBI before the training, which may be the reason why the t-test results were not significant. During the MBI training, PST learned that they learned MOMBI and its steps rather than models and that they should present models within the theoretical framework when using them. However, in the future, PST will not use models haphazardly and will make the lesson more meaningful by presenting models in a theoretical framework.

Before the training, all of the PST had positive attitudes towards models and all of them argued that it was a method that should be used in lessons. In addition, the majority of the PST stated that they had not prepared models and MBI lesson plans before. With this training, PST was informed about how the design process should be and what to pay attention to. After the training, the majority of the PST felt themselves competent to prepare models and MBI lesson plans. In addition, the training process entertained the PST and provided them with different perspectives.

References

[1] Bozdemir-Yüzbaşıoğlu, H., Sarıkaya, R. (2019). Mikroskobik canlılar konusunda model tabanlı öğrenme yaklaşımının öğrencilerin zihinsel model gelişimine etkisi. Kalem Eğitim ve İnsan Bilimleri Dergisi, 9(2), 357-384.

[2] İspir, B. (2021). Dördüncü sinif basit elektrik devreleri ünitesinde öğrenme amaçli yazma ve model tabanli öğrenme etkinliklerinin başariya etkisi.

[3] Gülçiçek, Ç., Güneş, B. (2004). Fen öğretiminde kavramların somutlaştırılması: modelleme stratejisi, bilgisayar simülasyonları ve analojiler. Eğitim ve Bilim, 29(134).

[4] Okumuş, S., Doymuş, K. (2017). İşbirlikli öğrenme ve modellerin yedi ilkeyle birlikte uygulanmasinin kavramsal anlamaya etkisi. Mustafa Kemal Üniversitesi Sosyal Bilimler Enstitüsü Dergisi, 14(39), 431-457.

[5] Gobert, J. D., Buckley, B. C. (2000). Introduction to model-based teaching and learning in science education. International Journal of Science Education, 22(9), 891-894.

[6] Düşkün, İ., İbrahim, Ü. (2015). Modelle öğretim yönteminin fen eğitimindeki yeri ve önemi. Mehmet Akif Ersoy Üniversitesi Eğitim Bilimleri Enstitüsü Dergisi, 4(6), 1-18.

[7] Kurnaz, M. A., & Sağlam Arslan, A. (2011). Model tabanli öğrenme yaklaşimini temel alan öğrenme ortaminin öğrencilerin enerji kavramini anlama düzeylerine etkisi.

[8] Oğan-Bekiroğlu, F. (2007). Model temelli öğretimin fizik öğretmeni adaylarının ay, ayın evreleri ve diğer ay olayları hakkındaki kavramlarına etkisi. Uluslararası Fen Eğitimi Dergisi , 29 (5), 555-593.

[9] Hanke, U., Huber, E. (2008, December). Acceptance of model-based instruction among students. in iadis international conference on cognition and exploratory learning in digital age.

[10] Jondeau, E., Rockinger, M. (2003). Conditional volatility, skewness, and kurtosis: existence, persistence, and comovements. Journal of Economic dynamics and Control, 27(10), 1699-1737.

[11] Miles, M. B., Huberman, A. M. (1994). Qualitative data analysis: An expanded sourcebook. sage.

[12] Baltacı, A. (2017). Nitel veri analizinde Miles-Huberman modeli. Ahi Evran Üniversitesi Sosyal Bilimler Enstitüsü Dergisi, 3(1), 1-14.

[13] Harman, G. ve Alat, K. (2015). Fen bilgisi öğretmen adaylarının fen ve teknoloji derslerinde model kullanımına yönelik tutum ölçeğinin geliştirilmesi ve doğrulanması. *Eğitim Fakültesi Dergisi, 17* (1), 30-54.

Measuring Digital Technology Competencies of Pre-Service Science Teachers

B. Yağsız[1], S. Okumuş[2]

[1]*Kazım Karabekir Educational Institute, Erzurum, Türkiye, ORCID: 0009-0005-8989-6572*
[2]*Kazım Karabekir Educational Institute, Erzurum, Türkiye, ORCID: 0000-0001-6271-8278*

Abstract

With the rapid progress in digital technologies, the competencies expected from students are also being updated. In this context, teachers need to develop their digital competencies to provide students with certain competencies. For this purpose, it is important to reveal the status of pre-service teachers' digital competencies during the undergraduate period. This study aimed to measure whether pre-service science teachers' digital competencies differ in terms of grade level and gender factors. In the study, survey design was selected from quantitative research methods. The sample of the study consisted of 170 pre-service science teachers studying at Atatürk University Kazım Karabekir Faculty of Education. Random sampling was used in sample selection. Digital Technology Competencies of Teachers Scale (DTECS) adapted into Turkish by Ergül and Taşar (2023) was used as a data collection tool in the study. For the analysis of the data obtained from the scale, normality analysis was performed first. Since 3rd-grade data did not provide normal distribution, Kruskal-Wallis and Mann-Whitney U tests were used to make comparisons in terms of grade level. Mann Whitney U test was also used to compare the data in terms of gender. In the study, a significant difference was observed between 1st and 3rd grades in favor of 3rd grades and between 2nd and 3rd grades in favor of 3rd grades (p<.05). There was no significant difference in terms of gender (p>.05). To increase the digital competencies of pre-service science teachers, it is predicted that providing training in various fields related to digitalization (augmented reality, educational digital games, etc.) will be effective.

Keywords: Digital competencies, pre-service science teachers, gender, grade level

Introduction

Today, the use of digital technologies in the field of education is increasing. Since there is no specific hierarchy of competencies, competencies are of equal importance. Each competence has a great contribution to our social life and society. Competencies complement each other and can be applied in different ways, and concepts that are important in one field may not have the same importance in the other field. Individuals

with such competencies have problem-solving, teamwork, critical thinking, analytical competencies, communication skills, creativity, and intercultural communication competencies [1].

The concept of digital competence is explained as a concept used at certain levels of learning, especially in the training of teachers [2]. On the other hand, digital competence is considered to be more than knowing how to use complex and interconnected devices and technology [3]. According to Ferrari (2012), the concept of digital competence is used as the use of all attitudes, skills, knowledge, strategies, and awareness to communicate, socialize, and problem-solve [4]. In some studies, it is known that digital competence is examined according to some variables (such as field, gender, teaching period, education level, and daily internet use) [5, 6, 7, 8, 9].

In some of these studies, for example, in the research conducted by Arslan (2019) with teachers working in primary and secondary schools, it was seen that there was no difference in the level of digital literacy when the variables were examined in terms of education levels and gender [5]. In another aspect of the research, the digital literacy levels of information technologies, science, and mathematics teachers were higher. In the research conducted by Demirdağ (2021), internet usage time increased the level of digital literacy [6].

With the rapid progress in digital technologies, the competencies expected from students are also being updated. In this context, teachers need to develop their digital competencies to provide students with certain competencies. For this purpose, it is important to reveal the status of pre-service teachers' digital competencies during the undergraduate period. This study aimed to measure whether pre-service science teachers' digital competencies differ in terms of grade level and gender factors.

The problem statement of the research is as follows: Do pre-service science teachers' (PST) digital competencies vary in terms of grade level and gender factors?

METHOD

Research Design

A survey design, one of the quantitative research approaches, was used. In quantitative research, mathematical models and statistical data are used to analyze the data and the findings are presented in a neutral, third-person language [10]. Therefore, since this study aims to determine the level of digital technology competencies of PST, the most appropriate design is survey design.

Data Collection Tool

The Scale of Digital Technology Competencies of Teachers (SDTCT) adapted into Turkish by Ergül and Taşar (2023) was used as a data collection tool in the study [11]. The SDTCT aimed to determine the digital technology competencies of PST for different situations. Cronbach's Alpha coefficient was calculated to determine the reliability coefficient of the SDTCT. Cronbach's Alpha was determined as .949 for this 19-item scale.

Application

This research was carried out in 1st, 2nd, 3rd, and 4th grades studying at undergraduate level in the 2023-2024 academic year. In this 19-item scale, prospective teachers were given 1 lesson hour to answer the questions.

Analysing the Data

For the analysis of the data in the study, normality analyses were performed first. The normality results of the data according to the grade level are given in Table 1.

Table 1. Normality results (grade level)

Normality test	Grade	Statistics	df	p
Kolmogorov-Smirnov	1	,098	52	,200
Shapiro- Wilk	2	,977	47	,480
	3	,790	45	**,000**
	4	,981	25	,900

According to Table 1, since 3rd-grade data did not provide normal distribution, Kruskal Wallis and Mann Whitney U tests were used for comparison in terms of grade level.

Mann Whitney U test was also used to compare the data in terms of gender.

Table 2. Normality results (gender)

Normality test	Gender	Statistics	df	p
Kolmogorov- Smirnov	Women	,132	142	**,000**
Shapiro-Wilk	Men	,967	26	,537

According to Table 2, since the data of women PST did not meet the normal distribution, Mann Whitney U test was used to compare the data in terms of gender.

Findings

In this section, firstly, descriptive statistics of the data obtained from the classes are given in Table 3.

Table 3. Descriptive statistics- grade level

Grade	n	X	SS
1	52	68,54	16,932
2	47	71,74	10,337
3	45	75,44	10,902
4	26	75,44	9,928
Total	170	72,36	13,041

According to Table 3, the digital competencies of the PST are above average. The highest average is seen in the 3rd and 4th grades.

In Table 4, the digital competencies of the PST were compared in terms of grade level.

Table 4. Kruskal-Wallis results- grade level

Grade	n	Mean Rank	SD	X^2	p
1	52	74,00	3	8,643	**0,034**
2	47	78,81			
3	45	99,60			
4	26	96,19			

According to Table 4, there was a difference between the groups. Mann Whitney U test was performed to determine which group was in favor of the difference. Mann Whitney U test results are given in Table 5.

Table 5. Mann Whitney U Test results - grade level

Grade	n	Mean rank	Sum of ranks	U	p
1	52	47,98	2495,00	1017,000	,461
2	47	52,23	2455,00		
1	52	42,80	2225,50	847,500	**,020**
3	45	56,17	2527,50		
1	52	36,22	1883,50	505,500	,071
4	26	46,06	1197,50		
2	47	40,38	1898,00	770,000	**,024**
3	45	52,89	2380,00		
2	47	34,19	1607,00	479,000	,128
4	26	42,08	1094,00		

According to Table 5, there was a significant difference between the 1st and 3rd grades in favor of the 3rd grades and between the 2nd and 3rd grades in favor of the 3rd grades (p<.05).

The digital competencies of PST were compared in terms of gender. For this, a comparison was made with Mann Whitney U test. The results are given in Table 6.

Table 6. Mann Whitney U Test results- gender

Group	n	Mean rank	Sum of ranks	U	p
Men	27	77,70	2098,00	1720,000	0,369
Women	143	86,97	12437,00		

According to Table 5, there was no significant difference between the digital competencies of the PST in terms of gender (p>.05).

Conclusion and Discussion

This study aimed to measure whether the digital competencies of the PST differ in terms of grade level and gender factors. In the study, the digital competencies of the PST were above normal. This may be because PST is Generation Z. In addition, the teaching method-technical courses on digitalization may be effective. In the study, a significant difference was observed between 1st and 3rd grades in favor of 3rd grades and between 2nd and 3rd grades in favor of 3rd grades (p<.05). The emergence of this situation may be influenced by the fact that the PST started to take courses related to technology until the 3rd-grade level. Especially at the 3rd grade level, the use of Web 2. tools such as Canva, Padlet, etc. in courses on science teaching may be effective.

There was no significant difference in terms of gender (p>.05). The fact that the PST of different genders at the same grade level are in similar age groups and go through similar educational processes may be effective in the emergence of this situation. To increase the digital competencies of PST, it is predicted that providing training in various fields related to digitalization (augmented reality, digital games, etc.) will be effective.

References

[1] Selimi, A., & Üseini, A. (2019, April). Yenilikçi eğitim ile dijital yetkinlik ve girişimcilik becerilerinin geliştirilmesi–Kuzey Makedonya örneği. In ICEB'19-International Congress of Economics and Business (pp. 11-13).

[2] Spante, M., Hashemi, S. S., Lundin, M., & Algers, A. (2018). Digital competence and digital literacy in higher education research: Systematic review of concept use. Cogent education, 5(1), 1519143.

[3] Falloon, G. (2020). From digital literacy to digital competence: the teacher digital competency (TDC) framework. Educational technology research and development, 68(5), 2449-2472.

[4] Vandeputte, P., Ferrari, S., & Coste, A. T. (2012). Antifungal resistance and new strategies to control fungal infections. International journal of microbiology, 2012.

[5]   Arslan, G. (2019). Mediating role of the self–esteem and resilience in the association between social exclusion and life satisfaction among adolescents. Personality and Individual Differences, 151, 109514.

[6] Demirdağ, S. (2021). Communication skills and time management as the predictors of student motivation. International Journal of Psychology and Educational Studies, 8(1), 38-50.

[7] Budak, F., & Korkmaz, Ş. (2020). COVID-19 pandemi sürecine yönelik genel bir değerlendirme: Türkiye örneği. Sosyal Araştırmalar ve Yönetim Dergisi, (1), 62-79.

[8] Rohde, H., Futrell, R., & Lucas, C. G. (2021). What's new? A comprehension bias in favor of informativity. *Cognition*, *209*, 104491.

[9] Karakuş, G., & Ocak, G. (2019). Öğretmen adaylarının dijital okuryazarlık öz-yeterlilik becerilerinin farklı değişkenler açısından incelenmesi. Afyon Kocatepe Üniversitesi Sosyal Bilimler Dergisi, 21(1), 129-147.

[10] Ma, P. C., Tretiakova, M. S., MacKinnon, A. C., Ramnath, N., Johnson, C., Dietrich, S., ... & Salgia, R. (2008). Expression and mutational analysis of MET in human solid cancers. Genes, Chromosomes and Cancer, 47(12), 1025-1037.

[11] Ergül, D. Y., & TAŞAR, M. F. (2023). Development and validation of the teachers' digital competence scale (TDiCoS). Journal of Learning and Teaching in Digital Age, 8(1), 148-160.

Antioxidant Property Investigation of a Novel Plant Species Discovered from Türkiye: Rheum Telianum

K. Aslan[1], A.Z. Tel[2], M.A. Ylmaz[3], O. Cakir[4] and I. Gulcin[5]

[1]Atatürk University, Erzurum, Türkiye, ORCID: 0000-0001-8388-5470
[2]Adıyaman University, Adıyaman, Türkiye, ORCID: 0000-0002- 1204-3839
[3]Dicle University, Diyarbakır, Türkiye, ORCID: 0000-0002-4090-7227
[4]Dicle University, Diyarbakır, Türkiye, ORCID: 0000-0002-8006-2054
[5] Atatürk University, Erzurum, Türkiye, ORCID: 0000-0001-5993-1668

Abstract

Rhubarb, formally known as *Rheum* spp, is a genus of plant *Polygonaceae* and is well-known for its rich antioxidant source [1]. The present study reveals *in vitro* antioxidant properties and the phytochemical content of a novel *Rheum* species (*Rheum telianum)* isolated from Southeastern Anatolia. To perform the analysis, dried leaves and seeds of the plants were ground and extracted with ethanol to obtain plant secondary metabolites. Then, dried extracts were subjected to *in vitro* 2,2-Diphenyl-1-picrylhydrazyl (DPPH) radical scavenging and Cupric reducing antioxidant capacity (CUPRAC), Fe^{3+}, and the ferric reducing antioxidant power (FRAP)-reducing assays and all results were compared with the commercially available synthetic and natural antioxidants [2-4]. In addition to the antioxidant capacity assays, quantitative phenolic, flavonoid, and secondary metabolite were determined through colorimetric and LC-MS/MS chromatographic methods [2-5]. Results showed that both leaves and the seeds of the *R. telianum* have high inhibitory properties over DPPH radicals with 20.79 µg/mL, r^2=0.9884 and 5.67 µg/mL, r^2=0.9969 IC_{50} values, respectively. Similarly, metal-reducing capacities for the extracts were determined as high as standard antioxidants in the CUPRAC, Fe^{+3}, and FRAP assays. The total phenolic and flavonoid content of the leaves and the seeds was determined as directly proportional to the extracts' antioxidant properties. The samples' dominant secondary metabolites were evaluated using the LC-MS/MS analysis results. In conclusion, the extracts' structure and functional relationship and the plants' possible usage in the food, medicine, and cosmetic industries were made.

Keywords: *Rheum telianum*, Rhubarb, Antioxidant, LC-MS/MS

Introduction

Rheum spp., rhubarb in folk linguistics, is a genus that species-rich type of the *Polygonacae* family. This genus is mostly native to Asian countries like China, India, Nepal, Korea, Bhutan, Pakistan, Turkey, Iran, Russia and Tibet [1]. Currently, there are

forty-five accepted different species, among them 25 of those species have been reported to have biological importance. Among them *R. australe, R. palmatum, R. ribes,* and *R. webbianum* have the highest number of citations in the world [1]. These species have important usage in traditional medicine as they have been reported to be effective in liver, kidney, gastrointestinal, and reproductive system-related diseases. Also, due to their proven biological activity, they have a great potential to be used as sources in herbal medicine [1–4].

Rheum telianum is a novel rhubarb species that is s described as a new species from Kayatepe village (south-eastern Anatolia, Turkey). It is morphologically related to the west-central Asiatic *R. ribes* and *R. rhizostachyum* [3]. Here, it was aimed to determine the antioxidant properties and phytochemical content of this novel *Rheum* sp. to evaluate their biological activity relativeness to other important *Rheum* sp. and provide an insight into possible future biological activity with this preliminary study.

Experimental Part

Materials and Chemicals

1,1-diphenyl-2-picryl-hydrazyl (DPPH), neocuproine (2,9-dimethyl-1,10-phenanthroline), Ascorbic acid, butylated hydroxytoluene (BHT), butylated hydroxyanisole (BHA), α-tocopherol, Trolox, Folin Ciocalteu's and Ellman's Reagent (5,5'-Dithio-bis-(2-nitrobenzoic Acid) were purchased from Sigma-Aldrich GmbH, Steinheim, Germany. Standard phenolic compounds for LC-MS/MS were purchased from Sigma.

Preparation of the Plant Samples

Rheum telianum leaves and the seeds were collected from Kayatepe (Rezip) village of Adıyaman province in Türkiye, rocky serpentine soils, 37°87′ N, 38°27′ E, 1350 m TURKEY[5]. Water and ethanol extracts of the samples were prepared by weighing 10 gr of dried leaves and the seeds after grinding pieces up to 0,5 -10 mm. Then, 50 mL of ethanol was added to the milled plant material in a beaker and the samples were mixed for 5 hours. Solid particles were decanted from both clean cheesecloth, and Whatmann paper No.1, and centrifugation at 3000 rpm for 10 minutes until transparent extracts were obtained. Desolvation was performed with either a rotary evaporator [6]. The overall extraction yields were calculated from the amount of remaining extracts. 100 mg of dry extracts were separated for LC-MS/MS analysis and ethanol solution of extracts was prepared in known concentrations for further antioxidant capacity testing.

Phytochemical Analysis of The Extracts

Determination of total flavonoid and total phenol of the extracts

Total flavone and flavonol contents were determined by analyzing through the colorimetric method [6]. Three different concentrations (15-45 µg/mL) of 0.5 mL of the samples in ethanol were mixed with 1.5 mL of 95% methanol. Then, 0.5 mL of 1.0 M

potassium acetate, 2.3 mL of distilled water, and 1.5 mL of 10% Aluminum nitrate were added to the reaction mixture, and the samples were incubated at 25°C for 40 min after vigorously shaking. Absorbances at 415 nm of each reaction were recorded and the results were expressed as µg quercetin equivalents (QE) /mg of the extracts. A standard curve of quercetin was obtained within a concentration range of 1-500 µg/mL (y = 0,004614x + 0,01149, r2=0.9909). The total phenolic contents of the three different concentrations (15-45 µg/mL) of the plant extracts were determined by the Folin–Ciocalteu method applied by Karagecili et al. splitting the volumes of each component by half [6]. The results were expressed as µg gallic acid equivalents (GAE) /mg of the extracts with concentrations ranging between 0-200 µg/mL (y = 0,007993x - 0,1509, r^2= 0,9824).

Determination of Phytochemicals by LC-MS/MS

Screening of ethanol extract of the samples was performed against 53 standard phytochemical standards whose chromatographic conditions were validated and optimized for A Shimadzu-Nexera model ultrahigh performance liquid chromatography (UHPLC) coupled with a tandem mass spectrometer (Shimadzu LC/MS-8040) in the previously reported study [7]. LC-MS/MS method was applied as previously reported [6], [19] and adopted for dried samples of ethanol extract of *Rheum telianum* leaves (EERL), and the *Rheum telianum* seeds (EERS).

Determination of Antioxidant Properties of the Extracts

DPPH Radical Scavenging Activity

The DPPH radical scavenging activity determination assay was performed as previously applied [6,8]. An ethanol solution of 0.1 mM DPPH was prepared and incubated in the dark by mixing overnight for preradicalization. Then, 0.5 mL of DPPH and 0.5 mL of the samples in ethanol (15-45 µg/mL) were mixed and incubated at 30 °C for 30 minutes. The absorbances of each sample were recorded at 517 nm. Ascorbic acid, BHA, BHT, α - Tocopherol, and Trolox were used as positive controls in ABTS assays. Each sample was performed in triplicate.

Fe^{+3}, Cu^{2+} and Fe^{+3}-TPTZ Reducing Capacity

Fe^{+3}-reducing assay, Fe^{+3} ion-reducing antioxidant power (FRAP), and Cu^{2+}-reducing antioxidant capacity assay (CUPRAC) methods were employed to determine the ability of the samples to reduce metal complexes. Three different concentrations of the samples (0.75 mL in distilled water) were mixed with 1.25 mL of 0.20 M phosphate buffer solution (pH 6.6) and 1 % (w/w) potassium ferrocyanide. Then, the mixture was acidified with 1. 25 mL of 10 % trichloroacetic acid (w/w), and incubated at 50°C for 30 min. Lastly, 0.25 mL of 0.1 % Iron (III) chloride was added to form the blue complex and the absorbances of each sample were recorded at 700 nm via Shimadzu UV-1800 UV spectrophotometer [6]. CUPRAC assay was performed by combining an equal volume of 10 mM of copper (II) chloride, 7.5 mM neocuproine, and 1.0 M ammonium acetate buffer and the samples

were added by adjusting the final volume to 2 mL with distilled water [9]. The mixture was incubated for 30 min at 25 °C and was measured spectrophotometrically using the blue-colored final reaction mixture at 450 nm. FRAP reagent containing acidic 10 mM: 20 mM iron (III) chloride: 0.3 M sodium acetate buffer (pH=3.6) in a ratio of 1:1:10 was prepared before use. 0.5 mL of the samples in buffer mixed with an equal volume of 20 mM iron (III) chloride and FRAP reagent resulting in 5 mL final reaction volume. The absorbance of each reaction was measured at wavelength 593 nm after 30 min incubation at 37 °C [9]. Ascorbic acid, BHA, BHT, α -Tocopherol, and Trolox were used as positive controls in ABTS assays. Each sample was performed in triplicate.

Statistical Analysis

All experiments are repeated three times for each sample. The results are reported as the mean ± SD. (n = 3) and were evaluated using one-way ANOVA followed by Tukey's post hoc test; $p < 0.05$ was considered statistically significant.

Results and Discussion

The phytochemistry of *Rheum telianum* was investigated in terms of total phenolic and flavonoid content. Also, plant secondary metabolites were determined through LC-MS/MS against 53 phytochemical standards (thirty-three medicinal and 10 aromatic compounds) that were most commonly reported with their biological activity [7]. Since the significant biological activities such as antioxidant, antimicrobial, and anti-inflammatory properties of natural compounds were associated with phenolic contents, their analysis is inevitable for food, medicine, and cosmetic industries when determining the value of the herbal extract [10]. According to the results obtained from the quantitative assays, the total phenolic content of EERL and EERS was determined as 583 and 753 μg GAE /mg. Even though the flavonoids have same application field as phenolic compounds such as cosmetic and food industry, the most pronounced applications of these compounds, are in the field of medicine. Therefore, the determination of the total flavonoid content will significantly express the medicinal value of the plant extract [11]. The total flavonoid contents were also found as 298 and 238 QE μg/mg. Plant-to-extract ratios were defined by simple calculation of the extract production yield of dried plants. Based on this assumption, the DER (Dry extracts ratio of the leaves and the seeds was calculated as 10:5.9 and 10:3.9, respectively. This ratio may be used to partly determine the amount of active material extracted from plant biomass relative to the starting amount of biomass, thus, useful to define 'standardized extracts' for herbal formulations and dietary supplements [12].

LC-MS/MS Analysis of the *Rheum* extracts revealed a total of ten different compounds in the leaves and the seeds with high amounts. In the leaves of *Rheum telianum*, gallic acid gentisic acid, epicatechin gallate, rutin, isoquercitrin, hesperidin quercitrin, nicotiflorin, and acacetin; in the seeds gallic acid, catechin, gentisic acid, epicatechin gallate, rutin, isoquercitrin, hesperidin, and quercitrin were detected. Even though the quantities differed, a total of eight compounds were in common in both of

the extracts. Quantitative and chromatographic representations of the results are given in Figure 1.

_	Quantitative Results of *Rheum telianum* (mg/g)		
No	Analytes	EERS	EERL
4	Gallic acid	1	0,09
7	Catechin	0,552	N.D.
8	Gentisic acid	0,02	0,027
22	Epicatechin gallate	1,12	0,109
33	Rutin	0,868	2,149
34	isoquercitrin	0,117	0,026
35	Hesperidin	0,519	1,357
41	Quercitrin	0,43	0,984
43	Nicotiflorin	N.D.	0,034
56	Acacetin	N.D.	0,003
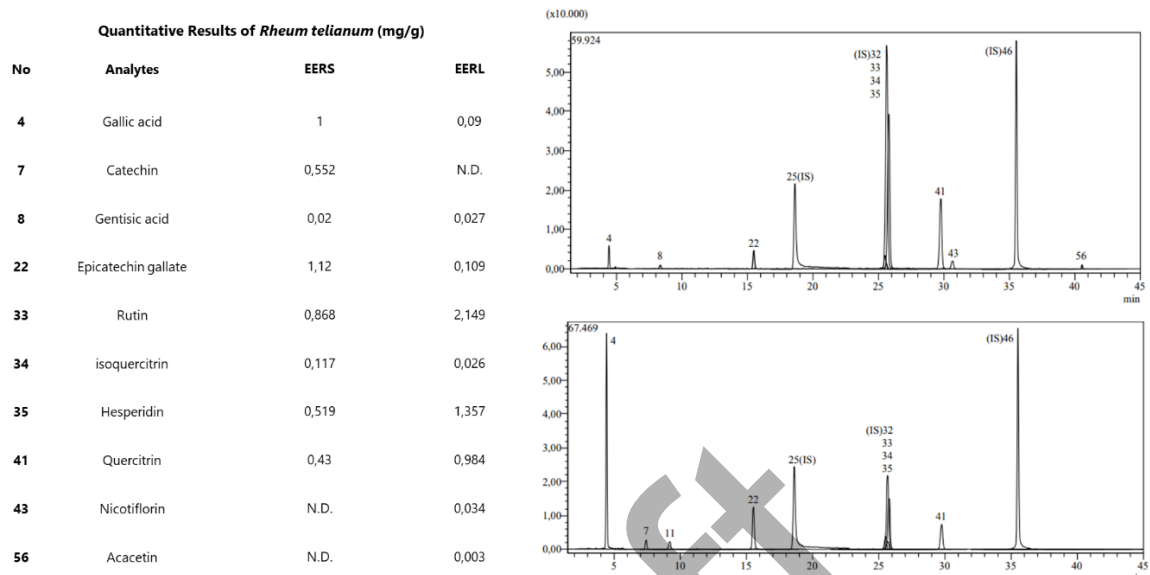
Figure 1. LC-MS/MS quantitative and chromatographic results of *Rheum telianum* leaves (EERL) and the seeds (EERS)

The antioxidant activity of the *Rheum telianum* plant was investigated through four different methods with two different mechanisms since combining different methods would be a more realistic approach regarding different antioxidant properties. Here, radical scavenging activity was determined by employing the DPPH radical scavenging assay, and the percentage of the inhibition was calculated by simply portioning with the control reaction that does not involve the samples. Results showed that both of the samples scavenged the DPPH radical up to 90 %, and even the seed extracts reached up to 98 %, which is greater activity than those ascorbic acid, BHA, BHT, Trolox were inhibited maximum with 94 %. Metal-reducing capacities were determined through three different methods and quite similar results were obtained from each of the assays. The Cu^{2+}-reducing capacity of the EERS was evaluated as being the highest and EERL, BHA, BHT, and Trolox were followed that result in descending order. In Fe^{3+}-TPTZ reducing results, the order was evaluated from the highest to the lowest, such as EERS, BHT, Trolox, BHA, and EERL. Lastly, the order was EERS, BHA, BHT, EERL, and Trolox from the highest to lowest in Fe^{3+}-reducing assay. A graphical representation of the antioxidant capacity results is shown in Figure 2.
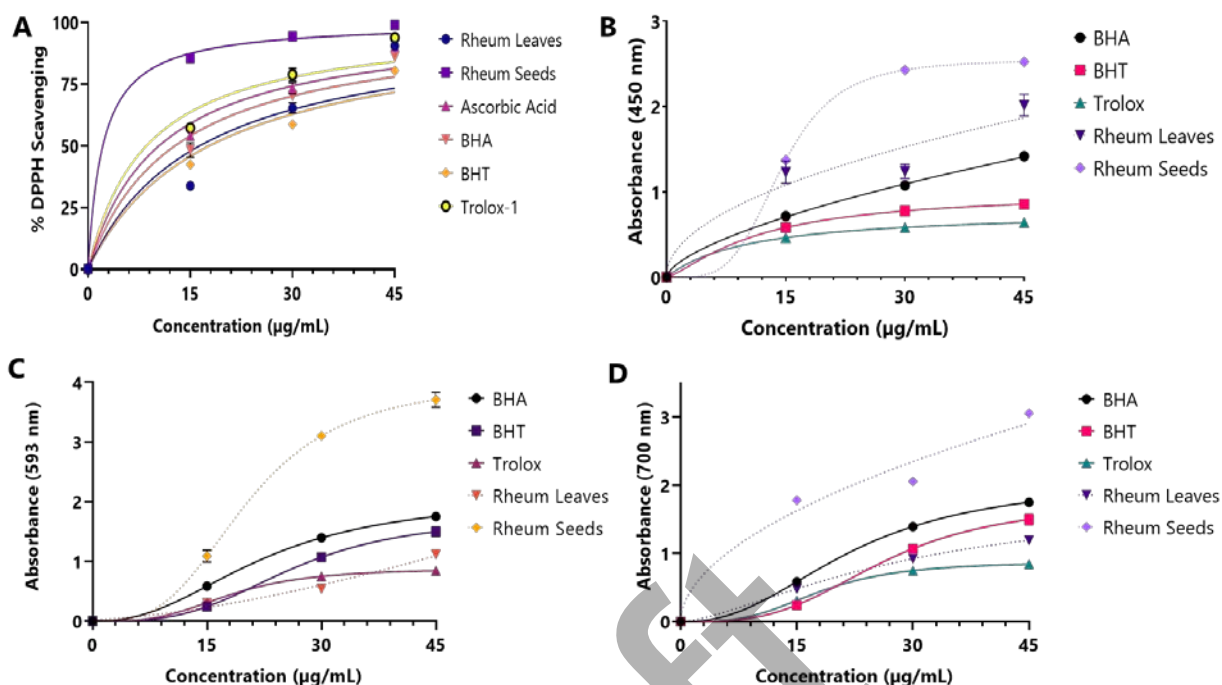
Figure 2. Graphical representation of antioxidant capacity results from A; DPPH radical scavenging assay B; CUPRAC assay C; FRAP assay D; Fe^{3+}-reducing assay.

IC$_{50}$ values of each sample in the DPPH assay were calculated using GraphPad Prism 8.4.0 using a non-linear regression model for normalized parameters. Mean absorbance values obtained from the metal-reducing tests were also tested by row statistics. Results obtained using 45 µg/mL of sample concentration were represented in Table 1.

Table 1. Antioxidant Activity Results

	DPPH· scavenging assay (IC$_{50}$)	CUPRAC assay (λ_{450})	FRAP assay (λ_{593})	Fe^{+3} reducing assay (λ_{700})
BHA (45 µg/mL)	16.00, r^2=0.9948	1.41±0.07, r^2=0.9948	2.33±0.01, r^2=0.9986	1.75±0.04, r^2=0.9983
BHT (45 µg/mL)	19.76, r^2=0.9883	0.86±0.02, r^2=0.9989	2.87±0.06, r^2=0.9938	1.50±0.08, r^2=0.9972
Trolox (45 µg/mL)	12.99, r^2=0.9946	0.64±0.01, r^2=0.9988	2.48±0.12, r^2=0.9558	0.84±0.01, r^2=0.9990
Ascorbic Acid (45 µg/mL)	13.92, r^2=0.9926	-	-	-
***Rheum* Leaves (45 µg/mL)**	20.79, r^2=0.9884	2.02±0.13, r^2=0.9272	1.12±0.07, r^2=0.9789	1.19±0.02, r^2=0.9979
***Rheum* Seeds (45 µg/mL)**	5.67, r^2=0.9969	2.53±0.01, r^2=0.9997	3.70±0.12, r^2=0.9981	3.07±0.03 r^2=0.9725

Conclusion

Rheum species have great importance due to their rich contents of bioactive metabolites, however, according to the latest advances, several *Rheum* species are under immense risk and have been considered as "threatened" due to overharvesting and habitat destruction. Therefore, suggestions for good applications to cultivate them have been made. Besides, the discovery of novel *Rheum* sp. with wide biological activity is promising in many industries such as food, medicine, and cosmetics. Here, it was evaluated that *Rheum telianum* species possess promising antioxidant activity, by having characteristics of the *Rheum* genus and *Polygonacae* family. Industrially important metabolites of the species were revealed in remarkable quantity. This study can be concluded as a preliminary study and evaluated as seminal for future activity investigation of *Rheum telianum* species.

Bibliography

[1]   G. E. Barreto, A. Sahebkar (eds.)., 2021 Pharmacological Properties of Plant-Derived Natural Products and Implications for Human Health, Advances in Experimental Medicine and Biology 1308., (2021) 309–346 pp.

[2]   G.R. Takeoka, L. Dao, L. Harden, A. Pantoja, J.C. Kuhl., 2013, Antioxidant activity, phenolic and anthocyanin contents of various rhubarb (*Rheum* spp.) varieties, Int J Food Sci Technol., (48) (2013) 172–178 pp.

[3]   A. Ilçim, F. Karahan, 2020, Rheum telianum (Polygonaceae), a new species from Southeastern Anatolia (Turkey), Phytotaxa (477) (2020) 81–89 pp.

[4]   O. Liudvytska, M. Bandyszewska, T. Skirecki, J. Krzyżanowska-Kowalczyk, M. Kowalczyk, J. Kolodziejczyk-Czepas, 2023. Anti-inflammatory and antioxidant actions of extracts from *Rheum rhaponticum* and *Rheum rhabarbarum* in human blood plasma and cells in vitro, Biomedicine and Pharmacotherapy., (165) (2023).

[5]   A A. Ilçim, F. Karahan, 2020, *Rheum telianum* (Polygonaceae), a new species from Southeastern Anatolia (Turkey), Phytotaxa., (477) (2020) 81–89 pp.

[6]   H. Karagecili, E. İzol, E. Kirecci, İ. Gulcin, 2023. Determination of Antioxidant, Anti-Alzheimer, Antidiabetic, Antiglaucoma and Antimicrobial Effects of *Zivzik Pomegranate (Punica granatum)*—A Chemical Profiling by LC-MS/MS, Life., (13) (2023)

[7]   M.A. Yilmaz, 2020. Simultaneous quantitative screening of 53 phytochemicals in 33 species of medicinal and aromatic plants: A detailed, robust and comprehensive LC–MS/MS method validation, Ind Crops Prod., (149) (2020).

[8]   İ. Gulcin, S.H. Alwasel, 2023. DPPH Radical Scavenging Assay, Processes 11., (2023) 2248 p.

[9]   L. Güven, U. Behbudbayli, A. Ertürk, H. Hancı, B. Yılmaz, Y. Kaya, İ. Gülçin, 2023. Determination of antioxidant, antimicrobial, anticholinesterase, antityrosinase, antidiabetic and antiglaucoma activities of essential oils from three different Thymus species and their chemical characterization by GC-MS analysis, Journal of Essential Oil-Bearing Plants., (26) (2023) 1424–1446 pp.

[10] H.H. Al Mamari, 2022. Phenolic Compounds: Classification, Chemistry, and Updated Techniques of Analysis and Synthesis

[11] A. Ullah, S. Munir, S.L. Badshah, N. Khan, L. Ghani, B.G. Poulson, A.H. Emwas, M. Jaremko, 2020. Important flavonoids and their role as a therapeutic agent, Molecules., (25) (2020).

[12] E. Medicines Agency, Committee on Herbal Medicinal Products (HMPC) Committee for Medicinal Products for Human Use (CHMP) Committee for Veterinary Medicinal Products (CVMP) Guideline on quality of herbal medicinal products 2 /traditional herbal medicinal products Final, 2022. www.ema.europa.eu/contact.

Applications of CRISPR-Cas Systems on Lactic Acid Bacteria

S. Doğan[1], T.Y. Koç[2], Y. Gülşahin[3], B. Alaylar[4], M. Karadayı[5] and M. Güllüce [6]

[1]Atatürk University, Department of Biology, Erzurum, Türkiye, ORCID: 0000-0003-0499-2169
[2]Atatürk University, Graduate School of Natural and Applied Sciences, Erzurum, Türkiye, ORCID: 0000-0002-7786-5462
[3]Atatürk University, Graduate School of Natural and Applied Sciences, Erzurum, Türkiye, ORCID: 0000-0002-3770-2116
[4]Agri Ibrahim Cecen University, Department of Molecular Biology and Genetics, Ağrı, Türkiye ORCID: 0000-0001-6737-3440
[5]Atatürk University, Department of Biology, Erzurum, Türkiye, ORCID: 0000-0002-2473-0409
[6]Atatürk University, Department of Biology, Erzurum, Türkiye, ORCID: 0000-0002-5957-8259

Abstract

CRISPR technologies, considered one of the greatest discoveries of the last decade, were developed by examining bacterial defense systems [1-3]. This technique is designed to make desired changes to specific DNA segments in cells' genomes, allowing the DNA within the cell to be replaced efficiently and error-free. The main reason why this technique is widely used and attracts the attention of researchers is that it can be easily customized and applied to various cell types [4]. However, the use of CRISPR technologies in the food industry is a relatively new field that needs to be investigated [5].

Food science is defined as a field that studies physical, chemical and biological processes, aiming to improve safe and sustainable food production as the world population increases rapidly [6]. While some of the microorganisms found in foods provide benefits in product processes, some need to be kept under control due to their harmful effects [7, 8].

Lactic acid bacteria are among the most important microorganisms for the food industry. Lactic acid bacteria, a very diverse group both phenotypically and phylogenetically, are very important for the food industry as starter cultures or probiotics. In recent studies, CRISPR-Cas systems have begun to be used as tools to perform operations such as gene deletion, insertion, and point mutation in various LAB types. With the use of these systems, studies have begun to develop new strains with functional properties [9-11]. In this study, current applications of CRISPR-Cas Systems on Lactic Acid Bacteria will be discussed.

Keywords: CRISPR, food application, genetic tool, lactic acid bacteria

Introduction

Genetics has been and continues to be a fundamental tool for understanding molecular and biological functions in various forms of life. Temperature-sensitive lethal genetic screens performed on microorganisms in the 1960s and 1970s laid the foundation for our current understanding of how DNA replication, transcription, and translation occur within the cell [12].

While the 1990s were known as the internet age, the 2000s attracted attention with biotechnology and genes as the dominant technologies of a new era. In 2012, French geneticist Emmanuelle Charpentier and American biochemist Jennifer Doudna developed a method called "genetic scissors" or "molecular scissors", one of the most powerful tools of gene technology [13]. This development provided a significant breakthrough in genetic science. Now, the DNA of plants, animals and microorganisms can be changed extremely easily and with high precision, and various gene edits can be made [14-16].

CRISPR is an acronym for "Clustered Regularly Interspaced Short Palindromic Repeats" and stands for clusters of regularly spaced palindromic repeats. This revolutionary term in the field of gene editing describes a method that allows precisely altering the DNA of organisms [13,17]. The existence of CRISPR has been known since 1987, but the biological functions of this structure became clear about a decade ago while investigating phage resistance in the starter culture *Streptococcus thermophilus* used in dairy products [18-20]. This discovery sparked interest in CRISPR loci and the Cas nucleases that work with them. Although much of the scientific literature focuses on the use of CRISPR-Cas9 for genetic engineering in eukaryotes, these systems have great potential across microbiology and specifically for engineering food cultures. Eventually, CRISPR-associated protein (Cas) systems turned into genome engineering tools that are frequently used in studies of microorganisms today [20-21].

CRISPR-Cas systems are found in approximately 85% of archaea and 40% of bacteria. These systems are found in approximately 63% of Lactobacillus species, 77% of Bifidobacterium, and all (100%) *Streptococcus thermophilus* strains, which are among the microorganisms of critical importance for the food industry [9, 20, 22, 23]. The CRISPR component of the CRISPR-Cas system contains a set of conserved repetitive sequences separated by unique spacers that represent the genetic record of foreign invaders such as phages and plasmids, helping microorganisms recognize foreign DNA and develop defenses against potential threats [9, 19].

Industrially important microorganisms, such as starter cultures and probiotic strains, are a desirable target to leverage CRISPR-Cas systems for genome engineering, especially given their important role in the food supply chain and their many biological functions ranging from food fermentation to promotion of human health. Based on this issue, current applications of CRISPR-Cas Systems on lactic acid bacteria, which are the cornerstone of fermentation, are discussed.

LABs and CRISPR Applications

General characteristics of lactic acid bacteria

Lactic acid bacteria, identified by Orlo-Jensen in 1919; They are rod- or cocci-shaped, gram-positive, catalase and nitrate reductase negative microorganisms that do not form spores and generally produce lactic acid as the end product of carbohydrate fermentation. Although they are generally aerotolerant, those that live in the human and animal digestive systems are anaerobic. Since they do not have the ability to synthesize the necessary enzymes and cytochromes, they cannot perform oxidative phosphorylation in the presence of oxygen. However, flavoproteins can carry out limited non-phosphorylating oxidation thanks to oxidase and peroxidase enzymes. Lactic acid bacteria can live at temperatures between 5-10 °C, and it is also known that some species are tolerant to salt, acid or alkyls [24-27].

Lactic acid bacteria play important roles in the biocycle of meats, vegetables and fermented dairy products; It ensures the production of safe foods that are resistant to pathogens, have a long shelf life. In addition, they are widely found in nature, are the basic element of fermented product production, provide textural structure such as taste, smell and aroma to foods, and enable the production and ripening of some foods; It is a group of microorganisms that have been widely researched due to their important industrial properties such as their ability to produce organic acids, exopolysaccharides, hydrogen peroxide and similar substances, antibacterial and aromatic compounds [27-30].

In recent years, lactic acid bacteria (LAB) have become widely used in various fields due to their economic value and functional properties [31]. LAB can be used to produce organic acids and prepare fermented foods, and some types may also contribute to the repair and growth of the intestinal barrier of animals [27, 32-35]. However, the incomplete metabolic pathways and low stability of LAB may hinder meeting increasing production demands. Thanks to advances in genome editing approaches, strategies have begun to be developed that can help LAB overcome these limitations and increase their beneficial properties [36-39].

The CRISPR-Cas system, one of the most popular technologies of recent times, has been thoroughly researched for use in genome editing of LAB [40]. This technology has enabled the development of flexible and high-throughput genome engineering tools for bacteria, archaea, and eukaryotes. Various scientific studies have shown that various genome editing targets have been successfully achieved in different LAB strains using the CRISPR-Cas system [9, 41-45].

CRISPR-Cas systems of lactic acid bacteria

Several studies have determined that CRISPR-Cas systems are common in LAB and that these systems are found in many *Lactobacillus*, *Streptococcus*, and *Bifidobacterium*

species. While the observed genomic incidence rate in LAB is estimated to be around 45%, rates of occurrence of CRISPR-Cas systems vary greatly at the species level [23, 46]. For example, the strain *L. reuteri* has a CRISPR-Cas system formation rate of only 17%, while strains such as *L. crispatus* and *L. delbrueckii* have rates as high as 96%. While *L. acidophilus* has at least one CRISPR locus, it lacks cas genes. In contrast, *L. paracollinoides* strains have cas genes but lack CRISPR loci [9, 23].

Overall, the most common type of CRISPR-Cas system among lactic acid bacteria is Type II. However, significant differences are observed in the distribution of these systems among species. Type I systems are common in L. parabuchneri, while Type II systems are more common in L. casei [9, 47]. Only Type I systems are found in L. helveticus, while Type II systems predominate in L. rhamnosus. Type III systems are rare among lactic acid bacteria and occur only in a few specific species. However, L. salivarius and L. ruminis appear to be reservoirs of Type III systems; Type III systems were detected in 32% of L. salivarius strains and 41% of L. ruminis strains [9, 23, 46].

If we talk about the common subtypes in lactic acid bacteria, Type II-A subtypes are found in approximately 30% of *lactobacilli*, while this rate is approximately 5% among bacteria in general. Subtype IE is known as the most common Type I subtype in nature and is therefore also the most common Type I subtype in the *Lactobacillus* and *Bifidobacterium* genera. Moreover, subtypes IE, IC, IU, II-A, and II-C are common subtypes found in both *Lactobacillus* and *Bifidobacterium* [9, 23].

CRISPR-Cas system and applications

While the CRISPR-Cas9 genome editing method is widely used in eukaryotes and some model bacteria, studies in this field in lactic acid bacteria (LAB) are still in their early stages [9, 48]. The limited availability of genetic tools that can be used effectively to insert or delete genes in LAB has caused limitations in the biotechnological applications of these bacteria. To overcome this deficiency, other genome editing tools are integrated into the CRISPR/Cas system to create a more effective genome editing design [49-51].

To perform genome editing in a bacterium, an endogenic CRISPR/Cas system is not necessarily required. If an endogenous CRISPR/Cas system is not available, an exogenic form (sgRNA: Cas9) can be introduced using genetic engineering into a plasmid containing guide RNA for genome editing. So far, only Type I and Type II systems have been used for endogenous CRISPR-based genome editing in LAB. However, L. salivarius and L. ruminis have the Type III system, indicating the potential of creating the first endogenous CRISPR genome editing tool based on the Type III system in LAB [20, 51].

Recently, genetic manipulation methods in lactic acid bacteria (LAB) have been significantly developed. These methods include plasmid-based homologous recombination, Red/RecET-mediated double-stranded DNA (dsDNA) recombination, single-stranded DNA (ssDNA) recombination, and CRISPR-based gene editing. These

advances have provided greater flexibility and efficiency for genomic modification and biotechnological applications in LAB [10, 52-54].

Among CRISPR-based techniques used in lactic acid bacteria (LAB), the most common method is classical homologous recombination, a plasmid-based double exchange process. This method involves a resistance screening marker and integration plasmid containing homologous arms of the target gene. The entire process usually involves a single exchange, followed by a second exchange supported by the host cell's endogenous RecA system LAB [10, 52, 55].

Another method used in gene regulation is Red/RecET-mediated double-stranded DNA recombination. This method offers a more precise approach to gene editing and has been used successfully in bacteria such as Escherichia coli, Lactococcus lactis, Pseudomonas syringae, Photorhabdus and Xenorhabdus. However, because this method relies on specific interactions between the recombinase system and proteins encoded by the host cell, recombination efficiency can often be limited when applied to different bacteria [10, 56-59].

CRISPR-based gene editing tools can be used for gene deletion, insertion and silencing in lactic acid bacteria (LAB). The most commonly used CRISPR-Cas9 systems require Cas9 as the effector protein and use a single guide RNA (sgRNA) to recognize target DNA. sgRNA consists of crRNA, which binds to target DNA, and tracrRNA, which interacts with the Cas9 protein. crRNA has a replaceable sequence of 20 to 24 nucleotides at its 5' end that fits perfectly with the target DNA, while tracrRNA has a hairpin structure at its 3' end that binds with Cas9. By designing more than one sgRNA, regulation can be made on more than one gene at the same time [60, 61].

Additionally, the CRISPR-Cas9 system can perform gene editing using different recombination techniques. Methods such as plasmid-based recombination, single-stranded DNA (ssDNA) recombination, and double-stranded DNA (dsDNA) recombination can be used for gene editing with this system [10, 62].

Result

The CRISPR/Cas9 system attracted attention with the discovery that repetitive sequences in the DNA of bacteria are a defense mechanism against bacteriophages. Studies carried out since this discovery have enabled the development of the CRISPR/Cas system as a technology with a wide range of applications.

In the field of biotechnology and genetic engineering related to LABs, many studies are being carried out for the use of the CRISPR/Cas system. These systems can be used in industry to increase product properties and redesign existing strains. However, there are some difficulties in developing industrial strains with new properties. In particular, problems such as cutting unwanted off-target DNA regions may arise due to the lack of

specificity of Cas9 to certain genomic regions. This can lead to ethical problems and have restrictive effects on the system.

However, it is hoped that with increased research, these problems can be resolved. Progressing work on the CRISPR/Cas system will help address the shortcomings and limitations of the system. In this way, it will be possible to use the CRISPR/Cas system more safely and effectively on LABs and other microorganisms.

References

[1] T. Zhan, N. Rindtorff, J. Betge, M.P. Ebert, & M. Boutros, 2019. CRISPR/Cas9 for cancer research and therapy. In Seminars in cancer biology 55 106-119. Academic Press.

[2] R. Luthra, S. Kaur, & K. Bhandari, 2021. Applications of CRISPR as a potential therapeutic. Life Sciences., 284 119908.

[3] H. Seok, R. Deng, D.B. Cowan, & D.Z. Wang, 2021. Application of CRISPR-Cas9 gene editing for congenital heart disease. Clinical and experimental pediatrics, 64(6) 269.

[4] J. Ruan, J. Xu, R.Y. Chen-Tsai, & K. Li, 2017. Genome editing in livestock: Are we ready for a revolution in animal breeding industry?. Transgenic research., 26(6) 715-726.

[5] A. Bölükbaş, & A. Gücükoğlu, 2022. CRISPR/Cas9 teknolojisi ve gıda alanında kullanımı. *Frontiers in Life Sciences and Related Technologies.*, *3*(1) 36-42.

[6] K. Selle, & R. Barrangou, 2015. CRISPR-Based technologies and the future of food science. Journal of food science., 80(11) 2367-2372.

[7] K. Papadimitriou, B. Pot, & E. Tsakalidou, 2015. How microbes adapt to a diversity of food niches. Current Opinion in Food Science., 2 29- 35.

[8] E. Stout, T. Klaenhammer, & R. Barrangou, 2017. CRISPR-Cas technologies and applications in food bacteria. Annual review of food science and technology., 8 413-437.

[9] A. Roberts, & R. Barrangou, (2020). Applications of CRISPR-Cas systems in lactic acid bacteria. *FEMS Microbiology Reviews.*, *44*(5) 523-537.

[10] X. Song, X.Y. Zhang, Z.Q. Xiong, X.X. Liu, Y. Xia, S.J. Wang, & L.Z. Ai, 2020, CRISPR–Cas-mediated gene editing in lactic acid bacteria. *Molecular Biology Reports*, *47*, 8133-8144.

[11] Y. Mu, C. Li, T. Zhang, F.J. Jin, Y.J. Sung, H.M. Oh, & L. Jin, 2022. Development and applications of CRISPR/Cas9-based genome editing in Lactobacillus. *International Journal of Molecular Sciences.*, *23*(21) 12852.

[12] J.P. Van Pijkeren, & R.A. Britton, 2014. Precision genome engineering in lactic acid bacteria. *Microbial Cell Factories*, *13*(Suppl 1), S10.

[13] T. SoysaL, 2021. Crispr Genom Düzenleme Teknolojileri: Patentlenebilirlikleri ve Covid-19 Salgınında Kullanımı. *Adalet Dergisi*, (66), 227-292.

[14] R. Barrangou & J.P. van Pijkeren, (2016). Exploiting CRISPR–Cas immune systems for genome editing in bacteria. *Current opinion in biotechnology*, *37*, 61-68.

[15] A.C. Komor, A.H. Badran, & D.R. Liu, 2017. CRISPR-based technologies for the manipulation of eukaryotic genomes. *Cell*, *168*(1), 20-36.

[16] M. Shwartz, 2018. CRISPR is a revolutionary gene-editing tool, but it's not without risk, Winter 2018, https://stanmed.stanford.edu/2018winter/CRISPR-for-gene-editing-isrevolutionary-but-it-comes-with-risks.html.

[17] A. Ergül, 2020. Bitkilerde Fonksiyonel Genombilim, Bitkilerde Genom Düzenlemesi (CRISPR/ Cas9), s. 5 vd.,

[18] Y. Ishino, H. Shinagawa, K. Makino, M. Amemura, & A. Nakata, 1987. Nucleotide sequence of the iap gene, responsible for alkaline phosphatase isozyme conversion in Escherichia coli, and identification of the gene product. *Journal of bacteriology*, *169*(12), 5429-5433.

[19] R. Barrangou, C. Fremaux, H, Deveau, M. Richards, P. Boyaval, S. Moineau,... & P. Horvath, 2007. CRISPR provides acquired resistance against viruses in prokaryotes. *Science*, *315*(5819), 1709-1712.

[20] C. Hidalgo-Cantabrana, S. O'Flaherty, & R. Barrangou, 2017. CRISPR-based engineering of next-generation lactic acid bacteria. *Current opinion in microbiology*, *37*, 79-87.

[21] R. Barrangou, & E.G. Dudley, 2016. CRISPR-based typing and next-generation tracking technologies. *Annual Review of Food Science and Technology*, *7*, 395-411.

[22] Z. Sun, H.M.B. Harris A. McCann, 2015. Expanding the biotechnology potential of lactobacilli through comparative genomics of 213 strains and associated genera. Nat Commun. 6, 1–13.

[23] A.B. Crawley, J.R. Henriksen, R. Barrangou, 2018. CRISPRdisco: An automated pipeline for the discovery and analysis of CRISPR-Cas systems. CRISPR J 1, 171–81.

[24] G. Kaban and M. Kaya, 2008. Identification of lactic acid bacteria and Gram-positive catalase-positive cocci isolated from naturally fermented sausage (sucuk). Journal of food science, 73(8), M385-M388.

[25] E. Dinçer, M. Kivanç, H. Karaca, 2009. Lactic acid bacteria and bacteriocins used as biopreservatives. Anadolu University, Faculty of Science, Department of Biology and Faculty of Pharmacy, Department of Microbiology, Eskişehir, GD08059.

[26] S. Hati, S. Mandal, J.B. Prajapati, 2013. Novel starters for value added fermented dairy products. Current Research in Nutrition and Food Science Journal, 1(1), 83-91.

[27] M.P. Mokoena, C.A. Omatola, A.O. Olaniran, 2021. Applications of lactic acid bacteria and their bacteriocins against food spoilage microorganisms and foodborne pathogens. Molecules, 26(22), 7055.

[28] E. Demir, 2014. Characterization of bacteriocin production in lactic acid bacteria isolated from fermented milk products. Master's Thesis, Adnan Menderes University, Institute of Science and Technology, Aydın.

[29] H. Özlü, 2015. Bacteriocin producing ability of lactic acid bacteria isolated from some cheeses, Doctoral Thesis, Atatürk University, Health Sciences Institute, Erzurum.

[30] E. Arsoy-Saraç, 2019. Determination of antifungal activity of sourdough lactic acid bacteria. Doctoral Thesis, Ondokuz Mayıs University, Institute of Science and Technology, Samsun.

[31] K. Makarova, A. Slesarev, Y. Wolf, A. Sorokin, B. Mirkin, E. Koonin,... & D. Mills, 2006. Comparative genomics of the lactic acid bacteria. *Proceedings of the National Academy of Sciences*, 103(42), 15611-15616.

[32] W.M. de Vos, 2011. Systems solutions by lactic acid bacteria: from paradigms to practice. *Microb Cell Fact* 10(Suppl 1), S2.

[33] P. Gaspar, A.L. Carvalho, S. Vinga, H. Santos, A.R. Neves, 2013. From physiology to systems metabolic engineering for the production of biochemicals by lactic acid bacteria. *Biotechnol Adv* 31, 764–788.

[34] M. Kleerebezem, O.P. Kuipers, E.J. Smid, 2017. Editorial: lactic acid bacteria-a continuing journey in science and application. *FEMS Microbiol Rev* 41, S1–S2.

[35] P. Filannino, R. Di Cagno, M. Gobbetti, 2018. Metabolic and functional paths of lactic acid bacteria in plant foods: get out of the labyrinth. *Curr Opin Biotechnol* 49, 64–72.

[36] J.P. van Pijkeren, R. Barrangou, 2017. Genome editing of food-grade lactobacilli to develop therapeutic probiotics. *Microbiol Spectr* 5.

[37] Y.S. Lee, T.Y. Kim, Y. Kim, S.H. Lee, S. Kim, S.W. Kang, J.Y. Yang, I.J. Baek, Y. Sung Y.Y. Park, S.W. O.E. Hwang, K.S. Kim, S. Liu, N. Kamada, N. Gao, M.N. Kweon, 2018. Microbiota-derived lactate accelerates intestinal stem-cell-mediated epithelial development. *Cell Host Microbe* 24, 833–846.e6.

[38] H. Xiao, Q. Wang, C.H. Bang-Berthelsen, P.R. Jensen, C. Solem, 2020. Harnessing adaptive evolution to achieve superior mannitol production by *Lactococcus lactis* using its native metabolism. *J Agric Food Chem* 68, 4912–4921.

[39] H. Wu, S. Xie, J. Miao, Y. Li, Z. Wang, M. Wang, Q. Yu, 2020. *Lactobacillus reuteri* maintains intestinal epithelial regeneration and repairs damaged intestinal mucosa. *Gut Microbes* 11, 997–1014.

[40] T.V. Plavecand A. Berlec, 2019. Engineering of lactic acid bacteria for delivery of therapeutic proteins and peptides. *Applied microbiology and biotechnology*, *103*, 2053-2066.

[41] D. Bhaya, M. Davison, R. Barrangou, 2011. CRISPR-Cas systems in bacteria and archaea: versatile small RNAs for adaptive defense and regulation. *Annu Rev Genet* 45, 273–297.

[42] P.D. Hsu, E.S. Lander, F. Zhang, 2014. Development and applications of CRISPR-Cas9 for genome engineering. *Cell* 157, 1262–1278.

[43] E. Choudhary, P. Thakur, M. Pareek, N. Agarwal, 2015. Gene silencing by CRISPR interference in mycobacteria. *Nat Commun* 6, 6267.

[44] Y. Li, S. Pan, Y. Zhang, M. Ren, M. Feng, N. Peng, L. Chen, Y.X. Liang, Q. She, 2016. Harnessing type I and type III CRISPR-Cas systems for genome editing. *Nucleic Acids Res* 44:e34.

[45] M. Adli, 2018. The CRISPR tool kit for genome editing and beyond. *Nat Commun* 9, 1911.

[46] A.E. Briner, G.A. Lugli, C. Milani, 20015. Occurrence and diversity of CRISPR-Cas systems in the genus Bifidobacterium. PLoS One 10, e0133661.

[47] E. Scaltriti, D. Carminati, C. Cortimiglia, 2019. Survey on the CRISPR arrays in Lactobacillus helveticus genomes. Lett Appl Microbiol, 68, 394–402.

[48] J. Muysson, L. Miller, R. Allie, D.L. Inglis, 2019. The Use of CRISPR-Cas9 Genome Editing to Determine the Importance of Glycerol Uptake in Wine Yeast During Icewine Fermentation. Fermentation, 5, 1-15.

[49] X. Song, H. Huang, Z. Xiong, L. Ai, S. Yang, 2017. CRISPR-Cas9D10A Nickase-Assisted Genome Editing in Lactobacillus casei. 83, 1–14.

[50] R.A. Börner, V. Kandasamy, A.M. Axelsen, A.T. Nielsen, E.F. Bosma, 2019. Genome editing of lactic acid bacteria: Opportunities for food, feed, pharma and biotech. FEMS Microbiology Letters, 366, 1–12.

[51] Ö.K. Ilıkkan, 2020. Laktik Asit Bakterilerinde CRISPR/Cas Sisteminin Biyoteknoloji ve Genetik Mühendisliğinde Kullanımı. *Akademik Gıda*, *18*(3), 303-311.

[52] G.L. Douglas, T.R. Klaenhammer, 2011. Directed chromosomal integration and expression of the reporter gene gusA3 in Laciobacillus acidophilus NCFM. Appl Environ Microbiol 77(20), 7365–7371. https://doi.org/10.1128/AEM.06028-11

[53] J.H. Oh, van J.P. Pijkeren, 2014. CRISPR-Cas9-assisted recombineering in Lactobacillus reuteri. Nucleic Acids Res 42(17), e131. https://doi.org/10.1093/nar/gku623

[54] P. Yang, J. Wang, Q. Qi, 2015. Prophage recombinases-mediated genome engineering in Lactobacillus plantarum. Microb Cell Fact 14(1), 154. https://doi.org/10.1186/s12934-015-0344-z

[55] W.M. Russell, T.R Klaenhammer, 2001. Efcient system for directed integration into the Lactobacillus acidophilus and Lactobacillus gasseri chromosomes via homologous recombination. Appl Environ Microbiol 67(9), 4361–4364. https://doi.org/10.1128/AEM.67.9.4361-4364.2001

[56] S. Datta, N. Costantino, X. Zhou, D.L. Court, 2008. Identifcation and analysis of recombineering functions from Gram-negative and Gram-positive bacteria and their phages. Proc Natl Acad Sci USA 105(5), 1626–1631. https://doi.org/10.1073/pnas.07090 89105

[57] B. Swingle, Z. Bao, E. Markel, A. Chambers, S. Cartinhour, 2010. Recombineering using RecTE from Pseudomonas syringae. Appl Environ Microbiol 76(5), 4960–4968. https://doi. org/10.1128/AEM.00911-10

[58] L.C. Thomason, J.A. Sawitzke, X. Li, N. Costantino, D.L. Court, 2014. Recombineering: genetic engineering in bacteria using homologous recombination. Curr Protoc Mol Biol. https://doi. org/10.1002/0471142727.mb0116s106

[59] J. Yin, H. Zhu, L. Xia, 2015. A new recombineering system for Photorhabdus and Xenorhabdus. Nucleic Acids Res 43(6), e36. https://doi.org/10.1093/nar/gku1336

[60] M. Jinek, K. Chylinski, I. Fonfara, M. Hauer, J.A. Doudna, E. Charpentier, 2012. A programmable dual-RNA-guided DNA endonuclease in adaptive bacterial immunity. Science 337(6096), 816– 821. https://doi.org/10.1126/science.1225829 45.

[61] J.A. Doudna and E. Charpentier, 2014. The new frontier of genome engineering with CRISPR-Cas9. Science 346(6213):1258096. https://doi.org/10.1126/science.1258096

[62] L. Guo, K. Xu, Z. Liu, C. Zhang, Y. Xin, Z. Zhang, 2015. Assembling the Streptococcus thermophilus clustered regularly interspaced short palindromic repeats (CRISPR) array for multiplex DNA targeting. Anal Biochem 478, 131–133. https://doi.org/10.1016/j. ab.2015.02.028

Microcontroller Based Automatic Watering System for Poultry or Indoor Ornamental Plants

M. Aksu

Kırşehir Ahi Evran Universty, Kırşehir, Turkey ORCID :0000-0001-8077-6383

Abstract

Automatic irrigation/humidification systems will provide savings as they will prevent both unnecessary water consumption and waste of manpower/time by automatically watering plants according to the humidity (water) rate in the environment where poultry/pets can drink water or ornamental plants. Thus, humidification/irrigation operations will be carried out automatically with the prepared system (depending on the humidity rate, at the desired time and amount) and according to the developed software. This study aims to use water resources in the most efficient way, maximize energy savings and prevent excessive or unnecessary irrigation. In this study, the data received from the humidity sensor / water level measurement sensor placed in the soil in the environment where the plant is located is processed in the microcontroller. According to this processed data, when irrigation is needed, the water pump / valve automatically works and replenishes the missing water in the watering can or the water needed by the plant in the soil. When the required water in the soil/container meets the need, the water pump/valve automatically turns off.

Keywords: Arduino uno, Microcontroller, Automatic watering, Poultry, Ornamental plants.

1. Introduction

As technology develops and advances, automation systems become a part of our lives and their facilitating effects on our lives increase day by day. The field of agriculture and animal husbandry also receives and must receive its share from the facilitating effects of these technological developments. Because agriculture and animal husbandry have an important place in human life. Biologically, the survival of the human species largely depends on these areas.

One of the most important factors in poultry farming, greenhouse cultivation and ornamental plants is irrigation/humidification. This process is done either manually by manpower or automatically using developing technologies.

One of the most important factors in achieving efficient results in both agriculture and animal husbandry is irrigation. It does not matter whether it is in poultry farming or livestock farming. Likewise, in agricultural areas, it does not matter whether there are large cultivated areas, greenhouses or small ornamental plants. Regular and homogeneous irrigation is required for the growing product/living being to be healthy and for economical irrigation. Regular and homogeneous irrigation can be easily done automatically with control elements and without manpower. These operations can be carried out on a small scale using microcontrollers such as Raspberry PI / Ardunio , or they can be prepared in medium and large scale projects.

2. Literature Review

There are many studies on subjects such as irrigation, air conditioning, humidity measurement and temperature measurement. However, there are not many studies in the literature on software-controlled greenhouse irrigation, ornamental plant irrigation, especially livestock and poultry irrigation with automatic systems.

In his study, Kırnak (2006) revealed that by measuring soil moisture with sensors, the problem of over- or insufficient irrigation can be solved with an automatic drip irrigation system in the right amount and at the right time.

Çakır et al. (2008) realized a remote controlled automatic irrigation system using PIC 16F877 microcontroller control circuit. The system irrigates manually or automatically remotely. In automatic irrigation, sensors compare the moisture value received from the soil with the moisture value needed by the plant and ensure that the plant is kept at the value it needs. In this way, the plant is provided with sufficient and homogeneous water that it needs. Thus, the system saves not only the amount of water by irrigating as needed, but also manpower and time because it works automatically.

In his study, Dukes (2003) achieved 50% water savings for the same type of products thanks to automatic control.

Öter et al. (2018) developed a PLC-controlled irrigation system that automatically irrigates according to ambient humidity and temperature values. In this way, they aimed to reduce irrigation errors and dependence on labor.

Pathak et al. (2017), in their prototype study, implemented an automatic irrigation system based on soil moisture measurements.

Millaa et al. (2006) designed an effective irrigation and erosion prevention system with a microprocessor-based infrared sensor. In addition, irrigation amount and times are recorded by the system and these data can be transferred to the computer for detailed analysis when necessary.

3. Material and Method
3.1. Microcontroller (Ardunio / Raspberry PI)

Arduino was used to take data from sensors in the soil or water container and perform the necessary control operations in line with this data. microcontroller was used. In the study, the Arduino device shown in Figure 1 was used for the automatic irrigation system. microcontroller was used. Arduino uno, Atmega328p microcontroller It has the chip. This microcontroller is equipped with digital and analog input/output (I/O) pins that can interact with other circuits. This microcontroller has 14 digital I/O pins (six PWM outputs), 6 analog I/O pins. Thanks to these pins, sensors, drivers, etc. can be controlled and data can be received from environmental components. It can be programmed on a computer using the Arduino IDE (integrated development environment) environment. Arduino UNO can be powered via USB or powered by an external battery. The ATmega328p on the controller comes programmed to boot without using external hardware.
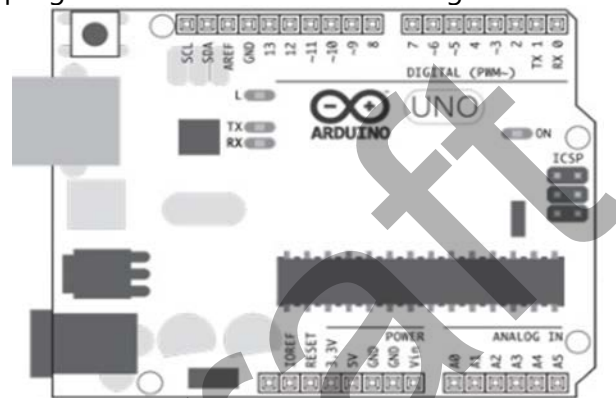
Figure 1. ArduinoUno controller used in the system

In this study, taking into account its cost and features, Arduno The Uno controller was decided to be suitable and used.

3.2. Sensors

Sensors are used to detect data or changes in the environment and transfer this information to other electronic devices. In the study, in addition to software, values such as soil moisture or water level in the container are needed in order to establish an automatic system. The only way to obtain information about these values is to measure the environment, and the measurement process is carried out through sensors. Sensors convert chemical, electrical or physical changes in the environment into measurable electrical signals. Data received through sensors are converted into electrical signals. These signals are then interpreted by electronic circuits and mechanical devices can be controlled. In this respect, sensors have an important place in our project. Arduino we use in our project The uno controller can take data from sensors as input and easily interpret it. Data from sensors that give analog output can be evaluated precisely by ArduinoUno.

3.2.1 Sensor Types

Sensors are the sensory organs of automatic systems, just like the sensory organs in humans. Automatic systems produce reactions according to the data they receive from sensors. In our study, sensors were used and the received data were processed and reactions were produced. In this context, a group of temperature / humidity / water level sensors (NTC, PTC, Rain Sensor ...) was used in the study. Sensors can be analog and digital. Data from analog sensors needs to be converted.

3.2.2. Soil Moisture Sensor and Water level measurement sensor

The sensor used in the study, shown in Figure 2 (a), which measures the moisture content of the soil, is buried in the soil. Soil moisture sensors are often integrated into other electronic devices such as microcontrollers or data acquisition systems. In this way, soil moisture data can be collected, processed and monitored. This information can be used for a variety of purposes, such as optimizing plant growing conditions, adjusting irrigation timing, and maintaining plant health. The system works automatically according to the moisture information obtained from the soil. The most important information required for the irrigation system is obtained by obtaining information about the moisture of the soil with the humidity sensor. The water level measurement sensor (Figure 2 (b)) is a sensor that we will measure depending on the decrease in the water level in a container.

a)   b)
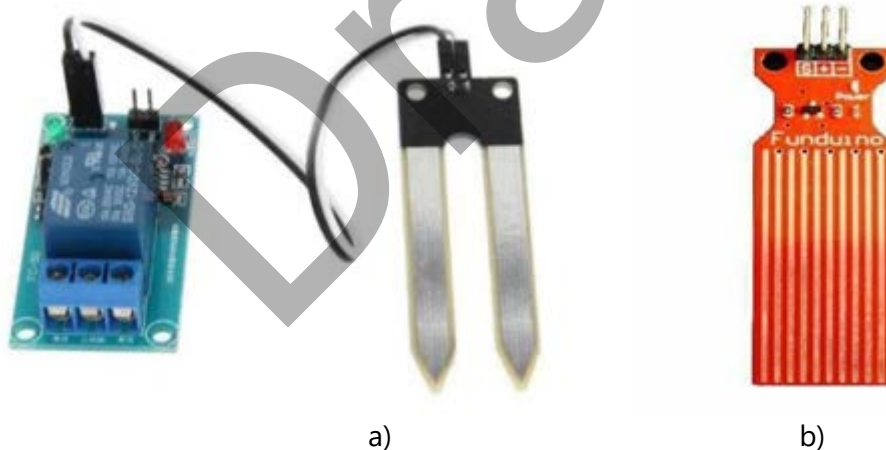
Figure 2. Humidity Sensor (a) and Water level measurement sensor (b)

3.3. Mini Water Pump and Driver card

Water pump is a motor used to transfer water to different locations. Viscous liquids such as water can be transferred up to 120 liters per hour with the water transfer motor (Figure 3), which operates silently and has very low power consumption.
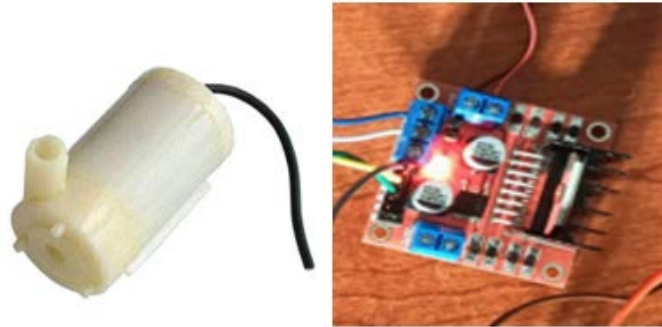
Figure 3. Mini Water Pump and Driver board

3.4. Automatic Watering System Circuit

In the automatic irrigation circuit (Figure 4), when the humidity value measured by the moisture meter exceeds a certain level, a signal is sent and the water pump starts to work. After the soil is irrigated, when the value measured by the moisture meter exceeds a certain moisture value, a signal is sent to the water pump again to stop and the water flow is cut off (Figure 5).

The water level measurement sensor is connected instead of the humidity sensor in the circuit in Figure 4, the water level in the water containers where pets, poultry or livestock meet their water needs is measured and when it decreases or runs out, the water pump/valve is activated and the missing water is automatically replenished.

Smart irrigation systems can be controlled remotely with the help of advanced digital technologies, and efficiency and resource use can be optimized with various smart irrigation sensors. Thanks to SIM card devices integrated into irrigation systems, irrigation system on-off operations can be easily controlled remotely via mobile devices. In addition, by accessing the control units of smart irrigation systems through applications that can be installed on mobile devices with various operating systems, many applications and parameters such as humidity monitoring, valve opening/closing and water monitoring can be controlled remotely.
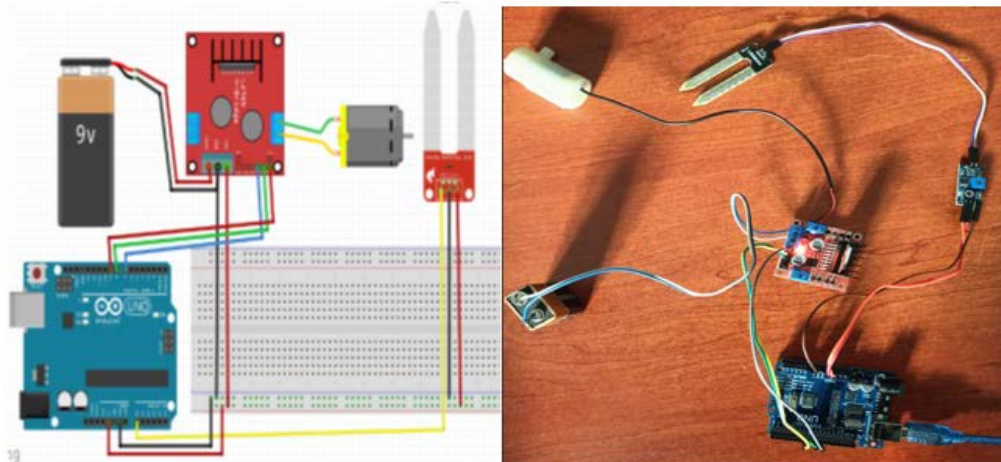
Figure 4. Automatic Irrigation System Circuit and Installed Circuit

Arduino Microcontroller coding was carried out in the Ardunio IDE environment. The system was previously established as a prototype in a virtual environment and the written codes were tested.

```
void loop() {
  veri=analogRead(sensor);
  Serial.println(veri);

if(veri>600)
{
  digitalWrite(motor,HIGH);
  delay(3000);
  digitalWrite(motor,LOW);
  delay(3000);
  veri=analogRead(sensor);
  if(veri>600){
    digitalWrite(motor,HIGH);
    delay(2000);
    digitalWrite(motor,LOW);
    delay(5000);
    }else {
      digitalWrite(motor,LOW);
      }
}else{
  digitalWrite(motor,LOW);
  }
}
```

Figure 5. Example of code block that operates the water engine according to the data from the sensor

4. Conclusions

Automatic irrigation systems will provide great benefits when used with the necessary transformations in the irrigation of livestock and large agricultural areas.

Additionally, this study is extremely important in terms of a sustainable environment and effective use of resources. Such studies save water by preventing unnecessary consumption of natural water resources and contribute to the sustainable use of water resources around the world.

Smart automatic irrigation solutions save water while increasing product efficiency by combining drip irrigation and automation systems by feeding the plant, not the soil. Drip irrigation systems deliver water directly to the root zone of the plant, maintaining optimum humidity levels, while offering balanced irrigation in integration with automation systems.

Smart automatic irrigation systems above and below ground reduce water losses such as evaporation, surface runoff and seepage deep into the soil. Irrigation process managed by automation units is carried out at the desired time or according to the water needs of the plant. Smart irrigation automation systems, which can be used in open field agriculture and greenhouse cultivation, save water and contribute to the efficient growth of the plant.

Especially in greenhouse irrigation automation, the irrigation algorithm must be created correctly by experts. Automating irrigation by automatically turning on and off water motors or valves is important for savings.

livestock farms, poultry farms and pet shops will save on factors such as manpower and water. Automated systems will create fewer errors than manual systems.

References

[1] A. Çakır, H. Çalış, 2007. Remote Controlled Automatic Irrigation System Design and Application. Suleyman Demirel Univ . Science. Inst. Journal, 11(3) (2007) 258-26

[2] D.M. Dukes, H.E. Simonne, E.W. Davis, D.W. Studstill, R. Hochmuth 2003. Effect of Sensor-Based High Frequency Irrigation on Bell Pepper Yield and Water Use. Proceedings 2nd International Conference on Irrigation and Drainage, Phoenix, AZ, May 12-15, (2003) 665-674.

[3] H. Kırnak, 2006. Automatıc Irrigatıon Based on Soil Moisture for Nursery Crops. V. GAP Müh. Kongresi, Harran Üni. Müh. Fak., 26-28 Nisan, (2006) 1540-1547, Şanlıurfa.

[4] A. Öter, M.Ş. Bahar, 2018. Programmable Controller Controlled Irrigation System. Kahramanmaraş Sütçü İmam Univ . Journal of Engineering Sciences, 21(4) (2018) 329-333.

[5] M. Pathak, R Pandya, S. Rudrawar, K.P. Agte, 2017. Automated Irrigation Using PLC Programming. International Conference on Ideas, Impact and Innovation in Mechanical Engineering (ICIIIME) 5(6): (2017) 696-700.

[6] K. Millaa, S. Kishb, 2006. A Low-cost Microprocessor and Infrared Sensor System for Automating Water Infiltration Measurements. Computers and Electronics in Agriculture, 53, (2006) 122-129.

The Impacts of Industrial Pollution on Environmental and Public Health: A Case Study on Heavy Metal Contamination in Altınoluk and Edremit

Z.Ü. Yümün[1], M. Önce[2], H. Ozen[3]

[1]Tekirdağ Namık Kemal University, Çorlu Faculty of Engineering, Department of Environmental Engineering, Tekirdağ, Türkiye. ORCID: 0000-0003-0658-0416
[2]Tekirdağ Namık Kemal University, Saray Vocational School, Department of Land Registry and Cadastre, Tekirdağ, Türkiye, ORCID: 0000-0001-9621-3630
[3]Topkapı Istanbul University Management and Information Systems, Istanbul, Turkiye. ORCID: 0009-0005-5594-621X

Abstract

This research investigates the presence and effects of industrial pollution, focusing on heavy metal and radiation contamination in the Altınoluk and Edremit regions. With the backdrop of the Industrial Revolution and continuous population growth, this study delves into the exacerbated dispersion of harmful chemical components into the environment, spotlighting the significant increase in heavy metal pollution. Utilizing Laser-Induced Breakdown Spectroscopy (LIBS), we assess the levels of heavy metal contamination, aiming to underscore the urgency of continuous monitoring and the implementation of mitigative strategies to protect public health and preserve environmental integrity. The LIBS method has increased its use in environmental analysis because it performs analysis quickly, on-site and with a small number of samples.

Keyword: LIBS, Altınoluk, Edremit, Heavy Metal, Radyoaktivite

Introduction

The advent of the Industrial Revolution marked a pivotal shift in human history, catalyzing rapid industrialization and unprecedented population growth. This progress, however, has been shadowed by the insidious spread of industrial pollution, including heavy metals and radioactive contaminants, into our natural environment. Elements that have existed since the earth's formation, like arsenic, lead, and mercury, are now increasingly dispersed at toxic levels, posing grave threats to health and environmental well-being.

Heavy metal and radioactivity pollution, especially accumulated in marine environments, harms the environment. Sediments are the repositories of marine environments. Non-biodegradable heavy metals and radionuclides that enter the marine environment

accumulate in the sediment. Non-degradable pollutants accumulated in sediments harm immobile or less mobile living things [1].

The encroachment of heavy metals and radioactive materials into ecosystems presents a complex array of toxicological, ecological, and health-related challenges. These contaminants, often byproducts of industrial processes, mining, and improper waste disposal, do not degrade over time. Instead, they persist in the environment, accumulating in soil, water, and living organisms, thereby magnifying their impacts through the food chain [1,2].

The infiltration of heavy metals and radioactive materials into the environment has manifold implications. Beyond the direct toxicological effects on human health, these pollutants disrupt biological systems, leading to biodiversity loss and compromised ecosystem services. The public health implications are profound, with increased risks of chronic diseases, developmental disorders, and cancer [3].

In recent years, new methods have begun to be used to detect pollution in marine environments. The LIBS method is a useful method that is fast, requires few samples, and offers on-site analysis. The LIBS method is used in many fields such as environment, health, food and forensic medicine.

Radioactivity is of two types: natural and artificial. Radioactive materials, on the other hand, emit radiation that can cause cellular and DNA damage in organisms. This not only affects the growth and health of plants and animals but also can lead to mutations that have far-reaching effects on biodiversity. The Chernobyl disaster of 1986, for example, resulted in a significant increase in genetic mutations and population declines in the surrounding wildlife [2,3].

The contamination of ecosystems with heavy metals and radioactive materials significantly contributes to biodiversity loss. Species that cannot tolerate the increased levels of pollution are either killed or forced to migrate, leading to altered community compositions and the potential extinction of local species. This loss of biodiversity undermines the resilience of ecosystems, diminishing their ability to provide essential services such as pollination, water purification, and climate regulation.

Addressing the challenges posed by heavy metal and radiation pollution necessitates a multifaceted approach. This includes the development and implementation of stricter environmental regulations, the adoption of cleaner and more sustainable industrial practices, and the promotion of public awareness and education on the risks of exposure. Furthermore, the continued advancement and application of analytical methods like LIBS are crucial for the timely detection and management of these environmental hazards.

Methodology

This study leverages the capabilities of Laser-Induced Breakdown Spectroscopy (LIBS), an analytical technique renowned for its rapid, on-site analysis with minimal sample

requirements. LIBS has emerged as a formidable tool in environmental monitoring, enabling precise detection and analysis of heavy metal pollutants across various matrices. Laser Induced Plasma Spectroscopy (LIBS) is a method of optical emission spectroscopy used for multiple analysis of elements. This method is able to make elemental analysis of all conductive and nonconductive substances. The optimum instrumental parameters for soil analysis have been obtained when repetition rate, td, and tw equaled 10 Hz, 1 µs, and 10 µs, respectively. Standard reference material (SRM-2586) has been used to prepare pellets for the parameter analysis [4,5,6].
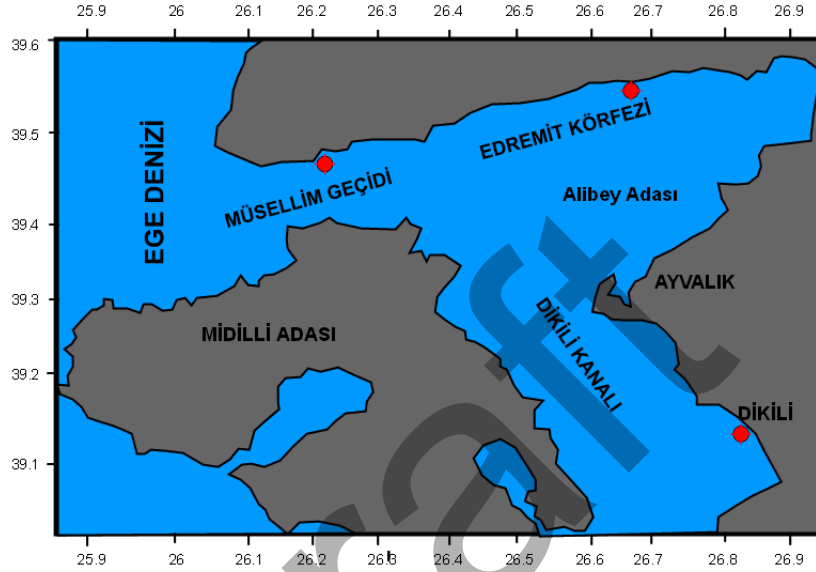
Figure 1. Work area location map

Sample preparation and Measurement: For elemental analysis, 25 g of samples were taken from each core from sediment samples. The sediment samples taken were placed in a specially made pellet container with 20-25 gr and compressed in the press machine under a pressure of about 100 bar for 5 seconds. This shape of the samples is called "pellet". Standard reference material (SRM-2586) was used to prepare pellets for the parameter analysis. The pelleted samples were placed in sealed bags and sent for LIBS analysis [1,7].

Gamma spectrometry analysis (Canberra GX5020) was used with an HPGe detector, which was joined to a coaxial high- purity germanium [5]. The setup was calibrated by using a solid, diverse gamma emitting reference sources in a 1 L Marinelli beaker. The sources were selected photo peaks for the full energy peak efficiency.

Results and Discussion

The application of LIBS in the Altınoluk and Edremit areas revealed concerning levels of heavy metal and radiation contamination. The findings not only corroborate the escalating threat of such pollutants on the ecosystem but also highlight the critical exposure levels in living organisms, including humans. The toxic and carcinogenic

properties of these contaminants, upon exceeding specific thresholds, underscore the dire need for comprehensive monitoring and evaluation mechanisms.

Table1. Libs analysis results

Sample No	A 1(%)	A 2(%)	A 3(%)	A 4(%)	A 5(%)	A 6(%)	A 7(%)
Ba	92	91	89	80	92	91	88
Li	90	91	88	89	89	91	88
Mg	89	88	86	86	87	90	88
O	88	87	85	89	90	87	88
Si	88	86	86	82	88	87	88
Ga	85	89	93	75	87	78	79
Rb	74	75	-	76	76	70	71
Al	74	73	73	72	73	85	84
Na	73	94	72	72	90	78	93
Sr	65	60	87	77	88	82	50
K	65	59	-	63	65	64	65
Ag	64	54	-	61	-	66	72
H	55	50	46	-	56	-	-
Fe	95	95	95	95	95	95	95
Ti	71	71	77	69	68	73	76
Ca	71	73	74	78	79	66	74
Be	-	-	72	-	46	64	50
N	-	-	63	68	68	71	69
Mn	-	-	49	-	-	-	-
F	-	-	-	57	-	-	-
Cl	-	-	-	-	-	-	-

Table 2. Radioactivity analysis results

Sample No	Radionüclide	Activity ± 2s (Bq/kg)	Measurable Lower (Bq/kg)	International Average Limit Values
A 1	K-40	555,2 ± 62,0	13.40	400
	Cs-137	5,4 ± 1,0	1.20	-
	Ra-226	32,6 ± 3,1	2.84	35
	Th-232	27,3 ± 2,9	2.25	30
A 2	K-40	542,3 ± 72,1	35.10	400
	Cs-137	2 ,0 ± 0,8	1.98	-
	Ra-226	20,6 ± 2,8	4.54	35
	Th-232	24,0 ± 3,1	3.18	30
A 3	**K-40**	**715,7 ± 79,6**	**19.80**	**400**
	Cs-137	< 2,0	1.98	-
	Ra-226	**48,6 ± 4,6**	**2.85**	**35**
	Th-232	**58,3 ± 5,5**	**1.95**	**30**

A 4	K-40	725,6 ± 111,3	46.30	400
	Cs-137	< 6,0	6.01	-
	Ra-226	47,4 ± 6,2	5.96	35
	Th-232	57,6 ± 7,2	7.14	30
A 5	K-40	443,7 ± 43,8	5.34	400
	Cs-137	1,8 ± 0,3	0.46	-
	Ra-226	16,9 ± 1,5	1.04	35
	Th-232	17,5 ± 1,6	0.89	30
A 6	**K-40**	**698,1 ± 83,7**	**18.40**	**400**
	Cs-137	3,9 ± 1,1	2.35	-
	Ra-226	**30,7 ± 3,4**	**3.68**	**35**
	Th-232	**37,0 ± 4,0**	**3.17**	**30**
A 7	K-40	510,3 ± 47,9	3.84	400
	Cs-137	20,4 ± 1,8	0.48	-
	Ra-226	20,8 ± 1,7	0.79	35
	Th-232	31,6 ± 2,5	0.62	30

Conclusion

The study illuminates the critical environmental and health impacts of heavy metal and radiation contamination, emphasizing the situation in Altınoluk and Edremit. The utilization of LIBS has proven instrumental in identifying and quantifying these pollutants, advocating for a sustained commitment to environmental monitoring and pollution mitigation. It is imperative that concerted efforts be made to reduce exposure to hazardous elements, safeguard public health, and ensure the preservation of our natural world for future generations.

References

[1] Z.Ü.Yümün, E. Kam, M. Önce, 2019. Analysis of toxic element with ICP-OES and Libs methods in marine sediments around the Sea of Marmara in Kapidağ Peninsula. Journal of Engineering Technology and Applied Sciences. 4(1) (2019) 43-50.

[2] Z.Ü. Yümün, E. Kam, A. R. Dinçer, M. Önce, S. Yümün, 2021. The investigation of toxic element pollution and radioactivity analyses of marine sediments in the Gulf of Gemlik (Bursa, Turkey). Applied ecology and environmental research. 19(2) (2021).

[3] E. Kam, M. Önce, Z.Ü. Yümün, 2020. Gamma Dose Values Of Stratıgraphıc Unıts Of Behramkale (Çanakkale)-Zeytinli (Edremit-Balıkesir) Sectıon Of Kaz Mountaıns. Journal of the Turkish Chemical Society, Section A: Chemistry. 7(1) (2020) 207-214.

[4] B. Çetin, F. Öner, I.Akkurt, 2016. Determination of Natural Radioactivity and Associated Radiological Hazard in Excavation Field in Turkey (Oluz Höyük), Acta Physica Polonıca. (2016) 130 (1) 475-478.

[5] A. Bozkurt, N. Yorulmaz, E. Kam, G. Karahan, A. E. Osmanlioglu, 2007. Assessment of Environmental Radioactivity for Sanliurfa Region of Southeastern Turkey. Radiation Measurements, 42 (8) (2007) 1387- 1391.

[6] D. Kurt, Z. U. Yümün, İ. F., Barut, E. Kam, 2016. Distribution of Gamma Radiation Levels in Core Sediment Samples in Gulf of Izmir: Eastern Aegean Sea. International Journal of Environmental, Chemical, Ecological,Geological and Geophysical Engineering. 10 (3) (2016).

[7] M. Önce, İ. Balnan, N. Kam, 2021. Determination of Heavy Metal Distribution of Yenikapı (Istanbul) Sea Sediments Using Libs Method. Journal of European Science and Technology, 22 (2021) 60-64.

Determination of Antioxidant Capacity, Anticholinergic Activity, and Phenolic Ingredients of Yellow Mustard (Sinapis alba), and Black Mustard (Brassica nigra) Extracts by LC-MS/MS

L. Polat Köse[1]

[1]Department of Pharmacy Services, Vocational School, Istanbul Beykent University, 34500, Istanbul, Turkey,
leylakose@beykent.edu.tr, ORCID: 0000-0001-5759-7889

Abstract

In the present work, it was aimed to evaluate water and ethanol extracts of the yellow mustard (*Sinapis alba*) and black mustard (*Brassica nigra*) seeds. Numerous bioanalytical methods were used to determine their antioxidant and radical scavenging capacity, total phenolic and flavonoid ingredients, and anticholinergic activity. In addition, the phenolic contents of each extracts were measured by LC-MS/MS analysis. The results obtained in the antioxidant studies were compared with reference standards. The reducing capability of yellow mustard (*Sinapis alba*) and black mustard (*Brassica nigra*) seeds extracts was evaluated using the cupric ion (Cu^{2+}), ferric ion (Fe^{3+}), and Fe^{3+}-TPTZ reducing methodologies. The half-maximal inhibition concentration (IC_{50}) values of *Sinapis alba* and *Brassica nigra* seeds extracts for 1,1-diphenyl-2-picryl-hydrazyl (DPPH•) free radical and 2,2´-azino-bis(3-ethylbenzthiazoline-6-sulfonic acid) (ABTS•+) cation radical removal activity was 1199.071-1798.606 µg/mL, and 786.639-1258.622 µg/mL, respectively. Besides, 28.823, 25.294, 20.588, and 12.353 µg of gallic acid equivalent of phenolic and 28.364, 24.909, 26.182, and 12.182 µg of quercetin equivalent of flavonoid contents were determined from 1 mg of *Sinapis alba* and *Brassica nigra* seeds water and ethanol extracts, respectively. For water and ethanol extracts of *Sinapis alba* and *Brassica nigra* seeds, IC_{50} values were calculated against acetylcholinesterase as 0.177 µg/mL, 0.185 µg/mL, 0.167 µg/mL, and 0.194 µg/mL, respectively. Thanks to they contain phytochemicals, extracts displayed substantial biological activity.

Keywords: Mustard, *Sinapis alba*, *Brassica nigra*, Antioxidant activity, Acetylcholinesterase

1. Introduction

Mustard is an annual plant belonging to the *Brassica* species, a member of the *Brassicaceae* family [1, 2]. The word mustard, which is the name of the plant, comes from the Latin word *Mustum ardens* because one of its metabolites that cause a sharp burning sensation is glucosinolates [3]. It is claimed that these glucosinolates, which are responsible for the sharp and bitter taste, also reduce the risk of cancer [4]. Although there are ten different species, the three most gastronomically preferred species are widely grown throughout the world. These are yellow or white mustard (*Sinapis alba*), black mustard (*Brassica nigra*), and eastern mustard (*Brassica juncea*) called as Indian

mustard [1]. Mustard seeds are grown in many regions around the world because they contain high amounts of edible oil. The leading countries in the production of this plant can be listed as India, Czech Republic, China, Bangladesh, Pakistan, Australia, Ukraine and some European countries [5]. Additionally, some mustard species grow in Turkey, too. Yellow mustard (*Sinapis alba*), wild mustard (*Sinapis arvensis*), Indian mustard (*Brassica juncea*) and black mustard (*Brassica nigra*) are among the species growing in the flora of Turkey [6]. The seeds of the mustard plant, which are of interest in gastronomy, are currently used in many areas, such as animal feed and biodiesel production [7]. It is reported that mustard seeds are beneficial in reducing the symptoms of rheumatoid arthritis, thanks to containing selenium and magnesium [8]. Mustard seeds are very effective in reducing migraine occurrence, thanks to their magnesium content, too [9, 10]. In general, mustard seeds or mustard are known to relieve respiratory congestion problems (). The mustard plant is mostly used as a spice in cooking. Whereas, mustard seed oil is used in alternative medicine thanks to its diuretic, appetite stimulant, stomach-soothing, expectorant, and waist and knee pain-relieving properties [11]. The natural resources provided by traditional medicine have always been the focus of attention since the synthetic drugs utilized in the therapeutic system given by modern medicine have many serious side effects in addition to their therapeutic effects [12]. On the other hand, unlike common product sources that are currently used only for therapeutic purposes in traditional medicine, cultivating natural resources that also serve spice, tea or aromatic purposes and using them more widely in daily life is also important for health [12, 13].

Herbs and spices with therapeutic effects have provided many benefits, such as treating diseases, providing mental relief, and providing taste and aroma for foods, from ancient times to the present. Today, spices and herbal sources are used to preserve food and beverages and extend their shelf life, thanks to their antimicrobial and antioxidant activities [14]. The important therapeutic properties of natural resources such as antioxidant and antimicrobial are due to their phytochemicals. Mustard contains phytochemicals such as glucosinolates and phenolic compounds [15]. For this reason, there is a need to prove the possible health potential of such medicinal and natural herb resources.

This study aimed to investigate the antioxidant, antiradical, and anticholinergic properties of water and ethanol extracts obtained from yellow mustard (*Sinapis alba*) and black mustard (*Brassica nigra*) seeds and determine their total phenolic and flavonoid contents. In addition, it was targeted to identify the phenolic substances responsible for the biological activities that the extracts may have by LC-MS/MS technique.

2. Materials and methods

2.1. *Chemicals*

All reagents and solvents used in the study were commercially obtained and used as purchased. Butylated hydroxyanisole (BHA), butylated hydroxytoluene (BHT), Trolox, and α-Tocopherol compounds, which are the reference standards used in antioxidant and radical scavenging studies, were commercially available. All extracts used in the study were prepared by grinding yellow mustard (*Sinapis alba*) and black mustard (*Brassica nigra*) seeds and mixing them in water and ethanol.

2.2. Preparation of extract solutions

2.2.1. Water extracts of Sinapis alba and Brassica nigra seeds

Ground *Sinapis alba* and *Brassica nigra* seeds were obtained by mixing separately in pure water at room temperature and in the dark overnight.

2.2.2. Ethanol extracts of Sinapis alba and Brassica nigra seeds

Ground *Sinapis alba* and *Brassica nigra* seeds were obtained by mixing separately in 96% ethanol at room temperature and in the dark overnight.

2.3. Preparation of standards and test solutions for LC-MS/MS

Both stock solutions used for standards and solutions used in calibration processes were prepared in the ethanol-water mixture at certain concentrations. Additionally, curcumin solution was used as internal standard. Details about the experiment have been reported in the previous papers [16-18]. Detailed information regarding the experimental parameters is served in Table 1A.

Table 1A. Validation and uncertainty parameters and LC-MS/MS parameters and of selected compounds

Compounds	Linear regression equation	r²	LOD (mg/L)	LOQ (mg/L)	RSD (%)	Parent ion	Daughter ion	Collision energy (V)
Gallic acid	y=(8.15E+15)x+(4.32E+14)	0.9848	0.002	0.008	4.85	168.6	124	13
Kaempferol	y=(8.11E+15)x+(4.07E+14)	0.9841	0.002	0.008	5.47	287	152.3	30
Fumaric acid	y=(2.02E+16)x+(6.21E+15)	0.9912	0.003	0.010	5.44	115	71	8
pyrogallol	y=(1.33E+15)x+(5.24E+15)	0.9803	0.001	0.002	5.47	125	80	16
p-OH benzoic acid	y=(4.35E+16)x+(9.83E+15)	0.9939	0.002	0.007	4.78	136.7	92.6	12
Vannilin	y=(3.47E+16)x+(5.62E+15)	0.9982	0.019	0.064	6.57	150.7	135.4	12
t-ferulic acid	y=(2.52E+15)x+(9.15E+15)	0.9822	0.047	0.158	5.21	193	133	15
Chlorogenic acid	y=(1.00E+17)x+(8.21E+15)	0.9894	0.445	1.483	5.45	353	191	14
Rosmarinic acid	y=(6.29E+16)x+(4.94E+15)	0.9933	0.022	0.072	3.73	359.2	160.5	15
Ursolic acid	y=(4.78E+14)x+(2.26E+15)	0.9861	0.008	0.027	0.30	455.6	455.1	10
Rutin	y=(7.72E+15)x+(8.79E+07)	0.9901	0.010	0.034	7.90	609	301	16
Curcumin*	-	-	-	-	-	369.0	177.0	20

* Used as internal standard.

2.5. Validation of experiments and uncertainty evaluation

Curcumin was used as the standard in the validation experiments performed for the compounds. Confirmation parameters for linearity, reproducibility, limit of detection (LOD), and limit of quantity (LOQ) tests were determined. The LC-MS/MS parameters of both secondary metabolites and internal standards are detailed in Tables 1A and B. r^2, the correlation coefficient, was ≥0.98. Linear regression equations for the respective compounds are given in Table 1A, where y represents the peak area and x represents the concentration. The stages related to the test were detailed in the previous study [18].

Table 1B. Amount (mg/kg) of secondary metabolites in extracts of yellow mustard (*Sinapis alba*) and black mustard (*Brassica nigra*) seeds.

Compounds	WESA	EESA	WEBN	EEBN
Gallic acid	-	4.53 ± 0.31	10.47 ± 0.73	-
Kaempferol	-	-	17.48 ± 1.23	-
Fumaric acid	224.73 ± 15.58	108.97 ± 7.56	204.95 ± 14.75	-
Pyrogallol	10.66 ± 0.71	-	94.92 ± 6.32	-
p-OH benzoic acid	14.71 ± 1.17	79.61 ± 6.33	421.93 ± 33.52	-
Vannilin	16.17 ± 1.48	85.17 ± 7.79	393.81 ± 36.02	-
t-ferulic acid	-	-	87.04 ± 6.08	-
Chlorogenic acid	6.8 ± 0.94	6.81 ± 0.94	-	6.79 ± 0.94
Rosmarinic acid	3.66 ± 0.28	3.93 ± 0.3	12.01 ± 0.92	3.74 ± 0.29
Ursolic acid	-	199.64 ± 13.86	-	189.53 ± 13.15
Rutin	1.74 ± 0.11	1.67 ± 0.11	10.78 ± 0.71	1.61 ± 0.11

2.6. Determination of biological activities

2.6.1. Fe^{3+} reducing assay

To determine the Fe^{3+} reduction ability of yellow mustard (*Sinapis alba*) and black mustard (*Brassica nigra*) seeds, the $Fe^{3+}(CN^-)_6$ to $Fe^{2+}(CN^-)_6$ reduction method was used. In this method, extracts of yellow mustard (*Sinapis alba*) and black mustard (*Brassica nigra*) seeds at different concentrations (10-30 µg/mL) were transferred to test tubes according to the procedure described in previous studies and incubated under the necessary conditions. Then, trichloroacetic acid (TCA) and 0.5 mL $FeCl_3$ were added respectively and the absorbance values at 700 nm were measured using spectrophotometer. The results obtained showed that the absorbance value increased as the reducing capacity increased [14].

2.6.2. Cupric ion (Cu^{2+}) reducing-CUPRAC assay

Cu^{2+} reduction method was used as the second reduction method for yellow mustard (*Sinapis alba*) and black mustard (*Brassica nigra*) seeds extracts. This reduction method was carried out with a slight modification of the CUPRAC method developed by Apak *et al* [19]. Test solutions prepared as in the previous study were transferred to test tubes containing yellow mustard (*Sinapis alba*) and black mustard (*Brassica nigra*) seeds extracts at specific concentrations (10-30 µg/mL) according to the described procedure [12]. Then, the volumes of the test tubes were completed to the required volume with distilled water and incubated for 30 minutes. Finally, the absorbance values of the samples were measured at 450 nm and reported [20].

2.6.3. FRAP assay

FRAP method was used as another reduction method for yellow mustard (*Sinapis alba*) and black mustard (*Brassica nigra*) seeds extracts. This method is based on the reduction of the Fe^{3+}-TPTZ complex in acidic environment. The preparations of all solutions used for the FRAP methodology were discussed in detail in the earlier paper [18]. In the experiment, TPTZ and HCl solutions were prepared freshly and mixed in certain proportions according to the procedure [12]. Then, acetate buffer and Fe^{3+} solutions were also prepared, respectively. Solutions were pipetted into test tubes containing various concentrations (10-30 µg/mL) of yellow mustard (*Sinapis alba*) and black mustard (*Brassica nigra*) seeds extracts as required, vortexed, and incubated at 37°C for 30 min. As a result, the color intensity of the Fe^{2+}-TPTZ complex formed in the medium was measured and recorded spectrophotometrically at 593 nm [14].

2.6.4. DPPH-free radical scavenging assay

In the DPPH-free radical scavenging experiment, the method developed by Blois was used [21]. For this purpose, firstly the DPPH free radical solution was freshly prepared. The radical solution preparation procedure has been described in detail in previous work [22]. Then, radical solutions (10-30 mg/mL) were added to the test tubes containing certain concentrations of yellow mustard (*Sinapis alba*) and black mustard (*Brassica nigra*) seeds extracts and quickly vortexed. After incubating in the dark for 30 minutes, the absorbance value at 517 nm was measured and recorded for each sample [23].

2.6.5. ABTS$^{\bullet+}$ cation scavenging assay

This assay was tested on yellow mustard (Sinapis alba) and black mustard (Brassica nigra) seeds extracts according to the radical scavenging method developed by Re *et al*. [24]. In this method, the radical solution was freshly prepared. For this, 7 mM ABTS solution was prepared. $K_2S_2O_8$ was slowly added to the mixture to oxidate and stirred overnight. Then, 0.25 mL of ABTS$^{\bullet+}$ cation radical solution and 96% ethanol were added to test tubes containing various concentrations (10-30 µg/mL) of yellow mustard (*Sinapis alba*) and black mustard (*Brassica nigra*) seeds extracts. Each test tube was vortexed vigorously and incubated in the dark for 30 min. Finally, their absorbance at 734 nm was measured and recorded. A parallel radical scavenging capacity was observed with increasing

concentrations of yellow mustard (*Sinapis alba*) and black mustard (*Brassica nigra*) seeds extracts.

The percentage of radicals scavenging was computed using the following equation:

$$RSE\ (\%) = [1-(As/Ac)] \times 100,$$

where RSE is radical removal effects, A_C is the absorbance value of the control, and A_S is the absorbance value of the sample [25].

2.6.6. *Determination of total phenolic compounds*

The Folin-Ciocalteu method was used to determine the total phenolic content of the extracts of yellow mustard (*Sinapis alba*) and black mustard (*Brassica nigra*) seeds, which are natural sources. The essence of this spectrophotometric method is that the Folin-Ciocalteu reagent interacts with the polyphenols in the test medium and forms a blue complex that absorbs at 760 nm [26]. The preparation of the solutions and reagents used in the method was described in detail in the previous study. For the test, the prepared reagents and solutions were added to the experimental containers containing extracts at certain concentrations in accordance with the procedure and shaken vigorously [12, 14]. Then, the test dishes were incubated for 30 minutes at 20-24°C in the dark, and absorbance values at 760 nm were measured and recorded. In order to make a comparison in this method, absorbance values were measured at various concentrations ranging from 0 to 300 μg using gallic acid, a standard phenolic compound. A calibration curve was created with the data obtained and the total phenolic compound amount of each extract was calculated using this curve.

2.6.7. *Determination of total flavonoids*

A colorimetric method was used for the determination of total flavonoids in extracts of yellow mustard (*Sinapis alba*) and black mustard (*Brassica nigra*) seeds [22]. The procedure of the method has been described in previous work. Extract solutions at different concentrations were taken into the test tube and 100 μL of potassium acetate (1.0 M), 100 μL of 10% $Al(NO_3)_3$, and 4.3 mL of ethanol were added respectively. Finally, the samples were incubated for half an hour at 20-24°C and absorbance values were measured and recorded using spectrophotometer at 415 nm. Quercetin was used as the standard for this method. The absorbance values of different concentrations of quercetin between 0 and 80 μg were measured and the standard graph was obtained. Results were evaluated as micrograms of quercetin equivalent per gram of extract [18, 27].

2.7. *Enzyme inhibition studies*

2.7.1. *Anticholinergic assay*

Acetylcholinesterase (AChE) enzyme is an enzyme that catalyzes the hydrolysis of acetylcholine, a neurotransmitter, and therefore has neurologically important functions. Decreasing or increasing activity of this enzyme causes serious neurological diseases. It has a very important role in the symptoms of diseases such as Alzheimer's or Parkinson's. Studies on cholinergic or anticholinergic activity are of interest in order to benefit the symptomatic treatment of such neurological diseases [28-30]. For this purpose, in this part

of the study, AChE activity tests were performed to determine whether yellow mustard (*Sinapis alba*) and black mustard (*Brassica nigra*) seeds extracts had sympathetic or parasympathetic effects. For these tests, the method developed by Ellman et al., was used [31]. Acetylthiocholine iodide (AChI) solution, which is the substrate of AChE, and 5,5'-dithiobis (2-nitrobenzoic acid) (DTNB) solution, which provides the formation of the colored complex, were used as reagents in the procedure [32]. AChE was interacted with different concentrations of extracts in the test medium to determine the effects of yellow mustard (*Sinapis alba*) and black mustard (*Brassica nigra*) seeds extracts against this enzyme. Then, absorbance values were measured spectrophotometrically at 412 nm and recorded. With the data obtained, a graph of activity (%) and concentration of each mustard seeds extracts were created. Finally, the IC_{50} values were calculated from this graph.

2.7.3. *Determination of inhibition parameters*

IC_{50} values were calculated from activity-concentration graphs obtained from inhibition studies of ethanol and water extracts of yellow mustard (*Sinapis alba*) and black mustard (*Brassica nigra*) seeds.

2.8. *Statistical analysis*

Antioxidant assays studies were carried out by repeating 3 times. The data obtained were reported as mean ± standard deviation and analyzed by SPSS (version 11.5 for Windows 2000, SPSS Inc.). One-way analysis of variance (ANOVA) was applied. Significant distinctions between means were identified by Duncan's multiple range tests, and $p < 0.05$ was seen as significant and $p < 0.01$ as highly significant.

3. Results

Mustard is a very well-known plant globally. It attracts a lot of attention among the public because it gives flavor to foods and has known therapeutic activities. Here, the metal reduction, radical scavenging and AChE inhibition activities of yellow mustard (*Sinapis alba*) and black mustard (*Brassica nigra*) seeds were analyzed and determined. Additionally, total phenolic and total flavonoid contents of each extract were investigated. Furthermore, some phenolic contents that allow it to display bioactive properties were also elucidated using the LC-MS/MS technique. Within the scope of the study, methods applied in the literature were used [18].

### 3.1. *Reducing and radical scavenging assays*

Within the scope of the study, specific bioanalytical methods were used to determine the metal reducing and radical scavenging capacities of yellow mustard (*Sinapis alba*) and black mustard (*Brassica nigra*) seeds extracts [18, 33, 34].

As metal reduction and radical removal methods; Fe^{3+} reduction, Cu^{2+} reduction (CUPRAC method), FRAP, DPPH-free radical scavenging and $ABTS^{•+}$ cation radical scavenging methods were used and evaluated. Tests were performed in 3 repeats at concentrations of 10, 20 and 30 μg/mL of yellow mustard (*Sinapis alba*) and black mustard (*Brassica nigra*) seeds extracts. The results obtained with increasing concentration of the extracts showed a proportional correlation. BHA, BHT, Trolox and *α*-

Tocopherol compounds were used as standards for comparison in all metal reduction and radical scavenging studies. The results were remarkably reasonable. The Fe^{3+}-Fe^{2+} reducing power of 30 µg/mL concentration of standards and yellow mustard (*Sinapis alba*) and black mustard (*Brassica nigra*) seeds extracts was in the following order: BHA (2.095; r^2: 0.9561) > BHT (1.428; r^2: 0.8780) > Trolox (1.204; r^2: 0.9202) > α-Tocopherol (0.938; r^2: 0.9700) > WESA (0.301; r^2: 0.8837) > WEBN (0.251; r^2: 0.9007) > EEBN (0.234; r^2: 0.8266) > EESA (0.231; r^2: 0.7804). In the CUPRAC method, Cu^{2+} reducing power of the yellow mustard (*Sinapis alba*) and black mustard (*Brassica nigra*) seeds extracts and positive controls at the same concentration (30 µg/mL) were in the orderly: BHA (2.762; r^2: 0.9629) > BHT (1.753; r^2: 0.9005) > Trolox (1.567; r^2: 0.9855) > α-Tocopherol (0.992; r^2: 0.9768) > EEBN (0.416; r^2: 0.8424) > EESA (0.397; r^2: 0.8064) > WESA (0.325; r^2: 0.6726) > WEBN (0.289; r^2: 0.6300).

The FRAP method is a method that works similarly with the Fe^{3+} and Cu^{2+} reduction methods. The principle of the method is based on the increase in color intensity with increasing concentrations of antioxidant molecules added to the test medium. In the method, a dark complex with maximum absorbance at 593 nm is formed between the reduced Fe^{2+} ions and TPTZ. As the reducing power of antioxidant molecules increases, the amount of the complex formed and accordingly the absorbance value at 593 nm increases. The Fe^{3+}-TPTZ-Fe^{2+}-TPTZ reduction powers of yellow mustard (*Sinapis alba*) and black mustard (*Brassica nigra*) seeds extracts and the standards at the same concentrations are; BHA (2.944; r^2: 0.8113) > BHT (1.972; r^2: 0.8394) > α-Tocopherol (1.781; r^2: 0.9573) > Trolox (1.642; r^2: 0.9030) >EEBN (0.566; r^2: 0.6966) > EESA (0.520; r^2: 0.5753) > WESA (0.514; r^2: 0.5785) > WEBN (0.480; r^2: 0.5041). All reducing results are reported Table 2 and Figure 1 A, B, C.

In all three metal reduction methods, there was a similarity between the reducing powers of yellow mustard (*Sinapis alba*) and black mustard (*Brassica nigra*) seeds extracts. Moreover, in all reducing methods, all extracts exhibited similar reducing properties. These bioanalytical techniques are frequently used in these kinds of investigations due to their ease of use, affordability, and fast applicability [14, 19].
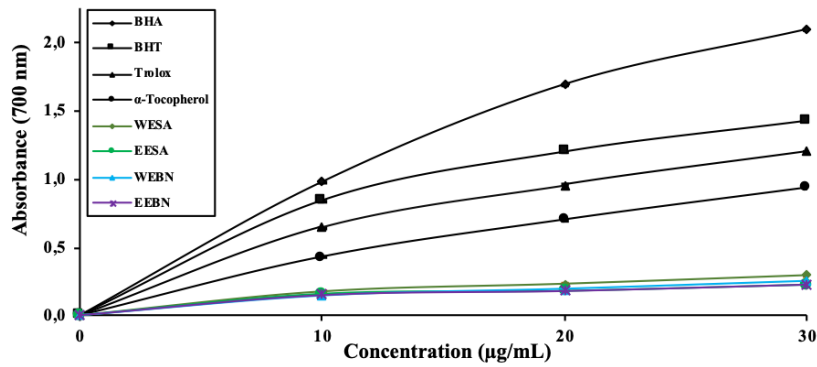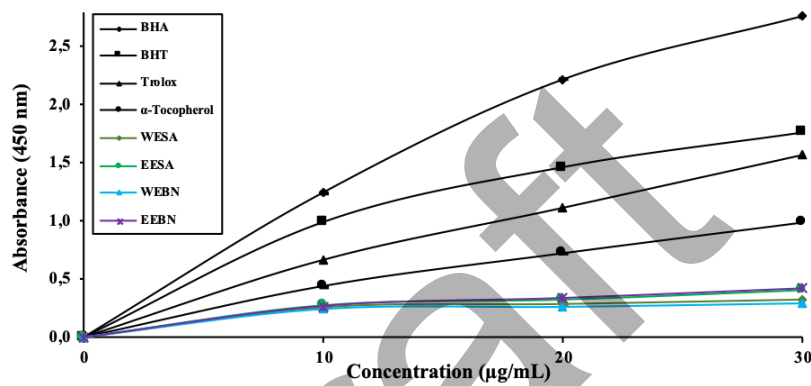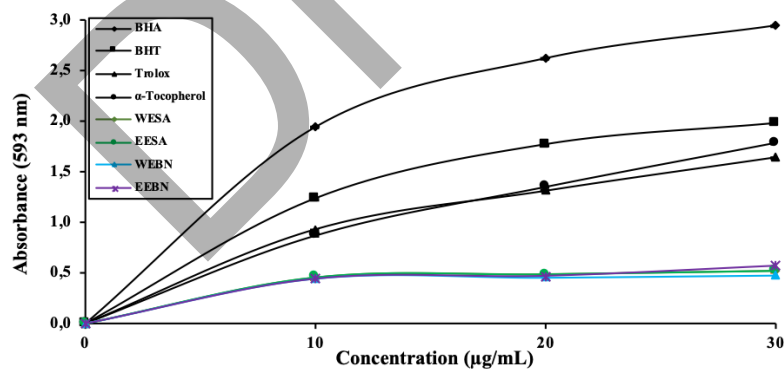
Figure 1. A, $Fe^{3+} \rightarrow Fe^{2+}$ reductive potential of different concentrations (10-30 µg/mL) of *Sinapis alba* and *Brassica nigra* seeds extracts and reference antioxidants. **B**, Cupric ions-Cu^{2+} reducing ability of different concentrations (10-30 µg/mL) of *Sinapis alba* and *Brassica nigra* seeds extracts and reference antioxidants. **C**, Fe^{3+}-TPTZ-Fe^{2+}-TPTZ reducing ability of different concentrations (10-30 µg/mL) of *Sinapis alba* and *Brassica nigra* seeds extracts and reference antioxidants [Butylated hydroxyanisole (BHA), Butylated hydroxytoluene (BHT), Trolox, α-Tocopherol, water extract of *Sinapis alba* (WESA), ethanol extract of *Sinapis alba* (EESA), water extract *Brassica nigra* (WEBN), and ethanol extract of *Brassica nigra* (EEBN)].

Table 2. Determination of reducing power by potassium ferric ion reduction, CUPRAC and FRAP methods of *Sinapis alba* and *Brassica nigra* seeds [water extract of *Sinapis alba* (WESA), ethanol extract of *Sinapis alba* (EESA), water extract *Brassica nigra* (WEBN), and ethanol extract of *Brassica nigra* (EEBN)] extracts.

Antioxidants	Fe^{3+}-Fe^{2+} reducing[a]		Cu^{2+}-Cu^+ reducing[a]		Fe^{3+}-TPTZ reducing[a]	
	λ_{700}	r^2	λ_{450}	r^2	λ_{593}	r^2
BHA	2.095 ± 0.004	0.9561	2.762 ± 0.002	0.9629	2.944 ± 0.002	0.8113
BHT	1.428 ± 0.003	0.8780	1.753 ± 0.002	0.9005	1.972 ± 0.002	0.8394
Trolox	1.204 ± 0.003	0.9202	1.567 ± 0.002	0.9855	1.642 ± 0.003	0.9030
α-Tocopherol	0.938 ± 0.002	0.9700	0.992 ± 0.002	0.9768	1.781 ± 0.003	0.9573
WESA	0.301 ± 0.003	0.8837	0.325 ± 0.004	0.6726	0.514 ± 0.003	0.5785
EESA	0.231 ± 0.003	0.7804	0.397 ± 0.003	0.8064	0.520 ± 0.004	0.5753
WEBN	0.251 ± 0.003	0.9007	0.289 ± 0.003	0.6300	0.480 ± 0.003	0.5041
EEBN	0.234 ± 0.002	0.8266	0.416 ± 0.002	0.8424	0.566 ± 0.004	0.6966

[a] expressed as absorbance values.

As well as synthetic molecules, the antioxidant properties of many pharmacological herbal sources, which are natural antioxidant sources and have been used from past to present, can be easily determined by such applicable methods [35].

Many radical scavenging methods are used to determine the antiradical properties of natural or synthetic sources. In this study, DPPH• free radical and ABTS•+ cation radical scavenging methods were used to determine the antiradical capacities of yellow mustard (*Sinapis alba*) and black mustard (*Brassica nigra*) seeds extracts. In both methods, radical solutions were prepared night before.

For the DPPH• free radical, non-radical 2,2-diphenyl-1-picrylhydrazyl (DPPH) was mixed with ethyl alcohol and a radical solution was formed [18, 34].

Increasing concentrations of yellow mustard (*Sinapis alba*) and black mustard (*Brassica nigra*) seeds extracts and standard antioxidant solutions were added to equal amounts of radical solutions in test tubes. Here, as the concentrations of the added antioxidant solutions increase, the intensity of the dark purple color of the radical solution decreases. This is due to the increase in electrons transferred to radicals as the amount of added antioxidant solutions increases [18]. The absorbance values of this method were measured at 517 nm.

Table 3 shows the radical scavenging (p<0.01) of standard antioxidants BHA, BHT, Trolox and α-Tocopherol, as well as yellow mustard (*Sinapis alba*) and black mustard (*Brassica nigra*) seeds extracts, in the certain concentration of DPPH• free radicals. As a result of the evaluation, the IC_{50} values obtained for each standard molecule and extract are 1199.071 µg/mL (r^2: 0.9151) for WESA, 1284.719 µg/mL (r^2: 0.8612) for EESA, 1712.958 µg/mL for

EEBN. (r^2: 0.8231), 1798.606 µg/mL for WEBN. (r^2: 0.8038), 45.534 µg/mL (r^2) (0.9313) for BHA, 58.020 µg/mL (r^2: 0.9803) for Trolox, 81.755 µg/mL (r^2: 0.9593) for BHT, and 87.737 µg/mL (r^2: 0 .9914) for α-Tocopherol. The order of DPPH$^•$ free radical scavenging activity was as follows: BHA > Trolox > BHT > α-Tocopherol > WESA > EESA > EEBN > WEBN. The low IC_{50} values calculated from the graphs obtained from the measurements indicate that the antioxidant solutions have a high radical scavenging capacity [22].

The second method applied to determine the radical scavenging activity of yellow mustard (*Sinapis alba*) and black mustard (*Brassica nigra*) seeds extracts was the ABTS$^{•+}$ cation radical scavenging activity. As a result of the procedures applied according to the procedure, it is seen that the extracts of yellow mustard (*Sinapis alba*) and black mustard (*Brassica nigra*) seeds have a significant ABTS$^{•+}$ cation radical scavenging capacity in parallel with the increase in their concentrations (Table 3 and Figure 2 A, B). It was determined that there was a significant decrease in ABTS$^{•+}$ (p<0.01) cation radical concentrations by adding yellow mustard (*Sinapis alba*) and black mustard (*Brassica nigra*) seeds extracts to the medium at different concentrations (10-30 µg/mL). IC_{50} values for each extract were 786.639 µg/mL (r^2: 0.8641) for WESA, 983.298 µg/mL (r^2: 0.8410) for WEBN, 1048.852 µg/mL (r^2: 0.8326) for EESA, and 1258.622 µg/mL (r^2: 0.8779) for EEBN. Additionally, IC_{50} values for BHA, BHT, Trolox, and α-Tocopherol were 19.423 µg/mL (r^2: 0.7720), 21.552 µg/mL (r^2: 0.8091), 31.154 µg/mL (r^2: 0.8871), and 73.176 µg/mL (r^2: 0.9161), respectively. The ABTS$^{•+}$ radical scavenging activity of yellow mustard (*Sinapis alba*) and black mustard (*Brassica nigra*) seeds extracts and standard antioxidant molecules was in the order: BHA > BHT > Trolox > α-Tocopherol > WESA > WEBN > EESA > EEBN.

Among the methods commonly used to elucidate antioxidant activities, DPPH$^•$ free radical and ABTS$^{•+}$ cation radical scavenging methods are very important determiners. Moreover, since these methods are mechanistically the same, the results obtained from the studies are expected to be similar [27]. In the study, ABTS$^{•+}$ cation radical solution should be prepared fresh. For this purpose, $K_2S_2O_8$ is added to the ABTS solution, which has an oxidant effect and accelerates the formation of the ABTS$^{•+}$ cation radical. As a result, an intense dark blue/green radical solution is obtained [32]. This color of the solution shows absorbance at 734 nm [18].

The results obtained from the applied reduction and radical scavenging experiments are presented in Tables 2 and 3, respectively.

Two mechanisms are proposed in the literature to explain the elimination of radicals. The first of them is based on single electron transfer (SET) and the other is based on hydrogen atom transfer (HAT) [36, 37].

In SET mechanism, a single electron from the antioxidant molecule is transferred to the radical during the removal of radicals. Thus, in a reaction based on the SET mechanism, the radical concentration decreases as the concentration of antioxidant molecules added to the medium increases. As a result, the color of the reducing radical solution changes [19, 37, 38].

In HAT mechanism, the radical scavenging effectiveness of antioxidants depends on their ability to donate hydrogen atoms. If a radical scavenging reaction is to operate via the

HAT mechanism, it proceeds very quickly as it occurs independently of both the solvent system and the pH of the environment. Mechanistically, reactions proceeding with SET occur more slowly [32, 39].

Within the scope of this study, CUPRAC, FRAP, Fe^{3+} reduction and DPPH$^•$ free radical scavenging reactions, which are among the methods used to determine the antioxidant activity of extracts, operate with the SET principle, but the ABTS$^{•+}$ cation radical scavenging test operates with both the SET and HAT principles.
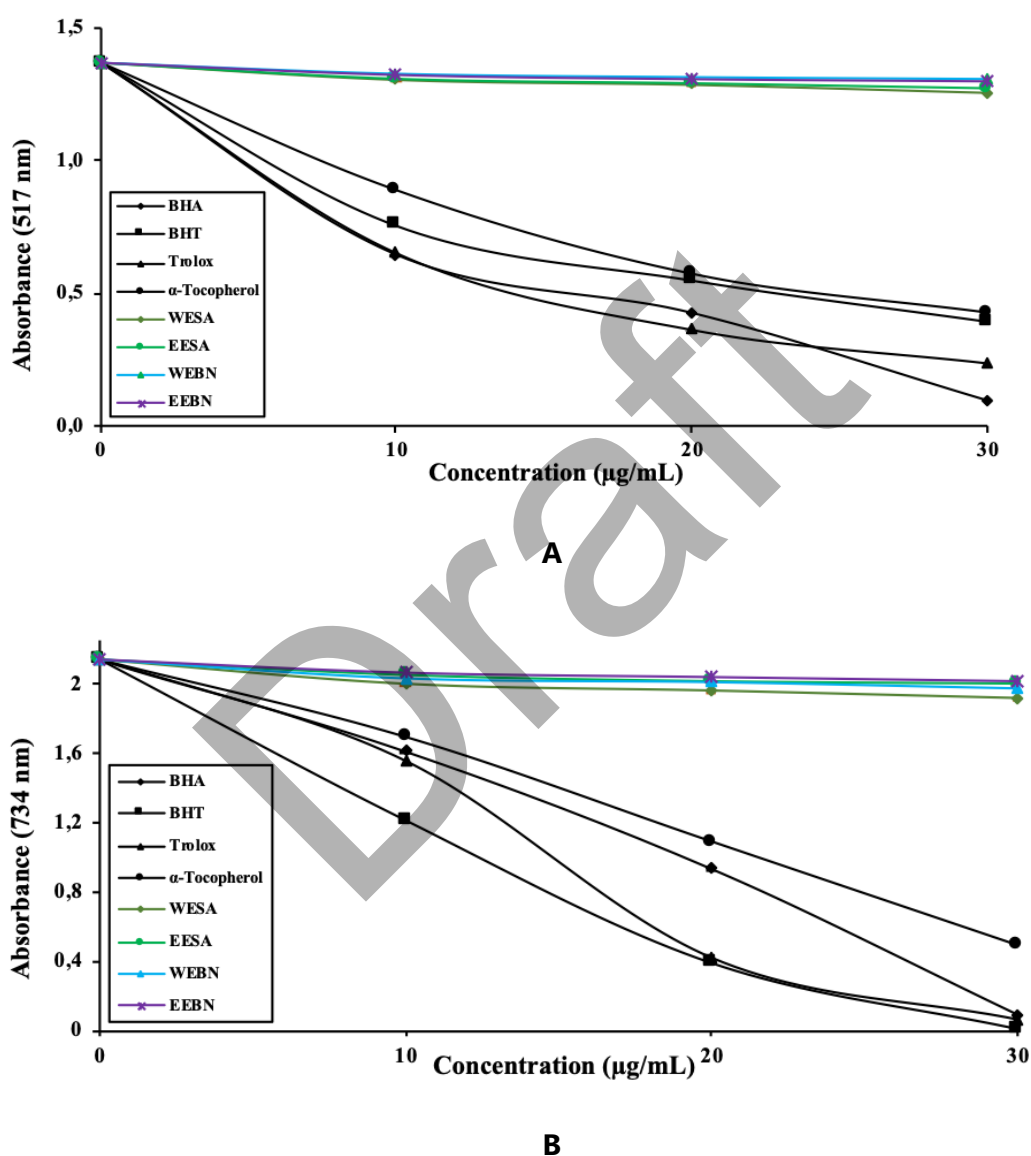
Figure 2. **A**, DPPH$^•$ free radical scavenging activity of different concentrations (10-30 µg/mL) of *Sinapis alba* and *Brassica nigra* seeds extracts and reference antioxidants. **B**, ABTS$^{•+}$ radical scavenging activity of different concentrations (10-30 µg/mL) of *Sinapis alba* and *Brassica nigra* seeds extracts and standard antioxidant compounds [Butylated hydroxyanisole (BHA), Butylated hydroxytoluene (BHT), Trolox, α-Tocopherol, water extract of *Sinapis alba* (WESA), ethanol extract of *Sinapis alba* (EESA), water extract *Brassica nigra* (WEBN), and ethanol extract of *Brassica nigra* (EEBN)].

Table 3. Determination of half maximal concentrations (IC_{50}) of standard radical scavenger, DPPH• and ABTS•+, scavenging and AChE inhibition assays in water extract of *Sinapis alba* seed (WESA), ethanol extract of *Sinapis alba* seed (EESA), water extract of *Brassica nigra* seed (WEBN), and ethanol extract of *Brassica nigra* seed (EEBN).

Antioxidants	DPPH• scavenging		ABTS•+ scavenging		AChE inhibition
	IC_{50} (µg/mL)	r^2	IC_{50} (µg/mL)	r^2	IC_{50} (µg/mL)
BHA	45.534	0.9313	19.423	0.7720	-
BHT	81.755	0.9637	21.552	0.8091	-
Trolox	58.020	0.9803	31.154	0.8871	-
α-Tocopherol	87.737	0.9914	73.176	0.9161	-
WESA	1199.071	0.9151	786.639	0.8641	0.177
EESA	1284.719	0.8612	1048.852	0.8326	0.185
WEBN	1798.606	0.8038	983.298	0.8410	0.167
EEBN	1712.958	0.8231	1258.622	0.8779	0.194
Tacrine*	-	-	-	-	0.044

*Tacrine was used as a standard inhibitor for AChE enzyme and its concentration mmol/L.

3.2. *Determination of total phenolic and flavonoid content assays*

Phytochemicals are naturally occurring substances that are used as remedies for diseases and as a means of preventing many other diseases. This group of molecules is beneficial in the prevention and healing process of many diseases that are common around the world. Flavonoids exhibit especially anticancer, cholesterol-lowering and blood lipid levels-lowering effects [14, 18]. Bioactive natural resources, which attracted attention through trial and error in the past, are now preferred more consciously.

Nowadays, polyphenolic compounds are in the class of antioxidants with very high bioavailability. Thanks to these pharmacological activities, sources of polyphenolic compounds attract a lot of attention [22].

The total phenolic contents of yellow mustard (*Sinapis alba*) and black mustard (*Brassica nigra*) seed extracts were determined. In the application of the method, a commercially available Folin-Ciocalteu reagent was used. First, a standard graph was prepared using gallic acid solution (r^2: 0.9907). Total phenolic contents of all extract samples were calculated as gallic acid equivalent per mg extract (GAE mg^{-1} extract) using this calibration curve [12]. Phenolic content of 28.823, 25.294, 20.588, and 12.353 µg GAE was calculated from 1 mg WESA, EESA, WEBN, and EEBN, respectively.

To determine the total flavonoid content of yellow mustard (*Sinapis alba*) and black mustard (*Brassica nigra*) seeds extracts, a standard graph was first obtained. For this, different concentrations of quercetin solution were used and a standard graph (r^2: 0.9988) was obtained. The total flavonoid content of yellow mustard (*Sinapis alba*) and

black mustard (*Brassica nigra*) seeds extracts was calculated as quercetin equivalent per 1 mg extract (QE mg^{-1} extract) using the equation calculated from this graph [12]. The results showed that they had flavonoid contents of 28.364, 24.909, 26.182, and 12.182 µg of QE from 1 mg of WESA, EESA, WEBN, and EEBN, respectively.

3.3. *Enzyme inhibition assays*

Studies of natural products with therapeutic properties through enzyme inhibition are extremely important from a pharmacological perspective. Because synthetic products designed and synthesized as medicines have serious side effects in addition to their therapeutic effectiveness. Additionally, if a drug is to be designed, having the drug-active ingredient be natural can minimize possible side effects. Today, the majority of drugs used for therapeutic purposes provide symptomatic treatment by affecting the activities of enzymes. This is especially valuable in terms of improving the quality of life of individuals with diseases such as Alzheimer's or Parkinson's, which are neurodegenerative diseases that do not have a radical treatment [40, 41]. For this, it is essential to prove the pharmacological activities of natural resources that will increase the quality of life [14, 18].

Both Alzheimer's and Parkinson's, which are types of dementia, are diseases that progress so insidiously that the symptoms that characterize the disease are noticed in the last stage of the disease. This process takes approximately 15-20 years [42, 43]. Until the final stage of the disease is reached, memory loss and behavioral disorders occur, which are expressed as irreversible and degenerative conditions in the brain [28]. Today, many people are trying to cope with this type of neurodegenerative diseases in the world. Moreover, it is predicted that the current number will increase several times in the coming years. According to the data obtained from many studies, it is stated that ROS (Reactive Oxygen Species) species, which are both exposed to individuals and stress-based, are associated with emerging dementias [18]. This being the case, it is of great importance that either synthetic molecules or natural sources to contain phytochemical, have cholinergic activity as well as antioxidant properties.

The findings regarding AChE inhibition of yellow mustard (*Sinapis alba*) and black mustard (*Brassica nigra*) seeds extracts were graphed and the IC$_{50}$ values calculated from this graph were tabled. The IC$_{50}$ values obtained for the extracts of both seeds were 0.177 µg/mL for WESA, 0.185 µg/mL for EESA, 0.167 µg/mL for WEBN, and 0.194 µg/mL for EEBN, respectively. Additionally, the measured IC$_{50}$ value for tacrine, used as a standard inhibitor of AChE, was 0.044 mmol/L. The IC$_{50}$ values obtained as a result of the studies are reasonable for the AChE inhibition. Looking at the results in Table 3, yellow mustard (*Sinapis alba*) and black mustard (*Brassica nigra*) seeds extracts appear to have a significant anticholinergic activity. It was determined that the relatively best inhibition result obtained belonged to WEBN and WESA extracts. Table 3 shows all the results. Linearity correlation coefficients (r^2) in the AChE inhibition study were determined to be >0.98. Herbal sources, which are frequently used in traditional treatment methods, have always been of interest because they safely show protective or therapeutic effects on metabolic enzymes [18].

4. Conclusion

In this study, the antioxidant, antiradical, and anticholinergic properties of yellow mustard (*Sinapis alba*) and black mustard (*Brassica nigra*) seeds extracts were investigated. For this, extracts were obtained by treating yellow mustard (*Sinapis alba*) and black mustard (*Brassica nigra*) seeds with water and 96% ethanol separately. All extracts were tested in antioxidant, radical scavenging and AChE enzyme inhibition assays with different bioanalytical methods. In addition, total phenolic and total flavonoid tests were applied to quantitatively determine some phytochemicals in its content. At last, the phenolic contents of each extract were determined using the LC-MS/MS technique. Generaly, WESA, EESA and WEBN exhibited better activity results than EEBN because it contained similar phenolic compounds in terms of both diversity and quantity. Yellow mustard (*Sinapis alba*) and black mustard (*Brassica nigra*) seeds extracts, which show a reasonable level of natural antioxidant activity, are currently used in areas such as gastronomy, therapeutic purposes, and animal feed support. In this study, more detailed and precise information were presented with proven data. Thanks to the data obtained, the potential effects of such natural resources were revealed. On account of, it is predicted that it will shed light on both more conscious implementation of traditional medicine practices and the design of natural product analogue drugs.

References

[1] M. Rahman, A. Khatun, L. Liu, B. J. Barkla, 2018. Brassicaceae Mustards: Traditional and Agronomic Uses in Australia and New Zealand, Molecules, 23 (2018).

[2] B. Sawicka, K. Ewa, 2007. Gorczyce jako rośliny wielofunkcyjne, Acta Scientiarum Polonorum, Technologia Alimentaria, 6 (2007) 17-27.

[3] P. Avato, M. P. Argentieri, 2015. Brassicaceae: a rich source of health improving phytochemicals, Phytochemistry Reviews, 14 (2015) 1019-1033.

[4] Y. Zhang, T. W. Kensler, C. G. Cho, G. H. Posner, P. Talalay, 1994. Anticarcinogenic activities of sulforaphane and structurally related synthetic norbornyl isothiocyanates, Proc Natl Acad Sci U S A, 91 (1994) 3147-3150.

[5] S. Choudhury, P. Asrani, A. Kashyap, M. Rao, L. Prasad, U. Pant, A. Gupta, R. Bhattacharya, G. Bhattacharya, 2023. Whole genome resequencing of advanced introgression lines of Brassica juncea L. Czern. for characterizing alien introgression from Diplotaxis erucoides L. DC, Indian Journal of Genetics and Plant Breeding, 83 (2023) 217-223.

[6] A. Guner, Aslan, S., Ekim, T., Vural, M., & Babac, M.T., *Turkey plant list (Vascular Plants)*. Istanbul: Nezahat Gökyiğit Botanical Garden and Flora Research Association Publication, 2012.

[7] P. Terpinc, B. Čeh, N. P. Ulrih, H. Abramovič, 2012. Studies of the correlation between antioxidant properties and the total phenolic content of different oil cake extracts, Industrial Crops and Products, 39 (2012) 210-217.

[8] R. Puthiyedath, R. Pushpan, S. Rohini, 2009. Mustard and its uses in Ayurveda, Indian Journal of Traditional Knowledge, 8 (2009) 400-404.

[9] Y. Sabah Abdulameer, H. Hamzah Ajeel, Z. Bakir Al-Hilli, 2021. Effects of Supplementation of Brassica Juncea Seed Extract in Drinking Water on Intestinal

Histomorphometry, Bacteriology, and Serum Biochemistry Parameters of Broiler Chicken, Arch Razi Inst, 76 (2021) 925-934.

[10] A. Mauskop, B. M. Altura, 1998. Role of magnesium in the pathogenesis and treatment of migraines, Clin Neurosci, 5 (1998) 24-27.

[11] E. A. A. Ikhlas A. Khan, *Leung's Encyclopedia of Common Natural Ingredients: Used in Food, Drugs and Cosmetics, 3rd Edition*. John Wiley & Sons: 2009; p 848.

[12] L. Polat Kose, Z. Bingol, R. Kaya, A. C. Goren, H. Akincioglu, L. Durmaz, E. Koksal, S. H. Alwasel, İ. Gülçin, 2020. Anticholinergic and antioxidant activities of avocado (Folium perseae) leaves – phytochemical content by LC-MS/MS analysis, International Journal of Food Properties, 23 (2020) 878-893.

[13] Ç. Olgun, O. Özkan, B. Güney, E. Pattabanoglu, K. Güney, M. Gür, 2017. Chemical Composition and Antimicrobial Activity in Cold Press Oil of Fennel, Anise, White and Black Mustard Seeds, Indian Journal of Pharmaceutical Education and Research, 51 (2017) s200-s204.

[14] L. P. Köse, İ. Gülçin, A. C. Gören, J. Namiesnik, A. L. Martinez-Ayala, S. Gorinstein, 2015. LC–MS/MS analysis, antioxidant and anticholinergic properties of galanga (Alpinia officinarum Hance) rhizomes, Industrial Crops and Products, 74 (2015) 712-721.

[15] M. Jahangir, H. Kim, Y. Choi, R. Verpoorte, 2009. Health-Affecting Compounds in Brassicaceae, Comprehensive Reviews in Food Science and Food Safety, 8 (2009) 31-43.

[16] A. C. Gören, S. Çıkrıkçı, M. Çergel, G. Bilsel, 2009. Rapid quantitation of curcumin in turmeric via NMR and LC–tandem mass spectrometry, Food Chemistry, 113 (2009) 1239-1242.

[17] A. Gören, G. Bilsel, M. Bilsel, 2012. Rapid and simultaneous determination of 25-OH-vitamin D 2 and D 3 in human serum by LC/MS/MS: Validation and uncertainty assessment, J Chem Metrl, 1 (2012).

[18] L. Polat Köse, 2024. Evaluation of Antioxidant Capacity, Anticholinergic and Antidiabetic Activities, and Phenolic Ingredients of Asphodelus aestivus by LC–MS/MS, Chemistry & Biodiversity, 21 (2024) e202301965.

[19] R. Apak, K. Güçlü, M. Ozyürek, S. Esin Karademir, E. Erçağ, 2006. The cupric ion reducing antioxidant capacity and polyphenolic content of some herbal teas, Int J Food Sci Nutr, 57 (2006) 292-304.

[20] I. Gülçin, 2008. Measurement of antioxidant ability of melatonin and serotonin by the DMPD and CUPRAC methods as trolox equivalent, Journal of Enzyme Inhibition and Medicinal Chemistry, 23 (2008) 871-876.

[21] M. S. Blois, 1958. Antioxidant Determinations by the Use of a Stable Free Radical, Nature, 181 (1958) 1199-1200.

[22] L. Polat Köse, 2021. Mısır İpeği'nin (Zea Mays L.) Antioksidan ve Antiradikal Özelliklerinin Belirlenmesi, Journal of the Institute of Science and Technology, 11 (2021) 402-412.

[23] İ. Gulcin, S. H. Alwasel. DPPH Radical Scavenging Assay *Processes* [Online], 2023.

[24] R. Re, N. Pellegrini, A. Proteggente, A. Pannala, M. Yang, C. Rice-Evans, 1999. Antioxidant activity applying an improved ABTS radical cation decolorization assay, Free Radic Biol Med, 26 (1999) 1231-1237.

[25] İ. Gülçin, V. Mshvildadze, A. Gepdiremen, R. Elias, 2006. Screening of antiradical and antioxidant activity of monodesmosides and crude extract from Leontice smirnowii tuber, Phytomedicine, 13 (2006) 343-351.

[26] Z. Bingol, H. Kızıltaş, A. C. Gören, L. P. Kose, M. Topal, L. Durmaz, S. H. Alwasel, İ. Gulcin, 2021. Antidiabetic, anticholinergic and antioxidant activities of aerial parts of shaggy bindweed (Convulvulus betonicifolia Miller subsp.) – profiling of phenolic compounds by LC-HRMS, Heliyon, 7 (2021) e06986.

[27] L. Durmaz, A. Erturk, M. Akyüz, L. Polat Kose, E. M. Uc, Z. Bingol, R. Saglamtas, S. Alwasel, İ. Gulcin, 2022. Screening of Carbonic Anhydrase, Acetylcholinesterase, Butyrylcholinesterase, and α-Glycosidase Enzyme Inhibition Effects and Antioxidant Activity of Coumestrol, Molecules, 27 (2022).

[28] C. J. C. Ortiz, C. M. Damasio, L. Pruccoli, N. F. Nadur, L. L. de Azevedo, I. A. Guedes, L. E. Dardenne, A. E. Kümmerle, A. Tarozzi, C. Viegas, Jr., 2020. Cinnamoyl-N-Acylhydrazone-Donepezil Hybrids: Synthesis and Evaluation of Novel Multifunctional Ligands Against Neurodegenerative Diseases, Neurochem Res, 45 (2020) 3003-3020.

[29] Y. Li, R. Fang, Z. Liu, L. Jiang, J. Zhang, H. Li, C. Liu, F. Li, 2021. The association between toxic pesticide environmental exposure and Alzheimer's disease: A scientometric and visualization analysis, Chemosphere, 263 (2021) 128238.

[30] S. Mitra, G. Turconi, T. Darreh-Shori, K. Mätlik, M. Aquilino, M. Eriksdotter, J. O. Andressoo, 2021. Increased Endogenous GDNF in Mice Protects Against Age-Related Decline in Neuronal Cholinergic Markers, Front Aging Neurosci, 13 (2021) 714186.

[31] G. L. Ellman, K. D. Courtney, V. Andres, R. M. Featherstone, 1961. A new and rapid colorimetric determination of acetylcholinesterase activity, Biochemical Pharmacology, 7 (1961) 88-95.

[32] M. Erdoğan, L. Polat Köse, S. Eşsiz, İ. Gülçin, 2021. Synthesis and biological evaluation of some 1-naphthol derivatives as antioxidants, acetylcholinesterase, and carbonic anhydrase inhibitors, Archiv der Pharmazie, 354 (2021) 2100113.

[33] İ. Gülçin, 2012. Antioxidant activity of food constituents: an overview, Arch Toxicol, 86 (2012) 345-391.

[34] İ. Gulcin, 2020. Antioxidants and antioxidant methods: an updated overview, Archives of Toxicology, 94 (2020) 651-715.

[35] A. Cavalli, M. L. Bolognesi, A. Minarini, M. Rosini, V. Tumiatti, M. Recanatini, C. Melchiorre, 2008. Multi-target-Directed Ligands To Combat Neurodegenerative Diseases, Journal of Medicinal Chemistry, 51 (2008) 347-372.

[36] J. S. Wright, E. R. Johnson, G. A. DiLabio, 2001. Predicting the Activity of Phenolic Antioxidants: Theoretical Method, Analysis of Substituent Effects, and Application to Major Families of Antioxidants, Journal of the American Chemical Society, 123 (2001) 1173-1183.

[37] F. Shahidi, P. Ambigaipalan, 2015. Phenolics and polyphenolics in foods, beverages and spices: Antioxidant activity and health effects – A review, Journal of Functional Foods, 18 (2015) 820-897.

[38] D. Huang, B. Ou, R. L. Prior, 2005. The Chemistry behind Antioxidant Capacity Assays, Journal of Agricultural and Food Chemistry, 53 (2005) 1841-1856.

[39] R. L. Prior, X. Wu, K. Schaich, 2005. Standardized Methods for the Determination of Antioxidant Capacity and Phenolics in Foods and Dietary Supplements, Journal of Agricultural and Food Chemistry, 53 (2005) 4290-4302.

[40] G. Luisi, A. Stefanucci, G. Zengin, M. P. Dimmito, A. Mollica, 2018. Anti-Oxidant and Tyrosinase Inhibitory In Vitro Activity of Amino Acids and Small Peptides: New Hints for the Multifaceted Treatment of Neurologic and Metabolic Disfunctions, Antioxidants (Basel), 8 (2018).

[41] L. Polat Köse, A. Köse, 2024. Identification of hCA I, hCA II, AChE and BChE Inhibitory Properties of Some Norcantharimide Derivatives; Molecular Docking, SAR and in silico ADME Studies, ChemistrySelect, 9 (2024) e202400684.

[42] H. Braak, D. R. Thal, E. Ghebremedhin, K. Del Tredici, 2011. Stages of the pathologic process in Alzheimer disease: age categories from 1 to 100 years, J Neuropathol Exp Neurol, 70 (2011) 960-969.

[43] R. J. Bateman, C. Xiong, T. L. Benzinger, A. M. Fagan, A. Goate, N. C. Fox, D. S. Marcus, N. J. Cairns, X. Xie, T. M. Blazey, D. M. Holtzman, A. Santacruz, V. Buckles, A. Oliver, K. Moulder, P. S. Aisen, B. Ghetti, W. E. Klunk, E. McDade, R. N. Martins, C. L. Masters, R. Mayeux, J. M. Ringman, M. N. Rossor, P. R. Schofield, R. A. Sperling, S. Salloway, J. C. Morris, 2012. Clinical and biomarker changes in dominantly inherited Alzheimer's disease, N Engl J Med, 367 (2012) 795-804.

Modelling and Analysis of STATCOM Based SEIG

A.S. Özer[1] and H. Karaca[2]

[1]Konya Technical University, Department of Control and Automation Technology, Konya/Türkiye, 0000-0002-8430-2887

[2]Selçuk University, Department of Electrical and Electronics Engineering, Konya/Türkiye, 0000-0002-5561-489X

Abstract

Regulation of the energy produced in renewable energy systems is of vital importance. Especially in wind energy systems, self-excited induction generator (SEIG) is frequently preferred due to its advantages such as brushless robust structure, low cost, less maintenance, self-protection against faults, no need for DC excitation, and the ability to generate electrical energy at variable speeds. However, the output voltage of the SEIG is extremely sensitive to load variation. One of the most suitable solutions to keep the voltage of the SEIG constant is the use of STATCOM structure. The performance of STATCOM depends on its control algorithm. In the literature, *dq*-based theory and instantaneous reactive power theory (IRPT) are widely used. In this study, modelling and analysis of a STATCOM based SEIG for voltage regulation of renewable energy systems is carried out. The mathematical expressions of *dq*-based theory required to control the STATCOM are clearly given. The modelled system is tested with linear and nonlinear loads. The obtained results demonstrate that the STATCOM keeps the SEIG voltage constant even under different loads.

Keywords: Static compensator (STATCOM), Self-excited induction generator (SEIG), Wind energy conversion systems (WECS), *dq*-based theory.

Introduction

In recent times, there has been a rapid increase in the inclination towards clean energy sources that can replace fossil fuels. Wind energy systems hold a significant share among renewable, clean energy sources [1]. Particularly in wind energy systems, the self-excited induction generator (SEIG) is often preferred due to its brushless robust structure, low cost, reduced maintenance requirements, self-protection against faults, lack of need for DC excitation, and ability to generate electricity at variable speeds [2]. The squirrel cage induction machine, externally driven and connected to a reactive power source through its stator terminals, is commonly referred to as a self-excited induction generator (SEIG). Despite its positive attributes, voltage variations occur in the voltages produced by the SEIG with changes in load and speed. Additionally, the output voltages of the SEIG are significantly affected by harmonics in the load. Therefore, voltage regulation is required in wind energy systems where SEIGs are used [3]. To achieve voltage regulation, reactive power needs to be provided. For this purpose, power electronics-based Static

Compensator (STATCOM) systems are widely used in SEIG applications to provide reactive power. The performance of STATCOM depends on the control algorithm that generates reference signals for the Voltage Source Inverter (VSI) [4].

In this study, modeling and analysis of a STATCOM-based SEIG for regulating the voltage obtained from renewable energy systems have been conducted. The mathematical expressions for the *dq*-based control algorithm necessary to control the STATCOM are explicitly provided. This will guide researchers interested in working in this field. The modeled system has been tested with linear and nonlinear loads. The results obtained demonstrate that the STATCOM maintains the voltage of the SEIG constant even under different loads.

System Configurations

The system configuration of the STATCOM-based SEIG is illustrated in Fig. 1. It comprises an induction generator, a star-connected three-phase capacitor bank utilized for self-excitation, various consumer loads, and a STATCOM. A capacitor bank is essential for supplying reactive power, ensuring the generation of rated voltage under no-load conditions [5]. Within the STATCOM, an IGBT-based Voltage Source Inverter (VSI) with a DC bus capacitor is integrated. Additionally, an inductor (L_f) is added in series with the point of common coupling (PCC) to mitigate high-frequency noise emanating from the VSI. The primary function of the STATCOM is to regulate the terminal voltage.
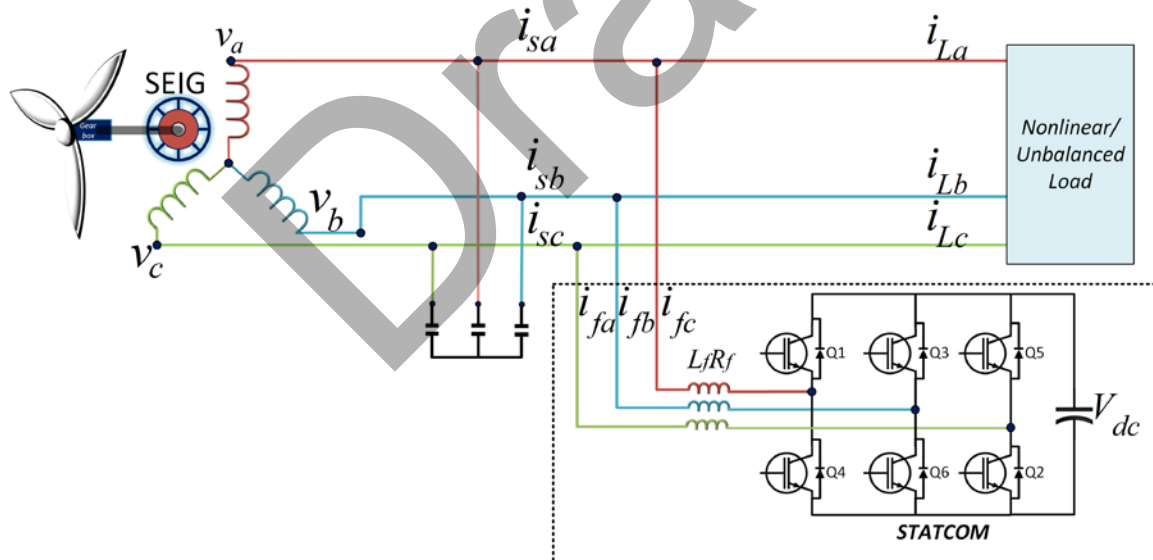

Figure 1. Schematic of STATCOM-based SEIG system

dq-BASED CONTROL ALGORITHM

dq-based control theory is also referred to as the synchronous reference frame (SRF) theory [6]. The block diagram of the *dq*-based theory is illustrated in Figure 2.
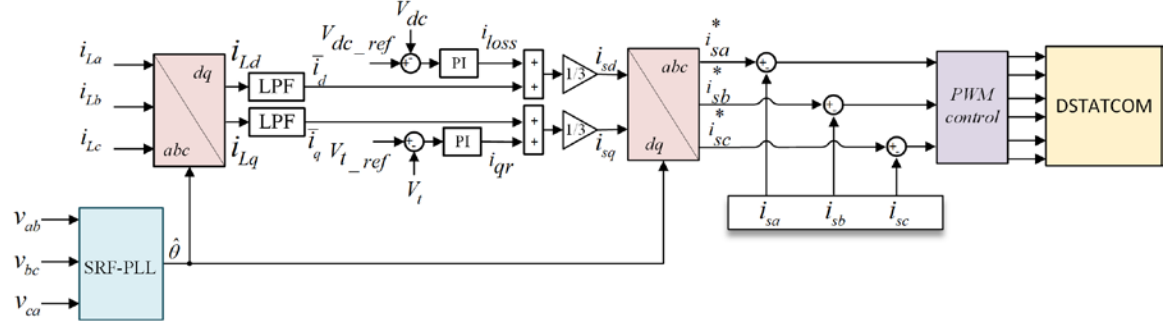

Figure 2. Schematic of *dq*-based method

In the SRF theory, measurements of load currents (i_{labc}), SEIG terminal voltages (v_{sabc}), and DC bus voltage (V_{dc}) are required. These measured signals are utilized as feedback signals. The *abc-dq* transformation is employed to convert the components of load currents from the synchronous reference frame to the *dq* reference frame. The currents i_{Ld} and i_{Lq} contain both fundamental and harmonic components. To remove the harmonic content from these currents, a Low Pass Filter (LPF) is employed. The fundamental components at the output of the LPF are expressed as $\overline{i_d}, \overline{i_q}$,

The Phase-Locked Loop provides the phase angle θ information necessary for the *abc* to *dq* plane conversion and inverse conversion. Additionally, the *dq*-based theory consists of two PI controllers. One PI controller is utilized to maintain the DC bus voltage of the VSI constant and stable, while the other is used to regulate the terminal voltage of the SEIG.

In the STATCOM, an active current is required to maintain the voltage level of the DC bus; otherwise, the DC bus voltage will collapse after a certain period. To regulate the DC bus voltage, the active component (i_{sd}) is utilized. These two components are calculated through $\overline{i_d}$ and $\overline{i_q}$.

For the active component (i_{sd}) current, the measured DC bus voltage (V_{dc}) is compared with the reference voltage value ($V_{dc\ ref}$), and the voltage error is entered into the PI controller.

The active component (i_{sd}) is calculated using the value generated at the output of the PI controller (i_{sd}), as per equation (1).

$$i_{sd} = \frac{i_{db} + \overline{i_d}}{3}$$

(1)

To prevent a drop in the SEIG voltage, reactive power must be provided. The reactive component (i_{sq}) of the source reference currents (i^*_{sa}, i^*_{sb}, i^*_{sc}) is used to control the magnitude of the SEIG voltage. To calculate this component, the peak value of the SEIG

voltage must first be determined. The peak magnitude of the SEIG voltage is calculated as follows:

$$V_t = \sqrt{\frac{2}{3}(v_{ab}^2 + v_{bc}^2 + v_{ca}^2)} \qquad (2)$$

This value is compared with the reference value of the voltage magnitude (V_{t_ref}), and the error is entered into the PI controller. The reactive component of the current (i_{sq}) is obtained using the value generated at the output of the PI controller (i_{qr}), as per equation (3)

$$i_{sq} = \frac{i_{qr} + \overline{i_q}}{3} \qquad (3)$$

The obtained i_{sd} and i_{sq} currents are utilized to derive the reference source currents (i^*_{sa}, i^*_{sb}, i^*_{sc}) through the *dq-abc* transformation.

After generating the reference source currents, the next step involves comparing these reference currents (i^*_{sabc}) with the measured currents of the SEIG (i_{sabc}) to generate PWM signals. These PWM signals are then fed to the IGBTs to provide the required active and reactive power.

PERFORMANCE OF STATCOM-BASED SEIG UNDER THE LINEAR AND NONLINEAR LOAD CONDITIONS

The performance of STATCOM with the proposed *dq*-based control algorithm is acquired under various linear and nonlinear load conditions. These conditions are given as follows.

Test condition-1: To examine the proposed *dq*-based controller under linear load, resistive load is connected.

Test condition-2: To examine the proposed SEIG-STATCOM controller under a nonlinear load, three-phase diode rectifier with resistive load is connected.

1.1. Performans of SEIG-STATCOM system under lineer load conditions

In Fig. 3, the load currents (i_{Labc}), STATCOM currents (i_{fabc}), SEIG currents (i_{sabc}), SEIG terminal voltages (v_{ab}, v_{bc}, v_{ca}), the magnitude of the SEIG voltages (V_t), and the DC bus voltage (V_{dc}) values are respectively displayed for the SEIG-STATCOM system operated under test-1 conditions.

In test-1, the load currents are balanced due to the linear load as shown in Fig. 3(a). Fig. 3(b) demonstrated the currents injected by STATCOM into the system to provide the reactive power needed by the SEIG. Thanks to the proposed *dq*-based controler, SEIG currents and voltages are obtained in sinusoidal and balanced form as illustrated in Fig. 3(c) and Fig. 3(d), respectively. Also, the amplitude of SEIG voltage (V_t) and DC bus voltage (V_{dc}) are also observed to be constant and maintained at reference values as shown in Fig. 3(e) and Fig. 3(f), respectively.
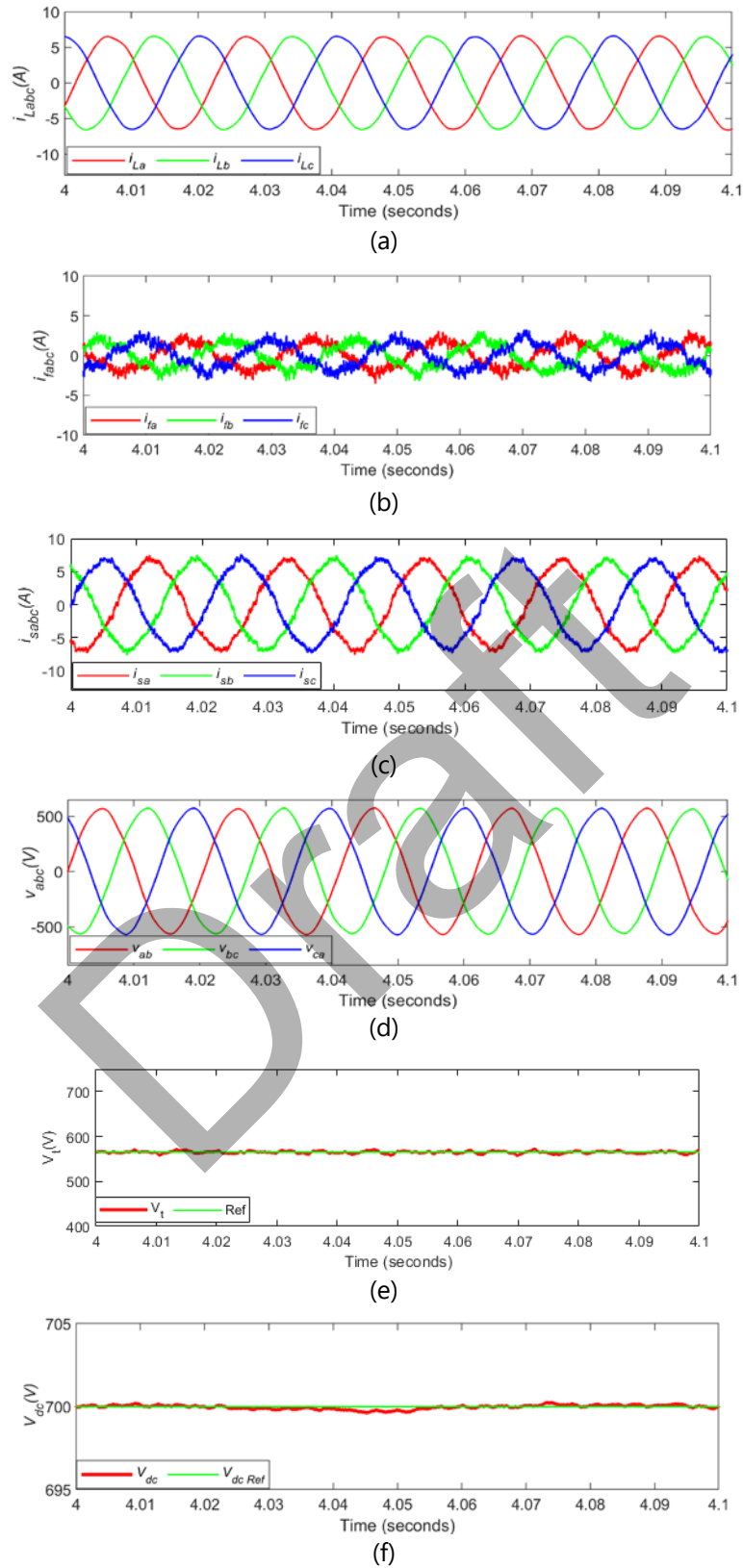
(a)

(b)

(c)

(d)

(e)

(f)

Figure 3. Performance of SEIG-STATCOM system under linear loads (a) Load currents, (b) STATCOM currents, (c) SEIG currents, (d) SEIG terminal voltages, (e) Amplitude of SEIG voltages and (f) DC bus voltage

1.2. Performans of SEIG-STATCOM system under nonlineer load conditions

In Fig. 4, the load currents (i_{Labc}), STATCOM currents (i_{fabc}), SEIG currents (i_{sabc}), SEIG terminal voltages (v_{ab}, v_{bc}, v_{ca}), the magnitude of the SEIG voltages (V_t), and the DC bus voltage (V_{dc}) values are respectively displayed for the SEIG-STATCOM system operated under test-2 conditions.

In Test-2, harmonics occur in the load currents due to the nonlinear load, as illustrated in Fig. 4(a). Therefore, the STATCOM suppresses the load harmonics and injects balancing currents, as shown in Fig. 4(b), to maintain the SEIG currents nearly sinusoidal. SEIG currents and voltages are obtained in a balanced manner, as depicted in Fig. 4(c) and Fig. 4(d), respectively. When examining the V_{dc} and V_t voltages, as seen in Fig. 4(e), the V_{dc} value exhibits only approximately 0.5 V oscillation despite the increase in harmonic levels in the load current. Additionally, the Vt voltage, as presented in Fig. 4(f), demonstrates an approximate 2V oscillation.

(a)

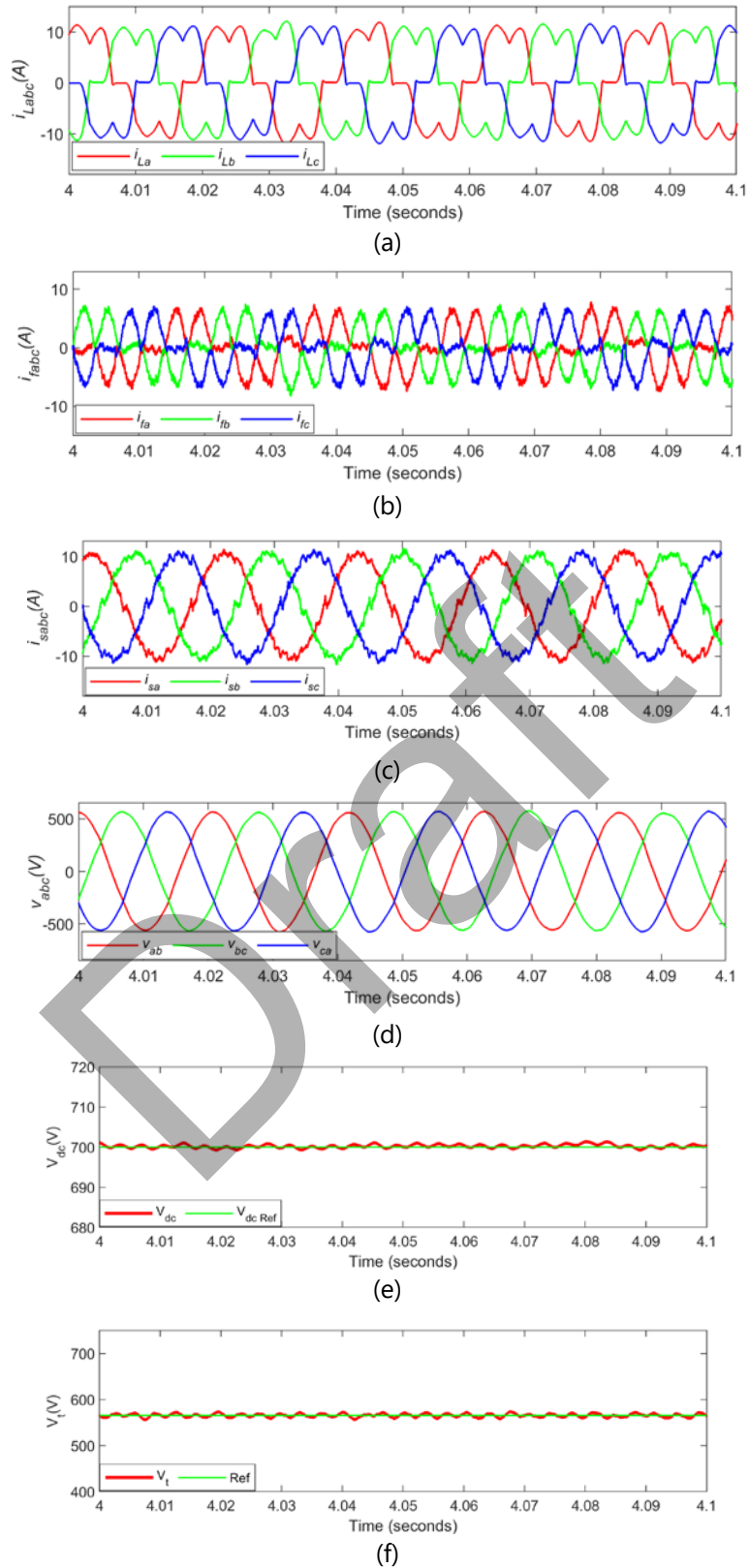

(b)

(c)

(d)

(e)

(f)

Figure 4. Performance of SEIG-STATCOM system under nonlinear loads (a) Load currents, (b) STATCOM currents, (c) SEIG currents, (d) SEIG terminal voltages, (e) Amplitude of SEIG voltages and (f) DC bus voltage

Conclusions

This study presents the modeling and analysis of a STATCOM-based SEIG for voltage regulation in renewable energy systems. Mathematical expressions of the *dq* based control algorithm necessary to manage the STATCOM are provided explicitly. The modeled system is tested under both linear and nonlinear loads. The results demonstrate that the STATCOM effectively maintains the SEIG voltage constant even under varying loads.

References

[1] B. Subhash,. and V. Rajagopal, 2023. Optimal Gains for Control Voltage and Frequency in Standalone Wind Energy Conversion System. Journal of The Institution of Engineers (India): Series B, 2023: p. 1-17.

[2] A.S. Satpathy, D. Kastha, and K. Kishore, 2019. Control of a STATCOM-assisted self-excited induction generator-based WECS feeding non-linear three-phase and single-phase loads. IET Power Electronics, 2019. 12(4): p. 829-839.

[3] A.S. Özer, F. Sevilmiş, H. Karaca, H. Arabacı., 2022. Enhanced control method for voltage regulation of DSTATCOM based SEIG. Energy Reports, 2022. 8: p. 839-847.

[4] A.S. Özer, H. Karaca, and F. Sevilmiş, 2023. APF Based Control Algorithm for Voltage Regulation of Self Excited Induction Generator Using DSTATCOM. a a. 2: p. 2.

[5] B. Singh., S. Murthy, S. Gupta, 2006. STATCOM-based voltage regulator for self-excited induction generator feeding nonlinear loads. IEEE transactions on industrial electronics, 53(5), 1437-1452.

[6] B. Singh. and J. Solanki, 2009. A comparison of control algorithms for DSTATCOM. IEEE transactions on Industrial Electronics, 2009. 56(7): p. 2738-2745.

A Comparative Study of Gated Recurrent Unit and Long-Short Term Memory for Li-Ion Batteries on State of Charge Estimation

O. Ozer[1] and H. Arabaci[1]

[1]Selçuk University, Konya, Turkey, 0000-0001-7489-1721: , 0000-0002-9212-0784:

Abstract

State of Charge (SOC) estimation is critical to safe operation for lithium-ion batteries which are being used in mobile devices in particular electric vehicles. Nonlinearity caused by the complexity in chemical structure of battery does not allow direct measurement of the SOC parameter. Estimating SOC by deep learning methods is very popular nowadays. In this study, the SOC estimation of the li-ion battery was made with two different deep learning algorithms, which are gated recurrent unit (GRU) and long-short term memory (LSTM). The voltage and current of the battery obtained as a result of the driving profile experiments conducted in the laboratory environment at 25 °C are the input of the algorithms, and the SOC is the output. Training, validation, and test data are completely different. Hyperparameters are the same for both algorithms. Since the LSTM is more complex, it also has extra parameters. The LSTM provides high accuracy than the GRU according to mean absolute error (MAE) and mean squared error (MSE). On the other hand, GRU gives better result in terms of calculation time.

Keywords: SOC, deep learning, GRU, LSTM.

Introduction

Climate change is a major problem that threatens world life today. Scientists are investigating various solutions to minimize this problem. With increasing investments in renewable energy sources, electric vehicles also stand out as an environmentally friendly alternative. Compared to traditional vehicles, there are no exhaust emissions in electric vehicles since fossil fuels are not used. In this way, the release of environmentally harmful gases into the atmosphere is prevented and air quality is improved. This means a cleaner environment and a healthier atmosphere. Additionally, electric vehicles help use energy resources more sustainably by reducing dependence on fossil fuels. Environmental problems of our age have accelerated the spread of electric vehicle technology. The studies, which first started with hybrid systems in which electric motors and internal combustion engines were used together, turned into the production of vehicles using

only electric motors, with the developments in battery technology. Lithium-ion (Li-ion) batteries are commonly used in a wide range of applications, from mobile devices to electric vehicles [1]. Battery management system (BMS) plays a critical role in the effective and safe use of advance battery technologies such as li-ion. These systems optimize the charging-discharging processes of batteries and ensure safety at the same time. BMS monitors and prevents dangerous situations such as overcharge, overdischarge, overtemperature and short circuit while improving battery performance. This extends the life of batteries, increases energy efficiency, and ensures safety standards [2]. BMS needs parameters to do its job well. The most important of these parameters is SOC. SOC is defined as the usable capacity of the battery until the next charge. When the BMS accurately estimates the SOC value, it prevents the battery from overcharging or overdischarging, providing healthy operating conditions. In addition, presenting the remaining available capacity as a parameter is very important for user experience. The user must be aware of when the device needs to be charged. Especially in electric vehicles, estimating the SOC accurately and indicating the range for the next charge plays an important role in arriving the desired point before the vehicle runs out of charge [3]. To avoid this undesirable situation, it is essential to make SOC estimation with high accuracy. In literature, three main methods are used for SOC estimation. These; ampere-hour integral method, model-based prediction methods (such as electrical equivalent circuit model) and data-based prediction methods. To make predictions in the first two methods, detailed electrical and chemical knowledge about batteries is needed. On the contrary, in data-based methods, predictions can be made with high accuracy without know how about batteries.

Chemali et al. introduced a new method to perform accurate SOC estimation for Li-ion batteries using a recurrent neural network (RNN) with LSTM. They trained an LSTM-RNN model over datasets recorded at various ambient temperatures [1]. How et al. proposed a deep neural network (DNN) with a sufficient number of hidden layers is capable of predicting the SOC of the unseen drive cycles during training [2]. Tian et al. proposed a method combining a LSTM network with an adaptive cubature Kalman filter (ACKF) [3]. Hong et al. presented a machine learning method to perform real-time SOC prediction for battery systems using a RNN with LSTM. They proposed joint-prediction strategy using LSTM and multiple linear regression algorithms [4]. Yang et al. proposed a RNN with GRU to estimate the battery SOC from measured current, voltage, and temperature values. The proposed method is robust against unknown initial SOC values and can be trained to learn the influence of ambient temperatures [5]. Yang et al. presented a study that estimates battery SOC from voltage, current, and temperature using a LSTM to model battery behaviors. They used an unscented Kalman filter (UKF) to filter out the noises and reduce the estimation errors [6]. Qin et al. presented a new design of SOC estimation to consider the influences of varying ambient temperatures. Transfer learning was used to estimate at new temperatures [7]. Du et al. proposed a unified deep learning method that could be implemented for both remaining useful lifetime and SOC. According to study the two parameters reflect the state of a battery in use [8]. Mamo and Wang presented a LSTM model with an attention mechanism to estimate the SOC of li-ion battery. They located an attention mechanism on the output layer of LSTM [9]. Yang

et al. proposed LSTM network to model the complex dynamics of lithium iron phosphate batteries and deduced SOC from current, voltage, and ambient temperatures [10].

In this study, the SoC prediction of the li-ion battery was made with two different deep learning algorithms, which are GRU and LSTM, with experimental data as inputs and output of the algorithms. The performances of the algorithms are compared by accuracy and computational cost.

State of Charge Estimation With Deep Learning

The SOC indicates the remaining usable capacity of a battery shown in Eq. 1 where *Q(t)* symbolizes available capacity at time t, Q_{max} symbolizes total capacity and *SOC(t)* symbolizes percentage of available capacity at time t. The SOC is employed to avoid excessive discharge or charging, while also managing the battery's operation to minimize the impact of aging [11]. Since the dynamic behaviour of li-ion batteries is nonlinear, it is not possible to measure SOC directly. Battery capacity has a nonlinear relationship with temperature and discharge current. Therefore, SOC measurement cannot be done directly.

$$SOC(t) = \frac{Q(t)}{Q_{max}} \qquad (1)$$

Cho and colleagues introduce a GRU approach that enables individual recurrent units to dynamically capture sequential dependencies across diverse time scales [12]. The GRU incorporates a gating mechanism to regulate information flow within each unit. In subsequent steps, we denote x[t] as the current input, h[t] as the current output, h[t -1] as the output from the previous step, z[t] as the update gate and r[t] as the reset gate. A graphical illustration of the GRU cell shown in Figure 1.
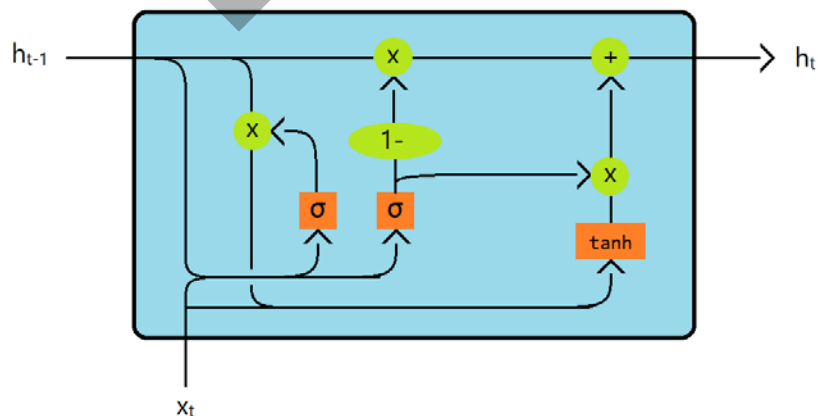

Figure 1. Structure of a GRU cell

GRU is an RNN architecture frequently used in forecasting time series problems. Gating mechanism allows to capture long-term dependencies effectively. Update gate controls how much of the previous hidden state should be retained, and reset gate determines how much of the past information to forget.

Hochreiter and Schmidhuber introduced the LSTM network as an advancement over classical RNNs [13]. Instead of conventional hidden nodes, LSTM utilizes memory units to mitigate the issues of gradient vanishing or explosion, particularly evident after numerous time steps, thereby addressing the challenges associated with traditional RNN training [14]. We denote x_t as the current input, h_t as the current output and c_t as the unit memory. A graphical illustration of LSTM structure is shown in Figure 2.
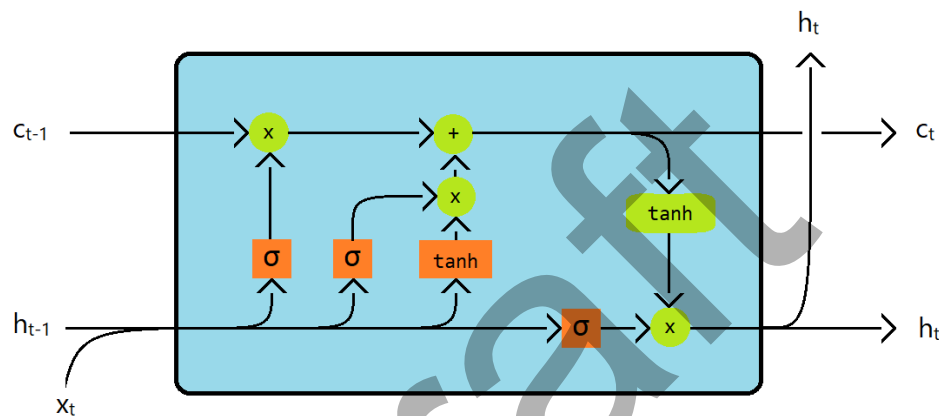

Figure 2. Structure of a LSTM cell

GRU and LSTM have similar structure. There is a main difference that LSTM includes cell state ct gives memory feature. While both algorithms can give similar results due to the similarity between them, differences emerge in the two cases. First, LSTM provides higher accuracy in longer time series because it has a memory cell. Secondly, since its structure is simpler, GRU has lower computational costs.

A series of vehicle drive cycle Cycle 1, Cycle 2, Cycle 3, Cycle 4, HWFTa, HWFTb, UDDS, LA92 and Neural Network were applied on a battery cell and data measured by Kollemeyer [15]. Neural network cycle was used for training, Cycle 1 was used for validating and the remaining cycles were also used to test the algorithm performance in our study. Voltage and current are the inputs, SOC is the output of the algorithms.

Results and Discussions

In this section, two deep learning methods GRU and LSTM are interpreted under similar conditions. All data used in training, validation and testing were recorded at 25 °C. Each network is trained and tested individually. All the hyperparameters are same for both networks. If the results don't meet the accuracy requirement, adjustments are made to

parameters like the number of layers and neurons. Through multiple rounds of training and parameter tweaking, the optimal model is achieved. We use Adam optimizer to improve convergence speed. The computations were run on a laptop configured with Intel® Alder Lake Core™ i7-12700H CPU and NVIDIA GeForce RTX 3070 Ti GPU. The SOC estimation of MAE and MSE of the two networks are given in Table 1.

Table 1. Accuracy of the networks

Drive Cycle	MAE of GRU	MAE of LSTM	MSE of GRU	MSE of LSTM
Cycle 2	0.0191	*0.0155*	0.000554	*0.000347*
Cycle 3	0.0175	*0.0130*	0.000504	*0.000257*
Cycle 4	0.0145	*0.0133*	0.000348	*0.000335*
HWFTa	0.1190	*0.1007*	0.016740	*0.012053*
HWFTb	0.1158	*0.0975*	0.015907	*0.011372*
UDDS	0.0548	*0.0436*	0.004313	*0.002599*
LA92	0.0223	*0.0134*	0.000889	*0.000340*

As can be seen from Table 1, the LSTM network estimated SOC with higher accuracy with lower MAE and MSE in all driving cycles than GRU network. The memory cell in the LSTM network led to better performance than GRU in long-term time series. Another criterion to compare is the computation time of the networks. The calculation times of GRU and LSTM networks in the testing phase are presented in Table 2.

Table 2. Test time of the networks (s)

Drive Cycle	GRU (s)	LSTM (s)
Cycle 2	*35.705*	40.032
Cycle 3	*31.855*	35.810
Cycle 4	*38.271*	42.445
HWFTa	*22.579*	25.710
HWFTb	*22.818*	25.970
UDDS	*73.759*	79.754
LA92	*46.191*	48.832

Table 2 demonstrates that the computational costs in seconds are reduced in the GRU network, attributed to its simpler internal structure. Since the neurons in the LSTM network performed more mathematical operations (see in Figure 2), it took longer to reach the result. On the other hand, it has been observed that as the processed data size increases, the test time increases linearly.

Conclusions

SOC estimation is very important for Li-ion batteries to operate safely and efficiently. Data driven SOC estimation methods are very popular nowadays. In this paper two SOC estimation networks deep learning based are investigated. The main object of this paper is comparing the accuracy of GRU and LSTM networks SOC estimation for li-ion battery. The results show that LSTM gives more accurate estimation than GRU for all data sets. On the other side, results show that computation time of networks are different. GRU network achieved results faster.

References

[1] E. Chemali, P. J. Kollmeyer, M. Periendl, R. Ahmed, A. Emadi, 2018. Long Short-Term Memory Networks for Accurate State-of-Charge Estimation of Li-ion Batteries, IEEE Trans. Ind. Electron. 65(8) (2018) 6730-6739.

[2] D. N. T. How, M. A. Hannan, M. S. H. Lipu, K. S. M. Sahari, P. J. Ker, K.M. Muttaqi, 2020. State-of-Charge Estimation of Li-Ion Battery in Electric Vehicles: A Deep Neural Network Approach, IEEE Trans. Ind. Appl. 56(5) (2020) 5565-5574.

[3] Y. Tian, R. Lai, X. Li, L. Xiang, J. Tian, 2020. A combined method for state-of-charge estimation for lithium-ion batteries using a long short-term memory network and an adaptive cubature Kalman filter, Appllied Energy 265 (2020) 114789.

[4] J. Hong, Z. Wang, W. Chen, L. Y. Wang, C. Qu, 2020. Online joint-prediction of multi-forward-step battery SOC using LSTM neural networks and multiple linear regression for real-world electric vehicles, Journal of Energy Storage 30 (2020) 101459.

[5] F. Yang, W. Li, C. Li, Q. Miao, 2019. State-of-charge estimation of lithium-ion batteries based on gated recurrent neural network, Energy 175 (2019) 66-75.

[6] F. Yang, S. Zhang, W. Li, Q. Miao, 2020. State-of-charge estimation of lithium-ion batteries using LSTM and UKF, Energy 201 (2020) 117664.

[7] Y. Qin, S. Adams, C. Yuen, 2021. Transfer Learning-Based State of Charge Estimation for Lithium-Ion Battery at Varying Ambient Temperatures, IEEE Trans. Ind. Informat. 17(11) (2021) 7304-7315.

[8] Z. Du, L. Zuo, J. Li, Y. Liu, H. T. Shen, 2021. Data-driven Estimation of Remaining Useful Lifetime and State of Charge for Lithium-ion Battery, IEEE Trans. Transpor. Electrific. 8(1) (2021) 356-367.

[9] T. Mamo, F. K. Wang, 2020. Long Short-Term Memory With Attention Mechanism for State of Charge Estimation of Lithium-Ion Batteries, IEEE Access 8 (2020) 94140-94151.

[10] F. Yang, X. Song, F. Xu, K. L. Tsui, 2019. State-of-Charge Estimation of Lithium-Ion Batteries via Long Short-Term Memory Network, IEEE Access 7 (2019) 53792-53799.

[11] J. P. R. Barrera, N. M. Galeano, H. O. S. Maldonado, 2017. SoC Estimation for Lithium-ion Batteries: Review and Future Challenges, Electronics 6(4) (2017) 102.

[12] K. Cho, B. V. Merriënboer, C. Gulcehre, D. Bahdanau, F. Bougares, H. Schwenk, Y. Bengio, 2014. Learning Phrase Representations using RNN Encoder-Decoder for Statistical Machine Translation, arXiv preprint (2014) arXiv:1406.1078.

[13] S. Hochreiter, J. Schmidhuber, 1997. Long short-term memory, Neural computation 9(8) (1997) 1735-1780.

[14] X. Song, F. Yang, D. Wang, K. L. Tsui, 2019. Combined CNN-LSTM Network for State-of-Charge Estimation of Lithium-Ion Batteries, IEEE Access 7 (2019) 88894-88902.

[15] P. Kollmeyer, Panasonic 18650PF Li-ion Battery Data, Mendeley Data 1 (2018) https://data.mendeley.com/datasets/wykht8y7tg/1.

Comparative Analysis of Database Technologies for IoT Environments

A. Ozmen[1], M. Ertugrul[2]

[1]Department of Electronics and Automation, Vocational High School, Agri Ibrahim Cecen University, Agri, Turkey, ORCID: https://orcid.org/0000-0002-3631-4883
[2]Department of Metallurgical and Materials Engineering, Karadeniz Technical University, Trabzon, Turkey, ORCID: https://orcid.org/0000-0003-1921-7704

Abstract

The Internet of Things (IoT) refers to systems composed of interconnected devices capable of exchanging data. These systems offer services for data collection and analysis, making both data collection and storage critically important in IoT environments. With the widespread adoption of IoT systems, the demand for data storage solutions has increased. Traditionally, Structured Query Language (SQL) based databases have been favored due to their simplicity, robustness, flexibility, scalability, and performance. However, with the rise of Big Data, NoSQL databases have emerged, providing alternatives to traditional relational databases. NoSQL databases are non-relational, schema-less, do not require joins, are easily replicable, and are horizontally scalable. In IoT systems, data is typically stored in cloud-based systems, but there are scenarios where offline data storage becomes necessary. Thus, the choice of database in IoT systems becomes a critical factor depending on the use scenarios. This study is based on experiments conducted using the ESP32 microcontroller to compare the performance differences between SQL and NoSQL databases utilized in IoT-based systems. During these experiments, data insertion and retrieval operations were measured using Google's NoSQL-based Firebase database and the local SQLite database. Our findings indicate that Firebase performs faster in data insertion operations compared to SQLite. In data retrieval operations, especially with smaller data sets, the SQLite database on the SPI Flash File Storage (SPIFFS) file system exhibited better performance. Additionally, it was observed that the Little File System (LittleFS) file system could handle larger data volumes more effectively compared to SPIFFS.

Keywords: IoT, NoSQL, IoT database, SQLite, ESP32 microcontroller

Introduction

The Internet of Things (IoT) represents a technological revolution enabling communication between various devices and applications via the internet. Offering advanced data analytics and real-time processing capabilities, IoT paves the way for innovations across a wide range of fields from industry to healthcare services. This expanding ecosystem generates large-scale data streams, introducing significant challenges in the management of database systems[1].

While IoT devices commonly store their data in cloud systems, in scenarios lacking internet access, with weak communication, or where highly secure data collection is necessary, data is stored directly on embedded systems. This necessitates the establishment of databases within these embedded systems. In this context, SQLite emerges as a free solution that facilitates the creation of SQL-based databases in embedded systems[2,3]. Moreover, the emergence of large datasets has paved the way for the development of NoSQL databases, which differ from traditional relational database systems by offering schema-less structures[2,4–6]. The capability of NoSQL databases to handle unstructured data (such as texts, images, videos, emails) [7] distinguishes these technologies from traditional SQL systems.

In their study, Rautmare et al. (2016) conducted a comparative analysis of SQL and NoSQL databases within the context of a small-scale IoT sprinkler system application, investigating whether NoSQL demonstrated superior performance to SQL across various scenarios. They utilized MongoDB, a NoSQL database, to measure the time expended in executing 'Select' and 'Insert' queries against varying numbers of records and threads. Their findings indicated that MongoDB occasionally required shorter response times compared to MySQL; however, MySQL responses were more consistent when compared with those from MongoDB [4]. Reetishwaree et al. (2020) Utilizing sensor data like temperature/humidity and water level, they monitored a facility environment in real-time. The results revealed that while NoSQL databases performed 'Update' and 'Delete' operations more swiftly, SQL databases excelled in 'Select' operations[1]. Mladenova et al. (2022) presented a study and performance comparison of SQL and NoSQL databases concerning data from IoT devices and sensors. They tested 'Insert' and 'Select' operations under various technical variables. Their research concluded that MySQL was the preferred choice when multiple 'Select' queries were needed, whereas MongoDB was more suitable for scenarios with fewer 'Insert' queries[5].

Although extensive comparisons between these two types of databases exist in the literature[1,4,5,8] direct comparisons using performance data from low-capacity embedded systems like the ESP32 on SQLite-based implementations have not been conducted. This study includes comparisons of data insertion, search, and error-free record times in IoT contexts using the ESP32 microcontroller, comparing SQLite and Firebase. The findings presented provide valuable insights into how these database systems can be optimized within IoT devices.

Material and Method

In our research, we utilized the widely used ESP32 microcontroller in IoT systems. Two systems were created for the experiment, with the first system (D1) used to examine data "INSERT" and "SELECT" parameters. In the D1 system, the ESP32 was operated with three algorithm versions. The reason for applying different algorithms is the availability of two different File Systems (FS) that we can use with ESP32, namely SPIFFS and LittleFS. The performance evaluation of the SQLite database in our study was separately analyzed based on these two FS. For comparison, the NoSQL-based Firebase database produced by Google was used. The C++ code was written to utilize randomly generated temperature, humidity, and time information for 10 and 100 records for 10 sensors. The difference between the system time at the start of the " INSERT" and " SELECT" processes (T1) and the system time at the completion of the processes, T2, was calculated in microseconds for all records, and the average was computed[9].

Table 1. Materials used in IoT system

Device/Sensor	Usage Feature
ESP32	Microcontroller
DS18B20	Temperature Measurement
DHT11	Humidity Measurement
DS3231	Real-Time Clock (RTC)

The second system (D2) was designed to showcase the performance of faltering records due to communication issues in IoT communication networks. As seen in Table 1, the IoT system comprises 2 DS18B20 sensors, 1 DHT11 humidity sensor, DS3231 RTC sensors, and an ESP32. A total of 10 devices are present in the created IoT network, and the system has been recording temperature, humidity, and time data to the Firebase database at a rate of 144 data points per day for 6 months.

Results and Discussion

In our study, a total of three analyses were conducted using two IoT systems. The performance indicators obtained from the "INSERT" operation performed with the D1 system are presented in Figure 1A. The data obtained indicate that for the "INSERT" operation, 100 records took 109961 µs to be stored in the SQLite database set up on the LittleFS system (LittleFS + SQLite), 56031 µs on the SPIFFS system (SPIFFS + SQLite), and 23971 µs when saved on Firebase for 100 records. Similarly, for 1000 records, it took 324706 µs on LittleFS + SQLite and 138964 µs on SPIFFS + SQLite. Firebase was excluded from this analysis due to its hourly limit of 100 data points (which applies to free usage). According to these results, the "INSERT" operation is much faster with the NoSQL

database Firebase compared to the SQL database. Additionally, it was concluded that SPIFFS is faster than LittleFS.

The second analysis conducted with the D1 system is the "SELECT" operation. The results obtained from this operation are presented in Figure 1B and Table2. For the "SELECT" operation from a dataset containing 100 records, it took 165142 µs on LittleFS + SQLite, 78951 µs on SPIFFS + SQLite, and 419907 µs on Firebase. This analysis involved a "GET" operation from the Firebase database. For 1000 records, it took 791866 µs on LittleFS + SQLite and 783602 µs on SPIFFS + SQLite. While the processing time for "SELECT" operations was close between LittleFS and SPIFFS systems with large datasets, SPIFFS was found to be faster with smaller datasets. Moreover, cloud-based systems take significantly longer to retrieve data compared to local systems. Possible reasons for this could be attributed to security measures in cloud systems and the impact of internet speed on latency.
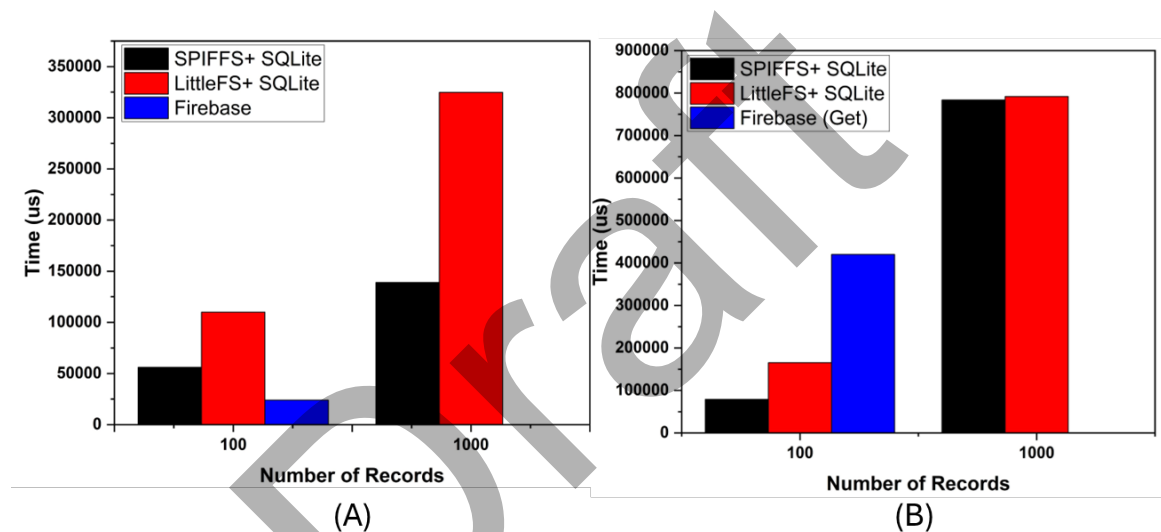

Figure 1. A) Latency in 'INSERT' Operations, Latency in 'SELECT' Operations

An additional investigation was conducted with the D1 system to determine the error-free record limit for LittleFS + SQLite and SPIFFS + SQLite. It was found that SPIFFS + SQLite becomes unresponsive after an average of 2000 records, while LittleFS + SQLite worked smoothly up to 10000 records. Since the system was configured for a maximum of 10000 records, the limit of LittleFS + SQLite was not reached. To conduct a similar analysis for Firebase, the D2 system was set up. With the D2 system, a Firebase data loss analysis was conducted, revealing a 2.46% data loss rate in 259200 records. This level of data loss can be attributed to communication and internet interruptions in the IoT system.

Table 2. Latency Times by Operation

Database	Number of Data	Operation Type	
		INSERT (µs)	SELECT (µs)
LittleFS+ SQLite	100	109961	165142
	1000	324706	791866
SPIFFS + SQLite	100	56031	78951
	1000	138964	783602
Firebase	100	23971	419907

Conclusions

This study presents a comprehensive comparison of SQL and NoSQL database systems within the context of IoT implementations, particularly focusing on embedded systems. The findings from our research using the ESP32 microcontroller highlight significant performance differences between the two types of databases in handling IoT data. Our experiments reveal that Firebase, a NoSQL database, demonstrates considerable speed advantages in "INSERT" operations compared to SQLite operating on both LittleFS and SPIFFS file systems. This suggests that for applications where rapid data entry is critical, and the system constraints allow, Firebase presents a more efficient option. In contrast, the "SELECT" operations show that SQLite on SPIFFS performs more efficiently than on LittleFS, especially with smaller datasets. This indicates that for systems where frequent data retrieval is necessary, SQLite on SPIFFS might offer better performance. Additionally, SPIFFS + SQLite systems become unresponsive at a lower data volume compared to LittleFS + SQLite, suggesting that LittleFS may be more suitable for applications requiring larger databases.

References

[1]   S. Reetishwaree, V. Hurbungs, 2020. Evaluating the performance of SQL and NoSQL databases in an IoT environment, in: 2020 3rd Int. Conf. Emerg. Trends Electr. Electron. Commun. Eng., IEEE, (2020) 229–234.

[2]   M. Slabinoha, S. Melnychuk, I. Manuliak, B. Pashkovskyi, 2022. Comparative analysis of embedded databases performance on single board computer systems using Python, in: 2022 IEEE 17th Int. Conf. Comput. Sci. Inf. Technol., IEEE, (2022) 222–225. https://doi.org/10.1109/CSIT56902.2022.10000475.

[3]   G. Rani, T. Sharma, A. Sharma, 2023. Future Database Technologies for Big Data Analytics, in: 2023 Int. Conf. Intell. Syst. Commun. IoT Secur., IEEE, (2023) 349–354. https://doi.org/10.1109/ICISCoIS56541.2023.10100525.

[4]   S. Rautmare, D.M. Bhalerao, 2016. MySQL and NoSQL database comparison for IoT application, in: 2016 IEEE Int. Conf. Adv. Comput. Appl., IEEE, (2016) 235–238. https://doi.org/10.1109/ICACA.2016.7887957.

[5]   T. Mladenova, I. Valova, 2022. Performance Study of MySQL and MongoDB for IoT Data Processing and Storage, in: 2022 Int. Conf. Autom. Informatics, IEEE, (2022) 60–63. https://doi.org/10.1109/ICAI55857.2022.9960134.

[6]   A. B. Moniruzzaman, S.A. Hossain, 2013. NoSQL Database: New Era of Databases for Big data Analytics - Classification, Characteristics and Comparison, International Journal of Database Theory and Application. 6 (2013) 43–45.

[7]   A. Al-Sakran, H. Qattous, M. Hijjawi, 2018. A proposed performance evaluation of NoSQL databases in the field of IoT, in: 2018 8th Int. Conf. Comput. Sci. Inf. Technol., IEEE, (2018) 32–37. https://doi.org/10.1109/CSIT.2018.8486199.

[8]   M. Muniswamaiah, T. Agerwala, C.C. Tappert, 2020. Performance of databases in IoT applications, in: 2020 7th IEEE Int. Conf. Cyber Secur. Cloud Comput. (CSCloud)/2020 6th IEEE Int. Conf. Edge Comput. Scalable Cloud, IEEE, (2020) 190–192. https://doi.org/10.1109/CSCloud-EdgeCom49738.2020.00041.

[9]   V. Pupezescu, M.-C. Pupezescu, L.-A. Perisoara, 2022. Optimizations of Database Management Systems for Real Time IoT Edge Applications, in: 2022 23rd Int. Carpathian Control Conf., IEEE, (2022) pp. 171–176.

Evaluation of Forage Quality Properties of Different Forest Rangeland Sites

T. Çomaklı[1], A. Bilgili[2], E. Çomaklı[3] and M.K. Güllap[4]

[1]*Eastern Anatolia Forestry Research Institute, Erzurum, Türkiye, ORCID: 0000-0002-0699-9818*
[2]*Eastern Anatolia Forestry Research Institute, Erzurum, Türkiye, ORCID: 0000-0002-2151-3521*
[3]*Atatürk University, Faculty of Agriculture, Erzurum, Türkiye, ORCID: 0000-0001-8477-7076*
[4]*Atatürk University, Faculty of Agriculture, Erzurum, Türkiye, ORCID: 0000-0002-6348-4335*

Abstract

Forest rangeland are among the forage sources that are very important and have rich potential for livestock farming. In this study conducted in Erzurum province Oltu district Kırdağı location during 2015, 2016 and 2017 concerning the above forest, forest interior and forest edge rangeland sites, the forage quality properties were emphasized. Rangeland sites were determined according to the full blocks trial design by random sampling. In this research, dry matter yield, crude protein ratio, acide detergent fiber (ADF), neutral detergent fiber (NDF) ratios were investigated. The amounts of dry matter are in the forest top rangeland (50.68 kg/da), in-forest rangeland (30.77 kg/da) and forest edge rangeland (24.81 kg/da), respectively. Crude protein averages of rangeland sites for all years varied between 8.33% and 11.37%. In all years of the research, the highest crude protein rate was obtained in the forest-side rangeland site, and the lowest crude protein rate was obtained in the forest edge rangeland site. According to the average of the years, the forest edge rangeland site had the highest ADF rate with 45.44%, while the lowest ADF rate was recorded in the forest edge rangeland site with 40.91%. According to the average of the years, the forest edge rangeland site had the highest NDF rate with 62.85%, while the lowest NDF rate was recorded in the forest edge rangeland site with 57.74%. According to the research results, lower crude protein and higher ADF and NDF ratios were detected in dry matter samples taken from forest edge rangeland cuttings. It was concluded that grazing, especially during the growth period, caused the forage quality in the rangeland to decrease. For this reason, in order to obtain quality forage in the rangeland, it is recommended that the rangeland be left to rest for certain periods.

Keywords: forest rangeland sites, forage quality, dry matter.

Introduction

Rangelands are the most important natural resources that have survived to the present day, meeting the various needs of wild animals, pets and humans, although they have been subjected to different utilization since the existence of the earth. While Türkiye's rangeland area was around 44 million hectares in the earliest years of the Republic, it decreased to 21.7 million hectares in the 1980s. According to the latest statistics, meadow-rangeland areas have decreased to approximately 14.6 million hectares. [1].

While there has been a decrease in rangeland areas, the change in cattle population has been the opposite and while Türkiye had 6.9 million cattle in 1928, this number increased to 18.1 million in 2021 [2]. Considering that animal husbandry is one of the most important sources of livelihood in the region and as real rangelands continue to lose their productivity, livestock owners are looking for alternative grazing areas and especially forest villages are forced to turn towards interior forest, forest edge and forest top rangeland areas for animal grazing. According to the inventory study conducted by the General Directorate of Forestry, there is a total of 1.5 million hectares of forest rangelands, of which 279 thousand hectares are in-forest rangelands, 718 thousand hectares are over-forest rangelands and 557 thousand hectares are forest edge rangelands [3]. Although sub-forest cover rangelands do not produce as much forage as open areas and differ in terms of fodder quality, they are important alternative forage sources for regions with summer dry fodder period, especially because they dry out later in the summer months. In order to protect forests, one of our most important natural resources, and especially forest regeneration, it is of great importance to reduce the pressure of livestock on forests by improving rangelands close to forest areas and increasing their productivity and quality. If this can be realized, it will be possible to protect both forest vegetation and our rangelands exposed to erosion, and as a result of the animals being able to find sufficient forage resources, the dependence of the farmers living around the forests on the forests and socio-economic conflicts will be prevented [4-5].

Material Medhod

Study area

The study was conducted in 3 different rangeland sites with the same aspect (north-west) and approximately the same slope (5%) in Kırdağı locality of Oltu district, Erzurum province. The study area was divided into 3 different groups as above forest (I. rangeland site), interior forest (II. rangeland site) and forest edge (III. rangeland site).
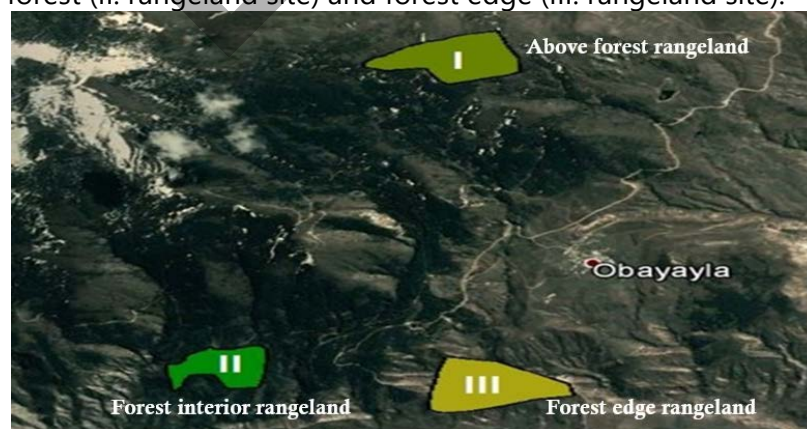

Figure 1. Location of the research area

The rangeland sites in the research areas are located at altitudes of 1810 m, 1930 m and 2370 m, respectively, and the average altitude was accepted as 2100 m.

Climate characteristics

In the region where the research area is located, there is a transitional climate between the continental climate and the Black Sea climate. Generally, the summer months are hot and dry, while precipitation intensifies in spring and fall. Climate data were evaluated by interpolating the data records (between 2014-2017) of the nearest meteorological station (1660 m) to the research area (2100 m). According to these data, the average temperature was determined as 6.9°C in 2015, 5.9°C in 2016, 7.1°C in 2017 and 7.0°C in the long-term average. The average annual precipitation was 590.3 mm in 2015, 640.9 mm in 2016, 529.1 mm in 2017, and the long-term average was 578.6 mm. According to the long-term average, the highest temperature was realized in July and August (19.4-20.6°C). The distribution of annual precipitation according to seasons and months is quite uneven. The wettest month of the year is May with an average of 121.3 mm and the wettest month is January with 13.6 mm. In 2015, the highest precipitation occurred in June (118.0 mm) and the lowest in September with 2.7 mm; in 2016, the highest precipitation occurred in May (128.2 mm) and the lowest in March and November with 16.7 mm; in 2017, the highest precipitation occurred in May (103.0 mm) and the lowest in January with 4.9 mm.

Using the interpolated values, temperature and precipitation diagrams was drawn and water deficit in the area evaluated [6]. It is seen that the beginning of the dry period (the first intersection point of the precipitation and temperature curves) starts in the first week of July and continues until the end of September (Figure 2).
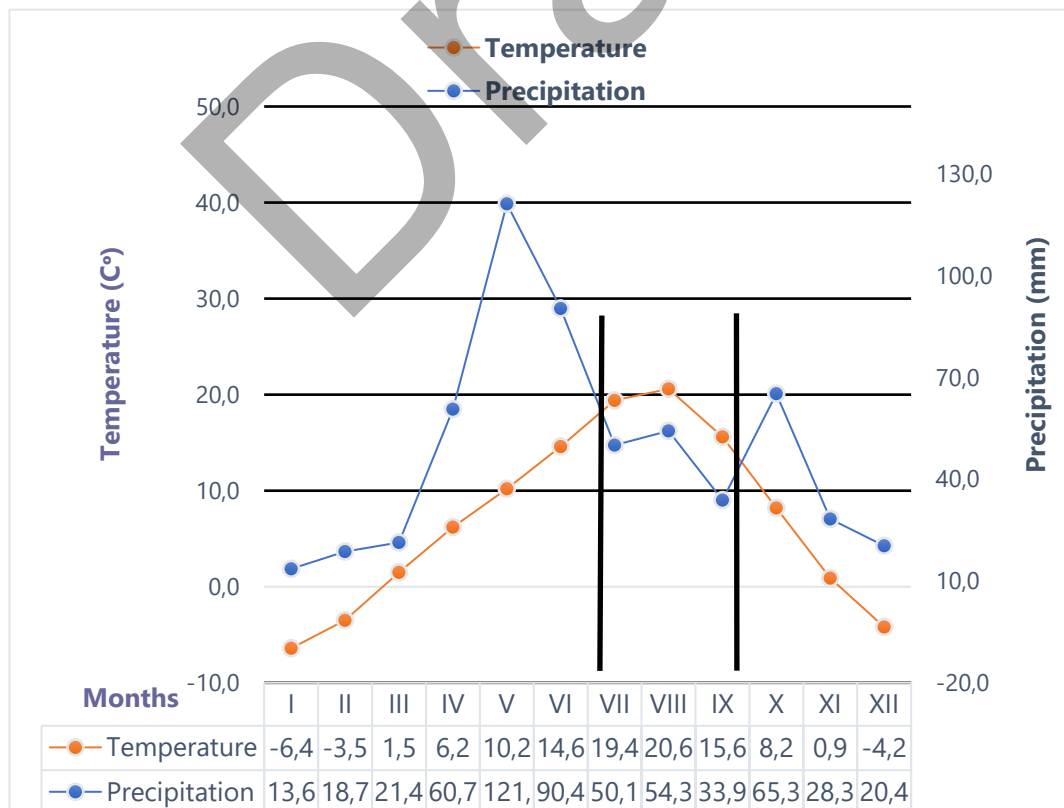

Months	I	II	III	IV	V	VI	VII	VIII	IX	X	XI	XII
Temperature	-6,4	-3,5	1,5	6,2	10,2	14,6	19,4	20,6	15,6	8,2	0,9	-4,2
Precipitation	13,6	18,7	21,4	60,7	121,	90,4	50,1	54,3	33,9	65,3	28,3	20,4

Figure 2. Rainfall-temperature relationship of the research area

Soil Properties

According to the soil analysis results of the rangeland sites where the study was conducted, it was determined that the texture class was clay loam (CL) and sandy clay loam (SCL). Ph values were recorded as 7.87, 7.76 and 7.36, respectively; electrical conductivity (EC) as 0.1, 0.08 and 0.07; organic matter as 4.05, 2.36 and 1.31; and phosphorus content as 14.9, 21.3 and 23.3, respectively (Table 1).

Table 1. Soil analysis results of the research area

Rangeland	Sand	Clay	Silt	Texture Class	pH	EC mmhos/cm	CaCO$_3$ %	OM %	K me/100 gr	Na ppm	Ca me/100 gr
I	42,84	29,21	27,93	CL	7,87	0,1	1,85	4,05	14,9	39,3	5,4
II	51,11	16,37	29,18	SCL	7,76	0,08	0,41	2,36	21,3	12	3,7
III	47,75	26,09	26,15	SCL	7,36	0,07	0,36	1,31	23,3	12	3,5

Method

The rangeland sites were arranged according to a randomized complete blocks experimental design by random sampling. Two different sampling methods, vegetation and soil, were used in the study. In order to determine dry matter quantity and forage quality (crude protein, ADF and NDF), six 50x50 cm quadrats were used to take matter samples from each rangeland site each year. In order to determine the chemical and physical properties of soil, soil samples were taken from 0-30 cm depth from 3 different rangeland sites. In the chemical analyses carried out to determine the forage quality, the forage samples subjected to analysis with ANKOM fiber analyzer were washed with acetone, dried overnight at 105°C, cooled in a desiccator and then weighed and ADF and NDF ratios were determined [7]. Nitrogen was determined using Kjeldahl method and crude protein ratio (%) was determined by multiplying the nitrogen found by 6.25 [8]. Dry matter yield was determined by weighing the mowed forages with a precision of 0.001 g after drying them in an oven set at 68°C for 24 hours [9]. For the comparison of the values obtained from rangeland site, the values were subjected to analysis of variance in SPSS package program after the ArcSinus transformation were applied to the values. Duncan multiple comparison test were used to compare the means [10].

Results

Amount of dry matter

The amount of dry matter in the rangeland sites and their changes over the years are presented in Table 2. The amount of dry matter varied between 33.08 kg/da and 37.86 kg/da according to the years. The average of the years was determined as 43.62 kg/da.

Table 2. Amount of dry matter (kg/da)

Rangeland/Year	2015	2016	2017	Mean
I	49,49 **A**	50,45 **ns**	52,09 **A**	**50,68 a**
II	33,11 **B**	24,35 **ns**	34,87 **B**	**30,77 b**
III	23,39 **C**	24,42 **ns**	26,63 **B**	**24,81 c**
Mean	**35,33 ns**	**33,08 ns**	**37,86 ns**	**43,62**

* The averages marked with a capital letter are significant at the 1% level, while those marked with a lower-case letter are significant at the 5% level.

In the first year of the study, the highest amount of dry matter was determined in site I (49.49 kg/ha) and the lowest amount of dry matter was determined in site III (23.39 kg/ha) (Table 2). In the third year of the study, as in the first year of the research, site I had the highest amount of dry matter while site III had the lowest amount of dry matter. These differences are thought to be due to the difference in altitude between the sites and the change in overgrazing pressure. The forest edge rangeland at low altitude, which is more exposed to grazing, produces less forage than the high-altitude areas because it does not have the opportunity to rest. In addition, it is thought that the increase in humidity in parallel with the increase in altitude increases the dry matter yield [11]. At the same time, the higher amount of soil organic matter in the first rangeland site compared to the other rangeland sites may be another factor affecting the amount of dry matter.

Crude protein ratios (%)

The crude protein ratios of the forage samples taken from the rangeland cutting are shown in Table 3. The crude protein ratios were 9.43% in the first year of the study, 9.57% in the second year and 10.20% in the third year. The crude protein average of all rangeland sites was determined as 9.73%.

Table 3. Crude protein ratios (%)

Rangeland/Year	2015	2016	2017	Mean
I	11,15 **ns**	11,39 **ns**	11,59 **a**	**11,37 a**
II	9,20 **ns**	9,3 **ns**	9,97 **b**	**9,49 b**
III	7,94 **ns**	8,02 **ns**	9,05 **b**	**8,33 c**
Mean	**9,43 B**	**9,57 B**	**10,20 A**	**9,73**

* The averages marked with a capital letter are significant at the 1% level, while those marked with a lower-case letter are significant at the 5% level.

The average crude protein ratios varied between 8.33% and 11.37% in the years of the research. In all the years of the study, the highest crude protein ratio was obtained in the first site, and the lowest crude protein ratio was obtained in the third site. The fact that site I was located at a higher altitude caused the crude protein ratio in the forage samples to be higher. As a matter of fact, it has been determined in other studies that the crude protein ratio in forage increases with increasing altitude [12-13]. This is because metabolic activity in plants increases with increasing altitude and as a result, forage quality is higher [14]. In addition, it is inevitable that the differences in species

composition will lead to changes in the crude protein content of the forage produced by rangelands [15].

Acide detergent fiber (ADF) ratios (%)

The ADF ratio was 42.50% in the first year of the study, 43.05% in the second year and 43.81% in the third year. This difference between the years was found to be statistically significant (p<0.01). According to the average of the years, the highest ADF rate was found in rangeland site III (45.44%) and the lowest ADF rate was found in site I (40.91%). This difference was statistically significant (p<0.05). In all years of the research, the highest ADF rates was found in site III and the lowest ADF rates was found in site I (Table 4).

Table 4. ADF ratios (%)

Rangeland/Year	2015	2016	2017	Mean
I	40,05 **b**	40,76 **C**	41,94 **b**	**40,91 c**
II	42,77 **a**	42,98 **B**	43,24 **b**	**42,99 a**
III	44,69 **a**	45,4 **A**	46,24 **a**	**45,44 a**
Mean	**42,50 B**	**43,05 B**	**43,81 A**	**43,11**

* The averages marked with a capital letter are significant at the 1% level, while those marked with a lower-case letter are significant at the 5% level.

It is known that forage quality in plants is affected by topography, climate, botanical composition, soil properties, season and grazing practices [16]. These results obtained from the study may be due to the differences in plant growth, plant composition and grazing intensity. As a matter of fact, it was stated that ADF ratio varied according to plant species, leaf-stem ratio [17], growth period and grazing intensity [18]. There was an increase in ADF ratio in the second and third years compared to the first year among the rangeland sites. This may be related to the drier second and third years and the early cessation of rainfall.

Neutral detergent fiber (NDF) ratios (%)

The NDF rate, which was an average of 60.49% in all research areas, was 60.19% in the first year of the study, 60.38% in the second year, and 60.94% in the third year (Table 5).

Table 5. NDF ratios (%)

Rangeland	2015	2016	2017	Mean
I	57,27 **b**	57,63 **C**	58,34 **C**	**57,74 C**
II	60,58 **a**	60,72 **B**	61,43 **B**	**60,90 B**
III	62,72 **a**	62,8 **A**	63,04 **A**	**62,85 A**
Mean	**60,19 B**	**60,38 B**	**60,94 A**	**60,49**

* The averages marked with a capital letter are significant at the 1% level, while those marked with a lower-case letter are significant at the 5% level.

According to the average of the years, site III was the highest NDF ratio with 62.85%, while the lowest NDF ratio was recorded in site I with 57.74%. It was determined that this change recorded in the rangeland sites according to the average of the years was statistically significant (p<0.01). In all the years of the research, the highest NDF rates was obtained in site III and the lowest NDF rates was obtained in site I (Table 5). The average NDF ratio in the forest edge rangeland sites was higher than the other rangeland sites. This may probably be due to the fact that this rangeland site was grazed for a longer period and more intensively than the other sites. Because in heavily grazed vegetation, plants have fewer leaves and therefore more stems due to the effect of grazing. In addition, due to grazing pressure, there is an increase in the proportion of plants with low forage value in these areas [19]. This may have resulted in a higher NDF ratio in the forest edge rangeland sites. As a matter of fact, the fact that it was stated that plant stems contain a higher proportion of NDF [17] confirms this idea. In the study, the NDF ratio was higher in the second and third years compared to the first year, as in the ADF ratio, and this may probably be due to the drier season in the second and third years.

Conclusions

As a result, when the rangeland sites above forest, forest edge and interior forest are compared in terms of the above characteristics, it is determined that the rangelands on the forest edge have been destroyed due to misuse and are of low quality in terms of rangeland evaluation criteria compared to other sites; and it is thought that this situation is caused by early and over-capacity grazing that is not in accordance with rangeland management principles. In order to prevent these negativities, it is thought that early grazing can be prevented by avoiding early spring grazing in areas with these and similar characteristics, not grazing before May 15 throughout the Eastern Anatolia Region and supporting the production of quality roughage by forest villagers. However, in areas with microclimate characteristics in the Eastern Anatolia Region, the grazing date can be moved to slightly earlier periods.

References

[1] TUİK, 2018. Bitkisel ve Hayvansal Üretim İstatistikleri. T.C. Başbakanlık Türkiye İstatistik Kurumu. http://www.tuik.gov.tr

[2] TUİK, 2021. Hayvansal Üretim İstatistikleri. Türkiye İstatistik Kurumu, Ankara, http://www.tuik.gov.tr

[3] Avcıoğlu, R., Tung T., Akbari N. ve Özel N., 1996. Seferihisar Yöresi Orman İçi ve Orman Kenarı Doğal Meralarının Islahı Olanakları Üzerinde Ön Araştırmalar. Orman Bakanlığı, Ege Ormancılık Araştırma Enstitüsü Müdürlüğü, Teknik Bülten No:2, İzmir.

[4] Çomaklı, B., 2001. Doğu Anadolu Bölgesinde Çayır-Mera Durumu ve Bölge Hayvancılığının Gelişmesindeki Önemi, Türkiye'nin Sorunlarına Çözüm Konferansları IV. 22 Mayıs, Erzurum.

[5] Uluocak, N., 1977. Doğal Meralar ve Orman Meraları. Gıda-Tarım ve Hayvancılık Bakanlığı, Ziraat İşletmeleri Genel Müdürlüğü, Çayır Mera ve Yem Bitkileri Semineri, 20-27 Haziran 1977, s. 1-19, Erzurum.

[6] Ustaoğlu, B., 2013. Oflak Dağı ve Çevresinin Fiziki Coğrafya Özellikleri. SAÜ Fen Edebiyat Dergisi II:169–190.

[7] Ankom Technology, 2004. The Ankom 200 Fiber Analyzer. Fairport, NY, https://www.ankom.com/product-catalog/ankom-200-fiber-analyzer

[8] Kacar, B., 1972. Bitki ve Topragın Kimyasal Analizleri: II. Bitki Analizleri. Ankara Üniv. Ziraat Fak. Yay. No:453, Ankara, 464 s.

[9] Sleugh, B., Moore, K.J., George, J.R. and Brummer, E.C., 2000. Brinary Legume-Grass Mixtures Improve Forage Yield, Quality and Seasonal. Distribution. Argon. J., 92: 24–29.

[10] Yıldız, N. ve Bircan H. 1994. Araştırma ve Deneme Metodları. Atatürk Üniv. No: 697, Zir. Fak. No: 305, Ders Kit. No: 57, Erzurum, 277 s.

[11] Terzioğlu, Ö. ve Yalvaç, N., 2004. Van Yöresi Doğal Meralarında Otlatmaya Başlama Zamanı, Kuru Ot Verimi ve Botanik Kompozisyonun Belirlenmesi Üzerine Bir Araştırma. Yüzüncü Yıl Üniversitesi, Ziraat Fakültesi, Tarım Bilimleri Dergisi (J. Agric. Sci.), 14(1): 23–26.

[12] Koç, A., Öztaş, T. ve Tahtacıoğlu, L., 2000. Palandöken meralarının farklı kesimlerinde alınan ot örneklerinde bazı kimyasal özelliklerinin otlatma mevsimindeki değişimi. Proc. Int. Animal Nutrition Congr, 471–478, Isparta.

[13] Mountousis, I., Papanikolaou, K., Stanogias, G., Chatzitheodoridis, F. and Karalazos, V., 2006. Altitudinal chemical composition variations in biomass of rangelands in Northern Greece. Livestock Research for Rural Development. Volume 18 Article # 106. Retrieved February 19, 2010, from,http: //www.lrrd 18/8/moun18106.htm (15-02-2008).

[14] Thilenius, J.F., 1979. Range management in the alphin zone: Practices and problems. In Special Management Needs of Alpine Ecosystems (ed: D.A Johnson), Soc. Range Manage., 5: 43–64.

[15] Holechek, J.L., Pieper, R.D. and Herbel, C.H., 2004. Range Management: Principles and Practicies. Prentice Hall, New Jersey, p. 607.

[16] Corona, G.L., Castrejón, F.P., Mendoza G.M., and Cobos, M.P., 1995. Ruminal degradability of NDF in corn stover using two cultures of Saccharomyces cerevisiae. Vet. Méx. 26: 276–285

[17] Ball, D.M., Collins, M., Lacefield, G.D., Martin, N.P., Mertens, D.A., Olson, K.E., Putnam, D.H., Undersander, D.J. and Wolf, M.W., 2001. Understanding forage quality. American Farm Bureau Federation Publication 1-01, Park Ridge, USA p. 21.

[18] Ainalis, A.B., Tsiouvaras, C.N. and Nastis, A.S., 2006. Effect of summer grazing on forage quality of woody and herbaceous species in a silvapastoral system in North Greece. J. of Arid Environ., 67: 90–99.

[19] Çomaklı, E., Güllap, M. K., Çomaklı, T., & Bilgili, A., (2021). The comparison of botanical composition and the condition and health class of different rangeland sites in forest ecosystem. Turkısh Journal Of Agrıculture And Forestry, vol.45, no.3, 349-355.

The Relationship between Nutrition Problems and Soil Profile in Afforestation Studies in Base Physiography

E. Çomaklı[1], M. Özgül[2], E. Yağanoğlu[3], M.A Başaran[4] and S. Öksüz[5]

[1]Atatürk University, Faculty of Agriculture, Erzurum, Türkiye, ORCID: 0000-0001-8477-7076
[2]Atatürk University, Faculty of Agriculture, Erzurum, Türkiye, ORCID: 0000-0002-5855-0086
[3]Atatürk University, Faculty of Agriculture, Erzurum, Türkiye, ORCID: 0000-0001-5963-3871
[4]Eastern Anatolia Forestry Research Institute, Erzurum, Türkiye, ORCID: 0000-0003-0878-0673
[5]Eastern Anatolia Forestry Research Institute, Erzurum, Türkiye

Abstract

The aim of the study is to evaluate the status of *Pinus sylvestris* L. (Scots pine) afforestation, which was brought by planting to the edge of the railway station in the base land. The relationship between physiography, climate and soil characteristics and the success of afforestation efforts in the base lands will be determined. In the study, trunk sections of Scots pine trees planted 55 years ago were examined. Physiographic conditions of the area were examined. Root depths were examined in the opened soil profile section. At the same time, some physical and chemical properties were determined in soil samples taken along the soil profile. The data taken together with the climate data were evaluated together. As a result of the annual ring and soil profile examination, it was concluded that Scots pine, due to its biological characteristics, tends to form taproot, which is required to form taproot, as a result of artificial irrigation. At the same time, the result that the average annual precipitation is not suitable for Scots pine development has been a factor limiting success. It appears that humidity and temperature regimes based on climate data cannot seasonally store sufficient water for perennial root development. It has been determined that in the dry period with water deficit, the soil is insufficient to meet the nutrient and water needs of the plant, especially from >50 cm depth. When the soil properties are examined, it is seen that the pH value is between 7.62-8.54, the lime content increases to 37.2% and the salinity increases to 0.27 (ds/m). These rates show that not only the development of Scots pine individuals is weak, but also the immune system of the individuals is vulnerable to diseases. In the evaluation of the data obtained, it becomes clear that the species appropriate to the region should be selected in afforestation studies and the physiographic conditions, climate conditions and soil profile should be evaluated integratedly. It will be important to consider land drainage, especially in afforestation planned on base lands.

Keywords: afforestation, soil profile, physiography, climate condutions.

Introduction

Afforestation activities are being carried out around the world as a low-cost and easily achievable option compared to other measures to mitigate the negative impacts of climate change. Especially in recent years, afforestation is presented as an important solution to limit climate change. In our country, afforestation activities have been carried out for many years and serious efforts have been made to expand our forest areas. Indeed, as a result of the studies carried out, forest areas increased from 20.2 million hectares (Mha) in 1973 to approximately 23.3 Mha by 2023 [1]. Afforestation activities include both forest afforestation and non-forest afforestation. A significant portion of the afforestation activities are located on transportation routes (highways and railways). However, it is also important to what extent the benefits to be obtained from afforestation activities can be achieved. In this context, site identification, species selection, and monitoring studies should be carried out in synchronization. The Food and Agriculture Organization of the United Nations (FAO) considers arid regions with annual rainfall of 300 mm or less and semi-arid regions with annual rainfall between 300-600 mm [2]. Especially in arid and semi-arid regions such as our country, it is important to examine the development of trees, climatic conditions, physiographic conditions and soil properties in an integrated manner.

Material Medhod

Study area

The research area located within the borders of Selim district of Kars province is geographically located at 40°27'37.44'' N latitude north latitude and 42°55'22.08'' D east longitude and has an average altitude of 1830 m (Figure 1).
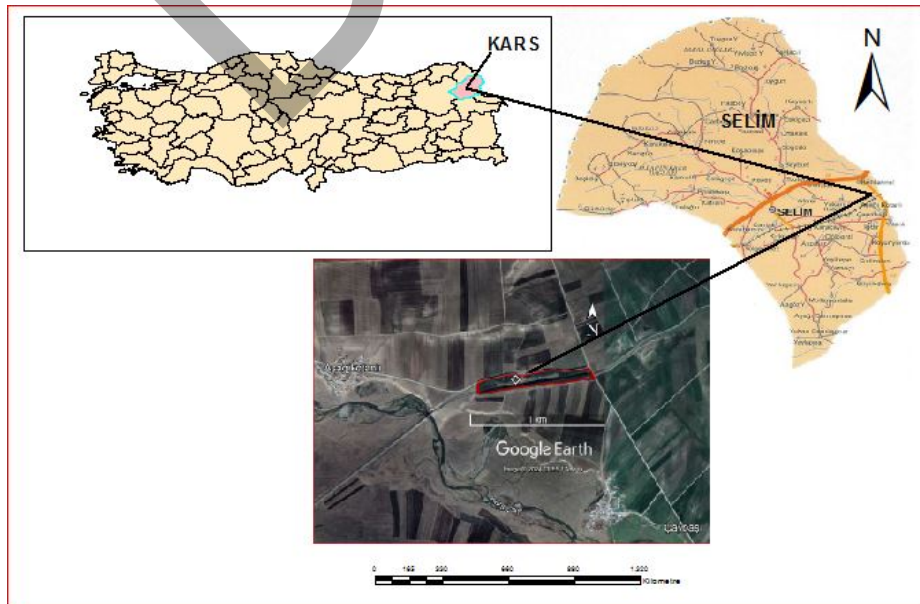

Figure 1. Location of the research area

The afforestation area is surrounded by dry agricultural lands and is generally flat and nearly flat in terms of physiographic characteristics. Within the land integrity, it consists of unified physiography including colluvial flats and basaltic volcanic deposits. Considering the area in general, it is covered with Neogene aged lake sediments and Quaternary aged alluvium [3]. Approximately 800 m south of the area is the Kars Stream. The area of approximately 8 ha around Benli Ahmet train station was afforested by planting yellow pine saplings in 1970. The average temperature is about 6°C, and the monthly average temperature ranges from −8.7° (January) to 18.8° (August). The average annual precipitation is about 370 mm and concentrated in May-July. The climate type of the research area was determined as arid according to the Erinç method. According to Köppen's method, it has the characteristics of Winter Severe, Summer Arid and Cool climate indicated by Dsb symbols.

Data Collection and Analysis Procedures

Soil samples were taken by excavating the soil profile, keeping a distance between dead and living trees. Soil samples were collected from four depth layers (0-7, 8-30, 31-60 and 61-90 cm). This profile were used to represent the horizon's chemical and physical properties. In addition, the soil profile was described according to the soil survey manual [4]. The sampling was carried out in the summer of 2023. Additionally, the physiographic conditions of the area were examined and evaluated. Soil samples were oven-dried at 105°C to constant weight. The soil sample was sieved to 2 mm, and plant residue particles were excluded from the samples for analysis. Particle size fractions were determined by the Bouyoucus's hydrometer method and soil texture was obtained with the textural triangle [5]. The amount of organic matter was determined by Walkey-Black methods using 5 g soil samples [6]. Soil pH was measured using a 1/2.5 soil sample and pure water ratio by pH meter [7]. EC was determined at 25 C° using saturated water by a conductivity bridge apparatus [8]. Total lime ($CaCO_3$) was determined by the Scheibler Kalsimeter method [9]. Exchangeable Cations (Ca, K and Na) were determined by shaking the soil samples with ammonium acetate to displace the cations [10]. Two trees selected from the area were cut down, their trunk cross sections were examined, and their development status over the years was evaluated taking into account climate and physiographic conditions.

Results

When the graph of precipitation amount according to the annual temperature distribution is analyzed, it is seen that the beginning of the dry period (the second intersection point of the precipitation and temperature curves) starts in the last week of June and continues until the beginning of November. It is understood that there is an absolute water deficit in the field during this dry period (Figure 2).
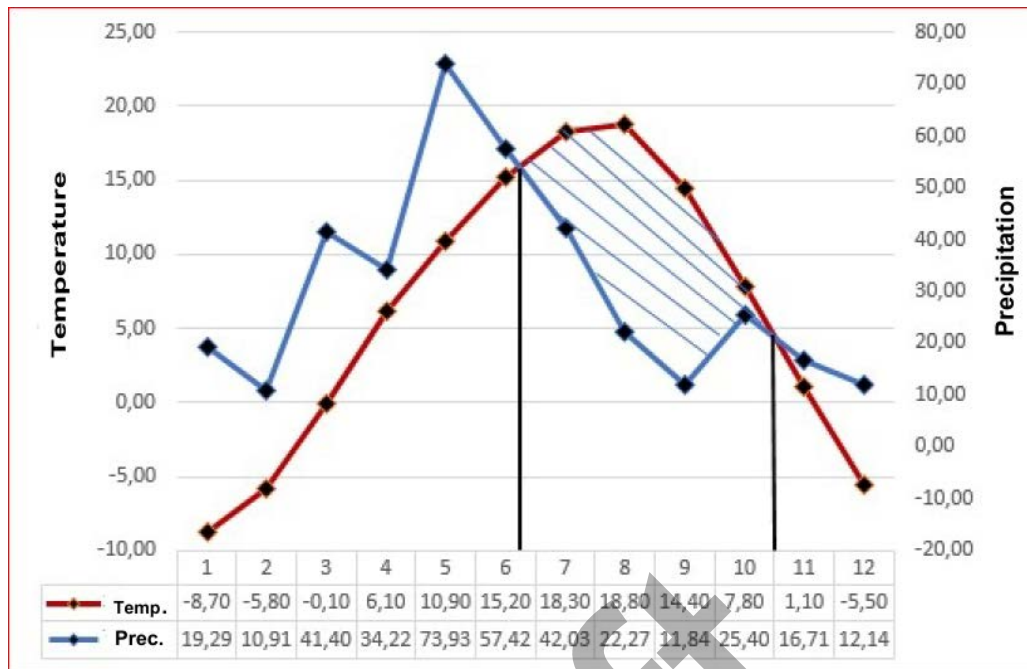
Figure 2. Precipitation-temperature relationship of the research area (2013-2022)

The analysis of the soil samples revealed that the pH of the soils was between 7.62-8.54, the lime content was 37.2% and the salinity was as high as 0.27 EC (ds/m). Soil particle size distribution varied very little in the profile (Table 1) and in general soils had a sandy and loam texture throughout their profile. The ranges of some exchangeable cations found in the soils were as follows: Na (1.4-7.1 me/100 gr), K (3.7-7.6 me/100 gr and Ca (19.5-42.2 me/100 gr), respectively (Table 1). Scots pine grows better in acidic soils and the optimum pH value in afforestation areas should be between 5.0-5.7 and salinity should be around 0.10 EC (ds/m) [11]. The research area has basic, alkaline and saline soil characteristics. In areas with these characteristics, it is inevitable that the development of Scots pine individuals will be weak and the immune system of the trees will be vulnerable to diseases. When these values are taken into consideration, it is concluded that the some soil characteristics of the current site do not provide a suitable environment for the growth of Scots pine trees. The average organic matter content of the soils taken from different depth levels in the research area was determined as 4.89% at 0-7 cm depth level, 2.39% at 8-30 cm depth level, 2.23% at 31-60 cm depth level and 1.96% at 61-90 cm depth level. It is desirable that the soil where the Scots pine tree is grown has high organic matter. These organic matter amounts are ideal for yellow pine growing environment. In addition, the amount of organic matter decreased from the upper layer of the soil to the lower layers. It is thought that this is due to the fall of dead branches and shoots under the stand.

Table 1. Some properties of the soil profile

Depth (cm)	pH (1:2,5)	EC (dS/m)	CaCO$_3$ (%)	OM (%)	Na (me/100 gr)	K (me/100 gr)	Ca (me/100 gr)	Texture Class
0-7	7.62	0.27	22.0	4.89	1.4	7.6	42.2	SL
8-30	8.25	0.25	37.2	2.39	7.1	4.6	23.0	L
31-60	8.54	0.15	33.8	2.23	4.8	3.7	24.4	SCL
61-90	8.42	0.16	30.4	1.96	2.8	3.9	19.5	L

The A horizon of the examined soil profile can be defined as two horizons in which the trees differ in terms of the density of their roots. The soils distributed in the research area were prevented by defective soil formation processes, the formation of which was caused by the parent material and topographical conditions. They are in the class of young profiled soils consisting of A and C horizons with inhibited profile development as a result of prolonged inundation (hydromorphic processes) due to the composition of the parent material (high lime content and cementation) and physiographic location. This is clearly observed when the density and thickness of the roots of trees and other plants in the surface horizons of the soils (horizon A), their distribution patterns on the surface and their presence in the parent material (horizon C) are examined. The C horizon is defined by the 2C horizon because the materials underlying the soils in the research area, depending on the depth, were deposited by different geological processes. The mineral particle size distribution of these materials varies significantly (lithologic discontinuity) (Figure 3).
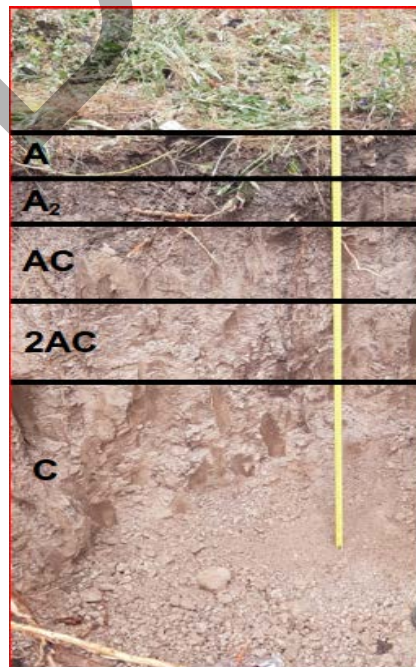

Figure 3. Soil profile

It was observed that the root development of both the dried and healthy individuals showed plate root development, while the yellow pine should have a tap root due to its biological characteristics. The reason for this root development was that the trees in the field were grown with irrigation for a certain period of time since the planting year, and accordingly, it was observed that the trees tended to make surface-orientated root system instead of tap roots (Figure 4). The increase in evaporation due to the increase in temperature in recent years has increased the ecological sensitivity of the environment. It is thought that especially summer drought has started to affect the development of trees negatively.

Figure 4. Broad root formation

This situation can be easily seen from the cross-sections in which the annual rings of the trees in the field are examined. It was observed that in the first years of irrigation, the spacing between the annual rings was wide, while in the non-irrigation period, the spacing between the annual rings was narrow (Figure 5b). In areas afforested with forest trees, irrigation in the form of irrigation disrupts the root and trunk balance by making the root of the tree lazy. For this reason, if the irrigation process is terminated, the immune system of the tree roots deteriorates. Individuals with weakened immunity are attacked by fungi and insects. These cause the individuals to die completely or get sick (Figure 5a).

Figure 5. Cross sections of the sample trees (a.dead tree- b. Healty tree)

It was determined that the planting interval was determined as 1.5 m x 2.0 m in the afforestation. However, the lack of any maintenance activities in the stand causes the trees to utilise less and less soil per unit area. In addition, stands that are not maintained in a timely manner lag behind in development [12,13].

Figure 6. Current status of the afforestation area

In order for the stand to have a healthy structure, thinning studies should be carried out and the distance between these trees should be increased over time. In this way, it is thought that individuals staying in the area may be more resistant to adverse conditions.

Conclusions

As a result of the evaluations made, it was determined that the ability of the soil to retain plant nutrients is poor and the soil properties are not in ideal conditions for the growth of Scots pine. Excessive irrigation, which will adversely affect root development, should be avoided especially in Scots pine plantations. As a matter of fact, it is thought that this situation has a great effect on the drying in the current area. In addition to all these, maintenance work should be carried out on time according to the development of the stand. However, in such areas where maintenance time has passed, it is necessary to avoid a harsh intervention and to carry out a moderate intervention over the years. First of all, it is necessary to prevent the spread of pests such as insects etc. throughout the area by removing dried individuals from the area. Especially in such physiographs where there is a ground water problem, it is necessary to make the necessary analyses in the soil profiles opened before starting afforestation works, taking into account the requirements of the species to be planted. As a result, physiographic conditions, climatic conditions (long years evaluation) and soil properties should be evaluated in an integrated manner.

References

[1] OGM, 2023. OGM Official Statistics. General Directorate of Forestry Web Page, http://www.ogm.gov.tr/tr/e-kutuphane/resmi-istatistikler. Access date: 22.02.2024).

[2] FAO, 1963. Tree planting practices for arid zones. food and agriculture organization of The United Nation, Rome.

[3] M. Demir, 2021. Geographical Principles of Agricultural Activities in Kars Province. Eastern Geographical Rewiew, 26(45), 77-106.

[4] Soil Survey Staff, 2014. Keys to Soil Taxonomy, 12th Edn. Texcoco: USDA NRCS.

[5] G.W. Gee and D. Or, 2002. Methods of soil analysis: Part 4 physical methods, Particle size analysis, 5, 255-293.

[6] D.W. Nelson and L.E. Sommers, 1982. Organic Matter. Methods Of Soil Analysis Part2. Chemical And Microbiological Properties Second Edition. Agronamy. No: 9 Part 2. Edition 574-579.

[7] G.W. Thomas, 1996. Soil pH and soil acidity. Methods of soil analysis: part 3 chemical methods, USA, 5, 475-490.

[8] S. Sonmez, D. Buyuktas, F. Okturen, S. Citak, 2008. Assessment of different soil to water ratios (1:1, 1:2.5, 1:5) in soil salinity studies. Geoderma. 144:361–369.

[9]   R.H. Loeppert, D.L. Suarez, 1996. Carbonate and gypsum. Methods of Soil Analysis: Part 3 Chemical Methods 5: 437-474. https://doi.org/10.2136/sssabookser5.3.c15

[10] D. Knudsen, G.A. Peterson, P.F. Pratt, 1982. Lithium. sodium and potasium. Methods of Soil Analysis Part 2. Chemical and Microbiological Properties Second Edition. American Society of Agronomy. Soil Science Society of America-Madison. Visconsin. USA. 225-245

[11] Anonymous, 1993. The Handbook Series of Scots pine: 7, Forestry Research Institute Publications, Miscellaneous Publications Series: 67, Ankara.

[12] E. Bayar, A. Deligöz, 2019. Three-Year Results of Precommercial Thinning in Burdur Region Natural Anatolian Black Pine Stand. Artvin Coruh University Journal of Forestry Faculty 20:18-27. https://doi.org/:10.17474/artvinofd.476662

[13] A. Göktürk, A. Demirci, S. Güner, 2010. Sarıçam (*Pinus silvestris* L.) Meşcerelerinde Aralama Uygulamalari. ''III. Ulusal Karadeniz Ormancılık Kongresi'', (3), 931-940. Artvin.

Determination of the Effect of Strigolactone on Pepper (*Capsicum annuum*) Seedlings under Zinc Toxicity

M. Yuce[1]

[1]*Ataturk University, Erzurum, Turkey, ORCID:* 0000-0002-0113-7071

Abstract

The zinc (Zn) content in the soil is increasing due to industrial activities and excessive use of Zn-containing fertilizers. Increasing Zn levels in the soil negatively affect human and animal health by affecting the production of vegetables and fruits. Strigolactone (SL), a carotenoid compound, is a phytohormone that has various roles in plants and has important effects in coordination with other hormones. Therefore, this study was conducted to evaluate the effect of SL in pepper grown under Zn stress. For this purpose, 10 µM SL was applied as a foliar spray three times at three-day intervals to pepper seedlings transferred to the hydroponic system. At the end of the period, the solutions in the hydroponic system were replaced with 5 mM $ZnSO_4$ solution. After 3 days, pepper seedlings were harvested and stored at -80 °C. Zn treatment (5 mM Zn) significantly has negatively affected pepper growth, the expression levels of antioxidant enzyme antioxidant enzyme and aquaporin genes. On the other hand, SL treatment (10 µM) increased pepper growth, antioxidant enzyme activity and stomatal movement. As a result of the study, it was found that SL affects the expression levels of antioxidant enzyme genes (*SOD* and *CAT*) and aquaporin genes (*CaPIP1-1, CaPIP1-2, CaTIP1-2* and *TIP5-1*) differently depending on the tissue and is especially more effective in roots. It has been determined that SL application can increase Zn tolerance by increasing growth parameters and affecting the expression levels of stress-sensitive genes.

Keywords: Zn, SL, heavy metal, gene expression, antioxidant enzyme

Introduction

Zn is a vital micronutrient, the most abundant after iron on earth [1]. Zn is an important plant micronutrient that functions as a cofactor for various enzymes such as carbonic anhydrase, alkaline phosphatases, aldolases, carboxypeptidases, alcohol dehydrogenases, superoxide dismutases, and is essential in various physiological processes such as electron transfer in photosynthesis and respiration [2]. While Zn levels act as antioxidants in optimum conditions, excessive amounts cause oxidative stress by increasing the formation of high concentrations of reactive oxygen species (ROS). Since common carriers serve for the uptake of divalent cations such as iron, calcium and Zn, increasing

Zn concentration also causes disruption of the homeostasis of other elements [3]. In addition, high Zn concentration significantly negatively affects various plant physiological, biochemical and molecular processes as it disrupts the structures of enzymes and proteins [4].

SL is endogenous hormones that play a vital role in the growth and development processes of many plants [5]. SL serves as a critical factor to increase the resilience of plants during stress by promoting basal root development, which plays an important role in plants' search for water and nutrients [6, 7]. SL may also regulate stomatal closure to minimize water loss through transpiration while maintaining gas exchange necessary for photosynthesis [8]. Additionally, strigolactone ensures stress tolerance by significantly increasing the plant's resilience by producing stress-related proteins and compounds [6].

Pepper is an important vegetable crop with high nutritional value [6]. Compared to other vegetables, pepper has a fragile root system and has a weaker water absorption capacity, making it more sensitive to environmental stresses [9]. Therefore, it is important to increase the resistance of pepper to heavy metal stress. For this purpose, in this study, the effect of SL on plant growth parameters of pepper grown under zinc toxicity, gene expression of antioxidant enzymes and the expression level of aquaporin genes were determined.

Materials and Methods

Pepper (*Capsicum annuum* L. cv Maraş) seeds were used as plant material in the study. Homogeneous seedlings, grown under controlled greenhouse conditions (diurnal the temperature of of day: 25±2°C; nocturnal temperatures of, night: 20±2°C and the humidity: 50±3%) until the seedling stage, were transferred to the hydroponic system. Three days after the transfer, SL treatment 10 (µM) as a foliar spray was made three times with three days intervals. At the end of the period, the hydroponic solution was replaced with 5 mM $ZnSO_4$ solution and the solutions containing only water was considered as the control group. One week after the stress conditions were applied, the plants were harvested and their growth parameters were taken, and the samples were frozen in liquid nitrogen at -80 °C for molecular analysis.

The fresh weight of the harvested plant samples was determined and the dry weight was calculated after being kept in the oven at 40 °C for 72 hours.

After powdered 0.1 g frozen pepper root and leaves in liquid nitrogen, Total RNA was extracted using Trizol (Invitrogen, USA). The concentrations of total RNA were determined by Nanodrop spectrophotometer and the integrity of was verified on 1% agarose gel.The RevertAid First Strand cDNA Synthesis Kit (Thermo Scientific) was used to synthesize cDNA from total RNAs. The synthesized cDNA was used to determine the expression levels of the genes identified using the A Maxima SYBR Green/ROX q-PCR Kit (Thermo Scientific) on the Rotor-Gene Q system (Qiagen, Germany). Specific PCR

products were confirmed by melting curve analysis and gel electrophoresis. Gene expression levels were determined using the $2-\Delta\Delta\Delta Ct$ method according to [10].

The one-way ANOVA was utilized to statistically analyze using SPSS. The difference among and between means were examined applying the Duncan test at the 0.05 ($p \leq 0.05$) probability level.

Results and Discussion

The study found that the treatment had a statistically significant effect on growth indicators. The findings of the study show that $ZnSO_4$ application significantly reduced all growth parameters (plant fresh weight (PFW), root fresh weight (RFW), plant dry weight (PDW) and root dry weight (RDW)) compared to the control group and SL application. SL application combined with Zn stress significantly increased these growth parameters compared to Zn application alone (Figure 1). The results obtained showed that SL pre-treatment to plants reduced the growth inhibition caused by Zn stress. Previous studies have shown that SL application can increase adaptation to Zn toxicity by reducing the effect of stress on growth [11, 12, 13].
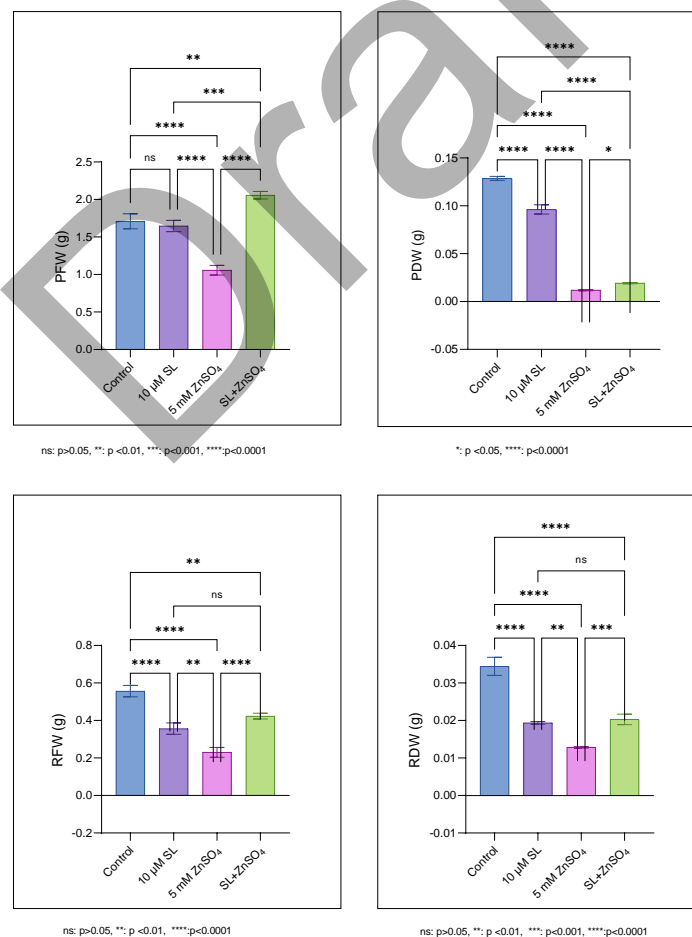

Figure 1. The effects of SL and Zn on growth parameters of pepper

Antioxidant enzymes such as SOD and CAT can prevent oxidative damage to plant cells by significantly reducing ROS accumulation. It has been observed that the gene expression levels of SOD and CAT enzymes vary depending on the tissue, and especially in roots, the expression level increases with Zn stress (Figure 2). It was observed that SL application combined with Zn stress reduced the expression level in roots compared to Zn stress alone. The possible reason for this may be that SL application acts as an antioxidant and therefore may significantly reduce the expression level of antioxidant enzymes. The results we obtained are similar to earlier studies [14, 15].
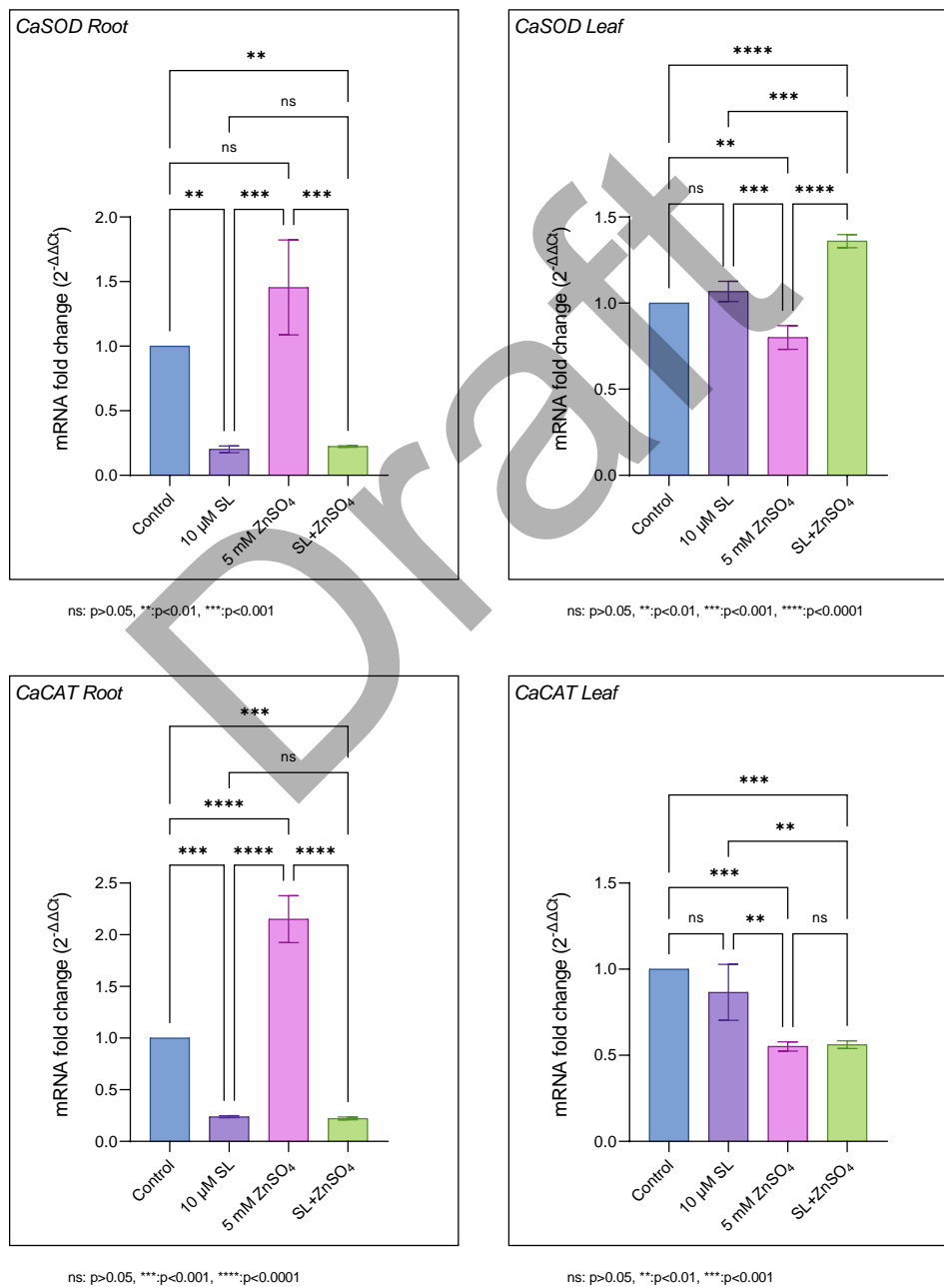

Figure 2. The effects of SL and Zn on the gene expression level of SOD and CAT enzyme

Zn toxicity significantly affects the water balance in plant cells. Increasing water availability in cells is an important step to increase the adaptation of plants to heavy metal toxicity [16]. Promoting bidirectional transmembrane movement of water, plant aquaporins function as small and highly hydrophobic transmembrane proteins that regulate the flow of intracellular or intercellular water molecules as well as cell elongation and differentiation and stomatal movement. Among aquaporins, plasma membrane intrinsic proteins (PIPs) are highly conserved and highly water-selective channel proteins. Tonoplast internal proteins (TIPs), which are localized on vacuolar membranes or vacuole formers, are key proteins in intracellular water transport and are responsible for the transport of not only water but also hydrogen peroxide, urea and glycerol [17].

It has been observed that the expression levels of aquaporin genes (*CaPIP1-1, CaPIP1-2, CaTIP1-2* and *TIP5-1*) vary according to tissue and increase with Zn stress, especially in roots. SL application significantly reduced the expression levels of these genes compared to Zn stress (Figure 3). The increase in the expression level of these genes with Zn stress may contribute to the maintenance of water availability under stress conditions [16]. Similarly, it was found that the expression levels of *PIP* and *TIP* genes were induced by various heavy metals and increased resistance to Cd and Zn metals [18, 19]. Exogenous SL can regulate stomatal conductance to compensate for water deficiency [20]. The decrease in the expression levels of aquaporin genes with SL application may mean that the water permeability of stem cells may be reduced to protect the cells from water loss [17].
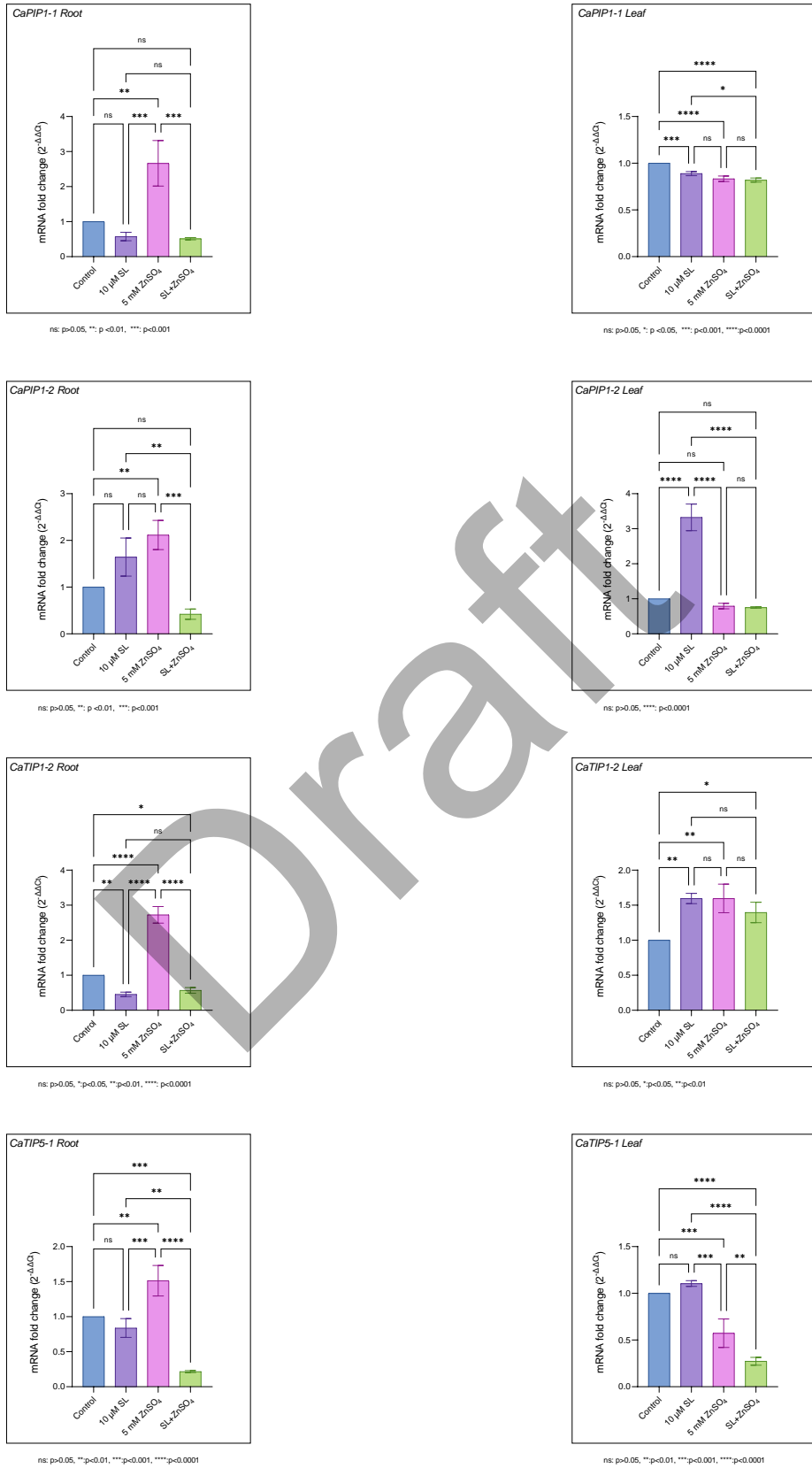
Figure 3. The effects of SL and Zn on expression level of aquaporine genes

Conclusions

The study shows that SL application can be used to obtain better growth in pepper seedlings grown under Zn stress and non-stress conditions and to obtain more resistant plants against various environmental stresses.

References

[1] M. Rizwan, S. Ali, M.Z.U. Rehman, A. Maqbool, 2019. A critical review on the effects of zinc at toxic levels of cadmium in plants. Environ. Sci. Pollut. Res. 26 (2019) 6279-6289.

[2] H. Kaur, S. Srivastava, N. Goyal, S. Walia, 2024. Behavior of zinc in soils and recent advances on strategies for ameliorating zinc phyto-toxicity. Environ. Exp. Bot. (2024) 105676.

[3] H. Kaur, S. Srivastava, 2023. The beneficial roles of trace and ultratrace elements in plants. Plant Growth Regul. 100(2) (2023) 219-236.

[4] H. Kaur, N. Garg, 2021. Zinc toxicity in plants: a review. Planta. 253(6) (2021) 129.

[5] E. Janeeshma, H. Habeeb, A.M. Shackira, A.K. Sinisha, P.P. Mirshad, B. Khoshru, D. Mitra, 2024. Strigolactone and analogues: a new generation of plant hormones with multifactorial benefits in environmental sustainability. Environ. Exp. Bot. (2024) 105775.

[6] S. Danish, M. Hareem, K. Dawar, T. Naz, M.M. Iqbal, M.J. Ansari, R. Datta, 2024. The role of strigolactone in alleviating salinity stress in chili pepper. BMC Plant Biol. 24(1) (2024) 209.

[7] M. Luqman, M. Shahbaz, M.F. Maqsood, F. Farhat, U. Zulfiqar, M.H. Siddiqui, F.U. Haider, 2023. Effect of strigolactone on growth, photosynthetic efficiency, antioxidant activity, and osmolytes accumulation in different maize (*Zea mays* L.) hybrids grown under drought stress. Plant Signal. Behav.18(1) (2023) 2262795.

[8] M. Sedaghat, Y. Emam, A. Mokhtassi-Bidgoli, S. Hazrati, C. Lovisolo, I. Visentin, Z. Tahmasebi-Sarvestani, 2021. The potential of the synthetic strigolactone analogue GR24 for the maintenance of photosynthesis and yield in winter wheat under drought: investigations on the mechanisms of action and delivery modes. Plants. 10(6) (2021) 1223.

[9] H. Shu, K. Xu, X. Li, J. Liu, M.A. Altaf, H. Fu, Z. Wang, 2024. Exogenous strigolactone enhanced the drought tolerance of pepper (Capsicum chinense) by mitigating oxidative damage and altering the antioxidant mechanism. Plant Cell Rep. 43(4) (2024) 1-13.

[10] K.J. Livak, T.D. Schmittgen, 2001. Analysis of relative gene expression data using real-time quantitative PCR and the 2− ΔΔCT method. Methods, 25(4) (2001) 402-408.

[11] Y. Li, S. Li, Q. Feng, J. Zhang, X. Han, L. Zhang, J. Zhou, 2022. Effects of exogenous Strigolactone on the physiological and ecological characteristics of Pennisetum purpureum Schum. Seedlings under drought stress. BMC Plant Biol. 22(1) (2022) 578.

[12] A. Sattar, S. Ul-Allah, M., Ijaz, A., Sher, M., Butt, T., Abbas, S.A. Alharbi, 2022. Exogenous application of strigolactone alleviates drought stress in maize seedlings by regulating the physiological and antioxidants defense mechanisms. Cereal Res. Commun. 50(2) (2022) 263-272.

[13] X. Liu, T. Gao, C. Liu, K. Mao, X. Gong, C. Li, F. Ma, 2023. Fruit crops combating drought: Physiological responses and regulatory pathways. Plant Physiol. 192(3) (2023) 1768-1784.

[14] Z. Min, R. Li, L. Chen, Y. Zhang, Z. Li, M., Liu, Y. Fang, 2019. Alleviation of drought stress in grapevine by foliar-applied strigolactones. Plant Physiol. Biochem. 135 (2019) 99-110.

[15] P. Garcia-Caparros, L. De Filippis, A. Gul, M. Hasanuzzaman, M. Ozturk, V. Altay, M.T. Lao, 2021. Oxidative stress and antioxidant metabolism under adverse environmental conditions: a review. Bot. Rev. 87 (2021) 421-466.

[16] K. Yin, R. Zhao, Z. Liu, S. Qi, Y. Zhang, Y. Liu, S. Chen, 2024. Populus euphratica CPK21 interacts with heavy metal stress-associated proteins to mediate Cd tolerance in Arabidopsis. Plant Stress. 11 (2024) 100328.

[17] M.Y. Liu, Q.S. Li, W.Y. Ding, L.W. Dong, M. Deng, J.H. Chen, Q.S. Wu, 2023. Arbuscular mycorrhizal fungi inoculation impacts expression of aquaporins and salt overly sensitive genes and enhances tolerance of salt stress in tomato. Chem. Biol. Technol. Agric. 10(1) (2023) 5.

[18] L.D. Zhang, L.Y. Song, M.J. Dai, Z.J. Guo, M.Y. Wei, J. Li, H.L. Zheng, 2022. Cadmium promotes the absorption of ammonium in hyperaccumulator Solanum nigrum L. mediated by ammonium transporters and aquaporins. Chemosphere. 307 (2022) 136031.

[19] Y. Zhang, Z. Wang, T. Chai, Z. Wen, H. Zhang, 2008. Indian mustard aquaporin improves drought and heavy-metal resistance in tobacco. Mol. Biotechnol. 40 (2008) 280-292.

[20] E.B. Aliche, C. Screpanti, A. De Mesmaeker, T. Munnik, H.J. Bouwmeester, 2020. Science and application of strigolactones. New Phytol. 227(4) (2020) 1001-1011.

Practical Augmented Reality Training for Academicians

B. Ispir[1], and S. Okumuş[2]

[1]*Atatürk University, Erzurum, Türkiye, ORCID: 0000-0002-0428-8887*
[2]*Atatürk University, Erzurum, Türkiye, ORCID: 0000-0001-6271-8278*

Abstract

This study was conducted to introduce augmented reality technology to academicians and to emphasize the potential of this technology in education. Twenty-six academicians assigned in different departments of the Faculty of Education participated in the study. From this point of view, 5 different groups were formed by taking into account the departments in which the academicians were assigned, and a 15-hour training was prepared. The training contents were realized in 3-hour sessions for each group. After the trainings were completed, 17 volunteer academicians evaluated both the training process and the trainer through a 5-point Likert-type questionnaire. A comprehensive evaluation was made to understand the impact of the training and the extent to which academicians benefited from the training and the data obtained were analyzed descriptively. As a result, the majority of the academicians stated that the training met their expectations and was understandable. Academicians reported that they were provided with sufficient opportunity to ask questions during the training, that they acquired new knowledge and skills, and that the training contributed to their professional development.

Keywords: Augmented reality, BlippAR, Educational technologies, Academicians.

Introduction

The use of teaching methods and textbooks alone doesn't attract students' attention and this leads to weak learning outcomes (Saidin et al., 2024). Therefore, it is seen that augmented reality (AR) technology, which emerged as a visualization method, is used more frequently to enrich students' learning experiences (Levy et al., 2024). AR is one of the advanced technologies that combines computer graphics with the real world interactively (Klopfer & Squire, 2008; Silva et al., 2003). Moreover, AR can be defined as a technology that enhances learning interaction by overlaying digital information in physical environments (Chen et al., 2022). However, to have this experience and thus create storable and accessible AR activities, some software is needed (Simon, 2023). In this context, software such as Unity Vuforia, HP Reveal, BuildAR, and BlippAR are generally used to design AR activities (Altıok, 2020; Chiang et al., 2022; Parmaxi & Demetriou, 2020).

BlippAR, one of the AR activity design software, is frequently used in education to enrich learning experiences (Striuk et al., 2018). Because the basic features of BlippAR can be used free of charge. In addition, BlippAR provides a user-friendly experience with its simple and understandable interface (Kharchenko & Babenko, 2021). In this respect, BlippAR makes it very fast and convenient for users to create powerful AR activities with drag-and-drop logic without requiring coding skills (Elivera & Palaoag, 2020; McNally & Kolivand, 2024). Therefore, this software enables non-professional developers to create engaging designs (Rosdi & Akhir, 2021; Wang et al., 2019). These tools and services enable AR to be brought into classroom environments to provide an immersive learning experience (van Arnhem, 2016). In fact, in BlippAR-supported education studies, it has been observed that students' motivation, interest, and understanding of concepts have increased. Also, it was stated that students' digital and technological competence levels improved as a result of the use of AR technologies such as BlippAR (Karnishyna et al., 2022). In another study, it was determined that learning became more interesting and enjoyable through BlippAR (Alizadeh et al., 2017).

Thus, introducing BlippAR technology to academicians is important for them to adopt contemporary education methods and design activities that will enrich the learning experience for their future students. Furthermore, it is thought that learning BlippAR will support academicians in developing technological skills. However, when the literature was examined, there was no study in which academicians were trained in a way to encourage them to design AR activities. Therefore, it is necessary to investigate how effective the features offered by BlippAR are in creating interactive learning environments and how academicians interact with such technologies. In line with the stated reasons, the study was conducted to introduce AR technology to academicians in practice and to emphasize the potential of this technology. Moreover, increasing the awareness of academicians about how AR can be used in education is among the aims of the study. In addition, the study aims to improve the qualifications of academicians and increase the quality of education.

Method

Considering the departments where the academicians are assigned, 5 different groups were formed to learn about AR. Thus, a 15-hour training program was prepared. In this study, 26 academicians assigned in different departments of the Faculty of Education participated. The training content was delivered in 3-hour sessions for each group. In the first hour of the training, information was given about the history of AR, the areas where it is used, and its positive and negative aspects. Then BlippAR, one of the AR software, was introduced. In this context, multimedia elements that can be used in the BlippAR program and the Sketchfab library were shown practically. In the second and third hours, a basic marker-based AR activity was gradually designed with the academicians through BlippAR. After the training, 17 volunteer academicians evaluated both the training process and the trainer through a form. For this, a Likert-type questionnaire was used as a data collection tool. In the questionnaire, 6 questions were asked to evaluate the training, 6 questions to evaluate the trainer, and 4 questions about the end of training

outcomes. In addition, the questionnaire included two questions about the general satisfaction level and whether AR would be used in the future. Also, a comment field was included for those who wished to provide an optional additional opinion. The comments were used to support or refute the questionnaire items. To understand the impact of the training through the questionnaire and the extent to which academicians benefit from the training, a comprehensive evaluation was made and the data obtained were analyzed descriptively. When presenting some of the findings of the participants, code names were given as A1, A2, A3, …, A17.

Findings

In the study, the averages of the questionnaire items were taken to evaluate the views of academicians on AR training and the instructor who conducted this training (Figure 1, Figure 2 & Figure 3). In this context, a decision was reached regarding the satisfaction levels of academicians by considering the relevant averages. On the other hand, items related to training, trainer, and end of training outcomes are shown in different colors.
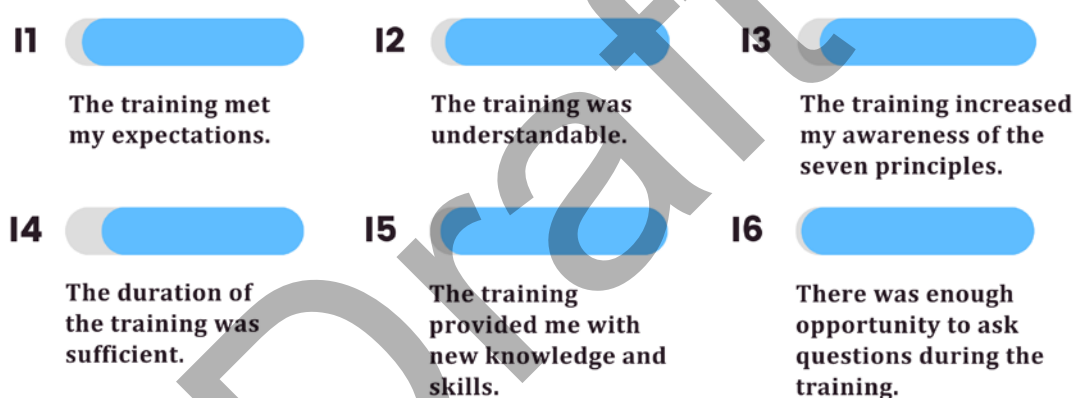

Figure 1. Academicians' views on augmented reality education

When Figure 1 is analyzed, it is determined that the training met the expectations of the academicians. Two academicians (A5 and A13) provided additional opinions that the training was very productive. In addition, all participants stated that the training was understandable and that they weren't confused. Besides this, academicians generally expressed positive opinions about the duration of the training. Likewise, the academicians stated that there was enough opportunity to ask questions during this period. Nevertheless, the academic coded A8 wanted the duration of the training to be increased. The same participant stated that it would be useful to briefly mention alternative AR tools. In addition, academicians stated that they gained new knowledge and skills through the training.
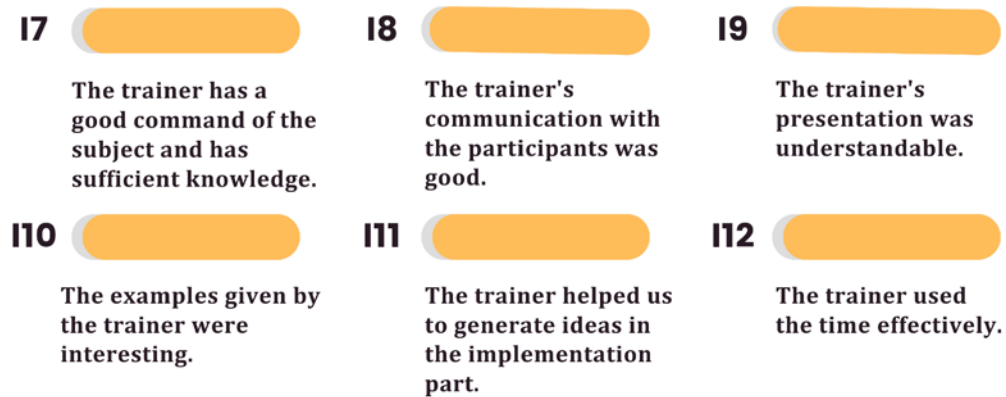
Figure 2. Academicians' views on the trainer

Looking at Figure 2, the academicians stated that the trainer had sufficient knowledge about AR and BlippAR. All academicians stated that the trainer communicated with the participants at an adequate level. It can be thought that this situation helped academicians to produce creative ideas in the implementation part. In addition, the academicians stated that the presentation prepared by the trainer was understandable and the examples given during the presentation were interesting. On the other hand, opinions were reached that the trainer used the time effectively.
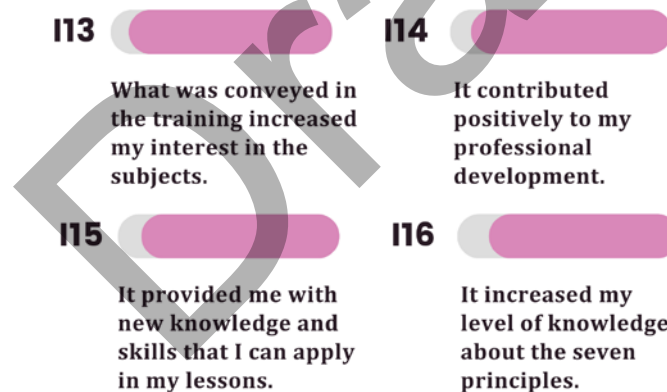

Figure 3. Academicians' views on end of training outcomes

Figure 3 shows that what was explained during the training increased academicians' interest in the subjects. In addition, academicians stated that the AR training contributed positively to their professional development. In this context, academics stated that they would use the new knowledge and skills they acquired in their courses. Finally, it was observed that academicians' general satisfaction levels regarding the training were high.

Conclusion and Discussion

The BlippAR training provided within the scope of the study met the expectations and was found to be understandable by the academicians. Participants generally spoke

positively about the duration of the training and emphasized that the opportunity to ask questions was sufficient. In addition, it was observed that academicians gained new knowledge and skills during the training process. On the other hand, it was concluded that the topics presented in the training increased the interest of the academicians and contributed positively to their professional development. As a result, academicians were highly satisfied with the training provided. Sat et al. (2023) found that BlippAR had a higher satisfaction score than Unity Vuforia. Similar to these results, Irshad and Rambli (2015) examined user satisfaction using BlippAR and two different AR software. The results showed that AR ads created using BlippAR had a positive impact on users. In another study, BlippAR was found to help students have a positive user experience (Alizadeh et al., 2017).

The fact that BlippAR is easier, functional, and user-friendly may have led to these results. This is because BlippAR is considered as a tool that can be used by non-programmers or designers with little background in computer programming to create activities (Dengel et al., 2022; Kazanidis & Pellas, 2019). Similarly, Cabero-Almenara and Llorente-Cejudo (2019) stated that BlippAR is one of the easiest AR software to use for designers. Roig-Vila et al. (2019) conducted training in which students were able to create AR objects using Aurasma, Augment, and BlippAR software. In this context, it was found that the students highly agreed that AR was easy to use. On the other hand, the direct web-based operation of BlippAR without downloading any files may have affected the satisfaction levels of academicians. The statement that BlippAR allows creating and organizing AR activities on web-based platforms supports this idea (BlippAR, 2024; Herpich et al., 2017).

Limitations and Recommendations

Although it makes important contributions to the literature, this study also has some limitations. The study was conducted only with academicians assigned in the faculty of education of a university located in the east of Turkey. This situation makes it difficult to generalize and obtain comparable results. Therefore, future research should be conducted in different universities and faculties. In addition, the use of only BlippAR in the training given to academicians constitutes another limitation of the study. Therefore, other AR activity design software such as Unity Vuforia, Fectar, Roar, and UniteAR can be used in future research. This may also help to identify the advantages and disadvantages of different platforms. On the other hand, the duration of the training was limited to three hours for each group. A longer training period may help to obtain more in-depth results. From this point of view, comprehensive training studies can be conducted to allow for the evaluation of the participants' long-term performance.

Acknowledgments

References

[1] Alizadeh, M., Mehran, P., Koguchi, I., & Takemura, H. (2017). Learning by design: Bringing poster carousels to life through augmented reality in a blended English course. *CALL in a Climate of Change: Adapting to Turbulent Global Conditions–Short Papers from EUROCALL*, 7-12. https://doi.org/10.14705/rpnet.2017.eurocall2017.680

[2] Altıok, S. (2020). The effects of augmented reality supported instruction on elementary students' academic achievement and the opinions of students. *Educational Technology Theory and Practice, 10*(1), 177-200. https://doi.org/10.17943/etku.622871

[3] BlippAR. (2024). *Blippbuilder*. Accessed from https://www.blippar.com/ on 23.04.2024.

[4] Cabero-Almenara, J., & Llorente-Cejudo, C. (2019). Evaluación de software de producción de objetos en Realidad Aumentada con fines educativos. *Revista de Educación a Distancia, 60*. http://doi.org/10.6018/red/60/01

[5] Chen, M. P., Wang, L. C., Zou, D., Lin, S. Y., Xie, H., & Tsai, C. C. (2022). Effects of captions and English proficiency on learning effectiveness, motivation and attitude in augmented-reality-enhanced theme-based contextualized EFL learning. *Computer Assisted Language Learning, 35*(3), 381-411. https://doi.org/10.1080/09588221.2019.1704787

[6] Chiang, F. K., Shang, X., & Qiao, L. (2022). Augmented reality in vocational training: A systematic review of research and applications. *Computers in Human Behavior, 129*, 107125. https://doi.org/10.1016/j.chb.2021.107125

[7] Dengel, A., Iqbal, M. Z., Grafe, S., & Mangina, E. (2022). A review on augmented reality authoring toolkits for education. *Frontiers in Virtual Reality, 3*, 798032. https://doi.org/10.3389/frvir.2022.798032

[8] Elivera, A., & Palaoag, T. (2020, April). *Development of an augmented reality mobile application to enhance the pedagogical approach in teaching history* [Paper presentation]. IOP Conference Series: Materials Science and Engineering (Vol. 803, No. 1, p. 012014). https://doi.org/10.1088/1757-899X/803/1/012014

[9] Herpich, F., Guarese, R. L. M., & Tarouco, L. M. R. (2017). A comparative analysis of augmented reality frameworks aimed at the development of educational applications. *Creative Education, 8*, 1433-1451. https://doi.org/10.4236/ce.2017.89101

[10] Irshad, S., & Rambli, D. R. A. (2015, 17-19 November). *User experience satisfaction of mobile-based AR advertising applications* [Paper presentation]. Advances in Visual Informatics: 4th International Visual Informatics Conference (pp. 432-442). Springer.

[11] Karnishyna, D. A., Selivanova, T. V., Nechypurenko, P. P., Starova, T. V., & Stoliarenko, V. G. (2022, June). The use of augmented reality in chemistry lessons in the study of "Oxygen-containing organic compounds" using the mobile application Blippar

[Paper presentation]. *Journal of Physics: Conference Series* (Vol. 2288, No. 1, p. 012018). IOP.

[12] Kazanidis, I., & Pellas, N. (2019). Developing and assessing augmented reality applications for mathematics with trainee instructional media designers: An exploratory study on user experience. *Journal of Universal Computer Science*, *25*(5), 489-514. https://doi.org/10.3217/jucs-025-05-0489

[13] Kharchenko, Y. V., & Babenko, O. M. (2021, July). *Using Blippar to create augmented reality in chemistry education* [Paper presentation]. CEUR Workshop Proceedings (pp. 213–229). https://doi.org/10.31812/123456789/4630

[14] Klopfer, E., & Squire, K. (2008). Environmental detectives the development of an augmented reality platform for environmental simulations. *Educational Technology Research and Development, 56*(2), 203-228. https://doi.org/10.1007/s11423-007-9037-6

[15] Levy, J., Chagunda, I. C., Iosub, V., Leitch, D. C., & McIndoe, J. S. (2024). MoleculAR: An augmented reality application for understanding 3D geometry. *Journal of Chemical Education,* 1-7. https://doi.org/10.1021/acs.jchemed.3c01045

[16] McNally, K. F., & Kolivand, H. (2024). A web-based augmented reality system. *EAI Endorsed Transactions on Scalable Information Systems*, 1-8. https://doi.org/10.4108/eetsis.5481

[17] Parmaxi, A., & Demetriou, A. A. (2020). Augmented reality in language learning: A state-of-the-art review of 2014–2019. *Journal of Computer Assisted Learning, 36*, 861-875. https://doi.org/10.1111/jcal.12486

[18] Roig-Vila, R., Lorenzo-Lledó, A., & Mengual-Andrés, S. (2019). Utilidad percibida de la realidad aumentada como recurso didáctico en Educación Infantil. *Campus Virtuales*, *8*(1), 19-35.

[19] Rosdi, M. M., & Akhir, M. A. S. B. M. (2021). *An innovation of augmented reality lab sheet for DEE30015 electronic equipment repair course by using blippar software* [Paper presentation]. International Congress of Eurasian Social Sciences-5 (pp. 402-408).

[20] Saidin, N. F., Abd Halim, N. D., Yahaya, N., & Zulkifli, N. N. (2024). Enhancing students' critical thinking and visualisation skills through mobile augmented reality. *Knowledge Management & E-Learning*, *16*(1), 1-41. https://doi.org/10.34105/j.kmel.2024.16.001

[21] Sat, M., Ilhan, F., & Yukselturk, E. (2023). Comparison and evaluation of augmented reality technologies for designing interactive materials. *Education and Information Technologies, 28*, 11545–11567. https://doi.org/10.1007/s10639-023-11646-3

[22] Silva, R., Oliveira, J. C., & Giraldi, G. A. (2003). Introduction to augmented reality. *National Laboratory for Scientific Computation*, 11, 1–11.

[23] Simon, J. (2023). Augmented reality application development using Unity and Vuforia. *Interdisciplinary Description of Complex Systems: INDECS*, *21*(1), 69-77. https://doi.org/10.7906/indecs.21.1.6

[24] Striuk, A., Rassovytska, M., & Shokaliuk, S. (2018). Using Blippar augmented reality browser in the practical training of mechanical engineers. *arXiv preprint.* https://doi.org/10.31812/0564%2F2252

[25] van Arnhem, J. P. J. (2016). Mobile apps for libraries: Exploring blippar for education. *The Charleston Advisor, 17*(4), 53-57. https://doi.org/10.5260/chara.17.4.53

[26] Wang, Q., Siedlaczek, M., Chen, Y. Y., Gormish, M., & Suel, T. (2019, December). *Forward index compression for instance retrieval in an augmented reality application* [Paper presentation]. International Conference on Big Data (pp. 1946-1952). IEEE.